

# Metallo-supramolecular architectures based on terpyridine metal complexes

**Citation for published version (APA):**

Hofmeier, H. (2004). *Metallo-supramolecular architectures based on terpyridine metal complexes*. [Phd Thesis 1 (Research TU/e / Graduation TU/e), Chemical Engineering and Chemistry]. Technische Universiteit Eindhoven. <https://doi.org/10.6100/IR573334>

**DOI:**

[10.6100/IR573334](https://doi.org/10.6100/IR573334)

**Document status and date:**

Published: 01/01/2004

**Document Version:**

Publisher's PDF, also known as Version of Record (includes final page, issue and volume numbers)

**Please check the document version of this publication:**

- A submitted manuscript is the version of the article upon submission and before peer-review. There can be important differences between the submitted version and the official published version of record. People interested in the research are advised to contact the author for the final version of the publication, or visit the DOI to the publisher's website.
- The final author version and the galley proof are versions of the publication after peer review.
- The final published version features the final layout of the paper including the volume, issue and page numbers.

[Link to publication](#)

**General rights**

Copyright and moral rights for the publications made accessible in the public portal are retained by the authors and/or other copyright owners and it is a condition of accessing publications that users recognise and abide by the legal requirements associated with these rights.

- Users may download and print one copy of any publication from the public portal for the purpose of private study or research.
- You may not further distribute the material or use it for any profit-making activity or commercial gain
- You may freely distribute the URL identifying the publication in the public portal.

If the publication is distributed under the terms of Article 25fa of the Dutch Copyright Act, indicated by the "Taverne" license above, please follow below link for the End User Agreement:

[www.tue.nl/taverne](http://www.tue.nl/taverne)

**Take down policy**

If you believe that this document breaches copyright please contact us at:

[openaccess@tue.nl](mailto:openaccess@tue.nl)

providing details and we will investigate your claim.

# Metallo-supramolecular architectures based on terpyridine metal complexes

## PROEFSCHRIFT

ter verkrijging van de graad van doctor aan de  
Technische Universiteit Eindhoven, op gezag van de  
Rector Magnificus, prof.dr. R.A. van Santen, voor  
een commissie aangewezen door het College voor  
Promoties in het openbaar te verdedigen op  
woensdag 3 maart 2004 om 16.00 uur

door

Harald Hofmeier

geboren te Heidelberg, Duitsland

Dit proefschrift is goedgekeurd door de promotoren:

prof.dr. U.S. Schubert

en

prof.dr. J.-F. Gohy

This research was financially supported by the Deutsche Forschungsgemeinschaft (SFB 486) and the Eindhoven University of Technology.

Omslagontwerp: Harald Hofmeier en Jan-Willem Luiten

Druk: Universiteitsdrukkerij, TUE

CIP-DATA LIBRARY TECHNISCHE UNIVERSITEIT EINDHOVEN

Hofmeier, Harald

Metallo-supramolecular architectures based on terpyridine metal complexes / by Harald Hofmeier.

Eindhoven: Technische Universiteit Eindhoven, 2004.

Proefschrift. – ISBN 90-386-2915-X

NUR 913

Trefwoorden: supramoleculaire chemie; amfifielen / metaalhoudende polymeren / overgangsmetaalcomplexen ; Ruthenium / coördinatieverbindingen; terpyridine / polymeren; morfologie / copolymeren; vernetting

Subject headings: supramolecular chemistry ; amphiphiles / organometallic polymers / transition metal complexes; Ruthenium / coordination compounds; terpyridine / polymer morphology / copolymers; crosslinking

Copyright 2004, H. Hofmeier

# Table of contents

<b>1</b>	<b>Recent developments in the supramolecular chemistry of terpyridine metal complexes</b>	<b>1</b>
1.1	Introduction	2
1.2	Synthetic strategies	3
1.3	Uninuclear terpyridine ruthenium complexes	7
1.4	Dyads and triads	22
1.5	Supramolecular assemblies	33
1.6	Cycles	46
1.7	Fullerene terpyridine complexes	53
1.8	Complexes containing biochemical groups	57
1.9	Conclusions	61
1.10	Aim and scope of this thesis	61
1.11	References	62
<b>2</b>	<b>New terpyridine ligands and model complexes</b>	<b>69</b>
2.1	Introduction	70
2.2	Functionalized terpyridine ligands	70
2.3	Synthesis and characterization of asymmetric ruthenium(II) terpyridine model complexes	72
2.4	Photophysical investigations and perylene-containing complexes	80
2.5	Chiral terpyridine-ruthenium complexes: supramolecular aggregates	84
2.6	Kinetic studies of the formation of the ruthenium complexes in water	93
2.7	Asymmetric bipyridine-terpyridine-copper(II) complexes: a different approach for supramolecular architectures	95
2.8	Conclusions	99
2.9	Experimental part	100
2.10	References	110
<b>3</b>	<b>Linear metallo-supramolecular polymers</b>	<b>115</b>
3.1	Linear terpyridine-ruthenium(II) poly(ethylene glycol) coordination polymers	116
3.2	Linear supramolecular polymers containing both terpyridine metal complexes and quadruple hydrogen bonding units	130
3.3	Conclusions	139
3.4	Experimental section	139
3.5	References	142



<b>4</b>	<b>Metallo-supramolecular graft copolymers</b>	<b>145</b>
4.1	Introduction	146
4.2	Supramolecular grafting: a novel approach for polymeranalogous reactions	147
4.3	Aqueous micelles from amphiphilic supramolecular graft copolymers	153
4.4	Conclusions	162
4.5	Experimental part	162
4.6	References	165
<b>5</b>	<b>Supramolecular cross-linking</b>	<b>167</b>
5.1	Introduction	168
5.2	Supramolecular branching and cross-linking of terpyridine-modified copolymers: complexation and decomplexation studies in diluted solution	169
5.3	Combining covalent and non-covalent cross-linking: a novel terpolymer for two-step curing applications	177
5.4	Combination of supramolecular cross-linking with covalent cross-linking through epoxide ring-opening reactions	185
5.5	Free-radical and thermal curing of terpyridine-modified terpolymers	190
5.6	Conclusions	196
5.7	Experimental part	197
5.8	References	202
	<b>Summary</b>	<b>205</b>
	<b>Zusammenfassung</b>	<b>207</b>
	<b>Acknowledgement</b>	<b>209</b>
	<b>Curriculum Vitae</b>	<b>211</b>
	<b>List of publications</b>	<b>212</b>

# 1

## Recent developments in the supramolecular chemistry of terpyridine metal complexes

**Abstract:** This chapter describes recent developments in the field of supramolecular chemistry of terpyridine metal complexes. The synthesis and characteristics of single as well as multiple homo- and heterometallic complexes is discussed. Furthermore, complexes containing fullerenes, biological building blocks, extended aggregates of different architectures as well as rings are presented. A special emphasis is related to the properties (e.g. redox properties, luminescence etc.) of functional systems. Potential applications in optical nano-devices, molecular storage units, molecular switches or solar cells are discussed.

*Parts of this work have been published:*

H. Hofmeier, U. S. Schubert, submitted.

## **1.1 Introduction**

Supramolecular chemistry has become one of the most interesting fields in modern chemistry. In 1987, J.-M. Lehn, C. J. Pederson and D. J. Cram received the Nobel Prize for their pioneering work.<sup>[1]</sup> Self-recognition and self-assembly processes represent the basic concept of supramolecular chemistry and the interactions involved are mainly of a non-covalent nature (e.g. van-der-Waals, hydrogen-bonding, ionic or coordinative interactions). Compared to covalent bonds, these interactions are weaker and usually reversible. Nature is the model for artificial supramolecular processes. Inter- and intramolecular non-covalent interactions are of major importance for most biological processes such as highly selective catalytic reactions and information storage:<sup>[2, 3]</sup> different non-covalent interactions are present in proteins, giving them their specific structures. DNA represents one of the most famous examples, where the self-recognition of the complementary base-pairs by hydrogen-bonding leads to the self-assembly of the double helix. Today, many synthetic supramolecular systems are known.<sup>[1, 4]</sup> The resulting compounds are expected to reveal new chemical, physical as well as biological properties. Starting from biomimetic systems, the concept was extended to "molecular machines"<sup>[5]</sup> and supramolecular polymers.<sup>[6]</sup>

Among the approaches to supramolecular polymers is the use of self-complementary multiple hydrogen-bonding units that are characterized by increased stability compared to single hydrogen bonds.<sup>[7-13]</sup> Supramolecular assemblies and fully reversible polymers have already been prepared in the past. Another type of interaction, which has been used extensively in supramolecular chemistry, is metal coordination. In particular, chelating ligands are of interest, since they allow the construction of defined supramolecular architectures and possess an increased stability compared to hydrogen-bonding. Besides bipyridines,<sup>[14]</sup> terpyridines have been utilized extensively.

Terpyridines were first discovered by Morgan and Burstall.<sup>[15]</sup> By heating pyridine with anhydrous iron(III) chloride at 340 °C in an autoclave (50 atms.) for 36 hours, 2,6':6',2"-terpyridine was produced (besides bipyridines and other products). It was subsequently discovered that the addition of iron(II) ions to a solution of terpyridine compounds gave rise to a purple color, giving the first indication for the formation of a metal complex. In the following sections, an overview of the synthesis of various functionalized terpyridine ligands (especially 4'-functionalized terpyridines) is given, followed by a description of the latest achievements in the field of terpyridine complexes, ranging from mononuclear complexes via dyads and triads (in this section, emphasis is directed to ruthenium(II) complexes and their optical properties) to extended supramolecular architectures. In this chapter only 2,6':6',2"-terpyridine and its complexes are discussed, the ligand is therefore abbreviated as "terpyridine".

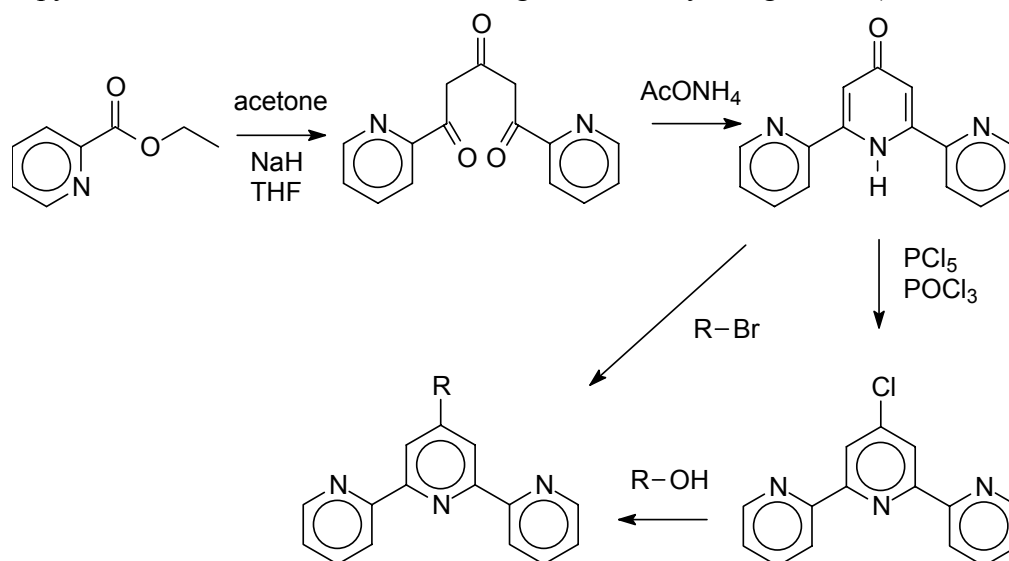
## 1.2 Synthetic strategies

### 1.2.1 Terpyridine ligands

Terpyridine ruthenium complexes of the type  $[\text{Ru}(\text{tpy})_2\text{X}_2]$  ( $\text{X} = \text{e.g. Cl}^-, \text{ClO}_4^-, \text{PF}_6^-$ ) are already known for a long time.<sup>[16, 17]</sup> A main characteristic is the strength of the metal-ligand coordinative bond in these complexes. With many transition metal ions in low oxidation states a *bis*-complex is formed, with a pseudo octahedral coordination at the metal center. The stability of this type of complexes can be explained by the strong metal-ligand ( $d-\pi^*$ ) back donation. Furthermore, a strong chelate effect is present. The common geometry of this type of complexes is a distorted octahedral geometry, because the most common coordinativity for transition metal ions is hexacoordination. The distorted octahedral coordination geometry has been determined in detail by X-ray structure analysis.<sup>[18]</sup>

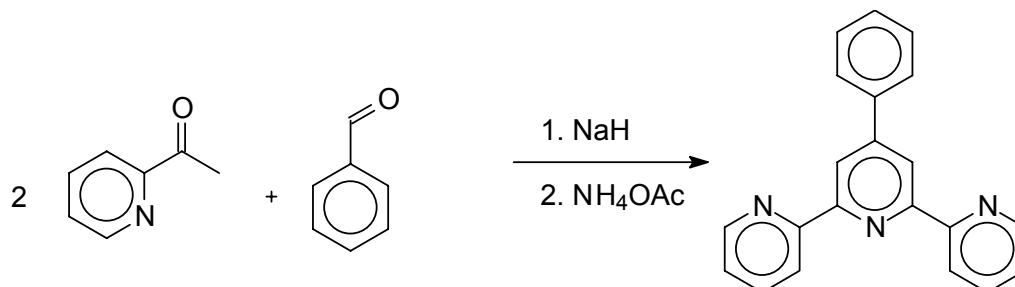
A variety of terpyridines, functionalized at different positions, has been prepared over the past years. Several reviews were published on that subject.<sup>[19, 20]</sup> Therefore, only a short overview over the most common functionalization procedures to the most frequently used 4'-functionalized terpyridines, including some recent publications, will be presented in this chapter.

4'-Functionalized terpyridines are versatile building blocks for supramolecular assemblies and polymers. Whereas asymmetrically functionalized bipyridines (*e.g.* bipyridines bearing a substituent on one pyridine ring) may lead to isomers (*fac* or *mer* (*tris*-bipyridine) diastereomers), depending on the orientation of the functional groups (*facial* or *meridional*) upon complexation with metal ions, the complexation of terpyridines leads to defined complexes because of a 4'-functionalized terpyridine possessing  $C_{2v}$  symmetry with a rotation axis through the 4'-position. Numerous examples are known for the reaction between 4'-chloro-terpyridine and alcohols in DMSO, using a base catalyst, *e.g.* KOH (Scheme 1.1).<sup>[21-23]</sup>



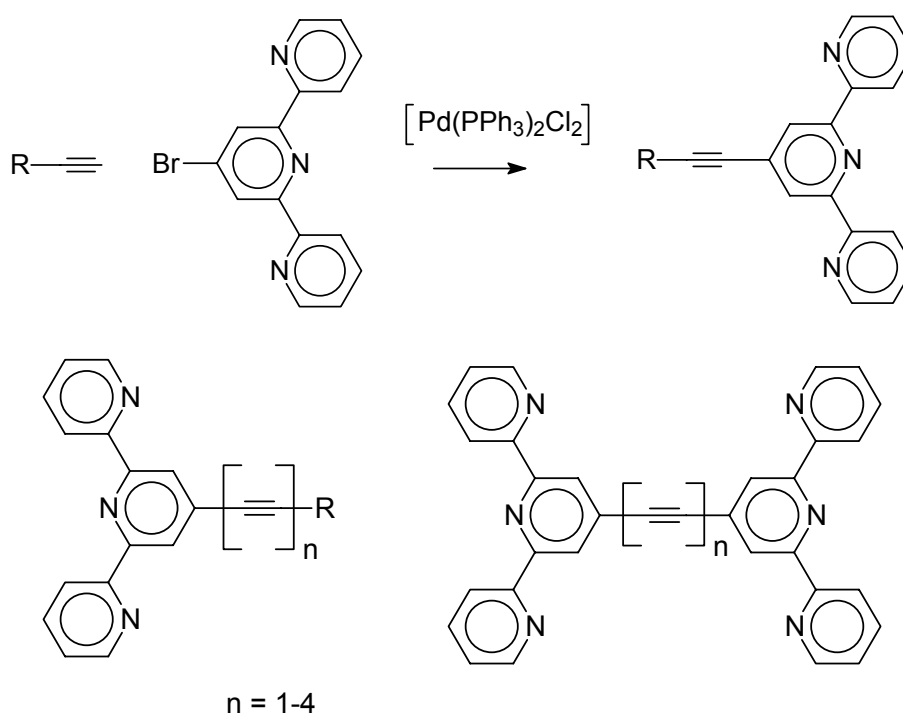
Scheme 1.1. Synthetic approach to 4'-functionalized terpyridines via the pyridone<sup>[24-26]</sup> and chloro-terpyridine<sup>[21-23]</sup> route.

Moreover, pyridone<sup>[27, 28]</sup> (the precursor of 4'-chloro-terpyridine) can be utilized for functionalization.<sup>[24, 25]</sup> For this type of reaction, bromides or tosylates are applied as starting material to react with the pyridone. More examples are presented in a recent publication,<sup>[26]</sup> where also a nitrile, an epoxide and various other moieties containing an olefinic group could be introduced in one step. 4'-Phenyl groups can be introduced by reacting acetopyridine with benzaldehyde (Scheme 1.2) in a so-called "Kröhnke" condensation reaction.<sup>[17, 29]</sup>



Scheme 1.2. Synthesis of 4'-phenylsubstituted terpyridines.<sup>[17, 29]</sup>

The cross-coupling of alkynes with bromo-terpyridines is straightforward and opens avenues to various polytopic terpyridine ligands that can be employed in the construction of supramolecular assemblies (Scheme 1.3). Due to the extended conjugation systems, these compounds are characterized by outstanding optical properties such as room-temperature fluorescence of the corresponding ruthenium complexes. Furthermore, they might be used as "nanowires". A large variety of these compounds has been prepared in the laboratory of R. Ziessel, who reviewed this topic in 1999.<sup>[30]</sup> This reaction is very versatile and allows the construction of a large variety of *mono*- and *bis*-terpyridines containing extended conjugated alkyne units.



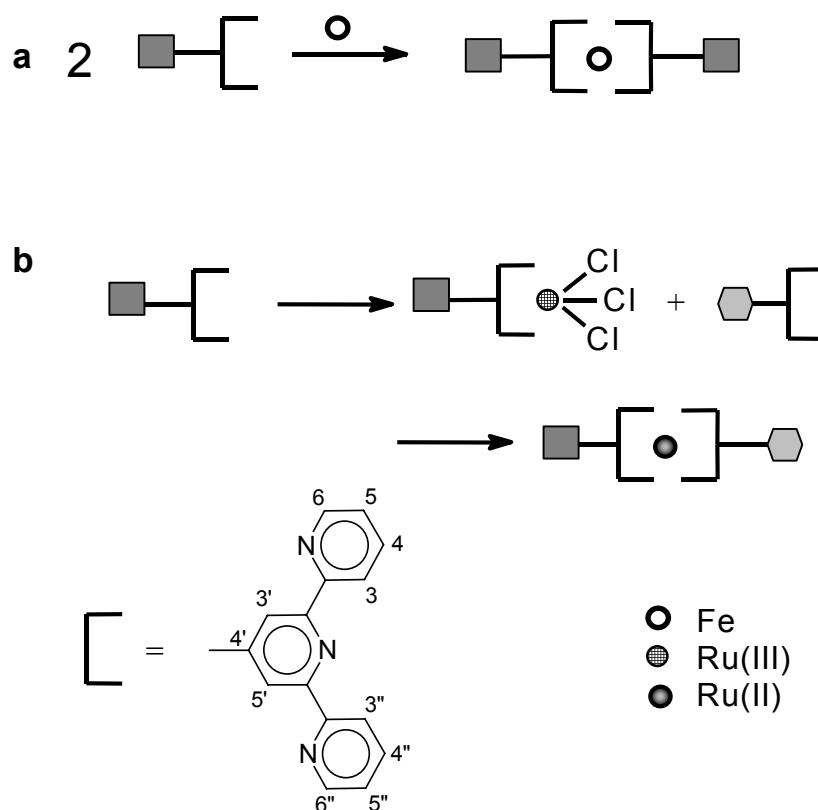
Scheme 1.3. Palladium-catalyzed cross-coupling of alkyne-derivatives.<sup>[30]</sup>

## 1.2.2 Metal complexes

In order to obtain *bis*-terpyridine metal complexes, metal-ions (e.g. zinc(II), cobalt(II), copper(II) nickel(II), iron(II)) are usually treated with the respective ligand in a 1:2 ratio (Scheme 1.4a). The complexes are subsequently purified by exchange of the counterions and recrystallization of the complex. Addition of metal salts to a mixture of two different terpyridines leads to a statistical mixture of homocomplexes and the hetero complex. In order to prepare exclusively asymmetric complexes, a directed strategy, where the two ligands are introduced in a two-step reaction (via a *mono*-complex intermediate, Scheme 1.4b) has to be used. Suitable metals for this strategy are ruthenium and osmium.

## 1.2.2.1 Ruthenium complexes

Complexation of terpyridine ligands to a ruthenium(II) center can be carried out in a two-step reaction (Scheme 1.5). The ruthenium(III) intermediate is subsequently reacted in the second step under reductive conditions to yield the corresponding asymmetric ruthenium(II) complex.<sup>[17]</sup>



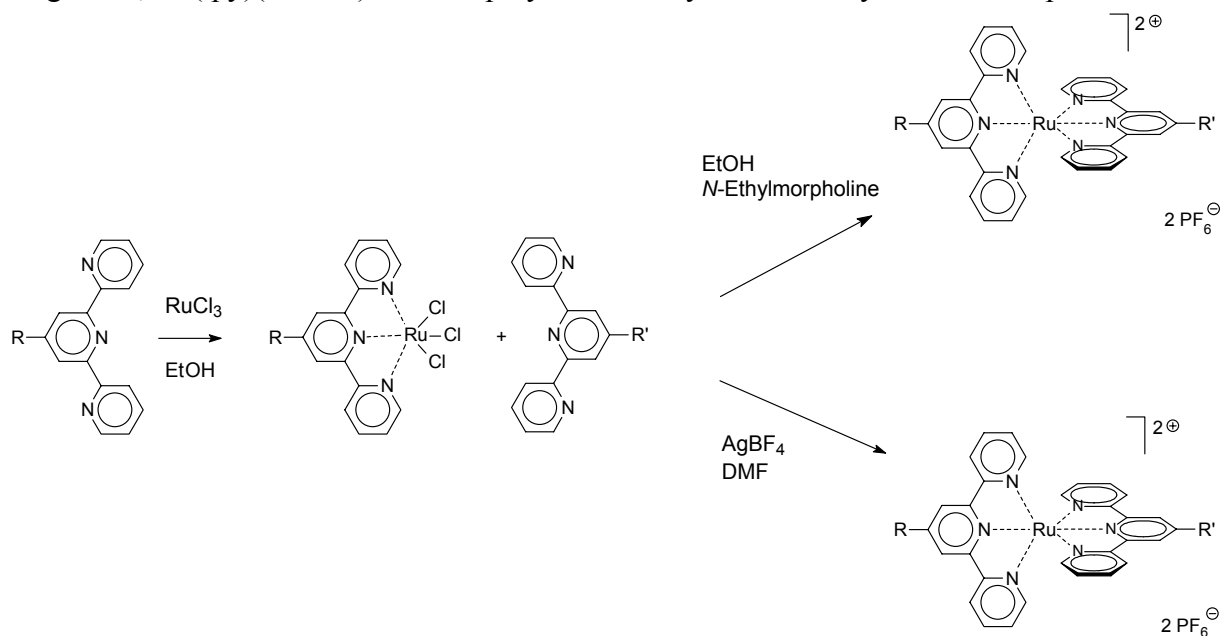
Scheme 1.4. Schematic representation of the formation of terpyridine complexes.

In the first step, ruthenium(III) trichloride hydrate is added to a methanolic or ethanolic solution of the first terpyridine ligand. The resulting *mono*-complex is poorly soluble in most cases and can be simply isolated by filtration. Subsequently, this intermediate is suspended with the second ligand in methanol, containing *N*-ethylmorpholine<sup>[31]</sup> and refluxed for 1-4

hours. The solvent also acts as reductive agent to reduce the ruthenium(III) to ruthenium(II), followed by loss of the chlorides and eventual coordination of the second terpyridine.

Alternatively, an equimolar amount of silver tetrafluoroborate is added to the ruthenium(III) *mono*-complex in DMF or acetone to remove the chlorides.<sup>[32]</sup> The vacant coordination sites are now occupied by the weakly binding solvent molecules, therefore activating the ruthenium(III) complex. Unlike terpyridine ruthenium(III) trichloride that is reacted in suspension, the activated species is soluble. This intermediate is reacted without isolation with the second terpyridine (after filtration of the formed silver chloride) to lead to the desired *bis*-terpyridine ruthenium(II) complex. Yields between 50% and 90% can usually be obtained. Although this is a directed method, the formation of a statistic mixture of hetero and homocomplexes has been reported in one specific case,<sup>[33]</sup> but this atypical behavior could not be explained by the authors.

In another method for endcapping functionalized terpyridines with terpyridine ruthenium(II) fragments, Ru(tpy)(DMSO)Cl<sub>2</sub> is employed for the synthesis of asymmetric complexes.<sup>[34]</sup>



Scheme 1.5. Synthetic strategy towards asymmetric terpyridine complexes.<sup>[17, 32]</sup>

Another, somewhat unusual method, was presented by D. Greene *et al.* who showed that microwave-assisted heating gave the desired product in yields up to 94% within one minute.<sup>[35]</sup>

Symmetric terpyridine complexes can be obtained by the RuCl<sub>3</sub>-*N*-ethylmorpholine method, either in a two-step reaction by applying the same ligand twice or in a one-pot reaction.

Another method described by Reahn starts from ruthenium trichloride, which is dechlorinated with AgBF<sub>4</sub> in acetone.<sup>[36]</sup> The resulting hexaacetone ruthenium(III) complex, where the ligands are loosely bound, is reacted with the ligand including reduction.

It has to be noted that the ruthenium(II) center can be reduced by electrocrystallization to result in neutral complexes. A crystal structure could be obtained, showing indeed only the *bis*-terpyridine ruthenium(0) complexes without any other ions.<sup>[37]</sup>

### 1.2.2.2 Photophysical properties

Absorption as well as emission spectra reveal that a metal-ligand charge transfer takes place in terpyridine-ruthenium complexes. As opposed to bipyridine complexes, where fluorescence phenomena can be observed over a wide temperature range, no fluorescence emission is detected at room temperature in the case of terpyridines due to a non-radiative transition of the excited triplet metal-to-ligand charge-transfer ( $^3\text{MLCT}$ ) state via a triplet metal-centered ( $^3\text{MC}$ ) state to the ground state (see e.g. ref.<sup>[16]</sup>). However, at low temperatures, this path becomes less efficient, and therefore luminescence could be observed.<sup>[38-40]</sup> For a sufficient observation of the emission properties, the material can be "dissolved" in a rigid glass at 77 K.<sup>[41]</sup>

The photophysical properties of the complexes can be fine-tuned by the introduction of donor, acceptor or both kinds of groups, leading to room-temperature fluorescent terpyridine ruthenium(II) complexes. Another method to improve the luminescence lifetime and quantum efficiency utilizes the attachment of aromatic groups. One of the first examples is represented by 4'-*p*-tolyl-terpyridine; an extension of this approach of connecting aromatic rings to the terpyridine moiety lead to 4,4',4''-tetraphenylterpyridine, which revealed further improved optical properties. For more detailed information on these kinds of systems, the reader is referred to a review by Sauvage.<sup>[16]</sup>

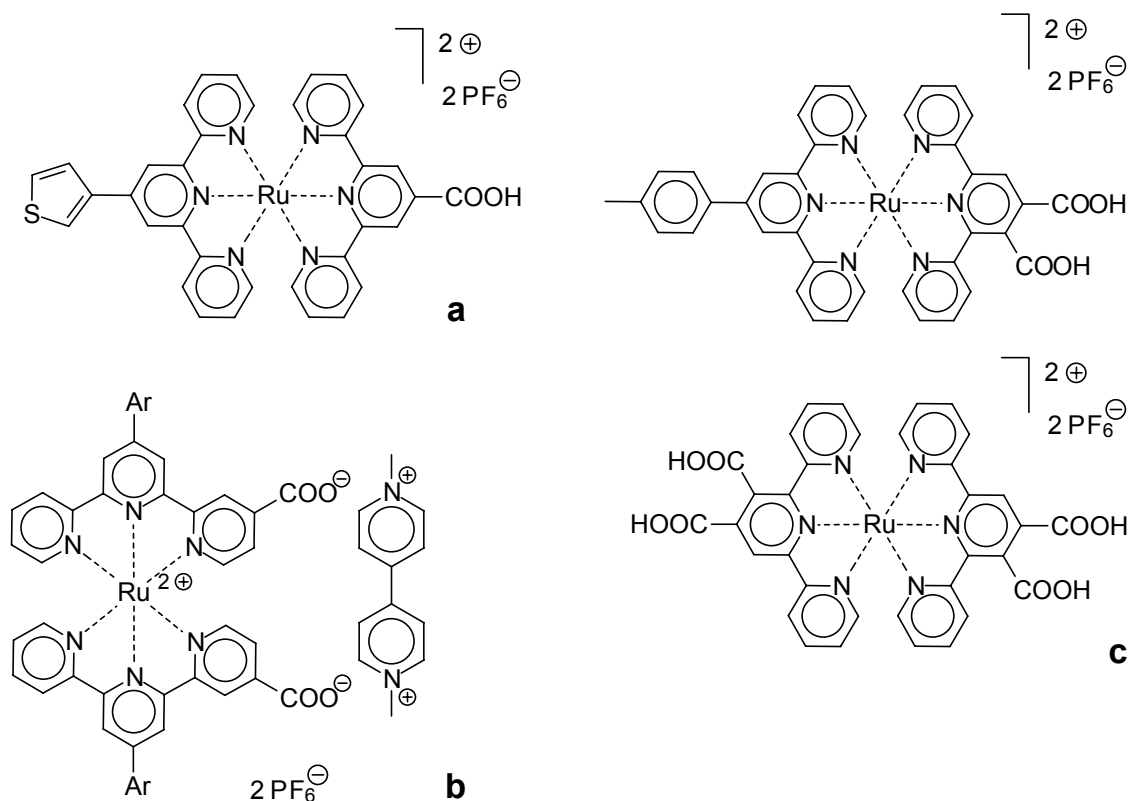
A very different approach to the preparation of room-temperature fluorescent ruthenium complexes is the entrapment of the compounds in zeolite cages.<sup>[42]</sup> The zeolite-induced destabilization of the ligand-field (LF) state resulted in a strongly enhanced room-temperature fluorescence of the terpyridine-ruthenium(II)-complex.

## 1.3 Uninuclear terpyridine ruthenium complexes

A lot of work has already been done in the field of terpyridine complexation chemistry. Still a significant amount of research is being performed on uninuclear terpyridine complexes. A huge potential lies in these compounds regarding the fine-tuning of optical properties or the use as precursors for supramolecular architectures.

Carboxy groups (Scheme 1.6) play an important role as substituents on terpyridine ligands due to their potential use as an anchoring group on surfaces. One example is  $\text{TiO}_2$ , which is widely used in solar cell applications.<sup>[43]</sup> Terpyridine ruthenium complexes, attached to  $\text{TiO}_2$ , could be used as sensitizers in novel solar cells. In the reported example, an electropolymerizable thienyl group has also been introduced into the terpyridine complex (Scheme 1.6a).<sup>[44]</sup>  $[\text{RuLL}'][\text{PF}_6]_2$  ( $\text{L} = 4'-(3\text{-thienyl})-2,2':6',2''\text{-terpyridine}$ ;  $\text{L}' = 4'\text{-carboxy-}2,2':6',2''\text{-terpyridine}$ ) was prepared following two different synthesis pathways. The first one involves a protection of the carboxylic group on the ligand before formation of the complex followed by hydrolysis in the final step.





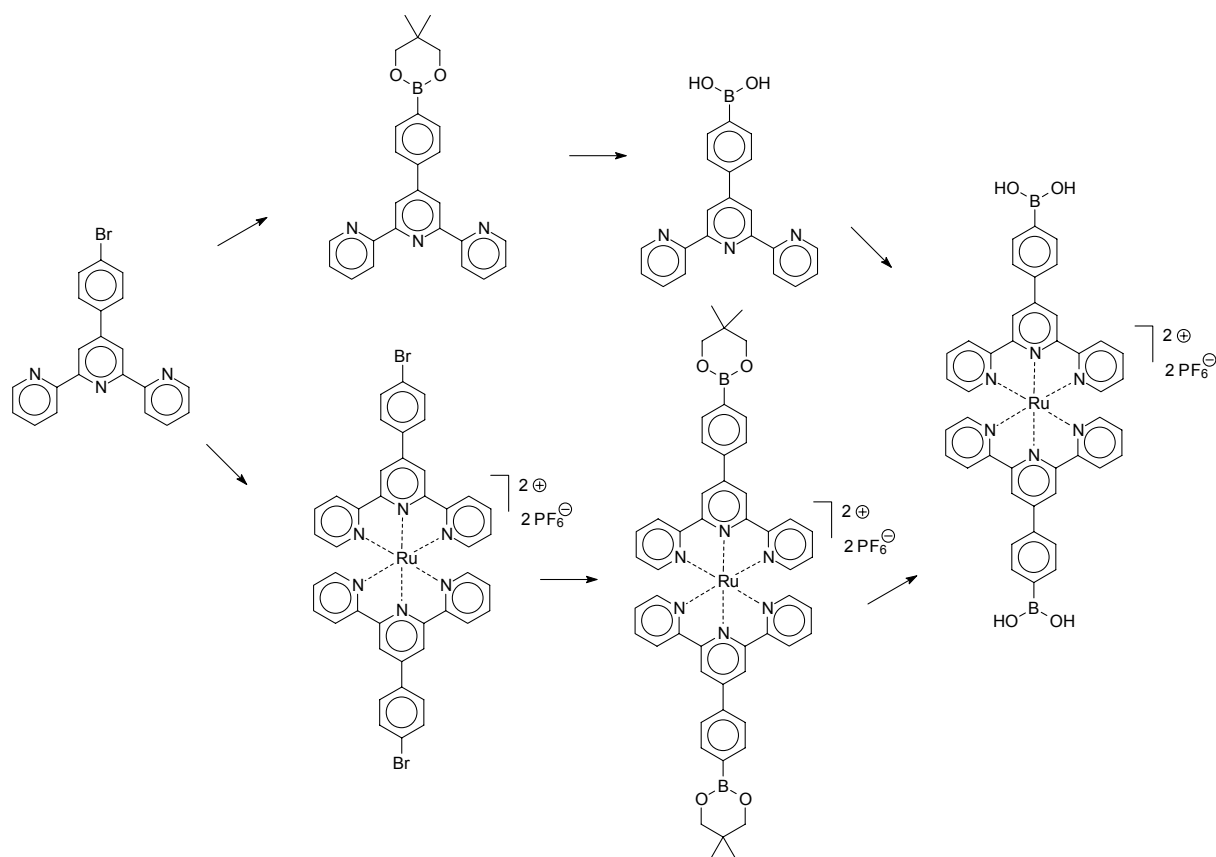
Scheme 1.6. Carboxy-functionalized terpyridine complexes.<sup>[44-46]</sup>

This route was chosen because the direct complexation of the free carboxylic acid resulted in a very low yield. The second approach is a new route, based on oxidation of a furan ring: 4'-(2-furyl)-terpyridine was reacted with 4'-(3-thienyl)-terpyridine ruthenium trichloride, followed by treatment of the resulting complex with KMnO<sub>4</sub> under basic conditions that leads to the carboxy compound. For the latter case, an even higher yield compared to the first route was obtained.

Carboxy-groups have also been introduced into the 4-position of terpyridines (Scheme 1.6b).<sup>[45]</sup> Due to their spatial orientation, they can easily coordinate to methyl viologen (4,4'-bis(methylpyridinium)) by ionic interactions, providing a photoinduced electron transfer.

In order to increase the electron injection efficiency and to reduce the chance of desorption of the complexes from the TiO<sub>2</sub> surface, asymmetric *bis*-terpyridinyl ruthenium(II) complexes carrying vicinal carboxylic acids were developed (Scheme 1.6c).<sup>[46]</sup> Because the complexation of the free di-acid resulted in the loss of one carboxylic group (decarboxylation), a protection of the acid groups by ester-formation was necessary. The resulting compounds showed room temperature luminescence and efficient sensitization of nanocrystalline TiO<sub>2</sub> films, with conversion yields (IPCE) of up to 70%.

A new versatile method for the preparation of functionalized terpyridines and their corresponding metal complexes is the use of boron chemistry.<sup>[47]</sup> In the following example 4'-(4-bromophenyl)-terpyridine and 4'-bromoterpyridine have been functionalized with boronate groups by a palladium-catalyzed Miyaura cross-coupling, resulting in the first example of a boronate ester-functionalized terpyridine (Scheme 1.7).

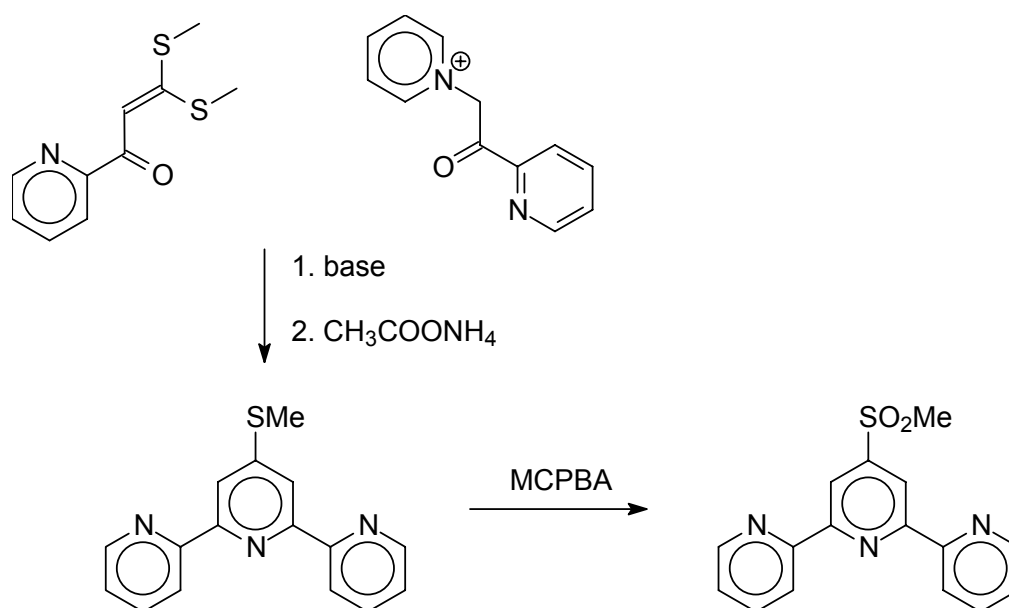


Scheme 1.7. Synthesis of boronate terpyridine complexes.<sup>[47]</sup>

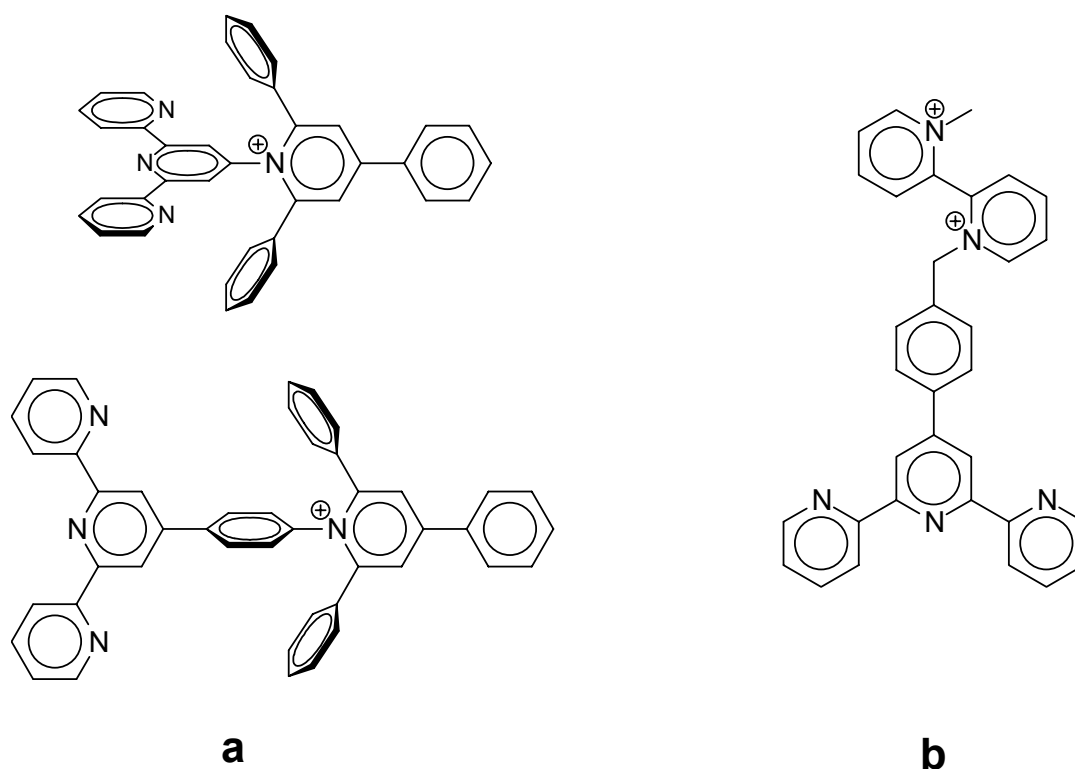
Subsequent hydrolysis of this intermediate led to the free boronic acid. The ligand, bearing the boronic ester, could be complexed with ruthenium(II), while the free acid disintegrated because of the destabilized boron bond. Furthermore, the boronation could also be performed on a preformed ruthenium(II) complex. The resulting boronate complexes are interesting starting materials for further reactions involving the boronate group (e.g. Suzuki-Miyaura cross-couplings).

Electron withdrawing groups in the 4'-position of terpyridines have been shown to result in room-temperature-fluorescent ruthenium(II) complexes.<sup>[31]</sup> Chloroterpyridine revealed a weak luminescence. In order to obtain a more efficient complex, a methylsulphone group was introduced via a methylthio terpyridine, followed by oxidation (Scheme 1.8).<sup>[48]</sup> The intermediate was prepared according to the Potts method<sup>[49]</sup> and oxidized to the sulphone using a per-acid.

Another acceptor moiety that has been reported recently is a triphenylpyridinium group.<sup>[50]</sup> Due to the steric demands of the aromatic rings, there is no conjugation of the whole system. Furthermore, rotation around the molecular axis is inhibited (Scheme 1.9a).



Scheme 1.8. Synthesis of a terpyridine sulphonate.<sup>[48]</sup>

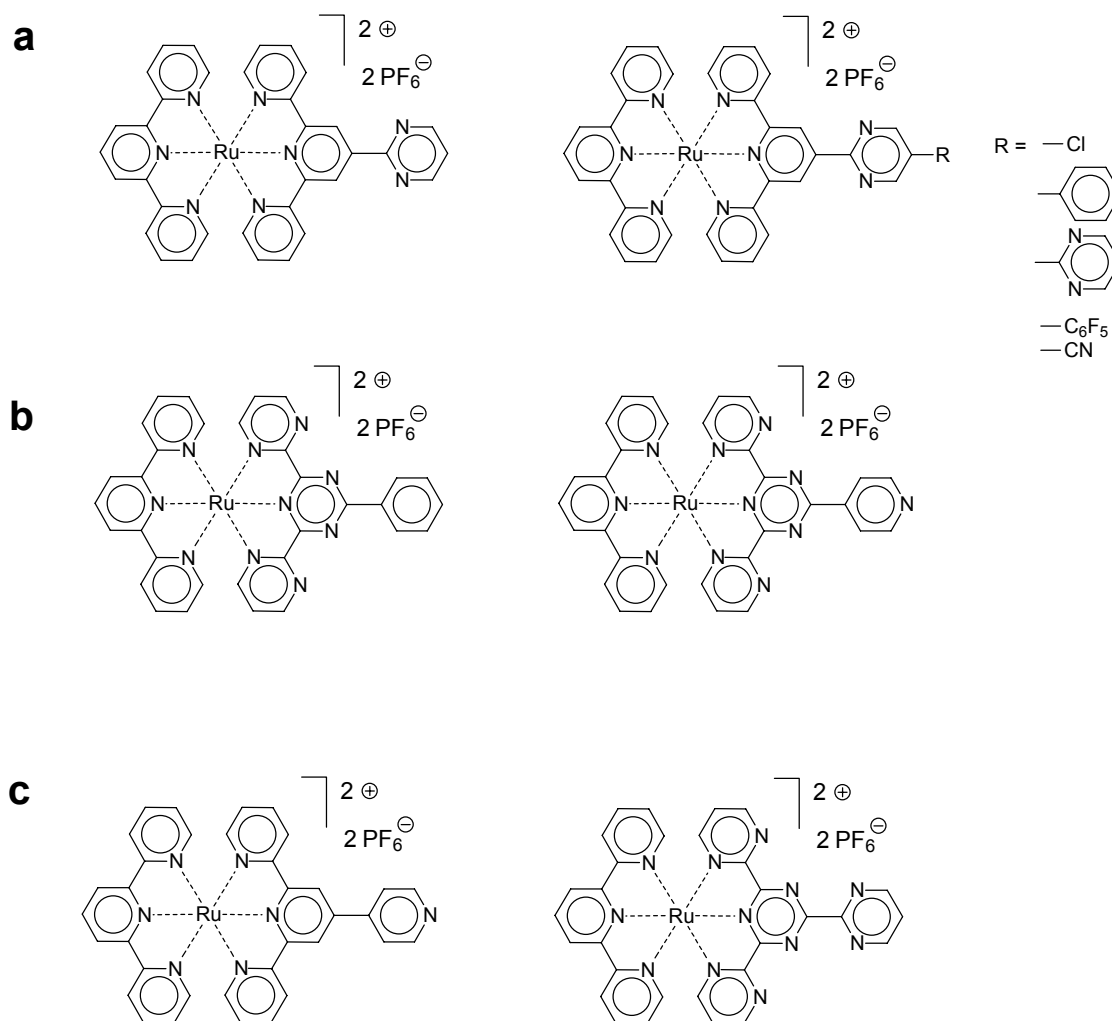


Scheme 1.9. (a) Triphenylpyrinium-<sup>[51]</sup> and (b) viologen<sup>[52]</sup> functionalized terpyridine ligands.

In spite of the lack of conjugation between the terpyridine and the triphenyl pyridinium moiety (due to the bulky phenyl rings), an enhanced room-temperature luminescence was observed.<sup>[51]</sup> This behavior was ascribed to a through-bond electronic substituent effect originating from the directly connected electron-withdrawing group. In the case where the unit is separated by a *para*-phenyl ring, the formation of photoinduced electron-transfer (PET) processes with the formation of charge-separated (CS) states is possible.

Another example, where a pyridinium moiety is connected to a terpyridine, is shown in Scheme 1.9b. In this case, a 1-methyl-1'-[4-(2,2':6',2''-terpyridin-4-yl)benzyl]-4,4'-bipyridine-dium was used to prepare an osmium complex, where the characteristic osmium fluorescence is efficiently quenched by the viologen moiety. The quenching most probably involves an intramolecular electron transfer.<sup>[52]</sup>

Besides the introduction of electron-withdrawing groups, the extension of the conjugated  $\pi$ -system of the ligand by one or more aromatic rings is also a promising approach (Scheme 1.10). One strategy towards such systems are connected benzoic aromatic rings. In the case shown in Scheme 1.10a, a pyrimidine moiety has been introduced into the 4'-position of a terpyridine.<sup>[53]</sup> In addition, analogous terpyridines bearing a second pyrimidine, phenyl or pentafluorophenyl groups in the *p*-position of the first aromatic ring, have been prepared to extend the conjugated  $\pi$ -system. This configuration leads to an increase of the gap between the metal-centered and the MLCT states. A luminescence at room temperature (lifetime up to 200 ns) is the result.



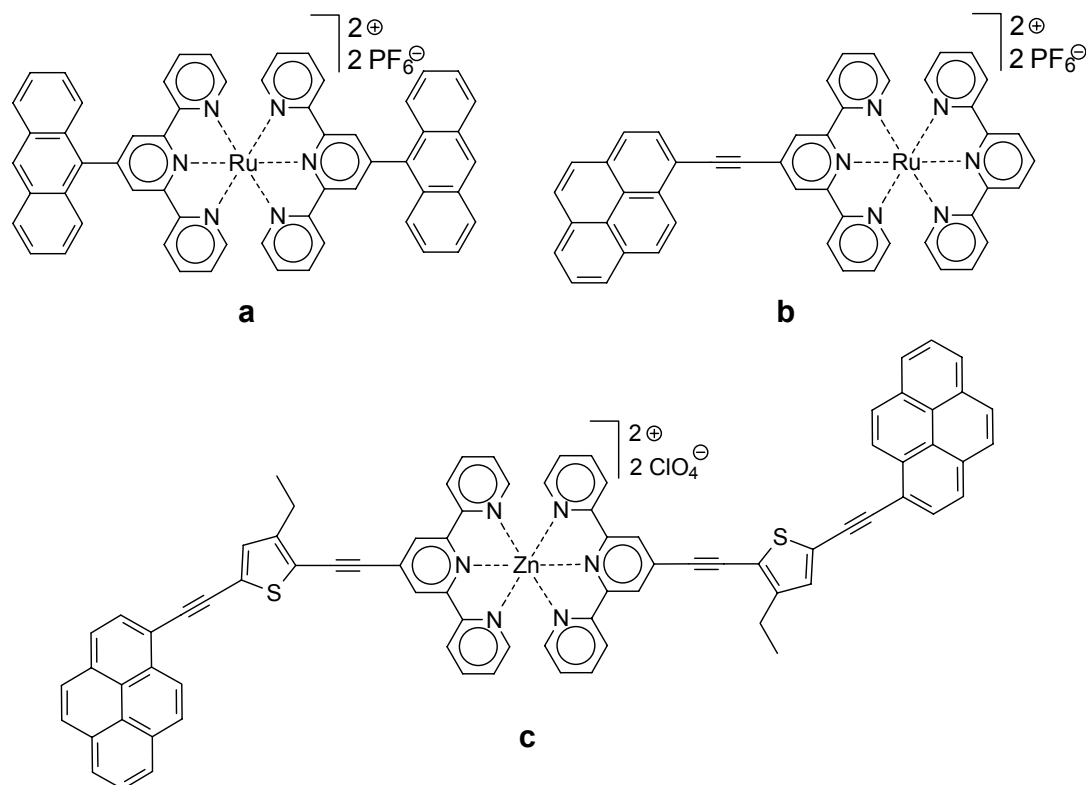
Scheme 1.10. Phenyl and pyridyl functionalized complexes of (hetero)terpyridines.<sup>[53-55]</sup>

Other examples of luminescent ruthenium complexes include complexes involving the ligand 2-(4'-pyridyl)-4,6-bis-(2'-pyridyl)-1,3,5-triazine. The bis(2'-pyrimidyl)-1,3,5-triazines can be

considered as "heteroterpyridines" (nitrogen atoms in the 3,3',5',3"-positions), which have the potential for room temperature luminescence (Scheme 1.10b).<sup>[54]</sup> Similar ruthenium(II) complexes of 4'-pyridyl and 4'-pyrimidyl functionalized terpyridines and *N*-heteroterpyridines have been prepared and characterized in the group of J. A. Thomas (Scheme 1.10c).<sup>[55]</sup> Despite the similarity to the previously described systems, the authors reported that these complexes are non-fluorescent.

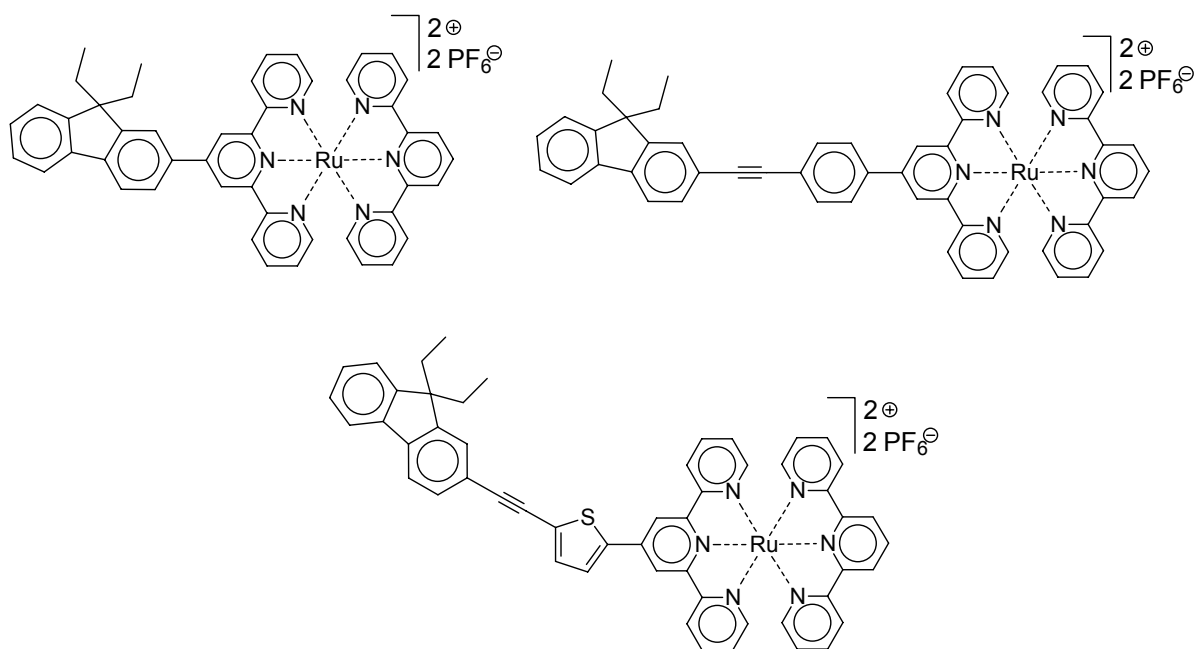
An interesting feature of the 2,4,6-*tris*(2-pyrimidyl)-1,3,5-triazine ligand is that it is actually composed of three terpyridine subunits, the reported complex thus contains two vacant complexing units. This architectural feature makes this system interesting for the construction of supramolecular assemblies as described later.

Besides benzoic aromates, annelled aromates have also been introduced into terpyridines, where the corresponding ruthenium complexes show the ability for room-temperature luminescence. Among the examples is a terpyridine bearing an anthracene in the 4'-position, which has been complexed to form ruthenium(II) and iron(II) complexes.<sup>[56]</sup> Other examples include the introduction of pyrene moieties (Scheme 1.11).<sup>[57]</sup> Recently, ethynyl-pyrene units have also been introduced in the 5,5"-positions of a terpyridine.<sup>[58]</sup> Moreover, pyrene moieties have been linked via a (*bis*-ethynyl)-thiophene bridge to the terpyridine.<sup>[59]</sup> This ligand is luminescent at room temperature due to the efficient population of an intramolecular charge transfer excited state. However, addition of zinc(II) ions results in quenching of the fluorescence, making such systems interesting as "sensors" for metal ions.



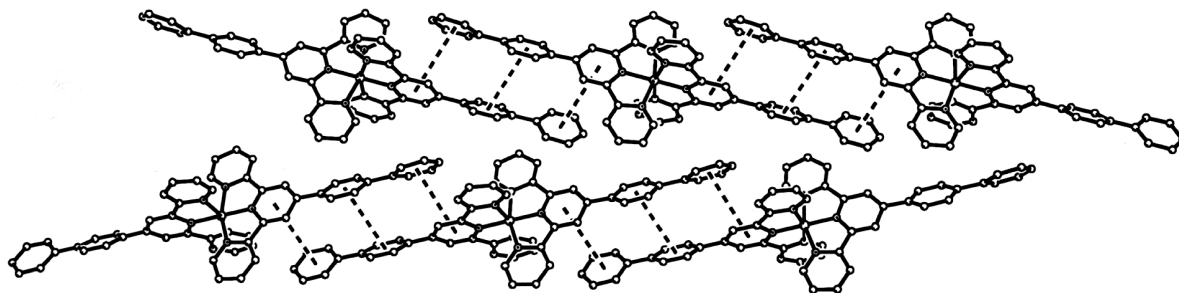
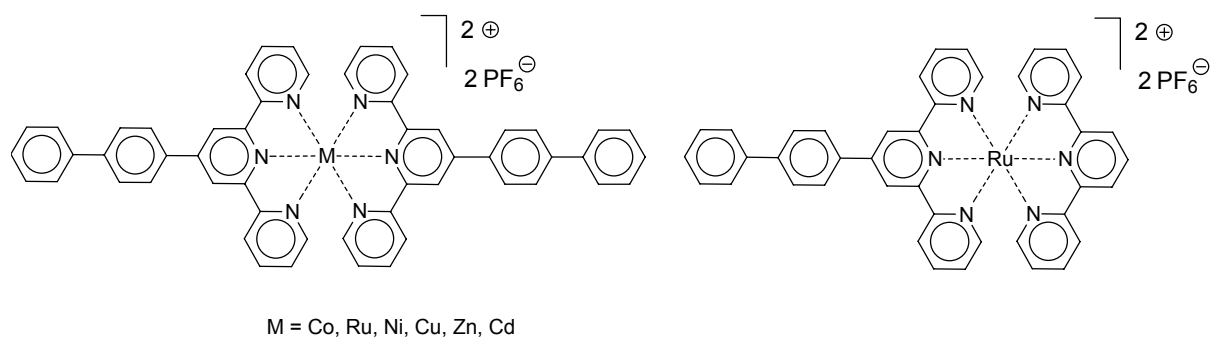
Scheme 1.11. Terpyridine ruthenium complexes, containing extended aromatic functions: (a) anthryl,<sup>[56]</sup> (b) pyrene-1-ylethynyl,<sup>[57]</sup> (c) 4-ethyl-5-pyren-1-ylethynylthiophen-2-ylethynyl.<sup>[59]</sup>

Furthermore, alkyne cross-coupling reactions have also been used to obtain fluorene-functionalized terpyridine complexes.<sup>[60]</sup> Fluorene units have been coupled to terpyridines directly or via phenylene-ethynylene or thiophenyl-ethynylene connectors, applying Kröhnke synthesis and Sonogashira coupling reactions. The ruthenium(II) complexes, formed from these ligands, are shown in Scheme 1.12. These ruthenium complexes are non-luminescent despite the attached conjugated groups, whereas the corresponding zinc complexes are highly luminous.



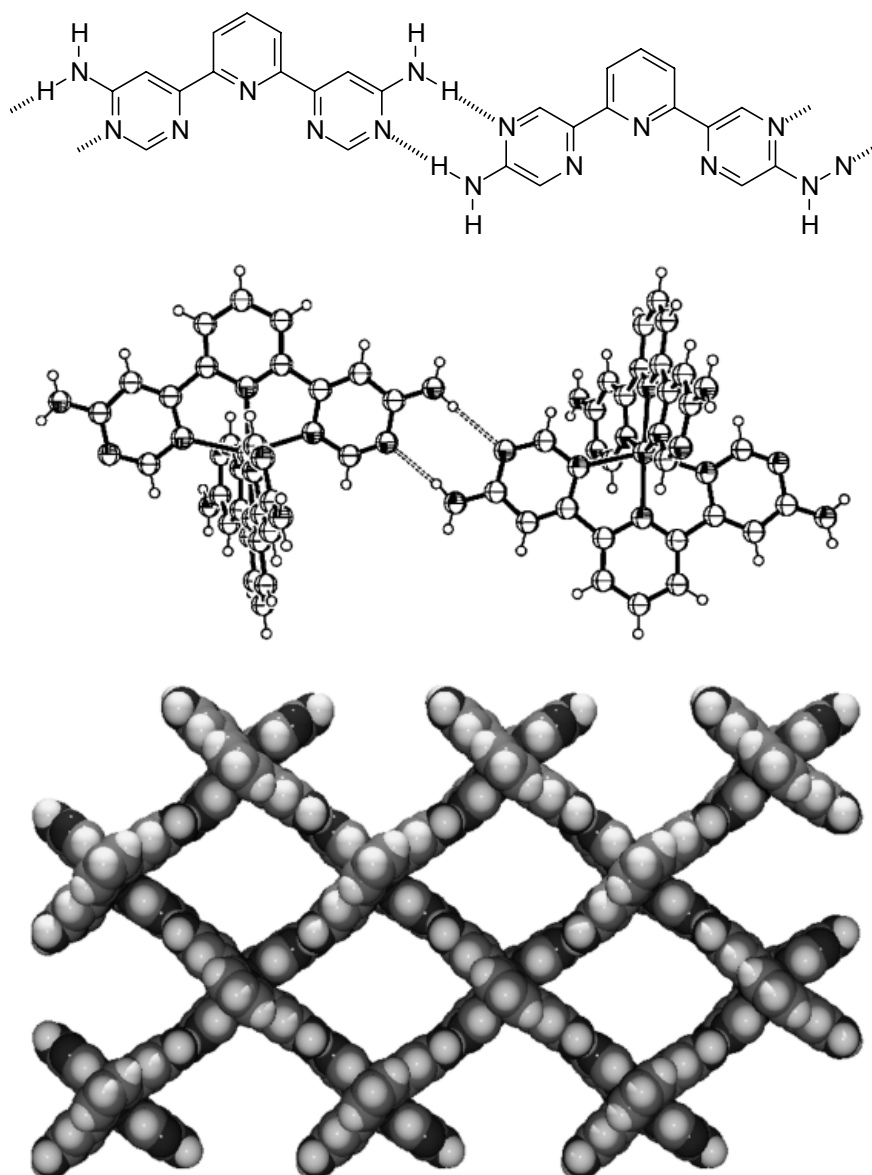
Scheme 1.12. Fluorene-functionalized terpyridine ruthenium(II) complexes.<sup>[60]</sup>

Besides photophysical properties originating from delocalization phenomena, the intermolecular interactions of such compounds are also of interest. Extended aromatic systems are known to give rise to  $\pi$ - $\pi$  interactions, which could be relatively strong for large molecules. Such  $\pi$ -stacking could be exploited for the 3-dimensional arrangement of terpyridine complexes (Scheme 1.13). The group of Alcock reported the synthesis of 4'-biphenyl functionalized terpyridines and the preparation of the corresponding complexes using a variety of metal ions.<sup>[61]</sup> Furthermore, a ruthenium complex with one biphenyl-terpyridine and one unfunctionalized terpyridine was synthesized.  $\pi$ -Stacking interactions between the biphenyl and pyridyl rings were observed in the crystal structure, resulting in aggregation of the complexes in the solid state. Depending on the metal ion, different structures were found: while for cobalt, ruthenium, nickel and copper, biphenylene-biphenylene interactions lead to linear rod-like arrays, for complexes of zinc and cadmium, biphenylene-pyridyl interactions lead to two-dimensional sheets. Moreover, ruthenium, zinc and cadmium complexes showed room temperature luminescence both in solid state as well as in solution.



Scheme 1.13.  $\pi$ -stacking of 4'-(4-biphenyl)-terpyridine ruthenium complexes.<sup>[61]</sup>

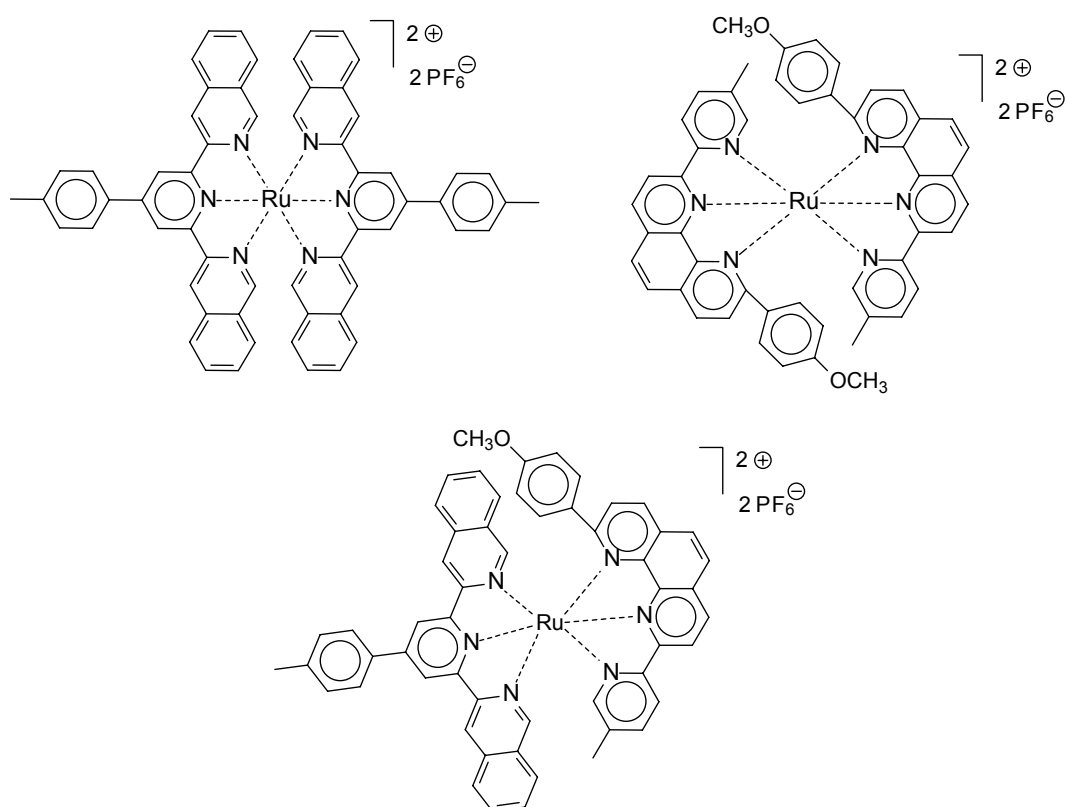
Another non-covalent interaction, which has been used in the chemistry of terpyridine complexes, is hydrogen bonding: in one particular example, two "heteroterpyridines", containing amino-pyrimidine and amino-pyrazine moieties, have been synthesized, which could form double hydrogen bonds.<sup>[62]</sup> The solid-state structures did indeed reveal the formation of extended grid-like structures through molecular recognition (Scheme 1.14). Whereas  $\text{PF}_6^-$  counterions of a cobalt complex resulted in a complete saturation of the hydrogen bonds,  $\text{BF}_4^-$  counterions led to partially broken networks. With zinc triflate, only half of the bonds are formed, leading to a chain-like assembly. An explanation is the different packing of the complexes in the crystal, influenced by the size of the respective counterions. These complexes could be considered as a prototype for the generation of novel organized arrays of terpyridine complexes through sequential self-assembly processes.



*Scheme 1.14. Terpyridines with hydrogen-bonding groups that assemble to a grid-like superstructure.*<sup>[62]</sup>

Numerous differently functionalized terpyridine analogues, where pyridine rings have been replaced by quinoline and phenanthroline moieties, have been used to form symmetric as well as asymmetric complexes.<sup>[63]</sup> Besides functional groups, connected by  $\sigma$ -bonds in various positions, fused phenyl rings were also introduced (Scheme 1.15). Among the species described is also a "terpyridine" consisting of a pyridylphenanthroline. Moreover, cyclometallated species have been prepared.<sup>[63]</sup> Here one *N*-atom is replaced by carbon, resulting in a Ru-C bond. Some of these complexes show long MLCT excited state lifetimes (70-106 ns) at room temperature.

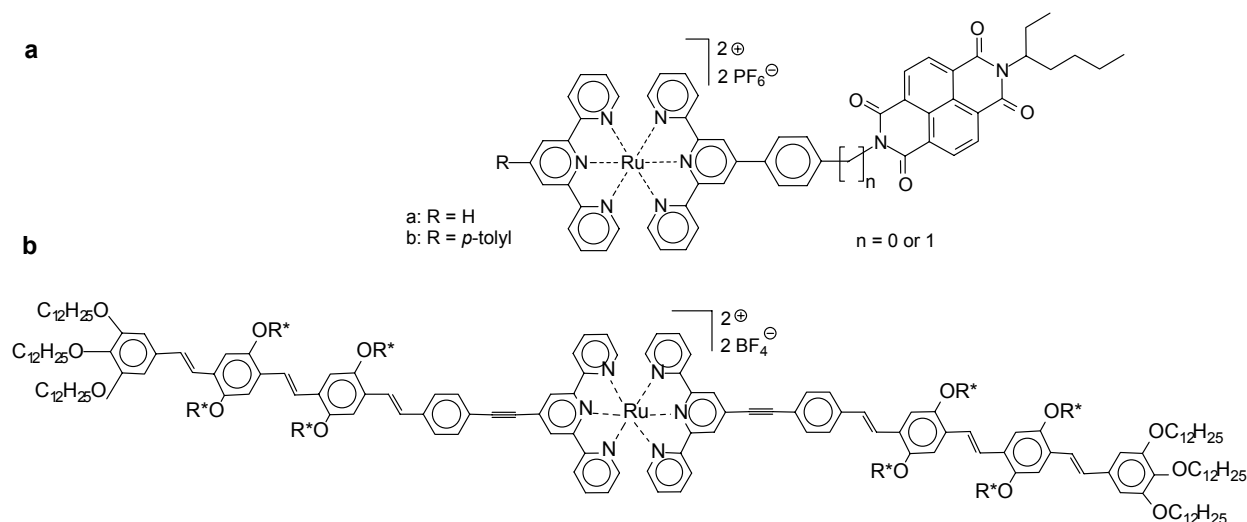




Scheme 1.15. Ruthenium complexes of terpyridines with fused aromatic rings.<sup>[63]</sup>

With a view to applications in solar cells or artificial photosynthesis, photosensitizer-electron acceptor systems have been prepared by connecting a naphthalene-diimide moiety to a terpyridine unit (reaction of the corresponding aminoterpyridines with the naphthalene anhydride) and subsequent formation of the corresponding ruthenium complexes. Unsubstituted terpyridine as well as 4'-*p*-tolyl-terpyridine have been applied as the second ligand and the acceptor unit has been attached in a rigid fashion via a phenylene-group or via an additional saturated carbon atom (Scheme 1.16a).<sup>[64]</sup> However, unlike the corresponding bipyridine complexes, no electron transfer was detected in the case of the terpyridine complexes, which was ascribed to the short lifetime of the excited state of the ruthenium-terpyridine complex.

*Oligo(p*-phenylene vinylene) (OPV) is of special interest due to its outstanding optical properties. Furthermore, it is known to act as a donor in an efficient photoinduced electron transfer, which is of interest for solar cell applications. In combination with fullerene compounds acting as acceptors, the photochemical generated charges could be separated and drained with suitable compounds.

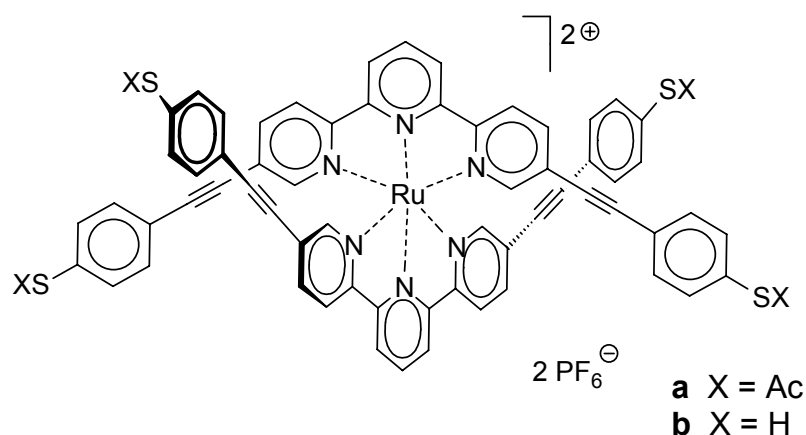


*Scheme 1.16. Naphthalenediimide<sup>[64]</sup> and oligo(*p*-phenylene vinylene)<sup>[65]</sup>-substituted terpyridine complexes.*

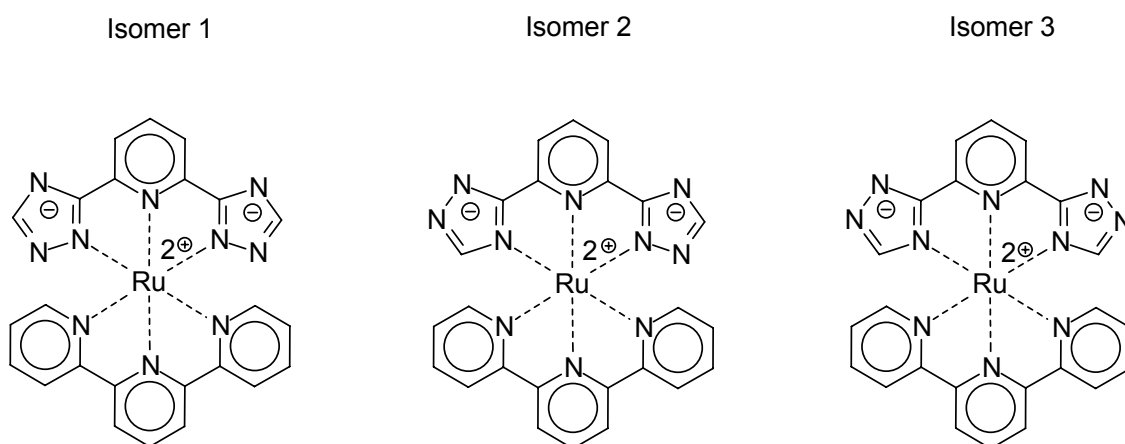
In order to improve this system, two OPV units bearing terpyridine ligands (synthesized by a palladium-catalyzed cross-coupling reaction), have been converted to a ruthenium(II) complex (Scheme 1.16b).<sup>[65]</sup> Near steady-state photoinduced absorption experiments did indeed reveal a charge-separated state, which was dependent from the polarity of the solvent. In further experiments, the OPV donor has been coupled directly to a fullerene via terpyridine ruthenium complexation.

Ruthenium complexes containing fully conjugated ligands terminated with thiol groups (substitution in the 5,5''-position) have been obtained by cross-coupling of the corresponding alkynes. The resulting compounds could subsequently be immobilized on gold surfaces (Scheme 1.17). Self-assembled monolayers of single molecules have been imaged using scanning tunneling microscopy.<sup>[66]</sup> The delocalized phenylene-ethynyl-moiety could act as molecular wire, which might eventually lead to applications in molecular electronics.

There are also numerous examples where terpyridines have been combined with tridentate terpyridine analogues (Scheme 1.18). In the case of *bis*-triazol pyridine, e.g., different isomers are possible, because this ligand possesses different sets of nitrogen atoms that are able to coordinate to the ruthenium ion.<sup>[67]</sup> Compared to  $[\text{Ru}(\text{tpy})_2]^{2+}$ , the fluorescence lifetime of the these systems showed a 300-fold increase and is explained by a rise of the energy of the  $^3\text{MC}$  level (in contrast to the previously described examples, where the  $^3\text{MLCT}$  state was lowered). Furthermore, 5-phenyl-*bis*-triazol and *bis*-tetrazol-pyridines have been reported. The triazol rings are deprotonated in the complexes ( $6\pi$ -aromat), and a reprotonation results in quenching of the fluorescence.<sup>[68]</sup>



Scheme 1.17. Conjugated thiol terpyridine complex.<sup>[66]</sup>



Scheme 1.18. Different coordination isomers of the complex  $Ru(tpy)(bis\text{-}triazol\text{ pyridine})$ .<sup>[67]</sup>

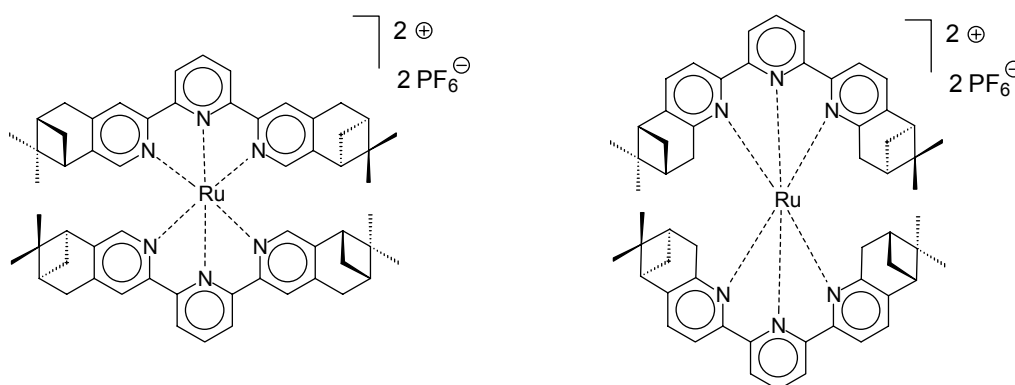
Attempts have been undertaken to prepare liquid crystals containing metal complexes in order to obtain mesophases where the characteristic properties of such complexes are incorporated. One approach to achieve this goal consists of a terpyridine ruthenium(II) complex, bearing a long alkyl chain.  $C_{19}H_{31}$  and  $C_{31}H_{63}$ -tails have been introduced, resulting in amphiphilic complexes, which could also act as surfactants.<sup>[69]</sup> For the complex containing the short chain, lyotropic mesomorphism was found in water, while a similar behavior was detected for the long-chain-complex in ethylene glycol.

### 1.3.1 Chiral complexes

First attempts to introduce chirality into terpyridines were undertaken by the group of Abruña et al.<sup>[70]</sup> A 4',4''''-bis(methylthio)-4'',4''''-bis(*n*-propylthio)septipyridine was synthesized, which upon complexation with copper forms double-helices involving two ligand moieties and two copper(II) ions. In these complexes, the ligand strands act as double terpyridine-units, leaving two pyridine rings uncoordinated. The same group reported the preparation of 6,6''-diphenyl-4,4''-bis(alkylthio)-2,2':6',2''-terpyridines, which forms helical complexes with

Cu(I)-ions.<sup>[71]</sup> In this case, the terpyridine serves as a *bis*-dentate and a *mono*-dentate ligand, whereas with Cu(II)-ions a regular terpyridine complex is formed.

Another system is described in ref.<sup>[72]</sup> In this case chirality is introduced by a 2,2-*bis*[2-(4(S)- or 4(R)-phenyl-1,3-oxazoliny)]propane that was coordinated together with unfunctionalized terpyridine to an oxo-ruthenium(IV) complex. The approach of von Zelewsky consists of the utilization of a chiral 'dipineno'-(5,6:5'',6'')-fused 2,2':6',2''-terpyridine ligand as well as of the analogous (4,5:4'',5'')-fused derivatives.<sup>[33]</sup> Here, chirality is introduced by fusing a chiral pinene-cycle in 5,6-position onto the terpyridine ring, thus making the ligand itself chiral (Scheme 1.19). The ligands were synthesized in an enantiomerically pure fashion.



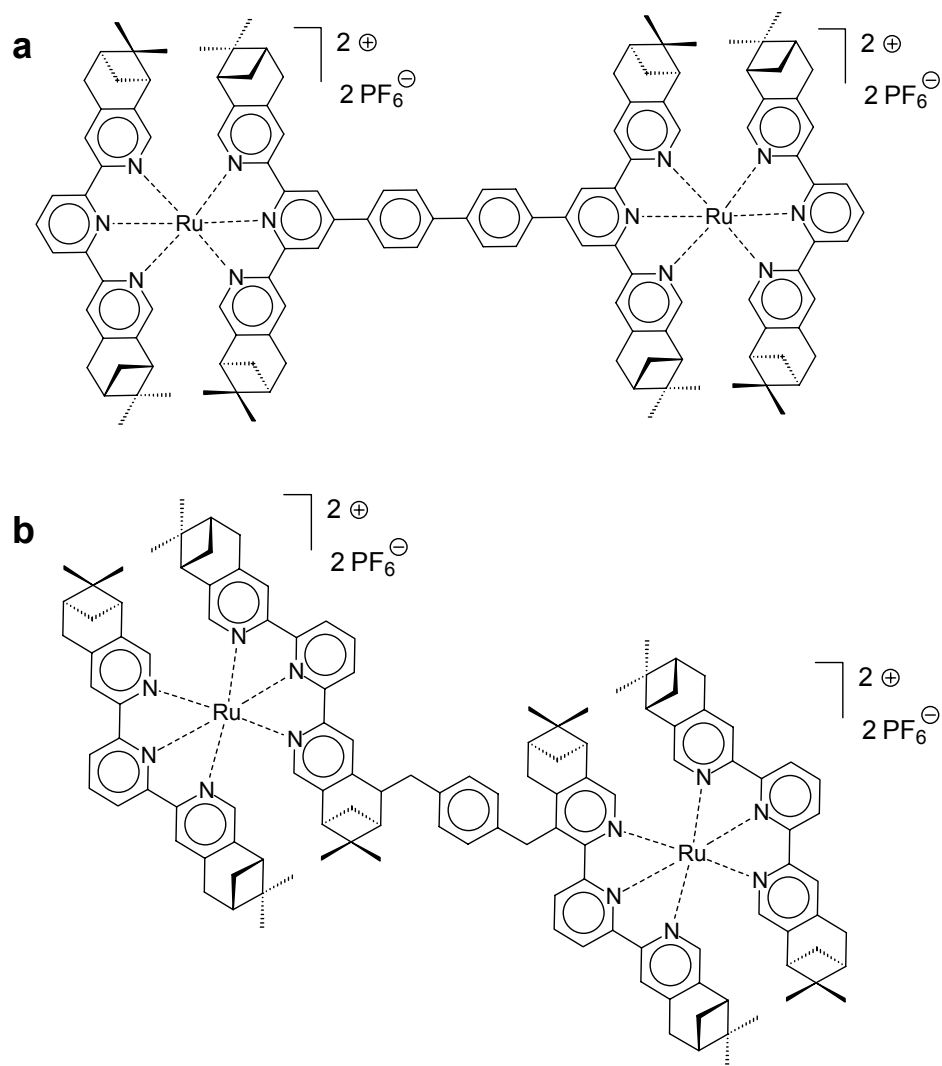
Scheme 1.19. Chiral terpyridine complexes with fused pinene units.<sup>[33]</sup>

Circular dichroism (CD) investigations showed that the resulting complexes are helically distorted in a chiral fashion. These and other pinene-functionalized terpyridines have been investigated regarding stereoselective catalysis.<sup>[73]</sup>

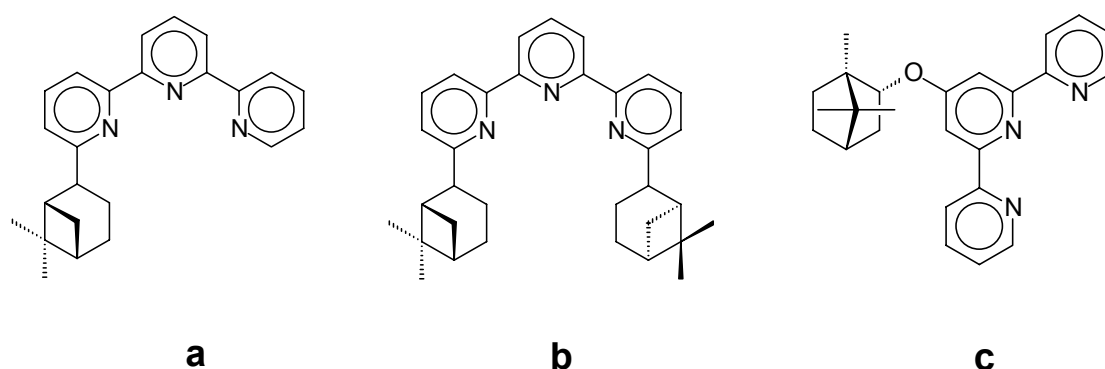
Subsequently, this work has been continued to investigate multinuclear and polymeric systems. The group of Abruña *et al.* reported the linking of two 'dipineno'-(5,6:5'',6'')-fused 2,2':6',2''-terpyridine ligands in the 4'-position by a biphenyl moiety (Scheme 1.20a).<sup>[74]</sup>

A slightly different approach consists of the connection via the dipineno-groups and a *p*-xylene linker (Scheme 1.20b). Both ligand systems have been used to obtain dinuclear ruthenium(II) complexes and coordination polymers that exhibit room-temperature fluorescence due to the aromatic connector. The ligands have also been applied in the preparation of iron(II) coordination polymers.<sup>[75, 76]</sup>

Furthermore, attempts were undertaken to introduce chirality in side groups, which are connected only via one  $\sigma$ -bond (instead of the previously described fused systems). Besides an example of 6,6''-substituted terpyridines (Scheme 1.21a-b),<sup>[73]</sup> another example was reported by Constable *et al.*,<sup>[77]</sup> where a bornyl-group acted as the substituent in the 4'-position of the terpyridine (Scheme 1.21c).



Scheme 1.20. Chiral terpyridine-ruthenium complex dyads.<sup>[74]</sup>

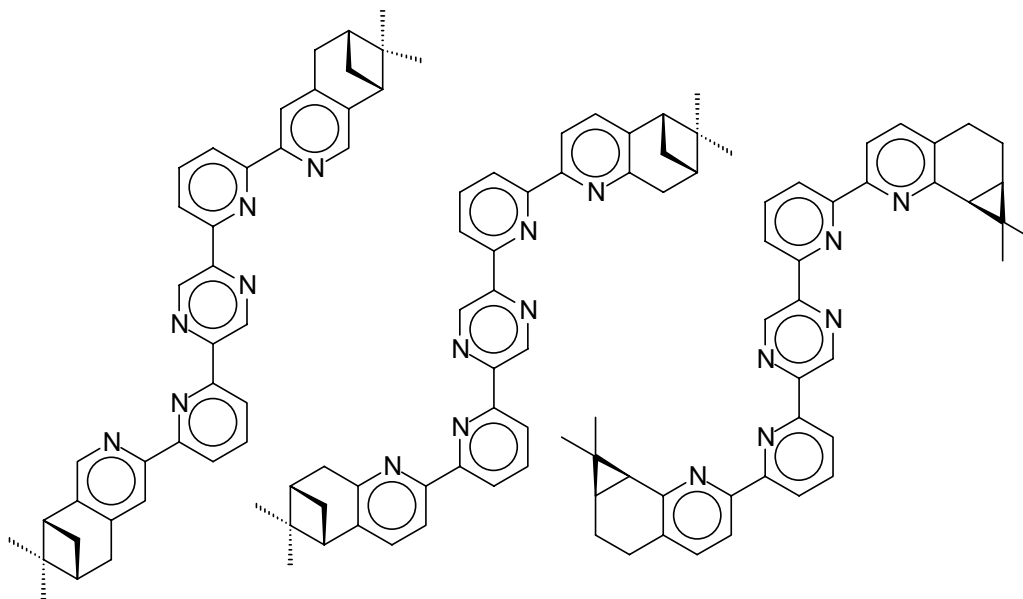


Scheme 1.21. Connecting a chiral unit via a single bond.<sup>[73, 77]</sup>

Ruthenium(II) as well as cobalt(II)-complexes were synthesized using these type of ligands. However, transfer of chiral information to the complex core was minimal.

Novel ligands that contain a central pyrazine ring connected to peripheral bipyridine moieties have been prepared, providing terpyridine-like binding moieties.<sup>[78]</sup> The coordination sites are pointing in opposite directions. Annellated terpene fragments render these metal chelators

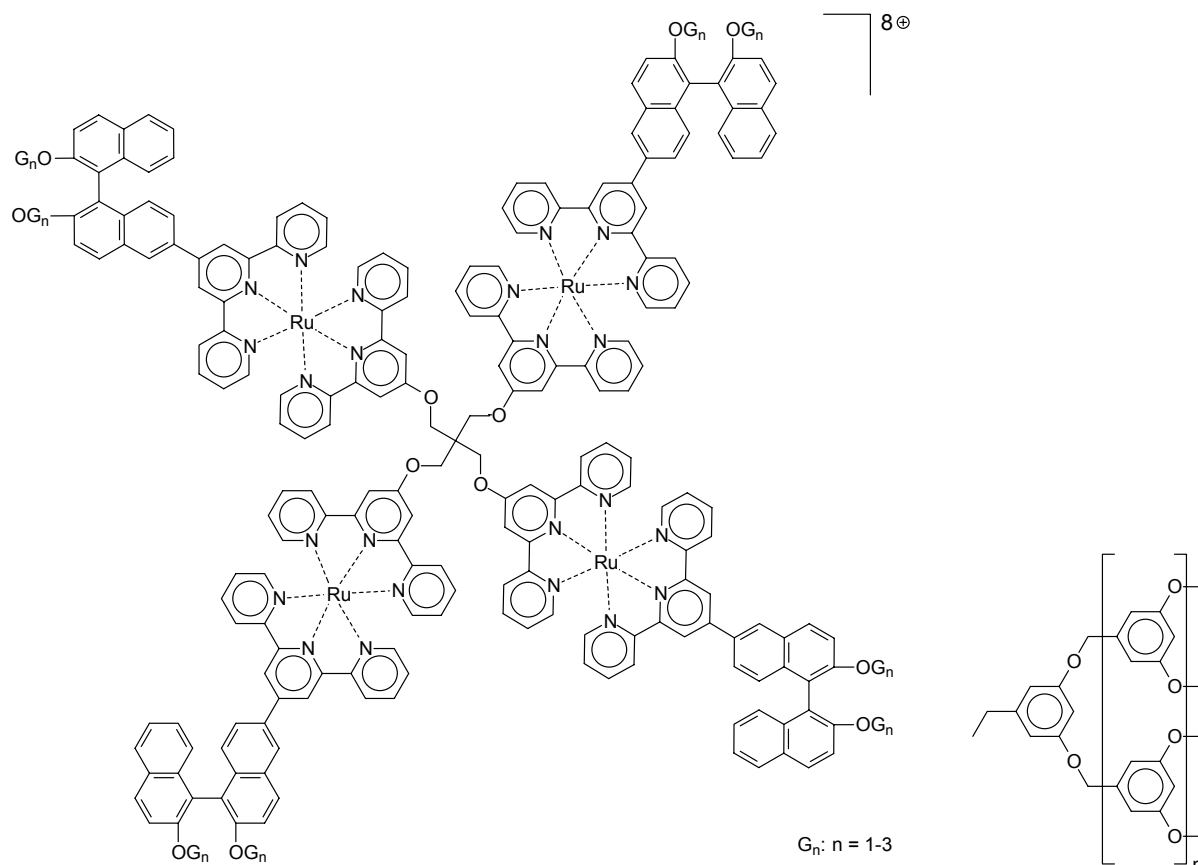
chiral (Scheme 1.22). Thus, stereoselectivity is introduced into the formation of chiral, multinuclear coordination species.



Scheme 1.22. Biscoordinating ligand, bearing chiral groups.<sup>[78]</sup>

An interesting extended chiral architecture was achieved by Jiang *et al.*<sup>[79, 80]</sup> by the successful preparation of a chiral terpyridine-dendrimer molecule, consisting of four terpyridine-Ru(II) complexes (Scheme 1.23).

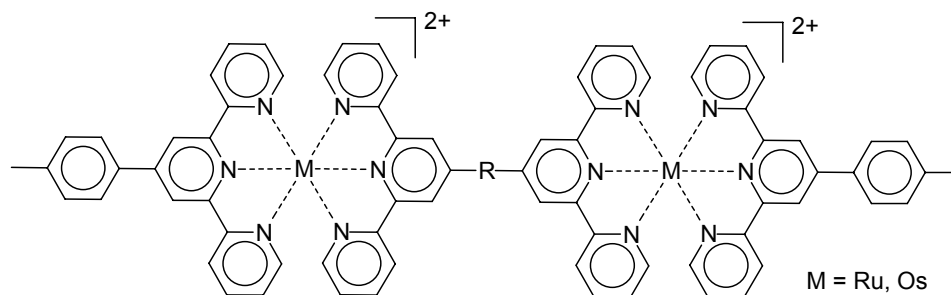
Terpyridine groups were attached to the binaphthyl units, subsequently reacted with RuCl<sub>3</sub> and further complexed to the terpyridinyl-functionalized pentaerythrol, which acts as the dendrimer core. CD spectroscopy revealed an enantiomerically pure compound.



Scheme 1.23. Tetranuclear terpyridine ruthenium complex, bearing chiral binaphthyl groups.<sup>[79, 80]</sup>

## 1.4 Dyads and triads

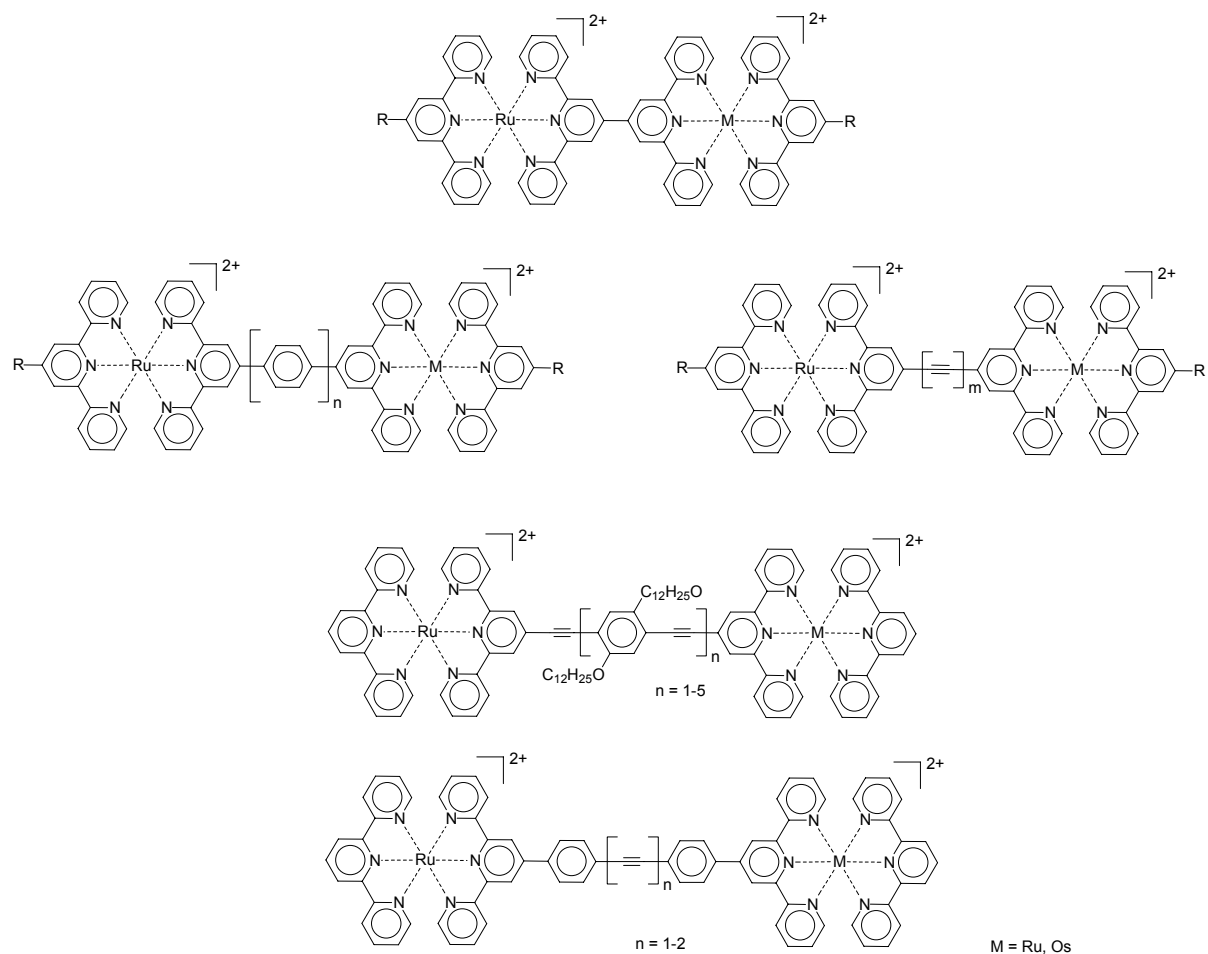
Many systems containing two or three terpyridine complex units, linked by different spacers, have been synthesized. Both homodyads (same metal ions) and heterodyads (different metal ions) are known. Interesting examples are represented by the combination of the metals ruthenium and osmium. A variety of such compounds and their properties is reviewed by Sauvage *et al.*<sup>[16]</sup> in 1994. The general formula is depicted in Scheme 1.24.



Scheme 1.24. Schematic representation of a dyad.

If a ruthenium complex is connected to an osmium complex, then an energy transfer from Ru to Os can be observed when exciting the ruthenium(II) complex unit. Many dyads have been

synthesized using rigid *bis*-terpyridine ligands. Therefore, the resulting complexes have a rod-like structure (Scheme 1.25).



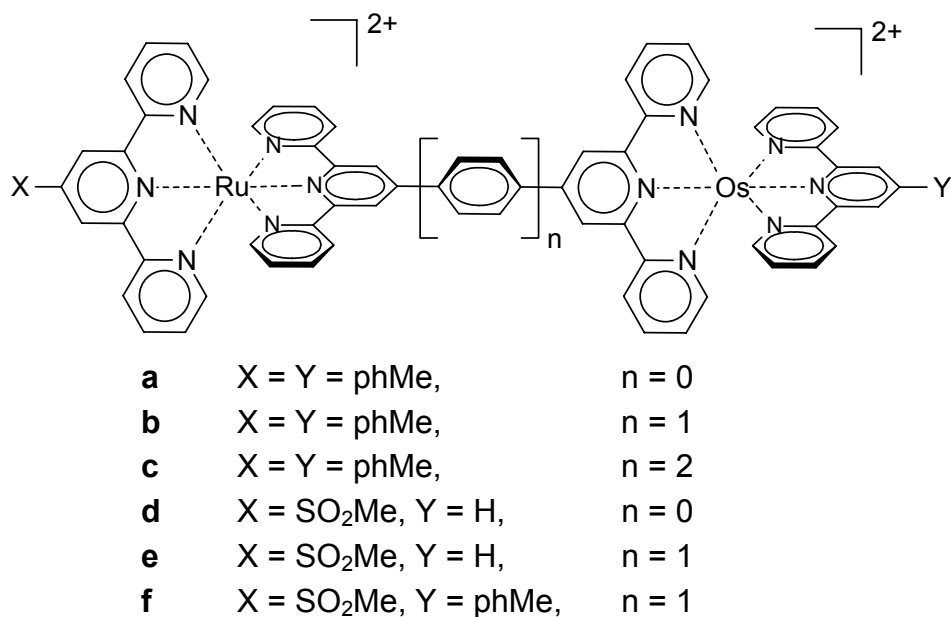
Scheme 1.25. Dyads, linked by *p*-phenylene and/or ethynyl moieties.<sup>[16, 30, 81, 82]</sup>

Starting from a dyad with directly connected terpyridines, various spacer groups have been introduced. Intensive work has been performed on a wide range of conjugated spacers of different length and composition, allowing the photophysical properties of the corresponding complexes to be fine-tuned. Phenylene-linked dyads have been reviewed in ref.<sup>[16]</sup> and the alkyne-linked complexes in ref.<sup>[30]</sup> Complexes of the mixed alkyne-phenylene linked ligands have been reported more recently.<sup>[81]</sup> For the *p*-phenylene-bridged dyads (with  $n = 0-2$ ) it has been shown that conjugation enhances the luminescence lifetime.<sup>[82]</sup> However, the phenylene-bridged system shows less luminescence than the directly linked one because the phenyl-ring is not coplanar to the terpyridine moieties and therefore preventing complete delocalization.

Besides homometallic ruthenium complexes, also ruthenium-osmium-dyads have been prepared using the bridging ligands. The synthesis of these systems has been performed by first complexing only one coordinating site with a ruthenium fragment, followed by a reaction with an osmium precursor as a second step. An energy-transfer from the ruthenium center to the osmium could be observed in the products.

The basics of the system depicted in Scheme 1.26 have already been reported in the literature,<sup>[16]</sup> but nevertheless, a lot of research is still being carried out on this system.





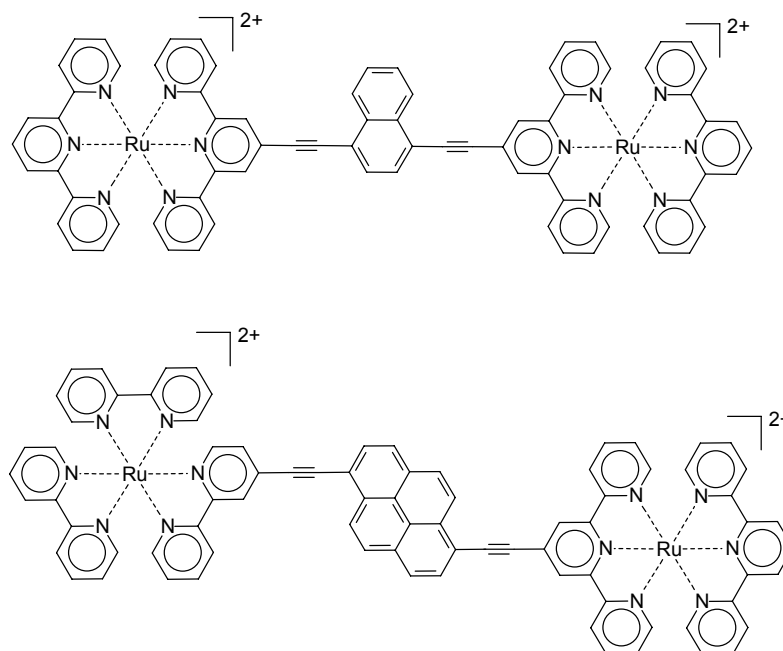
Scheme 1.26. *p*-Phenylene-linked dyads with donor and acceptor groups.<sup>[16]</sup>

Further adjustment and fine-tuning of the optical properties could be achieved by introducing donor or acceptor groups into the terminal ligands.<sup>[83]</sup> Electrochemical experiments revealed both metal-metal and ligand-ligand interactions and photophysical studies showed a very efficient energy transfer mechanism, which is most likely based on an electron exchange mechanism to be operational.

Architectures of terpyridine complexes, connected to ethynyl groups, are of major importance due to their enhanced photophysical properties. Because of an enhanced delocalization of the electrons in such systems, the triplet energy state is lowered, resulting in efficient luminescence at room temperature.

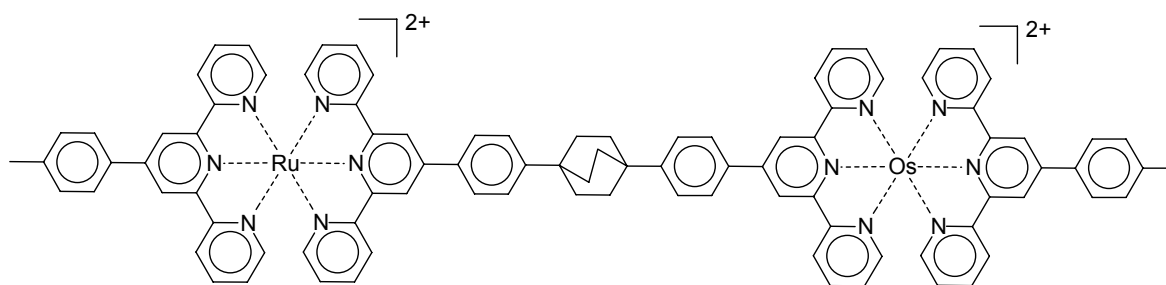
In a different experiment, rhodium(III) has been introduced into an analogous series of phenylene-bridged binuclear complexes.<sup>[84]</sup> Compared to the Ru-Os system, an energy transfer from Rh(III) to Ru(II) was found. In the case of direct linkage, an electron transfer from Ru(II) to Rh(III) was observed. Analogous dyads have been prepared using Ru(II) and Co(III) complexes.<sup>[85]</sup> For these systems, an electron transfer from ruthenium to cobalt was found.

In order to study the effect of different central aromatic units on the photophysical properties of the dyad, naphthalene has been introduced into the backbone of the bridging ligand, which was subsequently converted to the ruthenium dyad (Scheme 1.27).<sup>[86]</sup> Compared to the analogous phenylene linked dyad, the triplet lifetime is prolonged. In the same laboratory, a pyrene that connects a terpyridine ruthenium(II) complex moiety with a bipyridine, has been reported recently.<sup>[87]</sup>



Scheme 1.27. Dyads, linked by various aromatic groups.<sup>[86, 87]</sup>

In the dyads discussed up to now, rigidity in the spacer is maintained by conjugated systems such as aromates or alkynes. In order to investigate the effect of conjugation on the photophysical and electrochemical properties of rod-like dinuclear complexes, a saturated bicyclic compound was introduced into the linker unit of a ruthenium(II)-osmium(II) dyad (Scheme 1.28).<sup>[88]</sup> In this system, the electronic interactions are completely decoupled without affecting the rigidity of the spacer.

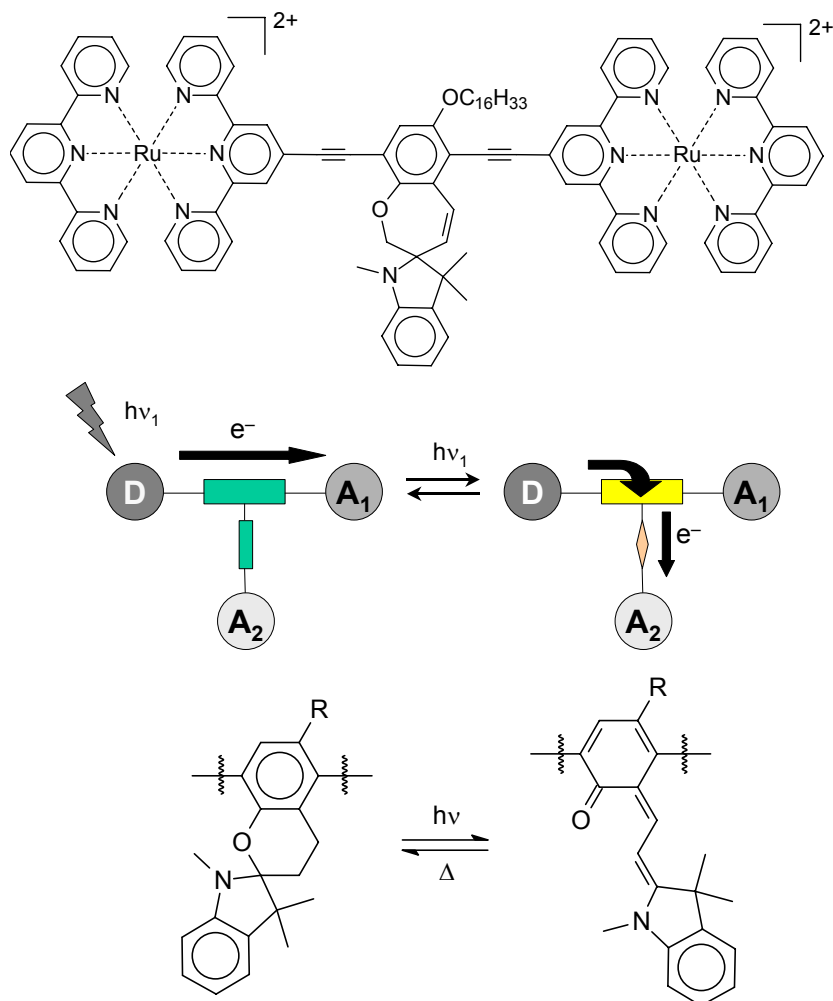


Scheme 1.28. Ruthenium-osmium dyad containing an insulating bicyclo[2.2.2]octane.<sup>[88]</sup>

The central bicyclo[2.2.2]octane acts as an insulator between the two complex moieties, preventing electronic communication between the metal centers. Therefore, the electrochemistry of such a dyad resembles that of the isolated parent complexes. At room temperature, no energy transfer was found due to the distance of the complex units. At low temperatures (77 K) in a matrix, however, the triplet-lifetime was long enough to allow an energy transfer. As expected, no electron transfer was detected due to the isolating linker.

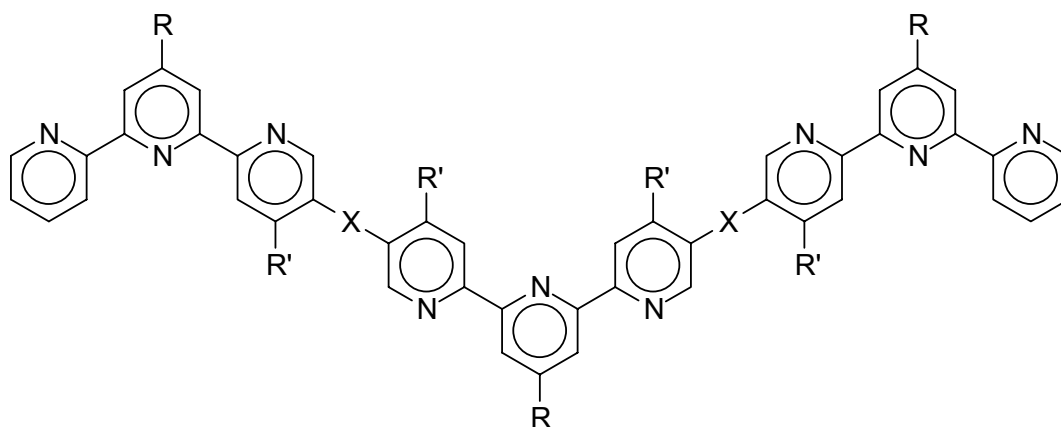
On the way to molecular devices, a dyad was designed which could act as a T-junction relay (molecular switch).<sup>[89]</sup> The spiropyran moiety in the bridge undergoes light-activated ring-opening to the merocyanine form and reforms thermally. Whereas in the closed form the delocalized bridge could act as a "molecular wire" (it is known that the MLCT state involves

the LUMO, which spans across both terminals), in the merocyanine form the alternative pathway to the side-group is opened (Scheme 1.29).



Scheme 1.29. Dyad, containing a spiropyrane, which could act as a molecular switch (*T*-junction relay) and schematic representation of the switching process.<sup>[89]</sup>

All the multinuclear complexes reported previously herein were composed of 4'-functionalized terpyridines, giving rise to rod-like complex arrays. In contrast to these approaches, the bridging ligand depicted in Scheme 1.30 consists of three terpyridines, which are linked in the 4 and 4''-positions. Different structures are therefore accessible.<sup>[90]</sup> Compared to the *tris*-ligands described before, in this case individual terpyridine moieties are linked in the 5 and 5''-positions by ethyl and ethylene groups, respectively. Trinuclear ruthenium(II) complexes with unfunctionalized terpyridine have been synthesized which revealed luminescence at room temperature for the ethylene-linked complex and no fluorescence for the alkylspacer-separated triad.

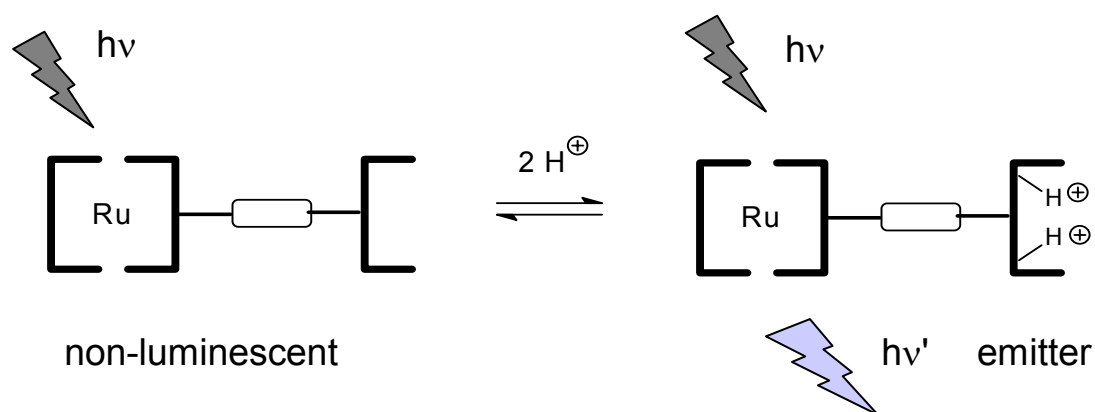


Scheme 1.30. Ligand for a 5,5'-linked triad.<sup>[90]</sup>

#### 1.4.1 Switchable dyads and triads

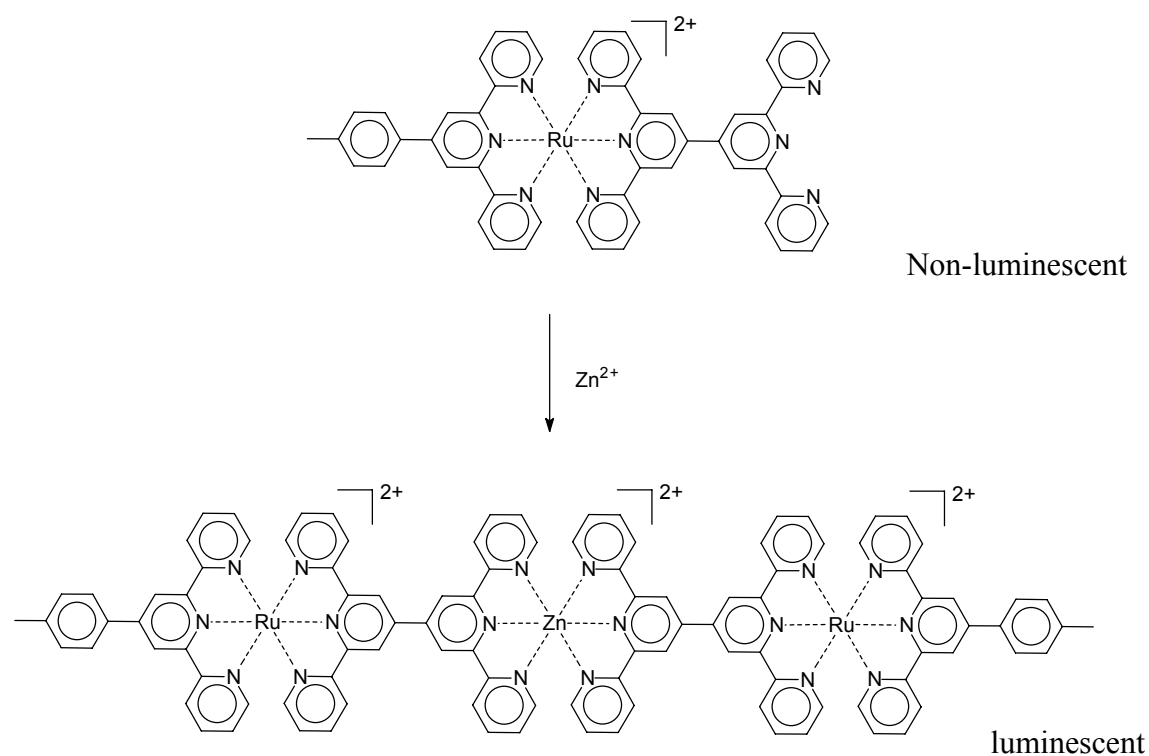
Multinuclear terpyridine complexes, especially those capable of energy and/or electron transfer, are promising compounds for future applications in optical nano-devices or solar cells. In the field of devices, molecular switches, where electrochemical or optical activities can be switched simply and reversibly, are of special importance.

The *mono*-ruthenium(II) complex of a bridging ligand (separated by zero to two phenylene rings, as described in the previous references) could not only be used for further complexation, it also possesses other interesting properties: by protonation of the non-coordinating free terpyridine moiety, the luminescence properties could be modulated in a reversible manner. In this example, the non-luminescent complex became luminescent after protonation initiated by pH-change, giving access to "switchable" luminescence (Scheme 1.31).<sup>[91]</sup>



Scheme 1.31. Fluorescence switching by protonation of a free terpyridine moiety.<sup>[91]</sup>

Moreover, complexes of this type can be extended further, through complexation by addition of different metal ions like iron(II) or zinc(II) to result in ABA-triads (Scheme 1.32).

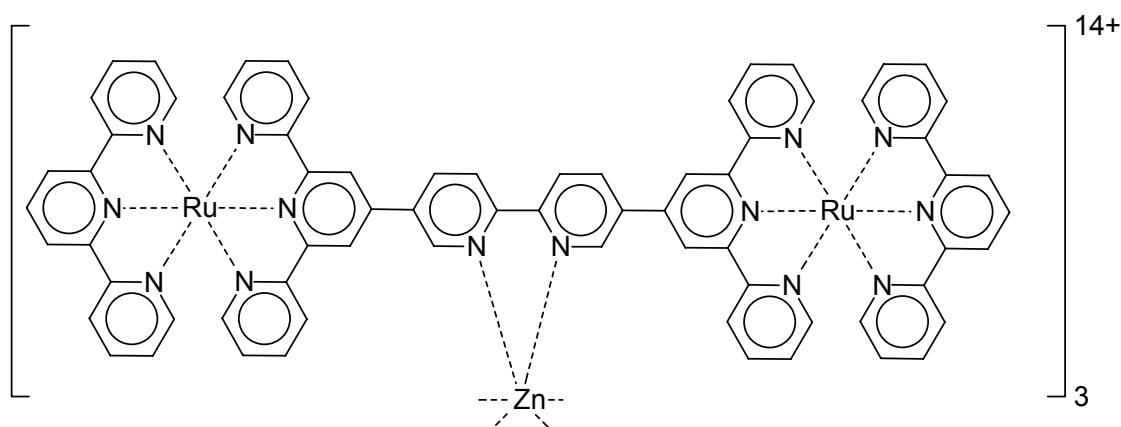


*Scheme 1.32. Switching of luminescence by complexation with zinc(II) ions.*<sup>[83]</sup>

The almost non-luminescent ruthenium(II)-terpyridine chromophore, functionalized with an uncoordinated terpyridine fragment, has been complexed with Zn(II)-ions, leading to a luminescent rod-like complex array revealing a luminescence enhancement factor (EF) larger than 10.<sup>[83]</sup> Due to the reversible, relatively weakly coordinated zinc complex, this system also gives rise to "switchable" emitters.

A different approach to tunable metal complex arrays includes the incorporation of a different complexing moiety such as bipyridine within the bridging ligand. One of the first compounds to be synthesized was a dyad, bridged by a 2,2'-bipyridine-5,5'-diethynyl group.<sup>[30, 92]</sup> The bipyridine moiety in the bridging ligand has been complexed with various metal ions. By this method the luminescence properties of the parent complex can be tuned. Whereas weakly binding ions cause an increase in the luminescence of the Ru(tpy)<sub>2</sub>-units, strong binders like Ag<sup>+</sup> or Hg<sup>2+</sup> are decreasing the luminescence. The cause for this behavior is the reducibility of these metal centers, making a photoinduced electron transfer possible, which, in turn, results in luminescence quenching. As described in the same publications, the nitrogen atoms have been methylated to lead to a viologen-moiety, resulting in a luminescence quenching through electron transfer processes.

In a dyad recently reported by Loiseau,<sup>[93]</sup> the terpyridine complexes were attached directly to a bridging bipyridine moiety (see Scheme 1.33). An enhancement of the luminescence was found for protonation of the bipyridine by addition of acids as well as after complexation with zinc(II). Utilizing cyclic voltammetry, it has been found that the electronic interaction between the peripheral chromophores is enhanced by zinc coordination.

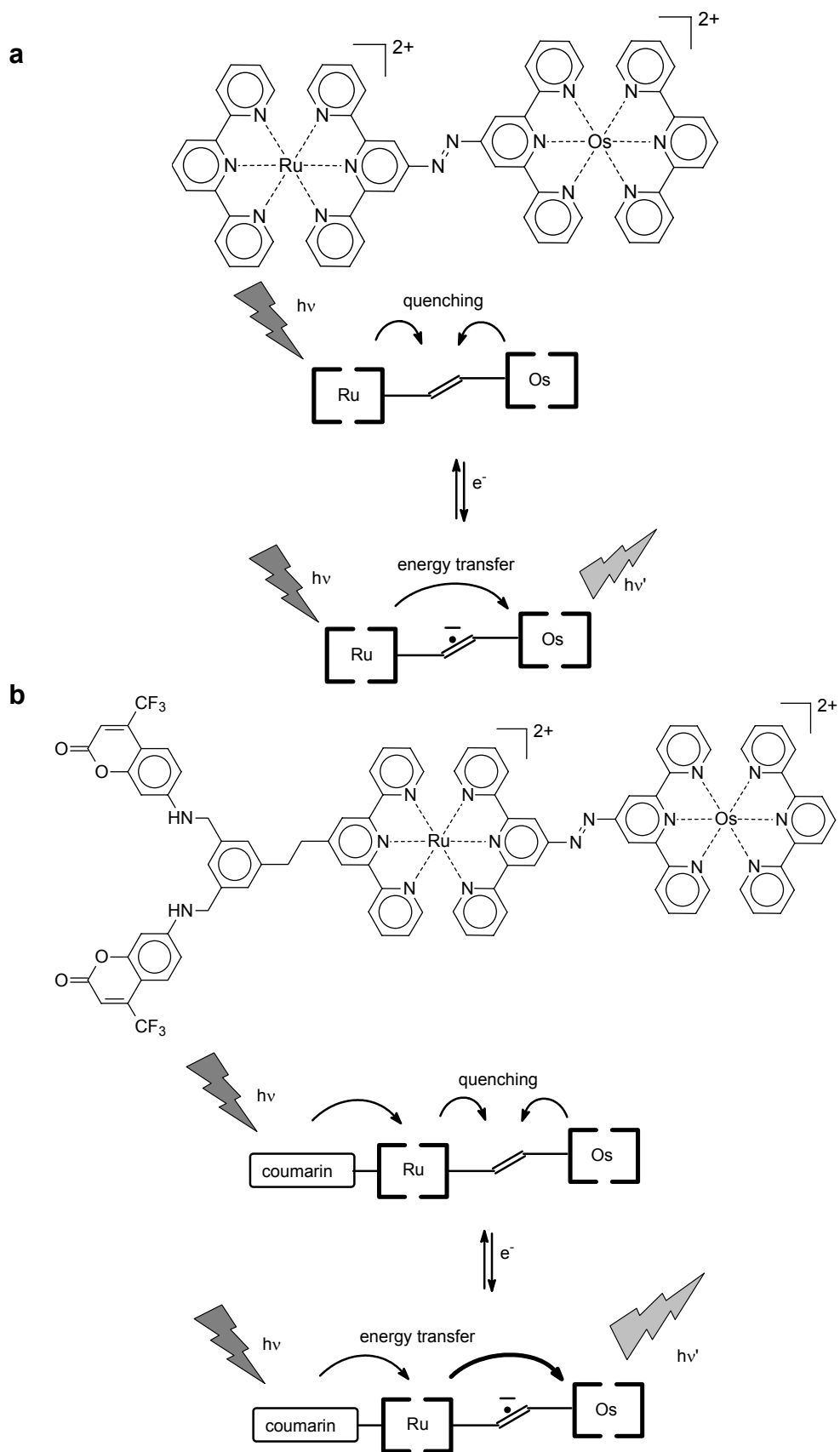


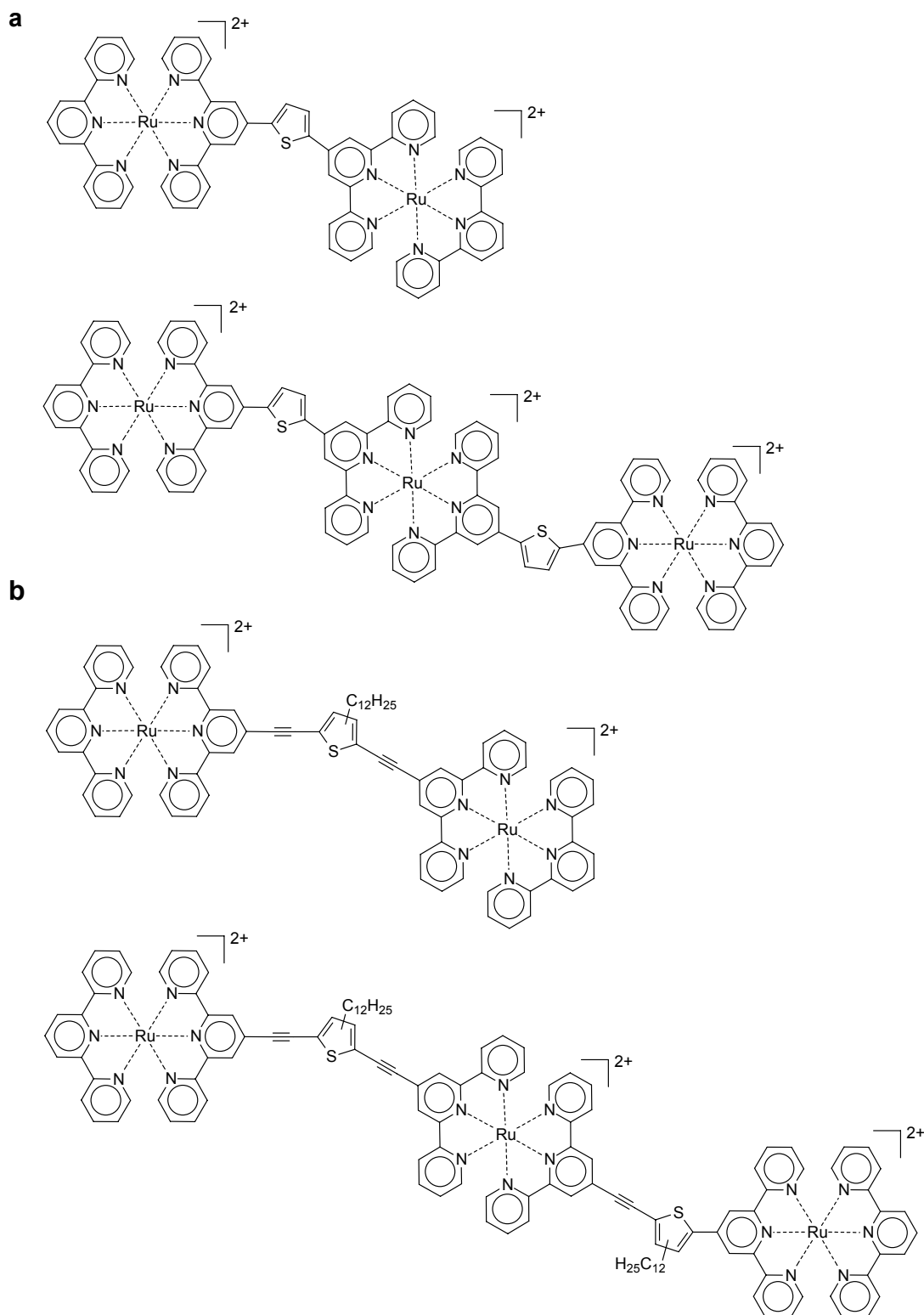
Scheme 1.33. Switchable dyad, containing a bipyridine fragment in the bridging ligand.<sup>[93]</sup>

A promising approach towards switchable fluorescent chromophores are azo-linked ruthenium-osmium dyads.<sup>[94]</sup> Besides *bis*-ruthenium and *bis*-osmium also a mixed ruthenium-osmium dyad has been synthesized (Scheme 1.34). In these systems, the energy transfer can be switched, triggered by a redox reaction. In its neutral state, the azo-group quenches the luminescence of both ruthenium and osmium. Reduction of the linker, however, leads to a luminescent homodinuclear Os(II) complex at room temperature. The corresponding homodinuclear Ru(II) complex shows a luminescence at 77 K. In the heterodinuclear complex, an energy transfer from ruthenium to osmium can take place, resulting in a strong osmium luminescence (Scheme 1.34a).

By attaching a coumarin group, the efficiency could be improved further.<sup>[95]</sup> An energy transfer from the coumarin *via* the ruthenium complex to osmium was observed (Scheme 1.34b). While the simple Ru-azo-Os dyad revealed an energy transfer of 40%, the coumarin-Ru-azo-Os triad showed an efficiency of more than 70%. Redox-stimulated switching could be performed efficiently.

Besides phenyl and pyridine groups, other aromatic groups have also been introduced into multinuclear complex arrays. A prominent example for a new class of dyads and triads is the "family" of compounds where thiophenes have been introduced (Scheme 1.35a). Besides model complexes (uninuclear complexes bearing one or two thiophenes), dyads and triads with ruthenium ions have been prepared successfully.<sup>[96]</sup> While the mononuclear complexes already showed an enhanced fluorescence, the multinuclear complexes revealed a luminescence similar to bipyridine ruthenium(II) complexes. This behavior can be explained by the stabilization of a cluster of luminescent <sup>3</sup>MLCT levels in the array by intermetal electronic communication of the complex units, leading to a higher energy gap and therefore to a lower probability of non-radiative deactivation.





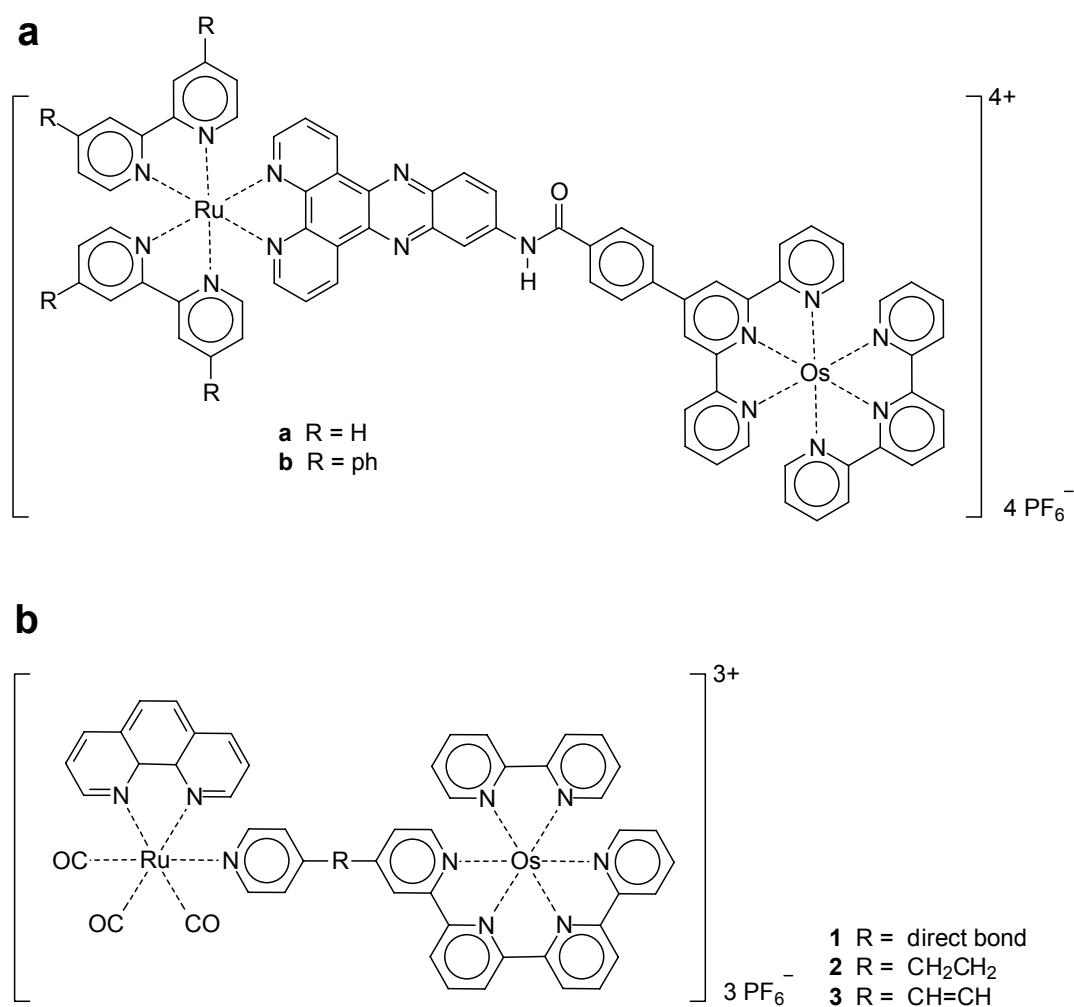
*Scheme 1.35. Thiophene-bridged dyads and triads.*<sup>[96]</sup>

Consequently, this approach has been extended to dyads and triads where the ruthenium complexes have been combined with osmium complexes in order to study energy- and electron transfer processes.<sup>[97]</sup> The mixed complexes are also luminescent, and an energy transfer from ruthenium to osmium could be observed. As a result, luminescence is enhanced when compared to the *homometallic* complexes. Thus, a five-fold enhancement was found for the Ru-Os-Ru triad.



The well-known chemistry of coupling alkynes to terpyridine has also been applied to couple terpyridine moieties to thiophenes (Scheme 1.35b).<sup>[98]</sup> In this way, systems where the terpyridine and thiophene moieties are separated by an alkyne were obtained. *Homometallic* ruthenium dyads as well as an ABA-triad (Ru-Zn-Ru) have been prepared. The thiophene unit was found to act as an insulator, preventing full delocalization. An enhanced luminescence was found compared with the uncomplexed mother compounds and compared with the phenylene analogues due to an improved stabilization of the triplet state. The thiophene-linked multinuclear complexes may eventually lead to applications such as molecular wires or as light-harvesting devices.

Bipyridine ruthenium(II) complexes have also been employed in a dyad with terpyridine osmium complexes as photosensitizer for an enhanced fluorescence.<sup>[99]</sup> This system has been made switchable by the introduction of an aminodipyrido[3,2-a:2',3'-c]phenazine moiety as a linker (Scheme 1.36a). The osmium emission could even be increased by the application of 4,4'-diphenyl-2,2'-bipyridine instead of native bipyridine. "Switching" was easily performed through protonation of the connecting unit.

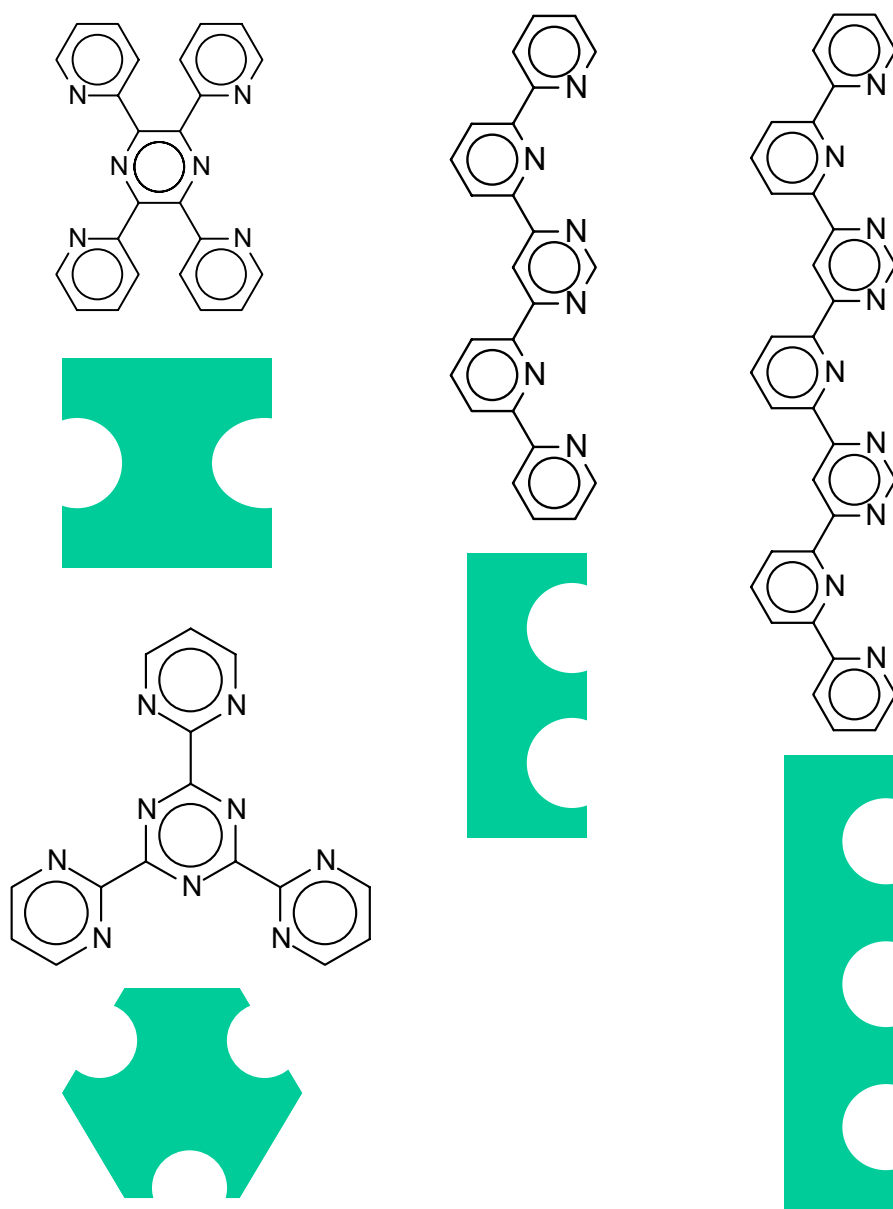


Scheme 1.36. Bipyridine ruthenium-terpyridine osmium dyad, linked by a amide bond (a)<sup>[99]</sup> and rhenium-carbonyl-osmium dyads (b).<sup>[100]</sup>

The energy transfer system containing an osmium center as receiving unit has been extended to a "hetero"-system consisting of a pyridine-bipyridine-terpyridine complex (Scheme 1.36b), to which a rhenium(II) pyridine-phenanthroline-tricarbonyl complex has been connected via an ethylene and a vinylene group. An efficient energy transfer was observed in this case.<sup>[100]</sup>

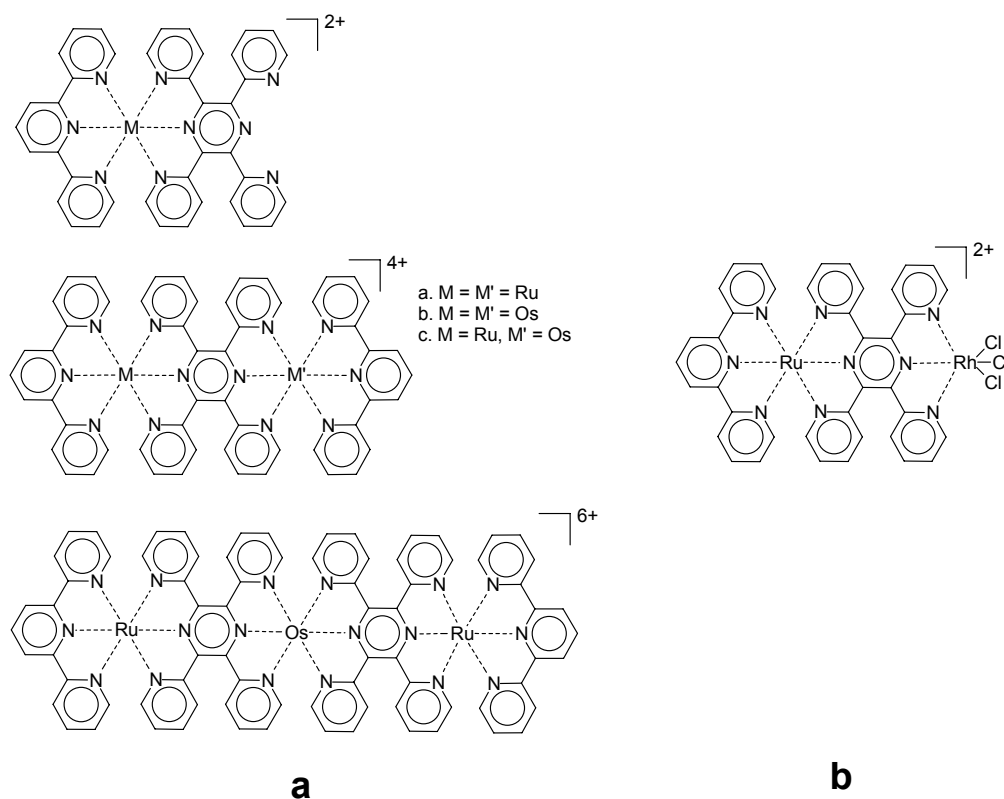
### 1.5 Supramolecular assemblies

So far, oligonuclear complexes were discussed, where two separated terpyridine complexes have been linked together by spacers of various types and lengths. Another possibility for constructing extended complex architectures are ligands, where two or more terpyridine motives are combined with sharing one or more nitrogen atoms (Scheme 1.37). Because the geometry is well defined, these kinds of ligands have been used as building blocks for the construction of extended supramolecular architectures.



Scheme 1.37. Building blocks for supramolecular architectures.

One example is the ligand *tetra*-2-pyridyl-1,4-pyrazine (tppz). This molecule can be considered as consisting of two fused terpyridines sharing the central aromatic ring. This allows the construction of rigid rod-like structures (Scheme 1.38a).<sup>[16]</sup>



Scheme 1.38. Complexes of the pyrazine ligand.<sup>[16, 101]</sup>

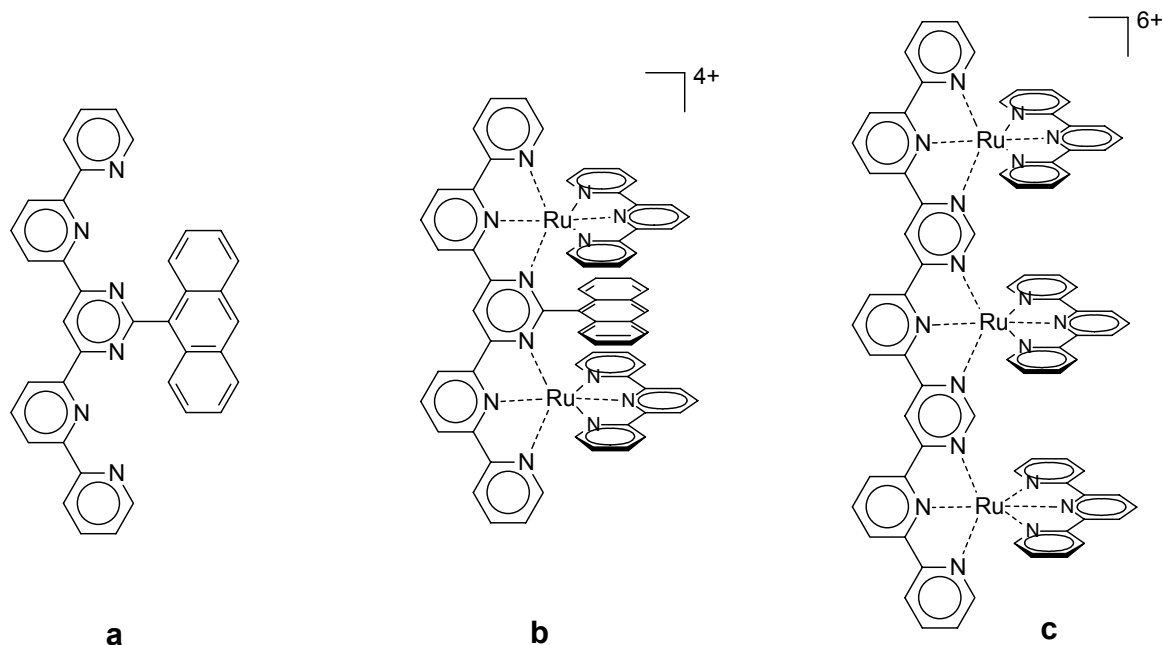
Whereas the *monometallic* compounds and the spacer-separated polyads described before show luminescence, the *multimetallic* complexes do not emit at room temperature due to metal-metal interaction.

Pyrazine ligands have also been used to synthesize mixed Ru(II)/Rh(III) complexes (Scheme 1.38b).<sup>[101]</sup> In this case, a *monometallic* tppz-tpy ruthenium(II) complex has been further complexed with rhenium(III) trichloride. With the rhenium complex known to be an electron acceptor, quenching of luminescence takes place in 80% efficiency via an electron transfer.

### 1.5.1 Grids and racks

The pyrazine ligand is composed of two fused terpyridines, pointing in 180° directions, allowing the formation of rod-like assemblies. Pyridine rings can also be combined with pyrimidine rings, resulting in ligand systems with fused terpyridine subunits. As opposed to the previously described systems, the coordinating sites are now pointing in the same direction. Two different kinds of assemblies can be obtained from these ligand types, namely grids and racks. In its free, uncomplexed form, the molecule has a helical shape,<sup>[102, 103]</sup> because only this form allows the favored *trans*-conformation of the nitrogen atoms. Therefore, the ligand has to unfold to form complexes.

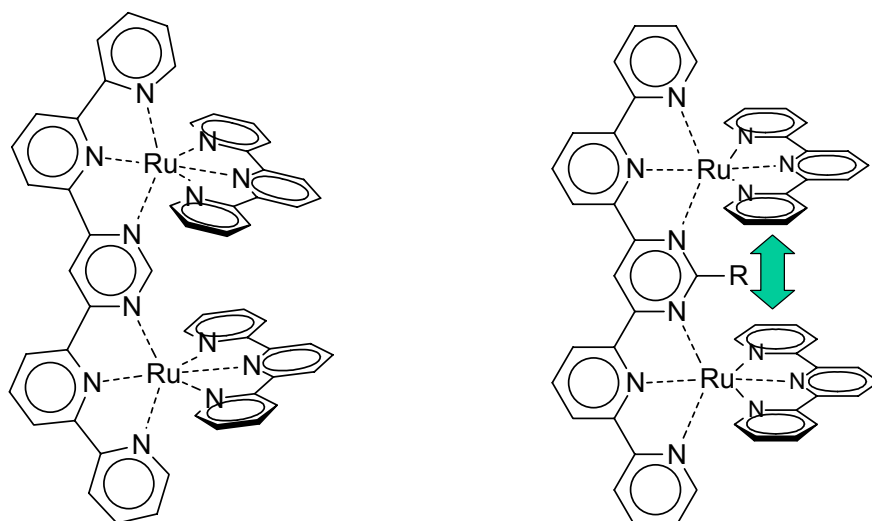
This type of ligand was first reported by J.-M. Lehn *et al.* in 1995 and prepared *via* a Stille-type cross-coupling of 6-stannylated bipyridine with 4,6-dichloropyrimidines.<sup>[104]</sup> Besides a ligand with no further substitution, a molecule bearing an anthryl-substituent in the 5-position of the pyrimidine ring was also synthesized (Scheme 1.39a). Di- and trinuclear rack-like structures can be achieved by endcapping the terpyridine subunits with the ruthenium(III) *mono*-complex of unfunctionalized terpyridine (Scheme 1.39b and c).



Scheme 1.39. Rack-like complexes.<sup>[104]</sup>

Crystal structure analysis revealed that the ligand axis is bent due to the not exactly octahedral geometry of the complex unit. This bend is reduced in the case of the anthracene-containing complexes because of the steric repulsion between this moiety and the terpyridine units (Scheme 1.40). Therefore, the anthryl group is arranged parallel to the neighboring terpyridines. A green color was found for the complexes, which could be explained by the nature of the bridging ligands and metal-metal interactions. UV-vis spectroscopy showed three MLCT absorption bands due to a splitting of the  $\pi^*$ -level.

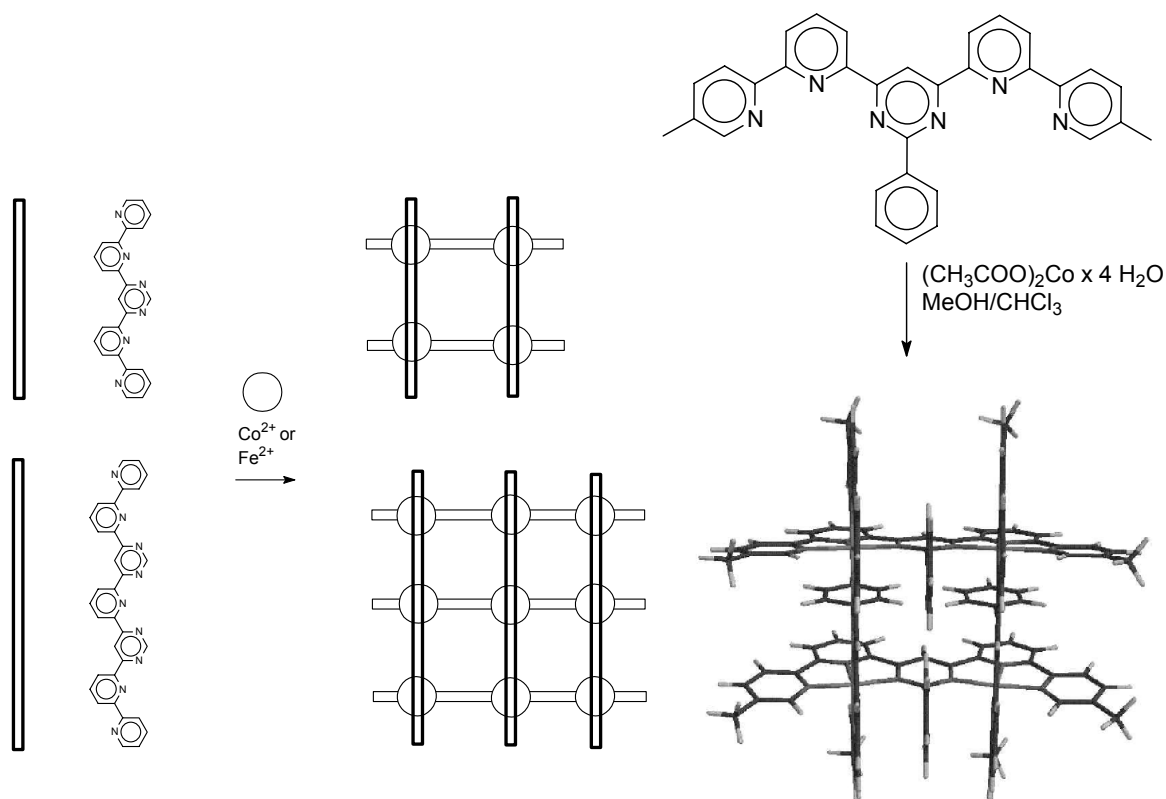
In further work, different substituents such methyl and phenyl groups, have been introduced into the 5-position of the pyrimidine, leading to different bending angles of the bridging ligand and convergence angles of the terpyridines, with a methyl group being found to be the best option for a straightened geometry.<sup>[105]</sup> In the same publication, *mononuclear* complexes where only one site of the bridging ligand is coordinated to a metal ion, were reported. However, the synthesis is more challenging due to activation of the second donor site after metal coordination at the first site.



Scheme 1.40. Distorted geometry of rack-like complexes and its reduction by a bulky substituent in the 5-position of the pyrimidine ring.

Photophysical experiments revealed an emission originating from the anthracene-containing rack-complex in the infrared region.<sup>[106]</sup> Comparison of the luminescence spectra and lifetimes with the luminescence properties of the subunits showed that in the supramolecular species, excitation energy flows with unitary efficiency to the lowest excited state, regardless of which chromophoric subunit is excited. Luminescence could be observed at room temperature as well as at low temperatures in a rigid matrix and the absorption as well as the luminescence properties could be fine-tuned by changing the substituent at the pyrimidine ring. An energy transfer from the central complexes to the peripheral ones could be observed.<sup>[107]</sup>

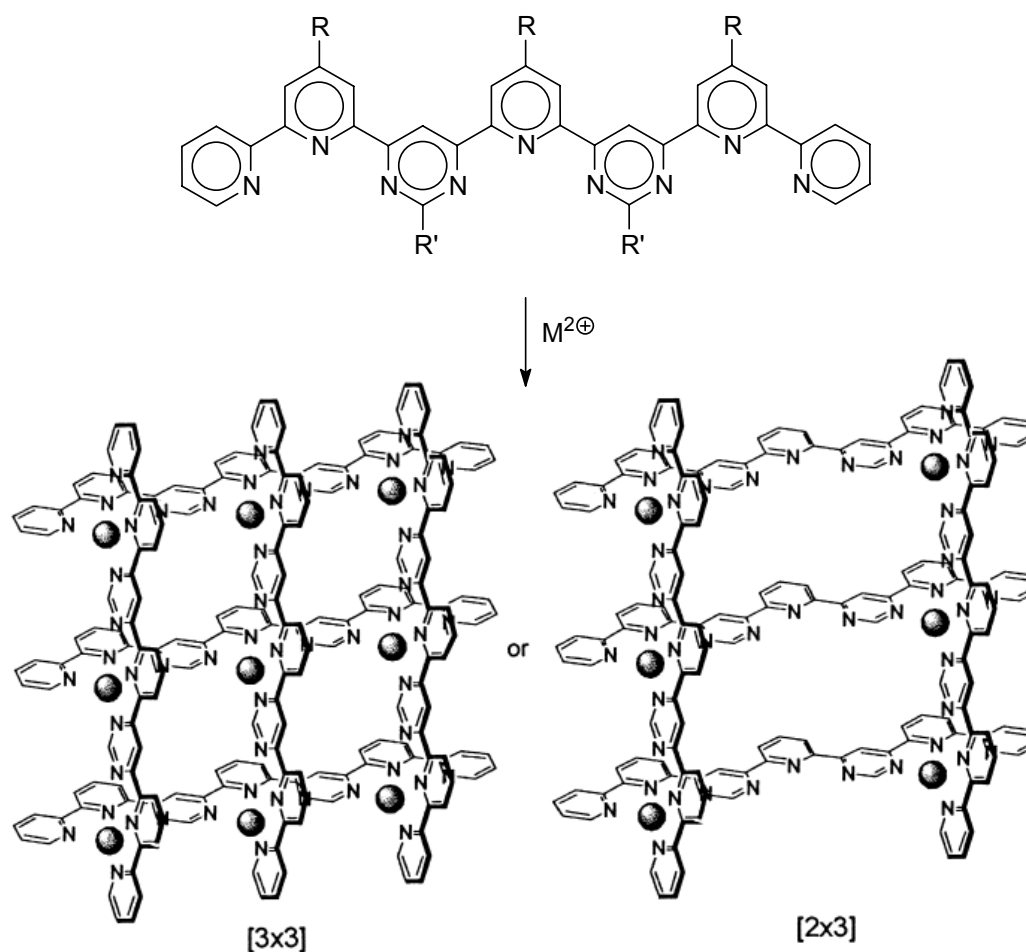
The first examples of grid-like assemblies, based on bipyridine subunits complexed by Ag(I) or Cu(I) ions, were reported in 1992 by Youinou *et al.* ( $[2 \times 2]$  grids)<sup>[108]</sup> and in 1994 by the group of J. M. Lehn ( $[3 \times 3]$  grids).<sup>[109]</sup> Most of the work up to now on these architectures has been performed in the laboratories of Lehn and still a lot of research is being carried out today. The principal structure of these complexes is shown in Scheme 1.41. First publications on grids from *tris*dentate ligands were published in 1997.<sup>[102, 103]</sup> Through addition of an equimolar amount of hexacoordinating metal ions to the *bis*coordinating ligands, analogous coordination arrays are obtained by self-assembly. Supramolecular grids have also been synthesized in the laboratories of Schubert.<sup>[110]</sup> 4,6-*Bis*(5''-methyl-2'',2'-bipyrid-6'-yl)-2-phenylpyrimidine was synthesized using a Stille-type coupling in two steps from 2,6-*bis*(trimethyltin)pyridine (*via* a stannylated bipyridine) and 4,6-dichloro-2-phenylpyrimidine. The product assembled into  $[2 \times 2]$  grids by addition of cobalt(II) acetate, and the complex array has been successfully detected in an unfragmented form by MALDI-TOF-MS.<sup>[111]</sup>



Scheme 1.41.  $[2 \times 2]$  and  $[3 \times 3]$  grid-like complexes.<sup>[102, 103]</sup>

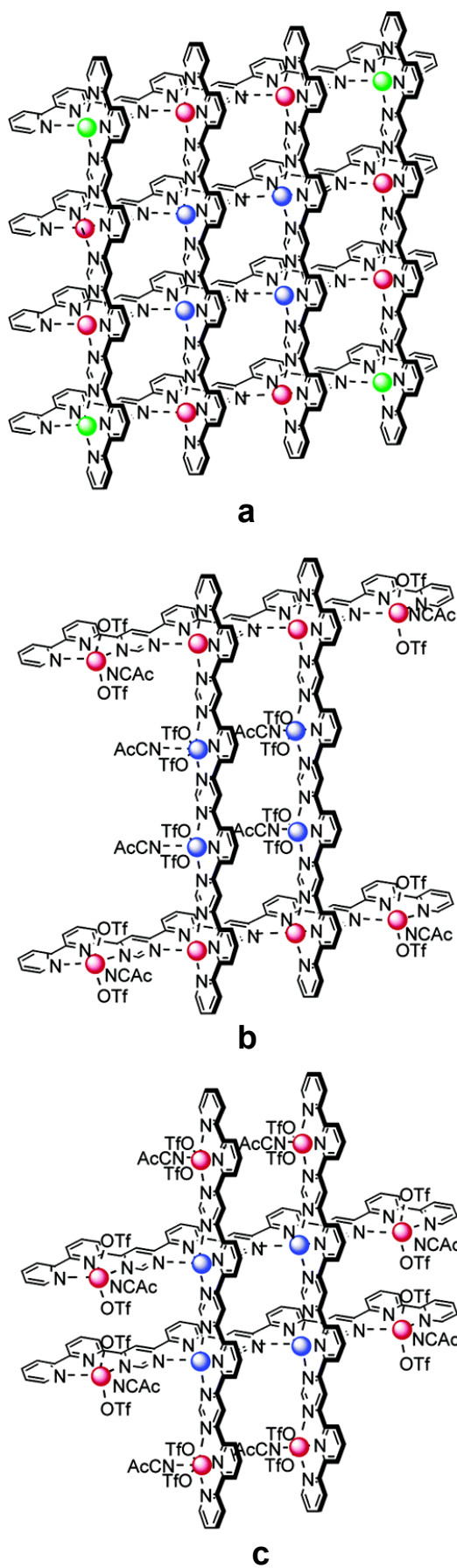
The ligand has been prepared in an improved synthesis: the originally described synthesis included a lithiation using butyllithium prior to reaction with trialkyltin chloride, resulting in lower yields, especially when the steps were repeated multiple times. In the new route, sodium stannane was applied, avoiding the lithiation step of the older route and resulting in significantly improved yields. An antiferromagnetic spin coupling could be found in the cobalt grid.<sup>[112]</sup> In the case of iron(II) grids, a spin-crossover from high spin to low spin could be triggered by temperature, pressure and light.<sup>[113]</sup>

In order to extend the grid-like structures, the synthetic approach was expanded from *bis*coordinating to *tris*coordinating ligands that are able to form  $[3 \times 3]$ -grids (Scheme 1.42).<sup>[114]</sup> Depending on the used ligands, metal ions and reaction conditions, different grid architectures can be formed. The *tris*terdentate ligand composed of three terpyridine subunits could form either  $[3 \times 3]$  or incomplete  $[2 \times 3]$  grids. Whereas zinc(II) tetrafluoroborate with ligand **a** (Scheme 1.42) and mercury(II) triflate with ligand **b** lead to  $[3 \times 3]$  structures, the other ligands or other metal ions, such as cobalt, form incomplete grids. Crystal structure analysis revealed the central non-coordinating complex moieties to be in a transoid conformation, which is more stable than the cisoid one due to steric hindrance of the ligands and also influenced by the type of metal ions or counterions used.



Scheme 1.42.  $[3 \times 3]$  and  $[2 \times 3]$  grids (a:  $R = R' = H$ , b:  $R = H$ ,  $R' = S^{\text{t}}Pr$ , c:  $R = Me$ ,  $R' = H$ , d:  $R = Ph$ ,  $R' = H$ ).<sup>[114]</sup>

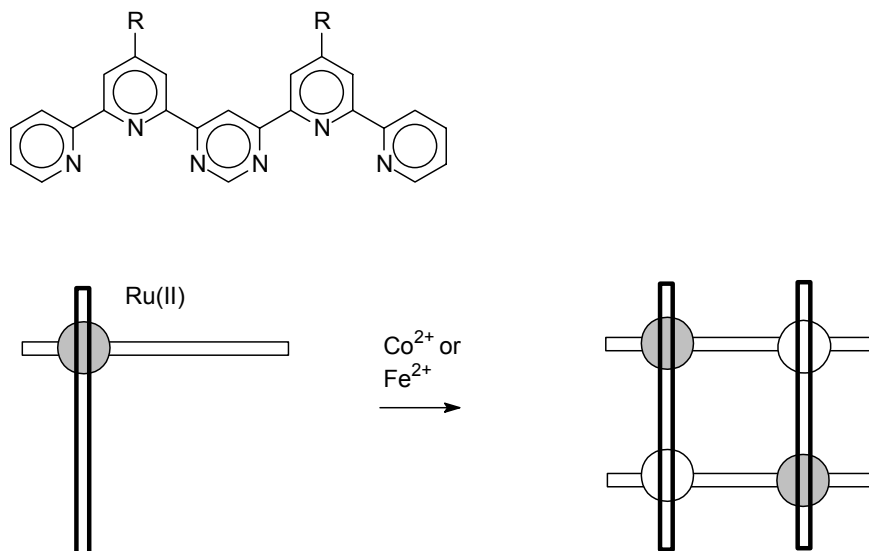
Due to their larger size resulting in less ligand distortion, lead(II) ions were found to be the most suitable metal ions for the assembly of extended grid structures. Using this metal, some very large structures have been reported:<sup>[115]</sup> a tetracoordinating ligand has been assembled into  $[4 \times 4]$ -grids by lead(II) ions. By adjusting the stoichiometry, also in this case different structures could be obtained, as shown in Scheme 1.43.<sup>[116]</sup> a complete  $[4 \times 4]$  grid was converted into a double-cross shaped structure *via* a double-T shaped  $[2 \times 2]$  grid structure through addition of lead triflate to a solution of the ligand. Besides X-ray structure analysis, NMR is a suitable tool for the investigation of such complexes. The structure of the  $[4 \times 4]$  grid has been determined by  $^{207}\text{Pb}$ -NMR, which revealed four different metal centers. Moreover, the existence of all types of grids up to the  $[4 \times 4]$  systems could be shown by electrospray-MS.<sup>[117]</sup>



Scheme 1.43. Grid structures from a tetracoordinating ligand.<sup>[115, 116]</sup>

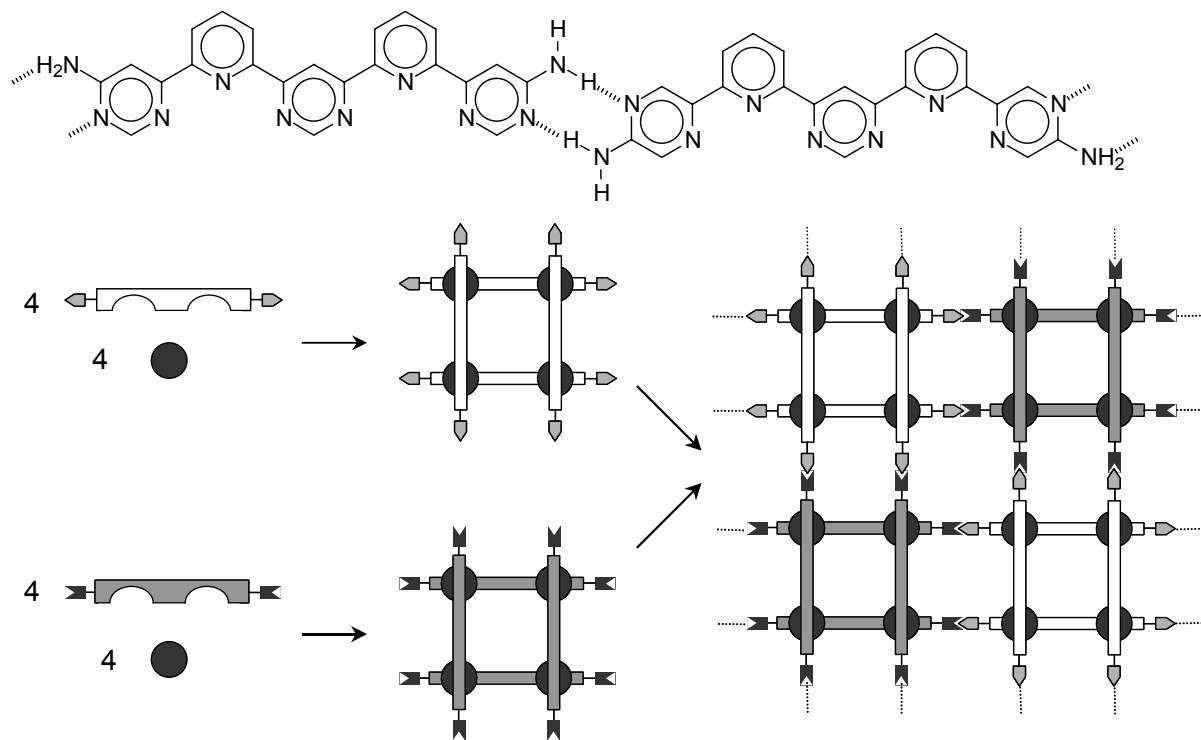


Apart from the homometallic grids, which are self-assembled from stoichiometric amounts of ligands and metal ions, attempts have also been undertaken to prepare heterometallic grid structures. These reactions need to be performed in a stepwise manner. First, one complexation site of the *biscoordinating* ligand was converted to a ruthenium(II) complex.<sup>[118]</sup> Subsequently, iron(II) or cobalt(II) ions were added to this intermediate (which is chiral), resulting in self-assembly to a grid-like complex (Scheme 1.44).



Scheme 1.44. Heterometallic grid complex.<sup>[118]</sup>

In an extension of the self-assembly principle, a two-level self-organization can be achieved by the use of two different ligands that bear complementary hydrogen bonding units at the periphery (Scheme 1.45).<sup>[119]</sup>

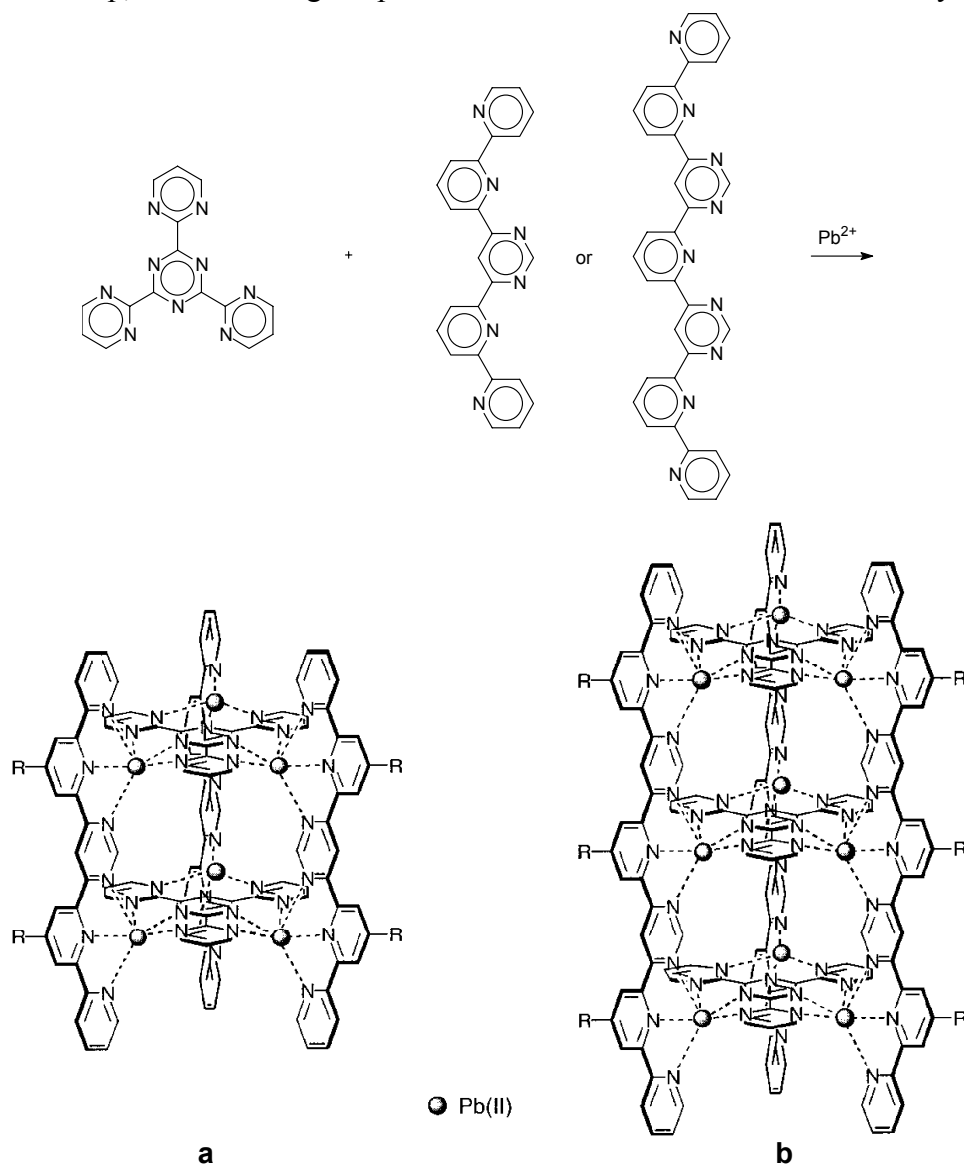


Scheme 1.45. Two-step self-assembly to a "hypergrid" by hydrogen-bonding.<sup>[119]</sup>

These compounds were converted to the grid-like complexes, respectively. Mixing stoichiometric amounts of each complex resulted in a highly organized "grid of grids".

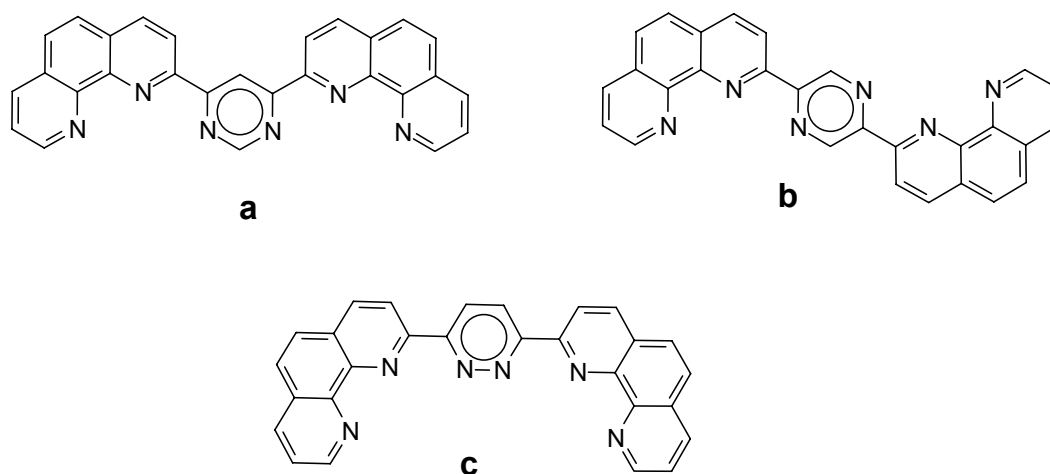
Complexes composed of different metal centers could be assembled in this fashion, giving rise to chessboard like layers. Another approach consisted of the introduction of pyridine rings in the 4'-position of the terpyridine subunits.<sup>[120]</sup> The free ligand as well as the resulting grid-complexes could be assembled on graphite surfaces. Weak CH-N hydrogen bonding interactions were also postulated by the authors, based on STM observations and comparisons with molecular modeling results.

Besides racks and grids, other architectures are also conceivable. When adding lead(II) ions to a mixture of *tris*-2,4,6-(2-pyrimidyl)-1,3,5-triazine and bridged ligands consisting of two or three fused terpyridine moieties, self-assembly took place, resulting in cylindrical cage-like complexes, constructed of either 6 or 9 metal centers, respectively (Scheme 1.46).<sup>[121]</sup> In this case, 36 respective 54 coordination bonds between 11 respective 15 components are formed in one reaction step, demonstrating the power and selectiveness of the self-assembly reaction.



Scheme 1.46. Cylindrical complex array.<sup>[121]</sup>

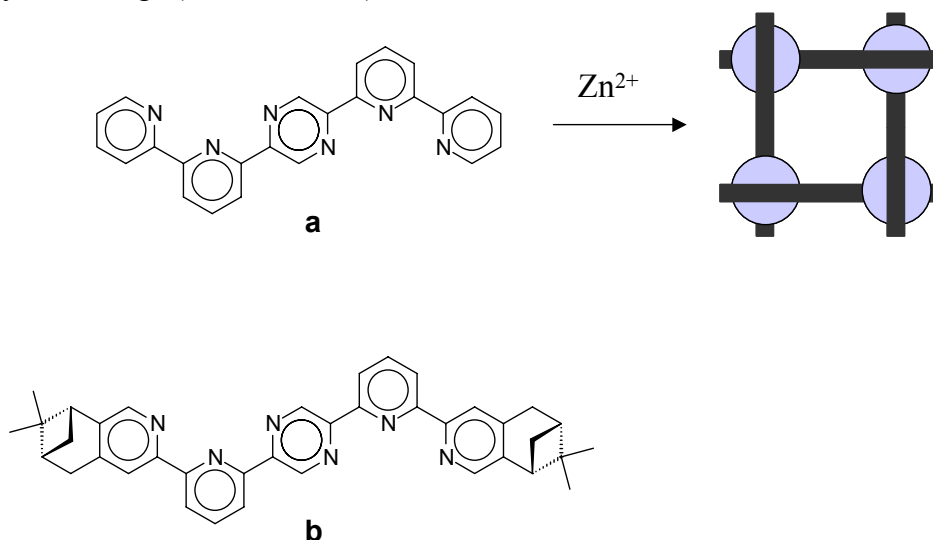
The concept of multiple chelators has been continued by the synthesis of phenanthroline-based systems.<sup>[122]</sup> *Bis*-tridentate ligands of the "Lehn-type" as well as molecules where the chelating moieties are pointing in 180° directions have been prepared (Scheme 1.47).



Scheme 1.47. Phenanthroline-based biscoordinating ligands.<sup>[122]</sup>

All the corresponding *mono*- and dimetallic Ru(II)-terpyridine complexes could be prepared, only in the case of the pincer-shaped ligand **c**, the dinuclear complex was not accessible because of steric hindrance.

Ligands of the structure as shown in Scheme 1.47b are able to form supramolecular assemblies consisting of four ligands and four metal ions. Unlike the "Lehn-type"-grids, these structures possess a  $D_4$ -symmetry and are therefore chiral.<sup>[123]</sup> Whereas the unsubstituted ligand (Scheme 1.48a) forms a racemic mixture of the supramolecular compound, the self-assembly could be directed in a stereoselective fashion by attaching pinene groups onto the terminal pyridine rings (Scheme 1.48b).

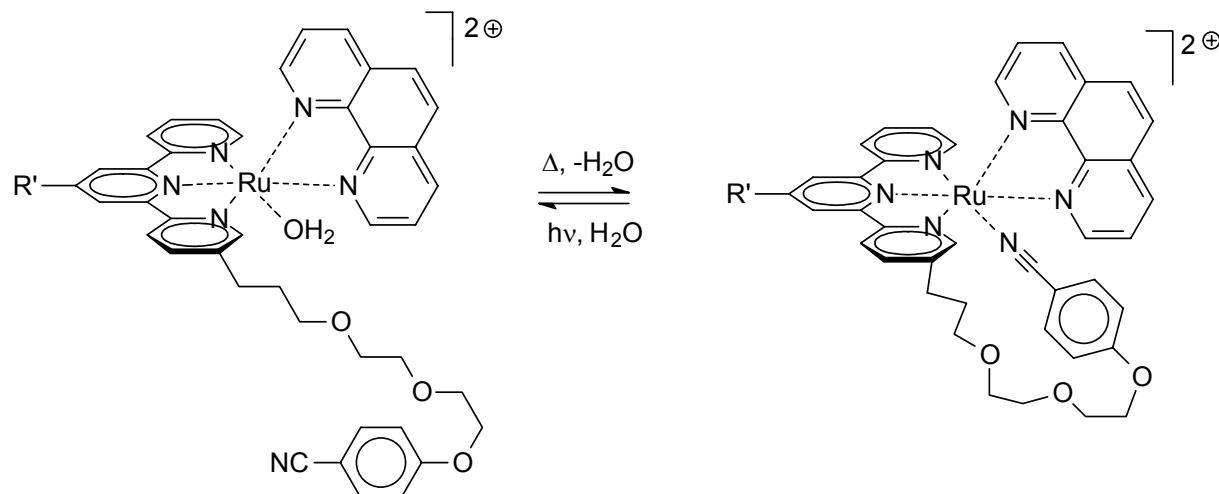


Scheme 1.48. Formation of chiral "grid"-like assemblies.<sup>[123]</sup>

### 1.5.2 Other assemblies

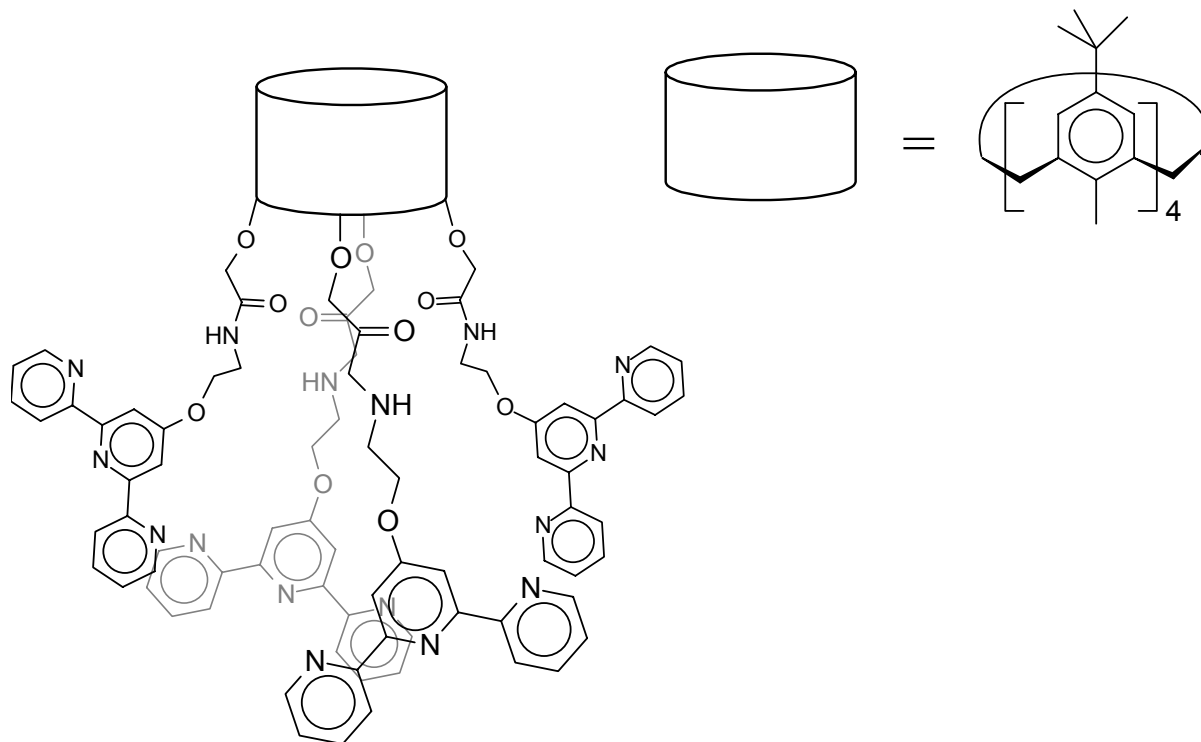
A novel switchable ruthenium complex is represented by the "scorpionate" system depicted in Scheme 1.49.<sup>[124]</sup> A Ru(II) complex was synthesized from a 1,10-phenanthroline unit and a

terpyridine ligand, linked to a benzonitrile. The latter, in turn, is able to coordinate to the ruthenium metal center, in a "back-biting" manner. The coordinated benzonitrile group can be reversibly replaced by water either through thermal or photochemical induction (Scheme 1.49).



Scheme 1.49. Scorpionate terpyridine complex.<sup>[124]</sup>

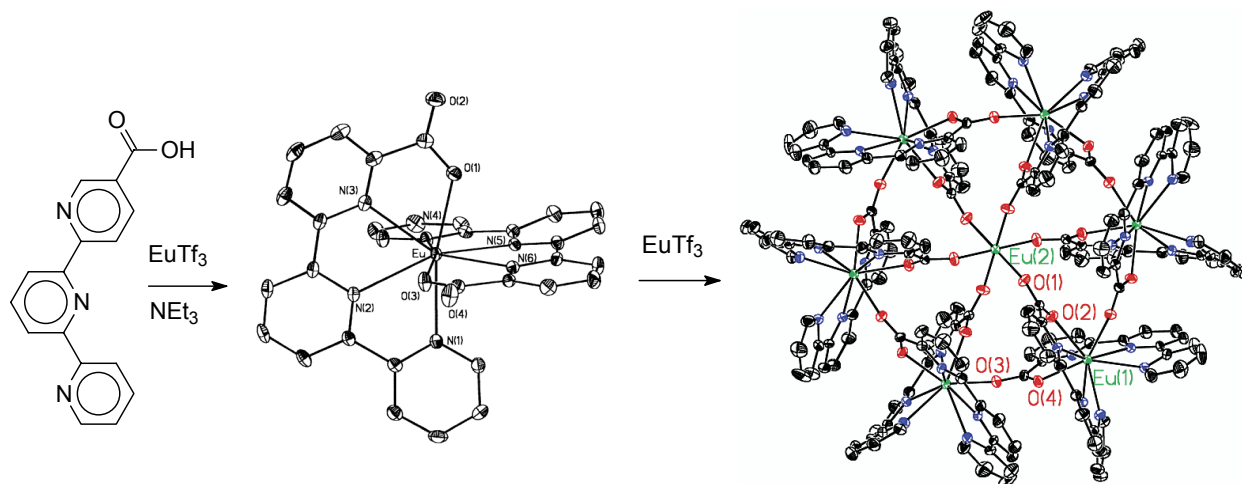
A calix[4]arene that has been modified with four terpyridine moieties can be prepared to act as a scaffold-like "pre-organizer" for supramolecular architectures (Scheme 1.50).<sup>[125]</sup> Complexation with nickel(II), copper(II) and cobalt(II) led to the formation of intramolecular complexes incorporating two metal ions.



Scheme 1.50. Calixarene-tetraterpyridine.<sup>[125]</sup>

A wheel-like self-assembled structure has been achieved using 6-carboxy terpyridine, which acts as a tetradentate ligand.<sup>[126]</sup> At a 2:1 ratio of the ligand to europium triflate, a

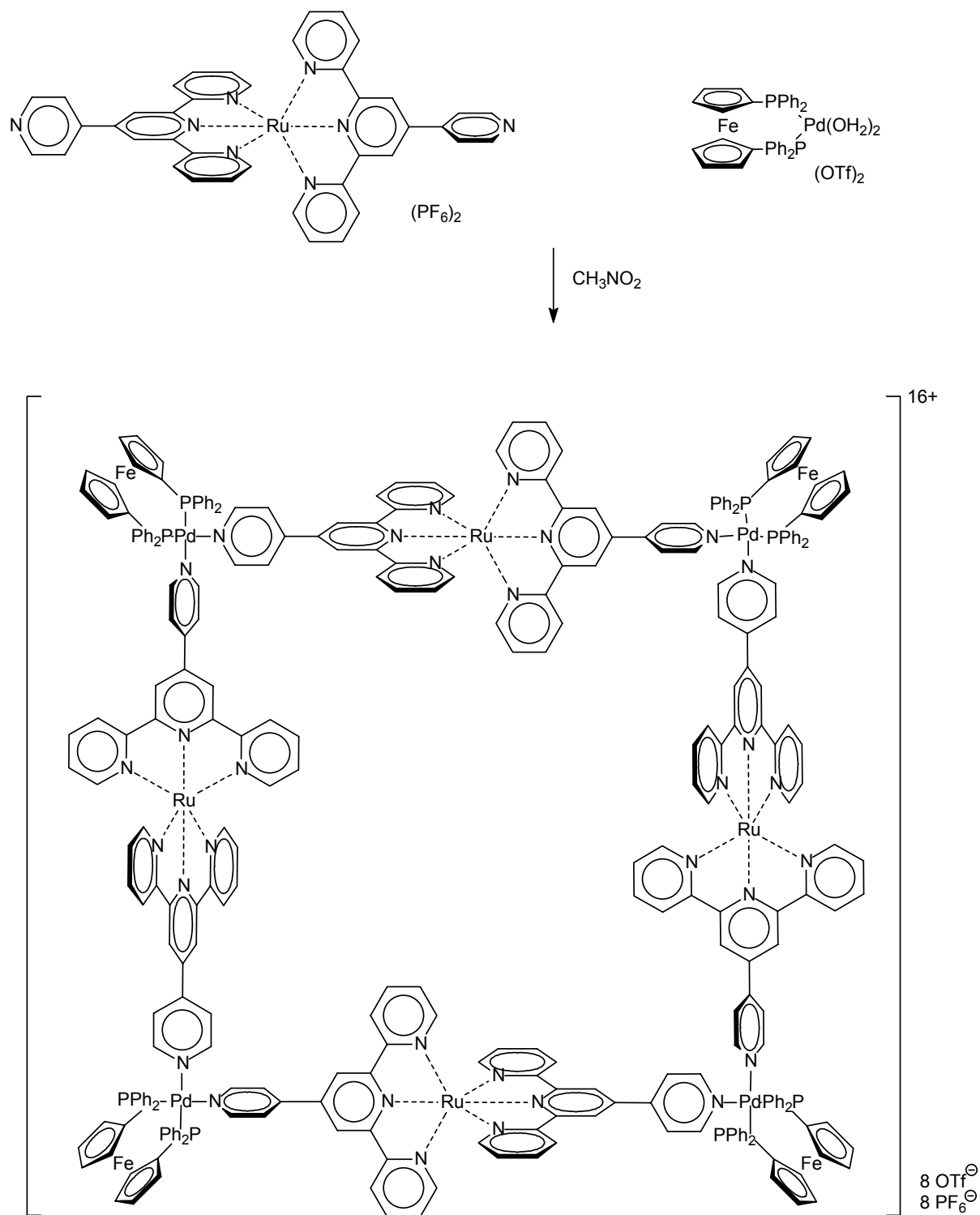
*mononuclear bis-complex* was formed. Addition of more europium ions resulted in self-assembly to the hexanuclear complex of wheel structure, where the carboxylates act as bridging ligands between the subunits. An octahedrally coordinated seventh europium ion lies in the center, coordinating to all six complex units (Scheme 1.51).



Scheme 1.51. Wheel-like europium terpyridine complex.<sup>[126]</sup>

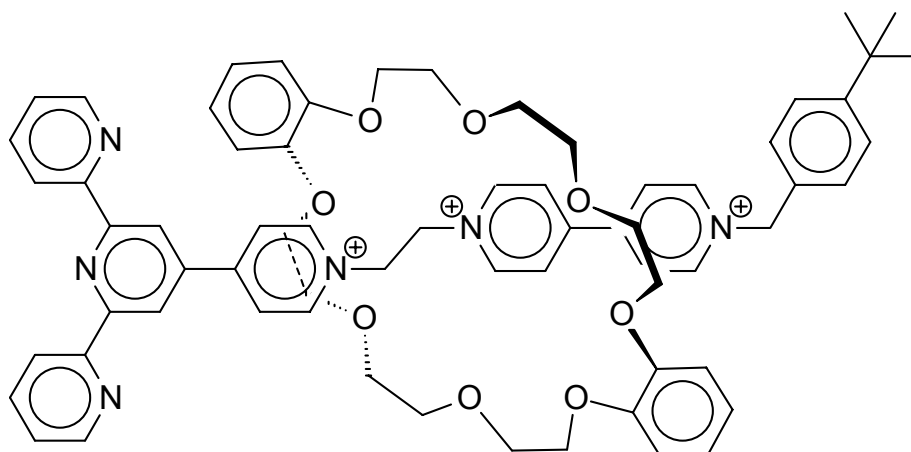
Large molecular squares have been obtained, which contained platinum or rhenium complexes in the corners and terpyridine complexes as bridging ligands (Scheme 1.52).<sup>[127, 128]</sup> Pyridyl terpyridine complexes of iron, ruthenium and osmium have been employed in a self-assembly reaction with  $\text{BrRe}(\text{CO})_5$  or  $(\text{dppf})\text{Pd}(\text{H}_2\text{O})_2(\text{OTf})_2$  (with  $\text{dppf} = 1,1'$ -*bis*(diphenylphosphino) ferrocene). These complexes act as corner-points and possess a square-planar coordination geometry, therefore leading to square-shaped structures. Multi-electron redox processes were observed in the assemblies, and fluorescence was detected for the osmium-containing compound but not for the others.

Rotaxanes of 4'-functionalized terpyridine are presented in a recent publication:<sup>[129]</sup> a cationic (dipyridinium)ethane system acts as an axle in a supramolecular system with crown ethers, which has been eventually locked by end-capping the axle with a bulky endgroup after the self-assembly process (Scheme 1.53).



Scheme 1.52. Multimetallic supramolecular squares.<sup>[127, 128]</sup>

Unsubstituted 24-crown-8 as well as the dibenzo- and dinaphthyl-analogues have been employed. Iron(II) complexes of all ligands have been prepared, showing a significant red-shift of the metal-ligand charge transfer absorption band for the complexes containing the crown ethers with the aromatic substituents. The crystal structure of the ligand revealed a  $\pi$ -interaction of the substituent of the crown ether with the terpyridine unit. This interaction causes a stabilization of the MLCT in the complex.

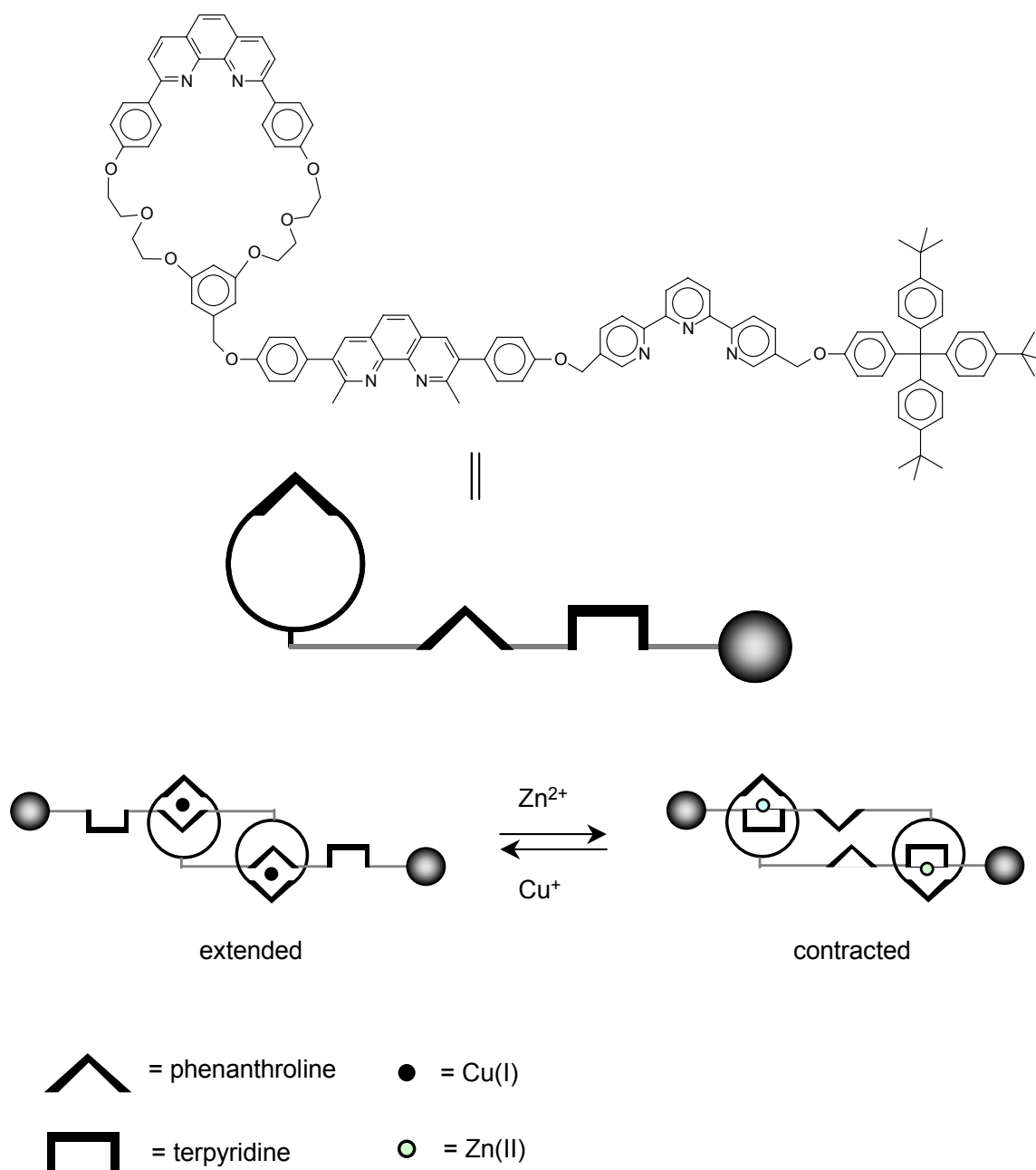


Scheme 1.53. Schematic representation of a terpyridine, consisting of a rotaxane assembly with a crown ether.<sup>[129]</sup>

An extended molecule consisting of a phenanthroline-moiety within a crown ether-like ring structure, connected to another phenanthroline which is bound to a terpyridine moiety (bearing a bulky endgroup in the 5"-position) in the 5-position has been prepared and subsequently self-assembled with copper(I) ions to form a linked *bis*-rotaxane.<sup>[130]</sup> After exchanging the metal ion to zinc, the coordination switched from a *tetracoordinated* to a *pentacoordinated* system, involving the terpyridine moiety (Scheme 1.54). The resulting reversible extension and contraction represents a first step towards novel applications such as artificial muscles or molecular machines.

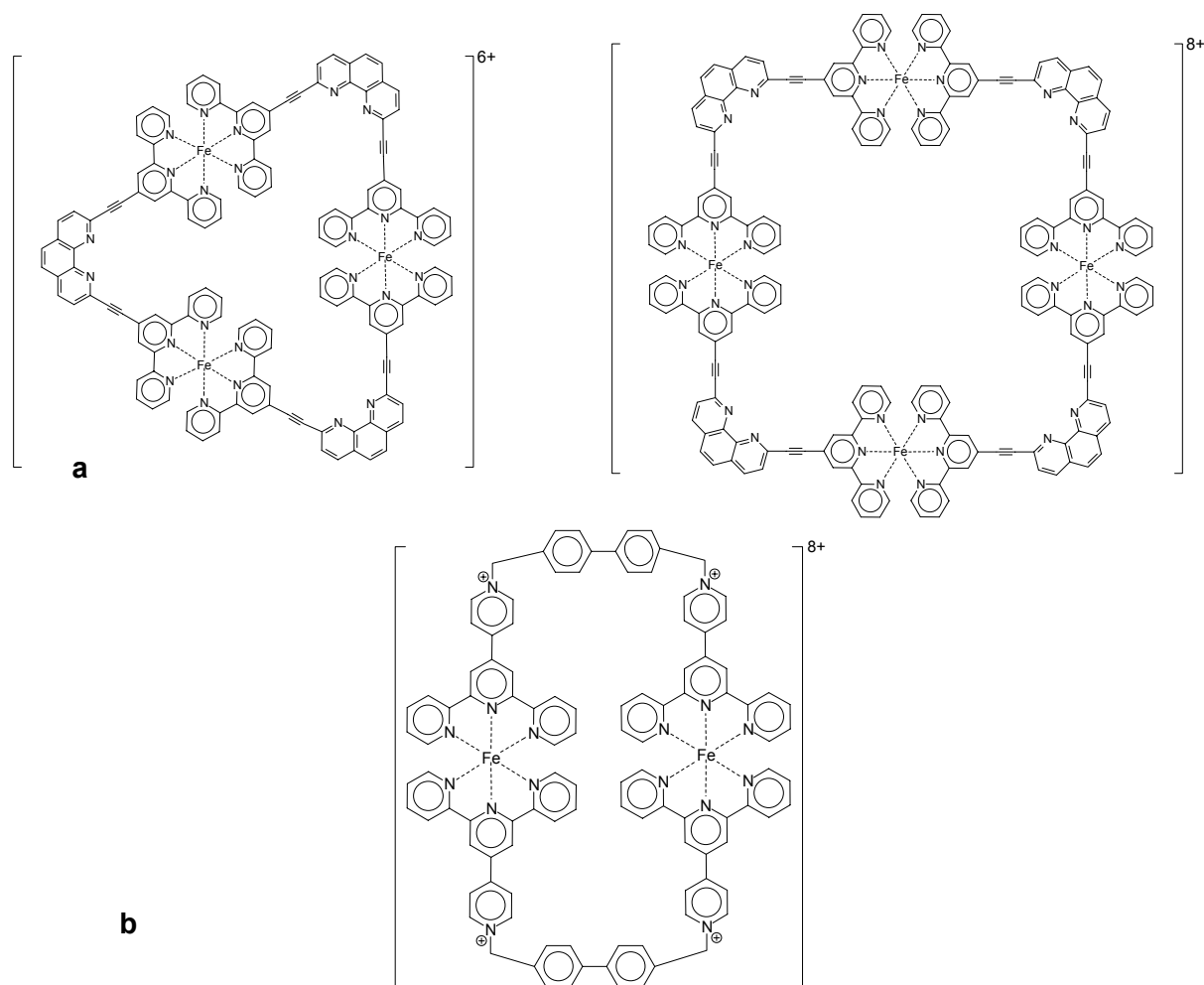
## 1.6 Cycles

*Bis*-terpyridines with suitable spacers are able to form ring structures by complexation with metal ions. Cycles based on rigid *bis*-terpyridines were the first reported examples. Whereas linear rigid systems form polymers, groups with an angle in the spacer group result in cyclic complexes. Due to the given geometry, the size of the rings is predetermined. Synthetically easily accessible linkers are the rigid ethynyl group, which was already reviewed by Ziesel (Scheme 1.55a).<sup>[30]</sup> The 60° angle of the two ethynyl-terpyridines, connected to the phenanthroline, favor a tricyclic structure, but also the less stable *tetracyclic* analogue was formed.



Scheme 1.54. "Molecular muscle" by redox-switchable terpyridine-phenanthroline complexes.<sup>[130]</sup>

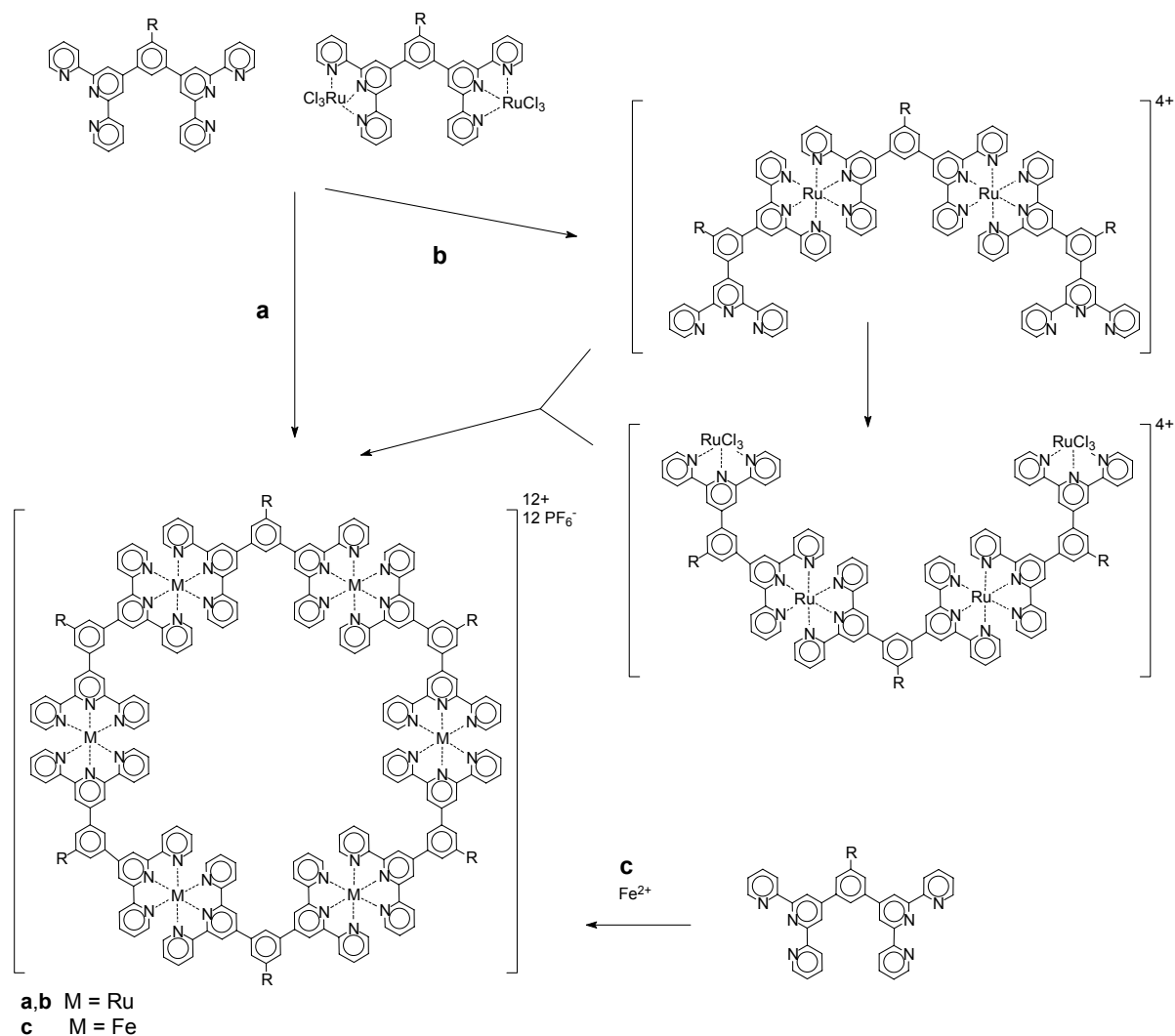




Scheme 1.55. Dimeric, trimeric and tetrameric cycles from rigid bis-terpyridines.<sup>[30, 131]</sup>

In another example, the synthesis of box-like cycles has been reported.<sup>[131]</sup> The *bis*-terpyridine ligand was obtained by alkylation of the pyridyl-*N*-atom of 4'-(4-pyridyl) terpyridine with 4,4'-*bis*-(bromomethyl)biphenyl. Complexation with iron(II) ions yielded a bicyclic compound as the main product (Scheme 1.55b).

An interesting cycle was presented by Newkome *et al.*<sup>[132]</sup> A *meta*-*bis*-terpyridyl phenyl ring was complexed with iron and ruthenium, leading to a hexameric cycle. This geometry is favored due to the 120° angle present in the ligand. Two approaches were used to obtain the ruthenium cycle (Scheme 1.56): in a self-assembly by reacting stoichiometric amounts of free ligand and of the ruthenium(III) *monocomplex* of the ligand (route a), the product was obtained. In the second approach (b), the macrocycle was constructed by a stepwise reaction via "half-rings" as intermediate. Moreover, an analogous cycle was prepared by adding iron(II) ions to the ligand, leading to exclusive formation of the hexameric cycle. Beside standard techniques and cyclic voltammetry, the existence of the macrocycles was also proven by TEM.



Scheme 1.56. Hexameric cycle by Newkome et al.<sup>[132]</sup>

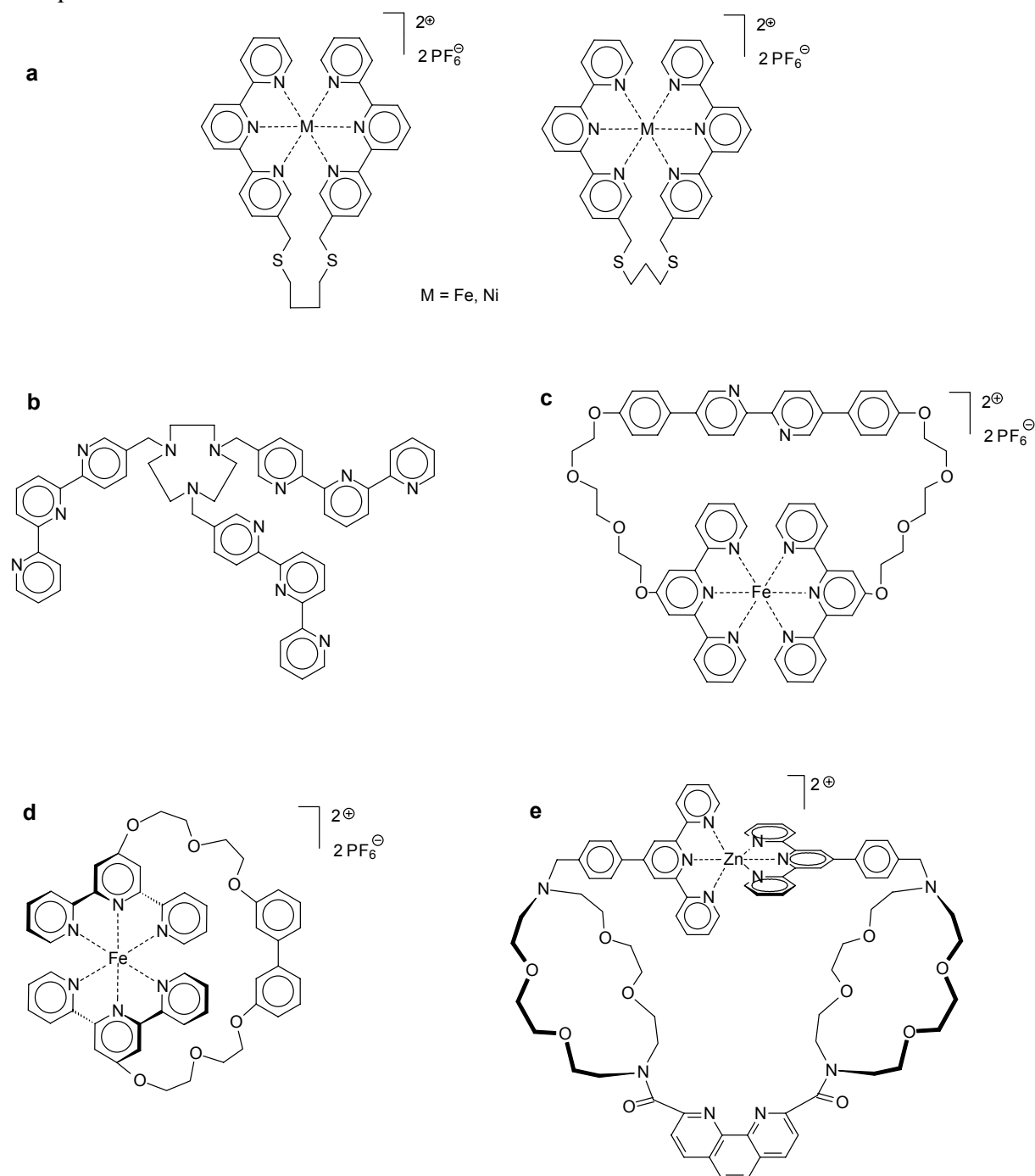
So far, most cycles were constructed from building blocks consisting of a rigid spacer, in which also the direction of complexation is predetermined by the angle within the spacer group. Therefore, cycles were obtained exclusively in well-defined sizes.

The formation of cyclic products from *bis*-terpyridines linked by flexible spacers is much more challenging, because these telechelics allow the formation of differently-sized rings as well as polymeric compounds. Despite these difficulties, different flexible groups have been employed in the synthesis of rings. Due to the flexibility, a mixture of various rings and coordination polymers were obtained in most cases. Therefore, low concentrations had to be applied in order to push the ring-chain-equilibrium to the side of ring formation. Furthermore, purification of the product by column chromatography mixture is necessary.

*Monocycles* can only be formed if the spacer possesses sufficient flexibility and an appropriate length. In the following example from the group of Moore, the terpyridines are linked in the 5-position by a 1,3-*bis*(2,2':6',2''-terpyridyl-5-ylmethylsulfanyl)propane and a 1,4-*bis*(2,2':6',2''-terpyridyl-5-ylmethylsulfanyl)butane spacer, each of which are 7 or 8 atoms long.<sup>[133]</sup> This length was predicted to be optimal by molecular modeling. The addition of Fe(II) or Ni(II)-ions resulted indeed in an intramolecular cyclization, which was verified by

X-ray structure analysis (Scheme 1.57a). When adding the free ligand to a solution of an iron(II) complex of unfunctionalized terpyridine, a ligand exchange was observed, leading to the cyclic complex. This behavior can be explained by the chelate effect.

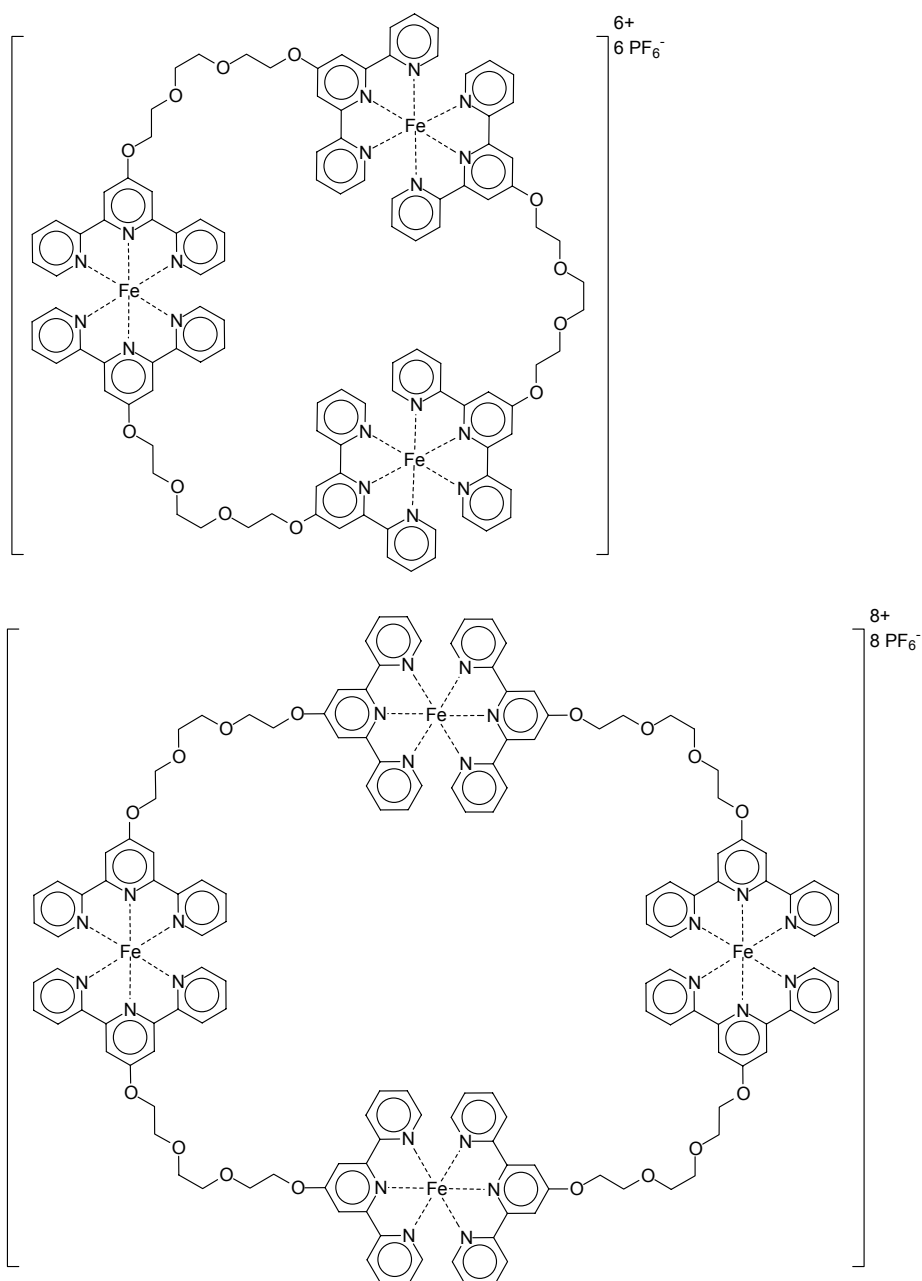
In the same manner, three terpyridine moieties could be connected to a cyclic triamine (Scheme 1.57b).<sup>[134]</sup> Complexation of this ligand to europium(III) led to a room-temperature luminescent bicyclic complex involving all terpyridine groups. In all of these cases, the terpyridines are connected in the 5-position. Due to this fact, the connecting points of the resulting complex are in close proximity, therefore even short spacers allow a successful complexation.



Scheme 1.57. Monocycles of 5- and 4'-linked bis-terpyridines.<sup>[133-136]</sup>

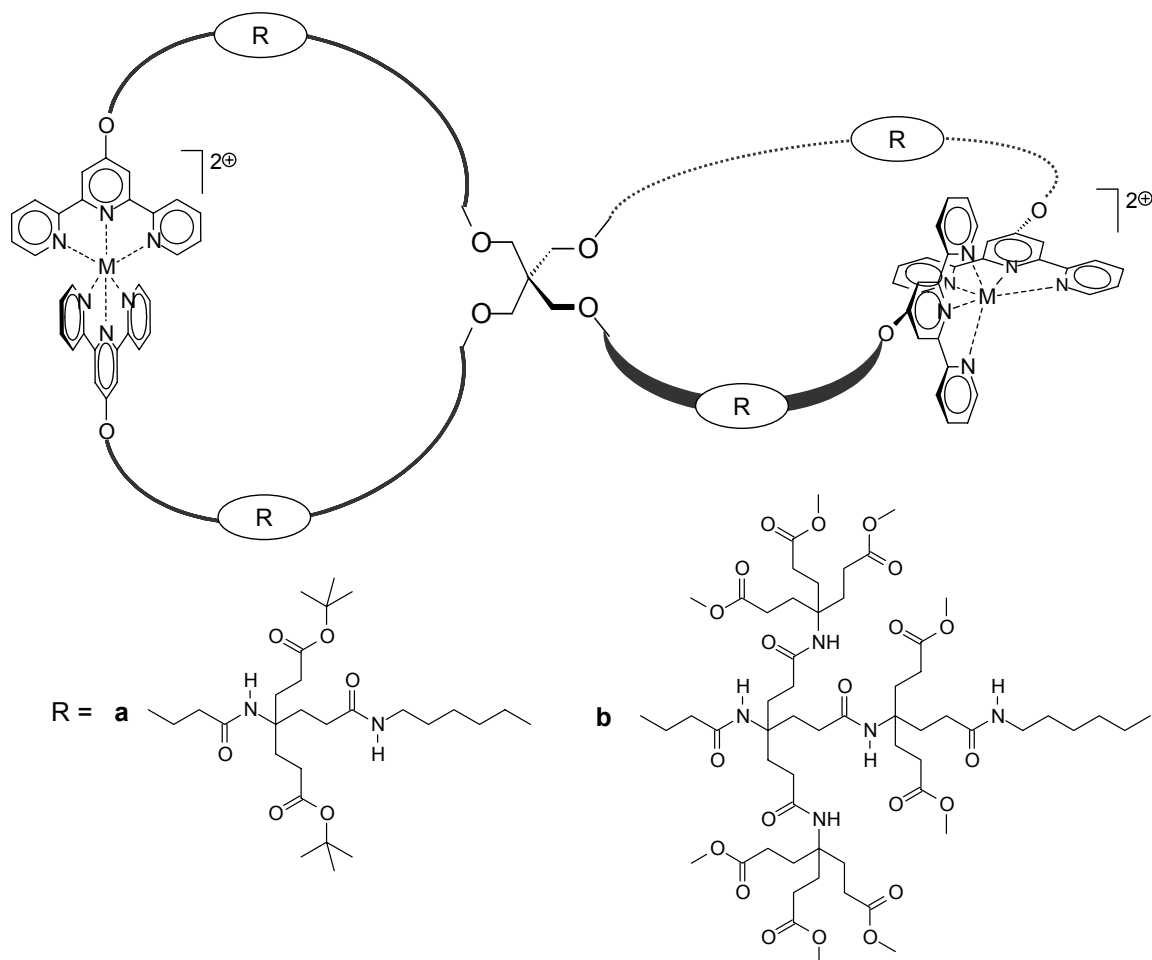
4'-Functionalized terpyridines, where the functionalities are on the opposite faces of the complex, require much longer spacers or a special geometry. The system shown in Scheme 1.57c, where the terpyridine-moieties are linked via tri(ethylene glycol) spacers to a rigid 5,5'-*bisphenyl* bipyridine domain, has been synthesized in the group of Constable.<sup>[135]</sup> Flexible chains are protruding in 120° angles from the rod-like central unit, thus the terpyridine groups are able to embrace the metal ions, allowing the formation of *monocycles*. This was confirmed by X-ray crystal structure analysis. The bipyridine unit is accessible for further complexation in order to construct extended supramolecular systems. In continuing experiments a *monocycle*, containing a 2,7-(diethylene glycol)-naphthalene linker, has been prepared (Scheme 1.57d). The "handle" is conformationally locked in the cleft between the terpyridine moieties, resulting in a chiral structure.<sup>[137]</sup> Another unimolecular ring structure was obtained from a multifunctional ligand (Scheme 1.57e): an extended polytopic ligand, containing two terpyridine moieties that were linked *via* crown ether moieties to a central phenanthroline unit, was complexed to Zn(II) ions to form a *monocyclic* complex.<sup>[136]</sup> In a different experiment, the terpyridine endgroups were complexed to bipyridine-ruthenium(II) fragments.

A recent result reported by Constable *et al.* describes the synthesis of cycles of different sizes.<sup>[138]</sup> The terpyridines were linked by flexible triethylene glycol chains in the 4'-position. This geometry does not allow the formation of *monocycles*, because the linker is too short. Therefore *tris*- and *tetracycles* were obtained besides some polymeric material (Scheme 1.58). To minimize the amount of polymeric product, the concentration was kept low (0.4 M), and the products were isolated by column chromatography. The composition of the products was analyzed by ESI-MS, furthermore a shift of the <sup>1</sup>H-NMR signals of the terpyridine protons compared to the polymer was found, which was attributed to the different chemical environment of the aromatic protons in the rings. Similar cycles, in this case with hexyl-spacers linking the terpyridine moieties, have been prepared recently.<sup>[139]</sup> A *tris*- and a *tetracycle* could be isolated and identified by MALDI-TOF mass spectrometry.



*Scheme 1.58. Flexible oligocycles by Constable.*<sup>[138]</sup>

The first examples of metallodendritic spiranes (spiro-metallodendrimers) were obtained in the group of Newkome<sup>[140]</sup> via incorporation of four terpyridine units within each dendritic quadrant of dendrimers with a pentaerythrol core (Scheme 1.59). These moieties were subsequently complexed to iron(II) and ruthenium(II) ions, leading to intramolecular cyclization of the spiro type.



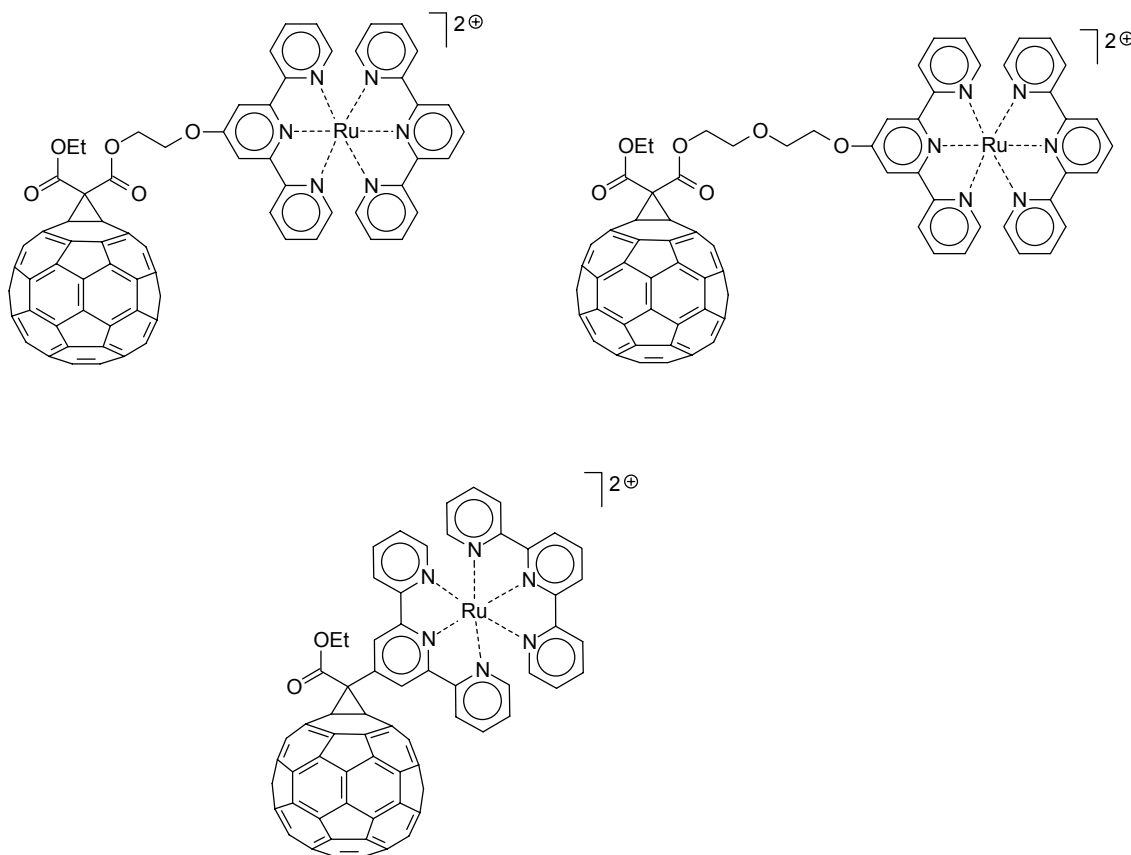
Scheme 1.59. Dendritic spirocycle.<sup>[140]</sup>

## 1.7 Fullerene terpyridine complexes

Fullerenes are of special interest in contemporary chemistry due to their photophysical and electrochemical properties, which make them interesting in the context of the development of novel molecular electronics or light harvesting devices and may eventually lead to potential applications such as organic solar cells. Most of the current research into these particular kinds of solar cells includes fullerenes due to their electron-accepting properties.

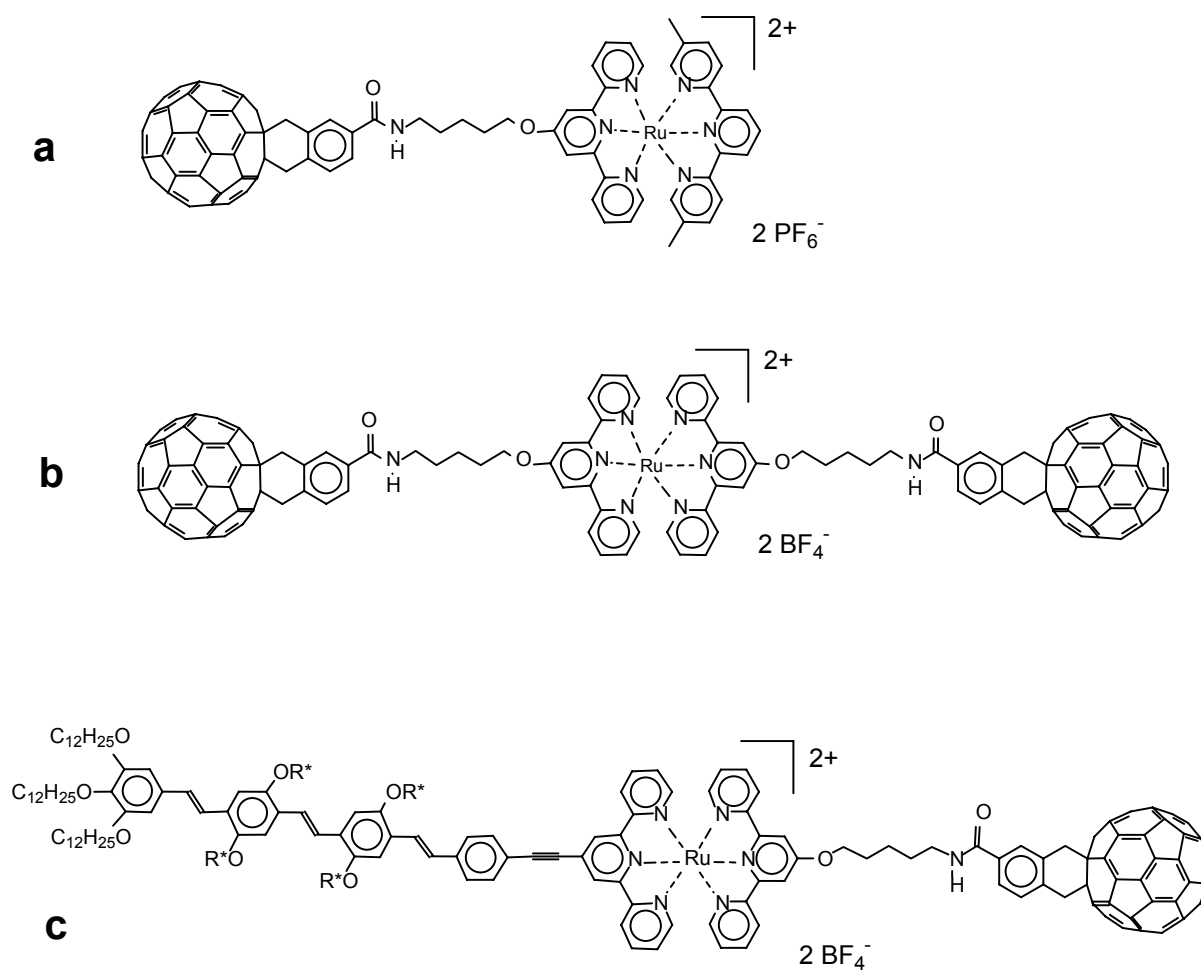
One approach has been the combination of fullerenes with terpyridine ruthenium(II) complexes. The pioneering work in the field was performed in the group of Constable.<sup>[141, 142]</sup> Terpyridines, bearing a malonate ester group linked by *oligo*(ethylene glycol)s were prepared in two-step reactions (Scheme 1.60). A Bingel reaction of brominated malonates with C<sub>60</sub> (loss of the bromine and addition to an unsaturated fullerene bond) led to the fullereno-terpyridines. In another reaction, the terpyridine was directly attached to the fullerene by adding a brominated terpyridinyl acetic acid ethyl ester under Bingel conditions to C<sub>60</sub>. The functional ligands were subsequently converted to the corresponding Ru(II)-complexes by ruthenium(III)/(II) chemistry. In the case of the compound where the units are spatially close,

a strong interaction between the fullerene and the terpyridine complex was found by cyclic voltammetry.



*Scheme 1.60. Fullerenes, containing terpyridine complexes, linked by spacers of various length.*<sup>[141, 142]</sup>

The approach was continued in the group of Schubert.<sup>[143]</sup> A functionalized fullerene (obtained in several steps including a Diels-Alder reaction) that contains an acid chloride has been reacted with an aminoterpyridine, resulting in a terpyridinyl-fullerene, linked by an alkyl group. AB-dyads and ABA triads were prepared by complexing the ligand to a terpyridine Ru(III) *mono*-complex or a second equivalent of the functional ligand and RuCl<sub>3</sub> (Scheme 1.61a-b).

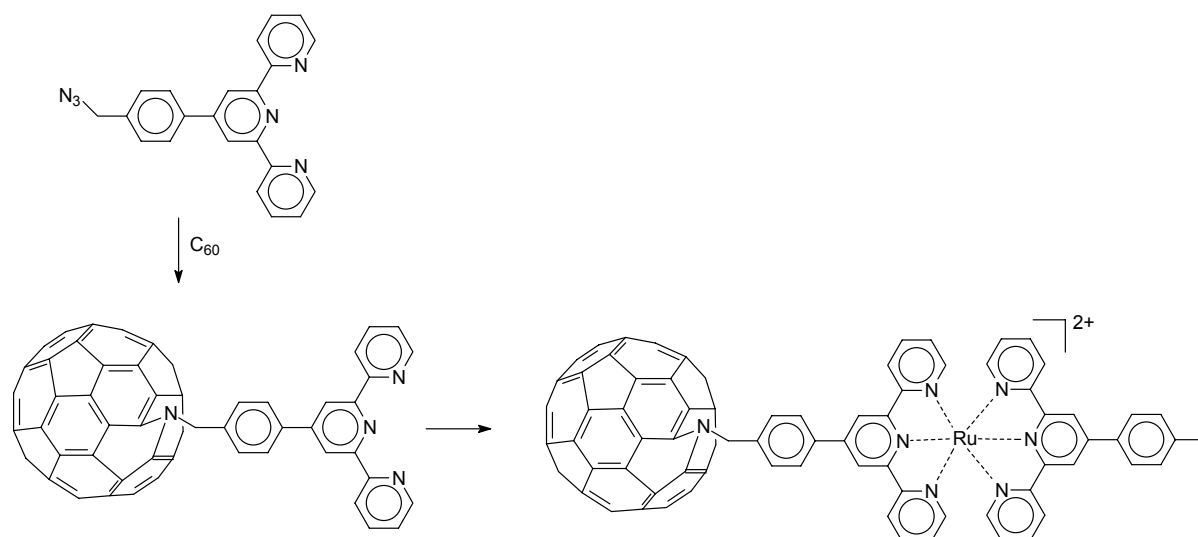


Scheme 1.61. Fullerene-terpyridine ruthenium(II) dyads and triads.<sup>[65, 143]</sup>

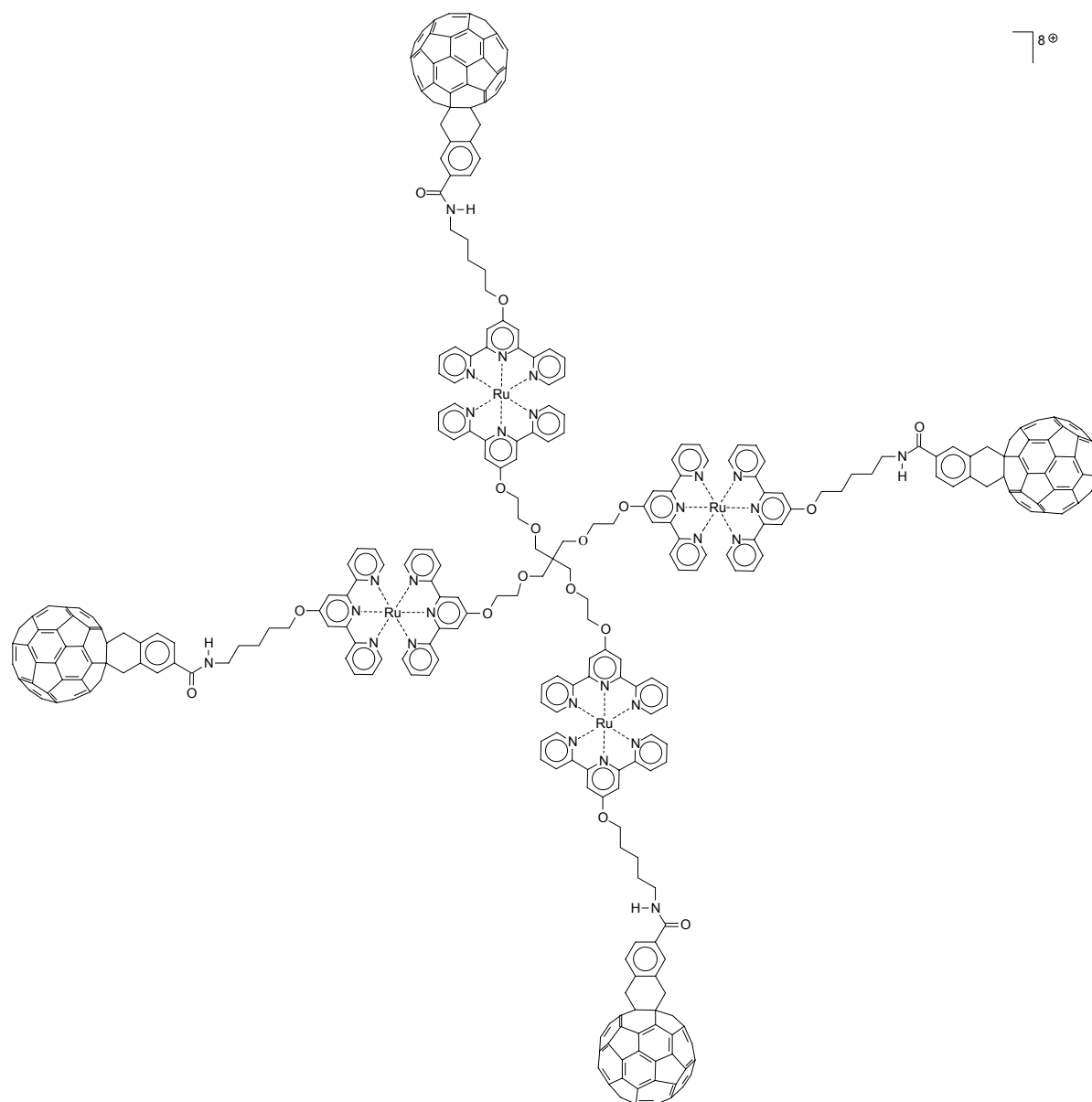
Another molecular moiety that has been studied intensively in the context of organic solar cells, is the highly luminescent and electron-donating *oligo(p-phenylene vinylene)* (OPV), that has already been covalently linked to fullerenes. Recently, the combination of these two units has been achieved *via* the formation of a terpyridine ruthenium(II) complex, leading to an ABC-triad (Scheme 1.61c).<sup>[65]</sup> Photoinduced absorption experiments revealed a lifetime of the charge-separated state of less than 100  $\mu$ s. Energy transfer from the OPV to the fullerene resulted in the quenching of the OPV luminescence.

In the group of Li, tolyl-terpyridine has been converted to an azide.<sup>[144]</sup> The cycloaddition reaction of this intermediate to the fullerene resulted in a ring-opening of the fullerene cage (1.6-aza-bridged, Scheme 1.62). Subsequent complexation with tolyl-terpyridine-ruthenium led to the fullerene-ruthenium complex dyad. In the group of Schubert, even a *tetra*fullerene adduct was successfully prepared. A *tetraterpyridine*, based on pentaerythrol, was reacted with the terpyridine-containing fullerene derivative (Scheme 1.63). The result is a star-shaped complex with buckyballs in the periphery.<sup>[145]</sup>





Scheme 1.62. Coupling of an azide-functionalized terpyridine to a fullerene.<sup>[144]</sup>

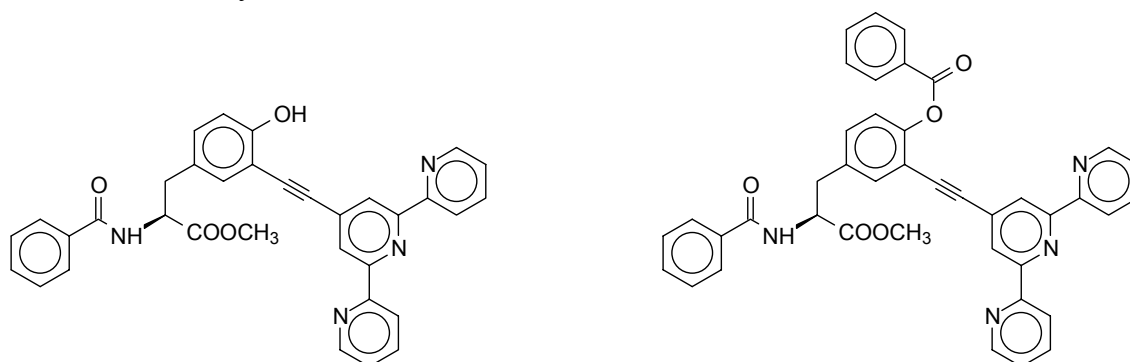


Scheme 1.63. Star-shaped tetrafullerene complex array.<sup>[145]</sup>

## 1.8 Complexes containing biochemical groups

An interesting approach is the combination of terpyridine-complex chromophores with biomolecules, which could act as luminescent labels for biological processes. Furthermore, the ability of electron transfer could help to study electron transfer processes in biological systems.

Ziessel *et al.* reported the synthesis of a terpyridine, containing an L-tyrosine group (Scheme 1.64) and the subsequent formation of the corresponding ruthenium(II) complexes.<sup>[146]</sup> This combination was chosen for future studies of "Photosystem II" (where water is oxidized to oxygen), a large membrane bounded protein system. It could also help to construct artificial water oxidation catalysts.

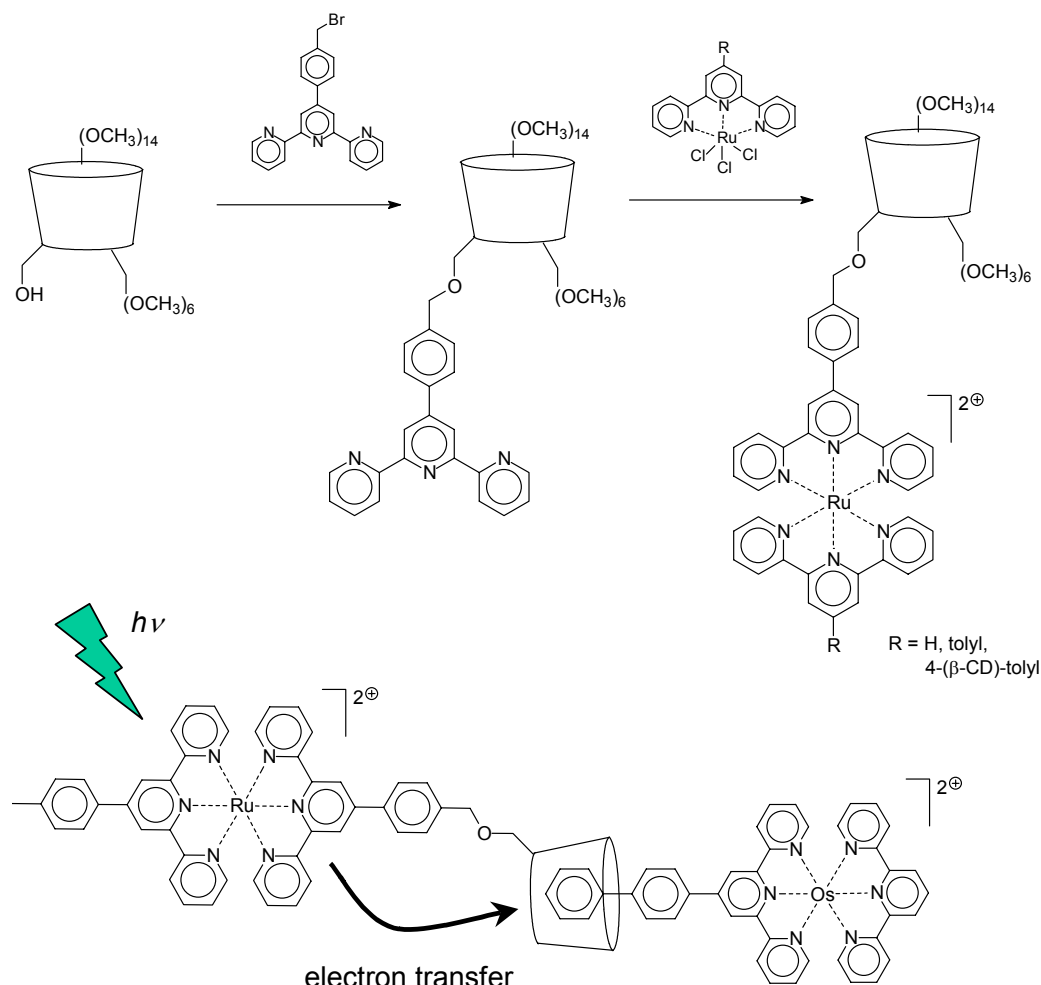


Scheme 1.64. Terpyridine, bearing an L-tyrosine group.<sup>[146]</sup>

An ethynyl group was chosen as linker and the palladium-catalyzed coupling of the iodide of the tyrosine group with the 4'-triflyl-terpyridine. Besides a compound containing a free phenolic group, also a complex, bearing a protected group was prepared.

While a solution of the unprotected complex in acetonitrile shows luminescence even at room temperature, it is quenched in a  $K_2CO_3$ -containing DMF solution, indicating an electron transfer from the phenolic group of the tyrosine moiety in basic conditions by photoexcitation, followed by back-electron transfer. In the protected compound, the phenol is blocked, therefore no electron transfer is possible and as a result, fluorescence was observed.

Cyclodextrin cups were employed to build supramolecular systems, consisting of a 4'-tolylterpyridine ruthenium complex and a guest-binding moiety (Scheme 1.65).<sup>[147]</sup> All but one of the methyl groups of the cyclodextrin were protected before attachment of the terpyridine fragment (4'-*p*-(bromomethyl)phenyl-terpyridine) by a Williamson type ether coupling.



Scheme 1.65. Cyclodextrin-functionalized terpyridine complexes and binding of a metallo-guest.<sup>[147, 148]</sup>

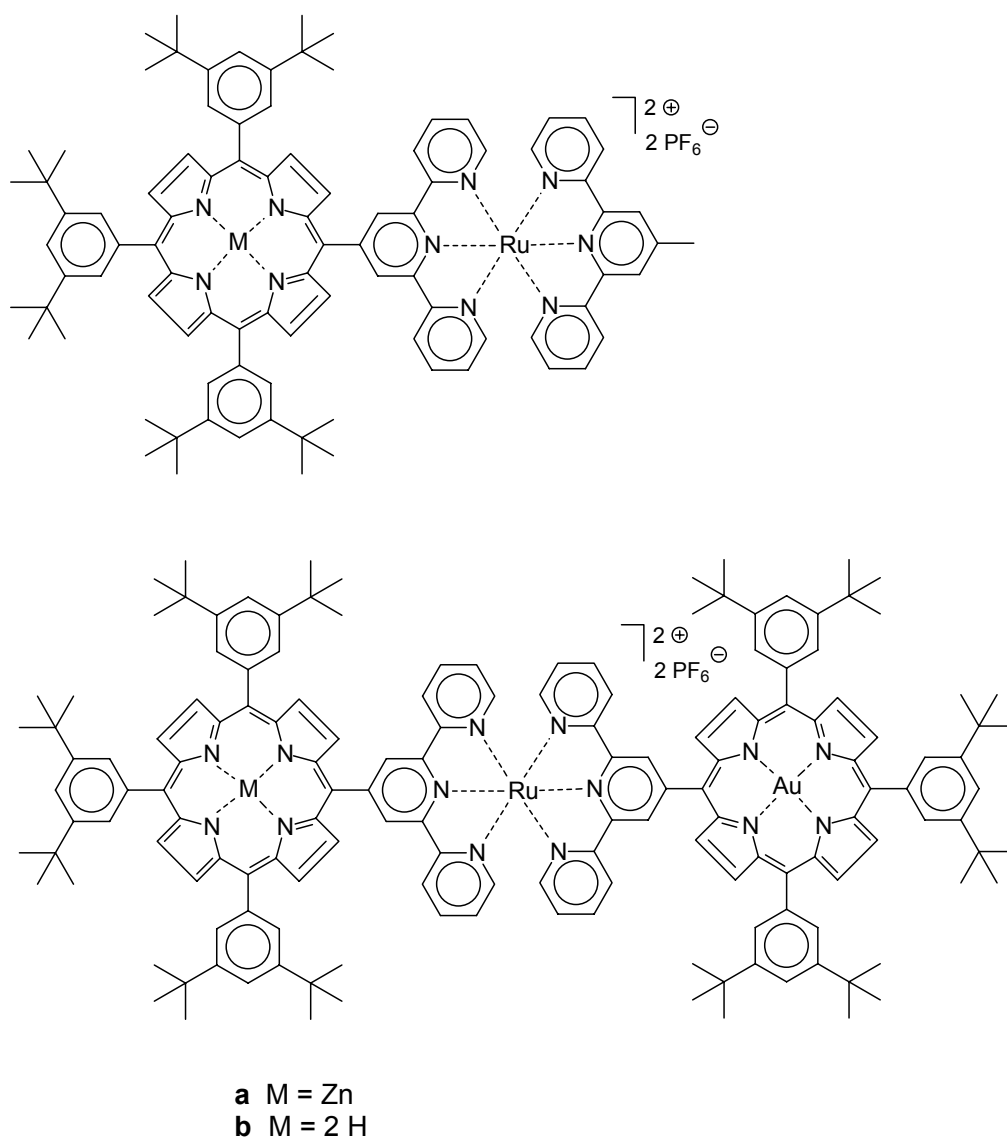
This functional ligand was subsequently complexed with terpyridine ruthenium(III) trichloride and 4'-*p*-tolyl-terpyridine ruthenium(III) trichloride, respectively, with the latter known to be room-temperature fluorescent. The final product may act as an optical sensor for the hydrophobic binding of guests to the cyclodextrin, as shown for the addition of anthraquinone-2-carboxylic acid: a quenching of the fluorescence was observed, caused by an intermolecular electron transfer from the ruthenium complex to the quinone.

In further studies (also including a *bis*(cyclodextrin) complex), different quinone guests were used, leading to a fluorescence quenching of different intensities, depending on the kind of quinone.<sup>[148]</sup> In another experiment, a biphenylterpyridine-terpyridine-osmium(II) complex (biphenyl-group as guest) was added to the host system. In the resulting Ru-Os system, an electron transfer from ruthenium to osmium could be observed after oxidation of the osmium center. However, a Ru(II)-Os(II) energy transfer was not detected due to the short lifetime of the ruthenium emission (in accordance with covalent dyads, linked by saturated spacers).

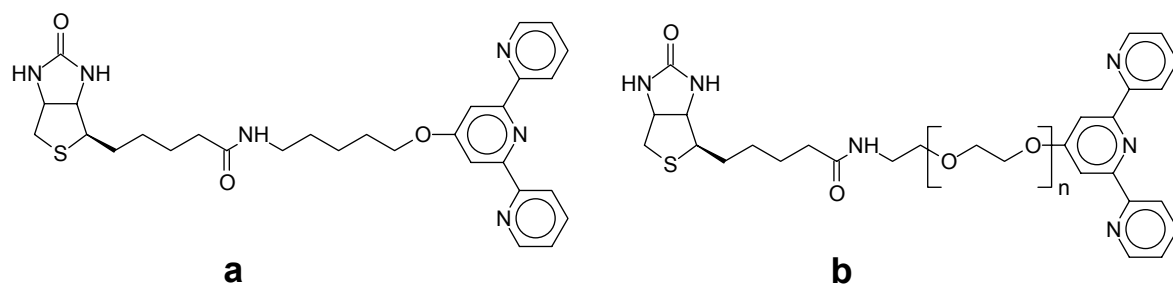
The novelty of this host-guest system, compared to the ones previously described (dyads), is that both donor and acceptor are being brought together spatially *via* non-covalent interactions.

A variety of porphyrin-ruthenium complex conjugates, AB dyads, ABA and ABC triads were constructed by Flamigni *et al.*, the ruthenium-based component being a strong electron and energy acceptor.<sup>[149-152]</sup> The porphyrin site has been studied when both uncomplexed as well as complexed to either zinc(II) or gold(II) ions (Scheme 1.66). A photoinduced two-step electron and energy transfer could be observed. The singlet excited state porphyrin is first quenched by the ruthenium component, leading to a ruthenium complex localized triplet excited state (<sup>3</sup>MLCT) which, in turn, transfers its triplet energy back to the porphyrin unit attached to it so as to generate the porphyrin triplet excited state.

Another approach in combining biochemistry with terpyridine supramolecular chemistry is the coupling of biotin to a 4'-aminoterpyridine, applying the well-known isocyanate coupling reaction.<sup>[153]</sup> Besides a short alkyl-spacer, a polymeric poly(ethylene glycol) chain has also been introduced (Scheme 1.67). Biotin is known to bind strongly to the protein avidine via multiple hydrogen bonding, with a geometry comparable to a "key and lock" system.



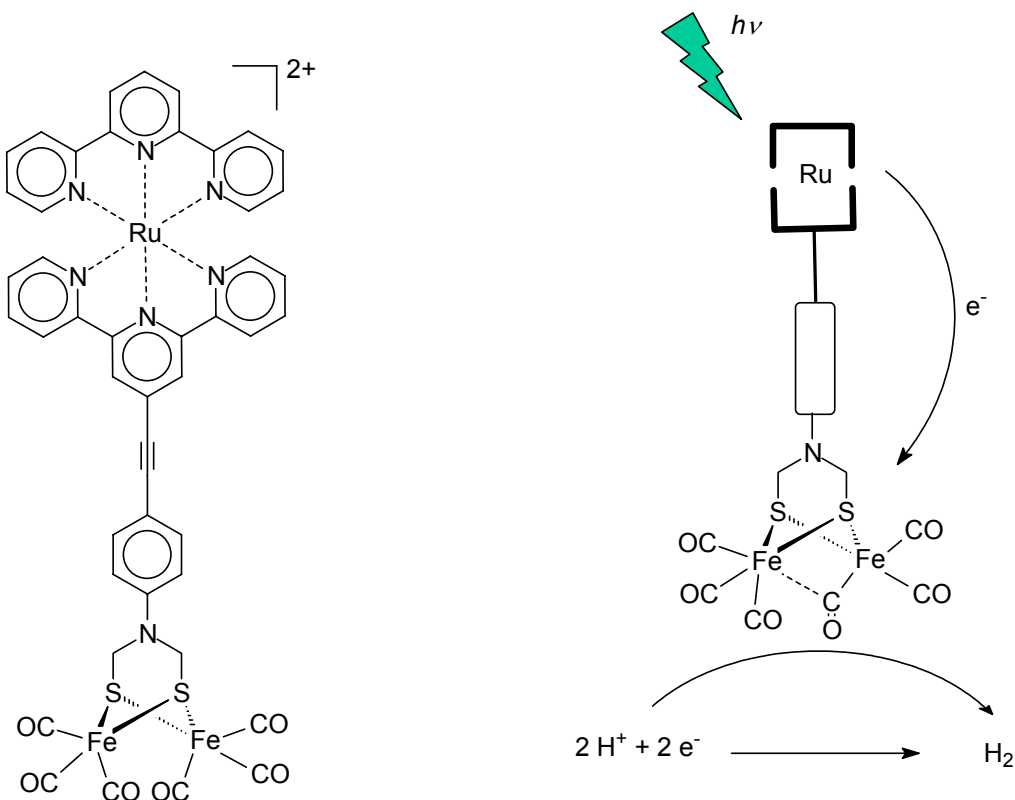
Scheme 1.66. Porphyrin terpyridine complexes.<sup>[149-152]</sup>



Scheme 1.67. Biotin-functionalized terpyridine ligands.<sup>[153]</sup>

In a recent publication, a dinuclear iron carbonyl complex was attached to a terpyridine ruthenium complex, mimicking the active site of iron-hydrogenase (Scheme 1.68).<sup>[154]</sup> Irradiation of the complex resulted in an electron transfer, which could be utilized to produce hydrogen.

Another recent contribution describes the connection of DNA-fragments to terpyridine complexes.<sup>[155]</sup> Two complementary DNA sequences (20 base pairs) were connected via a tri(ethylene glycol) to a terpyridine moiety, respectively, and subsequently the corresponding symmetric ruthenium(II) complexes were prepared. The mixing of these two complexes resulted in long linear arrays through self-assembly, where the length could be adjusted by the molar ratios of the ligands in the mixture.



Scheme 1.68. Terpyridine-ruthenium iron carbonyl dyad.<sup>[154]</sup>

## 1.9 Conclusions

In conclusion, terpyridine is one of the most suitable ligands for the construction of supramolecular systems through metal coordination due to the relative strong and directed metal bonding. Extended architectures can be obtained by directed reaction as well as self-assembly. Among the advantages of such complexes is the reversibility, which makes the terpyridine-containing compounds interesting in materials research and for the introduction into polymers. Finally, the electronic and optical properties, especially of ruthenium(II) and osmium(II), are of importance for potential applications such as solar cells and nano-devices because they allow the exploitation of the "light-harvesting properties" of the complexes through energy and electron transfer processes as well as through their inherent switchability.

## 1.10 Aim and scope of this thesis

The introduction of terpyridines into polymeric systems has grown to a visible field in modern macromolecular research. Different terpyridine-containing oligomeric and polymeric building blocks are easily synthesized and can be used for the construction of various architectures. The aim of this thesis was the preparation of new metallo-supramolecular architectures, ranging from linear coordination polymers and grafted architectures to cross-linked systems. In **chapter 1** the field of defined terpyridine-metal complexes has been reviewed with a special emphasis on architectures and properties.

**Chapter 2** describes a new convenient synthetic strategy for the preparation of 4'-functionalized terpyridine ligands, starting from pyridone. Subsequently, various functionalized terpyridine ligands have been converted into asymmetric ruthenium complexes as model compounds for supramolecular architectures, including complexes bearing chiral side chains. Finally, the approach of asymmetric chelate complexes was extended to mixed bipyridine-terpyridine-copper(II) systems.

Linear coordination polymers are presented in **chapter 3**. *Oligo-* and polymeric *bis-*terpyridine telechelics were complexed with ruthenium(II) ions, resulting in novel metallopolymers. One coordination polymer, constructed from poly(ethylene glycol)<sub>180</sub>-units, was investigated in more detail. Viscometry revealed the presence of high-molecular-weight polymers with a pronounced polyelectrolyte behavior. Moreover, thermogravimetric and rheological investigations were carried out. In addition, coordination polymers with alternating terpyridine complexes and quadruple hydrogen-bonding units were prepared and investigated for the first time.

Using the thus obtained knowledge of the directed synthesis of asymmetric ruthenium complexes, metallo-supramolecular graft copolymers were prepared, which are described in **chapter 4**. Among the examples is an amphiphilic, micelle-forming system, which was investigated using atomic force microscopy, TEM and dynamic light scattering.

In **chapter 5**, supramolecular cross-linking of terpyridine-containing copolymers is discussed. Initially, the viscosity of dilute solutions was investigated. Subsequently, higher concentrations were studied, where gel-formation occurred. Finally, supramolecular cross-linking was successfully combined with covalent cross-linking, which represents a new approach towards two-step curing in "smart coatings" and other applications.

## 1.11 References

- [1] J.-M. Lehn, *Supramolecular Chemistry, Concepts and Perspectives*, **1995**.
- [2] D. Philp, F. J. Stoddart, *Angew. Chem.* **1996**, *108*, 1242-1284; *Angew. Chem. Int. Ed.* **1996**, *35*, 1154-1196.
- [3] J. Darnell, H. Lodish, B. Baltimore, *Molecular Cell Biology*, Scientific American Books, New York, **1990**.
- [4] U. S. Schubert, in *Tailored Polymers & Applications* (Eds.: M. K. M. Y. Yagci, O. Nuyken, K. Ito, G. Wnek), VSP Publishers, Utrecht, **2000**, pp. 63-85.
- [5] V. Balzani, A. Credi, F. M. Raymo, J. F. Stoddart, *Angew. Chem.* **2000**, *112*, 3484-3530; *Angew. Chem. Int. Ed.* **2000**, *39*, 3348-3391.
- [6] U. S. Schubert, C. Eschbaumer, *Angew. Chem.* **2002**, *114*, 3016-3050; *Angew. Chem. Int. Ed.* **2002**, *41*, 2892-2926.
- [7] L. Brunsveld, B. J. B. Folmer, E. W. Meijer, R. P. Sijbesma, *Chem. Rev.* **2001**, *101*, 4071-4097.
- [8] G. Cooke, V. M. Rotello, *Chem. Soc. Rev.* **2002**, *31*, 275-286.
- [9] F. Ilhan, M. Gray, V. M. Rotello, *Macromolecules* **2001**, *34*, 2597-2601.
- [10] L. R. Rieth, R. F. Eaton, G. W. Coates, *Angew. Chem.* **2001**, *113*, 2211-2214; *Angew. Chem. Int. Ed.* **2001**, *40*, 2153-2156.
- [11] R. P. Sijbesma, F. H. Beijer, L. Brunsveld, B. J. Folmer, J. H. Hirschberg, R. F. Lange, J. K. Lowe, E. W. Meijer, *Science* **1997**, *278*, 1601-1604.
- [12] K. Yamauchi, J. R. Lizotte, D. M. Hercules, M. J. Vergne, T. E. Long, *J. Am. Chem. Soc.* **2002**, *124*, 8599-8604.
- [13] K. Yamauchi, J. R. Lizotte, T. E. Long, *Macromolecules* **2003**, *36*, 1083-1088.
- [14] G. R. Newkome, A. K. Patri, E. Holder, U. S. Schubert, *Eur. J. Org. Chem.* **2003**, in press (available online DOI: 10.1002/ejoc.200300399).
- [15] G. T. Morgan, F. H. Burstall, *J. Chem. Soc., Abstr.* **1932**, 20-30.
- [16] J. P. Sauvage, J. P. Collin, J. C. Chambron, S. Guillerez, C. Coudret, V. Balzani, F. Barigelletti, L. De Cola, L. Flamigni, *Chem. Rev.* **1994**, *94*, 993-1019.
- [17] E. C. Constable, M. W. C. Thompson, *New J. Chem.* **1992**, *16*, 855-876.
- [18] K. Lashgari, M. Kritikos, R. Norrestam, T. Norrby, *Acta Cryst. C* **1999**, *C55*, 64-67.
- [19] M. Heller, U. S. Schubert, *Eur. J. Org. Chem.* **2003**, 947-961.
- [20] R.-A. Fallahpour, *Synthesis* **2003**, 155-184.
- [21] U. S. Schubert, C. Eschbaumer, O. Hien, P. R. Andres, *Tetrahedr. Lett.* **2001**, *42*, 4705-4707.
- [22] G. R. Newkome, E. He, *J. Mater. Chem.* **1997**, *7*, 1237-1244.
- [23] R.-A. Fallahpour, *Synthesis* **2003**, 155-184.
- [24] D. Armspach, E. C. Constable, C. E. Housecroft, M. Neuburger, M. Zehnder, *J. Organomet. Chem.* **1998**, *550*, 193-206.

- [25] X. Liu, E. J. L. McInnes, C. A. Kilner, M. Thornton-Pett, M. A. Halcrow, *Polyhedr.* **2001**, *20*, 2889-2900.
- [26] P. R. Andres, H. Hofmeier, B. G. G. Lohmeijer, U. S. Schubert, *Synthesis* **2003**, 2865-2871.
- [27] U. S. Schubert, S. Schmatloch, A. A. Precup, *Design. Monom. Polym.* **2002**, *5*, 211-221.
- [28] E. C. Constable, M. D. Ward, *J. Chem. Soc., Dalton Trans.* **1990**, 1405-1409.
- [29] E. C. Constable, J. Lewis, M. C. Liptrot, P. R. Raithby, *Inorg. Chim. Acta.* **1990**, *178*, 47-54.
- [30] R. Ziessel, *Synthesis* **1999**, *11*, 1839-1865.
- [31] M. Maestri, N. Armaroli, V. Balzani, E. C. Constable, A. M. W. C. Thompson, *Inorg. Chem.* **1995**, *34*, 2759-2767.
- [32] M. Beley, J. P. Collin, R. Louis, B. Metz, J. P. Sauvage, *J. Am. Chem. Soc.* **1991**, *113*, 8521-8522.
- [33] M. Ziegler, V. Monney, H. Stoeckli-Evans, A. von Zelewsky, I. Sasaki, G. Dupic, J.-C. Daran, G. G. A. Balavoine, *J. Chem. Soc., Dalton Trans.* **1999**, 667-676.
- [34] V. Grosshenny, R. Ziessel, *J. Organomet. Chem.* **1993**, *453*, C19-C22.
- [35] D. L. Greene, D. M. P. Mingos, *Transition Met. Chem.* **1991**, *16*, 71-72.
- [36] S. Kelch, M. Rehahn, *Macromolecules* **1997**, *30*, 6185-6193.
- [37] S. Pyo, E. Pérez-Cordero, S. G. Bott, L. Echegoyen, *Inorg. Chem.* **1999**, *38*, 3337-3343.
- [38] A. Islam, N. Ikeda, K. Nozaki, Y. Okamoto, B. Gholamkhash, A. Yoshimura, T. Ohno, *Coord. Chem. Rev.* **1998**, *171*, 355-363.
- [39] M. L. Stone, G. A. Crosby, *Chem. Phys. Lett.* **1981**, *79*, 169-173.
- [40] U. S. Schubert, C. Eschbaumer, P. Andres, H. Hofmeier, C. H. Weidl, E. Herdtweck, E. Dulkeith, A. Morteani, N. E. Hecker, J. Feldmann, *Synth. Met.* **2001**, *121*, 1249-1252.
- [41] D. M. Klassen, G. A. Crosby, *J. Chem. Phys.* **1968**, *48*, 1853-1858.
- [42] A. A. Bhuiyan, J. R. Kincaid, *Inorg. Chem.* **1998**, *37*, 2525-2530.
- [43] M. Grätzel, *Prog. Photovolt. Res. Appl.* **2000**, *8*, 171-185.
- [44] J. Husson, M. Beley, G. Kirsch, *Tetrahedr. Lett.* **2003**, *44*, 1767-1770.
- [45] C. Mikel, P. G. Potvin, *Polyhedron* **2002**, *21*, 49-54.
- [46] M. Beley, C. A. Bignozzi, G. Kirsch, M. Alebbi, J. C. Raboin, *Inorg. Chim. Acta* **2001**, *318*, 197-200.
- [47] C. J. Aspley, J. A. G. Williams, *New. J. Chem.* **2001**, *25*, 1136-1147.
- [48] E. C. Constable, A. M. W. C. Thompson, N. Armaroli, V. Balzani, M. Maestri, *Polyhedr.* **1992**, *11*, 2707-2709.
- [49] K. T. Potts, M. J. Cipullo, P. Ralli, G. Theodoridis, *J. Org. Chem.* **1982**, *47*, 3027-3038.
- [50] P. Lainé, F. Bedioui, P. Ochsenbein, V. Marvaud, M. Bonin, E. Amouyal, *J. Am. Chem. Soc.* **2002**, *124*, 1364-1377.
- [51] P. Laine, F. Bedioui, E. Amouyal, V. Albin, F. Berruyer-Penaud, *Chem. Eur. J.* **2002**, *8*, 3162-3176.
- [52] E. Amouyal, M. Moullem-Bahout, *J. Chem. Soc., Dalton Trans.* **1992**, 509-513.
- [53] Y.-Q. Fang, N. J. Taylor, G. S. Hanan, F. Loiseau, R. Passalacqua, S. Campagna, H. Nierengarten, A. van Dorsselaer, *J. Am. Chem. Soc.* **2002**, *124*, 7912-7913.
- [54] M. I. J. Polson, N. J. Taylor, G. S. Hanan, *Chem. Commun.* **2002**, 1356-1357.
- [55] C. Metcalfe, S. Spey, H. Adams, J. A. Thomas, *J. Chem. Soc., Dalton Trans.* **2002**, 4732-4739.
- [56] E. C. Constable, D. R. Smith, *Supramol. Chem.* **1994**, *4*, 5-7.
- [57] M. Hissler, A. Harriman, A. Khatyr, R. Ziessel, *Chem. Eur. J.* **1999**, *5*, 3366-3381.



- [58] C. Goze, D. V. Kozlov, F. N. Castellano, J. Suffert, R. Ziessel, *Tetrahedr. Lett.* **2003**, *44*, 8713-8716.
- [59] A. C. Benniston, A. Harriman, D. J. Lawrie, A. Mayeux, K. Rafferty, O. D. Russel, *J. Chem. Soc., Dalton Trans.* **2003**, 4762-4769.
- [60] K. R. J. Thomas, J. T. Lin, C.-P. Chang, C.-H. Chuen, C.-C. Cheng, *J. Chin. Chem. Soc.* **2002**, *49*, 833-840.
- [61] N. W. Alcock, P. R. Barker, J. M. Haider, M. J. Hannon, C. L. Painting, Z. Pikramenou, E. A. Plummer, K. Rissanen, P. Saarenketo, *J. Chem. Soc., Dalton Trans.* **2000**, 1447-1462.
- [62] U. Ziener, E. Breuning, J.-M. Lehn, E. Wegelius, K. Rissanen, G. Baum, D. Fenske, G. Vaughan, *Chem. Eur. J.* **2000**, *6*, 4132-4139.
- [63] F. Barigelletti, B. Ventura, J.-P. Collin, R. Kayhanian, P. Gavina, J.-P. Sauvage, *Eur. J. Inorg. Chem.* **2000**, 113-119.
- [64] O. Johansson, M. Borgstroem, R. Lomoth, M. Palmblad, J. Bergquist, L. Hammarstroem, L. Sun, B. Kermark, *Inorg. Chem.* **2003**, *42*, 2908-2918.
- [65] A. El-Ghayoury, A. P. H. J. Schenning, P. A. van Hal, C. H. Weidl, J. L. J. van Dongen, R. A. J. Janssen, U. S. Schubert, E. W. Meijer, *Thin Solid Films* **2002**, *403-404*, 97-101.
- [66] J. Otsuki, H. Kameda, S. Tomihira, H. Sakaguchi, T. Takido, *Chem. Lett.* **2002**, *31*, 610-611.
- [67] M. Duati, S. Fanni, J. G. Vos, *Inorg. Chem. Commun.* **2000**, *3*, 68-70.
- [68] M. Duati, S. Tasca, F. C. Lynch, H. Bohlen, J. G. Vos, S. Stagni, M. D. Ward, *Inorg. Chem.* **2003**, *42*, 8377-8384.
- [69] J. D. Holbrey, G. J. T. Tiddy, D. W. Bruce, *J. Chem. Soc., Dalton Trans.* **1995**, 1769-1774.
- [70] K. T. Potts, M. Keshavarz-K, F. S. Tham, K. A. G. Raiford, C. Arana, H. D. Abruna, *Inorg. Chem.* **1993**, *32*, 5477-5484.
- [71] K. T. Potts, M. Keshavarz-K, F. S. Tham, H. D. Abruna, C. Arana, *Inorg. Chem.* **1993**, *32*, 4450-4456.
- [72] L. F. Szczepura, S. M. Maricich, R. F. See, M. R. Churchill, K. J. Takeuchi, *Inorg. Chem.* **1995**, *34*, 4198-4205.
- [73] G. Chelucci, A. Saba, D. Vignola, C. Solinas, *Tetrahedr.* **2001**, *57*, 1099-1104.
- [74] J. A. Barron, S. Glazier, S. Bernhard, K. Takada, P. L. Houston, H. D. Abruna, *Inorg. Chem.* **2003**, *42*, 1448-1455.
- [75] S. Bernhard, K. Takada, D. J. Diaz, H. D. Abruna, H. Murner, *J. Am. Chem. Soc.* **2001**, *123*, 10265-10271.
- [76] S. Bernhard, J. I. Goldsmith, K. Takada, H. D. Abruna, *Inorg. Chem.* **2003**, *42*, 4389-4393.
- [77] E. C. Constable, T. Kulke, M. Neuburger, M. Zehnder, *New. J. Chem.* **1997**, *21*, 1091-1102.
- [78] T. Bark, H. Stoeckli-Evans, A. von Zelewsky, *J. Chem. Soc., Perkin Trans. 1* **2002**, *16*, 1881-1886.
- [79] H. Jiang, S. J. Lee, W. Lin, *Org. Lett.* **2002**, *4*, 2149-2152.
- [80] H. Jiang, S. J. Lee, W. Lin, *J. Chem. Soc., Dalton Trans.* **2002**, 3429-3433.
- [81] A. Harriman, A. Khatyr, R. Ziessel, A. C. Benniston, *Angew. Chem.* **2000**, *112*, 4457-4460; *Angew. Chem. Int. Ed.* **2000**, *39*, 4287-4290.
- [82] L. Hammarstroem, F. Barigelletti, L. Flamigni, M. T. Indelli, N. Armaroli, G. Calogero, M. Guardigli, A. Sour, J.-P. Collin, J.-P. Sauvage, *J. Phys. Chem. A* **1997**, *101*, 9061-9069.
- [83] F. Barigelletti, L. Flamigni, V. Balzani, J.-P. Collin, J.-P. Sauvage, A. Sour, E. C. Constable, A. M. W. C. Thompson, *J. Am. Chem. Soc.* **1994**, *116*, 7692-7699.

- [84] M. T. Indelli, F. Scandola, J.-P. Collin, J.-P. Sauvage, A. Sour, *Inorg. Chem.* **1996**, *35*, 303-312.
- [85] H. Torieda, A. Yoshimura, K. Nozaki, S. Sakai, T. Ohno, *J. Phys. Chem. A* **2002**, *106*, 11034-11044.
- [86] A. El-ghayoury, A. Harriman, A. Khatyr, R. Ziessel, *J. Phys. Chem. A* **2000**, *104*, 1512-1523.
- [87] A. Harriman, A. Khatyr, R. Ziessel, *J. Chem. Soc., Dalton Trans.* **2003**, 2061-2068.
- [88] F. Barigelletti, L. Flamigni, V. Balzani, J.-P. Collin, J.-P. Sauvage, A. Sour, *New. J. Chem.* **1995**, *19*, 793-798.
- [89] A. Amini, K. Bates, A. C. Benniston, D. J. Lawrie, E. Soubeyrand-Lenoir, *Tetrahedr. Lett.* **2003**, *44*, 8245-8247.
- [90] B. Hasenknopf, J. Hall, J.-M. Lehn, V. Balzani, A. Credi, S. Campagna, *New. J. Chem.* **1996**, *20*, 725-730.
- [91] F. Barigelletti, L. Flamigni, M. Guardigli, J.-P. Sauvage, J.-P. Collin, A. Sour, *Chem. Commun.* **1996**, 1329-1330.
- [92] M. Hissler, A. El-ghayoury, A. Harriman, R. Ziessel, *Angew. Chem.* **1998**, *110*, 1804-1807; *Angew. Chem. Int. Ed.* **1998**, *37*, 1717-1720.
- [93] F. Loiseau, R. Passalacqua, S. Campagna, M. I. J. Polson, Y.-Q. Fang, G. S. Hanan, *Photochem. Photobiol. Sci.* **2002**, *1*, 982-990.
- [94] T. Akasaka, J. Otsuki, K. Araki, *Chem. Eur. J.* **2002**, *8*, 130-136.
- [95] T. Akasaka, T. Mutai, J. Otsuki, K. Araki, *J. Chem. Soc., Dalton Trans.* **2003**, 1537-1544.
- [96] E. C. Constable, C. E. Housecroft, E. Schofield, S. Encinas, N. Armaroli, F. Barigelletti, L. Flamigni, E. Figgemeier, J. G. Vos, *Chem. Commun.* **1999**, 869-870.
- [97] S. Encinas, L. Flamigni, F. Barigelletti, E. C. Constable, C. E. Housecroft, E. R. Schofield, E. Figgemeier, D. Fenske, M. Neuburger, J. G. Vos, M. Zehnder, *Chem. Eur. J.* **2002**, *8*, 137-150.
- [98] A. Harriman, A. Mayeux, A. De Nicola, R. Ziessel, *Phys. Chem. Chem. Phys.* **2002**, *4*, 2229-2235.
- [99] T. Akasaka, H. Inoue, M. Kuwabara, T. Mutai, J. Otsuki, K. Araki, *J. Chem. Soc., Dalton Trans.* **2003**, 815-821.
- [100] R. Argazzi, E. Bertolasi, C. Chiorboli, C. A. Bignozzi, M. K. Itokazu, N. Y. M. Iha, *Inorg. Chem.* **2001**, *40*, 6885-6891.
- [101] J.-D. Lee, L. M. Vrana, E. R. Bullock, K. J. Brewer, *Inorg. Chem.* **1998**, *37*, 3575-3580.
- [102] G. S. Hanan, D. Volkmer, U. S. Schubert, J.-M. Lehn, G. Baum, D. Fenske, *Angew. Chem.* **1997**, *109*, 1929-1931; *Angew. Chem. Int. Ed.* **1997**, *36*, 1842-1844.
- [103] G. S. Hanan, U. S. Schubert, D. Volkmer, E. Rivière, J. M. Lehn, N. Kyritsakas, J. Fischer, *Can. J. Chem.* **1997**, *75*, 169-182.
- [104] G. S. Hanan, C. R. Arana, J. M. Lehn, D. Fenske, *Angew. Chem.* **1995**, *107*, 1191-1193; *Angew. Chem. Int. Ed.* **1995**, *34*, 1122-1124.
- [105] G. S. Hanan, C. R. Arana, J. M. Lehn, G. Baum, D. Fenske, *Chem. Eur. J.* **1996**, *2*, 1292-1302.
- [106] A. Credi, V. Balzani, S. Campagna, G. S. Hanan, C. R. Arana, J.-M. Lehn, *Chem. Phys. Lett.* **1995**, *243*, 102-107.
- [107] P. Ceroni, A. Credi, V. Balzani, S. Campagna, G. S. Hanan, C. R. Arana, J.-M. Lehn, *Eur. J. Inorg. Chem.* **1999**, 1409-1414.
- [108] M.-T. Youinou, N. Rahmouny, J. Fischer, J. A. Osborn, *Angew. Chem.* **1992**, *104*, 771-773; *Angew. Chem. Int. Ed.* **1992**, *31*, 733-735.
- [109] P. N. W. Baxter, J. M. Lehn, J. Fischer, M.-T. Youinou, *Angew. Chem.* **1994**, *106*, 2432-2434; *Angew. Chem. Int. Ed.* **1994**, *33*, 2284-2286.

- [110] U. S. Schubert, C. Eschbaumer, *Org. Lett.* **1999**, *1*, 1027-1029.
- [111] U. S. Schubert, C. Eschbaumer, *J. Incl. Phenom. Macrocycl. Chem.* **1999**, *35*, 101-109.
- [112] O. Waldmann, J. Hassmann, P. Muller, G. S. Hanan, D. Volkmer, U. S. Schubert, J. M. Lehn, *Phys. Rev. Lett.* **1997**, *78*, 3390-3393.
- [113] E. Breuning, M. Ruben, J.-M. Lehn, F. Renz, Y. Garcia, V. Ksenofontov, P. Gütllich, E. Wegelius, K. Rissanen, *Angew. Chem.* **2000**, *112*, 2563-2566; *Angew. Chem. Int. Ed.* **2000**, *39*, 2504-2507.
- [114] E. Breuning, G. S. Hanan, F. J. Romero-Salguero, A. M. Garcia, P. N. W. Baxter, J.-M. Lehn, E. Wegelius, K. Rissanen, H. Nierengarten, A. van Dorsselaer, *Chem. Eur. J.* **2002**, *8*, 3458-3466.
- [115] A. M. Garcia, F. J. Romero-Salguero, D. M. Bassani, J.-M. Lehn, G. Baum, D. Fenske, *Chem. Eur. J.* **1999**, *5*, 1803-1808.
- [116] M. Barboiu, G. Vaughan, R. Graff, J.-M. Lehn, *J. Am. Chem. Soc.* **2003**, *125*, 10257-10265.
- [117] H. Nierengarten, E. Leize, E. Breuning, A. Garcia, F. Romero-Salguero, J. Rojo, J.-M. Lehn, A. van Dorsselaer, *J. Mass. Spectrom.* **2002**, *37*, 56-62.
- [118] D. M. Bassani, J.-M. Lehn, K. Fromm, D. Fenske, *Angew. Chem.* **1998**, *110*, 2534-2537; *Angew. Chem. Int. Ed.* **1998**, *37*, 2364-2367.
- [119] E. Breuning, U. Ziener, J.-M. Lehn, E. Wegelius, K. Rissanen, *Eur. J. Inorg. Chem.* **2001**, 1515-1521.
- [120] U. Ziener, J.-M. Lehn, A. Mourran, M. Möller, *Chem. Eur. J.* **2002**, *8*, 951-957.
- [121] A. M. Garcia, D. M. Bassani, J.-M. Lehn, G. Baum, D. Fenske, *Chem. Eur. J.* **1999**, *5*, 1234-1238.
- [122] D. Brown, S. Muranjan, Y. Jang, R. Thummel, *Org. Lett.* **2002**, *4*, 1253-1256.
- [123] T. Bark, M. Düggeli, H. Stoeckli-Evans, A. von Zelewsky, *Angew. Chem.* **2001**, *113*, 2924-2927; *Angew. Chem. Int. Ed.* **2001**, *40*, 2848-2851.
- [124] E. R. Schofield, J.-P. Collin, N. Gruber, J.-P. Sauvage, *Chem. Commun.* **2003**, 188-189.
- [125] Y. Molard, H. Parrot-Lopez, *Tetrahedr. Lett.* **2002**, *43*, 6355-6358.
- [126] Y. Bretonniere, M. Mazzanti, J. Pecaut, M. M. Olmstead, *J. Am. Chem. Soc.* **2002**, *124*, 9012-9013.
- [127] S.-S. Sun, A. J. Lees, *Inorg. Chem.* **2001**, *40*, 3154-3160.
- [128] S.-S. Sun, A. S. Silva, I. M. Brinn, A. J. Lees, *Inorg. Chem.* **2000**, *39*, 1344-1345.
- [129] G. J. E. Davidson, S. J. Loeb, *J. Chem. Soc., Dalton Trans.* **2003**, 4319-4323.
- [130] M. C. Jimenez-Molero, C. Dietrich-Buchecker, J.-P. Sauvage, *Chem. Eur. J.* **2002**, *8*, 1456-1466.
- [131] E. C. Constable, E. Schofield, *Chem. Commun.* **1998**, 403-404.
- [132] G. R. Newkome, T. J. Cho, C. N. Moorefield, R. Cush, P. S. Russo, L. A. Godínez, M. J. Saunders, P. Mohapatra, *Chem. Eur. J.* **2002**, *8*, 2946-2954.
- [133] P. M. Gleb U. Priimov, P. K. Maritim, P. K. Butalanyi, N. W. Alcock, *J. Chem. Soc., Dalton Trans.* **2000**, 445-449.
- [134] N. W. Alcock, A. J. Clarke, W. Errington, A. M. Josceanu, P. Moore, S. C. Rawle, P. Sheldon, S. M. Smith, M. L. Turonek, *Supramol. Chem.* **1996**, *6*, 281-291.
- [135] C. B. Smith, E. C. Constable, C. E. Housecroft, B. M. Kariuki, *Chem. Commun.* **2002**, 2068-2069.
- [136] F. Loiseau, C. D. Pietro, S. Serroni, S. Campagna, A. Licciardello, A. Manfredi, G. Pozzi, S. Quici, *Inorg. Chem.* **2001**, *40*, 6901-6909.
- [137] H. S. Chow, E. C. Constable, C. E. Housecroft, M. Neuburger, *J. Chem. Soc., Dalton Trans.* **2003**, 4568-4569.

- [138] E. C. Constable, C. E. Housecroft, C. B. Smith, *Inorg. Chem. Commun.* **2003**, *6*, 1011-1013.
- [139] P. R. Andres, U. S. Schubert, submitted.
- [140] G. R. Newkome, K. S. Yoo, C. N. Moorefield, *Chem. Commun.* **2002**, 2164-2165.
- [141] D. Armspach, E. C. Constable, F. Diederich, C. E. Housecroft, J.-F. Nierengarten, *Chem. Commun.* **1996**, 2009-2010.
- [142] D. Armspach, E. C. Constable, F. Diederich, C. E. Housecroft, J.-F. Nierengarten, *Chem. Eur. J.* **1998**, *4*, 723-733.
- [143] U. S. Schubert, C. H. Weidl, A. Cattani, C. Eschbaumer, G. R. Newkome, E. He, E. Harth, K. Müllen, *Polym. Prepr.* **2000**, *41*, 229-230.
- [144] C. Du, Y. Li, S. Wang, Z. Shi, S. Xiao, D. Zhu, *Synth. Met.* **2001**, *124*, 287-289.
- [145] R. Dagani, *Chem. Engin. News* **1999**, *77*, 54-59.
- [146] A. Khatyr, R. Ziessel, *Synthesis* **2001**, 1665-1670.
- [147] S. Weidner, Z. Pikramenou, *Chem. Commun.* **1998**, 1473-1474.
- [148] J. M. Haider, M. Chavarot, S. Weidner, I. Sadler, R. M. Williams, L. De Cola, Z. Pikramenou, *Inorg. Chem.* **2001**, *40*, 3912-3921.
- [149] J.-P. Collin, J.-O. Dalbavie, V. Heitz, J.-P. Sauvage, L. Flamigni, N. Armaroli, V. Balzani, F. Barigelletti, I. Montanari, *Bull. Soc. Chim. Fr.* **1996**, *133*, 749-754.
- [150] L. Flamigni, F. Barigelletti, N. Armaroli, B. Ventura, J.-P. Collin, J.-P. Sauvage, J. A. G. Williams, *Inorg. Chem.* **1999**, *38*, 661-667.
- [151] L. Flamigni, F. Barigelletti, N. Armaroli, J.-P. Collin, J.-P. Sauvage, J. A. G. Williams, *Chem. Eur. J.* **1998**, *4*, 1744-1754.
- [152] L. Flamigni, F. Barigelletti, N. Armaroli, J.-P. Colli, I. M. Dixon, J.-P. Sauvage, J. A. G. Williams, *Coord. Chem. Rev.* **1999**, 671-682.
- [153] S. Schmatloch, C. H. Weidl, I. van Baal, J. Pahnke, U. S. Schubert, *Polym. Prepr.* **2002**, *43*, 684-685.
- [154] S. Ott, M. Kritikos, B. Åkermark, L. Sun, *Angew. Chem.* **2003**, *115*, 3407-3410; *Angew. Chem. Int. Ed.* **2003**, *42*, 3285-3288.
- [155] K. M. Stewart, L. W. McLaughlin, *Chem. Commun.* **2003**, 2934-2935.



# 2

## New terpyridine ligands and model complexes

**Abstract:** Supramolecular architectures are of great interest in modern materials research. The directed construction of asymmetric 2,2':6',2''-terpyridine ruthenium(II) complexes is an important tool towards such systems. In this chapter, the synthesis of functionalized terpyridine ligands and asymmetric terpyridine ruthenium(II) complexes as models for supramolecular architectures and polymers is described. Terpyridines, bearing different functional groups in the 4'-position, were complexed with unfunctionalized terpyridine ligands utilizing Ru(III)/Ru(II) chemistry. The resulting compounds were characterized by UV-vis, one- and two-dimensional NMR spectroscopy as well as MALDI-TOF mass spectrometry. In addition, X-ray structure analysis on several compounds was performed. Moreover, the synthesis and characterization of room-temperature-fluorescent perylene-terpyridine ruthenium complexes and of chiral systems is described. Finally, asymmetric terpyridine-bipyridine-copper complexes were prepared and investigated.

*Parts of this work have been published:*

U. S. Schubert, C. Eschbaumer, P. Andres, H. Hofmeier, C. H. Weidl, E. Herdtweck, E. Dulkeith, A. Morteani, N. E. Hecker, J. Feldmann, *Synth. Met.* **2001**, *121*, 1249-1252; P. R. Andres, H. Hofmeier, B. G. G. Lohmeijer, U. S. Schubert, *Synthesis* **2003**, 2865-2871; A. El-Ghayoury, H. Hofmeier, A. P. H. J. Schenning, U. S. Schubert, *Tetrahedr. Lett.* **2004**, *45*, 261-264; H. Hofmeier, E. Herdtweck, U. S. Schubert, *Zeitschr. Anorg. Allg. Chem.* **2004**, *630*, in press; H. Hofmeier, P. R. Andres, R. Hoogenboom, E. Herdtweck, U. S. Schubert, submitted; H. Hofmeier, A. El-Ghayoury, A. P. H. J. Schenning, U. S. Schubert, submitted.

## 2.1 Introduction

Within the field of supramolecular chemistry,<sup>[1]</sup> 2,2':6',2''-terpyridines with a chemical functionality in the 4'-position<sup>[2]</sup> are a well-suited tool for the construction of metallo-supramolecular architectures, where the metal centers are used to control self-organization processes<sup>[1a,3]</sup> or metallo-polymerizations. In the latter case, telechelic terpyridine-functionalized polymeric<sup>[4]</sup> or non-polymeric building blocks<sup>[5]</sup> are extended to long chains or networks via metal complexation. Metal-ions suitable for the build-up of such metallo-polymers are transition metals such as Fe(II), Co(II), Ru(II) or Ni(II), which lead to octahedral *bis*-terpyridyl complexes<sup>[6,7]</sup> with high stability constants.<sup>[8]</sup> In this context, the well-known directed coupling method utilizing Ru(III)/Ru(II) chemistry is of special interest. Ligand A is first complexed with Ru(III) in order to form a *mono*-terpyridine complex and subsequently free terpyridine containing ligand B is added under reductive conditions in order to form A-terpyridine-Ru(II)-terpyridine-B structures.<sup>[9]</sup> Other applications, in particular concerning 2,2':6',2''-terpyridines with a synthetic handle in the 4'-position, lie in the fields of metallo-dendrimers,<sup>[10]</sup> surface science<sup>[11]</sup> and biochemistry.<sup>[12]</sup> Utilizing terpyridines with functionality in the 4'-position as building block offers the advantage of creating linear systems in which the octahedral metal complex is located in the backbone of the metallo-polymer.<sup>[5]</sup> Also no additional diastereomeric metal complex centers are added due to the  $C_{2v}$  symmetry of the terpyridine with a rotation axis through the 4'-position, thus leading to no *fac* or *mer* (*bis*-terpyridine) diastereomers upon complexation of 4'-functionalized terpyridines.

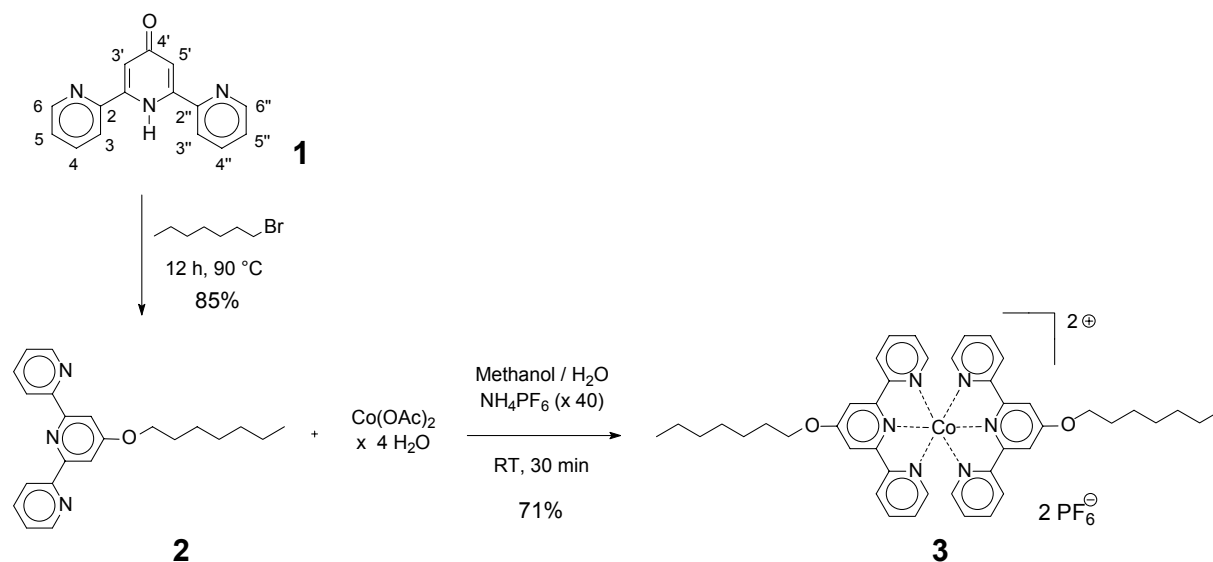
## 2.2 Functionalized terpyridine ligands

For functionalization in the 4'-position mainly two intermediates have been used up to now: 4'-chloro-2,2':6',2''-terpyridine and its precursor 2,6-*bis*-(pyrid-2-yl)-4-pyridone.<sup>[13]</sup> Surprisingly, for the latter one there are only few examples reported.<sup>[14,15]</sup> In contrast, there are numerous examples utilizing the nucleophilic aromatic substitution of the chloro-function in the 4'-chloro-2,2':6',2''-terpyridine, leading e.g. to 4'-R-alkoxy-2,2':6',2''-terpyridines.<sup>[16]</sup> The direct synthesis of 4'-functionalized 2,2':6',2''-terpyridines is also possible *via* the "Kröhnke-method", for which suitable precursors would have to be designed first.<sup>[17]</sup> As an example for the direct functionalization of the 2,6-*bis*-(pyrid-2-yl)-4-pyridone, the preparation of a heptoxy-terpyridine is described (Scheme 2.1). The ligand has been subsequently complexed with Co(II)-acetate to form a symmetric complex. Co(II) can be reduced to lower oxidation states (e.g. Co(I)), which preferably form *mono*-terpyridine complexes.<sup>[18]</sup> Therefore cobalt could be a metal-ion suitable for reversible metallo-supramolecular structures.

As already reported in literature, the alcoholate of the tautomeric form of the 2,6-*bis*-(pyrid-2-yl)-4-pyridone **1**, the 4'-hydroxy-terpyridine, can be prepared *in situ* in a  $K_2CO_3$ -basic DMF suspension and acts as nucleophile for  $S_N2$  type nucleophilic substitutions.<sup>[14]</sup> For a

nucleophilic attack onto alkyl chains good anionic leaving groups such as halides or tosylates are required. The heptyloxy-terpyridine **2** was easily prepared in high yield starting from the commercially available heptyl-bromide through extraction after pouring the reaction mixture into a 10-fold excess of water and subsequent column chromatography. It should be mentioned that the introduction of sensitive groups such as bromides, double bonds or epoxides has also been carried out successfully, which has not been feasible using the functionalization route *via* the 4'-chloro-2,2':6',2''-terpyridine.<sup>[16c]</sup> Apart from the availability of nucleophilic starting material in the latter case, this also has to do with the stronger basic system KOH/DMSO, which is required for the nucleophilic aromatic substitution compared to K<sub>2</sub>CO<sub>3</sub>/DMF for the S<sub>N</sub>2-type reaction used here.

The symmetric complex **3** was formed by the reaction of two equivalents 4'-(heptyloxy)-terpyridine with one equivalent of Co(II)acetate (Scheme 2).



Scheme 2.1 Synthesis of ligand **2** and the symmetric Co(II) complex **3**.

The addition of excess NH<sub>4</sub>PF<sub>6</sub> then immediately produced quantitative precipitation of the crude product. After filtration and washing with MeOH as well as water the pure complex was obtained after recrystallization from acetonitrile/diethyl ether. The shifts in the <sup>1</sup>H-NMR are influenced by the paramagnetism of Co(II) (Figure 2.1). Due to the hyperfine interaction of the unpaired Co(II) electrons with the ligand protons a shift to low field is observed with the signals still being sharp enough for integration.<sup>[19]</sup> Through comparison with similar complexes reported by Constable et al. the spin-state of the Co(II) could be assigned as low-spin.<sup>[20]</sup> The existence of the complex **3** was proven by MALDI-TOF mass spectrometry and verified by elemental analysis. The mass spectrum shows three isotope distributions which could all be assigned. All fragments refer to singly positive charged compounds. The peaks at *m/z* 898 and 753 represent the complex without one and none counter-ions, respectively. These fragment types are often observed for *bis*-terpyridyl complexes.<sup>[21,22]</sup> The fragment at *m/z* 631 refers to the complex without the counter-ions and without one ligand plus matrix minus a proton.



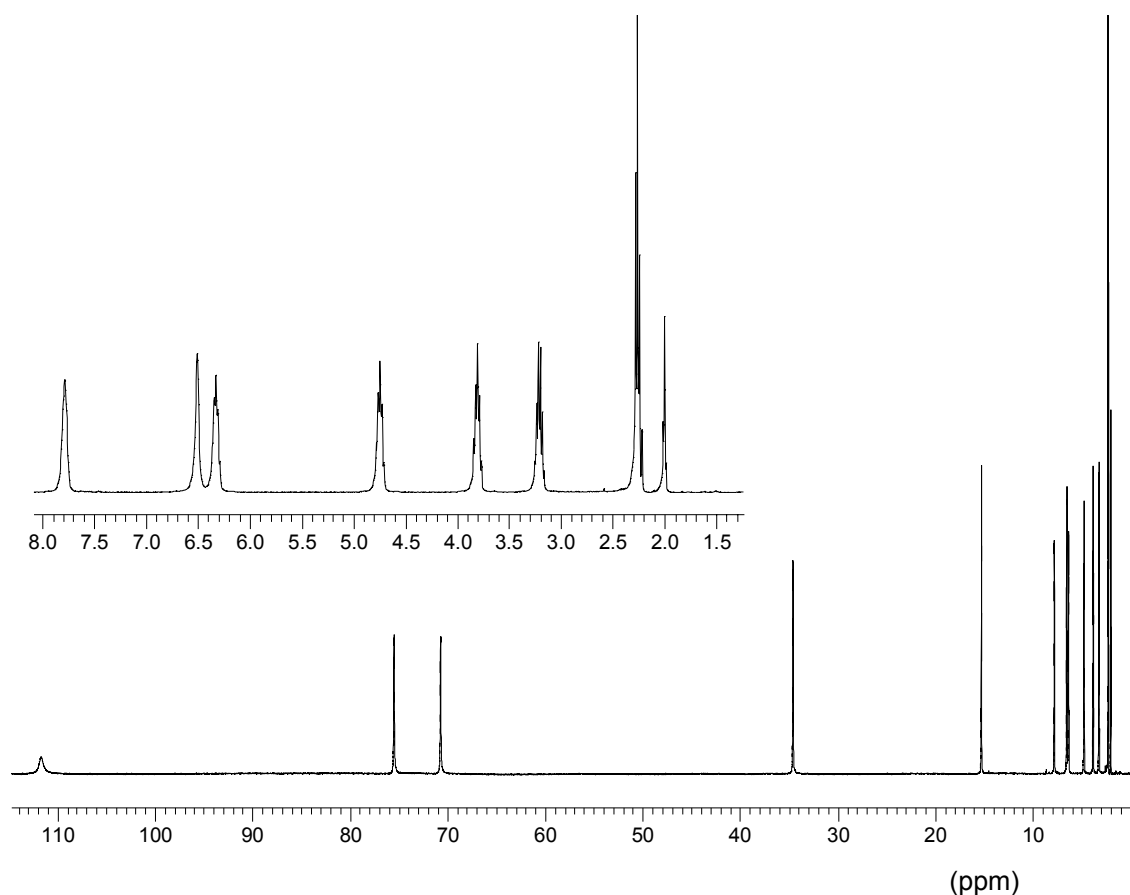
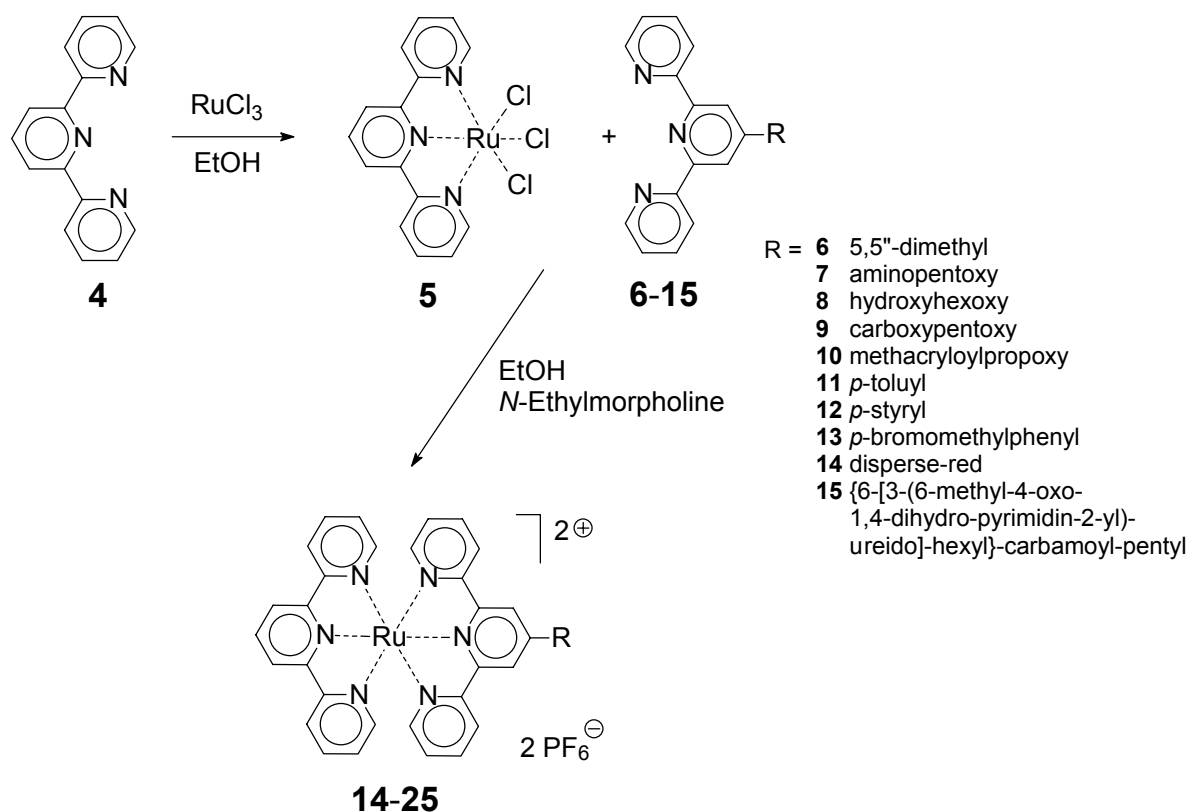


Figure 2.1 Knight shift  $^1\text{H}$ -NMR spectrum of cobalt complex **3** (in acetonitrile).

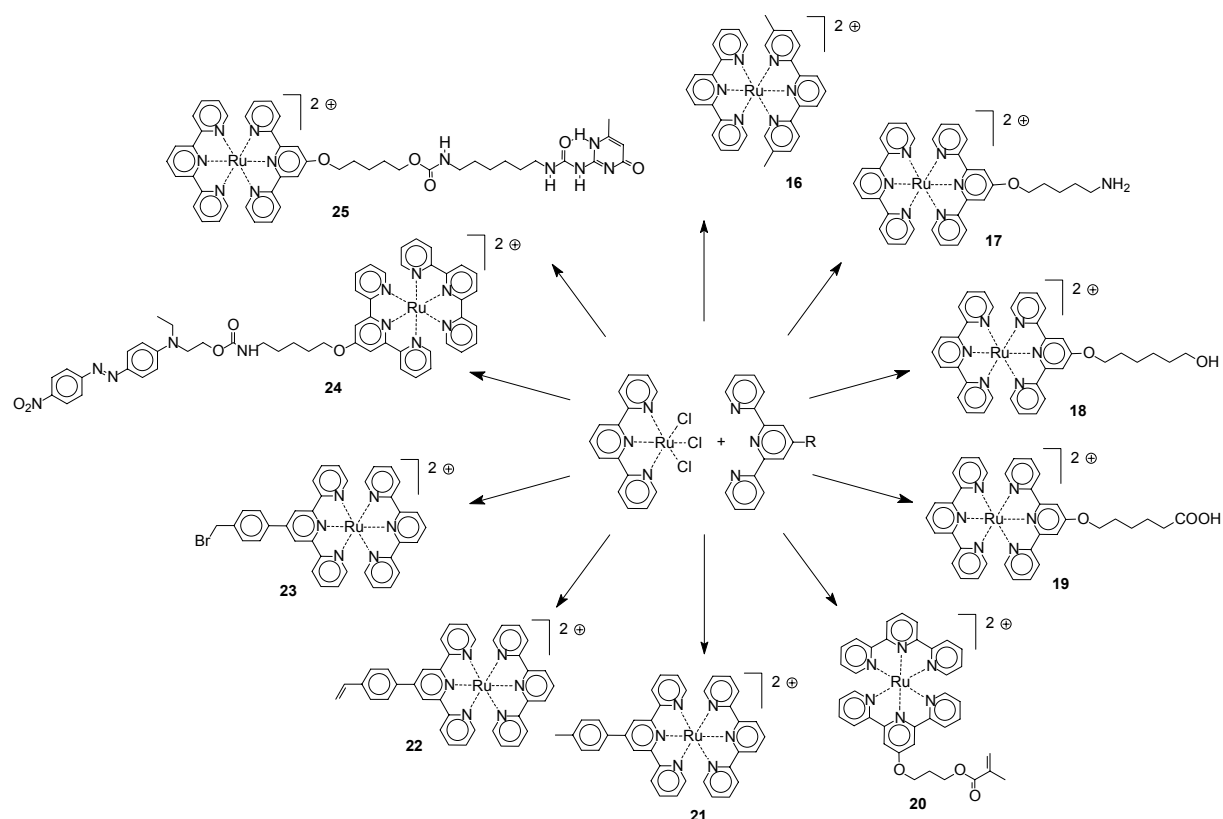
### 2.3 Synthesis and characterization of asymmetric ruthenium(II) terpyridine model complexes

Ruthenium complexes are of major importance for the construction of extended metallo-supramolecular systems. Especially the directed coupling of two different terpyridines to asymmetric *bis*-terpyridine complexes represents a very powerful method.<sup>[4b]</sup> Here the synthesis and characterization of model complexes, combining unfunctionalized terpyridine with terpyridines bearing different functional groups is presented. In a first step, 2,2':6',2''-terpyridine **4** was reacted with ruthenium(III) trichloride in refluxing methanol to obtain the terpyridine-ruthenium(III) *mono*-complex **5** as a brown precipitate (Scheme 2.2). This intermediate was reacted in the second step with various functionalized 2,2':6',2''-terpyridines (**6-15**) to yield the corresponding complexes **14-25** (Scheme 2.2 and 2.3). The reactions were performed in refluxing methanol, containing *N*-ethylmorpholine,<sup>[23]</sup> resulting in red solutions.



Scheme 2.2. Schematic representation of the complex synthesis.

The pure complexes were precipitated after exchange of the counterions by addition of a tenfold excess of ammoniumhexafluorophosphate. Subsequently, crystalline materials were obtained in 50-80% yield after crystallization by diffusion of diethyl ether into an acetonitrile solution of the crude material. In the case of the *p*-bromomethylphenyl-terpyridine complex **23**,  $^1\text{H-NMR}$  and MALDI-TOF mass spectrometry indicated that the bromo-substituents were partially substituted by methoxy-groups, derived from the solvent. Therefore, the compound was purified by column chromatography (silica), using acetonitrile containing aqueous  $\text{KNO}_3$  as mobile phase. Due to similar elution properties of the by-product, only the first fraction (5%) was pure according to elemental analysis. The amino (**17**), hydroxy (**18**) and carboxy groups (**19**) of the functionalized complexes could be used for subsequent reactions. Terpyridines containing polymerizable groups (based on methyl methacrylate (**20**) or styrene (**22**)) were also complexed successfully and previous work had already shown that these kinds of complexes could be used for co-polymerizations.<sup>[24]</sup> Moreover, the bromomethyl group is a well-known initiator for ring-opening polymerizations of oxazolines and hydroxy-groups could be used as co-initiator for the polymerization of lactones and lactides; the introduction of such a group into complexes leads to "metallo-supramolecular" initiators.<sup>[25]</sup> Finally, even more complicated functional groups like the dye "disperse-red" could be connected to a terpyridine ruthenium complex (**24**). This dye has a strong absorption at 480 nm, which is much stronger than the ruthenium MLCT band, which lies at the same wavelength (see also below).



Scheme 2.3. Schematic overview over the synthesized ruthenium(II) complexes ( $\text{PF}_6^-$  counterions omitted).

UV-vis spectroscopy revealed the formation of the terpyridine ruthenium(II) complexes (Figure 2.2): the characteristic bathochromic shift of the  $\pi$ - $\pi^*$ -absorption bands of the ligands at around 270 and 305 nm was found for all complexes.

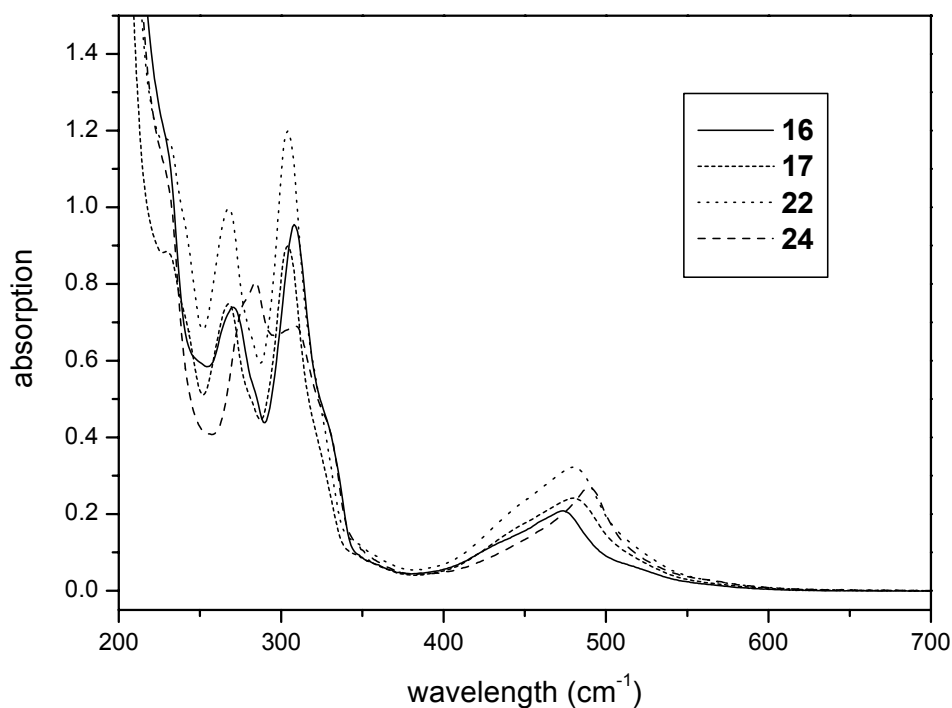


Figure 2.2. UV-vis spectra of the terpyridine complexes **16**, **17**, **22** and **24** (in acetonitrile).

In addition, the appearance of the metal-to-ligand charge transfer (MLCT) band of the complex at around 480 nm was detected. When comparing the position of this band in the spectra of the alkyl, oxo and phenyl substituted terpyridine complexes, a slight redshift of this band was observed in the mentioned order.

MALDI-TOF mass spectrometry is a powerful tool for the analysis of terpyridine metal complexes.<sup>[22]</sup> This technique allows the ionization and detection of terpyridine complexes: the cation without counterions as well as an ion pair with one PF<sub>6</sub> ion and sometimes with both counterions could be detected. Furthermore, matrix adducts were found in some cases. All species carry a single positive charge.<sup>[26]</sup> As an example, the spectrogram of compound **21** is shown in Figure 2.3. The observed isotopic pattern fits exactly to the simulated distribution (insert in Figure 2.3)

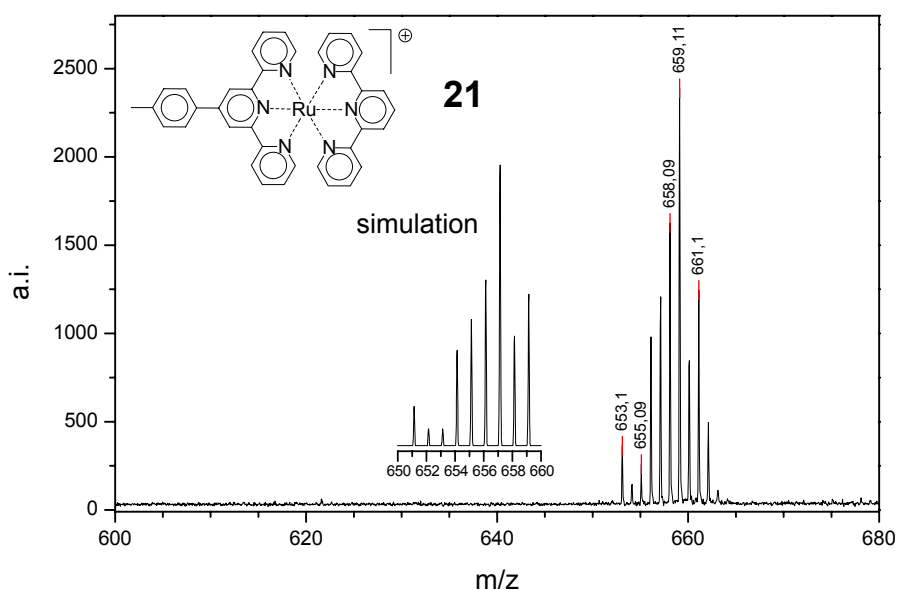


Figure 2.3. MALDI-TOF mass spectrum of complex **21** (insert: simulation of the isotopic pattern).

All complexes were also analyzed by <sup>1</sup>H-NMR spectroscopy. The resonances in the aromatic region could be assigned to the protons of the complexed terpyridine moieties: in particular the upfield shift of the 6,6''-signal is characteristic for *bis*-terpyridine complexes, due to the different chemical environment of the 6,6''-protons compared to the free ligand. Asymmetric terpyridine complexes, in particular complexes with additional phenyl groups, resulted in rather complicated NMR patterns. Therefore, two-dimensional <sup>1</sup>H-<sup>1</sup>H COSY spectroscopy was performed. All signals could be assigned properly via their cross-peaks, as shown for the spectra of the complexes **16** (Figure 2.4, middle) and **22** (Figure 2.4, bottom).

Ureidopyrimidinone moieties are of special interest since they are able to form strong self-complementary quadruple hydrogen-bonds.<sup>[27]</sup> Compounds containing this functional group have been extensively utilized for the construction of supramolecular assemblies<sup>[28]</sup> and polymers.<sup>[29]</sup> However, the combination of metal complexes with the hydrogen-bonding unit has not been reported until now. The ruthenium(II) complex **25** was sufficiently soluble in

dichloromethane so that a quantitative formation of supramolecular dimers took place as confirmed by  $^1\text{H-NMR}$  spectroscopy: the downfield shift of the NH-protons of the ureidopyrimidinone moiety clearly indicated the formation of the quadruple hydrogen bonds (Figure 2.5).<sup>[30]</sup>

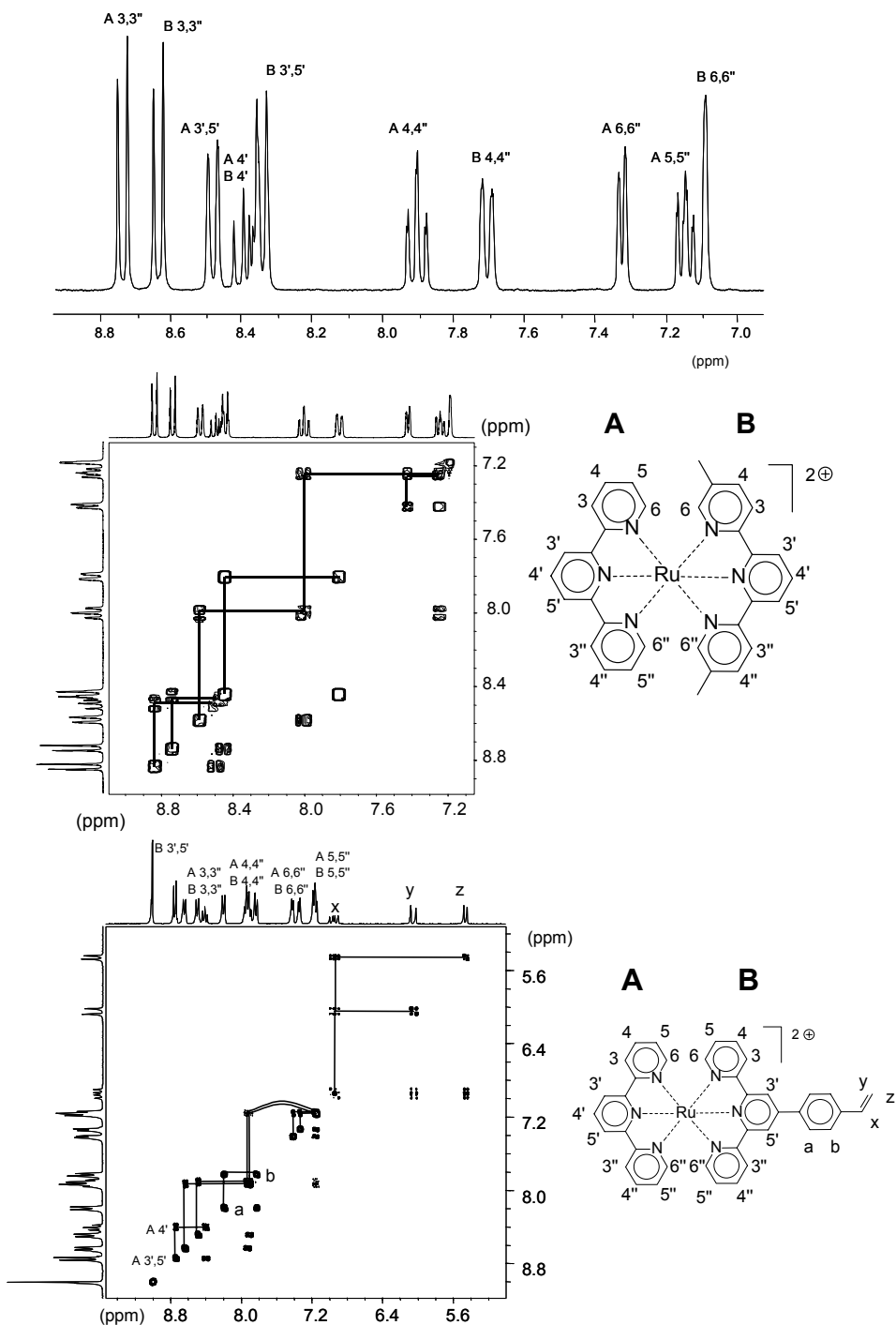


Figure 2.4.  $^1\text{H-NMR}$  spectrum and  $^1\text{H-}^1\text{H}$  COSY spectrum of **16**,  $^1\text{H-}^1\text{H}$  COSY of **22** (all in acetonitrile).

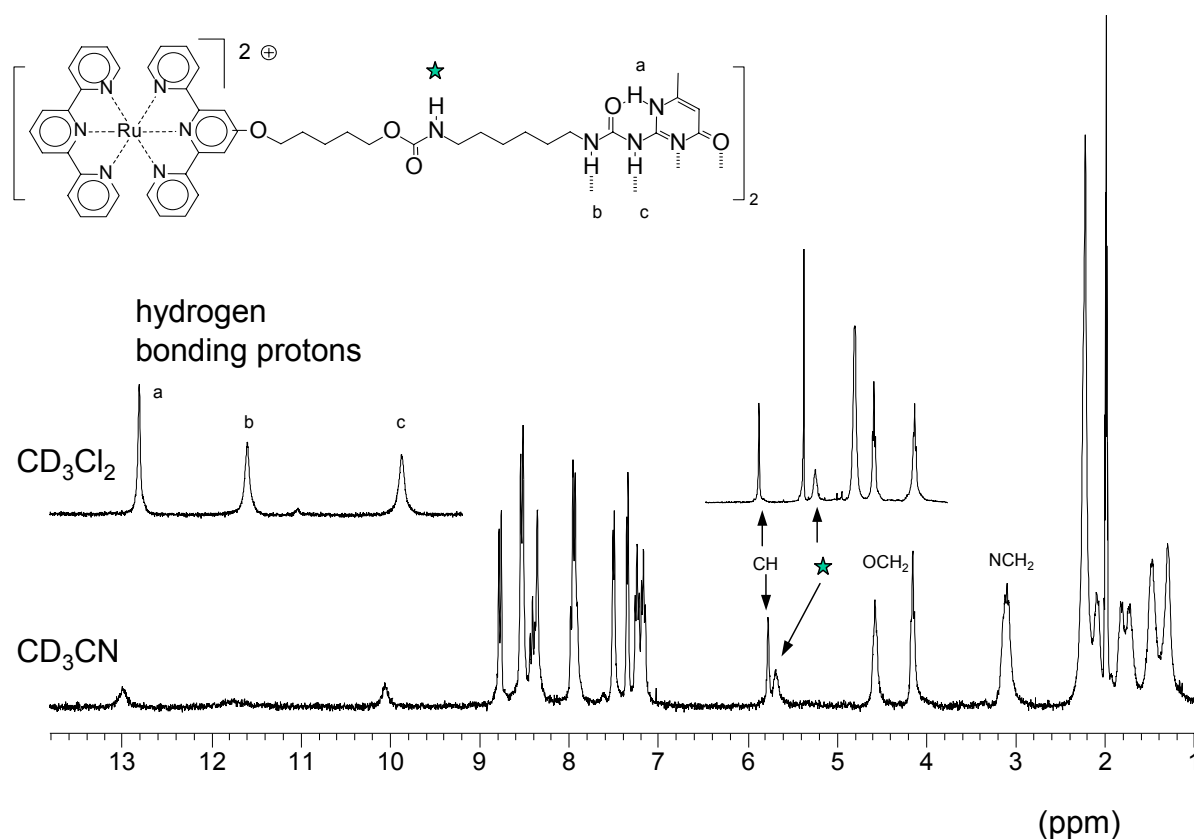


Figure 2.5.  $^1\text{H-NMR}$  spectrum of **25** in acetonitrile (insert: dichloromethane).

In the case of the hydroxy-compound **19**, single crystals were obtained by slow diffusion of diethyl ether into an acetonitrile solution of the complex, which were suitable for X-ray diffraction analysis. Figure 2.6 shows the molecular structure (ORTEP-representation) of the complex **19**, revealing an octahedral coordination at the metal center and the hydroxyalkyl group linearly protruding from the complex core. The detailed crystal characteristics are displayed in Table 2.1.

Besides the preparation of functionalized complexes containing unfunctionalized terpyridine ligands, also a complex of two 4'-functionalized terpyridine ligands was prepared. The heptyloxy functionalized terpyridine **2** was first converted into the heptyloxy-terpyridine-ruthenium(III) *mono*-complex **26** and subsequently reacted with 4'-(methoxy di(ethylene glycol))-2,2':6',2''-terpyridine **27** to yield the asymmetric complex **28** (Scheme 2.4). This complex represents a model compound for the corresponding supramolecular block copolymers: the comparison of the characteristics of supramolecular polymers and their model complexes (e.g. NMR-signals or UV-vis absorptions) are very helpful for the investigation of the success of the reaction and the purity of the obtained extended supramolecular systems.

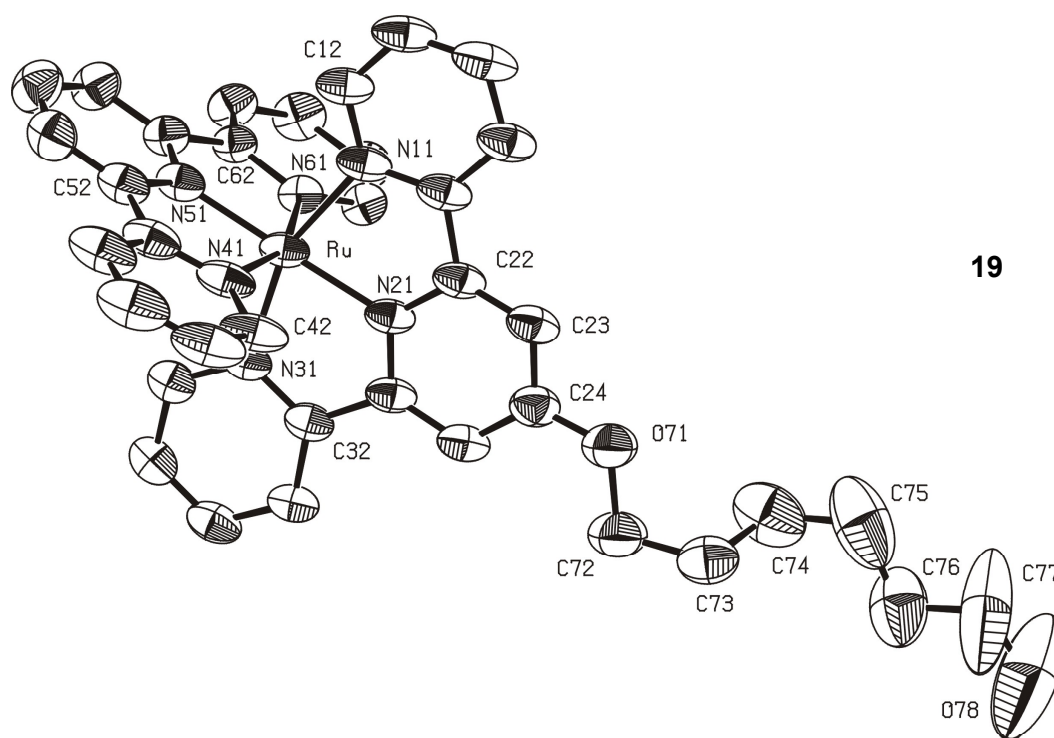
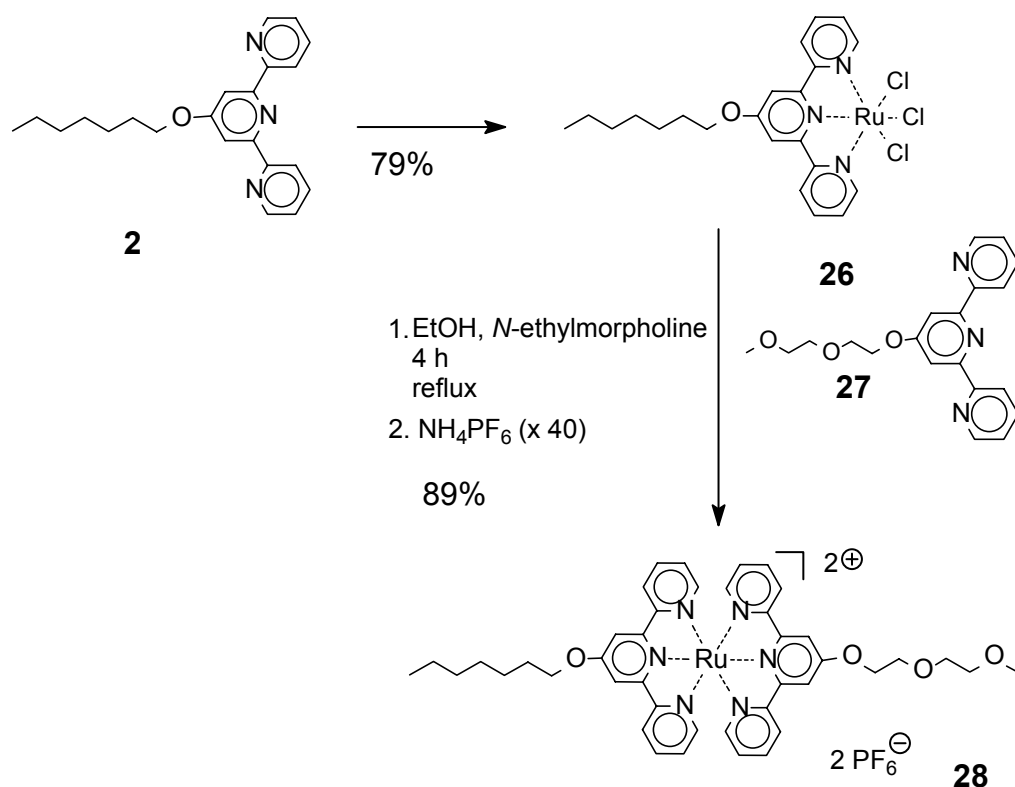


Figure 2.6. ORTEP style plot of the cationic part in the solid state of compound **19**\*1.083(CH<sub>3</sub>CN). Thermal ellipsoids are drawn at the 50% probability level. Hydrogen atoms are omitted for clarity. Selected bond lengths [ $\text{\AA}$ ] and bond angles [ $^\circ$ ]: Ru–N11 2.076(4), Ru–N21 1.980(5) Ru–N31 2.073(4) Ru–N41 2.086(4) Ru–N51 1.968(5) Ru–N61 2.074(4), N11–Ru–N21 79.0(2), N11–Ru–N31 157.7(2), N11–Ru–N41 91.9(2), N11–Ru–N51 100.3(2), N11–Ru–N61 92.4(2), N21–Ru–N31 78.7(2), N21–Ru–N41 101.5(2), N21–Ru–N51 179.1(2), N21–Ru–N61 100.4(2), N31–Ru–N41 91.9(2) N31–Ru–N51 102.0(2), N31–Ru–N61 92.1(2), N41–Ru–N51 79.0(2), N41–Ru–N61 158.2(2), N51–Ru–N61 79.2(2).



Scheme 2.4. Schematic representation of the synthesis of complex **28**.

Apart from characterization including  $^1\text{H}$ -,  $^{13}\text{C}$ -NMR, MALDI-TOF mass spectrometry and elemental analysis, 2-dimensional  $^1\text{H}$ - $^1\text{H}$ -COSY NMR was used for the characterization of the asymmetric *bis*-complex **28** (Figure 2.7). In the terpyridine region, all signals could be assigned via the cross-peaks (Figure 2.7, inset). It could be shown that the two peaks at 8.28 and 8.33 ppm are actually two singlets for the 3',5'-protons of the two different terpyridine ligands. Furthermore, the  $\text{CH}_2$  signals of the (methoxyethoxy)-ethoxy and the  $\text{CH}_2\text{O}$  signal of the heptoxy-rest could be distinguished. Also all aliphatic methylene groups were assigned properly.



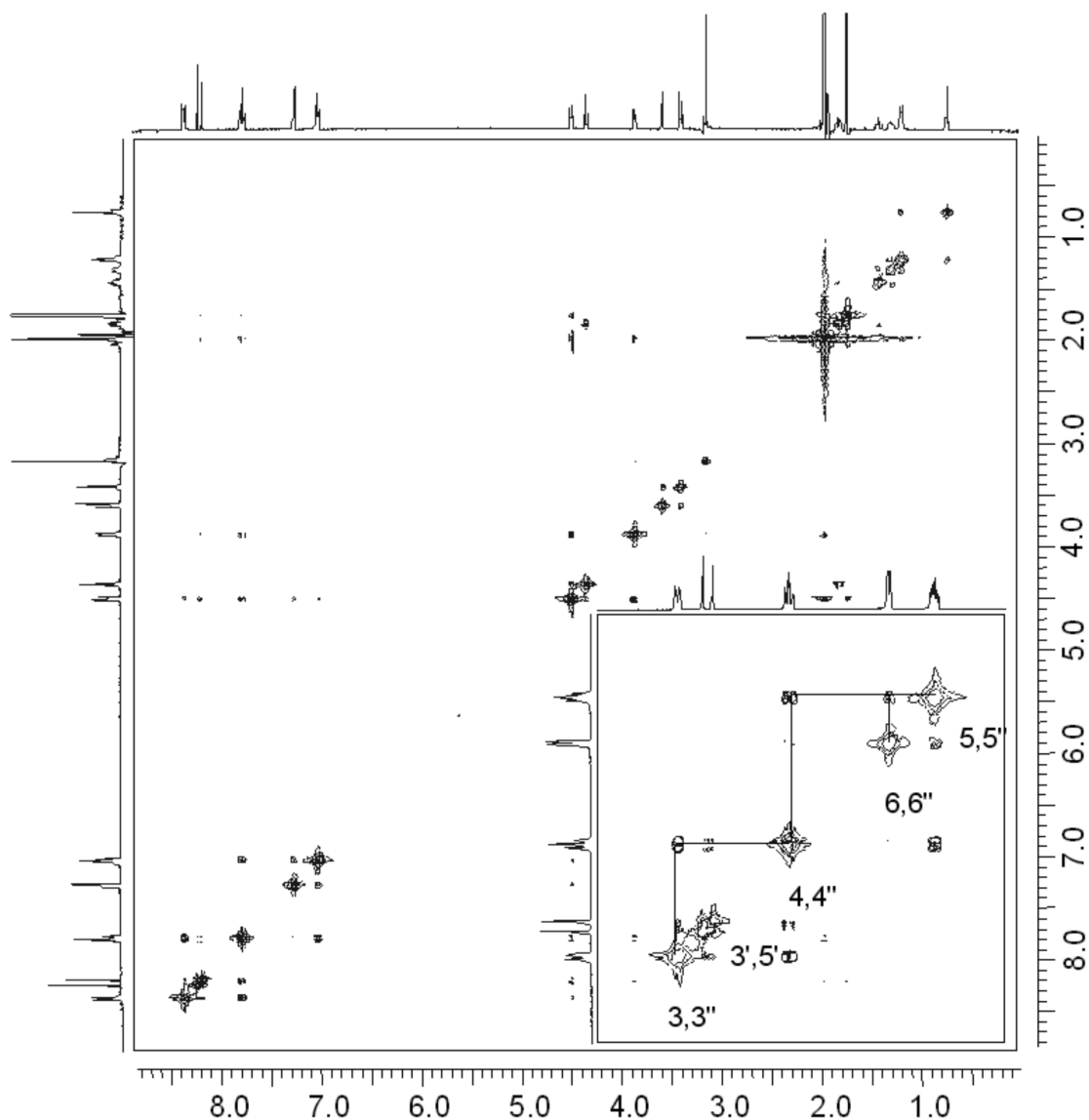


Figure 2.7.  $^1\text{H}$ - $^1\text{H}$ -COSY-NMR of the asymmetric complex **28** (in  $\text{CD}_3\text{CN}$ ).

## 2.4 Photophysical investigations and perylene-containing complexes

From investigations performed by several groups it is known that terpyridine-ruthenium(II) complexes show no or at least only very weak luminescence at room temperature. The lowest excited state is a triplet metal-to-ligand charge-transfer state ( $^3\text{MLCT}$ ), which undergoes a fast thermally activated radiation-less decay to an upper lying triplet metal-centered state ( $^3\text{MC}$ ) of the ruthenium-ion. Thus only at low temperatures excitation within the absorption bands of these complexes leads to the  $^3\text{MLCT}$  emission.<sup>[31]</sup> With an emission quantum yield of only  $3 \times 10^{-3}$  a free terpyridine moiety reveals similar weak emission properties at room temperature.<sup>[32]</sup> Furthermore, the ruthenium(III) complex **5** as well does not show any

significant luminescence. Therefore, the low temperature luminescence behavior of the ruthenium(II) complex has been investigated in more detail (Figure 2.8).

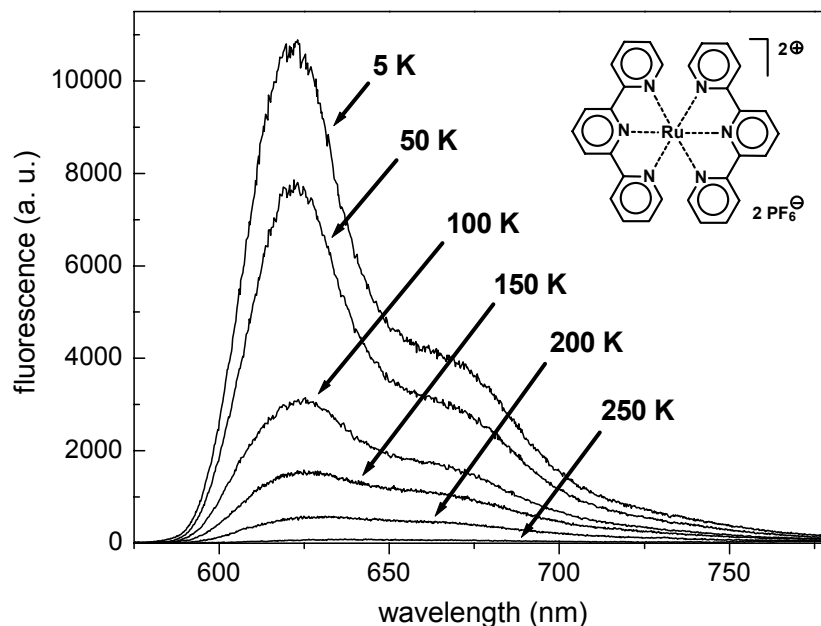
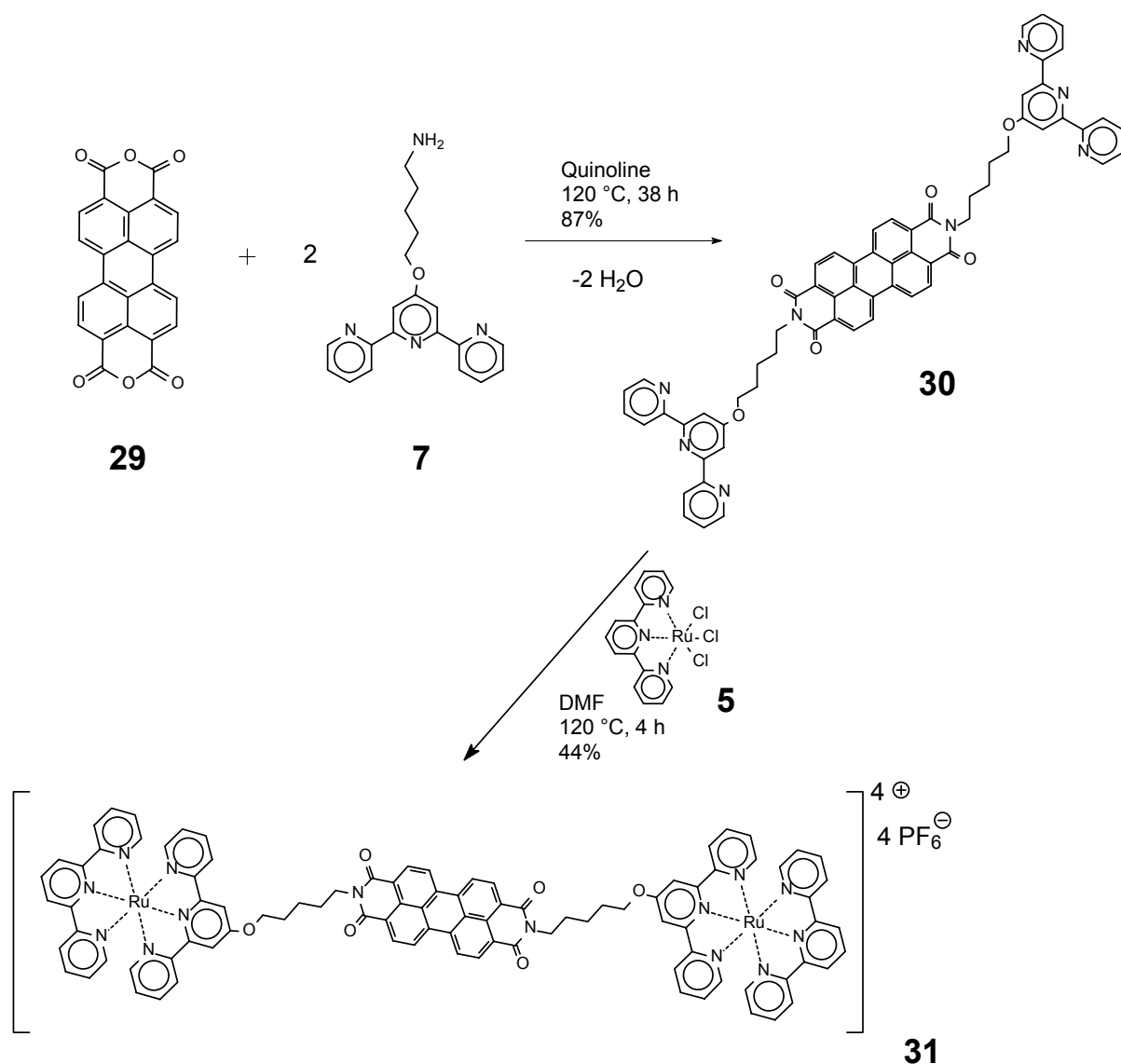


Figure 2.8. Temperature dependent luminescence of bis-terpyridine-ruthenium(II) hexafluorophosphate due to thermally activated nonradiative deactivation via the  $^3MC$  states.

At room temperature the ruthenium(II) of unfunctionalized terpyridine complex does not show luminescence, whereas a long living luminescence around 600 nm appears with decreasing temperature (Figure 2.8). In contrast to previously reported examples, where rigid-glass-matrices were utilized, a confocal setup was used for this experiment.<sup>[7]</sup> The sample was measured in solid state on a quartz glass substrate and the measurement setup was cooled down to 5 K in steps of 50 K.

In another experiment, a room-temperature-fluorescent perylene moiety was introduced (for a different approach towards such perylene-terpyridine compounds see ref.<sup>[33]</sup>): perylenetetracarboxylic dianhydride **29** has been reacted with the amino-functionalized 2,2':6',2''-terpyridine **7** in quinoline yielding the bis-terpyridine-terminated perylene dye **29** in 87% yield (Scheme 2.5). Compound **30** could be characterized in detail using NMR (in d-TFA), elemental analysis and MALDI-TOF mass spectrometry. Addition of the preformed terpyridine-ruthenium(III) complex **5** to ligand **30** resulted in the bis-terpyridine-ruthenium(II) complex **31** in 44% yield (after anion exchange with hexafluorophosphate counterions).



Scheme 2.5. Schematic representation of the synthesis of the perylene-containing terpyridine ruthenium(II) complex **31**.

The complex **31** with a molar mass of 2273 g/mol could be detected without fragmentation with MALDI-TOF mass spectrometry (Figure 2.9, bottom,  $M^+$  without the four hexafluorophosphate counterions; all species are singly charged, for this phenomenon see also ref.<sup>[26]</sup>). In addition, NMR proved the existence of the *bis*complex **31**.

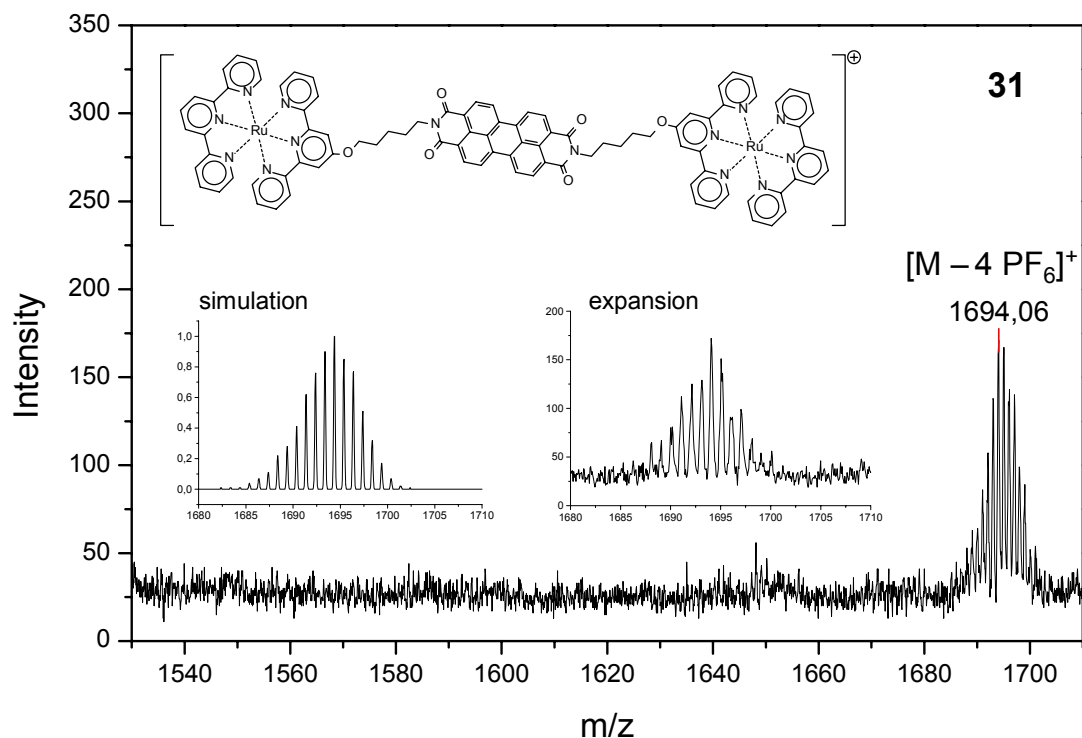


Figure 2.9. MALDI-TOF mass spectrum of the perylene terpyridine complex **31**.

The UV-vis spectrum clearly revealed the characteristic absorption bands of the perylene (Figure 2.10). It should be mentioned that the spin-allowed metal-to-ligand charge-transfer transition (MLCT) of the ruthenium terpyridine complex at about 480 nm lies beneath the perylene absorption in **31**. Perylene is known to be fluorescent at room temperature. The emission spectrum (insert in Figure 2.10) shows the emission maximum at 545 nm.

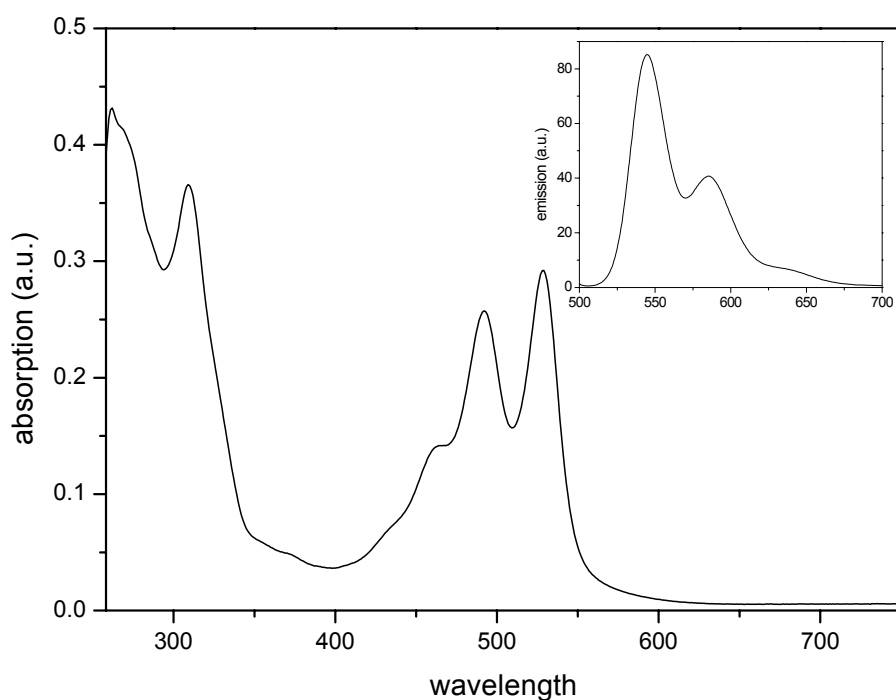


Figure 2.10. UV-vis absorption and fluorescence emission (insert) spectrum of the perylene complex **31** (DMSO).

## 2.5 Chiral terpyridine-ruthenium complexes: Supramolecular aggregates

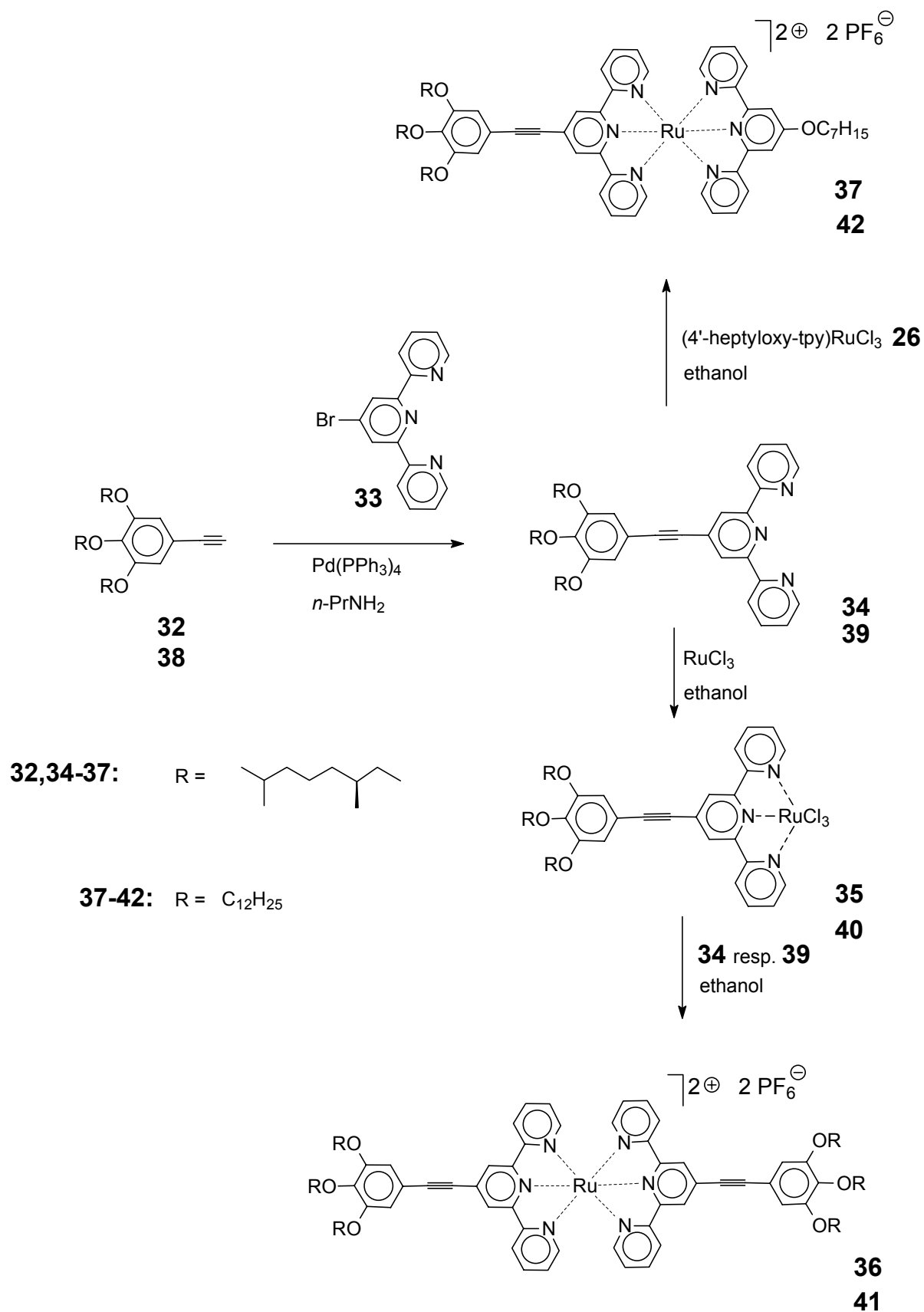
Spontaneous self-organization processes<sup>[1]</sup> of functional molecules into nanostructured assemblies are of growing interest due to their potential application in nanotechnology. Non-covalent interactions such as hydrogen-bonding,<sup>[29]</sup>  $\pi$ -interaction<sup>[34]</sup> or metal coordination<sup>[35]</sup> are utilized to form various types of aggregates. Chiral non-covalent compounds are an important research-field on the way to new materials. Among the recent examples are dimers of ureido-triazines carrying chiral trialkoxybenzene chains, formed by self-complementary quadruple hydrogen bonding, which subsequently assembled to helical columnar aggregates in apolar solvents.<sup>[28]</sup>

Chiral terpyridines are of special interest due to their ability of forming stable complexes with many transition metal ions (see before). The resulting complexes are promising materials due to their specific electrochemical, photophysical and photochemical properties (see chapter 1).<sup>[7,36]</sup> Few attempts to obtain chiral terpyridine complexes have already been described.<sup>[37,38]</sup> However, in most of these systems, the chiral groups were directly connected to the aromatic pyridine rings by fused terpene or pinene rings. In this way, distorted terpyridine moieties were obtained leading therefore to chiral distorted complexes. In addition, attempts have been undertaken to introduce chirality into moieties, which are connected via a single bond to the terpyridine.<sup>[39]</sup> However, transfer of chiral information to the complex core was minimal. In our approach, the chirality is located in the lateral alkyl chains of a 4'-phenylethynyl substituted terpyridine.<sup>[40]</sup>

In this section the synthesis of the chiral ligand and the subsequent formation of corresponding symmetric and asymmetric ruthenium(II) complexes as well as their supramolecular helical aggregation is described in detail. The obtained results are compared to the analogous achiral compounds.

### 2.5.1 *Synthesis and characterization*

In order to obtain complexes which could form helical aggregates in non-polar solvents, a rigid terpyridine ligand bearing chiral groups was synthesized by palladium cross-coupling between a trialkyloxybenzyl-alkyne **32** with 4'-bromo-2,2':6',2''-terpyridine **33** (Scheme 2.6).



Scheme 2.6. Schematic representation of the synthesis of the ruthenium(II) complexes 36, 37, 41 and 42.

The obtained compound 4'-[3,4,5-*tris*-(3,7-dimethyl-octyloxy)-phenylethynyl]-2,2':6,2''-terpyridine **34** was purified by column chromatography (alumina) and characterized by NMR, UV-vis, MALDI-TOF-MS and elemental analysis. Subsequently, the ligand was complexed with ruthenium(II)-ions. The Ru(III) *mono*-complex **35** was obtained as intermediate by reacting ligand **34** with RuCl<sub>3</sub>. Subsequently, a second equivalent of **34** was added under reductive conditions in refluxing ethanol containing *N*-ethylmorpholine. The pure compound **36** was isolated after exchange of the counterions by NH<sub>4</sub>PF<sub>6</sub> and preparative size exclusion on a Bio-Beads column.

Applying the ruthenium(III/II) chemistry, asymmetric terpyridine complexes are accessible in a directed way in a two-step reaction. The Ru(III)-*mono*-complex of heptylterpyridine **26**<sup>[41]</sup> was reacted with ligand **34**, leading to the asymmetric complex **37** under the same conditions as described above. In this case the complex was purified by recrystallization from acetonitrile/diethyl ether. Analogous symmetric and asymmetric complexes were prepared, where the chiral chains were replaced by achiral dodecyl-groups.

The UV-vis absorption spectra of the four complexes (in acetonitrile) are characterized by intense absorption bands attributed to the  $\pi$ - $\pi^*$  transitions associated with the aromatic rings of the ligands, which confirms for all cases the successful complex formation. Moreover, metal to ligand charge transfer (MLCT) transitions were observed for the ruthenium complexes at around 500 nm (Figure 2.11).

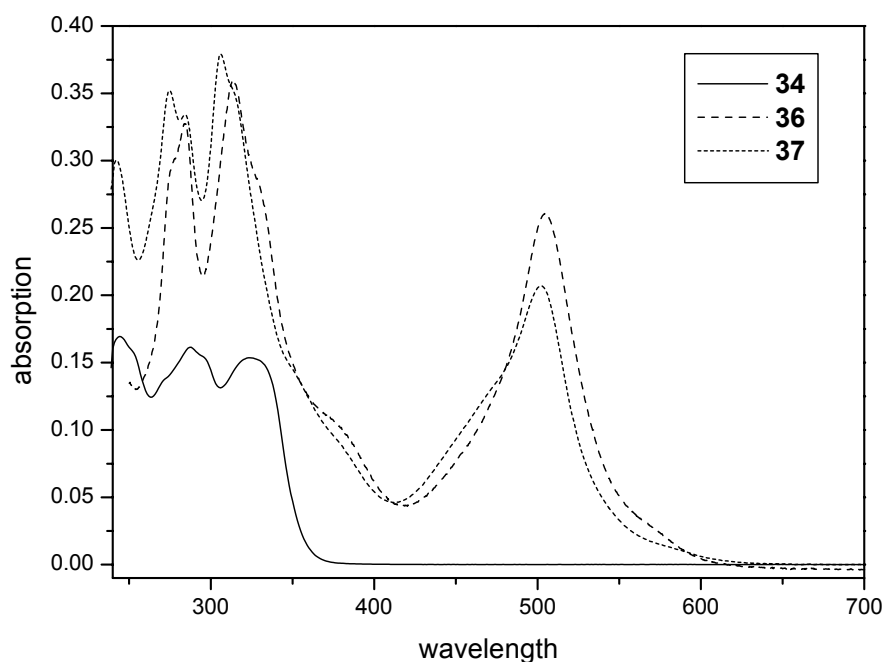


Figure 2.11. UV-vis spectra of **34**, **36** and **37** (in chloroform).

<sup>1</sup>H-NMR also demonstrated the successful formation of the complexes (Figure 2.12). The signals for the aromatic protons of the terpyridine rings can be found in the region from 7 to 9 ppm. A characteristic upfield shift of the peaks for the 6,6''-protons can be found when comparing the spectra of the ligands with the corresponding complexes. The OCH<sub>2</sub>-signals

can be found at 4 to 4.5 ppm and the aliphatic resonances between 0.8 and 2.3 ppm. Utilizing  $^1\text{H}$ ,  $^1\text{H}$ -COSY-NMR spectroscopy, the pattern of the asymmetric complexes could be interpreted and the signals assigned (Figure 2.13 and experimental part).

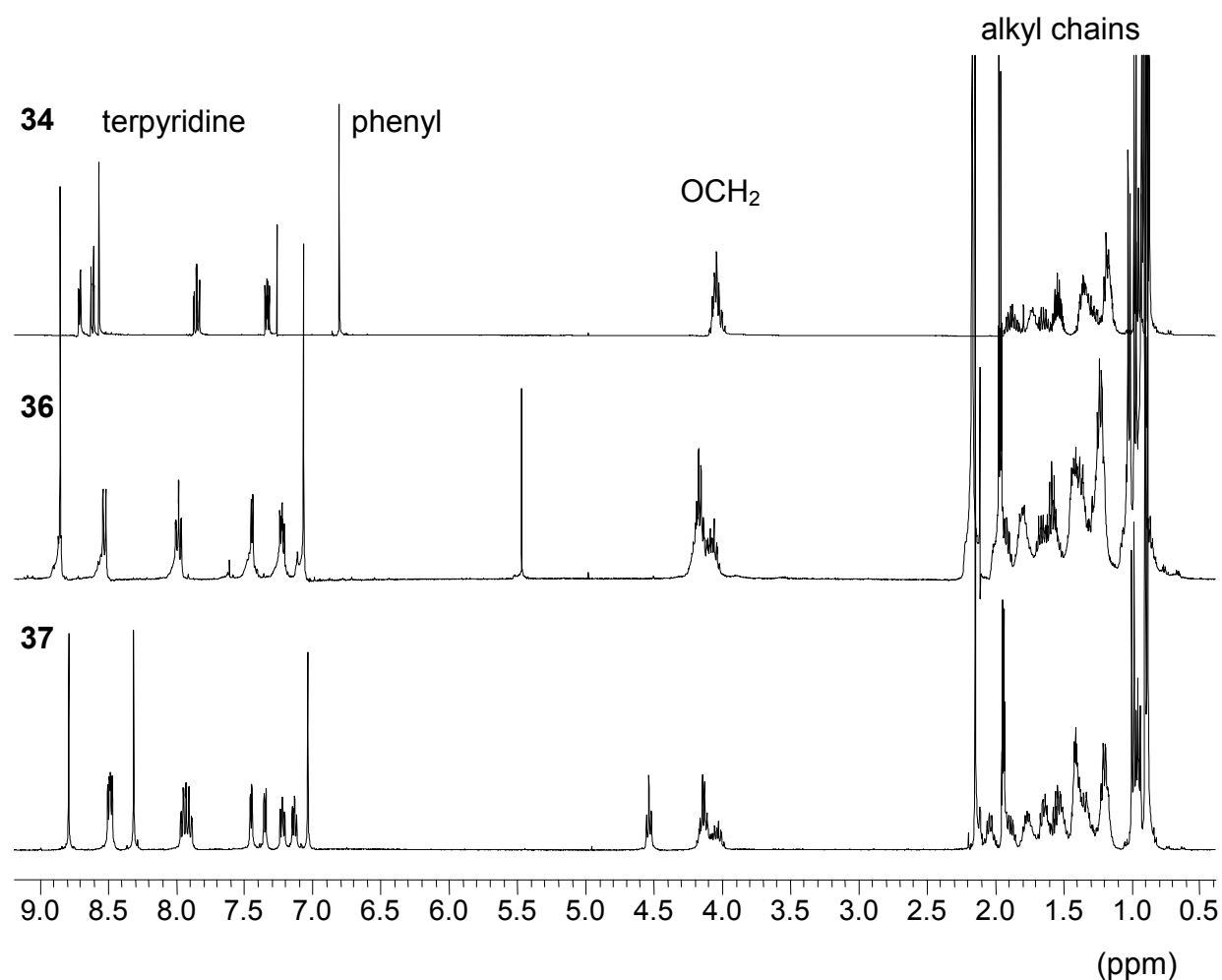


Figure 2.12.  $^1\text{H}$ -NMR spectra of ligand **34** (chloroform) and the complexes **36** and **37** (in acetonitrile).



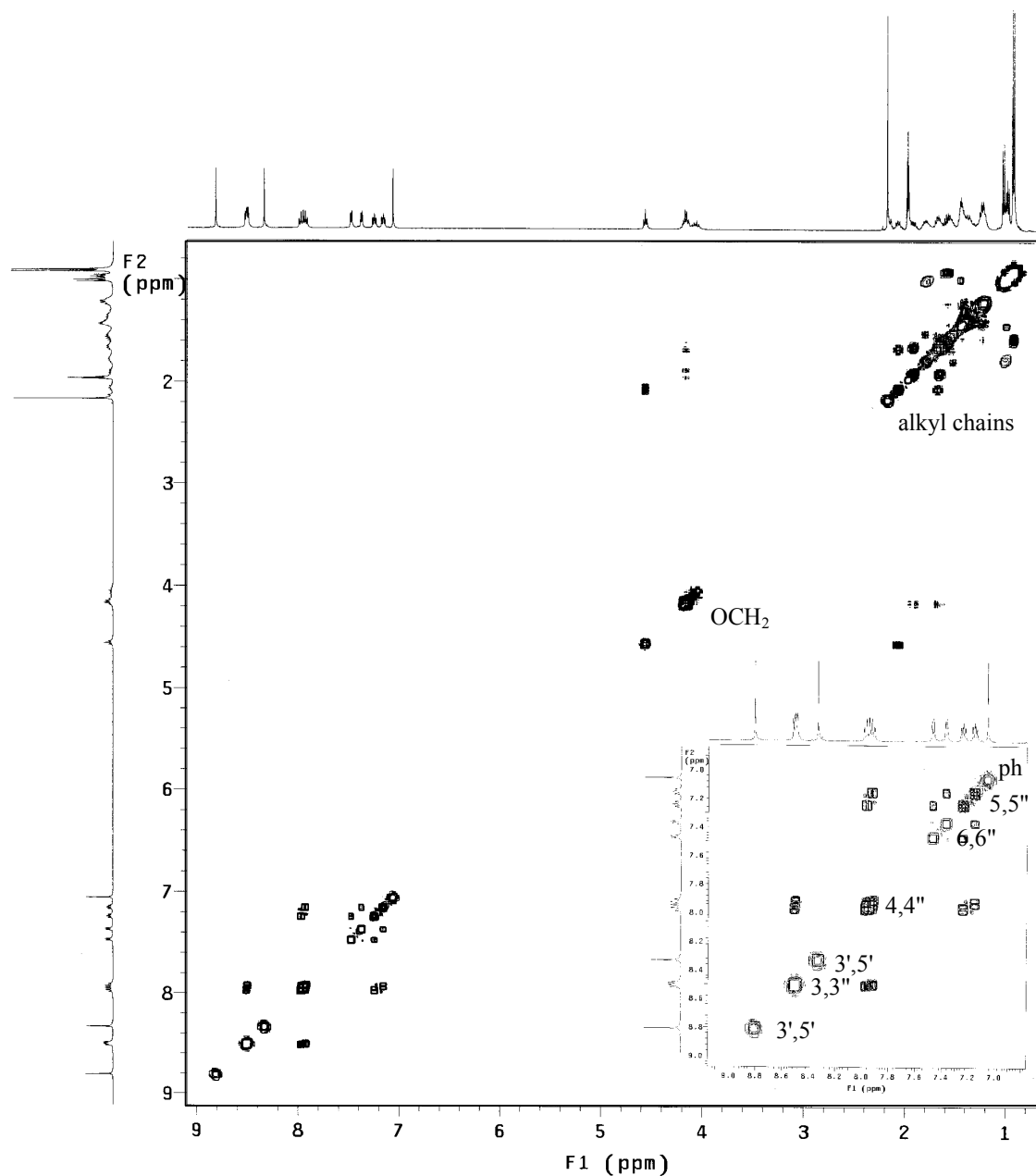


Figure 2.13.  $^1\text{H}$ -COSY-NMR spectrum of complex **37** (acetonitrile).

MALDI-TOF mass spectrometry is an excellent tool for proving the existence of such complexes.<sup>[22]</sup> Besides the unfragmented complex cations, also ion pairs of the cation with one  $\text{PF}_6^-$ -counterion were observed for **36** and **37** (Figure 2.14). All detected species carry the charge +1 (for this effect see ref.<sup>[26]</sup>). Furthermore, in electrospray-mass spectrometry both the singly as well as the doubly charged species were observed.

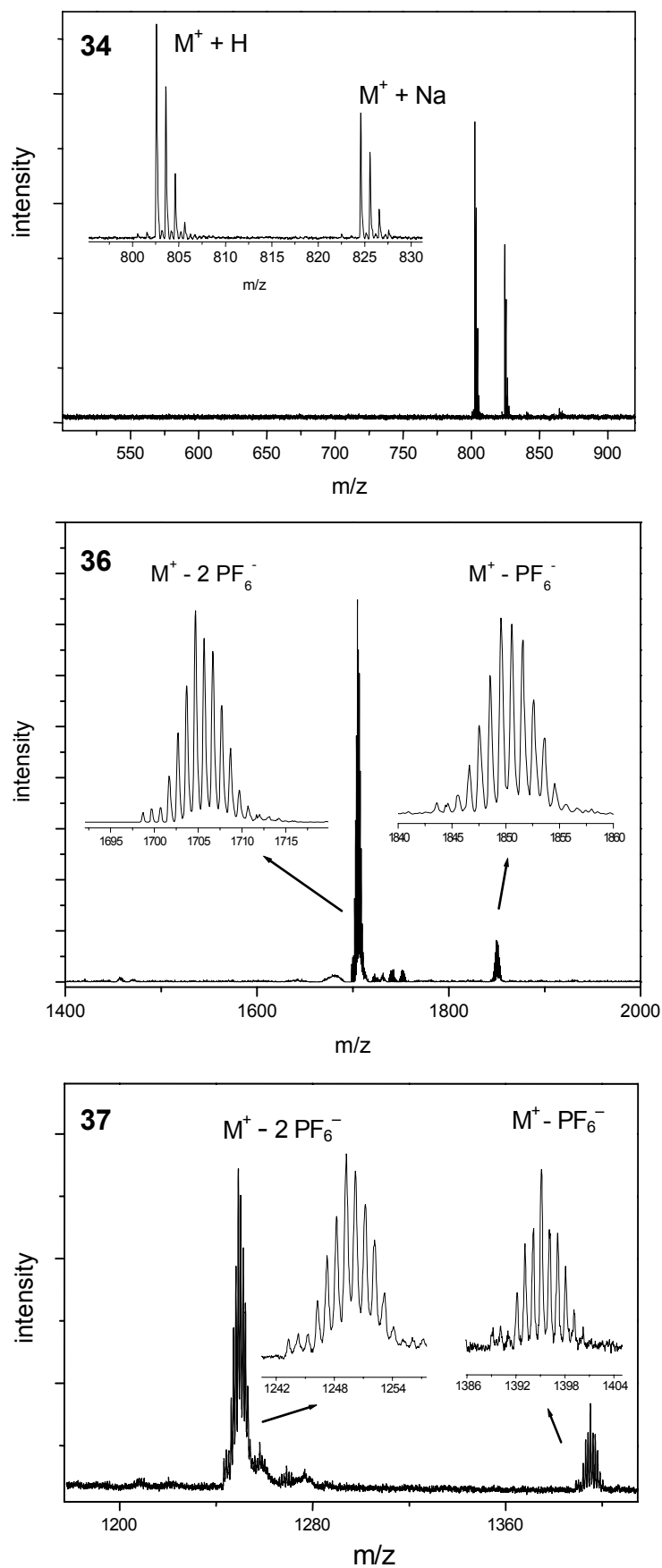


Figure 2.14. MALDI-TOF-MS of ligand 34 and the complexes 36 and 37 (matrix: dithranol).

### 2.5.2 Circular dichroism spectroscopy

In order to investigate the chiral characteristics of the ligand as well as of the complexes, UV-vis and circular dichroism (CD) measurements were performed. In acetonitrile and in chloroform no CD effect was found, suggesting that both the ligand and the complexes are molecularly dissolved and therefore no transfer of chiral information to the UV-active parts (the complex) is present.

To study the formation of chiral aggregates, dodecane as a less good solvent for the terpyridine metal complexes was employed in order to stimulate aggregation of the complexes.<sup>[28]</sup> A UV-vis spectrum of **36** in dodecane revealed a small shift of the absorption bands from 505 nm (chloroform) to 502 nm (dodecane). CD spectroscopy was performed on the ligand **34** as well as on the complexes **36** and **37**. In the case of the free ligand, no Cotton effect was observed, corresponding to an absence of aggregation processes. In contrast to these findings, the complexes showed a different behavior: a strong CD effect was detected for the complexes **36** and **37** (Figure 2.15).

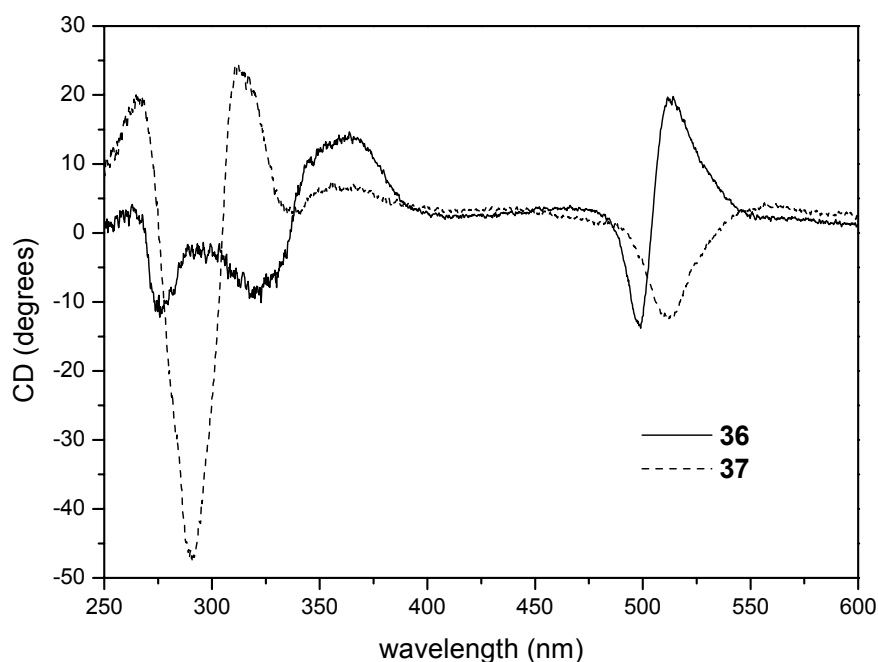


Figure 2.15. CD spectrum of **36** and **37** (dodecane, room temperature).

The effect appeared at the absorption bands of the ligand as well as the MLCT-bands. This suggests that the chirality of the side-chains can be transferred to the metal center, inducing chirality into the whole complex. Due to the aggregation, the geometry at the metal center is distorted in a chiral fashion. Such a behavior of a CD effect initiated by aggregation, involving metal centers, has been found in helical platinum "wires".<sup>[42]</sup> In the case of the symmetric complex **36**, a bisignate CD effect was found: at the maxima of the UV-bands, the CD signals are changing from positive to negative values, with positive values at higher and negative values at lower wavelengths than the absorption maxima. This behavior indicates an exciton coupling and suggests the presence of right-handed helical aggregates for the complex

**36**,<sup>[42,43]</sup> probably by intermolecular  $\pi$ -stacking of the aromatic groups. In addition, hydrophobic interactions of the alkyl groups may play a role. On the other hand, complex **37** possesses only one chiral ligand and furthermore lacks one moiety that is able to undergo stacking. Therefore, chiral aggregates of a different architecture can be expected, as shown by the different (non-bisignate) CD spectrum of compound **37**, where no exciton coupling was found. In addition, a different UV-vis behavior was observed: a small shift of the MLCT-band from 502 nm (in chloroform) to 504 (dodecane) was found.

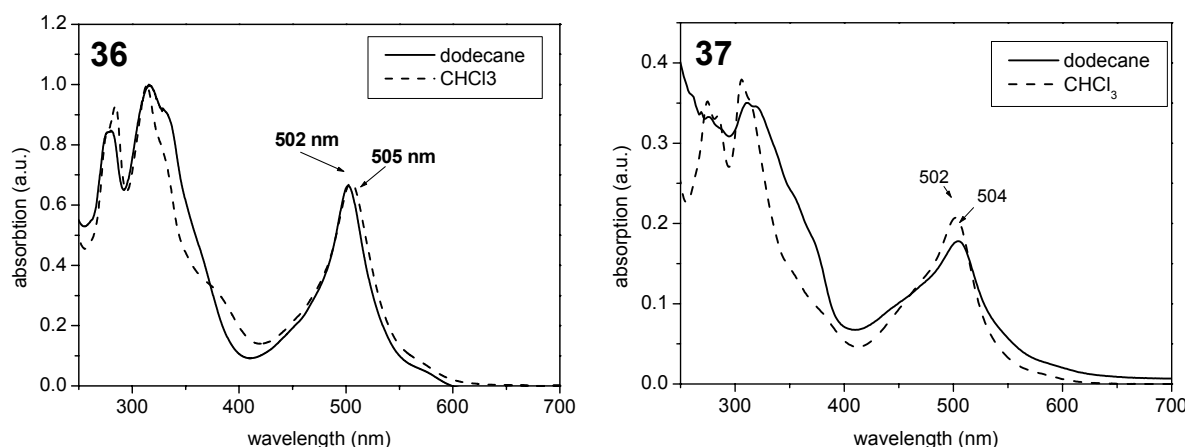


Figure 2.16. UV-vis spectra of the complexes **36** (right) and **37** (left) in dodecane and chloroform, respectively.

CD spectroscopy at higher temperatures showed that the aggregates of complexes **36** and **37** are stable up to 110 °C (Figure 2.17). The stepwise addition of chloroform to the dodecane solution resulted in a stepwise decrease of the CD effect (Figure 2.18). This indicates a subsequent breakup of the aggregates upon chloroform addition.

The corresponding achiral complexes **41** and **42** did not reveal any CD effect. In order to investigate if a similar aggregation is taking place, the absorption spectra of both complexes were recorded in dodecane. The comparison clearly showed as expected similar absorption spectra as in the case of **36** and **37** that suggest the same aggregation behavior for both chiral and achiral complexes. These results provide the evidence that the chirality is indeed induced exclusively by the chiral side chains and that the chirality is transferred to the complex moiety, caused by aggregation of the complexes.

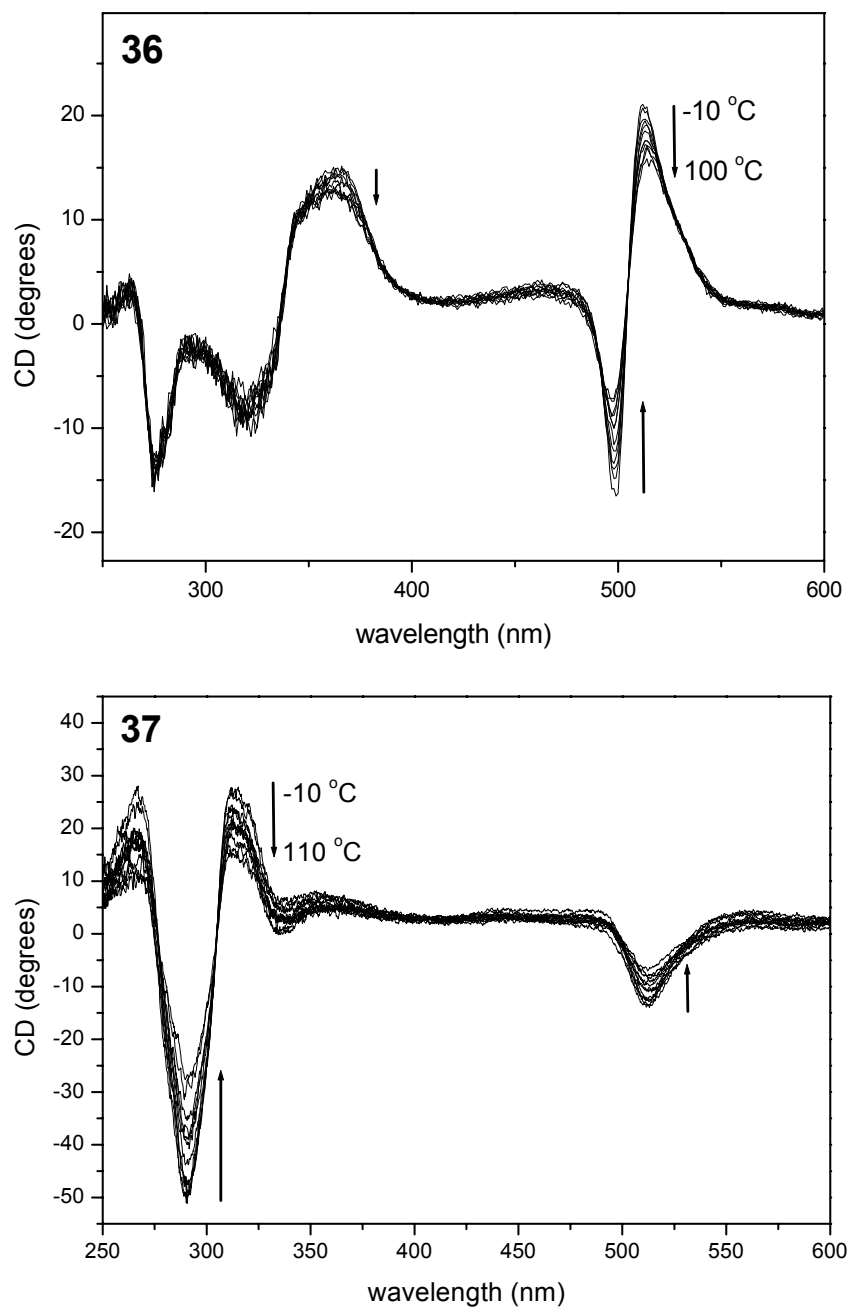


Figure 2.17. Temperature dependant ( $-10$  to  $110$  °C) CD measurements of **36** and **37** (dodecane), showing a decrease in the intensity of the CD-signal (arrow).

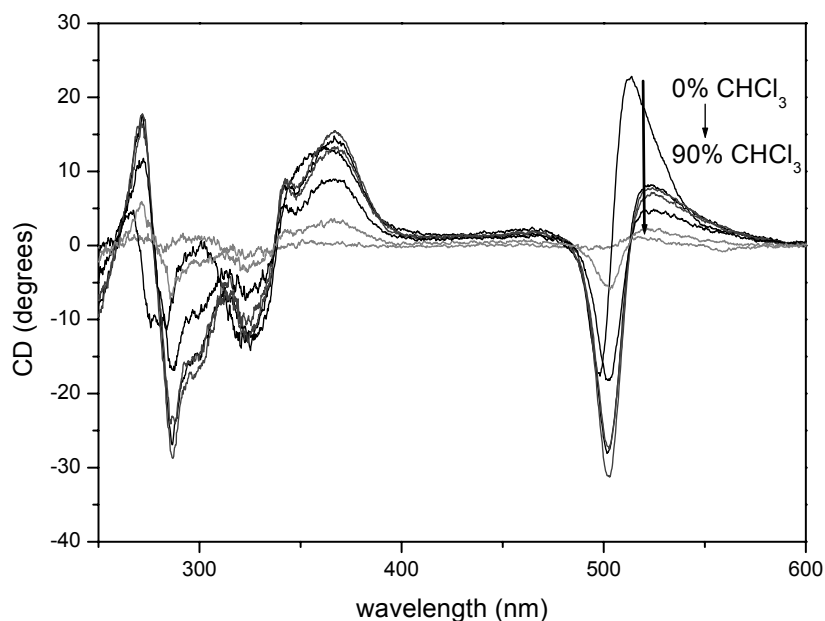


Figure 2.18. Solvent dependant CD measurements of **36** (dodecane  $\rightarrow$  chloroform).

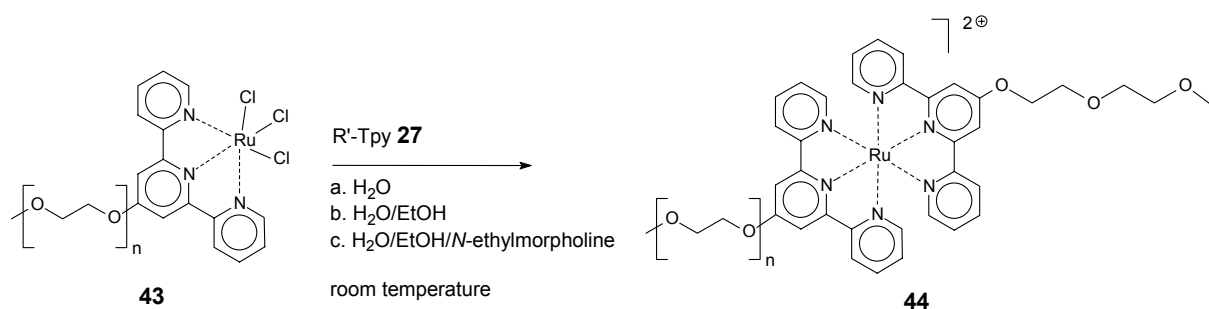
## 2.6 Kinetic studies of the formation of the ruthenium complexes in water

Bioreactions and biocompatible reactions are usually carried out in aqueous solutions. Because proteins are often degrading at elevated temperatures, room temperature is normally applied to this kind of reactions. The chemistry of terpyridine ruthenium complexes is a promising method to obtain novel materials, for example the combination of supramolecular chemistry with polymer chemistry or even biochemistry. Thus attempts were undertaken to make this reaction compatible to biomolecules by changing from alcoholic to aqueous solutions and avoiding the need of heating the mixture.

For this purpose, water-soluble educts were utilized and the complex formation was monitored by means of UV-vis spectroscopy. The intensity of the absorption band at 483 nm was used to obtain kinetic data. In all reactions, a solution of 4'-( $\omega$ -methoxy-poly(ethylene glycol))-terpyridine ruthenium(III) trichloride **43** ( $M_n = 3400$ ) and 4'-(methoxy di(ethylene glycol))-2,2':6',2''-terpyridine **27** in water was stirred at room temperature (Scheme 2.7). Three different reactions were performed:

- no more ingredients were added, the reaction was performed in pure water.
- 0.1 mL ethanol was added.
- 0.1 mL ethanol and 1 drop of *N*-ethylmorpholine were added.

In regular intervals a sample was taken from the solution and a UV-vis spectrum was recorded. In all three reactions, a complexation to compound **44** took place. The characteristic bathochromic shift of the ligand-centered absorptions could be detected.



*Scheme 2.7. Formation of the Ru(II) terpyridine complex 44 in aqueous solution.*

Furthermore, the metal-ligand charge transfer band characteristic for terpyridine ruthenium(II) complexes was observed. An increase of this band during the reaction was seen. The UV-spectra are shown in Figure 2.19 and the absorption of the MLCT band with time is plotted in Figure 2.20. Even in pure water, the appearance of the complex bands can be observed. However, the reaction is very slow: after 6 days the conversion is about 65% (32% after 2 days). Addition of 5% ethanol, which acts as reducing agent for Ru(III), increases the reaction speed significantly. After two days 50% conversion is reached and after 8 days the reaction is completed. The most remarkable increase can be observed after addition of *N*-ethylmorpholine. In this case, 80% of the reaction is completed after 8 hours and 100% conversion occurred after 48 hours.

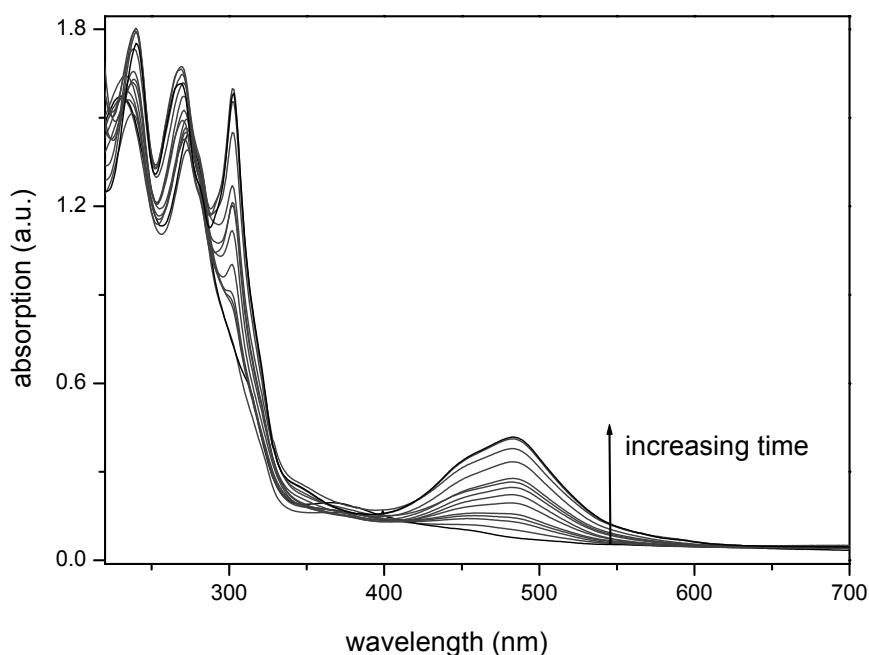


*Figure 2.19. UV-vis spectra of the monitoring of reaction b (in water/ethanol 95:5).*

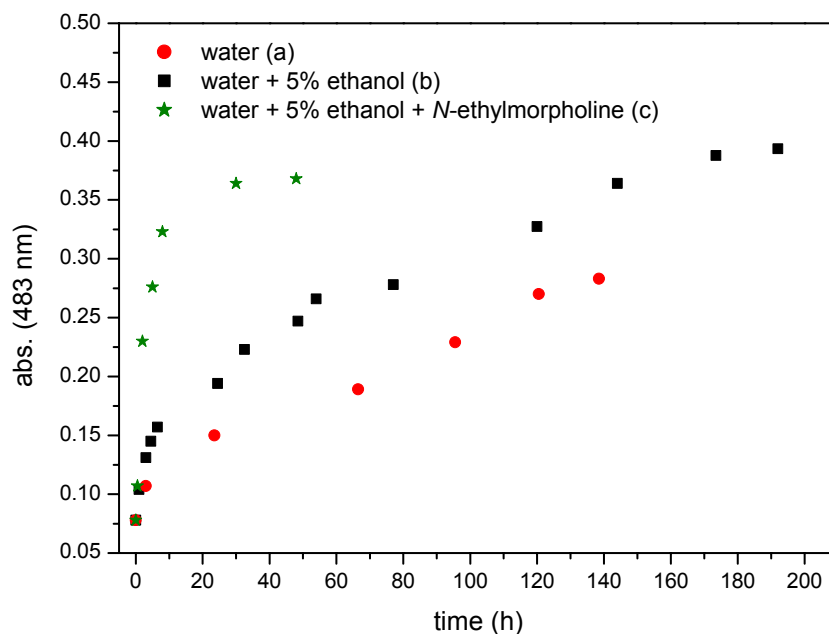


Figure 2.20. Kinetic curves of the complexation of ruthenium-terpyridine in water.

## 2.7 Asymmetric bipyridine-terpyridine-copper(II) complexes: a different approach for supramolecular architectures

Up to now, the directed synthesis of asymmetric terpyridine complexes utilizing the ruthenium(III)/(II)-chemistry<sup>[9a,44]</sup> has been discussed, which is the most commonly known method for the preparation of terpyridine-based supramolecular systems.

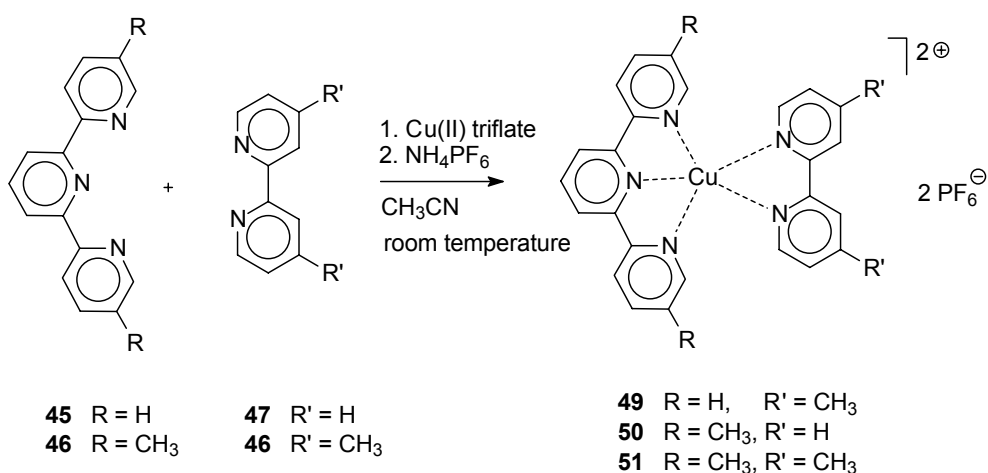
Another approach to asymmetric complexes utilizes copper ions. It has been shown that copper(II) forms asymmetric complexes with one terpyridine and one bipyridine ligand, leading to a pentacoordinated metal center.<sup>[45]</sup> In this case, the desired complex can be formed in one step by simply adding stoichiometric amounts of both ligands to a solution of copper(II) triflate (also a two-step reaction has been performed to obtain the complexes<sup>[45a]</sup>). The asymmetric complex can be isolated in nearly quantitative yields. This approach has already been applied to obtain helical compounds, where a *tris*-terpyridine ligand and a *tris*-bipyridine ligand have been assembled to a trinuclear complex.<sup>[46]</sup> In order to construct even more complex metallo-supramolecular architectures based on this connection system, a detailed knowledge of the influence of substituents onto the complexation behavior is a prerequisite. For this purpose, several complexes of methyl-functionalized ligands have been synthesized, characterized and their structure investigated by X-ray analysis. The methyl groups allow a future functionalization and therefore the implementation into extended assemblies and polymers.

### 2.7.1 Synthesis and characterization of the copper complexes

An important aspect on the way towards novel supramolecular assemblies is represented in the directed synthesis of asymmetric complexes of functionalized chelate ligands. In this



section the formation of copper(II) complexes containing one terpyridine and one bipyridine chelating ligand is described. The bipyridines as well as unfunctionalized terpyridine was commercially available. 5,5''-Dimethyl-2,2':6',2''-terpyridine has been synthesized in a Stille-type coupling reaction of two equivalents of 5-methyl-2-tributylstannyl pyridine with 2,6-dibromopyridine.<sup>[47]</sup> To obtain the complexes, a solution of copper(II) triflate in acetonitrile was added at room temperature to an equimolar mixture of the ligands in acetonitrile (Scheme 2.8).



*Scheme 2.8. Synthesis of the complexes 49-51.*

A sudden appearance of a blue color indicated an instant complex formation and the exclusive formation of the asymmetric species in solution has been found earlier by thermodynamic investigations.<sup>[45b]</sup> The complexes were precipitated after exchange of the counterions with hexafluorophosphate and addition of diethyl ether. A blue powder was obtained, which was recrystallized through diffusion of diethyl ether into an acetonitrile solution. Large plate-shaped deep blue crystals were obtained in all cases with yields of around 80%. UV-vis spectroscopy showed the ligand-centered band from 270 to 340 nm. At around 644 nm a weak metal-to-ligand charge transfer band (MLCT) was observed (Figure 2.21), which is consistent with the literature values.<sup>[45a]</sup>

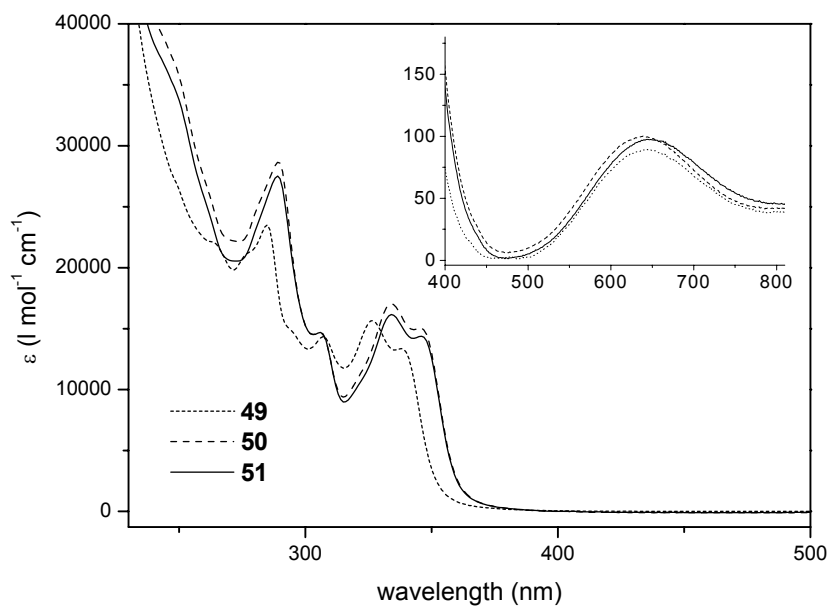


Figure 2.21. UV-vis spectra of the complexes **49-51** (in acetonitrile).

The successful formation of the asymmetric complexes could be confirmed by MALDI-TOF mass spectrometry (Figure 2.22). In all cases, the cation carried a singly positive charge. This effect was already observed earlier for *bis*-terpyridine complexes (see ref.<sup>[26]</sup>). Furthermore, the purity was proven by elemental analysis.

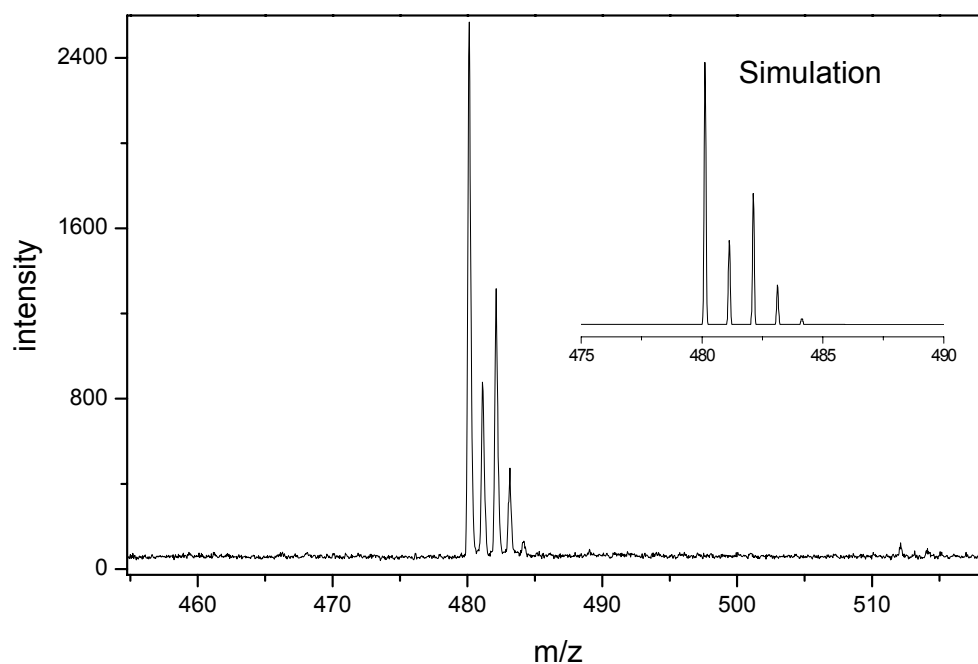


Figure 2.22 MALDI-TOF-MS of **49** (matrix: dithranol).

### 2.7.2 X-ray structure analysis

X-ray analysis was utilized in order to determine the crystal structure of the complexes. For all complex cations, a (distorted) square-pyramidal coordination of the N-atoms was found with N-Cu-N bond angles around  $80^\circ$  within the chelate ligands (Figure 2.23). The sixth

coordination site was occupied by a loosely coordinated PF<sub>6</sub>-counterion. Another possible configuration of pentacoordinated complexes would be a trigonal bipyramid. However, it is less favorable for these types of chelate complexes because of the binding angles set by the chelate ligands.<sup>[45a]</sup> This geometry would require N-Cu-N bond angles of 90° (as for the square pyramid) for the terpyridine, but 120° for the bipyridine ligand, requiring a stronger distortion of this ligand. Nevertheless, this geometry has been found in the crystal structure of the helical assembly<sup>[46]</sup> for the central complex unit of the trinuclear array and probably arises from the predetermined geometry of the helical assembly. On the other hand, the peripheral complex units show a similar square-pyramidal coordination as found for the mononuclear complexes. Triflate ions were used as counterions. Though not explicitly mentioned in the publication, a similar loose coordination can be expected. The square-pyramidal geometry has also been suggested earlier, deduced from electron resonance spectroscopy.<sup>[45b]</sup>

In the case of compound **49**, an acetonitrile solvent molecule was found in the crystal unit. Complexes **49** and **50**, which contain one cation per unit cell, showed only little influence of the position of the methyl group onto the structure. However, complex **51**, which contains two methylated ligands, possesses a different structure: in the unit cell, two complex cations are linked via one PF<sub>6</sub>-counterion (Figure 2.23, bottom). This different structure is probably derived from a different spatial demand of this complex. The coordination geometry of the metal center is similar as for the complexes **49** and **50**, showing no influence of the substituents.

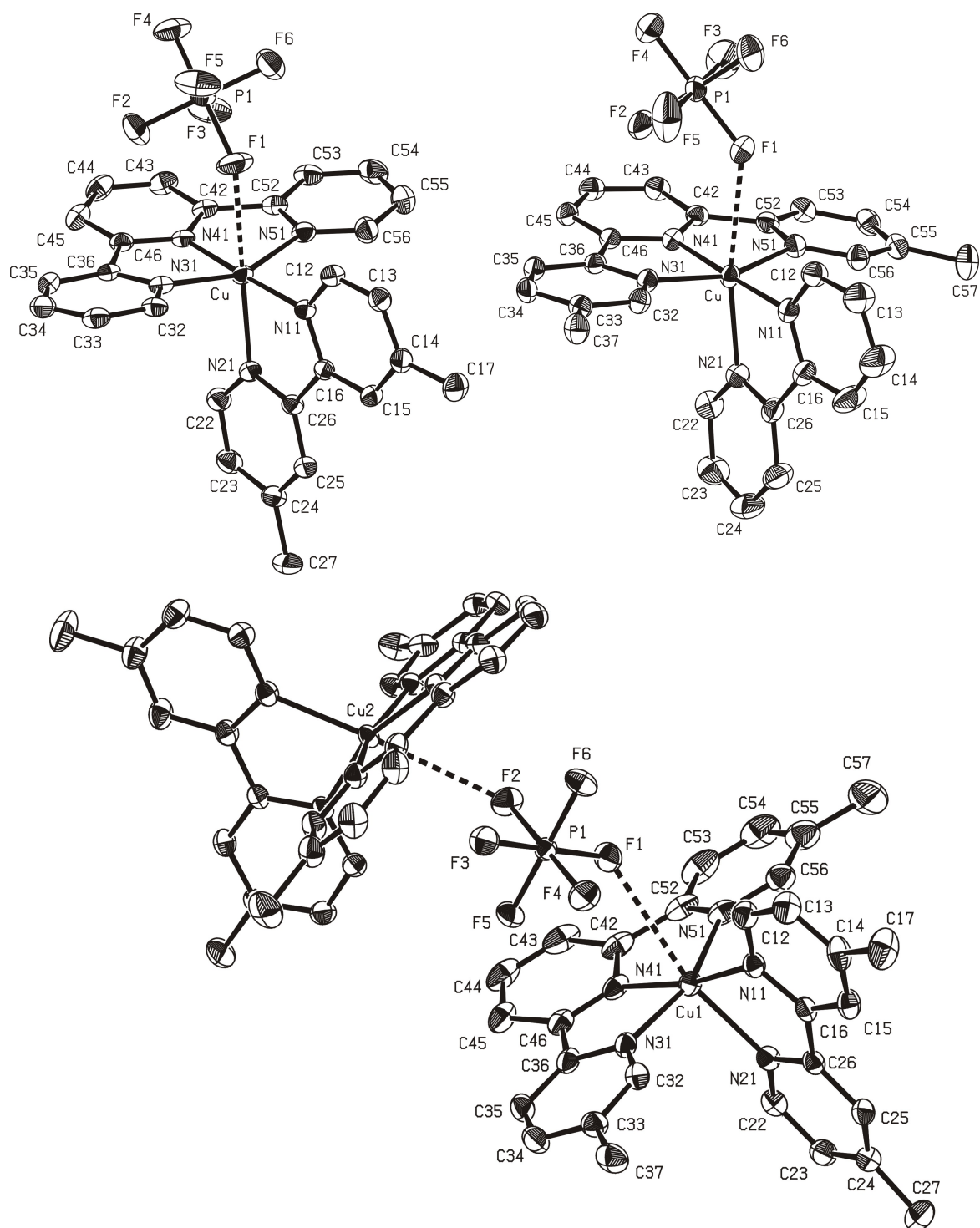


Figure 2.23 X-ray structure of the copper complexes **49** (top left), **50** (top right) and **51** (bottom). Thermal ellipsoids are drawn at the 50% probability level. Hydrogen atoms are omitted for clarity.

## 2.8 Conclusions

In this part of the work, functional terpyridine ligands were synthesized, followed by the subsequent preparation of their corresponding complexes. First, asymmetric terpyridine

ruthenium(II) complexes were prepared as models for supramolecular systems and polymers, utilizing ruthenium(III)/(II) chemistry. A variety of different functional groups was introduced into these complexes following this strategy. The compounds were characterized by UV-vis, MALDI-TOF-MS and NMR including  $^1\text{H}$ - $^1\text{H}$ -COSY spectroscopy and X-ray analysis. Subsequently, chiral terpyridine ruthenium(II) complexes were synthesized and their aggregation into chiral assemblies was investigated in detail utilizing CD-spectroscopy. Finally, mixed terpyridine-bipyridine-copper(II) complexes were prepared as a different approach towards defined supramolecular assemblies by metal complexation.

## 2.9 Experimental part

### Materials and instrumentation

Basic chemicals were obtained from Sigma-Aldrich. 2,6-Bis-(pyrid-2-yl)-4-pyridone was synthesized according to ref.<sup>[13b]</sup>. 4'-(2-[1-Methoxyethoxy]ethoxy)-2,2',6',2''-terpyridine (**27**) is described in ref.<sup>[41]</sup>. Compound **5** was synthesized according to a literature procedure.<sup>[48]</sup> The 4'-functionalized terpyridines were synthesized from 4'-chloro-2,2':6',2''-terpyridine<sup>[13b]</sup> as described elsewhere (**6** see ref.<sup>[49]</sup>, **7-9** see ref.<sup>[16]</sup>, **14** see ref.<sup>[50]</sup> and **15** see ref.<sup>[51]</sup>). Ligand **16** was available commercially and used as received. The acetylenes **32** and **38** have been synthesized as described elsewhere.<sup>[52]</sup> Preparative size exclusion chromatography was carried out on BioBeads SX1 columns ( $\text{CH}_2\text{Cl}_2$ ).

NMR spectra were recorded on a Bruker ARX 300 ( $^1\text{H}$ : 300 MHz,  $^{13}\text{C}$ : 75 MHz) and on a Varian Mercury 400 ( $^1\text{H}$ : 400 MHz,  $^{13}\text{C}$ : 100 MHz) NMR spectrometer. The chemical shifts were calibrated to the residual solvent peaks. UV-vis spectra were recorded on a Varian Cary 50 and on a Perkin Elmer Lambda-45 (1 cm cuvettes), and IR spectra were measured on a Bruker IFS55 FT-IR spectrometer (KBr tablets) or a Perkin Elmer Spectrum-1 ATR-FT-IR-spectrometer. Low temperature fluorescence measurements were performed using a confocal setup equipped with a helium-cryostat; detection was carried out by a Princeton Instr. CCD using a two minute integration time and an Actron 0.2 m spectrometer. An optical excitation power of 80 mW/cm<sup>2</sup> with a wavelength of 400 nm was supplied by a frequency doubled 120 fs pulsed laser system (Coherent Mira900). The solid state samples were prepared by drying a 10  $\mu\text{L}$  drop of 0.1 mol solution on a non-fluorescent quartz glass substrate. Solution fluorescence has been performed on a Perkin Elmer LS 50B luminescence spectrometer (1 cm cuvettes). MALDI-TOF mass spectra were recorded on a Bruker Biflex II and on a BioSystems Perseptive Voyager 2000 instrument with dithranol as matrix. Elemental analyses were measured on a Perkin Elmer Series II 2400 and melting points were obtained from a Büchi Melting Point B-540. CD-measurements were carried out on a Jasco J600 CD-machine and DSC investigations have been performed on a Perkin Elmer Pyris-1 DSC system with a heating rate of 40 K/min ( $T_g$ ).

### 4'-Heptyloxy-2,2':6',2''-terpyridine **2**

$\text{K}_2\text{CO}_3$  (3.5 g, 2.5 mmol) and **1** (3.15 g, 12.7 mmol) were mixed with 25 mL DMF and heated to 90 °C for 30 min. Then 1-bromoheptane (2.06 g, 11.5 mmol) in 12 mL DMF was added dropwise to the mixture and stirring was continued overnight. The resulting mixture was poured into water and extracted with 3  $\times$  25 mL chloroform. After drying the organic layer with  $\text{Na}_2\text{SO}_4$  the product was purified by column chromatography (alox N,  $\text{CHCl}_3$ ) to yield 3.0 g (68%) of compound **2**; mp 64 °C.

UV-vis ( $\text{CH}_3\text{CN}$ ):  $\lambda_{\text{max}}$  ( $\epsilon$ ) = 277 (25300), 240 nm (27900) nm ( $\text{L mol}^{-1}\text{cm}^{-1}$ ).

IR (ATR):  $1/\lambda$  ( $\text{cm}^{-1}$ ): 2941, 2920, 2867, 2853 (C-C); 1597, 1580, 1562 (C=C, C=N, terpyridine).

$^1\text{H}$ -NMR (400 MHz,  $\text{CDCl}_3$ ):  $\delta$  = 0.90 (3 H, t,  $J$  = 6.59 Hz,  $\text{H}_a$ ), 1.36 (6 H, m, H-alkyl), 1.50 (2 H, m, H-alkyl), 1.85 (2 H, m, H-alkyl), 4.22 (2 H, t,  $J$  = 6.59 Hz,  $\text{H}_b$ ), 7.32 (2 H, ddd,  $J$  = 8.1, 5.1, 1.5 Hz,  $\text{H}_{5,5''}$ ), 7.84 (2 H, ddd,  $J$  = 8.1, 8.1, 1.5 Hz,  $\text{H}_{4,4''}$ ), 8.01 (2 H, s,  $\text{H}_{3,5}$ ), 8.62 (2 H, dd,  $J$  = 8.1, 1.5 Hz,  $\text{H}_{3,3''}$ ), 8.69 (2 H, d,  $J$  = 5.9 Hz,  $\text{H}_{6,6''}$ ).

$^{13}\text{C}$ -NMR (100 MHz,  $\text{CDCl}_3$ ):  $\delta$  = 14.1 ( $\text{C}_a$ ), 22.6, 25.9, 29.0, 29.0, 31.8 (C-alkyl), 68.2 ( $\text{C}_b$ ), 107.4 ( $\text{C}_{5,5''}$ ), 121.3 ( $\text{C}_{4,4''}$ ), 123.7 ( $\text{C}_{3,3''}$ ), 136.7 ( $\text{C}_{3,5}$ ), 149.0 ( $\text{C}_{6,6''}$ ), 156.2 ( $\text{C}_{2,2''}$ ), 157.0 ( $\text{C}_{2,6}$ ), 167.3 ( $\text{C}_4$ ).

MS (MALDI-TOF, matrix: dithranol):  $m/z$  = 348 [ $\text{M} + \text{H}$ ]<sup>+</sup>.

Anal. Calcd for  $\text{C}_{22}\text{H}_{25}\text{N}_3\text{O}_6$  (347.46): C, 76.05; H, 7.25; N, 12.09. Found: C, 76.26; H, 6.91; N, 12.19.

**Bis(4'-heptylmethoxy-2,2':6',2''-terpyridine) cobalt(II) hexafluorophosphate 3**

To a stirred suspension of **2** (100 mg, 0.29 mmol) in MeOH (10 mL)  $\text{Co}(\text{OAc})_2 \times 4 \text{H}_2\text{O}$  (35.8 mg, 0.15 mmol) was added at room temperature. After 30 min  $\text{NH}_4\text{PF}_6$  (95 mg, 0.58 mmol) in 10 mL MeOH was added upon which an orange-brown precipitate was formed. The mixture was stirred for another 10 min and the precipitate was filtered off and washed with MeOH ( $3 \times 30 \text{ mL}$ ) and  $\text{CHCl}_3$  ( $3 \times 30 \text{ mL}$ ). Solvent rests were evaporated under reduced pressure. The crude product was then recrystallized by diffusion of diethyl ether into an acetonitrile solution and then dried under high vacuum yielding 113 mg (72%) of an orange solid.

UV-vis ( $\text{CH}_3\text{CN}$ ):  $\lambda_{\text{max}}$  ( $\epsilon$ ) = 306 (25800), 274 (38800), 244 nm (49400) nm ( $\text{L mol}^{-1}\text{cm}^{-1}$ ).

IR (ATR):  $1/\lambda$  ( $\text{cm}^{-1}$ ): 1615, 1603, 1571, 1558 (C=C, C=N, terpyridine); 827 (P-F,  $\text{PF}_6$ ).

$^1\text{H-NMR}$  (300 MHz,  $\text{CH}_3\text{CN}$ ):  $\delta$  = 2.20 (3 H, t,  $J$  = 7.31 Hz,  $\text{CH}_3$ ), 3.15 (2 H, m,  $\text{CH}_3$ ), 3.74 (2 H, m,  $\text{CH}_3$ ), 4.69 (2 H, m,  $\text{CH}_3$ ), 6.26 (2 H, m,  $\text{CH}_3$ ), 6.45 (2 H, m,  $\text{CH}_3$ ), 7.73 (2 H, m,  $\text{CH}_3$ ), 15.20, 34.20, 70.65, 75.42, 111.59 (10 H, H-terpyridine).

MS (MALDI-TOF, matrix: dithranol):  $m/z$  = 631.3 [ $\text{M} - \text{ligand} - 2 \text{PF}_6 + \text{dithranol} - \text{H}$ ] $^+$ , 753.4 [ $\text{M} - 2 \text{PF}_6$ ] $^+$ , 898.2 [ $\text{M} - \text{PF}_6$ ] $^+$ .

Anal. Calcd for  $\text{C}_{44}\text{H}_{50}\text{N}_6\text{O}_2\text{P}_2\text{F}_{12}\text{Co}$  (1043.78): C, 50.63; H, 4.83; N, 8.05. Found: C, 50.45; H, 4.71; N, 7.97.

**General method of preparation for the ruthenium complexes 16-25**

Equimolar amounts of free ligand and Ru(III) *mono*-complex were mixed with 10 mL ethanol and 30  $\mu\text{L}$  of *N*-ethylmorpholine and refluxed for 3 hours. A tenfold excess of ammoniumhexafluorophosphate was added and the precipitate collected by filtration. The crude product was dissolved in acetonitrile and crystallized through diffusion of diethyl ether.

**(5,5''-Dimethyl-2,2':6',2''-terpyridine) (2,2':6',2''-terpyridine) ruthenium(II) hexafluorophosphate 16**

90 mg (0.204 mmol) 2,2':6',2''-terpyridine ruthenium(III) trichloride **5**, 53 mg (0.204 mmol) 5,5''-dimethyl-2,2':6',2''-terpyridine **6**. Yield: 126 mg (70%).

UV-vis ( $\text{CH}_3\text{CN}$ ):  $\lambda_{\text{max}}$  ( $\epsilon$ ) = 270 (56400), 308 (72900), 474 (15800) nm ( $\text{L mol}^{-1}\text{cm}^{-1}$ ).

IR (KBr):  $1/\lambda$  ( $\text{cm}^{-1}$ ) = 1615, 1601 (C=C, C=N, terpyridine); 823 (P-F,  $\text{NH}_4\text{PF}_6$ ).

$^1\text{H-NMR}$  (300 MHz,  $\text{CDCl}_3$ ):  $\delta$  = 2.02 (6 H, s,  $\text{CH}_3$ ), 7.10 (2 H, d,  $J$  = 0.57 Hz,  $\text{H}_{6,6''}$ ), 7.15 (2 H, ddd,  $J$  = 6.87, 5.72, 1.14 Hz,  $\text{H}_{5,5''}$ ), 7.32 (2 H, dd,  $J$  = 5.72 Hz, 0.76 Hz,  $\text{H}_{6,6''}$ ), 7.71 (2 H, dd,  $J$  = 8.39, 0.76 Hz,  $\text{H}_{4,4''}$ ), 7.91 (2 H, ddd,  $J$  = 8.01, 8.01, 1.14 Hz,  $\text{H}_{4,4''}$ ), 8.35 (2 H, d,  $J$  = 8.39 Hz,  $\text{H}_{3,3''}$ ), 8.40 (1 H, t,  $J$  = 8.39 Hz,  $\text{H}_4$ ), 8.49 (2 H, dd,  $J$  = 8.01, 0.76 Hz,  $\text{H}_{3,3''}$ ), 8.64 (2 H, d,  $J$  = 8.01 Hz,  $\text{H}_{3,3''}$ ), 8.74 (2 H, d,  $J$  = 8.01 Hz,  $\text{H}_{3,3''}$ ).

$^{13}\text{C-NMR}$  (75 MHz,  $\text{CD}_3\text{CN}$ ):  $\delta$  = 17.02 ( $\text{CH}_3$ ), 122.46, 123.39, 123.48, 124.98, 127.01, 135.18, 135.39, 137.58, 138.17, 138.50, 151.96, 152.11, 154.98, 155.13, 157.97 (all tpy).

MS (MALDI-TOF, dithranol):  $m/z$  = 595.49 [ $\text{M} - 2 \text{PF}_6$ ] $^+$ .

Anal. Calcd for  $\text{C}_{32}\text{H}_{26}\text{N}_6\text{RuP}_2\text{F}_{12}$  (885.57 g/mol): C, 43.40; H, 2.96; N, 9.49. Found: C, 43.04; H, 2.89; N, 9.52.

**(4'-5-Aminopentyl-2,2':6',2''-terpyridine) (2,2':6',2''-terpyridine) ruthenium(II) hexafluorophosphate 17**

154.4 mg (0.47 mmol) 4'-5-aminopentyl-2,2':6',2''-terpyridine **7**, 209 mg (0.47 mmol) 2,2':6',2''-terpyridine ruthenium(III) trichloride **5**. Yield: 277 mg (61%) of a red crystalline solid.

UV-vis ( $\text{CH}_3\text{CN}$ ),  $\lambda_{\text{max}}$  ( $\epsilon$ ) = 268 (102400), 304 (123200), 480 (33100) nm ( $\text{L mol}^{-1}\text{cm}^{-1}$ ).

$^1\text{H-NMR}$  (300 MHz,  $\text{CD}_3\text{CN}$ ):  $\delta$  = 1.69 (2 H, m,  $\text{CH}_2$ ), 1.84 (2 H, q,  $J$  = 7.25 Hz,  $\text{CH}_2$ ), 2.05 (2 H, q,  $J$  = 7.63 Hz,  $\text{CH}_2$ ), 3.07 (2 H, t,  $J$  = 7.63 Hz,  $\text{CH}_2\text{N}$ ), 4.53 (2 H, t,  $J$  = 6.49 Hz,  $\text{CH}_2\text{O}$ ), 7.15 (4 H, m,  $\text{H}_{5,5''}$ ), 7.29 (2 H, dd,  $J$  = 4.96, 0.76 Hz,  $\text{H}_{6,6''}$ ), 7.42 (2 H, d,  $J$  = 5.34 Hz,  $\text{H}_{6,6''}$ ), 7.9 (4 H, ddd,  $J$  = 7.63, 7.63, 1.53 Hz,  $\text{H}_{4,4''}$ ), 8.30 (2 H, s,  $\text{H}_{3,3''}$ ), 8.36 (1 H, dd,  $J$  = 8.01, 8.01 Hz,  $\text{H}_4$ ), 8.48 (4 H, d,  $J$  = 8.01 Hz,  $\text{H}_{3,3''}$ ), 8.72 (2 H, d,  $J$  = 8.39 Hz,  $\text{H}_{3,3''}$ ).

$^{13}\text{C-NMR}$  (75 MHz,  $\text{CD}_3\text{CN}$ ):  $\delta$  = 24.43, 25.72, 26.86, 28.98 ( $\text{CH}_2$ ), 43.69 ( $\text{CH}_2\text{NH}_2$ ), 70.91 ( $\text{CH}_2\text{Otpy}$ ), 111.93, 124.52, 125.19, 125.32, 128.34, 138.79, 138.85, 153.17, 153.62, 156.81, 156.88, 159.01, 159.17, 167.41 ( $\text{C}_4\text{-O}$ ).

MS (MALDI-TOF, dithranol):  $m/z$  = 669.3 [ $\text{M} - 2 \text{PF}_6$ ] $^+$ .

**(4'-5-Hydroxyhexyl-2,2':6',2''-terpyridine) (2,2':6',2''-terpyridine) ruthenium(II) hexafluorophosphate 18**

70 mg (0.21 mmol) 4'-5-hydroxyhexyl-2,2':6',2''-terpyridine **8**, 92 mg (0.21 mmol) 2,2':6',2''-terpyridine ruthenium(III) trichloride **5**. Yield: 147 mg (72%).

UV-vis ( $\text{CH}_3\text{CN}$ ):  $\lambda_{\text{max}}$  ( $\epsilon$ ) = 242 (35500), 269 (41200), 305 (53500), 481 (15100) nm ( $\text{L mol}^{-1}\text{cm}^{-1}$ ).

IR (KBr):  $1/\lambda$  ( $\text{cm}^{-1}$ ) = 3404 (OH), 2935, 2854 (C-C); 1615, 1604 (C=C, C=N, terpyridine); 838 (P-F,  $\text{NH}_4\text{PF}_6$ ).

$^1\text{H-NMR}$  (300 MHz,  $\text{CD}_3\text{CN}$ ):  $\delta$  = 1.62 (6 H, m, 3  $\text{CH}_2$ ), 2.05 (2 H, q,  $J$  = 8.01 Hz,  $\text{CH}_2\text{CH}_2\text{O}$ ), 3.58 (2 H, t,  $J$  = 6.1 Hz,  $\text{CH}_2\text{OH}$ ), 3.54 (2 H, t,  $J$  = 6.5 Hz,  $\text{CH}_2\text{O}$ ), 7.19 (4 H, m,  $\text{H}_{5,5''}$ ), 7.29 (dd,  $J$  = 5.72, 1.53 Hz, 2 H,  $\text{H}_{6,6''}$ ), 7.43 (2 H, dd,  $J$  = 5.34, 1.53 Hz,  $\text{H}_{6,6''}$ ), 7.9 (4 H, ddd,  $J$  = 8.01, 1.53, 1.53 Hz,  $\text{H}_{4,4''}$ ), 8.30 (2 H, s,  $\text{H}_{3,3''}$ ), 8.36 (1 H, t,  $J$  = 8.01 Hz,  $\text{H}_4$ ), 8.34 (4 H, d,  $J$  = 8.02 Hz,  $\text{H}_{3,3''}$ ), 8.72 (2 H, d,  $J$  = 8.01 Hz,  $\text{H}_{3,3''}$ ).

$^{13}\text{C-NMR}$  (75 MHz,  $\text{CD}_3\text{CN}$ ):  $\delta$  = 26.37, 26.44, 29.59, 33.46 ( $\text{CH}_2$ ), 62.46 ( $\text{CH}_2\text{OH}$ ), 71.27 ( $\text{CH}_2\text{Otpy}$ ), 111.96, 124.49, 125.18, 128.30, 128.35, 136.05, 138.76, 153.18, 153.59, 156.82, 159.85, 159.04, 159.16, 167.41 ( $\text{C}_4\text{-O}$ ).

MS (MALDI-TOF, dithranol):  $m/z$  = 684.2 [ $\text{M} - 2 \text{PF}_6$ ] $^+$ , 828.14 [ $\text{M} - \text{PF}_6$ ] $^+$ .

**(4'-5-Carboxypentyl-2,2':6',2''-terpyridine) (2,2':6',2''-terpyridine) ruthenium(II) hexafluorophosphate 19**

50 mg (0.14 mmol) 4'-5-carboxypentyl-2,2':6',2''-terpyridine **9**, 61 mg (0.14 mmol) 2,2':6',2''-terpyridine ruthenium(III) trichloride **5**. Yield: 108 mg (79%).

UV-vis (CH<sub>3</sub>CN):  $\lambda_{\max}$  ( $\epsilon$ ) = 268 (102300) 304 (1231800), 481 (33200) nm (L mol<sup>-1</sup>cm<sup>-1</sup>).

<sup>1</sup>H-NMR (300 MHz, CD<sub>3</sub>CN):  $\delta$  = 1.69 (2 H, m, 3 CH<sub>2</sub>), 1.77 (m, 2 H, 3 CH<sub>2</sub>), 2.05 (2 H, tt,  $J$  = 7.25, 7.25 Hz, CH<sub>2</sub>), 2.42 (2 H, t,  $J$  = 7.25 Hz, CH<sub>2</sub>COOH), 4.54 (2 H, t,  $J$  = 6.68 Hz, CH<sub>2</sub>O), 7.16 (4 H, m, H<sub>5,5''</sub>), 7.29 (2 H, dd,  $J$  = 5.72, 1.53 Hz, H<sub>6,6''</sub>), 7.44 (2 H, dd,  $J$  = 5.34, 1.53 Hz, H<sub>6,6''</sub>), 7.90 (4 H, ddd,  $J$  = 8.01, 8.01, 1.53 Hz, H<sub>4,4''</sub>), 8.31 (2 H, s, H<sub>3,3''</sub>), 8.37 (1 H, t,  $J$  = 8.01 Hz, H<sub>4</sub>), 8.48 (4 H, dd,  $J$  = 8.01, 0.76 Hz, H<sub>3,3''</sub>), 8.73 (2 H, d,  $J$  = 8.01 Hz, H<sub>3,3''</sub>).

<sup>13</sup>C-NMR (75 MHz, CD<sub>3</sub>CN):  $\delta$  = 25.26 (CH<sub>2</sub>), 26.09 (CH<sub>2</sub>), 29.25 (CH<sub>2</sub>), 34.17 (CH<sub>2</sub>-COOH), 71.10 (CH<sub>2</sub>Otpy), 111.97, 124.97, 125.17, 125.32, 128.29, 128.34, 136.05, 138.76, 138.83, 153.18, 153.59, 156.81, 159.03, 159.15, 167.37, 175.16 (C<sub>4</sub>-O), 178.01 (COOH).

MS (MALDI-TOF, alpha-cyano):  $m/z$  = 698.18 [M - 2 PF<sub>6</sub>]<sup>+</sup>, 843.07 [M - PF<sub>6</sub>]<sup>+</sup>.

**(2-Methyl-acrylic acid 3-(2,2':6',2''-terpyridin-4'-yloxy)-propyl ester) (2,2':6',2''-terpyridine) ruthenium(II) hexafluorophosphate 20**

7 mg (0.016 mmol) 2,2':6',2''-terpyridine ruthenium(III) trichloride **5**, 6 mg (0.016 mmol) 2-methyl-acrylic acid 3-(2,2':6',2''-terpyridin-4'-yloxy)-propyl ester **10**. Yield: 10 mg (64%).

UV-vis (CH<sub>3</sub>CN):  $\lambda_{\max}$  ( $\epsilon$ ) = 241 (35500), 269 (41000), 305 (53500), 480 (15100) nm (L mol<sup>-1</sup>cm<sup>-1</sup>).

<sup>1</sup>H-NMR (400 MHz, CH<sub>3</sub>CN):  $\delta$  = 2.17 (1 H, s, CH<sub>3</sub>), 2.44 (2 H, tt,  $J$  = 6.8, 6.8 Hz, CH<sub>2</sub>), 4.50 (2 H, t,  $J$  = 6.8 Hz, OCH<sub>2</sub>), 4.66 (2 H, t,  $J$  = 6.8 Hz, OCH<sub>2</sub>), 5.71 (1 H, s, H<sub>olefinic</sub>), 6.19 (1 H, s, H<sub>olefinic</sub>), 7.19 (4 H, m, H<sub>5,5''</sub>), 7.30 (2 H, dd,  $J$  = 5.72, 1.53 Hz, H<sub>6,6''</sub>), 7.43 (2 H, dd,  $J$  = 5.34, 1.53 Hz, H<sub>6,6''</sub>), 7.92 (4 H, ddd,  $J$  = 8.01, 8.01, 1.53 Hz, H<sub>4,4''</sub>), 8.34 (2H, s, H<sub>3,3''</sub>), 8.38 (1 H, t,  $J$  = 9.2 Hz, H<sub>4</sub>), 8.49 (4 H, dd,  $J$  = 8.01, 8.01 Hz, H<sub>3,3''</sub>), 8.72 (2 H, d,  $J$  = 9.2 Hz, H<sub>3,3''</sub>).

<sup>13</sup>C-NMR (100 MHz, CD<sub>3</sub>CN):  $\delta$  = 17.75 (CH<sub>3</sub>), 28.36 (CH<sub>2</sub>), 61.94 (OCH<sub>2</sub>), 67.98 (CH<sub>2</sub>Otpy), 111.95, 124.47, 125.17, 125.28, 126.11, 128.31, 136.06, 138.76, 138.83, 153.15, 153.39, 153.59, 156.76, 163.38, 168.01 (C<sub>4</sub>-O).

MS (MALDI-TOF, dithranol):  $m/z$  = 710.83 [M - 2 PF<sub>6</sub>]<sup>+</sup>, 855.75 [M - PF<sub>6</sub>]<sup>+</sup>.

**(4'-p-Toluy-2,2':6',2''-terpyridine) (2,2':6',2''-terpyridine) ruthenium(II) hexafluorophosphate 21**

50 mg (0.09 mmol) 4'-p-toluy-2,2':6',2''-terpyridine **11**, 22 mg (0.09 mmol) 2,2':6',2''-terpyridine ruthenium(III) trichloride **5**. Yield 63.9 mg (75%).

UV-vis (CH<sub>3</sub>CN),  $\lambda_{\max}$  ( $\epsilon$ ) = 272 (66200), 281 (66300), 308 (59600), 483 (22800) nm (L mol<sup>-1</sup>cm<sup>-1</sup>).

IR (ATR):  $1/\lambda$  (cm<sup>-1</sup>) = 3114 (CH), 1605 (C=C, C=N, terpyridine); 832, 816 (P-F, NH<sub>4</sub>PF<sub>6</sub>).

<sup>1</sup>H-NMR (300 MHz, CD<sub>3</sub>CN):  $\delta$  = 2.54 (3 H, s, CH<sub>3</sub>), 7.16 (4 H, m, H<sub>5,5''</sub>), 7.34 (2 H, dd,  $J$  = 5.72, 0.76 Hz, H<sub>6,6''</sub>), 7.42 (2 H, dd,  $J$  = 5.72, 0.76 Hz, H<sub>6,6''</sub>), 7.58 (2 H, d,  $J$  = 8.58 Hz, C<sub>phenylic</sub>), 7.93 (4 H, m, H<sub>4,4''</sub>), 8.11 (2 H, d,  $J$  = 8.58 Hz, C<sub>phenylic</sub>), 8.41 (1 H, t,  $J$  = 8.01 Hz, H<sub>4</sub>), 8.49 (2 H, d,  $J$  = 8.20 Hz, H<sub>3,3''</sub>), 8.63 (2 H, d,  $J$  = 8.20 Hz, H<sub>3,3''</sub>), 8.75 (2 H, d,  $J$  = 8.20 Hz, H<sub>3,3''</sub>), 8.98 (2 H, s, H<sub>3,3''</sub>).

<sup>13</sup>C-NMR (75 MHz, CD<sub>3</sub>CN):  $\delta$  = 20.12 (CH<sub>3</sub>), 121.06, 123.39, 124.09, 124.16, 127.10, 127.14, 127.35, 129.99, 135.40, 137.74, 140.77, 152.05, 152.22, 155.11, 157.77, 157.89.

MS (MALDI-TOF, dithranol):  $m/z$  = 653.10 [M - 2 PF<sub>6</sub>]<sup>+</sup>, 692.13 [M - 2 PF<sub>6</sub> + K]<sup>+</sup>, 802.24 [M - PF<sub>6</sub>]<sup>+</sup>.

**(4'-p-Styryl-2,2':6',2''-terpyridine) (2,2':6',2''-terpyridine) ruthenium(II) hexafluorophosphate 22**

30 mg (0.092 mmol) 4'-p-styryl-2,2':6',2''-terpyridine **12**, 41 mg (0.092 mmol) 2,2':6',2''-terpyridine ruthenium(III) trichloride **5**. Yield: 54 mg (81%).

UV-vis (CH<sub>3</sub>CN),  $\lambda_{\max}$  ( $\epsilon$ ) = 271 (66100), 281 (66500), 308 (59600), 483 (22700) nm (L mol<sup>-1</sup>cm<sup>-1</sup>).

IR (KBr):  $1/\lambda$  (cm<sup>-1</sup>) = 2924, (C=C); 1603 (C=C, C=N, terpyridine); 843 (P-F, NH<sub>4</sub>PF<sub>6</sub>).

<sup>1</sup>H-NMR (300 MHz, CD<sub>3</sub>CN):  $\delta$  = 5.47 (1 H, d,  $J$  = 10.68 Hz, H<sub>olefinic</sub>), 6.07 (1 H, d,  $J$  = 17.93 Hz, H<sub>olefinic</sub>), 6.96 (1 H, dd,  $J$  = 17.93, 10.68 Hz, H<sub>olefinic</sub>), 7.17 (4 H, m, H<sub>5,5''</sub>), 7.35 (2 H, d,  $J$  = 5.34 Hz, H<sub>6,6''</sub>), 7.43 (2 H, d,  $J$  = 4.96 Hz, H<sub>6,6''</sub>), 7.84 (2 H, d,  $J$  = 8.19 Hz, C<sub>phenylic</sub>), 7.93 (4 H, m, H<sub>4,4''</sub>), 8.21 (2 H, d,  $J$  = 8.19 Hz, C<sub>phenylic</sub>), 8.42 (1 H, t,  $J$  = 8.01 Hz, H<sub>4</sub>), 8.50 (2 H, d,  $J$  = 8.01 Hz, H<sub>3,3''</sub>), 8.65 (2 H, d,  $J$  = 8.01 Hz, H<sub>3,3''</sub>), 8.76 (2 H, d,  $J$  = 8.01 Hz, H<sub>3,3''</sub>), 9.01 (2 H, s, H<sub>3,3''</sub>).

<sup>13</sup>C-NMR (75 MHz, CD<sub>3</sub>CN):  $\delta$  = 116.61 (olefinic), 122.29, 124.63, 125.34, 125.43, 128.26, 128.38, 128.99, 136.70, 136.86, 136.95, 138.96, 139.00, 140.62, 148.72, 153.31, 153.46, 156.31, 158.99, 160.38.

MS (MALDI-TOF, alpha-cyano):  $m/z$  = 671.04 [M - 2 PF<sub>6</sub>]<sup>+</sup>, 693.13 [M - 2 PF<sub>6</sub> + Na]<sup>+</sup>.

Anal. Calcd for C<sub>38</sub>H<sub>28</sub>N<sub>6</sub>RuP<sub>2</sub>F<sub>12</sub> + H<sub>2</sub>O (977.69 g/mol): C, 46.68; H, 3.09; N, 8.60. Found: C, 46.73; H, 3.05; N, 8.54.

**(4'-p-Bromomethylphenyl-2,2':6',2''-terpyridine) (2,2':6',2''-terpyridine) ruthenium(II) hexafluorophosphate 23**

104 mg (0.236 mmol) 2,2':6',2''-terpyridine ruthenium(III) trichloride **5**, 95 mg (0.236 mmol) 4'-p-bromomethylphenyl-2,2':6',2''-terpyridine **13**. The crystallized product was purified by column chromatography (silica), using an acetonitrile/aqueous KNO<sub>3</sub> mixture as mobile phase, followed by precipitation of the eluted fractions with NH<sub>4</sub>PF<sub>6</sub>. Yield: 130 mg (54%) of crude product; 12 mg (5%), pure product (first fraction from column chromatography).

UV-vis (CH<sub>3</sub>CN),  $\lambda_{\max}$  ( $\epsilon$ ) = 285 (66300), 309 (57000), 490 (22200) nm (L mol<sup>-1</sup>cm<sup>-1</sup>).

$^1\text{H-NMR}$  (300 MHz,  $\text{CD}_3\text{CN}$ ):  $\delta$  = 4.49 (2 H, s,  $\text{CH}_2\text{Br}$ ), 7.20 (4 H, m,  $\text{H}_{5,5''}$ ), 7.38 (2 H, dd,  $J$  = 5.72, 0.76 Hz,  $\text{H}_{6,6''}$ ), 7.45 (2 H, dd,  $J$  = 5.72, 0.76 Hz,  $\text{H}_{6,6''}$ ), 7.85 (2 H, d,  $J$  = 8.58 Hz,  $\text{C}_{\text{phenylic}}$ ), 7.96 (4 H, m,  $\text{H}_{4,4''}$ ), 8.23 (2 H, d,  $J$  = 8.58 Hz,  $\text{C}_{\text{phenylic}}$ ), 8.45 (1 H, t,  $J$  = 8.01 Hz,  $\text{H}_4$ ), 8.53 (4 H, d,  $J$  = 8.20 Hz,  $\text{H}_{3,3''}$ ), 8.66 (2 H, d,  $J$  = 8.20 Hz,  $\text{H}_{3,3''}$ ), 8.79 (2 H, d,  $J$  = 8.20 Hz,  $\text{H}_{3,5'}$ ), 9.04 (2 H, s,  $\text{H}_{3,5'}$ ).

$^{13}\text{C-NMR}$  (75 MHz,  $\text{CD}_3\text{CN}$ ):  $\delta$  = 46.50 ( $\text{CH}_2$ ), 122.64, 124.64, 125.35, 125.44, 128.38, 128.70, 129.18, 130.86, 136.73, 137.82, 138.98, 139.01, 141.24, 148.66, 153.30, 153.47, 156.28, 156.42, 158.98, 159.04.

MS (MALDI-TOF, dithranol):  $m/z$  = 736.99 [ $\text{M} - 2 \text{PF}_6$ ] $^+$ , 657.90 [ $\text{M} - 2 \text{PF}_6 - \text{Br}$ ] $^+$ .

Anal. Calcd for  $\text{C}_{37}\text{H}_{27}\text{BrF}_{12}\text{N}_6\text{P}_2\text{Ru}$  (1026.56 g/mol): C, 43.29; H, 2.65; N, 8.19. Found: C, 43.96; H, 2.71; N, 7.79.

**(4'-Disperse-red-2,2':6',2''-terpyridine) (2,2':6',2''-terpyridine) ruthenium(II) hexafluorophosphate 24**

21 mg (0.031 mmol) of [5-(2,2':6',2''-terpyridin-4'-yloxy)-pentyl]-carbamic acid 2-(ethyl-[4-(4-nitro-phenylazo)-phenyl]-amino)-ethyl ester **14**,<sup>[50]</sup> 14 mg (0.031 mmol) of 2,2':6',2''-terpyridine ruthenium(III) trichloride **5**. Yield: 23 mg (57%).

IR (ATR):  $1/\lambda$  ( $\text{cm}^{-1}$ ) = 3324 ( $\text{NH}_2$ ), 2941 (C–C); 1714 (C=O), 1600, 1587 (C=C, C=N, terpyridine); 830 (P–F,  $\text{NH}_4\text{PF}_6$ ).

UV-vis ( $\text{CH}_3\text{CN}$ ),  $\lambda_{\text{max}}$  ( $\epsilon$ ) = 241 (42000), 270 (49300), 305 (59000), 490 (40700) nm ( $\text{L mol}^{-1} \text{cm}^{-1}$ ).

$^1\text{H-NMR}$  (400 MHz,  $\text{CD}_3\text{CN}$ ):  $\delta$  = 1.21 (2 H, t,  $J$  = 7.32 Hz,  $\text{CH}_3$ ), 1.59 (2 H, m,  $\text{CH}_2$ ), 1.84 (2 H, q,  $J$  = 7.25 Hz,  $\text{CH}_2$ ), 2.05 (2 H, q,  $J$  = 7.63 Hz,  $\text{CH}_2$ ), 3.07 (2 H, t,  $J$  = 7.63 Hz,  $\text{CH}_2\text{NH}_2$ ), 3.53 (2 H, t,  $J$  = 6.49 Hz,  $\text{CH}_2\text{O}$ ), 4.32 (2 H, t,  $J$  = 6.49 Hz,  $\text{CH}_2\text{O}$ ), 6.95 (2 H, d,  $J$  = 8.79 Hz,  $\text{H}_{\text{phenylic}}$ ), 7.16 (2 H, dd,  $J$  = 6.59, 6.59 Hz,  $\text{H}_{5,5''}$ ), 7.23 (2 H, dd,  $J$  = 6.59, 6.59 Hz,  $\text{H}_{5,5''}$ ), 7.29 (2 H, dd,  $J$  = 4.96, 0.76 Hz,  $\text{H}_{6,6''}$ ), 7.42 (2 H, dd,  $J$  = 5.34, 0.76 Hz,  $\text{H}_{6,6''}$ ), 7.92 (8 H, m,  $\text{H}_{4,4''}$ ,  $\text{H}_{\text{phenylic}}$ ), 8.31 (4 H, m,  $\text{H}_{3,5'}$ ,  $\text{H}_{\text{phenylic}}$ ), 8.36 (1 H, t,  $J$  = 8.01 Hz,  $\text{H}_4$ ), 8.48 (4 H, d,  $J$  = 8.01 Hz,  $\text{H}_{3,3''}$ ), 8.72 (2 H, d,  $J$  = 8.39 Hz,  $\text{H}_{3,5'}$ ).

$^{13}\text{C-NMR}$  (100 MHz,  $\text{CD}_3\text{CN}$ ):  $\delta$  = 12.35, 23.58, 29.04, 30.31, ( $\text{CH}_2$ ), 41.20, 50.05 ( $\text{CH}_2\text{NH}_2$ ), 62.39, 71.18 ( $\text{CH}_2\text{Otpy}$ ), 111.91, 112.65, 123.26, 124.50, 125.17, 125.27, 125.73, 127.00, 128.30, 136.07, 138.78, 138.82, 144.23, 153.12, 153.57, 156.78, 158.96, 159.13, 167.28 ( $\text{C}_4\text{-O}$ ).

MS (MALDI-TOF, alpha-cyano):  $m/z$  = 1008.66 [ $\text{M} - 2 \text{PF}_6$ ] $^+$ , 1154.64 [ $\text{M} - \text{PF}_6$ ] $^+$ .

**({6-[3-(6-Methyl-4-oxo-1,4-dihydro-pyrimidin-2-yl)-ureido]-hexyl}-carbamic acid 5-(2,2':6',2''-terpyridin-4'-yloxy)-pentyl ester) (2,2':6',2''-terpyridine) ruthenium(II) hexafluorophosphate 25**

32 mg (0.051 mmol) of **15** and 32 mg (0.071 mmol) of 2,2':6',2''-terpyridine ruthenium(III) trichloride **5**. Yield: 46 mg (68%).

UV-vis ( $\text{CHCl}_3$ ):  $\lambda_{\text{max}}$  ( $\epsilon$ ) = 240 (49900), 270 (53900), 305 (60200), 481 (15200) nm ( $\text{L mol}^{-1} \text{cm}^{-1}$ ).

$^1\text{H-NMR}$  (400 MHz,  $\text{CD}_2\text{Cl}_2$ ):  $\delta$  = 1.35 (4 H, m,  $\text{CH}_2$ ), 1.51 - 1.56 (6 H,  $\text{CH}_2$ ), 1.73 - 1.80 (4 H, m,  $\text{CH}_2$ ), 2.09 (2 H, m,  $\text{CH}_2$ ), 2.22 (3 H, s,  $\text{CH}_3$ ), 3.14 (2 H, dd,  $J$  = 5.86, 6.59 Hz,  $\text{NHCH}_2$ ), 3.20 (2 H, dd,  $J$  = 5.86, 6.59 Hz,  $\text{NHCH}_2$ ), 4.14 (2 H, t,  $J$  = 5.86 Hz,  $\text{OCH}_2$ ), 4.58 (2 H, t,  $J$  = 5.86 Hz,  $\text{OCH}_2$ ), 5.21 (1 H, m, NH), 5.83 (1 H, s, CH), 7.15 (4 H, t,  $J$  = 6.59 Hz,  $\text{H}_{5,5''}$ ), 7.24 (2 H, d,  $J$  = 6.59 Hz,  $\text{H}_{6,6''}$ ), 7.43 (2 H, d,  $J$  = 4.39 Hz,  $\text{H}_{6,6''}$ ), 7.89 (4 H, m,  $\text{H}_{4,4''}$ ), 8.25 (2 H, s,  $\text{H}_{3,5'}$ ), 8.39 (1 H, t,  $J$  = 8.06 Hz,  $\text{H}_4$ ), 8.43 (4 H, d,  $J$  = 8.06 Hz,  $\text{H}_{3,3''}$ ), 8.68 (d, 2 H,  $J$  = 8.06 Hz,  $\text{H}_{3,5'}$ ), 10.09 (s, 1 H, NH), 11.85 (s, 1 H, NH), 13.08 (s, 1 H, NH).

MS (ESI):  $m/z$  = 481.0 [ $\text{M} - \text{PF}_6$ ] $^{2+}$ , 92%), 1104.9 [ $\text{M} - \text{PF}_6$ ] $^+$ , 100%).

MS (MALDI-TOF, dithranol):  $m/z$  = 963.05 [ $\text{M} - \text{PF}_6$ ] $^+$ , 1107.88 [ $\text{M} - 2 \text{PF}_6$ ] $^+$ .

Anal. Calcd for  $\text{C}_{48}\text{H}_{51}\text{F}_{12}\text{N}_{11}\text{O}_5\text{P}_2\text{Ru} + 2 \text{H}_2\text{O}$  (1253.00 g/mol): C, 44.73; H, 4.30; N, 11.95. Found: C, 44.45; H, 4.08; N, 11.81.

**4'-Heptyloxy-2,2':6',2''-terpyridine ruthenium(III) trichloride 26**

330 mg (1.01 mmol) of 4'-heptyloxy-2,2':6',2''-terpyridine **2** was mixed with 210 mg (1.01 mmol) of  $\text{RuCl}_3 \times \text{H}_2\text{O}$  and ethanol. The suspension was heated to 65 °C for 4 h. A brown precipitate occurred which was collected by filtration and washed with 50 mL of ethanol. Drying *in vacuo* yielded 438 mg (79%). The compound was used without further characterization.

**(4'-Heptyloxy-2,2':6',2''-terpyridine) (4'-(methoxy di(ethylene glycol))-2,2':6',2''-terpyridine) ruthenium(II) hexafluorophosphate 28**

79.1 mg (0.142 mmol) of the Ru(III) monocomplex **26** and 50 mg (0.142 mmol) of the free ligand **27** were mixed with 10 mL ethanol as well as 3 drops of *N*-ethylmorpholine and refluxed for 3 hours. After filtration, 230 mg (1.42 mmol) of ammoniumhexafluorophosphate was added to the red reaction solution. The formed precipitate was collected on a glass filter and washed with 20 mL of ethanol. The complex was redissolved in acetonitrile and crystallized by diffusion of diethyl ether yielding 137 mg (89%) of complex **28** as red crystals.

UV-vis ( $\text{CH}_3\text{CN}$ ):  $\lambda_{\text{max}}$  ( $\epsilon$ ) = 238.5 (67100), 264.4 (66200), 302.0 (74600), 486.0 nm (22900) nm ( $\text{L mol}^{-1} \text{cm}^{-1}$ ).

IR (ATR):  $1/\lambda$  ( $\text{cm}^{-1}$ ): 2933, 2853 (C–C); 1615, 1604 (C=C, C=N, terpyridine); 823 (P–F,  $\text{NH}_4\text{PF}_6$ ).

$^1\text{H-NMR}$  (400 MHz,  $\text{CD}_3\text{CN}$ ):  $\delta$  = 0.96 (3 H, t,  $J$  = 6.59,  $\text{H}_{\alpha(8)}$ ), 1.41 (4 H, m, H-alkyl (**2**)), 1.50 (2 H, m, H-alkyl), 1.63 (2 H, m, H-alkyl), 2.02 (2 H, m, H-alkyl), 3.33 (3 H, s,  $\text{H}_{\epsilon(8)}$ ), 3.58 (2 H, t,  $J$  = 4.4 Hz,  $\text{H}_{\delta(8)}$ ), 3.75 (2 H, t,  $J$  = 4.0 Hz,  $\text{H}_{\gamma(8)}$ ), 4.03 (2 H, m,  $\text{H}_{\beta(8)}$ ), 4.51 (2 H, t,  $J$  = 6.8 Hz,  $\text{H}_{\alpha(8)}$ ), 4.65 (2 H, t,  $J$  = 4.3 Hz,  $\text{H}_{\eta(3)}$ ), 7.14 (4



H, m, H<sub>5,5''</sub>), 7.38 (4 H, d,  $J = 5.1$  Hz, H<sub>6,6''</sub>), 7.89 (4 H, m, H<sub>4,4''</sub>), 8.28 (2 H, s, H<sub>3,5'</sub>), 8.33 (2 H, s, H<sub>3,5'</sub>), 8.46 (4 H, m, H<sub>3,3''</sub>).

<sup>13</sup>C-NMR (100 MHz, CD<sub>3</sub>CN):  $\delta = 14.28$  (C <sub>$\alpha$ (3)</sub>), 23.30, 26.53, 29.59, 29.66, 32.49 (C-alkyl(3)), 58.88 (C <sub>$\alpha$ (8)</sub>), 69.86, 70.72, 71.22, 71.32, 72.59 (C-ethoxy(27)), 111.81, 111.93, 125.17, 125.20, 128.25, 128.29, 138.57, 153.40, 157.39, 159.18, 166.98, 166.72 (all terpyridine).

MS (MALDI-TOF, matrix: dithranol):  $m/z = 800.09$  [M - 2 PF<sub>6</sub>]<sup>+</sup>, 945.03 [M - PF<sub>6</sub>]<sup>+</sup>.

MS (ESI):  $m/z = 399.2$  [M - 2 PF<sub>6</sub>]<sup>2+</sup>; 944.6 [M - PF<sub>6</sub>]<sup>+</sup>.

Anal. calcd for C<sub>42</sub>H<sub>46</sub>N<sub>6</sub>O<sub>4</sub>RuP<sub>2</sub>F<sub>12</sub> (1089.86): C, 46.29; H, 4.25; N, 7.71. Found: C, 46.13; H, 4.10; N, 7.55.

**[(2,2':6',2''-Terpyridin-4-yloxy pentyl)-perylene-tetracarboxylic diimide] [2,2';6',2''-terpyridine] ruthenium(II) hexafluorophosphate 31**

To a hot solution of terpyridine-RuCl<sub>3</sub> **5** (26 mg, 0.06 mmol) in 30 mL DMF, AgBF<sub>4</sub> (35 mg, 0.18 mmol) was added. The formed AgCl was removed by filtration. Compound **30** (30 mg, 0.029 mmol) was added and the mixture was heated to 120 °C for 4 hours. The crude product was precipitated by addition of an aqueous solution of NH<sub>4</sub>PH<sub>6</sub> (500 mg). After filtration the product was recrystallized from acetonitrile/diethyl ether yielding **31** (28 mg, 44%).

UV-vis (CH<sub>3</sub>CN):  $\lambda_{\max}$  ( $\epsilon$ ) = 217 (196500), 258 (110600), 303 (89330), 486 (62250), 521 (66540) nm (L mol<sup>-1</sup>cm<sup>-1</sup>).

<sup>1</sup>H-NMR (CD<sub>3</sub>CN):  $\delta = 1.82$  (4 H, m, CH<sub>2</sub>), 2.10 (4 H, m, CH<sub>2</sub>), 4.20 (2 H, m, CH<sub>2</sub>N), 4.59 (2 H, t,  $J = 6.49$  Hz, CH<sub>2</sub>O), 7.13 (4 H, m, H<sub>5,5''</sub>), 7.29 (2 H, d,  $J = 4.96$  Hz, H<sub>6,6''</sub>), 7.43 (2 H, d,  $J = 5.34$  Hz, H<sub>6,6''</sub>), 7.9 (6 H, m, H<sub>4,4''</sub> + perylene), 8.30 (2 H, m, H<sub>perylene</sub>), 8.32 (2 H, s, H<sub>3',5'</sub>), 8.36 (1 H, t,  $J = 8.01$  Hz, H<sub>4'</sub>), 8.46 (4 H, d,  $J = 8.01$  Hz, H<sub>3,3''</sub>), 8.72 (2 H, d,  $J = 8.39$  Hz, H<sub>3',5'</sub>).

MS (MALDI-TOF, matrix: dithranol):  $m/z = 1694.06$  [M - 4 PF<sub>6</sub>]<sup>+</sup>.

Anal. Calcd for C<sub>94</sub>H<sub>70</sub>N<sub>14</sub>O<sub>6</sub>Ru<sub>2</sub>P<sub>4</sub>F<sub>24</sub> + 2 diethyl ether (4971.96): C, 50.80; H, 3.89; N, 7.97. Found: C, 50.41; H, 4.01; N, 7.63.

**4'-[3,4,5-Tris-(3,7-dimethyl-octyloxy)-phenylethynyl]-2,2':6',2''-terpyridine 34**

250 mg (0.801 mmol) of 4'-bromo-2,2':6',2''-terpyridine **2** and 250 mg (0.438 mmol) of the acetylene **32** were dissolved in degassed *n*-PrNH<sub>2</sub>, and Pd(PPh<sub>3</sub>)<sub>4</sub> (6 mol %) was added. After heating up to 65 °C for 40 h the solvent was evaporated under vacuum and the product was purified through column chromatography using an alumina column and a 50/50 mixture of dichloromethane/hexane as eluent. Yield: 260 mg (74%).

UV-vis (acetonitrile):  $\lambda_{\max}$  ( $\epsilon$ ) = 238 (27700), 285 (25400), 320 (23700) nm (L mol<sup>-1</sup>cm<sup>-1</sup>).

<sup>1</sup>H-NMR (400 MHz, CDCl<sub>3</sub>):  $\delta = 0.88$  (18 H, d,  $J = 6.59$  Hz, 7-CH<sub>3</sub>), 0.94 (3 H, d,  $J = 6.59$  Hz, 3-CH<sub>3</sub> (para-chain)), 0.97 (6 H, d,  $J = 6.59$  Hz, CH<sub>3</sub> (meta-chains)), 1.18 (10 H, m, CH<sub>2</sub>), 1.35 (10 H, m, CH<sub>2</sub>), 1.54 (4 H, m, CH<sub>2</sub>), 1.64 (2 H, m, CH<sub>2</sub>), 1.73 (3 H, m, CH), 1.88 (3 H, m, CH), 4.04 (6 H, m, OCH<sub>2</sub>), 6.81 (2 H, s, H<sub>phenyl</sub>), 7.33 (2 H, ddd,  $J = 5.86, 4.39, 1.47$  Hz, H<sub>5,5''</sub>), 7.85 (2 H, ddd,  $J = 8.06, 8.06, 1.47$  Hz, H<sub>4,4''</sub>), 8.56 (2 H, s, H<sub>3',5'</sub>), 8.61 (2 H, dd,  $J = 8.06, 1.47$  Hz, H<sub>3,3''</sub>), 8.71 (2 H, d,  $J = 6.59$  Hz, H<sub>6,6''</sub>).

<sup>13</sup>C-NMR (100 MHz, CHCl<sub>3</sub>):  $\delta = 155.6, 155.4, 153.0, 149.1, 139.6, 136.9, 133.5, 123.9, 122.7, 121.2, 116.8, 110.3$  (aromatic), 94.4, 86.4 (alkyne), 71.8, 67.4 (OCH<sub>2</sub>), 39.3, 39.2, 37.5, 37.3, 37.0 (CH<sub>2</sub>), 29.8, 29.6, 28.0 (CH), 24.7 (CH<sub>2</sub>), 22.6, 22.7, 19.6 (CH<sub>3</sub>).

MS (MALDI-TOF, matrix: dithranol):  $m/z = 802.59$  [M + H]<sup>+</sup>, 824.56 [M + Na]<sup>+</sup>.

Anal. Calcd for C<sub>53</sub>H<sub>75</sub>N<sub>3</sub>O<sub>3</sub> (802.2), C, 79.35; H 9.42; N 5.24. Found: C, 79.39; H, 9.30; N, 5.05.

**[4'-[3,4,5-Tris-(3,7-dimethyl-octyloxy)-phenylethynyl]-2,2':6',2''-terpyridine] ruthenium(III) chloride 35**

126 mg (0.157 mmol) of 4'-[3,4,5-(tris-(3,7-dimethyl-octyloxy)-phenylethynyl)-2,2':6',2''-terpyridine **34** was mixed with 207 mg of RuCl<sub>3</sub> × H<sub>2</sub>O in ethanol. The suspension was heated to 65 °C for 4 h. A brown precipitate occurred which was collected by filtration and washed with ethanol. The compound was used without further purification or characterization. Yield: 143 mg (91%).

**Bis-[4'-[3,4,5-tris(3,7-dimethyl-octyloxy)-phenylethynyl]-2,2':6',2''-terpyridine] ruthenium(II) hexafluorophosphate 36**

32 mg (0.040 mmol) of **34** and 40 mg (0.040 mmol) of **35** were mixed in 20 mL of ethanol and 30  $\mu$ L of *N*-ethylmorpholine were added. The mixture was heated up to 70 °C for 4 h. After cooling to room temperature ammoniumhexafluorophosphate (in ethanol) was added. The compound was precipitated by adding water and evaporating the ethanol. A dark red solid was obtained, which was filtrated and further purified by size exclusion chromatography on a Bio-Beads SX1 column. Yield: 65.4 mg (82%).

UV-vis (acetonitrile):  $\lambda_{\max}$  ( $\epsilon$ ) = 282 (66200), 314 (65200), 501 (45300) nm (L mol<sup>-1</sup>cm<sup>-1</sup>).

<sup>1</sup>H-NMR (400 MHz, CDCl<sub>3</sub>):  $\delta = 0.88$  (27 H, dd,  $J = 6.59, 2.20$  Hz, CH<sub>3</sub>), 0.96 (12 H, t,  $J = 6.59$  Hz, CH<sub>3</sub>), 1.18 (10 H, m, CH<sub>2</sub>), 1.35 (10 H, m, CH<sub>2</sub>), 1.54 (4 H, m, CH<sub>2</sub>), 1.62 (2 H, m, CH<sub>2</sub>), 1.73 (3 H, m, CH), 1.89 (3 H, m, CH), 4.10 (6 H, m, OCH<sub>2</sub>), 7.00 (2 H, s, H<sub>phenyl</sub>), 7.21 (2 H, d,  $J = 6.59$  Hz, H<sub>5,5''</sub>), 7.31 (2 H, d,  $J = 5.86$  Hz, H<sub>6,6''</sub>), 7.85 (2 H, dd,  $J = 7.23, 7.23$  Hz, H<sub>4,4''</sub>), 8.38 (2 H, d,  $J = 8.06$  Hz, H<sub>3,3''</sub>), 8.65 (2 H, s, H<sub>3',5'</sub>).

$^{13}\text{C}$ -NMR (100 MHz,  $\text{CD}_3\text{CN}$ ):  $\delta$  = 158.4, 156.0, 154.2, 153.5, 141.1, 139.1, 131.4, 128.5, 125.9, 125.4, 116.7, 111.4 (aromatic), 98.6, 86.1 (alkyne), 72.4, 68.2 ( $\text{OCH}_2$ ), 40.0, 39.9, 38.1, 38.0, 37.9, 37.1 ( $\text{CH}_2$ ), 30.5, 30.4, 28.7 ( $\text{CH}$ ), 25.5, 25.4 ( $\text{CH}_2$ ), 22.9, 22.8, 20.0, 19.8 ( $\text{CH}_3$ ).

MS (ESI):  $m/z$  = 852.73 [ $\text{M} - 2 \text{PF}_6$ ] $^{2+}$ , 1850.7 [ $\text{M} - \text{PF}_6$ ] $^+$ .

MS (MALDI-TOF, matrix: dithranol):  $m/z$  = 1704.69 [ $\text{M} - 2 \text{PF}_6$ ] $^+$ , 1849.75 [ $\text{M} - \text{PF}_6$ ] $^+$ .

Anal. Calcd for  $\text{C}_{106}\text{H}_{150}\text{N}_6\text{O}_6\text{RuP}_2\text{F}_{12}$  (2053.5): C, 63.23; H 7.61; N 4.07. Found: C, 63.07; H, 7.24; N, 4.17.

**(4'-[3,4,5-Tris-(3,7-dimethyl-octyloxy)-phenylethynyl]-2,2':6',2''-terpyridine) (4'-heptyloxy 2,2':6',2''-terpyridine) ruthenium(II) hexafluorophosphate 37**

The compound was prepared following the procedure for **36**. 36 mg (0.046 mmol) **34**, 24.6 (0.046 mmol) **26**. In this case a precipitate was obtained after the addition of  $\text{NH}_4\text{PF}_6$  solution which was collected by filtration, washed with 50 mL of ethanol/water (50:50) and recrystallized from acetonitrile/diethyl ether. Yield: 53 mg (72%). This complex, however, was not readily soluble in dodecane. Therefore a solution in chloroform was mixed with dodecane and the chloroform was subsequently removed by evaporation. The obtained solution was used for the UV-vis and CD investigations.

UV-vis (acetonitrile):  $\lambda_{\text{max}}$  ( $\epsilon$ ) = 241 (61000), 273 (66300), 304 (68800), 502 (34100) nm ( $\text{L mol}^{-1}\text{cm}^{-1}$ ).

$^1\text{H}$ -NMR (400 MHz,  $\text{CD}_3\text{CN}$ ):  $\delta$  = 0.89 (18 H, d,  $J$  = 6.59 Hz,  $\text{CH}_3$ ), 0.95 (6 H, m,  $\text{CH}_3$ ), 0.99 (6 H, d,  $J$  = 6.59 Hz,  $\text{CH}_3$ ), 1.20 (10 H, m,  $\text{CH}_2$ ), 1.37 (14 H, m,  $\text{CH}_2$ ), 1.53 (6 H, m,  $\text{CH}_2$ ), 1.63 (4 H, m,  $\text{CH}_2$ ), 1.76 (2 H, m,  $\text{CH}_2$ ), 1.90 (3 H, m, CH), 2.04 (3 H, m, CH), 4.05 (2 H, m,  $\text{OCH}_2$ ), 4.13 (4 H, m,  $\text{OCH}_2$ ), 4.53 (2 H, t,  $J$  = 6.59 Hz,  $\text{OCH}_2$  (heptyl)), 7.03 (2 H, s,  $\text{H}_{\text{phenyl}}$ ), 7.13 (2 H, ddd,  $J$  = 7.32, 7.32, 1.46 Hz,  $\text{H}_{5,5''}$ ), 7.21, (2 H, ddd,  $J$  = 7.32, 7.32, 1.46 Hz,  $\text{H}_{5,5''}$ ), 7.35 (2 H, d,  $J$  = 5.13 Hz,  $\text{H}_{6,6''}$ ), 7.45 (2 H, d,  $J$  = 5.13 Hz,  $\text{H}_{6,6''}$ ), 7.90 (2 H, ddd,  $J$  = 8.06, 8.06, 1.46 Hz,  $\text{H}_{4,4''}$ ), 7.94 (2 H, ddd,  $J$  = 8.06, 8.06, 1.46 Hz,  $\text{H}_{4,4''}$ ), 8.31 (2 H, s,  $\text{H}_{3,3''}$ ), 8.48 (2 H, d,  $J$  = 8.06 Hz,  $\text{H}_{3,3''}$ ), 8.49 (2 H, d,  $J$  = 8.06 Hz,  $\text{H}_{3,3''}$ ), 8.79 (2 H, s,  $\text{H}_{3,3''}$ ).

$^{13}\text{C}$ -NMR (100 MHz,  $\text{CD}_3\text{CN}$ ):  $\delta$  = 178.9, 166.9, 158.3, 156.1, 153.6, 153.0, 152.6, 140.4, 138.3, 138.2, 127.9, 127.6, 125.1, 124.7, 124.6, 116.7, 111.3, 110.7, 98.6, 85.6 (alkyne), 71.7 ( $\text{OCH}_2$  (para-chain)), 70.7 ( $\text{OCH}_2$  (heptyl)), 67.5 ( $\text{OCH}_2$  (meta-chains)), 39.4, 39.4, 37.4, 37.35, 37.3, 36.4 ( $\text{CH}_2$ ), 31.8, 29.8 (CH (heptyl)), 29.7, 28.9, 28.0 (CH), 24.8, 25.4 ( $\text{CH}_2$ ), 22.6 (3- $\text{CH}_3$  (para-chain)), 22.2 (3- $\text{CH}_3$  (meta-chains)), 19.3 (7- $\text{CH}_3$  (para-chain)), 19.1 (7- $\text{CH}_3$  (meta-chains)), 13.7 ( $\text{CH}_3$  heptyl).

MS (ESI):  $m/z$  = 623.0 [ $\text{M} - 2 \text{PF}_6$ ] $^{2+}$ , 1393.8 [ $\text{M} - \text{PF}_6$ ] $^+$ .

MS (MALDI-TOF, matrix: dithranol):  $m/z$  = 1249.23 [ $\text{M} - 2 \text{PF}_6$ ] $^+$ , 1395.15 [ $\text{M} - \text{PF}_6$ ] $^+$ .

Anal. Calcd for  $\text{C}_{75}\text{H}_{100}\text{N}_6\text{O}_6\text{RuP}_2\text{F}_{12}$  (1598.8): C, 58.47; H 6.54; N 5.45. Found: C, 58.84; H, 6.35; N, 5.25.

**4'-(3,4,5-Tris-dodecyl-phenylethynyl)-2,2':6',2''-terpyridine 39**

The reactions were performed in the same way as described before. 500 mg (0.76 mmol) **38**, 217 mg (0.70 mmol) 4'-bromo-2,2':6',2''-terpyridine **33** and 53 mg (6% mol)  $\text{Pd}(\text{PPh}_3)_4$ . Yield: 530 mg (85%).

UV-vis (acetonitrile):  $\lambda_{\text{max}}$  ( $\epsilon$ ) = 238 (27700), 285 (25400), 320 (23700) nm ( $\text{L mol}^{-1}\text{cm}^{-1}$ ).

$^1\text{H}$ -NMR (400 MHz,  $\text{CDCl}_3$ ):  $\delta$  = 0.88 (9 H, m,  $\text{CH}_3$ ), 1.27 (49 H, m,  $\text{CH}_2$ ), 1.49 (6 H, m,  $\text{CH}_2$ ), 1.78 and 1.82 (6 H, m,  $\text{CH}_2$ ), 4.00 (6 H, m,  $\text{OCH}_2$ ), 6.78 (2 H, s,  $\text{H}_{\text{phenyl}}$ ), 7.30 (2 H, ddd,  $J$  = 5.86, 4.39, 1.47 Hz,  $\text{H}_{5,5''}$ ), 7.82 (2 H, ddd,  $J$  = 8.06, 8.06, 1.47 Hz,  $\text{H}_{4,4''}$ ), 8.55 (2 H, s,  $\text{H}_{3,3''}$ ), 8.59 (2 H, dd,  $J$  = 8.06, 1.47 Hz,  $\text{H}_{3,3''}$ ), 8.69 (2 H, d,  $J$  = 6.59 Hz,  $\text{H}_{6,6''}$ ).

$^{13}\text{C}$ -NMR (100 MHz,  $\text{CHCl}_3$ ):  $\delta$  = 155.6, 155.4, 153.0, 149.0, 139.6, 136.7, 133.4, 123.9, 122.6, 121.1, 116.7, 110.3 (arom.), 94.3, 86.4 (alkyne), 73.5 ( $\text{OCH}_2$  (para-chain)), 69.1 ( $\text{OCH}_2$  (meta-chains)), 31.9, 30.3, 29.7, 29.6, 29.4, 29.33, 29.28, 26.0 ( $\text{CH}_2$ ), 22.6 ( $\text{CH}_2\text{CH}_3$ ), 14.1 ( $\text{CH}_3$ ).

MS (MALDI-TOF, matrix: dithranol):  $m/z$  = 886.73 [ $\text{M} + \text{H}$ ] $^+$ , 908.85 [ $\text{M} + \text{Na}$ ] $^+$ .

Anal. Calcd for  $\text{C}_{59}\text{H}_{87}\text{N}_3\text{O}_3$  (886.4): C, 79.95; H 9.89; N 4.74. Found: C, 79.44; H, 9.98; N, 4.51.

**[4'-(3,4,5-Tris-dodecyl-phenylethynyl)-2,2':6',2''-terpyridine] ruthenium(III) chloride 40**

This compound has been prepared in the same manner as compound **35**. 82 mg (0.093 mmol) **39**, 130 mg (0.63 mmol)  $\text{RuCl}_3 \times \text{H}_2\text{O}$ . Yield: 99.7 mg (98%). The compound was used without further purification or characterization.

**Bis-[4'-(3,4,5-tris-dodecyl-phenylethynyl)-2,2':6',2''-terpyridine] ruthenium(II) hexafluorophosphate 41**

The compound was prepared following the procedure for **36**. 50 mg (0.045 mmol) **40**, 40 mg (0.045 mmol) **39**. Yield: 61 mg (62%).

UV-vis (acetonitrile):  $\lambda_{\text{max}}$  ( $\epsilon$ ) = 282 (66200), 314 (65200), 501 (45300) nm ( $\text{L mol}^{-1}\text{cm}^{-1}$ ).

$^1\text{H}$ -NMR (400 MHz,  $\text{CDCl}_3$ ):  $\delta$  = 0.89 (9 H, m,  $\text{CH}_3$ ), 1.27 (58 H, m,  $\text{CH}_2$ ), 1.50 and 1.57 (10 H, m,  $\text{CH}_2$ ), 1.77 and 1.84 (6 H, m,  $\text{CH}_2$ ), 4.05 (6 H, m,  $\text{OCH}_2$ ), 6.98 (2 H, s,  $\text{H}_{\text{phenyl}}$ ), 7.21 (2 H, t,  $J$  = 6.59 Hz,  $\text{H}_{5,5''}$ ), 7.32 (2 H, d,  $J$  = 5.13 Hz,  $\text{H}_{6,6''}$ ), 7.85 (2 H, dd,  $J$  = 7.23, 7.23 Hz,  $\text{H}_{4,4''}$ ), 8.37 (2 H, d,  $J$  = 8.06 Hz,  $\text{H}_{3,3''}$ ), 8.64 (2 H, s,  $\text{H}_{3,3''}$ ).

$^{13}\text{C}$ -NMR (100 MHz,  $\text{CHCl}_3$ ):  $\delta$  = 157.1, 154.6, 153.1, 152.0, 140.3, 138.3, 131.9, 124.7, 128.2, 125.1, 115.7, 110.8 (arom.), 99.8, 85.4 (alkyne), 73.6 ( $\text{OCH}_2$  (para-chain)), 69.2 ( $\text{OCH}_2$  (meta-chains)), 31.9, 30.3, 29.7, 29.6, 29.4, 29.3, 26.14, 26.07 ( $\text{CH}_2$ ), 22.7 ( $\text{CH}_2\text{CH}_3$ ), 14.1 ( $\text{CH}_3$ ).

MS (MALDI-TOF, matrix: dithranol):  $m/z$  = 1872.52 [ $\text{M} - 2 \text{PF}_6$ ] $^+$ , 2017.38 [ $\text{M} - \text{PF}_6$ ] $^+$ .

Anal. Calcd for  $C_{118}H_{174}N_6O_6RuP_2F_{12} + 1 H_2O$  (2163.7): C, 64.96; H 8.13; N 3.85. Found: C, 64.91; H, 8.03; N, 3.84.

**[4'-(3,4,5-Tris-dodecyl-phenylethynyl)-2,2':6',2''-terpyridine] [4'-heptyloxy 2,2':6',2''-terpyridine] ruthenium(II) hexafluorophosphate 42**

The compound was prepared following the procedure for **37**. 25 mg (0.028 mmol) **39**, 16 mg (0.028 mmol) **26**. Yield: 29 mg (63%). Dodecane solutions were obtained in a similar procedure as for **37**.

UV-vis (acetonitrile):  $\lambda_{max}$  ( $\epsilon$ ) = 241 (61000), 273 (66300), 304 (68800), 502 (34100) nm ( $L mol^{-1} cm^{-1}$ ).

$^1H$ -NMR (400 MHz,  $CD_3CN$ ):  $\delta$  = 0.88 (9 H, m,  $CH_3$ ), 0.96 (3 H, t,  $J$  = 6.86 Hz,  $CH_3$  (heptyl)), 1.11 (22 H, m,  $CH_2$ ), 1.29 (54 H, m,  $CH_2$ ), 1.42 (8 H, m,  $CH_2$ ), 1.52 (8 H, m,  $CH_2$ ), 1.66 (4 H, m,  $CH_2$ ), 1.82 (6 H, m,  $CH_2$ ), 3.98 (2 H, t,  $J$  = 6.59 Hz,  $OCH_2$ ), 4.08 (4 H, t,  $J$  = 6.04 Hz,  $OCH_2$ ), 4.53 (2 H, t,  $J$  = 6.59 Hz,  $OCH_2$ ), 7.01 (2 H, s,  $H_{phenyl}$ ), 7.13 (2 H, ddd,  $J$  = 6.59, 6.59, 1.46 Hz,  $H_{5,5''}$ ), 7.22, (2 H, ddd,  $J$  = 7.32, 7.32, 1.46 Hz,  $H_{5,5''}$ ), 7.35 (2 H, d,  $J$  = 5.13 Hz,  $H_{6,6''}$ ), 7.45 (2 H, d,  $J$  = 5.13 Hz,  $H_{6,6''}$ ), 7.90 (2 H, ddd,  $J$  = 8.06, 8.06, 1.46 Hz,  $H_{4,4''}$ ), 7.94 (2 H, ddd,  $J$  = 8.06, 8.06, 1.46 Hz,  $H_{4,4''}$ ), 8.31 (2 H, s,  $H_{3,5'}$ ), 8.48 (2 H, d,  $J$  = 8.06 Hz,  $H_{3,3''}$ ), 8.49 (2 H, d,  $J$  = 8.06 Hz,  $H_{3,3''}$ ), 8.78 (2 H, s,  $H_{3,5'}$ ).

MALDI-TOF-MS:  $m/z$  = 1335.02 [ $M - 2 PF_6$ ] $^+$ , 1480.00 [ $M - PF_6$ ] $^+$ .

**Kinetic studies of complex formation in aqueous media**

In all three reactions (a-b), 5 mg of 4'-( $\omega$ -methoxy-poly(ethylene glycol))-terpyridine ruthenium(III) trichloride **43** ( $M_n$  = 3400) and 0.5 mg of 4'-(methoxy di(ethylene glycol))-2,2':6',2''-terpyridine **27** were dissolved in 2 mL of water and stirred at room temperature.

(a) No more ingredients were added, the reaction was performed in pure water.

(b) 0.1 mL ethanol was added.

(c) 0.1 mL ethanol and 1 drop of *N*-ethylmorpholine were added.

In regular intervals, a sample was taken from the solution, diluted to a concentration of  $5 \times 10^{-5}$  and a UV-vis spectrum was recorded.

**General method for the preparation of the mixed terpyridine bipyridine copper complexes**

An equimolar amount of the ligands in 10 mL acetonitrile was added to a solution of Cu-triflate in 10 mL acetonitrile. After stirring for 2 h at room temperature, a tenfold excess of ammoniumhexafluorophosphate was added and the complex was precipitated by addition of 20 mL of diethyl ether. After washing with 20 mL of ethanol followed by 20 mL of diethyl ether the compound was recrystallized from acetonitrile/diethyl ether to yield blue crystals.

**(2,2':6',2''-Terpyridine) (4,4'-dimethyl-2,2'-bipyridine) copper(II) hexafluorophosphate 49**

100 mg (0.43 mmol) **45**, 77.4 mg (0.43 mmol) **48**, 155.5 mg coppertriflate. Yield: 267.5 mg (81%).

UV-vis:  $\lambda_{max}$  ( $\epsilon$ ) = 285 (23500), 307 (14300), 327 (15700), 337 (13400), 644 (100) nm ( $L mol^{-1} cm^{-1}$ ).

MS (MALDI-TOF, dithranol):  $m/z$  = 480.13 [ $M - 2 PF_6$ ] $^+$ , 296.33 [ $M - bpy - 2 PF_6$ ] $^+$ .

Anal. Calcd for  $C_{27}H_{23}N_5CuP_2F_{12}$  (771.99): C, 42.06; H, 3.01; N, 9.08. Found: C, 41.92; H, 2.96; N, 9.16.

**(5,5''-Dimethyl-2,2':6',2''-terpyridine) (2,2'-bipyridine) copper(II) hexafluorophosphate 50**

100 mg (0.38 mmol) **46**, 70.6 mg (0.38 mmol) **47**, 139 mg coppertriflate. Yield: 261.5 mg (80%).

UV-vis:  $\lambda_{max}$  ( $\epsilon$ ) = 289 (28700), 306 (14700), 334 (17100), 346 (15000), 640 (100) nm ( $L mol^{-1} cm^{-1}$ ).

MS (MALDI-TOF, dithranol):  $m/z$  = 479.9 [ $M - 2 PF_6$ ] $^+$ .

Anal. Calcd for  $C_{29}H_{27}N_5CuP_2F_{12} + H_2O$  (817.05): C, 42.63; H, 2.58; N, 8.57. Found: C, 42.41; H, 3.23; N, 8.44.

**(5,5''-Dimethyl-2,2':6',2''-terpyridine) (4,4'-dimethyl-2,2'-bipyridine) copper(II) hexafluorophosphate 51**

50 mg (0.19 mmol) **46**, 29.9 mg (0.19 mmol) **48**, 69.3 mg (0.19 mmol) coppertriflate. Yield: 266 mg (80%).

UV-vis:  $\lambda_{max}$  ( $\epsilon$ ) = 288 (27600), 305 (14700), 334 (16200), 346 (14400), 645 (100) nm ( $L mol^{-1} cm^{-1}$ ).

MS (MALDI-TOF, dithranol):  $m/z$  = 508.68 [ $M - 2 PF_6$ ] $^+$ .

Anal. Calcd for  $C_{27}H_{23}N_5CuP_2F_{12}$  (771.99): C, 42.06; H, 3.01; N, 9.08. Found: C, 41.88; H, 2.67; N, 9.16.

**Single crystal X-ray structure determination of compound 19\*1.083( $CH_3CN$ )**

Crystal data and details of the structure determination are presented in Table 1. Suitable single crystals for the X-ray diffraction study were grown by a slow diffusion of diethyl ether into a solution of **19** in acetonitrile at room temperature. A clear red needle (0.13  $\times$  0.25  $\times$  0.69 mm) was stored under perfluorinated ether, transferred in a Lindemann capillary, fixed and sealed. Preliminary examination and data collection were carried out on an area detecting system (NONIUS, MACH3  $\kappa$ -CCD) at the window of a rotating anode (NONIUS; FR591) and graphite monochromated  $MoK_{\alpha}$  radiation ( $\lambda$  = 0.71073 Å). The unit cell parameters were obtained by full-matrix least-squares refinement of 7640 reflections. Data collection were performed at 123 K within a  $\Theta$ -range of  $1.52^\circ < \Theta < 25.44^\circ$ . 8 data sets were measured in rotation scan modus with  $\Delta\phi / \Delta\Omega = 1.0^\circ$ . A total number of 45439 intensities were integrated. Raw data were corrected for Lorentz, polarization, and during the scaling procedure for latent decay and absorption effects. After merging ( $R_{int} = 0.048$ ) a sum of 7650 (all data) and 7034 ( $I > 2\sigma(I)$ ), resp., remained and all data were used. The structure was solved by a combination of direct methods

and difference Fourier syntheses. All non-hydrogen atoms were refined with anisotropic displacement parameters. All hydrogen atoms were calculated in ideal positions (riding model). Full-matrix least-squares refinements with 670 parameters were carried out by minimizing  $\Sigma w(F_o^2 - F_c^2)^2$  with SHELXL-97 weighting scheme and stopped at shift/err < 0.001. Small extinction effects had to be corrected. Besides the solvent molecules well located in the difference Fourier maps, but with incomplete site occupation factors, unresolved solvent molecules remained and had to be removed by the SQUEEZE procedure in addition. The final residual electron density maps showed no remarkable features. Neutral atom scattering factors for all atoms and anomalous dispersion corrections for the non-hydrogen atoms were taken from *International Tables for Crystallography*. All calculations were performed on an Intel Pentium II PC, with the STRUX-V system, including the programs PLATON, SHELXL-97, and SIR92.<sup>[53,54]</sup>

#### Single crystal X-ray structure determination of compound 49\*(CH<sub>3</sub>CN)

Crystal data and details of the structure determination are presented in Table 1, bond lengths and bond angles are listed in Table 2. Suitable single crystals for the X-ray diffraction study were grown by diffusion of diethyl ether into a solution of **49** in acetonitrile. A clear blue plate (0.10 × 0.66 × 1.02 mm) was stored under perfluorinated ether, transferred in a Lindemann capillary, fixed and sealed. Preliminary examination and data collection were carried out on an area detecting system (NONIUS, MACH3 κ-CCD) at the window of a rotating anode (NONIUS, FR591) and graphite monochromated MoK<sub>α</sub> radiation (λ = 0.71073 Å). The unit cell parameters were obtained by full-matrix least-squares refinement of 6075 reflections. Data collection were performed at 123 K within a Θ-range of 2.18° < Θ < 25.33°. Four data sets were measured in rotation scan modus with Δφ / ΔΩ = 1.0°. A total number of 17640 intensities were integrated. Raw data were corrected for Lorentz, polarization, and during the scaling procedure for latent decay and absorption effects. After merging ( $R_{\text{int}} = 0.072$ ) a sum of 5745 (all data) and 5189 ( $I > 2\sigma(I)$ ), respectively, remained and all data were used. The structure was solved by a combination of direct methods and difference Fourier syntheses. All non-hydrogen atoms were refined with anisotropic displacement parameters. All hydrogen atoms were found in the final difference Fourier maps and allowed to refine freely with isotropic displacement parameters. Full-matrix least-squares refinements with 555 parameters were carried out by minimizing  $\Sigma w(F_o^2 - F_c^2)^2$  with SHELXL-97 weighting scheme and stopped at shift/err < 0.001. The final residual electron density maps showed no remarkable features. Neutral atom scattering factors for all atoms and anomalous dispersion corrections for the non-hydrogen atoms were taken from *International Tables for Crystallography*. All calculations were performed on an Intel Pentium II PC, with the STRUX-V system, including the programs PLATON, SHELXL-97, and SIR92.<sup>[53,54]</sup>

#### Single crystal X-ray structure determination of compound 50

Crystal data and details of the structure determination are presented in Table 1, bond lengths and bond angles are listed in Table 2. Suitable single crystals for the X-ray diffraction study were grown by diffusion of diethyl ether into a solution of **50** in acetonitrile. A clear blue fragment (0.25 × 0.51 × 0.76 mm) was stored under perfluorinated ether, transferred in a Lindemann capillary, fixed and sealed. Preliminary examination and data collection were carried out on an area detecting system (NONIUS, MACH3 κ-CCD) at the window of a rotating anode (NONIUS, FR591) and graphite monochromated MoK<sub>α</sub> radiation (λ = 0.71073 Å). The unit cell parameters were obtained by full-matrix least-squares refinement of 5812 reflections. Data collection were performed at 123 K within a Θ-range of 2.14° < Θ < 25.37°. Eight data sets were measured in rotation scan modus with Δφ / ΔΩ = 1.0°. A total number of 45028 intensities were integrated. Raw data were corrected for Lorentz, polarization, and during the scaling procedure for latent decay and absorption effects. After merging ( $R_{\text{int}} = 0.050$ ) a sum of 5508 (all data) and 5178 ( $I > 2\sigma(I)$ ), respectively, remained and all data were used. The structure was solved by a combination of direct methods and difference Fourier syntheses. All non-hydrogen atoms were refined with anisotropic displacement parameters. All hydrogen atoms were found in the final difference Fourier maps and allowed to refine freely with isotropic displacement parameters. Full-matrix least-squares refinements with 516 parameters were carried out by minimizing  $\Sigma w(F_o^2 - F_c^2)^2$  with SHELXL-97 weighting scheme and stopped at shift/err < 0.001. The final residual electron density maps showed no remarkable features. Neutral atom scattering factors for all atoms and anomalous dispersion corrections for the non-hydrogen atoms were taken from *International Tables for Crystallography*. All calculations were performed on an Intel Pentium II PC, with the STRUX-V system, including the programs PLATON, SHELXL-97, and SIR92.<sup>[53,54]</sup>

#### Single crystal X-ray structure determination of compound 51

Crystal data and details of the structure determination are presented in Table 1, bond lengths and bond angles are listed in Table 2. Suitable single crystals for the X-ray diffraction study were grown by diffusion of diethyl ether into a solution of **51** in acetonitrile. A clear blue plate (0.25 × 0.38 × 0.76 mm) was stored under perfluorinated ether, transferred in a Lindemann capillary, fixed and sealed. Preliminary examination and data collection were carried out on an area detecting system (NONIUS, MACH3 κ-CCD) at the window of a rotating anode (NONIUS, FR591) and graphite monochromated MoK<sub>α</sub> radiation (λ = 0.71073 Å). The unit cell parameters were obtained by full-matrix least-squares refinement of 14786 reflections. Data collection were performed at 123 K

within a  $\Theta$ -range of  $1.47^\circ < \Theta < 25.56^\circ$ . Five data sets were measured in rotation scan modus with  $\Delta\varphi / \Delta\Omega = 1.0^\circ$ . A total number of 45920 intensities were integrated. Raw data were corrected for Lorentz, polarization, and during the scaling procedure for latent decay and absorption effects. After merging ( $R_{\text{int}} = 0.037$ ) a sum of 14786 (all data) and 12829 ( $I > 2\sigma(I)$ ), respectively, remained and all data were used. The structure was solved by a combination of direct methods and difference Fourier syntheses. All non-hydrogen atoms were refined with anisotropic displacement parameters. All hydrogen atoms were calculated in ideal positions (riding model). Full-matrix least-squares refinements with 892 parameters were carried out by minimizing  $\sum w(F_o^2 - F_c^2)^2$  with SHELXL-97 weighting scheme and stopped at shift/err  $< 0.001$ . Unresolvable solvent molecules had to be removed by the SQUEEZE procedure. A disorder over two positions (75:25) of the methyl group bound to C33 could be resolved clearly. The final residual electron density maps showed no remarkable features. Neutral atom scattering factors for all atoms and anomalous dispersion corrections for the non-hydrogen atoms were taken from *International Tables for Crystallography*. All calculations were performed on an Intel Pentium II PC, with the STRUX-V system, including the programs PLATON, SHELXL-97, and SIR92.<sup>[53,54]</sup>

Table 2.1. Crystal data and summary of intensity data collection and structure refinement of compound **19**\*1.083(CH<sub>3</sub>CN).

	<b>19</b> *1.083(CH <sub>3</sub> CN)
Empirical formula	[(C <sub>36</sub> H <sub>34</sub> N <sub>6</sub> O <sub>2</sub> Ru) <sup>2+</sup> ], 2[(PF <sub>6</sub> ) <sup>-</sup> ], 1.083(C <sub>2</sub> H <sub>3</sub> N)
Formula weight	1018.16
Shape, color	needle, red
Space group	$P \bar{1}$ (No. 2)
Unit cell dimensions	a = 8.7799(1) Å, b = 13.6908(3) Å, c = 17.7484(3) Å $\alpha = 86.133(1)^\circ$ , $\beta = 85.364(1)^\circ$ , $\gamma = 78.146(1)^\circ$
Volume	2078.23(6) Å <sup>3</sup>
Z	2
Density (calculated)	1.627 g/cm <sup>3</sup>
Absorption coefficient	0.553 mm <sup>-1</sup>
F(000)	1027.7
$\Theta$ -range for data collection	$1.52^\circ \leq \Theta \leq 25.44^\circ$
Index $\Theta$ -ranges	h: $\pm 10$ , k: $\pm 16$ , l: $\pm 21$
Reflections integrated	45439
Independent reflections (all data)	7650
Observed reflections [ $I > 2\sigma(I)$ ]	7034
Parameters refined	670
Final R indices <sup>a)</sup> [ $I > 2\sigma(I)$ ]	R1 = 0.0672, wR2 = 0.1702
R indices <sup>a)</sup> (all data)	R1 = 0.0726, wR2 = 0.1730
Goodness-of-fit on F <sup>2</sup>	1.147
Extinction coefficient, method	0.0038(8), SHELXL-97 isotropic
Largest diff. peak and hole	1.33 and -0.59 e/Å <sup>3</sup>

<sup>a)</sup> The high R-Values are caused by the disorder of the two PF<sub>6</sub>-anions and the solvent molecules (see above).

Table 2.2. Crystal data and summary of data collection and structure refinement of compounds 49\*(CH<sub>3</sub>CN), 50, and 51.

	49*(CH <sub>3</sub> CN)	50	51
Empirical formula	[(C <sub>27</sub> H <sub>23</sub> CuN <sub>5</sub> ) <sup>2+</sup> ], 2[(PF <sub>6</sub> ) <sup>-</sup> ], (C <sub>2</sub> H <sub>3</sub> N)	[(C <sub>27</sub> H <sub>23</sub> CuN <sub>5</sub> ) <sup>2+</sup> ], 2[(PF <sub>6</sub> ) <sup>-</sup> ]	[(C <sub>29</sub> H <sub>27</sub> CuN <sub>5</sub> ) <sup>2+</sup> ], 2[(PF <sub>6</sub> ) <sup>-</sup> ]
Formula weight	812.05	770.99	799.05
Shape, color	plate, blue	fragment, blue	plate, blue
Space group	<i>P</i> 2 <sub>1</sub> / <i>n</i> (No. 14)	<i>P</i> 2 <sub>1</sub> / <i>c</i> (No. 14)	<i>P</i> $\bar{1}$ (No. 2)
Unit cell dimensions	a = 8.6498(3) Å, b = 11.1494(6) Å, c = 34.205(2) Å β = 91.194(3)°	a = 17.6748(3) Å, b = 11.6226(2) Å, c = 15.6492(2) Å β = 109.9545(8)°	a = 14.0094(3) Å, b = 14.4069(2) Å, c = 21.4228(4) Å α = 71.3320(9)°, β = 82.2098(7)°, γ = 85.2098(9)°
Volume	3298.0(3) Å <sup>3</sup>	3021.77(8) Å <sup>3</sup>	4054.82(13) Å <sup>3</sup>
Z	4	4	4
Density (calculated)	1.635 g/cm <sup>3</sup>	1.695 g/cm <sup>3</sup>	1.309 g/cm <sup>3</sup>
Absorption coefficient	0.859 mm <sup>-1</sup>	0.932 mm <sup>-1</sup>	0.697 mm <sup>-1</sup>
F(000)	1636	1548	1612
Θ-range for data collection	2.18° ? Θ ? 25.33°	2.14° ? Θ ? 25.37°	1.47° ? Θ ? 25.56°
Index Θ-ranges	h: ±10, k: ±13, l: ±41	h: ±21, k: ±14, l: ±18	h: ±16, k: ±17, l: ±25
Reflections integrated	17640	45028	45920
Independent reflections (all data)	5745	5508	14786
Observed reflections [ <i>I</i> > 2σ( <i>I</i> )]	5189	5178	12829
Parameters refined	555	516	892
Final R indices [ <i>I</i> > 2σ( <i>I</i> )]	R1 = 0.0487, wR2 = 0.1196	R1 = 0.0408, wR2 = 0.1006	R1 = 0.0369, wR2 = 0.1077
R indices (all data)	R1 = 0.0545, wR2 = 0.1234	R1 = 0.0432, wR2 = 0.1023	R1 = 0.0428, wR2 = 0.1112
Goodness-of-fit on F <sup>2</sup>	1.041	1.042	1.062
Largest diff. peak and hole	0.71 and -0.54 e/Å <sup>3</sup>	1.29 and -0.77 e/Å <sup>3</sup>	0.59 and -0.47 e/Å <sup>3</sup>

Table 2.3. Characteristic bond lengths [ $\text{\AA}$ ] and bond angles [deg] for compounds **49\***( $\text{CH}_3\text{CN}$ ), **50** and **51**.

	<b>49*</b> ( $\text{CH}_3\text{CN}$ )	<b>50</b>	<b>51A</b>	<b>B</b> <sup>a)</sup>
Cu – N11	1.992(2)	1.984(2)	1.990(2)	1.993(2)
Cu – N21	2.180(2)	2.186(2)	2.171(2)	2.189(2)
Cu – N31	2.042(2)	2.022(2)	2.037(2)	2.045(2)
Cu – N41	1.924(2)	1.928(2)	1.933(2)	1.926(2)
Cu – N51	2.049(3)	2.044(2)	2.039(2)	2.049(2)
Cu ... F	2.823(2)	2.890(2)	2.990(1)	3.127(1)
N11 – Cu – N21	78.85(9)	79.45(9)	79.20(7)	78.73(7)
N11 – Cu – N31	101.02(10)	98.84(9)	97.25(8)	97.55(7)
N11 – Cu – N41	178.24(10)	177.51(9)	167.20(8)	162.37(7)
N11 – Cu – N51	98.42(11)	99.88(9)	99.76(8)	100.00(7)
N11 – Cu ... F	90.01(8)	89.97(8)	96.29(6)	87.90(5)
N21 – Cu – N31	97.49(9)	100.07(9)	97.88(7)	96.47(7)
N21 – Cu – N41	102.58(10)	103.01(9)	113.53(7)	118.84(7)
N21 – Cu – N51	99.36(10)	92.31(9)	96.94(7)	96.63(7)
N21 – Cu ... F	165.82(8)	168.77(8)	166.19(6)	159.24(6)
N31 – Cu – N41	79.85(10)	80.42(9)	80.18(8)	79.96(7)
N31 – Cu – N51	156.36(10)	159.15(10)	159.23(8)	159.84(7)
N31 – Cu ... F	75.87(8)	85.17(7)	95.64(6)	69.40(6)
N41 – Cu – N51	80.38(11)	80.49(9)	80.60(8)	80.31(7)
N41 – Cu ... F	88.73(9)	87.60(8)	71.64(6)	74.85(6)
N51 – Cu ... F	90.86(9)	85.74(8)	70.78(6)	101.31(6)

<sup>a)</sup> The unit cell of **51** contains two crystallographic independent molecules (**A**: Cu1, N11-N51 corresponds to **B**: Cu2, N61-N101).

## 2.10 References

- [1] [1a] J.-M. Lehn, *Supramolecular Chemistry, Concepts and Perspectives*, VCH, Weinheim, **1995**; [1b] U. S. Schubert, in *Tailored Polymers & Applications* (Ed.: M. K. M. Y. Yagci, O. Nuyken, K. Ito, G. Wnek), VSP Publishers, Utrecht, **2000**, 63-85.
- [2] M. Heller, U. S. Schubert, *Eur. J. Org. Chem.* **2003**, 947-961.
- [3] R. Ziessel, L. Douce, A. El-Ghayoury, A. Harriman, A. Skoulios, *Angew. Chem., Int. Ed.* **2000**, *39*, 1489-1493, *Angew. Chem.*, **2000**, *112*, 1549-1453.
- [4] [4a] M. Rehahn, *Acta Polym.* **1998**, *49*, 201-224; [4b] B. G. G. Lohmeijer, U. S. Schubert, *J. Polym. Sci., Part A: Polym. Chem.* **2003**, *41*, 1413-1427.
- [5] D. G. Kurth, M. Schütte, J. Wen, *Colloids Surf., A* **2002**, *198-200*, 633-643.
- [6] E. C. Constable, *Adv. Inorg. Chem. Radiochem.* **1986**, *30*, 69-121.

- [7] U. S. Schubert, C. Eschbaumer, P. R. Andres, H. Hofmeier, C. H. Weidl, E. Herdtweck, E. Dulkeith, A. Morteani, N. E. Hecker, J. Feldmann, *Synth. Met.* **2001**, *121*, 1249-1252.
- [8] R. H. Holyer, C. D. Hubbard, S. F. A. Kettle, R. G. Wilkins, *Inorg. Chem.* **1966**, *5*, 622-625.
- [9] [9a] B. P. Sullivan, J. M. Calvert, T. J. Meyer, *Inorg. Chem.* **1980**, *19*, 1404-1407; [9b] E. C. Constable, A. M. W. C. Thompson, D. A. Tocher, M. A. M. Daniels, *New J. Chem.* **1992**, *16*, 855-867; [9c] B. G. G. Lohmeijer, U. S. Schubert, *Angew. Chem.* **2002**, *114*, 3980-3984; *Angew. Chem. Int. Ed.* **2002**, *41*, 3825-3829.
- [10] G. R. Newkome, E. He, L. A. Godinez, *Macromolecules* **1998**, *31*, 4382-4386.
- [11] [11a] L. S. Pinheiro, M. L. A. Temperini, *Surf. Sci.* **2000**, *464*, 176-182; [11b] J. Park, A. N. Pasupathy, J. I. Goldsmith, C. Chang, Y. Yaish, J. R. Petta, M. Rinkoski, J. P. Sethna, H. D. Abruna, P. L. McEuen, D. C. Ralph, *Nature* **2002**, *417*, 722-725.
- [12] A. T. Daniher, J. K. Bashkin, *Chem. Commun.* **1998**, 1077-1078.
- [13] [13a] E. C. Constable, M. D. Ward, *J. Chem. Soc., Dalton Trans.* **1990**, 1405-1409; [13b] U. S. Schubert, S. Schmatloch, A. A. Precup, *Design. Monom. Polym.* **2002**, *5*, 211-221.
- [14] [14a] D. Armspach, E. C. Constable, C. E. Housecroft, M. Neuburger, M. Zehnder, *J. Organomet. Chem.* **1998**, *550*, 193-206; [14b] X. Liu, E. J. L. McInnes, C. A. Kilner, M. Thornton-Pett, M. A. Halcrow, *Polyhedr.* **2001**, *20*, 2889-2900.
- [15] E. C. Constable, C. E. Housecroft, C. B. Smith, *Inorg. Chem. Commun.* **2003**, *6*, 1011-1013.
- [16] [16a] G. R. Newkome, E. He, *J. Mater. Chem.* **1997**, *7*, 1237-1244; [16b] R.-A. Fallahpour, *Synthesis* **2003**, 155-184; [16c] U. S. Schubert, C. Eschbaumer, O. Hien, P. R. Andres, *Tetrahedr. Lett.* **2001**, *42*, 4705-4707; [16c] P. R. Andres, R. Lunkwitz, G. R. Pabst, K. Böhm, D. Wouters, S. Schmatloch, U. S. Schubert, *Eur. J. Org. Chem.* **2003**, 3769-3776.
- [17] F. Kröhnke, *Synthesis* **1976**, 1-24.
- [18] J. M. Rao, M. C. Hughes, D. J. Macero, *Inorg. Chim. Acta* **1976**, *16*, 231-236.
- [19] *Coord. Chem. Rev.* **1996**, *150*, ed. I. Bertini, C. Luchinat.
- [20] [20a] E. C. Constable, C. E. Housecroft, T. Kulke, C. Lazzarini, E. R. Schofield, Y. Zimmermann, *J. Chem. Soc., Dalton Trans.* **2001**, 2864-2871; [20b] E. C. Constable, C. P. Hart, C. E. Housecroft, *Appl. Organomet. Chem.* **2003**, *17*, 383-387.
- [21] U. S. Schubert, C. Eschbaumer, *J. Inclusion Phenom. Macrocyclic Chem.* **1999**, *35*, 101-109.
- [22] M. A. R. Meier, B. G. G. Lohmeijer, U. S. Schubert, *J. Mass Spectrom.* **2003**, *38*, 510-516.
- [23] M. Maestri, N. Armaroli, V. Balzani, E. C. Constable, A. M. W. C. Thompson, *Inorg. Chem.* **1995**, *34*, 2759-2767.
- [24] M. Heller, U. S. Schubert, *Macromol. Rapid Commun.* **2002**, *23*, 411-415.
- [25] [25a] U. S. Schubert, M. Heller, *Chem. Eur. J.* **2001**, *7*, 5252-5259; [25b] M. Heller, U. S. Schubert, *Macromol. Symp.* **2002**, *177*, 87-96.



- [26] [26a] U. S. Schubert, C. Eschbaumer, *Polym. Prepr.* **2000**, *41*, 676-677; [26b] M. Karas, M. Glückmann, J. Schäfer, *J. Mass Spectrom.* **2000**, *35*, 1-12.
- [27] L. Brunsveld, B. J. B. Folmer, E. W. Meijer, R. P. Sijbesma, *Chem. Rev.* **2001**, *101*, 4071-4097.
- [28] J. H. K. Hirschberg, L. Brunsveld, A. Ramzi, J. A. J. M. Vekemans, R. P. Sijbesma, E. W. Meijer, *Nature* **2000**, *407*, 167-170.
- [29] [29a] L. R. Rieth, R. F. Eaton, G. W. Coates, *Angew. Chem.* **2001**, *113*, 2211-2214; *Angew. Chem. Int. Ed.* **2001**, *40*, 2153-2156; [29b] R. P. Sijbesma, F. H. Beijer, L. Brunsveld, B. J. Folmer, J. H. Hirschberg, R. F. Lange, J. K. Lowe, E. W. Meijer, *Science* **1997**, *278*, 1601-1604; [29c] F. Ilhan, M. Gray, V. M. Rotello, *Macromolecules* **2001**, *34*, 2597-2601; [29d] G. Cooke, V. M. Rotello, *Chem. Soc. Rev.* **2002**, *31*, 275-286; [29e] K. Yamauchi, J. R. Lizotte, D. M. Hercules, M. J. Vergne, T. E. Long, *J. Am. Chem. Soc.* **2002**, *124*, 8599-8604; [29f] K. Yamauchi, J. R. Lizotte, T. E. Long, *Macromolecules* **2003**, *36*, 1083-1088.
- [30] F. H. Beijer, R. P. Sijbesma, H. Kooijman, A. L. Spek, E. W. Meijer, *J. Am. Chem. Soc.* **1998**, *120*, 6761-6769.
- [31] [31a] J.-P. Collin, S. Guillerez, J.-P. Sauvage, F. Barigelletti, L. Flamigni, L. De Cola, V. Balzani, *Coord. Chem. Rev.* **1991**, *111*, 291-296; [31b] M. Maestrie, N. Armaroli, V. Balzani, E.C. Constable, A. M. W. Cargill Thompson, *Inorg. Chem.* **1995**, *34*, 2759-2767.
- [32] B. Hasenknopf, J.-M. Lehn, *Helv. Chim. Acta* **1996**, *79*, 1643-1650
- [33] R. Dobraza, F. Würthner, *Chem Commun.* **2002**, 1878-1879.
- [34] L. Brunsveld, L. Zhang, M. Glasbeek, J. A. J. M. Vekemans, E. W. Meijer, *J. Am. Chem. Soc.* **2000**, *122*, 6175-6182.
- [35] [35a] U. S. Schubert, C. Eschbaumer, *Angew. Chem.* **2002**, *114*, 3016-3050; *Angew. Chem. Int. Ed.* **2002**, *41*, 2892-2926; [35b] J. E. McAlvin, S. B. Scott, C. L. Fraser, *Macromolecules* **2000**, *33*, 6953-6964; [35c] C. L. Fraser, A. P. Smith, *J. Polym. Sci., Part A: Polym. Chem.* **2000**, *38*, 4704-4716; [35d] S. Kelch, M. Rehahn, *Macromolecules* **1998**, *31*, 4102-4106; [35e] B. Lahn, M. Rehahn, *e-Polymers* **2002**, *001*, 1-33.
- [36] F. R. Keene, *Coord. Chem. Rev.* **1997**, *116*, 121-151.
- [37] M. Ziegler, V. Monney, H. Soeckli-Evans, A. von Zelewsky, I. Sasaki, G. Dupic, J.-C. Daran, G. G. A. Balavoine, *J. Chem. Soc., Dalton Trans.* **1999**, 667-675.
- [38] S. Bernhard, K. Takada, D. J. Díaz, H. D. Abruña, H. Mürner, *J. Am. Chem. Soc.* **2001**, *123*, 10265-10271.
- [39] [39a] G. Chelucci, A. Saba, D. Vignola, C. Solinas, *Tetrahedr.* **2001**, *57*, 1099-1104; [39b] E. C. Constable, T. Kulke, M. Neuburger, M. Zehnder, *New. J. Chem.* **1997**, *21*, 1091-1102.
- [40] A. El-Ghayoury, H. Hofmeier, A. P. H. J. Schenning, U. S. Schubert, *Tetrahedr. Lett.* **2004**, *45*, 261-264.
- [41] P. R. Andres, H. Hofmeier, B. G. G. Lohmeijer, U. S. Schubert, *Synthesis* **2003**, 2865-2871.
- [42] M. Fontana, W. R. Caseri, P. Smith, A. P. H. J. Schenning, E. W. Meijer, *Inorg. Chim. Acta* **2003**, *353*, 320-324.

- [43] N. Harada, K. Nakanishi, *Circular Dichroism Spectroscopy*, Oxford University Press, Oxford, **1983**.
- [44] T. Togano, N. Nagao, M. Tsuchida, H. Kumakura, K. Hisamatsu, F. S. Howell, M. Mukaida, *Inorg. Chim. Acta* **1992**, *195*, 221-225.
- [45] [45a] C. M. Harris, T. N. Lockyer, *Aust. J. Chem.* **1970**, *23*, 673-682; [45b] G. Arena, R. P. Bonomo, S. Museumeci, R. Purello, E. Rizzarelli, *J. Chem. Soc., Dalton Trans.* **1983**, 1279-1283.
- [46] B. Hasenknopf, J.-M. Lehn, G. Baum, D. Fenske, *Proc. Natl. Acad. Sci. USA* **1996**, *93*, 1397-1400.
- [47] U. S. Schubert, C. Eschbaumer, G. Hochwimmer, *Synthesis* **1999**, 779-782.
- [48] [48a] B. P. Sullivan, J. M. Calvert, *Inorg. Chem.* **1980**, *19*, 1404-1407; [48b] E. C. Constable, *Chem. Comm.* **1997**, 1073-1080.
- [49] U. S. Schubert, C. Eschbaumer, G. Hochwimmer, *Synthesis* **1999**, 779-782.
- [50] R. Hoogenboom, U. S. Schubert, unpublished results.
- [51] [51a] H. Hofmeier, A. El-Ghayoury, U. S. Schubert, *Polym. Prepr.* **2003**, *44*, 711-712; [51b] H. Hofmeier, A. El-Ghayoury, A. P. H. J. Schenning, U. S. Schubert, *Chem. Commun.* **2004**, in press.
- [52] A. P. H. J. Schenning, M. Fransen, E. W. Meijer, *Macromol. Rapid. Commun.* **2002**, *23*, 265-270.
- [53] Data Collection Software for NONIUS  $\kappa$ -CCD devices, Delft, The Netherlands **1999**.
- [54] [54a] Z. Otwinowski, W. Minor, *Methods in Enzymology* **1997**, *276*, 307-326; [54b] Th. Hahn, A. J. C. Wilson (Eds.), *International Tables for Crystallography*, Vol. C, 3<sup>rd</sup> Edition, Kluwer Academic Publisher, Dordrecht, Boston, London **1992**; [54c] G. Artus, W. Scherer, T. Priermeier, E. Herdtweck, *STRUX-V: A Program System to Handle X-Ray Data*, TU München, Garching, Germany **1997**; [54d] A. L. Spek, *PLATON: A Multipurpose Crystallographic Tool*, Utrecht University, Utrecht, The Netherlands, **2001**; [54e] A. Altomare, G. Cascarano, C. Giacovazzo, A. Guagliardi, M. C. Burla, G. Polidori, M. Camalli, *SIR92, J. Appl. Cryst.* **1994**, *27*, 435-436; [54f] G. M. Sheldrick, *SHELXL-97*, University of Göttingen, Göttingen, Germany, **1998**.



# 3

## Linear metallo-supramolecular polymers

**Abstract:** Supramolecular polymers are of great interest in modern materials research. Within this field, the construction of coordination polymers by complexation of oligomeric precursors bearing metal-coordinating groups at the chain ends is a promising approach. In this chapter, the synthesis of linear coordination polymers based on *oligo* as well as poly(ethylene glycol)s and terpyridine ruthenium(II) complexes is reported. Different reaction conditions (solvent, concentration) were used in order to obtain well-soluble high molecular weight polymers. The resulting compounds were characterized by UV-vis and NMR spectroscopy. Moreover, the viscosity of the materials was investigated with and without addition of salt. In addition to solution viscosimetry, the melt viscosity was determined by rheometry, which verified the presence of high-molecular weight polymers. The thermal characteristics of the polymers were investigated utilizing DSC and TGA. Imaging by AFM revealed a lamellar morphology. A double lamella structure could be found after annealing the sample. In subsequent experiments, telechelics containing terpyridine and ureidopyrimidinone moieties were prepared. Whereas the compounds form hydrogen-bonded dimers in chloroform solution, as shown by NMR spectroscopy, addition of metal ions leads to linear coordination polymers consisting of alternating terpyridine complexes and quadruple hydrogen bonding units, as indicated by NMR spectroscopy and viscosity measurements.

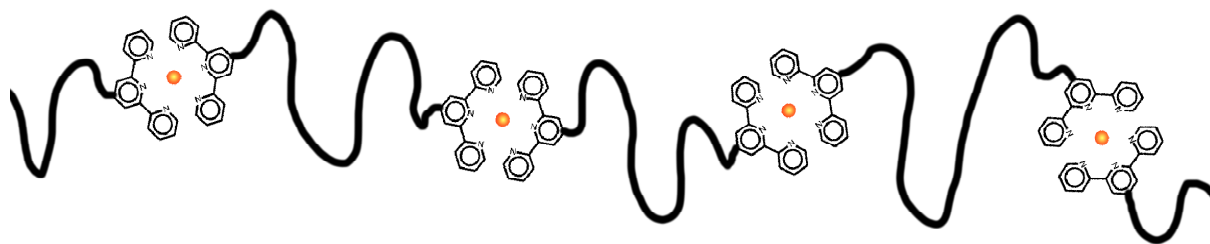
*Parts of this work have been published:*

H. Hofmeier, S. Schmatloch, D. Wouters, U. S. Schubert, *Macromol. Chem. Phys.* **2003**, *204*, 2197-2203; H. Hofmeier, A. El-Ghayoury, A. P. H. J. Schenning, U. S. Schubert, *Chem. Commun.* **2004**, in press.

## 3.1 Linear terpyridine-ruthenium(II) poly(ethylene glycol) coordination polymers

### 3.1.1 Introduction

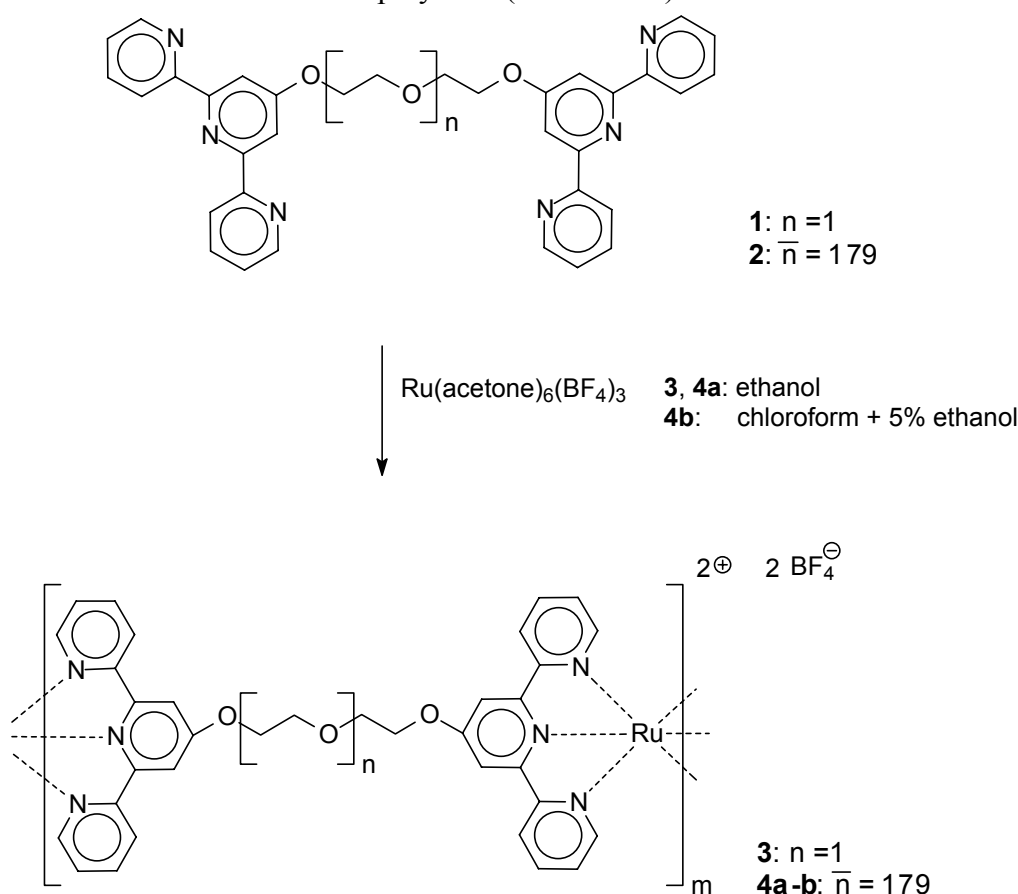
A significant effort in today's materials research is devoted to the synthesis and characterization of supramolecular polymers, which are expected to reveal new properties concerning film formation, surface activity and reversibility. Such polymers could also lead to "smart materials". In particular the introduction of supramolecular moieties into polymers by end-group modification of pre-polymers opens the way to new materials, as was already demonstrated for hydrogen bonding<sup>[1]</sup> and metal coordination systems.<sup>[2]</sup> With respect to the latter type of non-covalent interactions, a major role is played by 2,2':6',2''-terpyridine,<sup>[3]</sup> which acts as a chelating ligand for a variety of transition metal ions (e.g. Fe(II), Zn(II), Ru(II)). This complexing unit allows the construction of a variety of different architectures, such as AB and ABC block copolymers,<sup>[4]</sup> linear coordination polymers,<sup>[5-7]</sup> cross-linked systems<sup>[8]</sup> and even star-shaped<sup>[9]</sup> and grafted structures.<sup>[10]</sup> Linear terpyridine coordination polymers have so far been obtained by the use of metal ions like Fe(II), Zn(II) or Co(II),<sup>[7,11,12]</sup> some of them with chiral precursors. Coordination polymers with a rigid linker have been reported for Ru(II)<sup>[6,13]</sup> and Fe(II) ions.<sup>[14]</sup>



Moreover, the reversibility of the complexation under certain conditions can result in "switchable" systems.<sup>[15,16]</sup> An example is the thermal switching of an iron(II) terpyridine complex in a poly(ester) material.<sup>[17]</sup> Recently, the removal of the poly(ethylene glycol) corona in a supramolecular block copolymer micelle by the addition of a strong competing ligand was described.<sup>[16]</sup> Ruthenium is one of the most favorable ions in the engineering of coordination polymers, since it allows both the directed synthesis of asymmetric complexes as well as symmetric systems (see chapter 2). In addition, ruthenium complexes possess interesting optical and photophysical properties (see chapter 1). In this chapter the construction of highly soluble linear coordination polymers built-up from terpyridine-functionalized small organic as well as polymeric telechelics with ruthenium(II) ions is described. The obtained materials were investigated regarding their viscosity behavior including the polyelectrolyte effect<sup>[5,18]</sup> (increase of the reduced viscosity of charged polymers by dilution) as well as their morphology.

## 3.1.2 Synthesis and characterization

In this chapter, coordination polymers have been constructed by formation of ruthenium(II)-terpyridine complexes. Telechelics of di(ethylene glycol)<sup>[7]</sup> **1** and poly(ethylene glycol)<sub>180</sub><sup>[12,19]</sup> **2** ( $\bar{M}_n = 8000$ ), bearing terpyridine units at both chain ends, were used as precursors and were subsequently polymerized by complexation with ruthenium ions. In order to obtain an active ruthenium ion species, RuCl<sub>3</sub> was treated with AgBF<sub>4</sub> in refluxing acetone to yield the hexaacetone ruthenium(III) tetrafluoroborate, which is more active than RuCl<sub>3</sub> due to the loosely bound acetone ligands.<sup>[5]</sup> This intermediate was reacted with the terpyridine ligands resulting in a reduction of ruthenium(III) to ruthenium(II) ions by ethanol and the formation of the linear coordination polymers (Scheme 3.1).



Scheme 3.1. Schematic representation of the synthesis of the coordination polymers **3** and **4a-b**.

Polymers **3** and **4a** were synthesized in ethanolic solution and refluxed for 72 h. Monitoring by UV-vis spectroscopy was performed to determine the reaction progress. Polymer **3** was obtained as red precipitate, starting from the *bis*-terpyridine-modified di(ethylene glycol) **1**. The product was washed with methanol, dissolved in acetonitrile and precipitated again in methanol to yield a red polymer after filtration. In the case of **4a**, a film-like material was obtained after filtration and evaporation of the reaction solution (Figure 3.1).

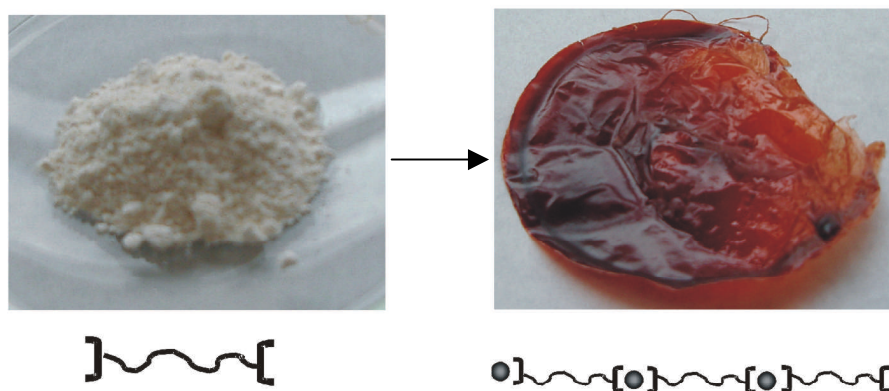


Figure 3.1. Film formation of coordination polymer **4b**.

In both cases, UV-vis spectroscopy revealed the characteristic red-shift of the  $\pi$ - $\pi^*$ -absorption bands of the ligands to 267 and 303 nm.<sup>[3]</sup> Furthermore, the appearance of the metal-to-ligand charge transfer (MLCT) band of the complex at 486 nm was detected for both polymers (Figure 3.2).

The *bis*-terpyridine-modified poly(ethylene glycol) **2** is of polymeric nature ( $\overline{M}_n = 8000$ ) with a flexible chain. Thus, the formation of rings could be possible in the case of **4a-b**. In order to minimize the probability of ring formation, the reaction conditions for **4b** were varied (see below and experimental part).

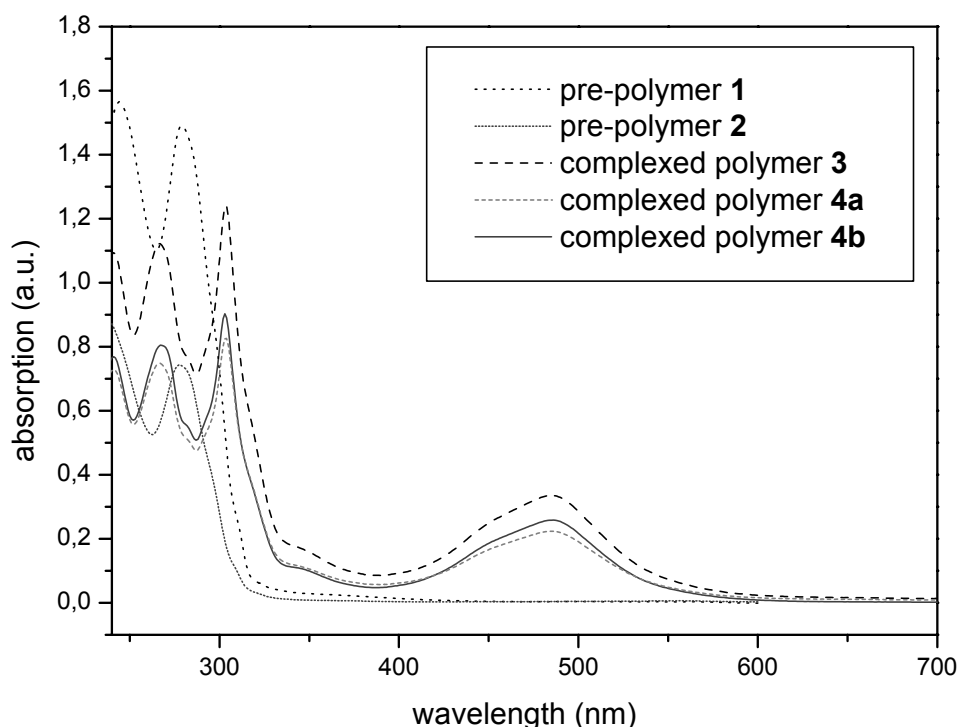


Figure 3.2. UV-vis spectra of the coordination polymers **3** and **4a-b** (in acetonitrile).

<sup>1</sup>H-NMR spectroscopy demonstrated the successful complexation of the telechelics (Figure 3.3). The signals in the aromatic region could be assigned to the complexed terpyridine protons and the chemical shifts were in accordance with the model complexes: in particular

the upfield shift of the 6,6''-signal is characteristic for *bis*-terpyridine complexes, due to the different chemical environment of the 6,6''-protons compared to the free ligand. No signals of uncomplexed terpyridines were found within the detectability of the NMR. The signals between 4 and 5 ppm could be attributed to the proton signals of the methylene groups next to the terpyridines ( $\alpha$ -methylenes) and the large signal around 3.5 in the case of **4a** and **4b** to the other methylene protons of the poly(ethylene glycol) chain.

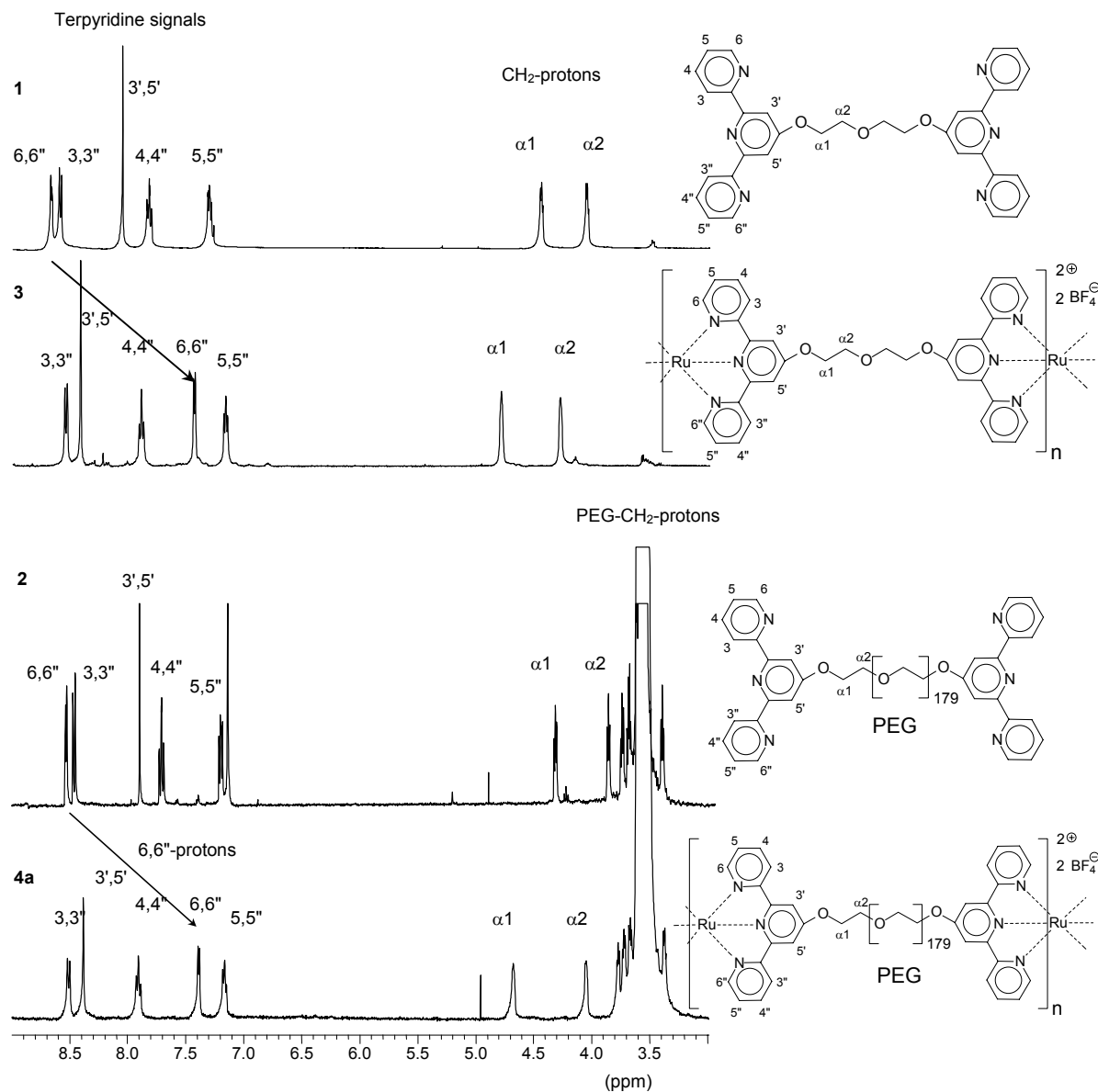


Figure 3.3.  $^1\text{H-NMR}$  spectra of the ligands **1-2** (in chloroform) and the coordination polymers **3-4a** (in acetonitrile).

### 3.1.3 Solution viscosimetry

To prove the formation of high molecular mass polymers, the solution viscosities were investigated by means of capillary viscosimetry utilizing an Ubbelohde viscosimeter. A concentration series was performed through stepwise dilution, starting from a concentration of 18-20 mg/mL (Figure 3.4).



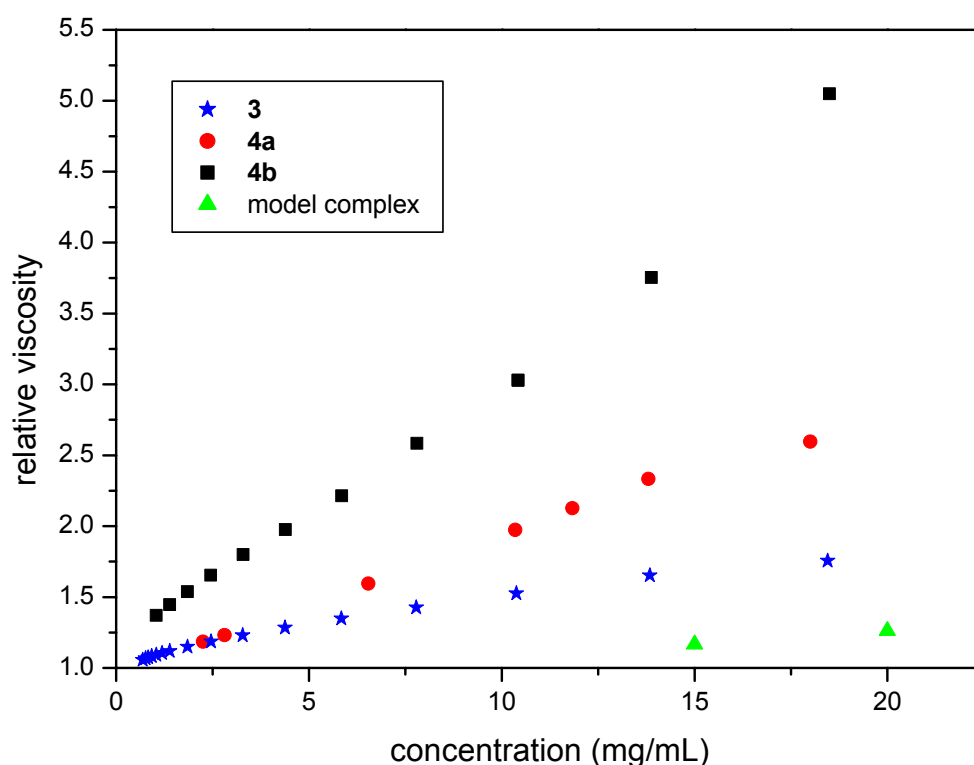


Figure 3.4. Relative viscosities of the coordination polymers **3** (acetonitrile), **4a-b** (methanol) and a model complex (bis[poly(ethylene glycol)<sub>76</sub>]iron(II) hexafluorophosphate;  $\bar{M}_n = 4000$ ; methanol).

A significant increase of the obtained relative viscosity was observed for the coordination polymers compared to the free ligands. Compound **3** reached a relative viscosity of 1.8 at 18.5 mg/mL and **4a** a relative viscosity of 2.6. The differently synthesized polymer **4b** revealed a relative viscosity of 5, twice as high as polymer **4a**. This is most likely a result of the reaction conditions: the concentration was increased 10 times, and therefore the possibility of ring formation was reduced. Rings are expected to possess a lower viscosity due to their lower molecular weight and compactness. On the other hand, if the lower viscosity would be caused by linear polymers with lower molecular weight, free terpyridine groups should be visible in the NMR spectrum, which is not the case. Possible macrocycles cannot be discerned by NMR spectroscopy and therefore not yet quantified. Furthermore, CHCl<sub>3</sub> with 5% ethanol was used as solvent for the synthesis of **4b**. Chloroform is a better solvent for the terpyridine moieties and it was therefore assumed that the terpyridine moieties should be better accessible for the complexation reaction under these conditions. Thus, a higher degree of polymerization should be obtained. The higher viscosity of **4b** compared to **4a** suggests that the fraction of real high molecular weight is indeed larger in the case of **4b**. As a reference experiment (to exclude other effects on the viscosity like ionic interactions, leading e.g. to a stacking of the complex moieties), an iron(II) bis-complex of terpyridine-*mono*-functionalized poly(ethylene glycol) ( $\bar{M}_n = 4000$ ) was investigated by viscosity measurements (the final complex dimer

revealed a  $\overline{M}_n = 8500$ , based on analytical ultracentrifugation experiments). Only a relative viscosity of 1.26 at 20 mg/mL was observed in this case.

Polymers **3**, **4a** and **4b** are expected to show a polyelectrolyte behavior due to the existence of charges in the polymer chain, as it has been shown for other metal coordination polymers.<sup>[5,6,20]</sup> Thus, the compounds were investigated concerning their polyelectrolyte effect. Therefore, the viscosity experiments were repeated in solutions of tetrabutylammonium tetrafluoroborate (20 mmol/L for **4b**; 50 mmol/L for **3**). The reduced viscosities were calculated for all measurements. In the absence of salt, a maximum at low concentrations was found (Figure 3.5, left): a reduced viscosity of 94 mL/g for polymer **3** was reached at a concentration of 0.83 mg/mL. In the case of **4b**, a maximum value of 720 mL/g was found at 0.16 mg/mL (Figure 3.5, right). For both systems, the values of the reduced viscosity decreased again at very low concentration, as has been shown before.<sup>[21]</sup> A possible explanation for this behavior is an increased dissociation of the polyelectrolyte counterions by dilution, causing an increase of the hydrodynamic volume. A stretching of the chains at low concentrations can therefore occur due to the repulsion of the positive charges within the chains, resulting in higher viscosities than uncharged polymers.<sup>[18]</sup> Furthermore, long-range intermolecular (attractive) electrostatic interactions between the cations of the polymer chains and the counterions (triple ion effect) can be expected.<sup>[21,22]</sup> By performing viscosity measurements in salt solution, the mean concentration of charge carriers in the solution remains constant and the polyelectrolyte effect is largely suppressed. The hydrodynamic volume remains constant and the intermolecular Coulomb interactions are screened out.<sup>[5]</sup>

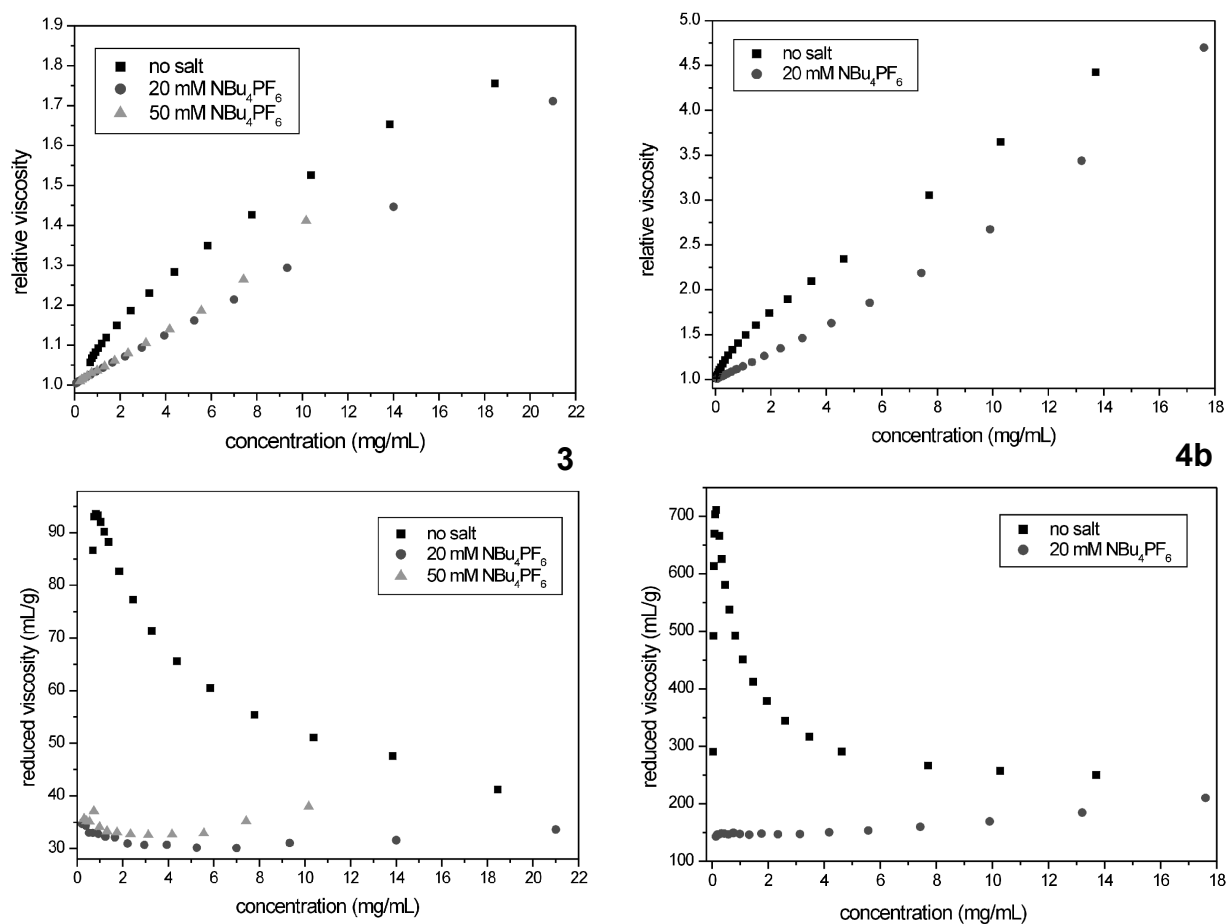


Figure 3.5. Relative (top) and reduced (bottom) viscosities of coordination polymer **3** (left) and **4b** (right, all in acetonitrile) as a function of salt addition (tetrabutylammonium tetrafluoroborate).

A concentration of 20 mmol/L salt was sufficient to suppress the polyelectrolyte behavior in the case of **4b**. However, in the case of compound **3**, a small increase remains in the low-concentration regime (in 20 mmol/L and also in 50 mmol/L salt), suggesting a remaining polyelectrolyte effect due to the higher charge density in this polymer (Figure 3.5, left). On the other hand, these values have to be taken with care because of the limits of the measurement accuracy at low concentrations, derived from the unavoidable error, caused by the multiple dilution steps. A non-linear behavior was found for the reduced viscosities at higher concentrations for the salt-measurements. Furthermore, the reduced viscosities were even higher at higher concentrations of the salt. These findings suggest an additional unspecific aggregation of the polymers.

Intrinsic viscosities of ~27 (**3**) and ~120 mL/g (**4b**) were extrapolated from the measurements where salt had been added. Taking these values into account, a viscosity average molecular weight of approximately 120 000 could be calculated for **4b**, suggesting the coupling of 14-15 units of **2** (utilizing equation (1)).<sup>[23]</sup>

$$[\eta] = 2.0 + 0.033M^{0.72} \quad (1)$$

Due to the relative small content of the complexes in the final coordination polymer, the known constants for covalent poly(ethylene glycol)s have been utilized for this calculation, which can certainly only represent a first assumption. However, the obtained values provide a first indication of the degree of polymerization. Due to the high flexibility of the polymer chains, also in this case ring formation cannot be excluded completely. For polymer **3**, based on di(ethylene glycol), a similar estimation of the molecular weight is not possible due to the much higher complex content.

#### 3.1.4 Differential scanning calorimetry

In order to investigate the thermal properties of the precursor **2** as well as the polymers **3** and **4b**, differential scanning calorimetry (DSC) experiments have been performed (Figure 3.6): whereas **3** showed no transition, not even at higher temperatures (the organic precursor **1** had a melting point of 185 °C), a glass transition of -50 °C and a melting peak at 51 °C was found for polymer **4b**. The lack of any transition of **3** could be explained with the high charge density, resulting in an amorphous material. In contrast to the brittle material **3**, polymers **4a** and **4b** formed flexible films. Covalent unfunctionalized poly(ethylene glycol) of an  $\overline{M}_n$  of 35 000 daltons is characterized by a  $T_g$  of -54 °C and a  $T_m$  of 66 °C.<sup>[24]</sup> Poly(ethylene glycol) of high molecular weight (200 000 daltons) was also investigated and similar values were found ( $T_g = -53$  °C;  $T_m = 65$  °C).

An explanation for the lower melting point and higher  $T_g$  of the coordination polymer **4b** could be a smaller size of the crystalline domains as a result of the bulky complex units, which may disturb the formation of larger domains. Precursor **2**, which contains free terpyridine units, revealed only a melting peak of 59 °C, which lies in between the melting points of coordination polymer **4b** and covalent poly(ethylene glycol). A comparison of the crystallization behavior revealed a lower crystallization temperature for the coordination polymer **4b** (30 °C), compared to a crystallization peak of 38 °C for precursor **2**. Again, no transitions were found for polymer **3**. These results support the conclusions drawn from the melting behavior.

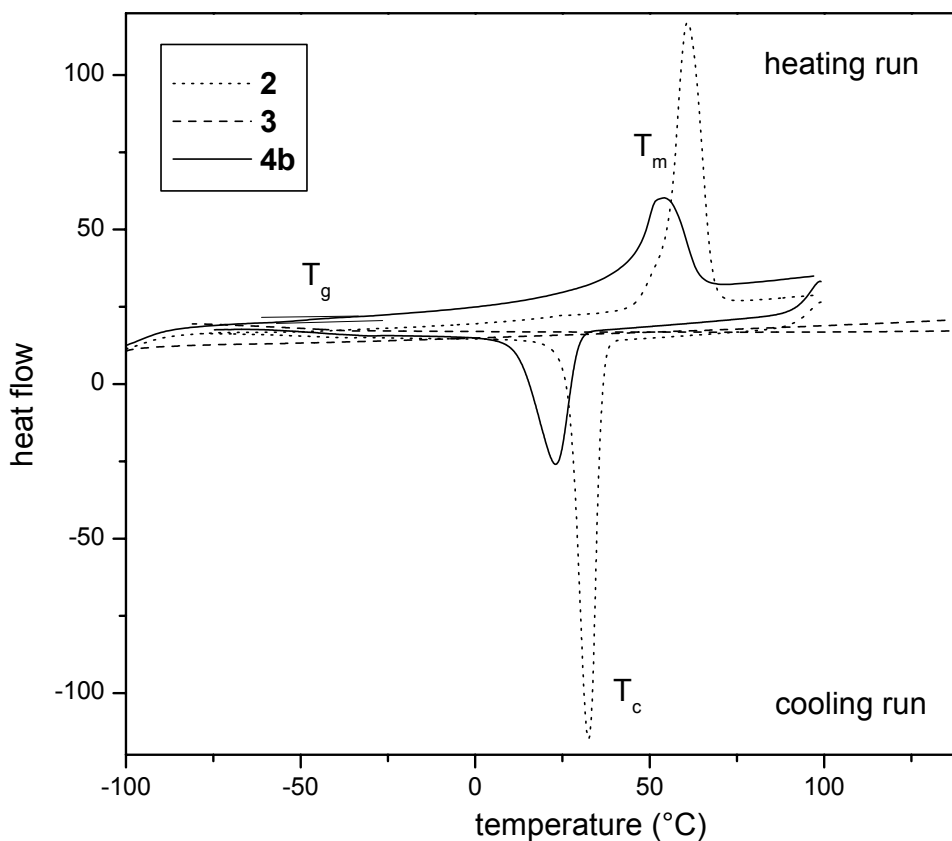


Figure 3.6. DSC curves of **2**, **3** and **4b** (second heating and cooling run, 40 °C/min).

### 3.1.5 Atomic force microscopy (AFM)

Thin films of polymers **3** and **4b** were also investigated by atomic force microscopy (AFM), utilizing the tapping mode (Figure 3.7). The phase image of polymer **4b** clearly revealed the presence of ordered lamellar domains (Figure 3.7, left), with the dark regions being a surface effect because the film was not completely flat. The observed repeat distance of perpendicular oriented lamellae was about 16 nm with 8-9 nm hard block sizes. The ordering is most probably caused by the poly(ethylene glycol) chain folding.<sup>[25]</sup> To confirm this assumption, a covalent poly(ethylene glycol) ( $\bar{M}_n$  of 100 000 dalton) was investigated using similar preparation conditions. Also in this case a lamellar morphology was observed (Figure 3.7, right) with similar periodicity (20 nm).

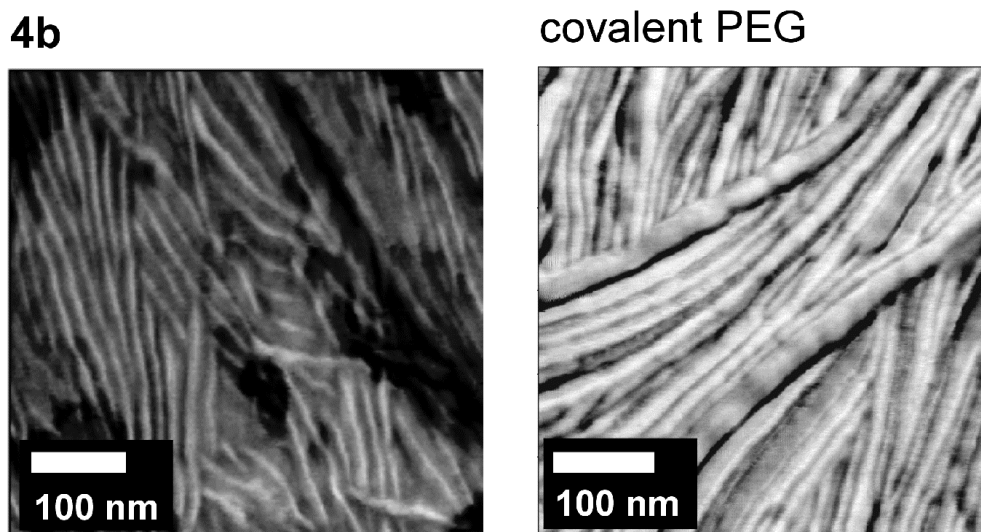


Figure 3.7 AFM phase images of **4b** and a covalent poly(ethylene glycol) ( $\overline{M}_n = 100\,000$  daltons).

However, the size of the crystalline poly(ethylene glycol) domains was larger (approximately 15 nm). Subsequently, a film was annealed at elevated temperature (on the heating stage of the AFM) and measured again at ambient temperature. Now a double lamella structure was found (Figure 3.8). The measurements could be repeated with a different AFM-tip to exclude a tip-convolution effect as a cause for the observed structures (however, it has to be mentioned that on some regions of the sample the features were not found).

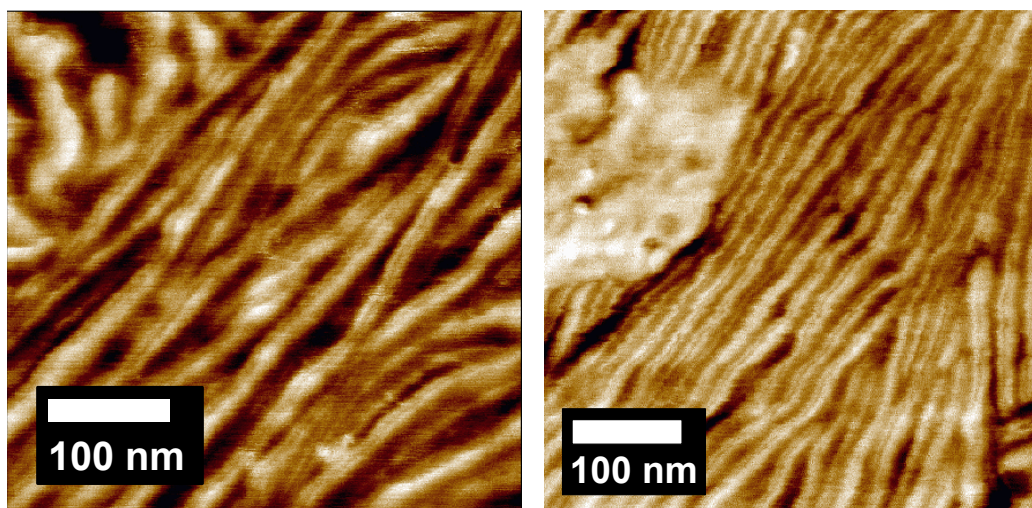
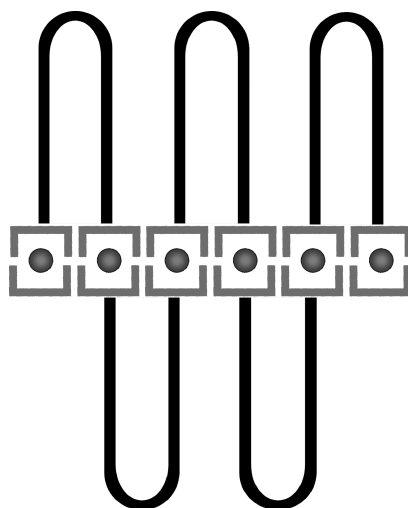


Figure 3.8. AFM phase images (two different experiments) of an annealed sample of **4b**, revealing a double lamella structure.

An explanation for this morphology could be the presence of once-folded poly(ethylene glycol) chains. For low molecular-weight PEGs, also double lamellae were found, which was explained by an arrangement of the chains by hydrogen-bonding of the terminal hydroxy

groups.<sup>[26]</sup> In the present case, the complex units could be responsible for this arrangement. Scheme 3.2 displays the basic concept. The polymer in the neighborhood of the complexes is expected to be amorphous because the complex moieties are much bulkier than hydroxy endgroups. Smaller crystalline domains could be the result, which is in accordance to the DSC data. The current findings for the ruthenium polymer are in agreement with the morphology found for an iron(II) coordination polymer of a similar constitution.<sup>[27]</sup>

For the di(ethylene glycol) system **3**, the observed phase image was less clear (z-scale was only 2° compared to 40° for **4b**) but still a semi-lamellar structure was observed with periodicities of about 5 nm (2.5 nm per line). In this case, the lamellar structure cannot be caused by the same origin due to the fact that the ethylene glycol spacer is only two units long. The observed 2.5 nm per line could therefore correspond to the size of a ruthenium-terpyridine-di(ethylene glycol) terpyridine unit (as obtained by molecular modeling).



*Scheme 3.2. Schematic representation of a potential poly(ethylene glycol) chain folding model, initiated by the terpyridine ruthenium(II) complex units.*

### 3.1.6 Thermogravimetric analysis

To investigate the thermal as well as the oxidative stability of **2**, **3** and **4b**, thermal gravimetric analysis (TGA) was performed in inert gas (nitrogen) and air atmosphere, respectively (Figure 3.9). For comparison, also  $\alpha,\omega$ -bishydroxy-poly(ethylene glycol)<sub>180</sub> (the precursor of **2**) and a poly(ethylene glycol) of high molecular weight (200 000 daltons) (abbreviated as PEG 200K) was investigated. In nitrogen atmosphere, the metal-free polymers revealed the fastest decompositions with 5% weight losses between 228 and 250 °C (Table 3.1), while the coordination polymer **4b** showed an increased stability (5% onset at 321 °C). Polymer **3** revealed an even higher decomposition temperature with a 5%-onset at 331 °C due to the large amount of complex units in the polymer. In addition, a flatter slope was found. As a result of the higher metal content in this polymer, a large amount of residue (20%) remained. The weight-percentage of ruthenium in the initial polymer **3** was 12%; the residue could contain compounds of boron and phosphorus besides ruthenium oxides.

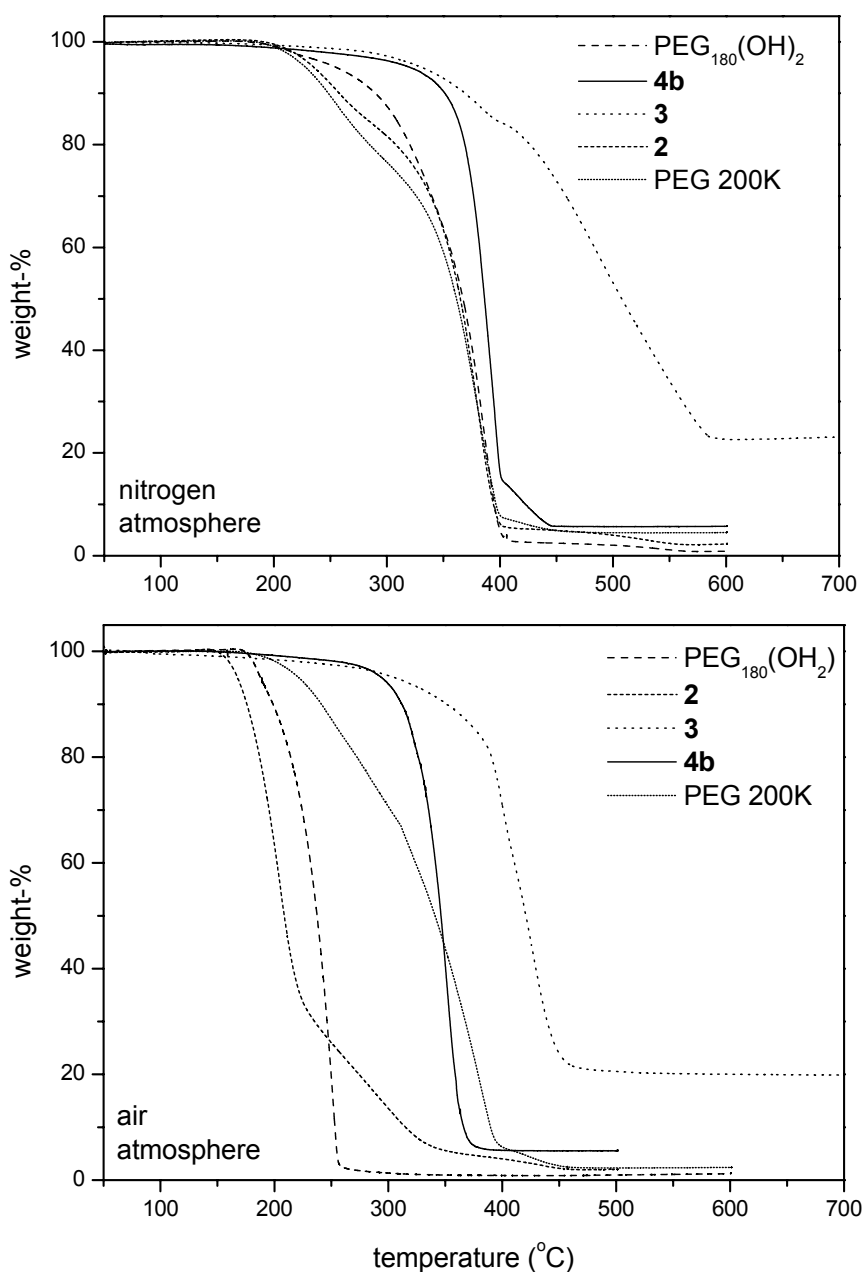


Figure 3.9. TGA traces of **2**, **3**, **4b** and hydroxy-terminated PEG<sub>180</sub> as well as PEG (200 000 daltons) in nitrogen (top) and air (bottom) atmospheres.

The mechanism of degradation of poly(ethylene glycol)s was found to be random scission of the polymer chains involving free radical species.<sup>[28]</sup> Therefore, the stabilization of the coordination polymer could be ascribed to trapment of the radicals by the metal complex moieties. Repetition of the TGA measurements in air showed that compound **2** is oxidized more easily with a 5%-onset of 168 °C (67 K less than the nitrogen-measurement) than coordination polymer **4b** (295 °C, 26 K less than in N<sub>2</sub>). The mechanism probably involves the addition of oxygen to form peroxy groups, which subsequently form radicals. More radicals can be formed, resulting in a faster decomposition.



The curve for **2** revealed a flattening slope between 230 and 320 °C, which was not found for the terpyridine-free analogue. An explanation could be an influence of the terpyridine moieties in the oxidative decomposition (terpyridines with short PEG-chains are formed, with have a decreased probability of chain scission). Finally, poly(ethylene glycol) of high molecular weight (200 000 daltons) was investigated to study the influence of the molecular weight on the decomposition behavior. Whereas thermal degradation of this polymer is similar to the corresponding molecular weight compound, the oxidative decomposition is slower than the low-molecular weight compounds, but it still faster than the coordination polymer. For oxidative decomposition, molecular weight shows a significant influence, because more scission steps are necessary to fully decompose the polymer. This effect should then be present also for thermal decomposition, however, since the process is much slower, it plays a minor role. Additionally, the heating rate is expecting to play a role. Finally, also the metal-rich coordination polymer **3** revealed a decreased onset (306 °C), indicating a faster decomposition in the oxidative atmosphere.

Table 3.1. 5% onsets (°C) by TGA for compounds **2**, **3**, **4b** PEG<sub>180</sub>(OH)<sub>2</sub> and PEG (200 000 daltons) in nitrogen and air atmospheres.

	nitrogen	air
PEG <sub>180</sub> (OH) <sub>2</sub>	255	188
<b>2</b>	235	168
<b>4b</b>	321	295
PEG 200K	228	222
<b>3</b>	337	307

The conclusion, drawn from the TGA results, is that the metallopolymers possess an increased stability towards thermal and oxidative decomposition due to the stable terpyridine-ruthenium complex moieties. Moreover, oxidative processes have a less drastic influence on the coordination polymer compared to the metal-free polymers due to radical trapping.

### 3.1.7 Melt viscosity

The melt viscosities (complex viscosity  $\eta^*(\omega)$ ) of the precursor **2** and coordination polymer **4b** were studied. Whereas the viscosity of the telechelic polymer **2** decreased by five orders of magnitude during the melting transition (from  $1.5 \times 10^6$  to 20 Pa.s), the viscosity of coordination polymer **4b** stayed at higher levels; 4 orders of magnitude higher than for the precursor. Only a decrease of less than two decades was observed (from  $7 \times 10^7$  to  $10^5$  Pa.s). A covalent poly(ethylene glycol) with an  $\bar{M}_n$  of 200 000 daltons (see TGA investigations) was also investigated for comparison. Its complex viscosity has the same order of magnitude as the coordination polymer **4b** before and after the transition. These findings give further

indication for the presence of high molecular weight polymer chains in polymer **4b**. The location of the melting transition is in accordance with the DSC results. To investigate the stability of the coordination polymer during the rheometry measurement (to exclude any chain rupture), the solution viscosity was measured before and after the rheometry measurement, revealing the same viscosities. Therefore, rupture of the polymer chains can be excluded, as expected for ruthenium(II) complexes.

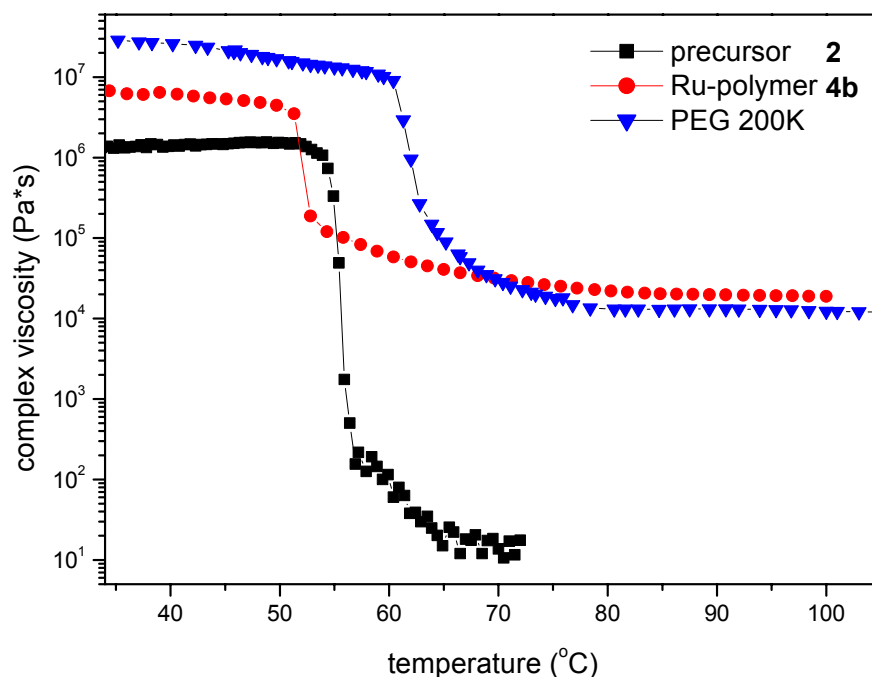


Figure 3.10. Temperature dependence of the absolute value of the complex viscosity of precursor **2**, coordination polymer **4b** and poly(ethylene glycol) ( $M_n = 200\,000$  daltons) at  $\omega = 1$  Hz.

Furthermore, the storage and the loss moduli were calculated. The storage modulus  $G'$  is a measure of the elasticity and measures the solid behavior of the substance, whereas the loss modulus  $G''$  is a measure of the fluid behavior. They are in relation to the dynamic viscosity as follows, where  $\omega$  denotes the angular frequency.

$$\eta^* \omega = G' + iG'' \quad (2)$$

A comparison of the moduli shows that for **4b** the storage modulus is always larger than the loss modulus, whereas for the covalent PEG the lines (moduli in dependence of temperature) cross after melting, as expected for conventional linear polymers (Figure 3.11). This behavior of the coordination polymer suggests the presence of intermolecular interactions (ionic interactions of the charges), which could remain largely intact after the melting transition (in agreement to the polyelectrolyte behavior of **4b**).

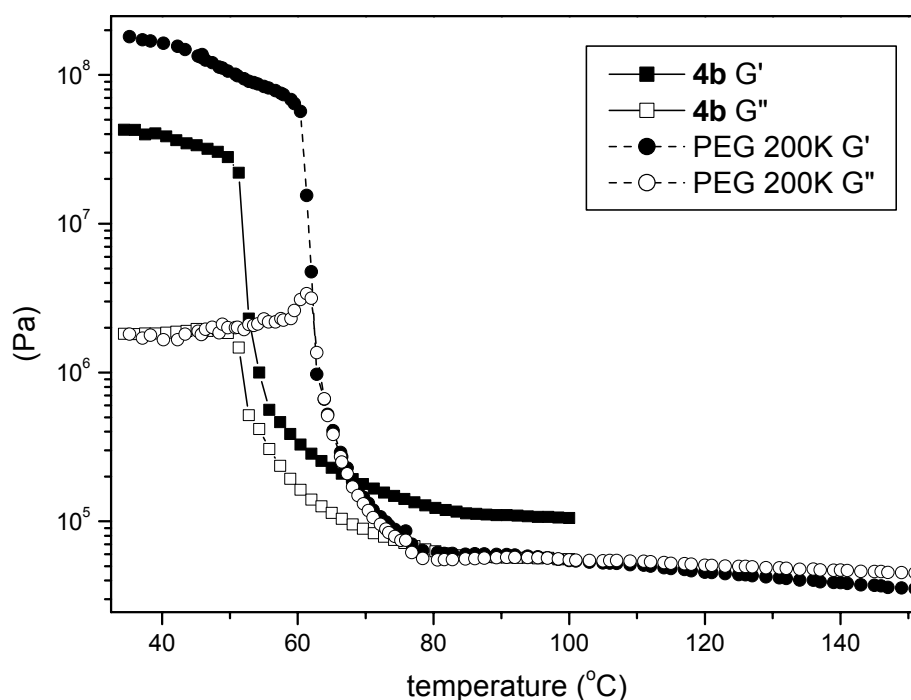


Figure 3.11.  $G'$  and  $G''$ -values of coordination polymer **4b** and PEG ( $M_n = 200\ 000$ ).

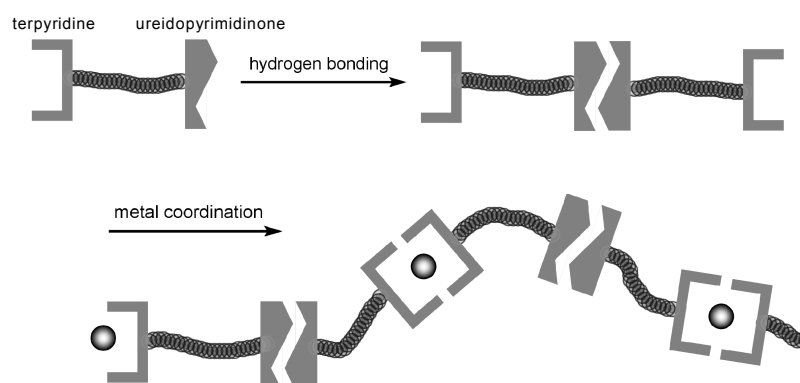
### 3.2 Linear supramolecular polymers containing both terpyridine metal complexes and quadruple hydrogen bonding units

One of the main approaches to the synthesis of supramolecular polymers consists of utilization of hydrogen bonding interactions. Recently, reversible supramolecular polymers, based on the strong dimerization of self-complementary 2-ureido-4[1H]-ureidopyrimidinone (UP) units, which exhibit real macroscopic polymeric properties, have been reported.<sup>[29]</sup> Improvement of the materials properties of low molecular weight telechelic polymers, bearing UP-units at the chain ends, was therefore achieved.<sup>[30]</sup> In such reversible systems, the degree of polymerization is strongly dependant on the utilized solvent, concentration and temperature.

In contrast to that, metal-to-ligand interactions<sup>[5,7]</sup> are usually stronger than the corresponding hydrogen bonding interactions and can be tuned by the choice of the metals or ligands used. Different specific features such as electrochemical, photophysical or magnetic properties, can be introduced into polymers (see previous chapters).

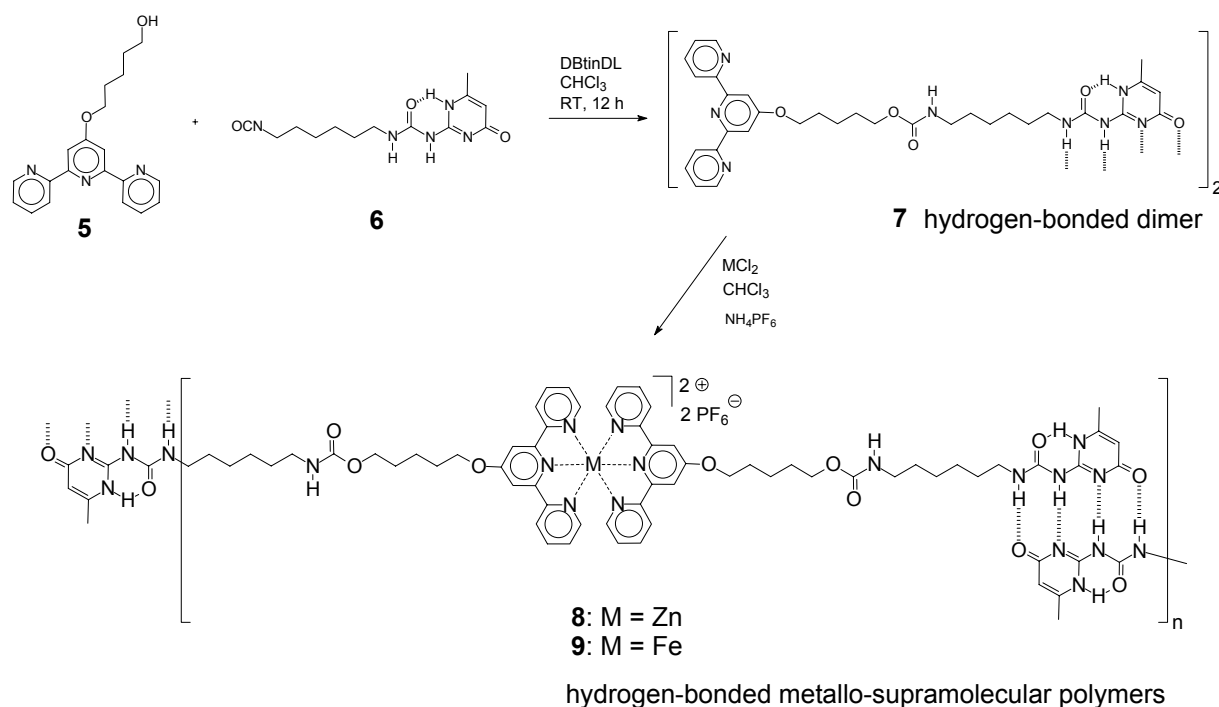
However, up to now usually only one directed supramolecular interaction (metal coordination or hydrogen bonding) was present within a certain polymer. The reported examples where both interactions have been introduced (which were called "coordination polymers") are actually solid-state structures.<sup>[31]</sup> Another example describes a terpolymer bearing side groups for hydrogen-bonding, metal coordination as well as ionic interactions.<sup>[32]</sup>

An interesting approach would therefore be the combination of both supramolecular interactions in the main chain of a synthetic polymer in order to gain access to a new class of reversible metallo-supramolecular polymers (Scheme 3.3).



*Scheme 3.3. Schematic representation of the supramolecular polymer containing both metal complex and hydrogen bonding units in the main chain.*

Here we report for the first time the design of novel molecules that contain a 2,2':6',2''-terpyridine<sup>[3]</sup> as well as a ureido-4[1H]-ureidopyrimidinone<sup>[33]</sup> group. The new compounds are capable of forming strong linear non-covalent polymers with alternating hydrogen-bonding and metal complex systems. In this approach, an isocyanate coupling reaction was used: the 4'-hydroxy-functionalized terpyridine **5**<sup>[34]</sup> was reacted with a ureidopyrimidinone bearing an isocyanate group **6**<sup>[30]</sup> (Scheme 3.4, top) to yield compound **7**.



*Scheme 3.4. Synthesis of the ligand 7 and complexation with Zn(II) and Fe(II).*

The reaction was performed at room temperature in chloroform using dibutyltindilaureate (DBTDL) as catalyst. Compound **7** was characterized by UV-vis, IR, MALDI-TOF-MS and

$^1\text{H-NMR}$  spectroscopy. The formation of quadruple hydrogen bonds was indicated by  $^1\text{H-NMR}$  spectroscopy. A large downfield shift for the N-H protons was observed (between 10 and 13 ppm), giving direct evidence for the involvement of these protons in strong hydrogen bonding,<sup>[35]</sup> leading to **DDAA**-dimers in solution (Figure 3.12, top).

Subsequently, the terpyridine moieties were complexed by addition of iron(II) and zinc(II) ions. In a UV-vis titration experiment, Fe(II) chloride in methanol was added to a chloroform solution of ligand **7** (leading to complex **9**). An increase of the MLCT charge transfer band of the iron complex at 558 nm was observed; a plateau was reached at the equivalence point after a linear increase (Figure 3.13).

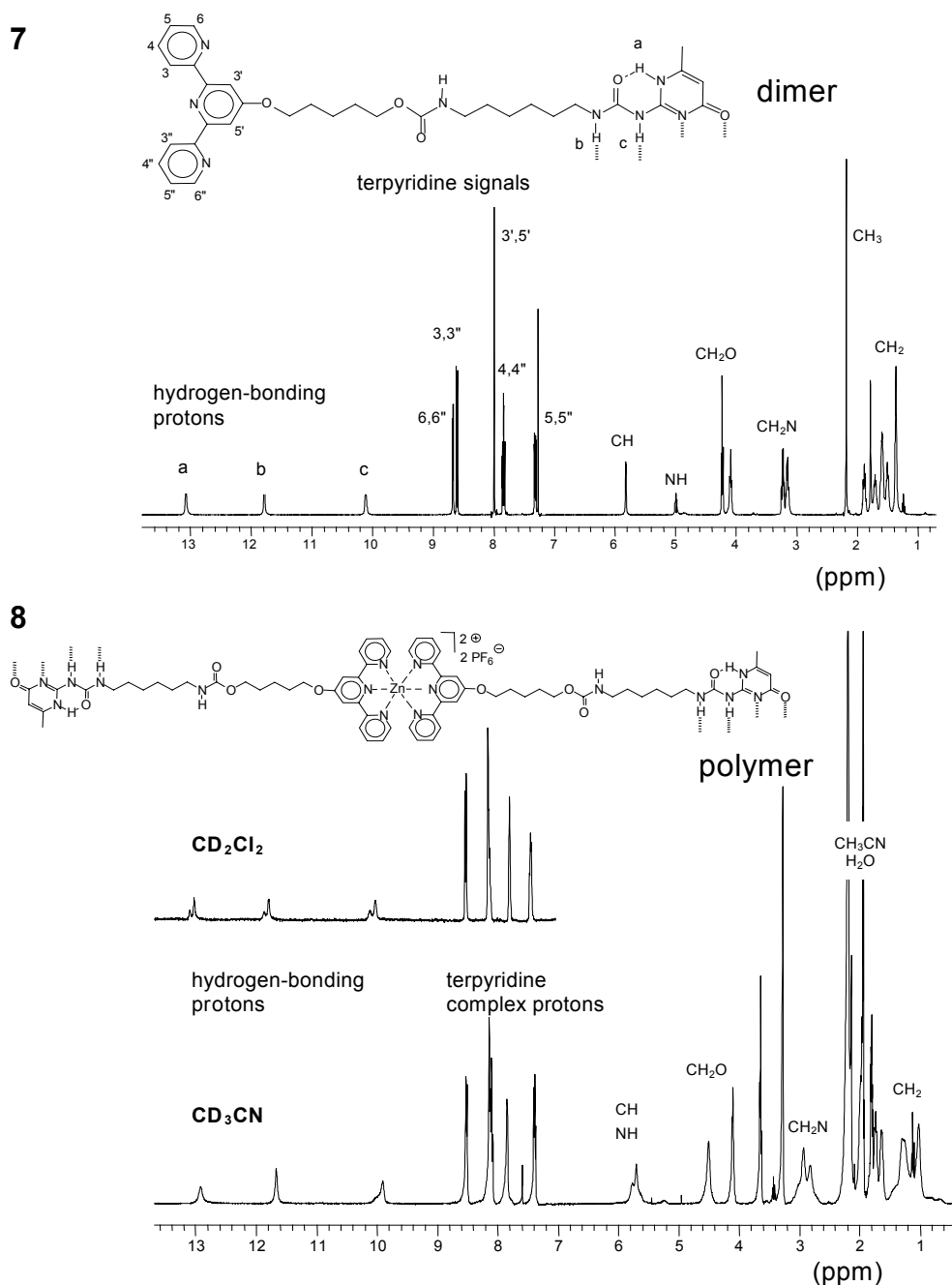


Figure 3.12.  $^1\text{H-NMR}$  spectra of ligand **7** ( $\text{CHCl}_3$ ) and complex **8** (in  $\text{CH}_3\text{CN}$ ; inset:  $\text{CH}_2\text{Cl}_2$ ).

The equivalence point was observed at a ligand:metal ratio of 2:1, indicating quantitative complexation. In a separate experiment, a methanolic solution of zinc(II) chloride was added to **7** in chloroform. After exchange of the counterions by addition of  $\text{NH}_4\text{PF}_6$ , the product was precipitated in diethyl ether in order to obtain compound **8** (Scheme 2, bottom).  $^1\text{H-NMR}$  spectroscopy showed a successful formation of the Zn-terpyridine complex as well as the hydrogen bonding interactions (Figure 3.12, bottom).

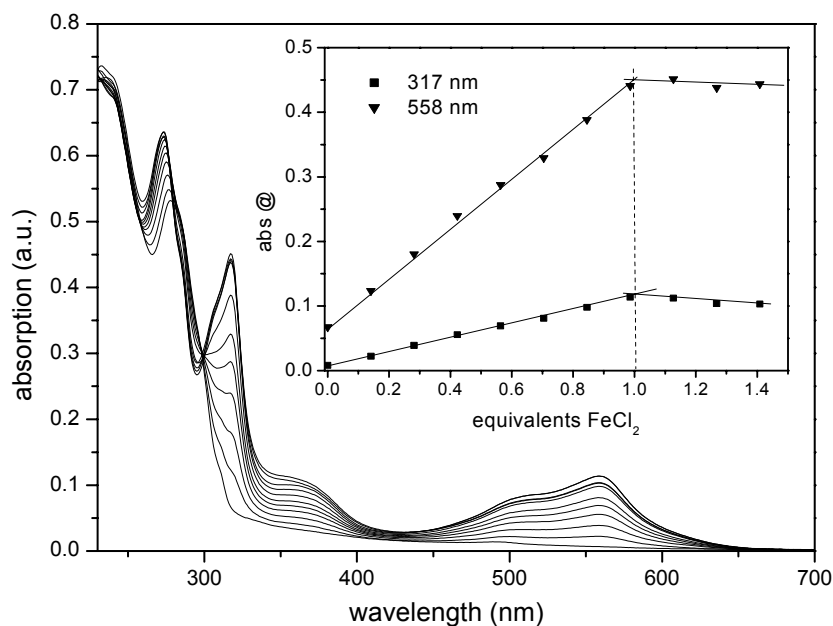
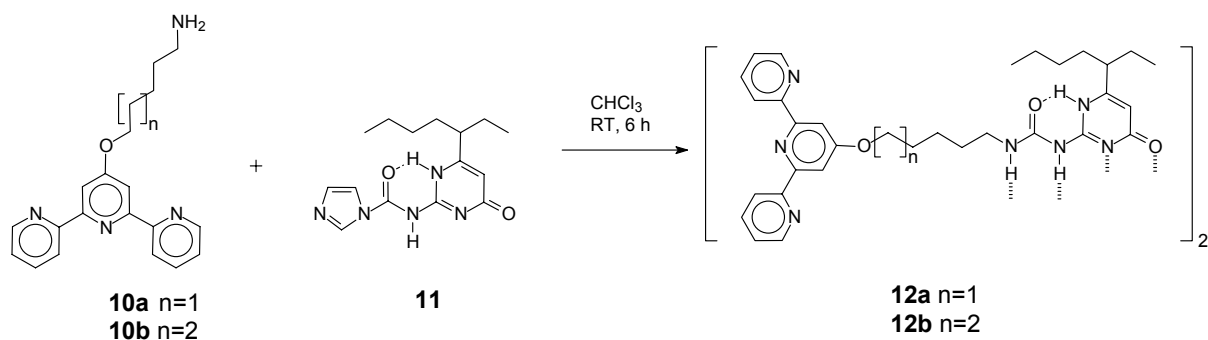


Figure 3.13. UV-vis titration of compound **7** with  $\text{FeCl}_2$  ( $\text{CHCl}_3$ ).

The signals in the aromatic region could be assigned to the terpyridine complex units and the resonances between 10 and 13.2 ppm to the N-H hydrogen bonding protons. In acetonitrile, the signals are clearly visible, but with a slightly lower intensity. The quadruple hydrogen bonds are not completely broken in this case and the absence of additional signals (of non-hydrogen-bonded NH-groups) indicates that hydrogen-bonds with residual water from the solvent are present. A  $^1\text{H-NMR}$  spectrum measured in dichloromethane revealed a quantitative formation of hydrogen bonds (insert in Figure 3.12). A splitting of the peaks was observed which could be explained by a partial formation of small cycles.<sup>[36]</sup>

Viscosity investigations are a suitable tool in order to show the formation of non-covalent polymers. However, this kind of characterization was critical for compound **7** due to the limited solubility of the ligands as well as the corresponding complexes. Therefore, a different compound (**12**) was prepared, which was expected to possess an increased solubility by introducing a branched alkyl chain into the ureidopyrimidinone group. 6-(1-Ethylpentyl)-isocytosine has been activated with carbonyldiimidazole (CDI).<sup>[37]</sup> This compound **11** was subsequently reacted with the amino functionalized terpyridines **10a-b** (Scheme 3.5). After washing with water and extraction, the compounds **12a-b** were obtained by recrystallization from chloroform/pentane. The compounds revealed indeed an increased solubility.



Scheme 3.5. Synthesis of compounds **12a-b**.

$^1\text{H-NMR}$  spectroscopy in chloroform proved the formation of hydrogen bonds with the typical signals between 10 and 13 ppm (Figure 3.15), showing the formation of dimeric species analogous to compound **7**. In addition, the terpyridine signals were found between 7 and 9 ppm, revealing the characteristic pattern. The olefinic signal of the UPy-group and all the aliphatic resonances are also present. Furthermore, MALDI-TOF-MS confirmed the proposed product (Figure 3.14). Hydrogen-bonded dimers could not be detected in MALDI-TOF, the quadruple hydrogen bond array is not strong enough to survive the desorption/ionization process.

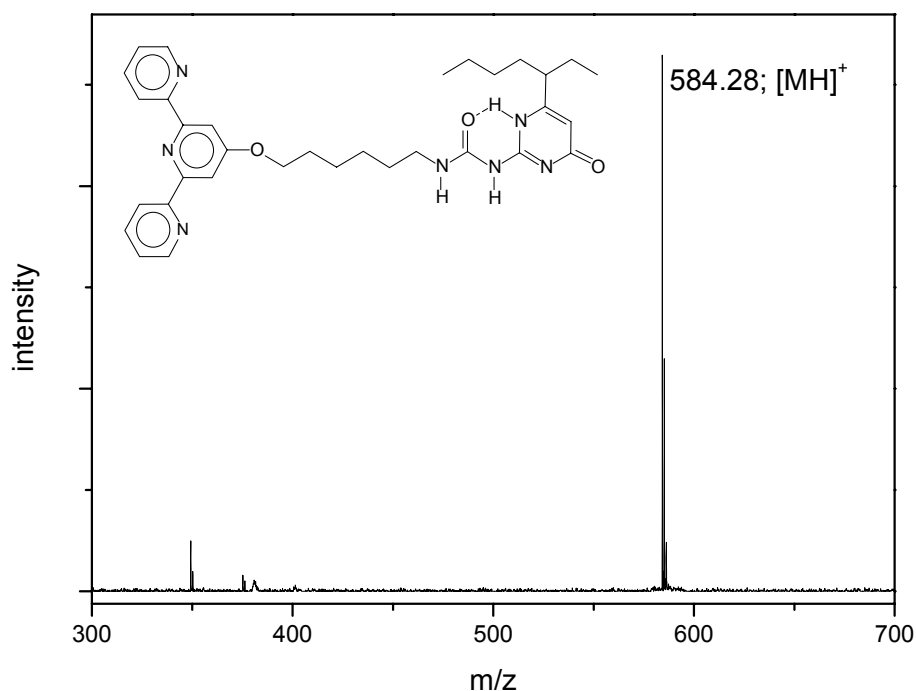


Figure 3.14. MALDI-TOF mass spectrum of ligand **12b** (matrix: dithranol).

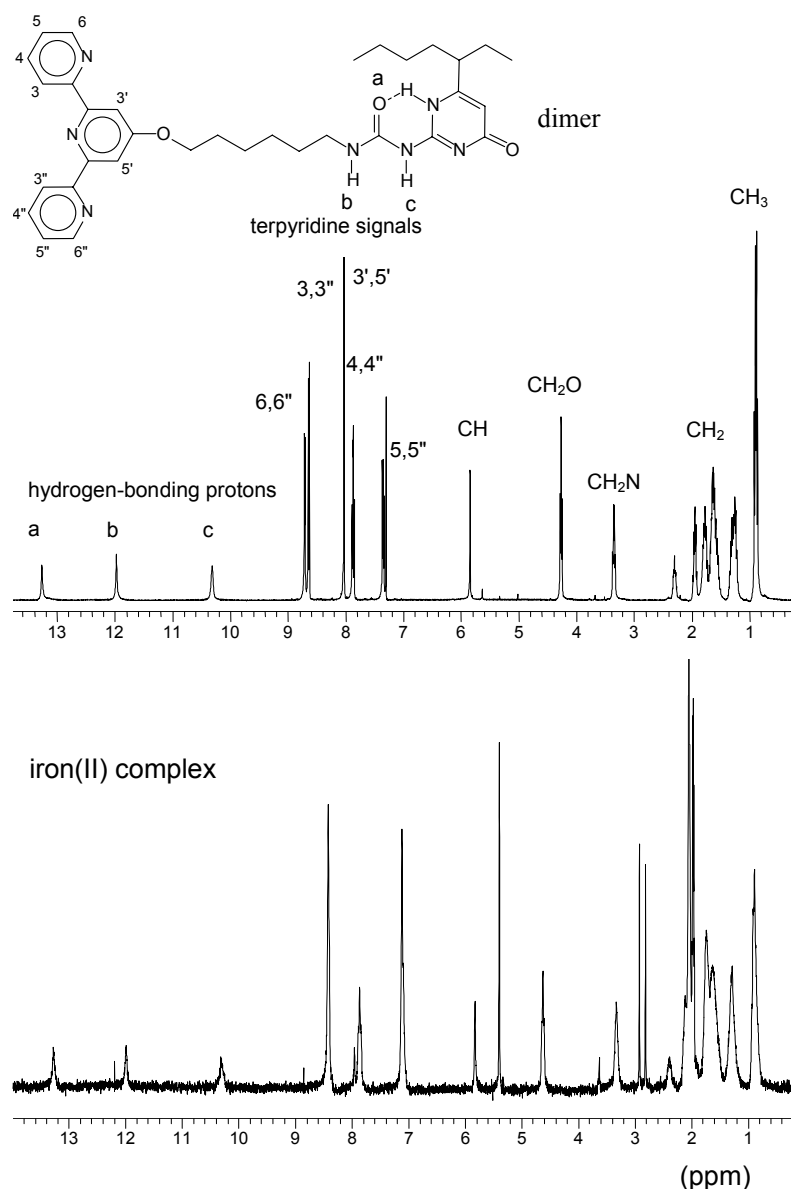


Figure 3.15.  $^1\text{H-NMR}$  spectra of ligand **12b** ( $\text{CHCl}_3$ ) and the corresponding iron(II) complexes (in an acetonitrile/ $\text{CD}_2\text{Cl}_2$ -mixture 20:80).

Solution viscosimetry experiments were performed during a stepwise addition of a  $\text{FeCl}_2$  solution in DMSO to a solution of **12a** in chloroform (0.044 mol/L). An increase of the relative viscosity from 1.05 to 1.8 at the equivalence point was observed, indicating the formation of polymeric species (Figure 3.16). The integrity of the hydrogen bonds under these solvent conditions (chloroform with 3% of DMSO) has been checked by NMR. Neither a decrease of the intensity nor a broadening or shift of the peaks was observed. Moreover, no new signals (of free hydrogen-bonding moieties) were found.



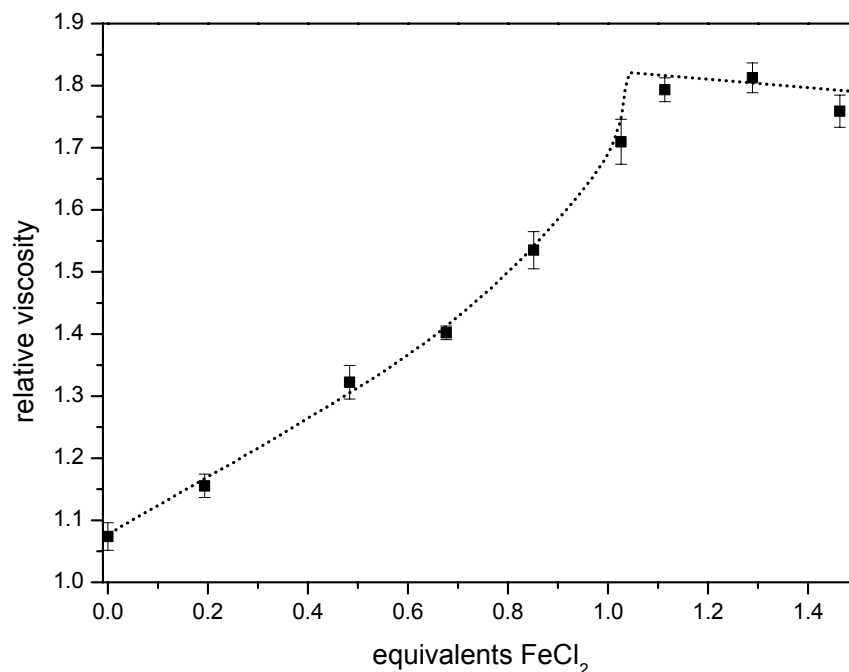
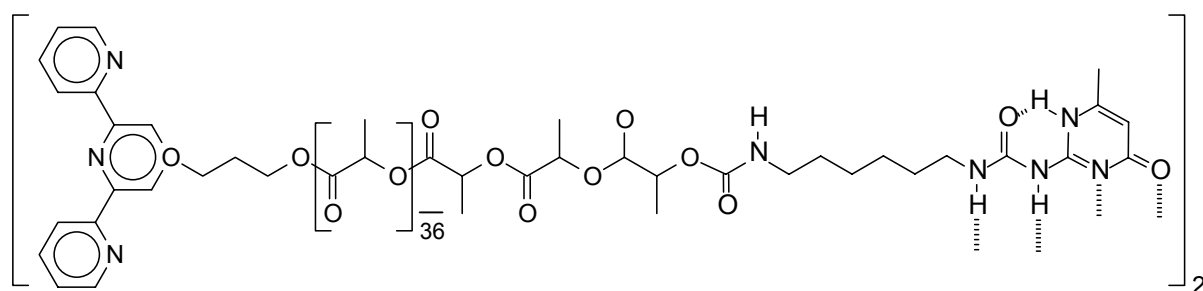


Figure 3.16. Viscosity titration of compound **12a** ( $\text{CHCl}_3$ ) with  $\text{FeCl}_2$ .

Nevertheless, DMSO is known to be a hydrogen bond acceptor solvent, but in small quantities the hydrogen bonds are still intact although the lifetime of the bond is shortened.<sup>[35]</sup> Up to now, these solvent-conditions were found to be the best option due to the solubility behavior of the titration agent ( $\text{FeCl}_2$ ), which was found to give the best results in terpyridine complexation titration experiments because of its ability for fast and complete complexation (leading exclusively to *bis*-complexes) and the purity of the compound.

However, at the equivalence point, the partial formation of a film-like material on the bottom of the viscosimeter was observed, showing that the solubility of the complex in apolar solvents is still problematic. Therefore, the degree of polymerization or the ring-chain equilibrium could not yet be quantified. Although the initial compound shows an improved solubility, the complex **13**, which has been isolated, revealed a similar solubility as the complexes **8** and **9**. An explanation is the high complex density of the coordination polymer in solid state, which is in the case of **13** even higher than for **8** because of the shorter spacer length. A  $^1\text{H-NMR}$  spectrum of the iron complex has been recorded in an dichloromethane/acetonitrile mixture. The hydrogen bonded protons could be detected similar to the previous results for **7** (Figure 3.15, bottom).

To overcome the solubility problems of the complex species and to improve the properties of the coordination polymer, a polymeric spacer has been introduced. A poly(lactide), bearing a terpyridine at one chain end (from a terpyridine-initiator) and a hydroxy group at the other end,<sup>[38]</sup> has been functionalized with a UP-group utilizing the isocyanate coupling reaction in a similar way as for **7** (Scheme 3.6, for the preparation approach see also Scheme 3.4).



Scheme 3.6. Poly(lactide) **15**, functionalized with a terpyridine and a quadruple hydrogen-bonding moiety.

The polymeric spacer is expected to reveal good solubility properties of the ligand as well as the corresponding coordination polymers. Polymer **15** showed indeed a good solubility in chloroform and the NMR spectrum revealed a complete functionalization (Figure 3.17, top). A methanolic solution of  $\text{FeCl}_2$  was added to the ligand solution and a purple product was isolated in quantitative yield after removal of the solvent *in vacuo*. The complex was well-soluble in chloroform and dichloromethane, and the hydrogen-bonding protons are clearly visible (Figure 3.17, bottom).

However, the terpyridine protons are not visible (with a poor resolution after addition of 10 vol-% of acetonitrile), which could be explained by a poor solvent-complex interaction. Probably the complex units are shielded by the polymer chains that contain polar CO-groups, which might interact with the charged complex moieties, making it less accessible for the apolar solvent. Already in visual appearance, the viscosity of the complex polymer in chloroform seems to be higher than in the free ligand. However, due to the synthesized small batch, detailed solution viscosimetry experiments could not yet be performed. A  $^1\text{H-NMR}$  spectrum recorded in pure acetonitrile revealed all terpyridine resonances, however, the signals were very broad. After changing the solvent to methanol, the resolution could be enhanced and the signal assigned to a terpyridine-iron(II) complex, as depicted in the insert in Figure 3.17 (bottom). The resonances of the hydrogen-bonding protons are not visible in this solvent, because methanol coordinates to the ureidopyrimidinone moieties, resulting in a cleavage of the quadruple hydrogen bonds. Due to exchange of these protons by deuterons from the solvent, no new signals appeared. In addition to the NMR-data, UV-vis spectroscopy showed the characteristic MLCT-band of the iron(II) complex, giving another evidence for the complex-formation. These first investigations show that the polymeric spacer is indeed better-suited for the construction of such supramolecular polymers.

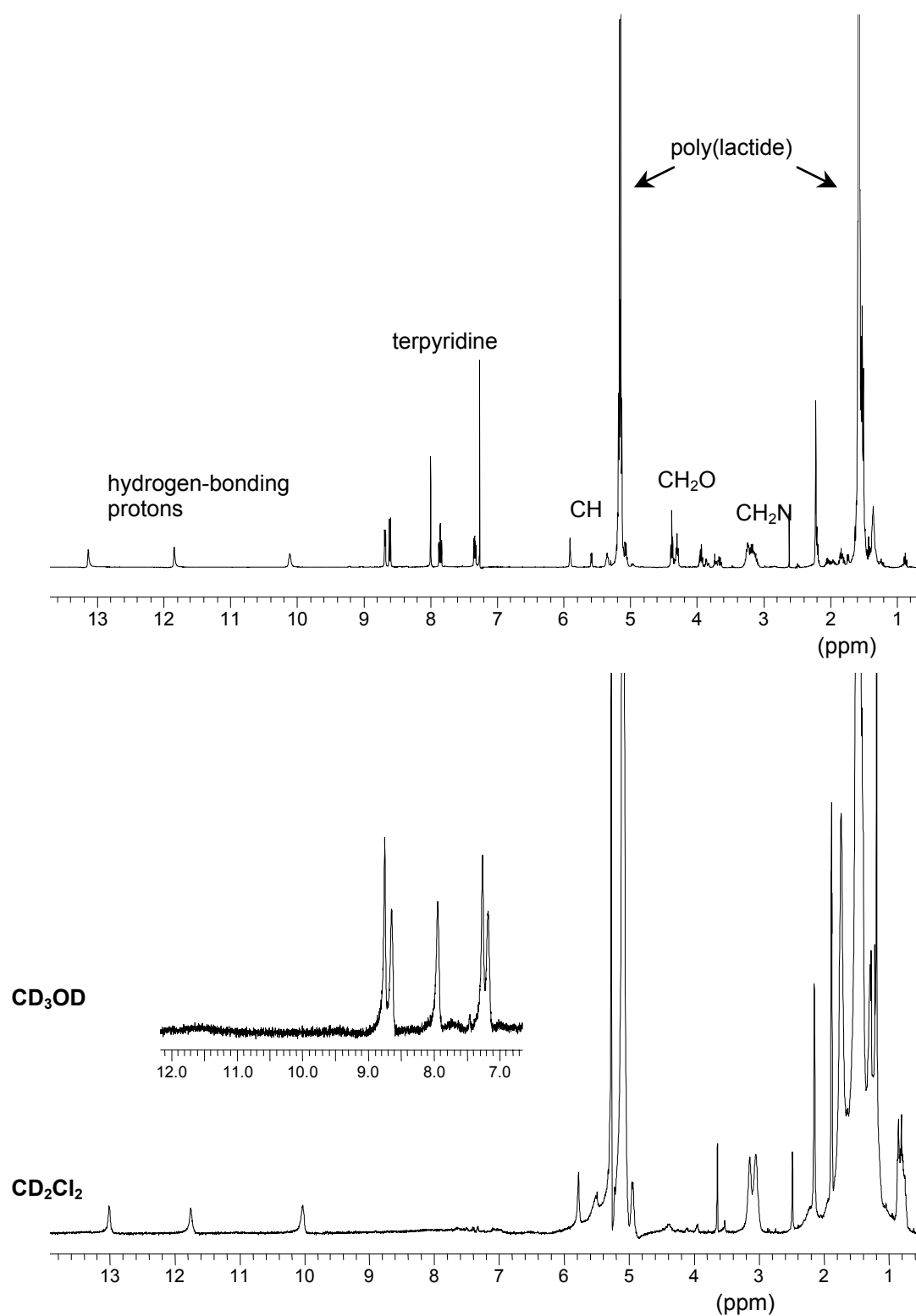


Figure 3.17.  $^1\text{H-NMR}$  of the functionalized poly(lactide) **15** (chloroform) and the corresponding Fe(II) complex **16** (dichloromethane, insert: methanol).

### 3.3 Conclusions

In this chapter selected interesting features of linear coordination polymers were presented. Metallo-supramolecular polymers containing terpyridine ruthenium(II) complexes in the main chain were synthesized and characterized by complexing *bis*-terpyridine-functionalized poly(ethylene glycol)s with ruthenium(II) ions. Fine-tuning of the reaction conditions led to an increase of the degree of polymerization. The polymeric nature was indicated by the film forming properties of the material and was proven by solution viscosimetry as well as rheometry. The polyelectrolyte effect was suppressed by addition of different salt quantities in case of the viscosity experiments. AFM imaging revealed a lamella-like organization of the polymer chains. In addition the thermic stability as well as the rheological properties were studied.

In further studies, metal coordination units were combined with hydrogen-bonding moieties. A series of new compounds containing, for the first time, terpyridine and ureidopyrimidinone moieties was synthesized which form linear supramolecular polymers involving both kinds of non-covalent interaction in the main chain, as demonstrated by UV-vis and NMR spectroscopy as well as viscosimetry.

### 3.4 Experimental section

#### Materials and instrumentation

Basic chemicals were obtained from Sigma-Aldrich. 2,2':6',2''-Terpyrid-4'-yl-di(ethylene glycol)<sup>[7]</sup> and 2,2':6',2''-terpyrid-4'-yl-poly(ethylene glycol)<sub>180</sub><sup>[12,19]</sup> were synthesized as described in literature. Hexaacetone ruthenium(III) tetrafluoroborate was prepared according to a literature procedure.<sup>[5]</sup> NMR spectra were measured on a Varian Mercury 400 spectrometer. The chemical shifts were calibrated to the residual solvent peaks or TMS. UV-vis spectra were recorded on a Perkin Elmer Lambda-45 (1 cm cuvettes, acetonitrile). The extinction coefficients ( $\epsilon$ -values) of the coordination polymers were calculated referred to one repeat unit. Solution viscosity investigations were performed at 20 °C on a Schott AVS 350 viscosimetry system using Micro-Ubbelohde viscosimeters with a capillary diameter of 0.4 mm (type I) and acetonitrile (**3**, **4b**) or methanol (**4a-b**, Figure 3.4) as solvent. Differential scanning calorimetry (DSC) investigations were performed on a Perkin Elmer Pyris-1 DSC system with a heating rate of 40 K/min (glass transitions,  $T_g$ ) and 10 K/min (melting points,  $T_m$  and crystallization points,  $T_c$ ), respectively. TGA analysis has been carried out on a Perkin Elmer Pyris-6 apparatus with a heating rate of 5 K/min. Atomic force microscopy (AFM) has been performed in tapping mode on a DI Multimode with a Nanoscope IIIa controller (Digital Instruments, Santa Barbara, CA, USA). The used cantilever was a "golden" silicon cantilever type NSG11-A (NT-MDT). Samples were prepared from dropcasting solutions (10 mg/mL) of **4b** (in chloroform) and **3** (in acetonitrile) onto silicon wafers. Furthermore, a Solver47H (NT-MDT, Moscow), equipped with a heating stage, was used. Rheological experiments were carried out on a Paar Physica UDS 200 rheometer. A Parallel plate with a diameter 8 mm was used and the measurements were performed within the linear viscoelastic regime at an oscillating frequency of 1 Hz and a strain amplitude of 1% temperature scan were carried out from 30 °C to 72 °C (**2**) respective 100 °C (**4b** and "PEG 200K") with a heating rate of 1 °C/min.

#### Poly(*bis*-2,2':6',2''-terpyrid-4'-yl-diethylene glycol ruthenium(II) tetrafluoroborate) **3**

100 mg (0.176 mmol) *bis*-2,2':6',2''-terpyrid-4'-yl-diethylene glycol **1** was mixed with 143 mg (0.176 mmol) hexaacetone ruthenium(III) tetrafluoroborate<sup>[5]</sup> and heated in 20 mL of ethanol to reflux for 72 h. The obtained red precipitate was washed with ethanol, dissolved in acetonitrile, filtrated, and re-precipitated in ethanol to yield 147 mg (0.174 mmol, 98%) of polymer **3**.

UV-vis (CH<sub>3</sub>CN)  $\lambda_{max}$  ( $\epsilon$ ) = 241 (42 700), 268 (44 700), 304 (50 100), 485 (14 300) nm (L·mol<sup>-1</sup>·cm<sup>-1</sup>)

<sup>1</sup>H-NMR (CD<sub>3</sub>CN):  $\delta$  (ppm) = 4.04 (t, 4 H,  $J$  = 4.39 Hz, OCH<sub>2</sub>), 4.44 (t, 4 H,  $J$  = 4.39 Hz, tpy-OCH<sub>2</sub>), 7.18 (m, 4 H, H<sub>5,5''</sub>), 7.41 (m, 4 H, H<sub>6,6''</sub>), 7.92 (m, 4 H, H<sub>4,4''</sub>), 8.37 (s, 4 H, H<sub>3,3''</sub>), 8.50 (m, 4 H, H<sub>3,3''</sub>).

**Poly(*bis*-2,2':6',2''-terpyrid-4'-yl-poly(ethylene glycol)<sub>180</sub> ruthenium(II) tetrafluoroborate) 4a**

117 mg (0.014 mmol) *bis*-2,2':6',2''-terpyrid-4'-yl-poly(ethylene glycol)<sub>180</sub> **2** was mixed with 9.0 mg (0.014 mmol) hexaacetone ruthenium(III) tetrafluoroborate and heated in 20 mL ethanol to reflux for 72 h. The reaction progress was monitored by UV-vis spectroscopy. Subsequently, the reaction mixture was filtered to remove the inorganic by-products. Finally, the solvent was removed *in vacuo* (18 mbar, 60 °C) to yield 114 mg (0.013 mmol, 96%) of a red polymer.

UV-vis (CH<sub>3</sub>CN)  $\lambda_{max}$  ( $\epsilon$ ) = 241 (58 200), 267 (56 000), 305 (60 100), 485 (15 700) nm (L·mol<sup>-1</sup>·cm<sup>-1</sup>).

<sup>1</sup>H-NMR (CD<sub>3</sub>CN):  $\delta$  (ppm) = 3.55 (m, 950 H, OCH<sub>2</sub>), 4.04 (t, 4 H,  $J$  = 4.39 Hz, tpy-OCH<sub>2</sub>CH<sub>2</sub>), 4.44 (t, 4 H,  $J$  = 4.67 Hz, tpy-OCH<sub>2</sub>), 7.18 (m, 4 H, H<sub>5,5''</sub>), 7.41 (m, 4 H, H<sub>6,6''</sub>), 7.92 (m, 4 H, H<sub>4,4''</sub>), 8.37 (s, 4 H, H<sub>3,3''</sub>), 8.50 (m, 4 H, H<sub>3,3''</sub>).

**Poly(*bis*-2,2':6',2''-terpyrid-4'-yl-poly(ethylene glycol)<sub>180</sub> ruthenium(II) tetrafluoroborate) 4b**

480 mg (0.058 mmol) *bis*-2,2':6',2''-terpyrid-4'-yl-poly(ethylene glycol)<sub>180</sub> **2** was mixed with 38 mg (0.054 mmol) hexaacetone ruthenium(III) tetrafluoroborate and heated in 5 mL chloroform containing 5% ethanol to reflux for 48 h and monitored by UV-vis spectroscopy. The reaction mixture became very viscous and was filtrated (after dilution) to yield 500 mg (0.057 mmol, 99%) of a red polymer after evaporation of the solvent at 18 mbar (60 °C).

UV-vis (CH<sub>3</sub>CN)  $\lambda_{max}$  ( $\epsilon$ ) = 242 (53 300), 268 (54 700), 304 (60 500), 485 (16 300) nm (L·mol<sup>-1</sup>·cm<sup>-1</sup>).

<sup>1</sup>H-NMR (CD<sub>3</sub>CN):  $\delta$  (ppm) = 3.55 (m, 950 H, OCH<sub>2</sub>), 4.04 (t, 4 H,  $J$  = 4.39 Hz, tpy-OCH<sub>2</sub>CH<sub>2</sub>), 4.44 (t, 4 H,  $J$  = 4.67 Hz, tpy-OCH<sub>2</sub>), 7.18 (m, 4 H, H<sub>5,5''</sub>), 7.41 (m, 4 H, H<sub>6,6''</sub>), 7.92 (m, 4 H, H<sub>4,4''</sub>), 8.37 (s, 4 H, H<sub>3,3''</sub>), 8.50 (m, 4 H, H<sub>3,3''</sub>).

DSC:  $T_g$  = -48.6 °C (second heating run, 40 °C/min),  $T_m$  = 50.3 °C (third heating run, 10 °C/min),  $T_c$  = 30.5 °C (third cooling run, 10 °C/min).

**Viscosity measurements**

Compound **3** (90 mg) was dissolved in 5 mL acetonitrile and the viscosity was measured utilizing an Ubbelohde viscosimeter. The solution was diluted stepwise to obtain the concentration curves. The measurements were repeated with 20 mM and 50 mM solutions of tetrabutylammonium tetrafluoroborate to eliminate the polyelectrolyte effect. Polymers **4a-b** were measured in the same way utilizing methanol as solvent.

**{6-[3-(6-Methyl-4-oxo-1,4-dihydro-pyrimidin-2-yl)-ureido]-hexyl}-carbamic acid 5-(2,2':6',2''-terpyridin-4'-yloxy)-pentyl ester 7a**

500 mg (1.49 mmol) of **5a** and 525 mg (1.75 mmol) of **6** were dissolved in 2 mL chloroform and heated to 65 °C. Then 12 mg (0.12 mmol) of dibutyltindelaureate (DBTDL) was added and stirring was continued overnight. A white precipitate formed (probably urea) which was removed by filtration and the solution was concentrated *in vacuo* yielding 607 mg (0.97 mmol, 65%) of **1** as a white solid.

UV-vis (CHCl<sub>3</sub>):  $\lambda_{max}$  ( $\epsilon$ ) = 280 (27800) nm (L mol<sup>-1</sup> cm<sup>-1</sup>).

<sup>1</sup>H-NMR (400 MHz, CHCl<sub>3</sub>):  $\delta$  (ppm) = 1.35-1.89 (m, 14 H, CH<sub>2</sub>), 2.18 (s, 3 H, CH<sub>3</sub>), 3.16 (dd, 2 H,  $J$  = 5.86 Hz, 6.59 Hz, NHCH<sub>2</sub>), 3.23 (dt, 2 H,  $J$  = 5.86, 6.59 Hz, NHCH<sub>2</sub>), 4.09 (t, 2 H,  $J$  = 6.59 Hz, OCH<sub>2</sub>), 4.23 (t, 2 H,  $J$  = 6.59 Hz, OCH<sub>2</sub>), 4.99 (s, 1 H, NH), 5.82 (s, 1 H, CH), 7.36 (m, 2 H, H<sub>5,5''</sub>), 7.88 (dd, 2 H,  $J$  = 7.32, 7.32 Hz, H<sub>4,4''</sub>), 8.06 (s, 2 H, H<sub>3,3''</sub>), 8.63 (d, 2 H,  $J$  = 7.32 Hz, H<sub>3,3''</sub>), 8.70 (d, 2 H,  $J$  = 5.86 Hz, H<sub>6,6''</sub>), 10.10 (s, 1 H, NH), 11.79 (s, 1 H, NH), 13.08 (s, 1 H, NH).

MALDI-TOF-MS:  $m/z$  = 630.01 [M+H]<sup>+</sup>, 652.00 [M+Na]<sup>+</sup>.

**{6-[3-(6-Methyl-4-oxo-1,4-dihydro-pyrimidin-2-yl)-ureido]-hexyl}-carbamic acid 5-(2,2':6',2''-terpyridin-4'-yloxy)-propyl ester 7b**

The synthesis was according to the preparation of **7a**. 458.2 mg (1.49 mmol) of **5b**, 525 mg (1.75 mmol) of **6** and 30  $\mu$ L of DBTL. Yield: 677 mg (77%).

UV-vis (CHCl<sub>3</sub>):  $\lambda_{max}$  ( $\epsilon$ ) = 278 (27500) nm (L mol<sup>-1</sup> cm<sup>-1</sup>).

IR:  $1/\lambda$  (cm<sup>-1</sup>) = 3320.4 (w), 3217.0 (w), 2933.1 (m), 2859.4 (m), 1698.0 (m), 1657.0 (s), 1580.2 (s), 1561.6 (s), 1522.1 (s), 1467.5 (m), 1442.7 (s), 1406.5 (s), 1360.2 (m), 1325.2 (w), 1246.6 (s), 1201.1 (s), 1138.0 (m), 1091.8 (m), 1047.6 (m), 1036.7 (s), 992.0 (w), 972.9 (w), 948.3 (w), 928.9 (w), 902.1 (w), 862.4 (w), 845.5 (m), 791.7 (s), 743.0 (s), 732.5 (s), 698.2 (m), 658.5 (m).

<sup>1</sup>H-NMR (400 MHz, CHCl<sub>3</sub>):  $\delta$  (ppm) = 1.36 (m, 4 H, CH<sub>2</sub>), 1.50 (m, 2 H, CH<sub>2</sub>), 1.58 (2 H, CH<sub>2</sub>), 2.16 (m, 3 H, CH<sub>2</sub> and CH<sub>3</sub>), 3.16 (dd, 2 H,  $J$  = 5.86, 6.59 Hz, NHCH<sub>2</sub>), 2.23 (dd, 2 H,  $J$  = 5.86, 6.59 Hz, NHCH<sub>2</sub>), 4.28 (t, 2 H,  $J$  = 5.86 Hz, OCH<sub>2</sub>), 4.32 (t, 2 H,  $J$  = 5.86 Hz, OCH<sub>2</sub>), 4.33 (s, 1 H, NH), 5.80 (s, 1 H, CH), 7.33 (dd, 2 H,  $J$  = 7.82, 4.89 Hz, H<sub>5,5''</sub>), 7.84 (dd, 2 H,  $J$  = 7.82, 7.82 Hz, H<sub>4,4''</sub>), 8.02 (s, 2 H, H<sub>3,3''</sub>), 8.61 (d, 2 H,  $J$  = 7.82 Hz, H<sub>3,3''</sub>), 8.67 (d, 2 H,  $J$  = 4.89 Hz, H<sub>6,6''</sub>), 10.08 (s, 1 H, NH), 11.74 (s, 1 H, NH), 13.05 (s, 1 H, NH).

<sup>13</sup>C-NMR (100 MHz, CHCl<sub>3</sub>):  $\delta$  (ppm) = 18.86, 25.91, 26.06, 28.86, 29.24, 39.43, 40.61, 64.74, 106.57, 107.38, 121.34, 123.82, 136.82, 148.19, 148.92, 154.59, 155.97, 156.48, 156.95, 167.04, 173.09.

MALDI-TOF-MS:  $m/z$  = 600.12 [M]<sup>+</sup>.

**4'-{6-[3-(6-Methyl-4-oxo-1,4-dihydro-3-heptyl-pyrimidin-2-yl)-ureido]-pentyl}-2,2':6',2''-terpyridine 12a**

The CDI-activated 6-(1-ethylpentyl)-isocytosine **11** (218 mg; 0.719 mmol) was mixed with 5-aminopentylterpyridine **10a** (200 mg; 0.598 mmol) in 20 mL of chloroform and reacted overnight at room temperature. The solution was extracted with water to remove unreacted **11**, dried over NaSO<sub>4</sub> and the solvent evaporated *in vacuo*. Finally, the compound was recrystallized from chloroform/pentane to yield 302 mg (89%) of **12a** as a white solid.

UV-vis (CHCl<sub>3</sub>):  $\lambda_{max}(\epsilon) = 277 (29400) \text{ nm (L mol}^{-1} \text{ cm}^{-1})$ .

IR:  $1/\lambda (\text{cm}^{-1}) = 3209.8 (\text{w}), 2929.4 (\text{m}), 2859.4 (\text{m}), 1698.0 (\text{m}), 1645.8 (\text{s}), 1577.8 (\text{s}), 1523.2 (\text{s}), 1457.0 (\text{s}), 1442.7 (\text{s}), 1406.2 (\text{s}), 1354.6 (\text{s}), 1312.7 (\text{m}), 1246.0 (\text{s}), 1232.1 (\text{m}), 1200.7 (\text{s}), 1146.7 (\text{w}), 1122.4 (\text{w}), 1091.3 (\text{m}), 1049.5 (\text{w}), 1023.1 (\text{s}), 989.2 (\text{w}), 952.2 (\text{w}), 922.8 (\text{m}), 902.0 (\text{w}), 872.7 (\text{m}), 847.5 (\text{m}), 793.4 (\text{s}), 774.7 (\text{m}), 744.4 (\text{s}), 734.9 (\text{s}), 697.6 (\text{m}), 658.9 (\text{m})$ .

<sup>1</sup>H-NMR (400 MHz, CHCl<sub>3</sub>):  $\delta (\text{ppm}) = 0.85 (\text{m}, 6 \text{ H}, \text{CH}_3), 1.24 (\text{m}, 4 \text{ H}, \text{CH}_2), 1.58 (\text{m}, 6 \text{ H}, \text{CH}_2), 1.73 (\text{m}, 2 \text{ H}, \text{CH}_2), 1.91 (\text{m}, 2 \text{ H}, \text{CH}_2), 2.26 (\text{m}, 1 \text{ H}, \text{CH}), 3.31 (\text{t}, 2 \text{ H}, J = 6.84 \text{ Hz}, \text{OCH}_2), 4.24 (\text{t}, 2 \text{ H}, J = 6.59 \text{ Hz}, \text{OCH}_2), 5.80 (\text{s}, 1 \text{ H}, \text{CH}), 7.36 (\text{dd}, 2 \text{ H}, J = 7.82, 4.89 \text{ Hz}, \text{H}_{5,5''}), 7.83 (\text{ddd}, 2 \text{ H}, J = 7.82, 7.82, 1.96 \text{ Hz}, \text{H}_{4,4''}), 7.99 (\text{s}, 2 \text{ H}, \text{H}_{3,5'}), 8.60 (\text{d}, 2 \text{ H}, J = 7.82 \text{ Hz}, \text{H}_{3,3''}), 8.67 (\text{d}, 2 \text{ H}, J = 4.89 \text{ Hz}, \text{H}_{6,6''}), 10.28 (\text{s}, 1 \text{ H}, \text{NH}), 11.94 (\text{s}, 1 \text{ H}, \text{NH}), 13.22 (\text{s}, 1 \text{ H}, \text{NH})$ .

<sup>13</sup>C-NMR (100 MHz, CHCl<sub>3</sub>):  $\delta (\text{ppm}) = 11.63, 13.84, 22.43, 25.61, 26.66, 26.51, 28.92, 28.9, 29.31, 29.23, 32.78, 39.92, 45.25, 68.11, 70.51, 106.16, 107.34, 121.28, 123.69, 136.70, 148.95, 154.82, 155.36, 156.14, 156.68, 156.96, 167.27, 173.12$ .

MALDI-TOF-MS:  $m/z = 584.28 [\text{MH}]^+$ .

**4'-{5-[3-(6-Methyl-4-oxo-1,4-dihydro-3-heptyl-pyrimidin-2-yl)-ureido]-hexyl}-2,2':6',2''-terpyridine 12b**

The synthesis was according to the preparation of **12a**. 100 mg (0.330 mmol) of **5**, 112.6 mg (0.323 mmol) of **4b** in 20 mL of chloroform. Yield: 183 mg (97 %).

UV-vis (CHCl<sub>3</sub>):  $\lambda_{max}(\epsilon) 277 (29500) \text{ nm (L mol}^{-1} \text{ cm}^{-1})$ .

IR:  $1/\lambda (\text{cm}^{-1}) = 3209.8 (\text{w}), 2929.4 (\text{m}), 2859.4 (\text{m}), 1698.0 (\text{m}), 1645.8 (\text{s}), 1577.8 (\text{s}), 1523.2 (\text{s}), 1457.0 (\text{s}), 1442.7 (\text{s}), 1406.2 (\text{s}), 1354.6 (\text{s}), 1312.7 (\text{m}), 1246.0 (\text{s}), 1232.1 (\text{m}), 1200.7 (\text{s}), 1146.7 (\text{w}), 1122.4 (\text{w}), 1091.3 (\text{m}), 1049.5 (\text{w}), 1023.1 (\text{s}), 989.2 (\text{w}), 952.2 (\text{w}), 922.8 (\text{m}), 902.0 (\text{w}), 872.7 (\text{m}), 847.5 (\text{m}), 793.4 (\text{s}), 774.7 (\text{m}), 744.4 (\text{s}), 734.9 (\text{s}), 697.6 (\text{m}), 658.9 (\text{m})$ .

<sup>1</sup>H-NMR (400 MHz, CHCl<sub>3</sub>):  $\delta (\text{ppm}) = 0.86 (\text{m}, 6 \text{ H}, \text{CH}_3), 1.25 (\text{m}, 4 \text{ H}, \text{CH}_2), 1.59 (\text{m}, 6 \text{ H}, \text{CH}_2), 1.74 (\text{m}, 2 \text{ H}, \text{CH}_2), 1.92 (\text{m}, 2 \text{ H}, \text{CH}_2), 2.27 (\text{m}, 1 \text{ H}, \text{CH}), 3.32 (\text{t}, 2 \text{ H}, J = 6.84 \text{ Hz}, \text{OCH}_2), 4.23 (\text{t}, 2 \text{ H}, J = 6.59 \text{ Hz}, \text{OCH}_2), 5.80 (\text{s}, 1 \text{ H}, \text{CH}), 7.32 (\text{dd}, 2 \text{ H}, J = 7.82, 4.89 \text{ Hz}, \text{H}_{5,5''}), 7.83 (\text{ddd}, 2 \text{ H}, J = 7.82, 7.82, 1.96 \text{ Hz}, \text{H}_{4,4''}), 7.99 (\text{s}, 2 \text{ H}, \text{H}_{3,5'}), 8.59 (\text{d}, 2 \text{ H}, J = 7.82 \text{ Hz}, \text{H}_{3,3''}), 8.67 (\text{d}, 2 \text{ H}, J = 4.89 \text{ Hz}, \text{H}_{6,6''}), 10.28 (\text{s}, 1 \text{ H}, \text{NH}), 11.94 (\text{s}, 1 \text{ H}, \text{NH}), 13.22 (\text{s}, 1 \text{ H}, \text{NH})$ .

<sup>13</sup>C-NMR (100 MHz, CHCl<sub>3</sub>):  $\delta (\text{ppm}) = 11.63, 13.83, 22.41, 23.36, 26.50, 28.68, 29.08, 29.24, 32.77, 39.82, 45.24, 68.04, 106.19, 107.36, 121.28, 123.71, 136.71, 148.97, 154.78, 155.42, 156.14, 156.72, 156.97, 167.27, 173.13$ .

MALDI-TOF-MS:  $m/z = 569.31 [\text{M}]^+$ .

**{6-[3-(6-Methyl-4-oxo-1,4-dihydro-pyrimidin-2-yl)-ureido]-hexyl}-carbamic acid 5-(2,2':6',2''-terpyridin-4'-yloxy)-pentyl ester zinc(II) hexafluorophosphate 8**

To a solution of 20 mg (0.032 mmol) of **6a** in chloroform was added a methanolic solution of Zn(II) acetate (3.5 mg, 0.032 mmol). Then an excess of ammonium hexafluorophosphate was added and the product **8** was precipitated in diethyl ether to yield 35.7 mg (0.022 mmol, 68%) of a white powder.

UV-vis (CHCl<sub>3</sub>):  $\lambda_{max}(\epsilon) = 241 (66400), 274 (47800), 310 (25800), 323 (27200) \text{ nm (L mol}^{-1} \text{ cm}^{-1})$ .

<sup>1</sup>H-NMR (400 MHz, CH<sub>2</sub>Cl<sub>2</sub>):  $\delta (\text{ppm}) = 0.95-1.41 (\text{m}, 8 \text{ H}, \text{CH}_2), 1.59-1.86 (\text{m}, 6 \text{ H}, \text{CH}_2), 2.14 (\text{s}, 3 \text{ H}, \text{CH}_3), 2.76-3.05 (\text{m}, 4 \text{ H}, \text{NHCH}_2), 4.10 (\text{m}, 2 \text{ H}, \text{OCH}_2), 4.50 (\text{m}, 2 \text{ H}, \text{OCH}_2), 5.63-5.79 (\text{m}, 2 \text{ H}, \text{NH}, \text{CH}), 7.40 (\text{m}, 2 \text{ H}, \text{H}_{5,5''}), 7.75 (\text{m}, 2 \text{ H}, \text{H}_{4,4''}), 8.11 (\text{m}, 4 \text{ H}, \text{H}_{3,5',6,6''}), 8.49 (\text{m}, 2 \text{ H}, \text{H}_{3,3''}), 10.03 (2s, 1 H, NH), 11.80 (2s, 1 H, NH), 13.04 (2s, 1 H, NH)$ .

MALDI-TOF-MS:  $m/z = 691.7 [\text{M} - 1 \text{ ligand } \mathbf{6a} - 2 \text{ PF}_6]^+$ .

**UV-vis titration of ligand 6**

0.743 mg (0.00124 mmol) of ligand **1** was dissolved in 25 mL of chloroform and 0.854 mg (0.0043 mmol) of iron(II) chloride was dissolved in 400  $\mu\text{L}$  methanol. This solution was added to the ligand in steps of 50  $\mu\text{L}$  and the formation of the iron complex was monitored by UV-vis spectroscopy after each addition.

**Viscosity titration of ligand 12**

102 mg (0.175 mmol) of compound **12** was dissolved in 4 mL of chloroform and 20 mg (0.158 mmol) of iron(II) chloride was dissolved in 400  $\mu\text{L}$  of DMSO. This solution was added in steps of 20 or 40  $\mu\text{L}$  to the ligand solution and measured in a micro-Ubbelohde viscosimeter.

The integrity of the hydrogen bonds under these solvent conditions (chloroform with 3% of DMSO) has been checked by NMR. Neither a decrease of the intensity nor a broadening nor a shift of the peaks nor the appearance of new signals was observed. Nevertheless, DMSO is known to be a hydrogen bond acceptor solvent,

but in small quantities the hydrogen bonds are still intact although the lifetime of the bond is shortened.<sup>[35]</sup> These solvent-conditions were found to be the best option due to the solubility behavior of the titration agent (FeCl<sub>2</sub>), which was found to give the best results in terpyridine complexation titration experiments due to its ability for fast and complete complexation (leading exclusively to *bis*-complexes) and the purity of the compound.

**{6-[3-(6-Methyl-4-oxo-1,4-dihydro-pyrimidin-2-yl)-ureido]-hexyl}-carbamic acid 5-(2,2':6',2''-terpyridin-4'-yloxy)-poly(lactide)-yl ester 15**

The synthesis was according to the preparation of **7a**. 64 mg (0.014 mmol) of **14**, 6 mg (0.02 mmol) of **6** and 10  $\mu$ l of DBTL. The mixture was refluxed for 48 hours. Then the product was precipitated into pentane, followed by two BioBeads SX-1 columns in dichloromethane and THF, respectively, and finally precipitated into methanol containing 10% of water. Yield: 58 mg (90%).

UV-vis (CHCl<sub>3</sub>):  $\lambda_{max}(\epsilon) = 277 (29400) \text{ nm (L mol}^{-1} \text{ cm}^{-1})$ .

<sup>1</sup>H-NMR (400 MHz, CHCl<sub>3</sub>):  $\delta$  (ppm) = 1.36 (m, 8 H, CH<sub>2</sub>), 1.57 (d, 114 H,  $J = 6.84 \text{ Hz}$ , CH<sub>3</sub> (polylactide)), 1.84 (2 H, CH<sub>2</sub>), 2.22 (m, 6 H, CH<sub>2</sub>), 3.17 (m, 2 H, NHCH<sub>2</sub>), 2.24 (m, 2 H, NHCH<sub>2</sub>), 4.30 (t, 2 H,  $J = 5.86 \text{ Hz}$ , OCH<sub>2</sub>), 4.38 (t, 2 H,  $J = 5.86 \text{ Hz}$ , OCH<sub>2</sub>), 5.15 (q, 38 H,  $J = 6.84 \text{ Hz}$ , CH (polylactide)), 5.90 (s, 1 H, CH), 5.35 (s, 1 H, NH), 7.33 (dd, 2 H,  $J = 7.82, 4.89 \text{ Hz}$ , H<sub>5,5''</sub>), 7.84 (dd, 2 H,  $J = 7.82, 7.82 \text{ Hz}$ , H<sub>4,4''</sub>), 8.02 (s, 2 H, H<sub>3',5'</sub>), 8.61 (d, 2 H,  $J = 7.82 \text{ Hz}$ , H<sub>3,3''</sub>), 8.67 (d, 2 H,  $J = 4.89 \text{ Hz}$ , H<sub>6,6''</sub>), 10.11 (s, 1 H, NH), 11.84 (s, 1 H, NH), 13.13 (s, 1 H, NH).

**Iron(II) complex of 15 (16)**

To a solution of **15** (7.0 mg) in chloroform (2 mL) a methanolic solution of FeCl<sub>2</sub> (0.3 mg) was added. The product **16** was isolated in quantitative yield after evaporation of the solvent.

UV-vis (CHCl<sub>3</sub>):  $\lambda_{max}(\epsilon) = 241 (66500), 274 (47900), 310 (25700), 323 (26800) \text{ nm (L mol}^{-1} \text{ cm}^{-1})$ .

<sup>1</sup>H-NMR (400 MHz, CHCl<sub>3</sub>):  $\delta$  (ppm) = 0.89 (m, 8 H, CH<sub>2</sub>), 1.39 (m, 2 H, CH<sub>2</sub>), 1.57 (d, 114 H,  $J = 6.84 \text{ Hz}$ , CH<sub>3</sub> (polylactide)), 2.16 (m, 2 H, CH<sub>2</sub>), 3.25 (m, 2 H, NHCH<sub>2</sub>), 4.48 and 4.56 (br, 2 H, OCH<sub>2</sub>), 4.72 (s, 1 H, NH), 5.15 (q, 38 H,  $J = 6.84 \text{ Hz}$ , CH (polylactide)), 5.91 (s, 1 H, CH), 10.14 (s, 1 H, NH), 11.87 (s, 1 H, NH), 13.14 (s, 1 H, NH). (CD<sub>3</sub>CN) 7.20 (br, 4 H, H<sub>5,5''</sub>, H<sub>6,6''</sub>), 7.89 (br, 2 H, H<sub>4,4''</sub>), 8.52 (br, 2 H, H<sub>3,3''</sub>, 3',5'').

### 3.5 References

- [1] [1a] L. R. Rieth, R. F. Eaton, G. W. Coates, *Angew. Chem.* **2001**, *113*, 2211-2214; *Angew. Chem. Int. Ed.* **2001**, *40*, 2153-2156; [1b] L. Brunsveld, B. J. B. Folmer, E. W. Meijer, R. P. Sijbesma, *Chem. Rev.* **2001**, *101*, 4071-4097; [1c] R. P. Sijbesma, F. H. Beijer, L. Brunsveld, B. J. Folmer, J. H. Hirschberg, R. F. Lange, J. K. Lowe, E. W. Meijer, *Science* **1997**, *278*, 1601-1604; [1d] F. Ilhan, M. Gray, V. M Rotello, *Macromolecules* **2001**, *34*, 2597-2601; [1e] G. Cooke, V. M Rotello, *Chem. Soc. Rev.* **2002**, *31*, 275-286; [1f] K. Yamauchi, J. R. Lizotte, D. M. Hercules, M. J. Vergne, T. E. Long, *J. Am. Chem. Soc.* **2002**, *124*, 8599-8604; [1g] K. Yamauchi, J. R. Lizotte, T. E. Long, *Macromolecules* **2003**, *36*, 1083-1088.
- [2] [2a] U. S. Schubert, C. Eschbaumer, *Angew. Chem.* **2002**, *114*, 3016-3050; *Angew. Chem. Int. Ed.* **2002**, *41*, 2892-2926; [2b] J. E. McAlvin, S. B. Scott, C. L. Fraser, *Macromolecules* **2000**, *33*, 6953-6964; [2c] C. L. Fraser, A. P. Smith, *J. Polym. Sci., Part A: Polym. Chem.* **2000**, *38*, 4704-4716; [2d] S. Kelch, M. Rehahn, *Macromolecules* **1998**, *31*, 4102-4106; [2e] B. Lahn, M. Rehahn, *e-Polymers* **2002**, *001*, 1-33.

- [3] U. S. Schubert, C. Eschbaumer, P. R. Andres, H. Hofmeier, C. H. Weidl, E. Herdtweck, E. Dulkeith, A. Morteani, N. E. Hecker, J. Feldmann, *Synth. Met.* **2001**, *121*, 1249-1252.
- [4] [4a] B. G. G. Lohmeijer, U. S. Schubert, *Angew. Chem.* **2002**, *114*, 3980-3984; *Angew. Chem. Int. Ed.* **2002**, *41*, 3825-3829; [4b] J.-F. Gohy, B. G. G. Lohmeijer, U. S. Schubert, *Macromolecules* **2002**, *35*, 4560-4563; [4c] J.-F. Gohy, B. G. G. Lohmeijer, S. K. Varshney, U. S. Schubert, *Macromolecules* **2002**, *35*, 7427-7435; [4d] J.-F. Gohy, B. G. G. Lohmeijer, S. K. Varshney, U. S. Schubert, B. Decamps, E. Leroy, S. Boileau, U. S. Schubert, *Macromolecules* **2002**, *35*, 9748-9755.
- [5] S. Kelch, M. Rehahn, *Macromolecules* **1997**, *30*, 6185-6193.
- [6] S. Kelch, M. Rehahn, *Macromolecules* **1999**, *32*, 5818-5828.
- [7] S. Schmatloch, M. Fernandez-González, U. S. Schubert, *Macromol. Rapid Commun.* **2002**, *23*, 957-961.
- [8] [8a] K. J. Calzia, G. N. Tew, *Macromolecules* **2002**, *35*, 6090-6093; [8b] A. Elghayoury, H. Hofmeier, B. de Ruyter, U. S. Schubert, *Macromolecules* **2003**, *36*, 3955-3959.
- [9] [9a] C. L. Fraser, A. P. Smith, X. Wu, *J. Am. Chem. Soc.* **2000**, *122*, 9026-9027; [9b] X. Wu, J. E. Collins, J. E. McAlvin, R. W. Cutts, C. L. Fraser, *Macromolecules* **2001**, *34*, 2812-2821; [9c] P. S. Corbin, M. P. Webb, J. E. McAlvin, C. L. Fraser, *Biomacromolecules* **2001**, *2*, 223-232; [9d] A. P. Smith, C. L. Fraser, *Macromolecules* **2002**, *35*, 594-596; [9e] U. S. Schubert, M. Heller, *Chem. Eur. J.* **2001**, *7*, 5252-5259.
- [10] U. S. Schubert, H. Hofmeier, *Macromol. Rapid Commun.* **2002**, *23*, 561-566.
- [11] [11a] S. Bernhard, K. Takada, D. Díaz, H. D. Abruña, H. Mürner, *J. Am. Chem. Soc.* **2001**, *123*, 10265-10271; [11b] S. Bernhard, J. I. Goldsmith, K. Takada, H. D. Abruña, *Inorg. Chem.* **2003**, *24*, 4389-4393.
- [12] U. S. Schubert, O. Hien, C. Eschbaumer, *Macromol. Rapid Commun.* **2000**, *21*, 1156-1161.
- [13] J. Hjelm, E. C. Constable, E. Figgemeier, A. Hagfeld, R. Handel, C. E. Housecroft, E. Mukhtar, E. Schofield, *Chem. Commun.* **2002**, 284-285.
- [14] M. Schütte, D. G. Kurth, M. R. Linford, H. Cölfen, H. Möhwald, *Angew. Chem.* **1998**, *110*, 3058-3061; *Angew. Chem. Int. Ed.* **1998**, *37*, 2891-2893.
- [15] B. G. G. Lohmeijer, U. S. Schubert, *Macromol. Chem. Phys.* **2003**, *204*, 1072-1078.
- [16] J.-F. Gohy, B. G. G. Lohmeijer, U. S. Schubert, *Macromol. Rapid Commun.* **2002**, *23*, 555-560.
- [17] M. Heller, U. S. Schubert, *Macromol. Rapid Commun.* **2001**, *22*, 1358-1363.
- [18] [18a] D. T. F. Pals, J. J. Hermans, *Rec. Trav. Chim.* **1952**, *71*, 433-457; [18b] H. Dautzenberg, W. Jaeger, J. Kötz, B. Philipp, C. Seidel, D. Stscherbina, *Polyelectrolytes*, Carl Hanser Verlag, Munich 1994.
- [19] [19a] U. S. Schubert, C. Eschbaumer, *Polym. Prepr.* **2000**, *41*, 542-543; [19b] S. Schmatloch, U. S. Schubert, *Macromol. Symp.* **2003**, *199*, 483-497.
- [20] M. Cazacu, A. Airinei, M. Marcu, *Appl. Organometal. Chem.* **2002**, *16*, 643-648.
- [21] J. Cohen, Z. Priel, *J. Chem. Phys.* **1988**, *88*, 7111-7116.
- [22] N. Ise, *Angew. Chem.* **1986**, *98*, 323-334; *Angew. Chem. Int. Ed.* **1986**, *25*, 323-334.
- [23] J. Brandrup, E. H. Immergut, E. A. Grulke, *Polymer Handbook (4th edition)*, Wiley Interscience, New York 1999 VII/32.
- [24] M. S. Park, J. K. Kim, *J. Polym. Sci., Part B* **2002**, *40*, 1673-1681.



- [25] [25a] L. G. M. Beekmans, D. W. van der Meer, G. J. Vansco, *Polymer* **2002**, *43*, 1887-1895; [25b] D. Snetivy, G. J. Vansco, *Polymer* **1992**, *33*, 432-434.
- [26] [26a] W. J. F. Barnes, P. Price, *Polymer* **1964**, *5*, 283-292; [26b] S. Z. D. Cheng, H. S. Bu, B. Wunderlich, *Polymer* **1988**, *29*, 579-583.
- [27] S. Schmatloch, A. M. J. v. d. Berg, A. S. Alexeev, H. Hofmeier, U. S. Schubert, *Macromolecules*, **2003**, *36*, 9943-9949.
- [28] [28a] S. L. Madorsky, S. Straus, *J. Polym. Sci.* **1959**, *36*, 183-194; [28b] C. G. Cameron, M. D. Ingram, M. Y. Qureshi, H. M. Gearing, L. Costa, G. Camino, *Eur. Polym. J.* **1989**, *25*, 779-784.
- [29] [29a] R. P. Sijbesma, F. H. Beijer, L. Brunsveld, B. J. B. Folmer, J. H. K. K. Hirschberg, R. F. M. Lange, J. K. L. Lowe, E. W. Meijer, *Science* **1997**, *278*, 1601-1604; [29b] J. H. K. K. Hirschberg, F. H. Beijer, H. A. van Aert, P. C. M. M. Magusin, R. P. Sijbesma E. W. Meijer, *Macromolecules* **1999**, *32*, 2696-2705.
- [30] B. J. B. Folmer, R. P. Sijbesma, R. M. Versteegen, J. A. J. van der Rijt, E. W. Meijer, *Adv. Mater.* **2000**, *12*, 874-878.
- [31] C. Naether, J. Greve, I. Jess, *Z. Naturforsch., B: Chemical Sciences* **2003**, *8*, 52-58.
- [32] J. M. Pollino, L. P. Stubbs, M. Weck, *Polym. Prepr.* **2003**, *44*, 730-731.
- [33] L. Brunsveld, B. J. B. Folmer, E. W. Meijer, R. P. Sijbesma, *Chem. Rev.* **2001**, *101*, 4071-4097
- [34] U. S. Schubert, C. Eschbaumer, O. Hien, P. R. Andres, *Tetrahedr. Lett.* **2001**, *42*, 4705-4707.
- [35] F. H. Beijer, R. P. Sijbesma, H. Kooijman, A. L. Spek, E. W. Meijer, *J. Am. Chem. Soc.* **1998**, *120*, 6761-6769.
- [36] [36a] A. T. ten Cate, R. P. Sijbesma, *Macromol. Rapid Commun.* **2002**, *23*, 1094-1112; [36b] S. H. M. Söntjens, R. P. Sijbesma, M. H. P. van Genderen, E. W. Meijer, *Macromolecules* **2000**, *34*, 3815-3818.
- [37] H. M. Keizer, A. Razmir, R. P. Sijbesma, E. W. Meijer, *Polym. Prepr.* **2003**, *44*, 596-597.
- [38] R. Hoogenboom, U. S. Schubert, unpublished results.

# 4

## Metallo-Supramolecular graft copolymers

**Abstract:** A copolymer of poly(methyl methacrylate) with terpyridine units in the side chains has been synthesized utilizing free radical polymerization. Subsequently, the free terpyridine units were complexed with several different terpyridine ruthenium *mono*-complexes, yielding metallo-supramolecular graft copolymers. Unfunctionalized terpyridine, 4'-hydroxy-propoxy terpyridine as well as poly(ethylene glycol) and poly(lactide) functionalized terpyridines have been employed in the grafting procedure. The obtained materials were characterized by NMR, UV-vis and GPC. Characterization by thermal analysis revealed distinct differences of these new materials compared to the initial copolymer. The poly(methyl methacrylate)-g-poly(ethylene glycol) turned out to be amphiphilic. Therefore, aqueous micelles could be prepared from these supramolecular graft copolymers. Three different graft copolymers were investigated, in which the average number of PEG branches (constant length) and the length of the PMMA backbone were varied. The successful formation of micelles was proven by dynamic light scattering (DLS), atomic force microscopy (AFM) and transmission electron microscopy (TEM). A good agreement was found between TEM and AFM observations, which show polydisperse spherical micelles. The hydrodynamic diameter measured by DLS was much larger, suggesting the formation of aggregates. No substantial difference in the micellar characteristic features was found between the three investigated samples.

*Parts of this work have been published:*

U. S. Schubert, H. Hofmeier, *Macromol. Rapid Commun.* **2002**, *23*, 561-566; J.-F. Gohy, H. Hofmeier, A. S. Alexeev, U. S. Schubert, *Macromol. Chem. Phys.* **2003**, *204*, 1524-1530.

## 4.1 Introduction

In the last decades, supramolecular chemistry has grown from an exotic subject to one of the main research fields in chemistry. Inter- and intramolecular supramolecular interactions are of major importance for most biological processes,<sup>[1]</sup> such as the formation of biomolecules, for catalytic processes, for the stabilization of specific structures and information storage. DNA represents one of the most famous examples. Today, many synthetic supramolecular systems are known, based on self-recognition and self-assembly processes.<sup>[2]</sup> The resulting compounds are expected to reveal new chemical, physical as well as biological properties. In addition, a growing field in chemistry is represented currently by the combination of supramolecular chemistry with classical polymer chemistry.<sup>[3-6]</sup> Besides hydrogen-bonds, metal-ligand interactions are of special interest. Several examples have been recently described for the defined introduction of such moieties into polymer backbones or side chains.<sup>[7]</sup> The combinations of such polymers with metal complexing units in the side chains open also new ways for the construction of graft copolymers. Grafting procedures on polymers and polymer-analogous reactions are well-known in polymer chemistry and play an important role for the design of materials.<sup>[8]</sup> For this purpose, covalent reactions are usually being utilized. However, combining this classical polymer approach with supramolecular chemistry allows the construction of new materials via self-organization processes.

During the last years, an interesting development in polymer chemistry has been observed regarding copolymers with supramolecular entities in the side chains. Several groups have reported on the preparation and investigation of systems, in which hydrogen bonds or metal complexes were utilized to introduce a cross-linking or an attachment of additional units. The work of Coates *et al.*<sup>[9]</sup> can be seen in this context as a logical extension of the pioneering work of Stadler at the end of the 1980's:<sup>[10]</sup> the combination of hydrogen bonding units in the side chain of a poly(1-hexene) resulted in the formation of thermoplastic elastomers, where the self-complementary quadruple hydrogen bonding unit acts as a cross-linker unit and forms the hard segments. Rotello *et al.*<sup>[11]</sup> described the synthesis of a side-chain functionalized polystyrene, where in this case the hydrogen bond moiety (D-A-D motive) is not self-complementary. Addition of suitable A-D-A units resulted in reversible side chain modification, called "plug and play" polymers.<sup>[11]</sup>

The authors described the complexation with small organic guest molecules. A similar approach – here based on metal complexes – was presented by Frechet *et al.*:<sup>[12]</sup> in this case a copolymer consisting of a coumarin-2 chromophore and a 2,2'-bipyridine ligand was used in order to graft a ruthenium-bipyridine complex onto the polymer chain. Complementary also a copolymerization of the already preformed ruthenium *tris*-bipyridine complex with the coumarin monomer was described. Comparing both routes, the authors reported a grafting efficiency of the small *bis*-bipyridine ruthenium complex of around 30%.<sup>[12]</sup> A similar experiment utilizing terpyridine ruthenium complexes was described recently by Schubert and Heller.<sup>[13]</sup>

In this chapter, the synthesis of a terpyridine side-chain functionalized poly(methyl methacrylate) is reported (Figure 4.1). Utilization of the ruthenium(III)/ruthenium(II) chemistry<sup>[14]</sup> allowed to engineer a new class of graft copolymers via metal-to-ligand self-organization processes.

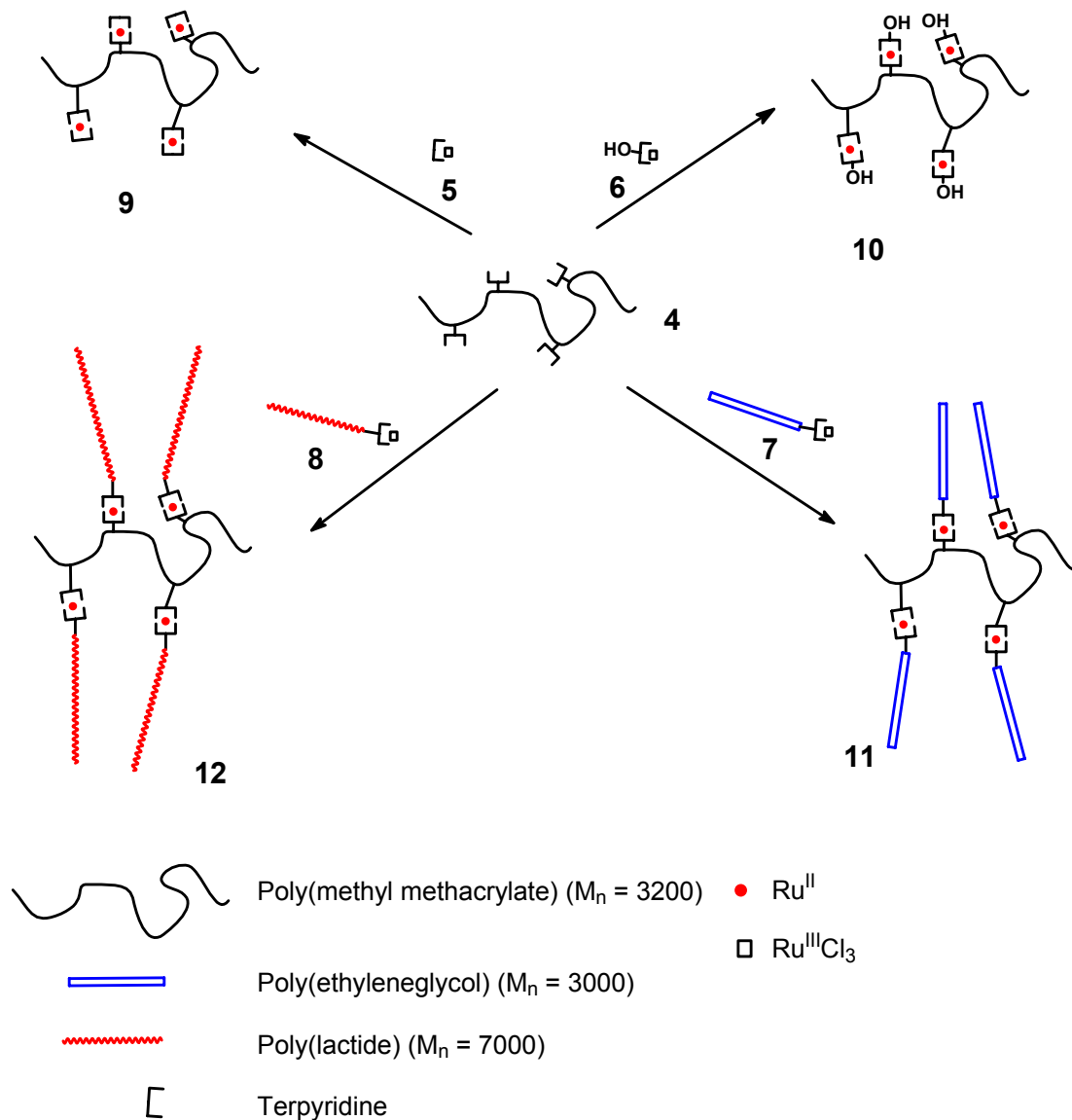


Figure 4.1. Schematic overview of the described graft copolymers 9 - 12.

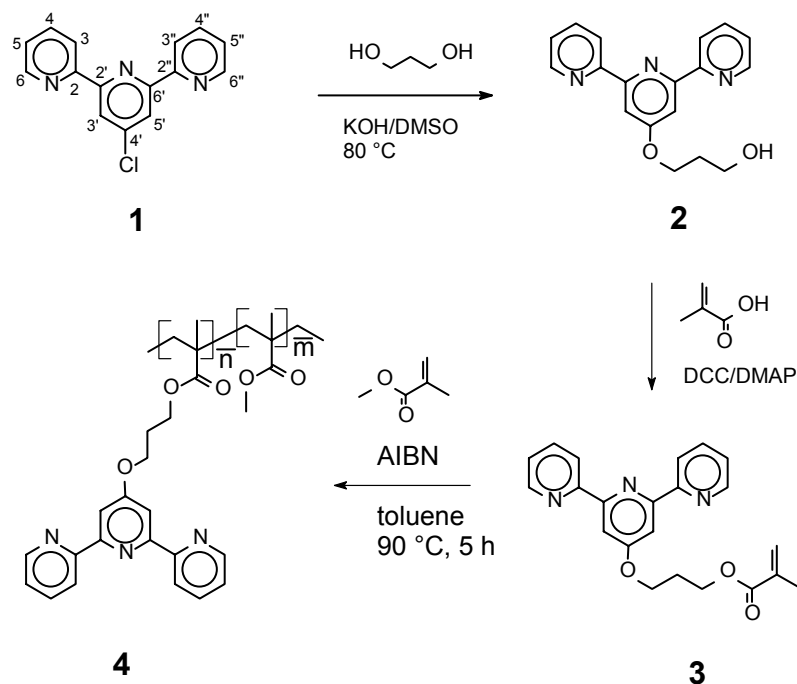
## 4.2 Supramolecular grafting: a novel approach for polymeranalogous reactions

### 4.2.1 Preparation of the graft copolymers

In this section a combination of the previously developed ruthenium chemistry for the formation of defined block copolymers and block copolymer micelles<sup>[15]</sup> (see also ref.<sup>[7a,16]</sup>) with a copolymer/grafting approach is described.

For this purpose a copolymer based on poly(methyl methacrylate) with a methacrylate-modified terpyridine moiety as functional unit, see also ref.<sup>[17]</sup>, was designed. Utilizing the

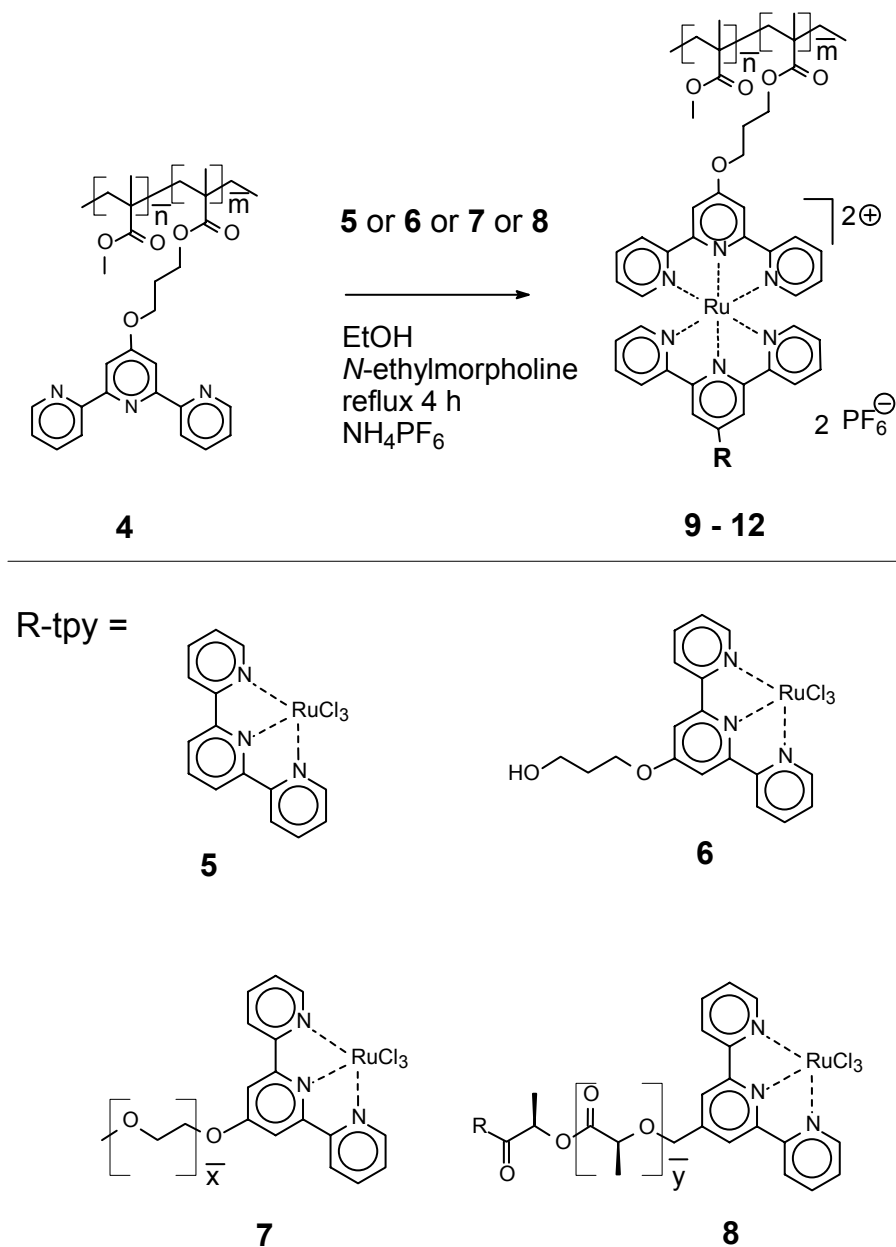
ruthenium(III)/(II) chemistry, different small organic as well as polymer blocks were grafted onto that PMMA backbone. The terpyridine-modified methacrylate **3** was synthesized in a two-step reaction starting from 4'-chloro-terpyridine **1**<sup>[34]</sup> (Scheme 4.1).



*Scheme 4.1. Synthesis of the terpyridine containing poly(methyl methacrylate) **4** (34:2, based on the  $\text{CHCl}_3$  GPC results).*

The hydroxy intermediate **2** could be obtained in high yields by the reaction of **1** with an excess of 1,3-propanediol. In the second step an ester coupling was performed with methacrylic acid to yield the terpyridine-functionalized methacrylate **3** in 66%. Free radical polymerization with AIBN as initiator was then utilized for the copolymerization of **3** with methyl methacrylate (Scheme 4.1, see also ref.<sup>[18]</sup>). The resulting copolymer **4** was characterized by NMR, GPC and UV-vis revealing an  $M_n$  of 1920 (THF GPC) or 3680 ( $\text{CHCl}_3$  GPC), a polydispersity of 1.46 or 1.61 and a terpyridine content of 6% (NMR). Therefore an average number of 2 units per polymer chain is calculated.

In order to construct a class of graft copolymers based on **4** a series of terpyridine modified compounds and oligomers were used, such as unsubstituted terpyridine, the hydroxy modified terpyridine **2**, a poly(ethylene glycol) modified terpyridine<sup>[37]</sup> as well as a poly(lactide) modified terpyridine (Scheme 4.2).<sup>[19]</sup>



Scheme 4.2. Synthesis of the supramolecular graft copolymers **9 – 12** ( $\bar{m} = 2$ ;  $\bar{n} = 34$ ;  $\bar{x} = 68$ ;  $\bar{y} = 87$ ).

Figure 4.1 shows a schematic overview over the graft copolymers. These four compounds were reacted with ruthenium(III)trichloride in a 1:1 ratio in order to synthesize the corresponding terpyridine-ruthenium(III) *mono*-complexes **5-8**, simply isolated via a precipitation procedure. The successful preparation could be easily checked by UV-vis spectroscopy. In all cases the characteristic metal-to-ligand-charge-transfer (MLCT) band for the *mono*-terpyridine ruthenium(III) complex at 390 nm could be detected. Compounds **5-8** were then utilized in a supramolecular grafting process (Scheme 4.2). For this purpose, ethanol was utilized as reducing agent and *N*-ethylmorpholine as catalyst to reduce the ruthenium(III) to ruthenium(II) ions. Only after that reduction a complex between the terpyridine-ruthenium-*mono*-complex and the uncomplexed terpyridine will be formed. The

supramolecular graft copolymers could be isolated after exchange of the counter-ions ( $\text{Cl}^-$ ) by addition of an excess of  $\text{NH}_4\text{PF}_6$  in 57 to 81% yield after an additional purification by size exclusion chromatography (BioBeads SX-1 in  $\text{CH}_2\text{Cl}_2$ ).

#### 4.2.2 Characterization

Investigation using UV-vis spectroscopy revealed the characteristic metal-to-ligand-charge-transfer (MLCT) band of the *bis*-terpyridine ruthenium(II) complex at 490 nm (Figure 4.2).

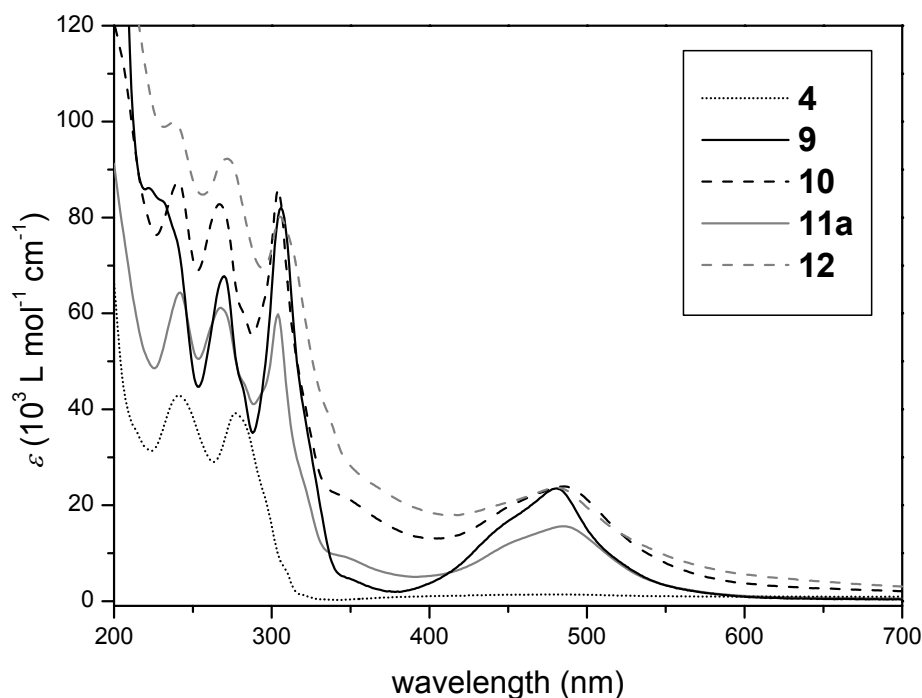


Figure 4.2. UV-vis spectra of the supramolecular graft copolymers **9** - **12** and the uncomplexed copolymer **4** (in acetonitrile).

In addition, the  $^1\text{H-NMR}$  spectra showed the characteristic shifts of all aromatic protons (Figure 4.3). In particular the upfield shift of the 6,6''-protons due to their different chemical neighborhood is typical for this kind of complexes. All signals could be assigned by a comparison with corresponding low-molar mass model complexes. In addition, the signals of all polymeric species were observed with integral ratios corresponding to the composition mentioned earlier. The graft copolymers were also analyzed by gel permeation chromatography (GPC). An increase in molar mass could be observed in all four cases (Table 4.1, see Figure 4.4 for an example). In addition, only a single peak could be detected.

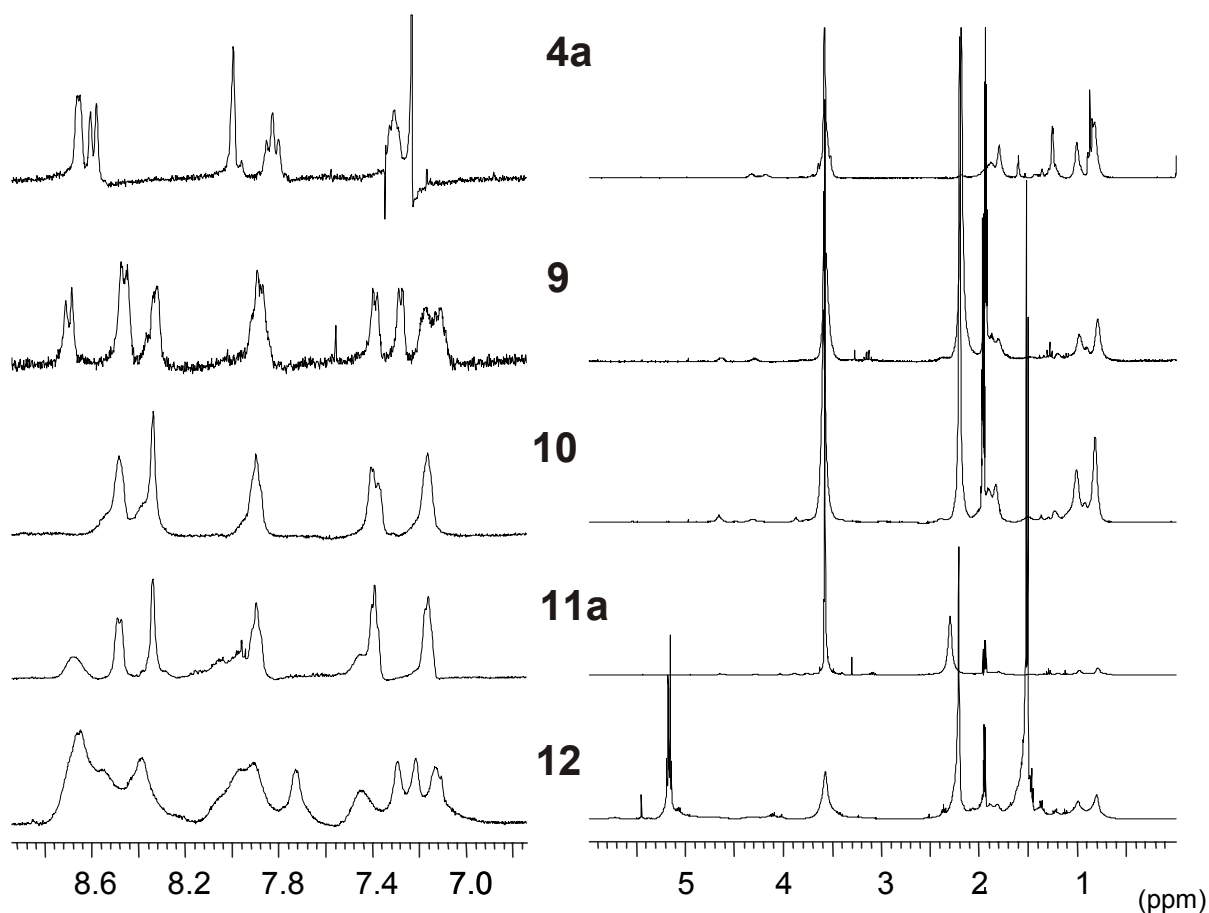


Figure 4.3.  $^1\text{H-NMR}$  spectra of **4** and **9** to **12** (in acetonitrile).

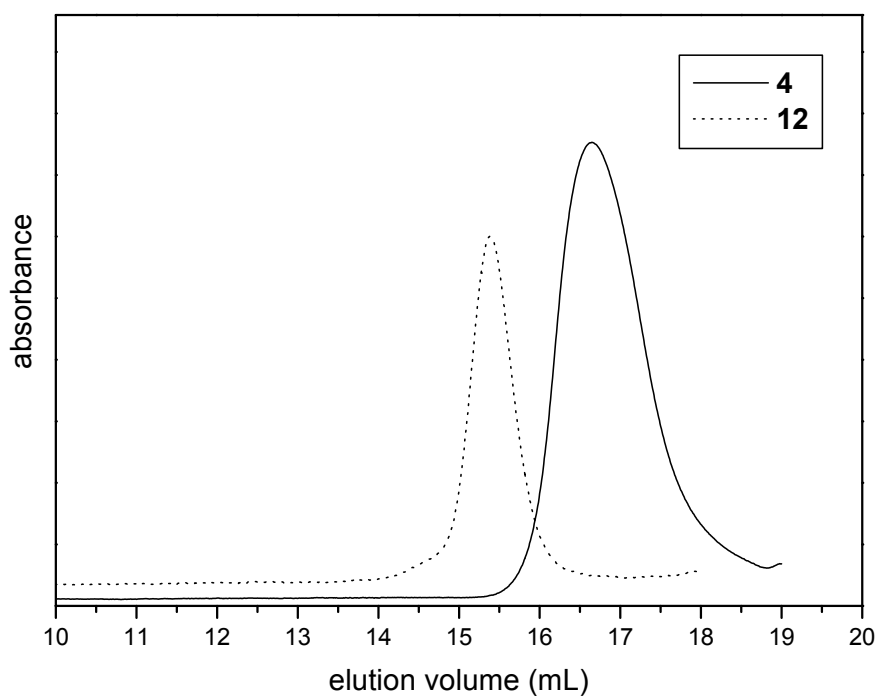


Figure 4.4. GPC-traces of the compounds **4** (---) and **12** (...), eluent THF.



Table 4.1. GPC results (THF).

Polymer	$\bar{M}_n$	PDI
<b>4</b>	1920	1.46
<b>4*</b>	3680*	1.61*
<b>9</b>	2100	1.21
<b>10</b>	3210	1.18
<b>PEG-tpy</b>	2750	1.39
<b>11a</b>	4820	1.05
<b>Poly(lactide)-tpy</b>	8170	1.17
<b>12</b>	9670	1.16

\* CHCl<sub>3</sub> as eluent

Thermal analysis using differential scanning calorimetry (DSC) was performed on the graft copolymer as well as the starting materials. In the case of PEG, also a blend of the starting polymers was investigated. While the copolymer **4** revealed a  $T_g$  of 93 °C, the graft copolymers with small terpyridines moieties (**9**, **10**) show no  $T_g$ . The poly(ethylenoxide)-terpyridine (PEG-tpy,  $T_m = 55$  °C) and its Ru<sup>III</sup> complex ( $T_m = 57$  °C) **7** revealed similar thermal behavior, whereas the graft copolymer **11a** showed a  $T_g$  of -11 °C. A polymer blend of **4** and PEG-tpy was prepared for comparison, revealing a melting peak at 55 °C and a  $T_g$  transition at -17 °C (Figure 4.5 and Table 4.2). This clearly demonstrated the influence of the grafting process on the thermal properties of the utilized polymers. At present it is unclear whether a superstructure is introduced by the terpyridine metal complexes (see, e.g., ref.<sup>[20]</sup>).

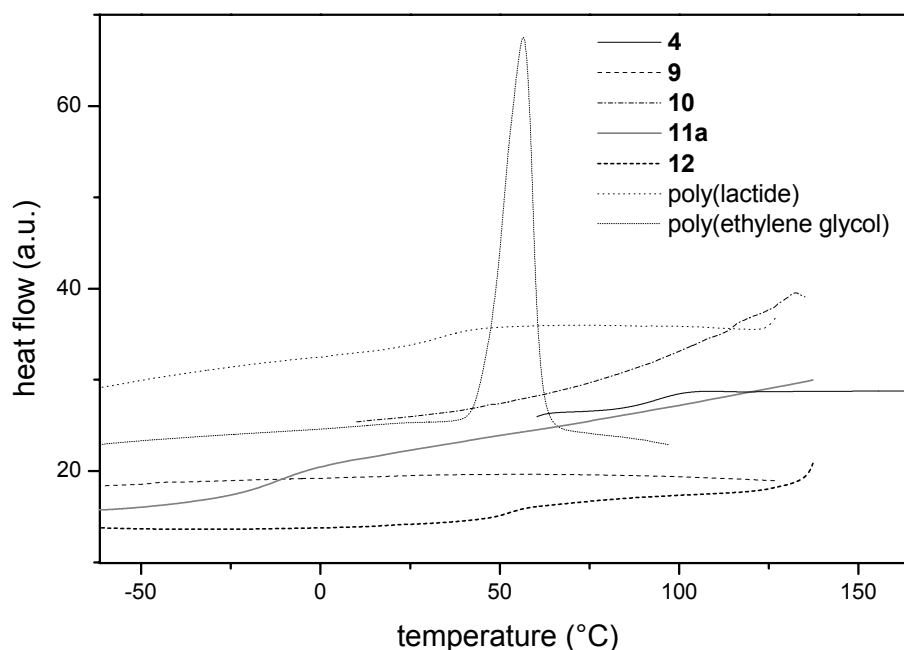


Figure 4.5. DSC traces of the graft copolymers (second heating run, 40 °C/min).

Table 4.2. Selected thermal properties (DSC measurements).

Compound	2 <sup>nd</sup> heating run	
	T <sub>g</sub> [°C]	T <sub>m</sub> [°C]
<b>4a</b>	93	---
<b>9</b>	---	---
<b>10</b>	---	---
<b>PEG-tpy</b>	---	55
<b>Blend of 4 + PEG-tpy</b>	-17	55
<b>7</b>	---	57
<b>11a</b>	-11	---
<b>Poly(lactide)-tpy</b>	---	11
<b>8</b>	35	---
<b>12</b>	51	---

### 4.3 Aqueous micelles from amphiphilic supramolecular graft copolymers

Nowadays, nanostructured materials have become a major field of research, in particular systems that are obtained by self-assembly processes. Prominent examples for such nanoobjects are micellar systems, which can be formed e.g. from amphiphilic block copolymers. In a protic solvent an aggregation of the hydrophobic blocks takes place to form the micelle core, surrounded by a corona of the hydrophilic part that provides colloidal stability.<sup>[21]</sup> Micelles can be used in applications such as drug-delivery systems<sup>[22]</sup> or as templates for the synthesis of inorganic nanoparticles.<sup>[23]</sup> The block copolymer approach has recently been expanded from covalent to supramolecular block copolymers.<sup>[6]</sup> A variety of different blocks has been combined utilizing the formation of heteroleptic *bis*-terpyridine ruthenium(II) complexes. Amphiphilic block copolymers based on PEG hydrophilic blocks and various hydrophobic blocks have been prepared utilizing the ruthenium(III)/(II)-chemistry which allows the directed synthesis of AB-block copolymers. Subsequently, aqueous metallo-supramolecular micelles have been prepared and characterized.<sup>[15]</sup> In contrast to covalent copolymer micelles, the supramolecular micelles can be reversibly modified. An example is the removal of the corona through decomplexation with hydroxyethyl ethylenediaminetriacetic acid (HEEDTA) to obtain only the spherical core.<sup>[24]</sup>

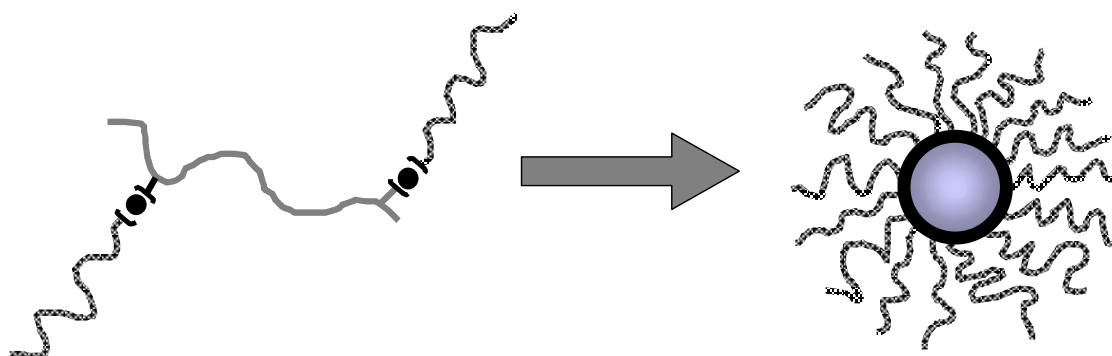
A different architectural approach for amphiphilic materials is resembled by graft copolymers. So far, these materials have been synthesized by conventional covalent chemistry. As an example, two methods have been applied to yield PMMA-*g*-PEG graft copolymers. The most popular reaction is a transesterification of a poly(methyl-*co*-isoheptyl methacrylate) with a potassium alkoxide of a PEG.<sup>[25]</sup> 10-15 grafts per 100 monomer units were obtained. Another approach to these materials is the copolymerization of MMA with a macromonomer consisting of a PEG bearing a methacrylate at one chain end.<sup>[26]</sup> In this specific case, micelles have not been reported so far. However, other graft copolymers of different chemical

composition have already been successfully used to prepare micelles.<sup>[27-13]</sup> Among the numerous examples previously reported are for example micelles obtained from graft copolymers containing inorganic (polyphosphazene<sup>[29]</sup>, siloxane<sup>[30]</sup>) or natural (chitin<sup>[31]</sup>) blocks. The dependence of the micellar size to the degree of grafting has been investigated in some of these previous contributions. Indeed, the aggregation number has been observed to decrease with higher grafting degree.<sup>[8]</sup> In sharp contrast, a weak dependence of the micelle size on grafting density has been noted by other authors.<sup>[12]</sup>

In the following sections of the present chapter, the synthesis and investigation of metallo-supramolecular aqueous micelles are reported, based on the foregoing described metallo-supramolecular PMMA-g-PEG graft copolymers.<sup>[32]</sup>

#### 4.3.1 Preparation of the micelles

One example of the previously described graft-copolymers **11a** contains water-soluble poly(ethylene glycol) side chains and is therefore amphiphilic. The material is therefore expected to form micelles in water (Scheme 4.3).



Scheme 4.3. Schematic representation of the micelle formation.

In order to explore this possibility, three graft copolymers with different degree of grafting (amount of side chains) have been synthesized according to the previously described procedure (ref.<sup>[32]</sup>) and investigated regarding their micellization behavior. In these three samples, the length of the PEG side chains was kept constant while the length of the PMMA backbone was varied (Table 4.3).

Table 4.3. Molecular characteristic features of the copolymers **4a-c**.

Copolymer	GPC data		Average degree of polymerization	Average number of terpyridine groups per chain <sup>1</sup>
	M <sub>n</sub> (g/mol)	PDI		
<b>4a</b>	3700	1.61	36	2
<b>4b</b>	5020	2.18	39	4
<b>4c</b>	6800	1.89	56	5

<sup>1</sup>Calculated from <sup>1</sup>H NMR data

The PEG chains were synthesized by living anionic polymerization and have a narrow polydispersity index while the PMMA backbones were prepared by free radical polymerization and are therefore characterized by a rather broad polydispersity index (Table 4.3). Since the graft copolymers were not readily soluble in water, pure water was added dropwise to a solution of the graft copolymers in DMF and the obtained solution was dialyzed against water, leading to frozen micelles. Details about this method can be found elsewhere.<sup>[18]</sup> Briefly, the graft copolymer chains are completely solvated in the initial DMF solution. As the added water content increases, the solvent quality for the PMMA backbone decreases progressively. At a critical water content, aggregation takes place. However, the structure of the accordingly formed aggregates is still labile. At higher added water content, the solubility and chain mobility of the PMMA chains is decreased and the kinetic process of polymer self-assembly and structural rearrangement of the aggregates can be very slow. After dialysis and elimination of DMF, the system is completely frozen. These systems are generally considered to be out of equilibrium since the kinetic process of aggregate rearrangement in the DMF/water mixture is difficult to control. The UV-spectra of the samples in DMF and in water revealed no significant changes in the shape and intensity of the absorption bands (Figure 4.6), suggesting that the integrity of the graft copolymers is kept during micelle preparation.

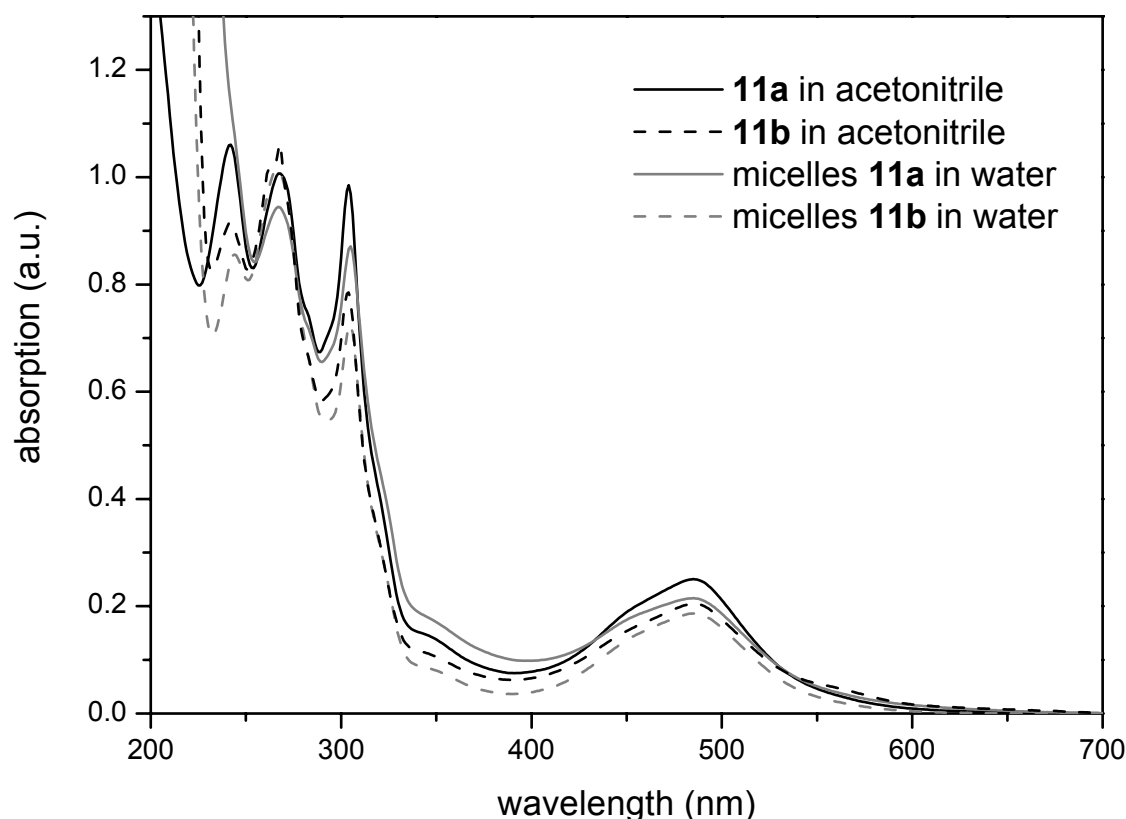


Figure 4.6. UV-Vis spectrum of samples **11a** and **11b** dissolved as unimers in acetonitrile and aggregated into micelles in water.

### 4.3.2 Dynamic light scattering

Light scattering (LS) was used as a tool to characterize the aqueous micelles formed by the three investigated graft copolymers. In a first experiment, the scattered intensity ( $I$ ) was recorded as a function of added water amount in order to determine the critical water concentration (cwc, see experimental part). Due to the preparation method used, it is meaningless to define a critical micelle concentration (cmc). It is however possible to extract information from the cwc. Because the cwc is strongly sensitive to the initial concentration of the copolymer in DMF,<sup>[17]</sup> the three investigated copolymers were dissolved at the same concentration in DMF, in order to make a comparison possible. The three curves shown in Figure 4.7 have a sigmoidal shape. At low added water content,  $I$  is low because the graft copolymer chains exist as unimers. Then, an increase in  $I$  is observed due to the formation of aggregates, as proven by the observation of a correlation function. Finally,  $I$  reaches a plateau value, as an indication that the aggregates are already frozen at these water contents and do not further modify their structure. The cwc has been found to be in the same range for the three investigated graft copolymers (400-600  $\mu\text{L}$ ). It should, however, be noted that the cwc was lowest for the **11a** sample, in agreement with a lower wt% of hydrophilic PEO blocks in this graft copolymer.

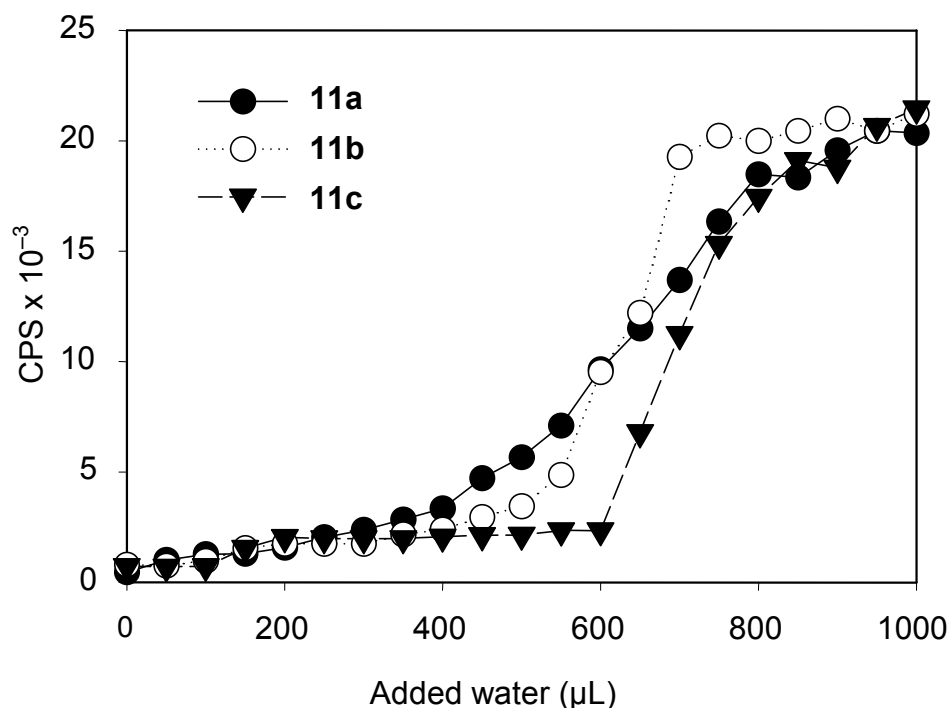


Figure 4.7. Scattered light intensity ( $I$ , counts per second CPS) as a function of the added water amount for the graft copolymers **11a-c** initially dissolved in DMF at a concentration of 1 g/L.

Dynamic light scattering (DLS) was then used in order to determine the characteristic size of the accordingly formed micellar objects. The DLS results were analyzed by several methods: the first cumulant of a cumulant expansion led to the mean hydrodynamic diameter ( $D_h$ ) and

the CONTIN routine allowed the distribution of hydrodynamic diameters to be calculated. The mean  $D_h$  calculated directly from the experimental correlation function is too large to fit to classical block copolymer micelles. Utilizing an analysis of the experimental correlation function by the CONTIN routine systematically showed two populations for the **11a** and **11b** samples, while only a single broad population was observed for **11c** (Figure 4.8).

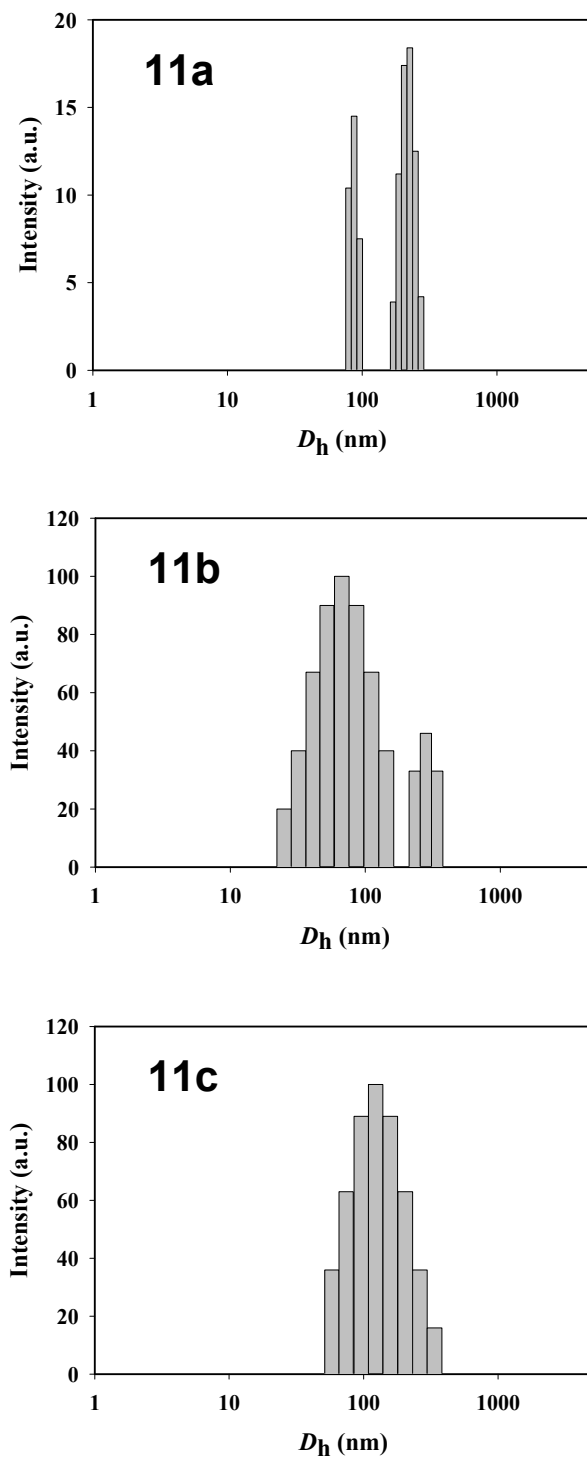


Figure 4.8. CONTIN size distribution histogram measured on aqueous micelles from **11a-c**.

The reproducibility of these results was checked, in order to eliminate any calculation artefact due to the CONTIN routine. Moreover, dilution of the sample did not modify the

characteristic sizes as measured by DLS, in agreement with the formation of frozen micelles. In analogy with previously reported results on micelles formed by metallo-supramolecular linear block copolymers,<sup>[15,24,33]</sup> the two populations were attributed to micelles (and small aggregates of micelles) and large aggregates of micelles (but this could also be caused by the utilized preparation method). However, in contrast to the results obtained from the linear supramolecular block copolymers, the polydispersity associated to each type of species was very large in the present case. Filtration of the samples (syringe filters with a porosity of 450 nm) resulted in a shift of the large aggregates population to smaller sizes, suggesting that the shearing effect induced by the filtration procedure disrupted partly the large aggregates.

The polydispersity found in the DLS results could originate from two factors: (i) the polydispersity of the primary micelles is broad resulting in broad aggregates (ii) the polydispersity of the primary micelles is narrow but a continuum of aggregates is formed. DLS is not the appropriate tool in order to gain deeper information on the system. For that purpose, transmission electron microscopy (TEM) and atomic force microscopy (AFM) have been utilized for a more detailed investigation of the morphology.

### 4.3.3 *Transmission electron microscopy*

TEM was first carried out directly on micelles dried on a formvar-coated copper grid. The results are shown in Figure 4.9 for samples **11a** and **11b**. Although no contrasting agent had been used, spherical micelles are seen in these pictures. The micelles appear as white spheres surrounded by a dark ring. The dark ring could be tentatively attributed to the presence of strongly electron adsorbing ruthenium ions found in the metallo-supramolecular complexes. The micelles are polydisperse in size but have all a spherical shape. The dark rings are not clear-cut, suggesting that the interface between the PMMA core and the PEG corona of the micelles is not sharp. The average size of these micelles lies in the 15-20 nm range and no clear difference can be seen between the micelles formed by sample **11a** and **11b**, due to the large size polydispersity. In the case of **11c**, the TEM results did not allow an identification of the structural features. The dark rings were very diffuse (data not shown because too blurry) and the mean size of the objects seemed to be larger than for samples **11a** and **11b**. In order to obtain more information, micelles from sample **11c** were negatively stained with phosphotungstic acid (Figure 4.10). This staining procedure leads to a dark ground onto which the micelles are observed as white spots. The TEM picture of Figure 4.10 clearly shows that very polydisperse spherical micelles with an average size of approx. 25-40 nm are formed in the case of sample **11c**.

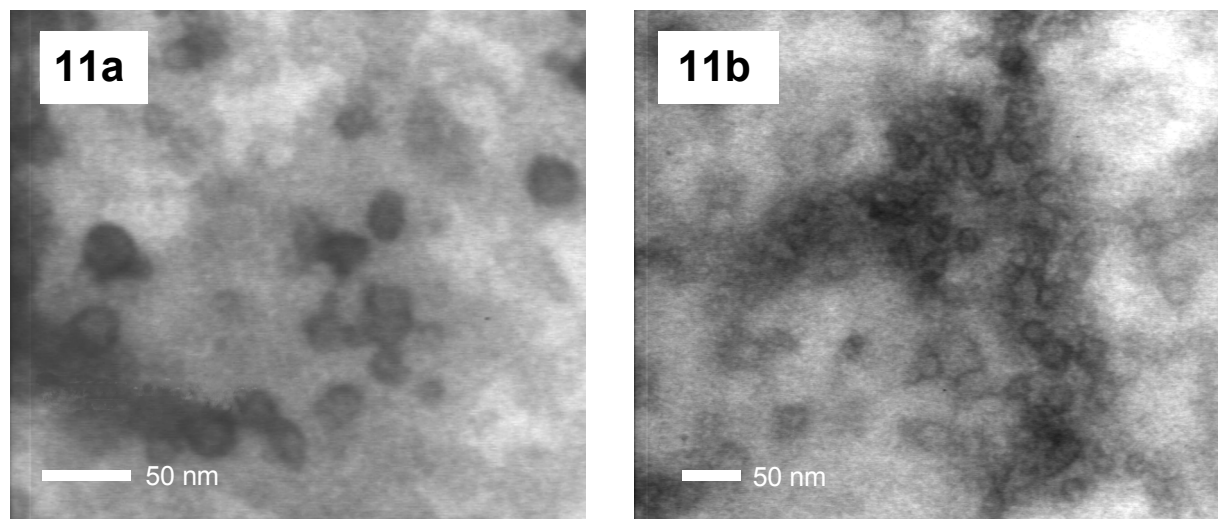


Figure 4.9. TEM images of micelles from **11a** and **11b** observed without contrasting.

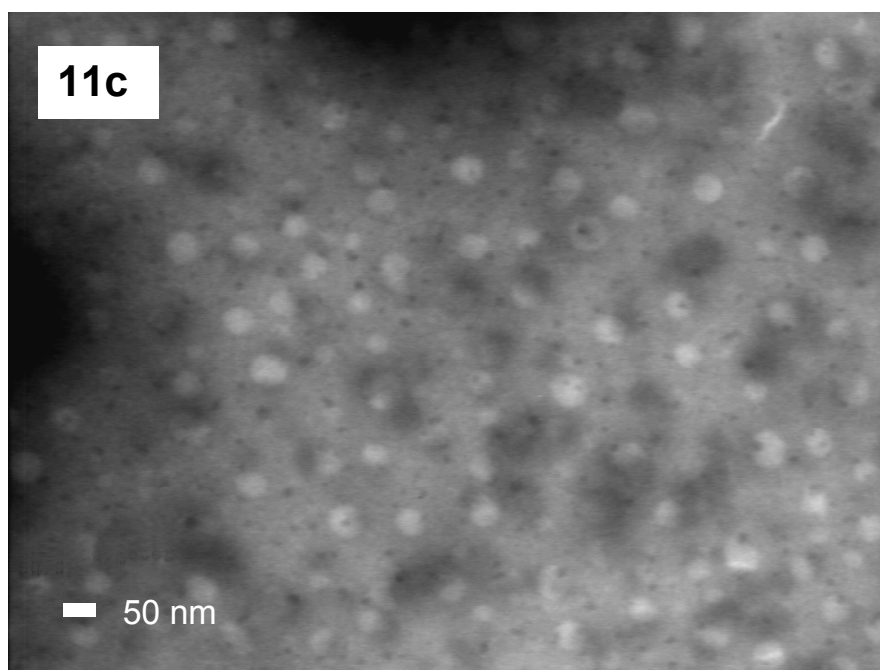


Figure 4.10. TEM image of micelles from **11c** (negative contrasting with  $H_3PO_4 \cdot 12WO_3$ ).

#### 4.3.4 Atomic force microscopy

Subsequently, AFM investigations were performed to confirm the TEM results. First, AFM measurements were performed on micelles spin-casted on a mica plate and therefore observed in the dried state. This is illustrated in Figure 4.11 for the sample **11a**. Polydisperse spherical micelles were observed on the substrate. Considering the tip-convolution effect, the lateral size is in agreement with the TEM pictures. The height of these micelles was around 5 nm. This small size can be explained by the collapse of coronal PEG chains on the PMMA core during the drying process. In this respect, the height of the micelles should be close to the diameter of the PMMA core of the micelles. Since drying can deeply affect the micellar



morphology, micelles from sample **11a-c** were also directly imaged under water by AFM. The results are shown in Figure 4.12, in which the inserts are high magnification pictures.

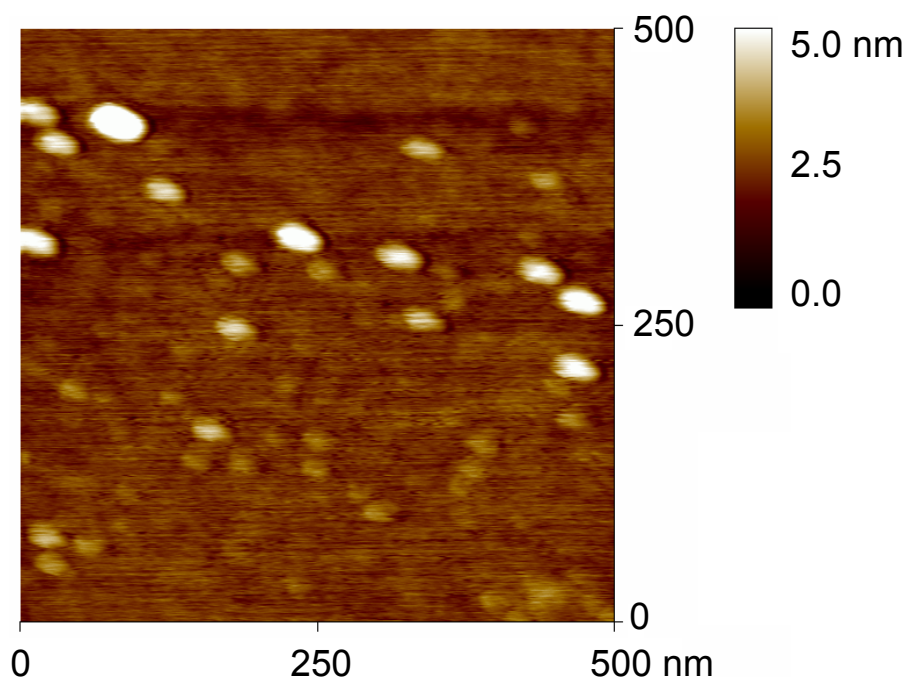


Figure 4.11. AFM image (height) of dried micelles from **11a**, spin-coated on a silicon wafer.

A dense layer of micelles on the surface was observed in each case. This could explain the significant decrease of the tip-convolution effects. The micelles are spherical and a broad polydispersity is again observed. The lateral sizes are in agreement with the previous TEM and AFM observations.

The height contrast revealed characteristic sizes in the 5 nm range, which is in agreement with the size of the PMMA core. This suggests that the AFM tip can more or less penetrate into the hydrated PEG corona and hits the PMMA core. The characteristic dimensions measured by TEM and AFM for the three investigated samples are summarized in Table 4.4.

Table 4.4. Characteristic dimensions (nm) of aqueous micelles formed by compounds **2a-c**, as determined by AFM in water, TEM and DLS ( $D_{xy}$ : lateral dimension of the micelles as measured by AFM or by TEM;  $D_z$ : height of the micelles as measured by AFM;  $D_h(\text{CONTIN})$  is the mean size of the small size population).

Sample	PEG wt%	AFM: $D_{xy}$	AFM: $D_z$	DLS: $D_h(\text{CONTIN})$	DLS: $D_h$ (mean)	TEM: $D_{xy}$
2a	62	~15	~5-7	79	165	~15-20
2b	71	~15	~5-7	67	110	~15-20
2c	69	~25	~6-8	123	188	~25-40

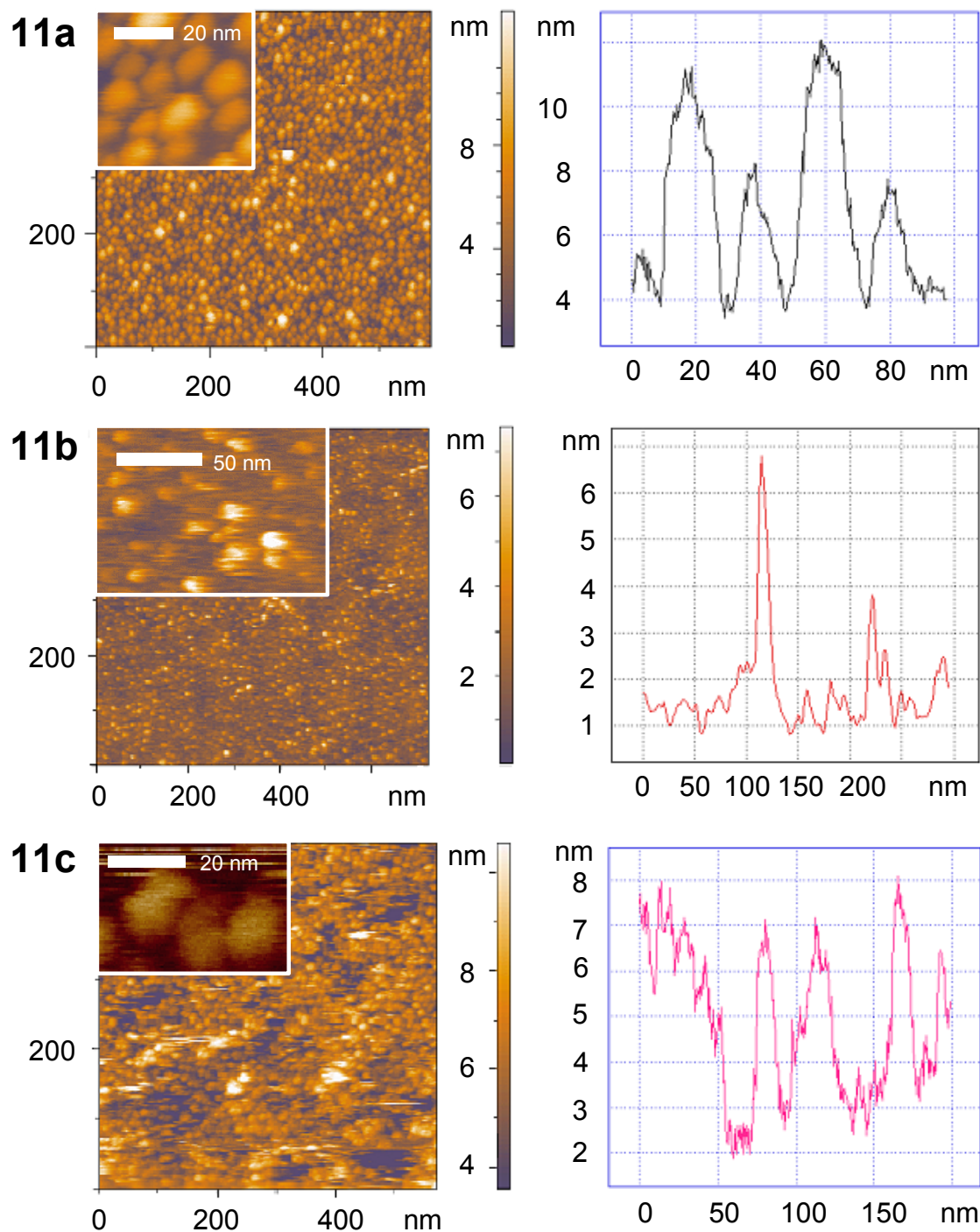


Figure 4.12. AFM images (height) and cross section of micelles from **11a-c** measured in aqueous solution.

Although the studied samples were characterized by different molecular parameters, their self-association is leading to rather similar types of micelles. The similarity of the results is obvious for samples **11a** and **11b**, while sample **11c** is different from the two others. However, because of the large polydispersity of the micelles, it is impossible to draw a clear trend.

## 4.4 Conclusions

In summary, we have synthesized poly(methyl methacrylate) based copolymers with terpyridine units in the side chain utilizing a free radical polymerization process. Using the ruthenium(III)/(II) chemistry known from supramolecular science, different organic and polymeric moieties were grafted onto that copolymer yielding a new class of compounds. The materials were characterized by NMR, UV-vis and GPC and revealed distinct changes in their thermal properties as compared to the starting materials. This route opens a new entry to graft copolymers using self-organization processes. Combinations of polymers that are not or not easily accessible with traditional methods could be prepared in future. Among the graft copolymer, which was investigated in more detail, is an amphiphilic system, containing PEG side chains. For this combination, graft copolymers that differ from the average number of grafted PEG blocks and the length of the PMMA backbone were investigated regarding micellation. Aqueous micelles have been prepared and analyzed by DLS, TEM and AFM. Polydisperse spherical micelles that are clustering into larger structures were observed. A good correlation was found between TEM and AFM measurements. These results are in agreement with previous investigations on aqueous micelles formed by linear metallo-supramolecular block copolymers. However, the polydispersity of the primary micelles is much larger than for these previously investigated samples. This is thought to result from the polydispersity of the samples both in the PMMA chain length and in the distribution of the grafted PEG along the PMMA backbone. Although they have different compositions, no clear difference was observed between the micelles formed by the three investigated samples.

## 4.5 Experimental part

### Materials and characterization

Basic chemicals were obtained from Sigma-Aldrich. For compound **1** see ref.<sup>[34]</sup> and for **2** see ref.<sup>[35]</sup>. The synthesis of **5** is described in ref.<sup>[14,36]</sup>, and for **7** see ref.<sup>[37]</sup>. Preparative size exclusion chromatography was carried out on BioBeads SX1 columns (CH<sub>2</sub>Cl<sub>2</sub>). NMR spectra were measured on a Bruker Mercury 400 and a Varian Gemini 300 NMR spectrometer. The chemical shifts were calibrated to the residual solvent peaks or TMS. UV-vis spectra were recorded on a Perkin Elmer Lambda-45 (1 cm cuvettes, CH<sub>3</sub>CN). DSC investigations were performed on a Perkin Elmer Pyris-1 DSC system with a heating rate of 40 K/min (T<sub>g</sub>) and 20 K/min (T<sub>m</sub>), respectively. GPC measurements were performed on a WATERS GPC equipped with a WATERS Model 510 pump, a Model 410 refractive index detector and a Model 486 UV detector (THF, flow rate of 1.0 mL/min, 2 mixed-C columns, Polymer Laboratories, polystyrene calibration) and in parts on a Shimadzu GPC-apparatus using a 5 μm PL-gel-mixed-D column (crosslinked polystyrene) with chloroform as eluent and an UV detector. Dynamic light scattering (DLS) measurements were performed on a Malvern 4700C apparatus equipped with a Malvern 7032 digital correlator and an Ion Laser Technology argon laser with a wavelength of 488 nm. A scattering angle of 90° was used for the measurements. The experimental correlation function was measured and analyzed with the CONTIN routine, which gives access to the distribution of hydrodynamic diameter ( $D_h$ ). The measurements were repeated and analyzed at least ten times, in order to verify the reproducibility of the CONTIN analysis. The mean  $D_h$  was also calculated from the first cumulant of a cumulant expansion of the correlation function, using the Stokes-Einstein approximation, as described elsewhere.<sup>[38]</sup> Transmission electron microscopy (TEM) observations have been carried out using a JEOL 2000 FX microscope operating at a voltage of 200 kV. Samples were prepared by drop-casting the aqueous micellar solution onto Formvar-coated copper TEM grid and directly observed without any further contrasting (sample **2a-b**), or contrasted with phosphotungstic acid (sample **2c**).

Atomic force microscopy (AFM) images were obtained either on a NT-MDT Smena-B or a Digital Instruments Nanoscope IIIa Multimode AFM-apparatus. Micelles were deposited on a mica plate by drop-casting on the plate and measured with the Multimode operated in air utilizing the Tapping Mode. Furthermore, direct imaging in aqueous solution was performed on a NT-MDT Smena-B, equipped with a solution-imaging head (DI Nanoprobe silicon nitride tip). The sample was deposited on a mica substrate and measured directly after the setup of the device (approx. 5 min).

### 2-Methyl-acrylic acid 3-(2,2':6',2''-terpyridin-4'-yloxy)-propyl ester **3**

To a solution of **2** (2.50 g, 8.13 mmol) in 50 mL CH<sub>2</sub>Cl<sub>2</sub> was added 1.86 g (9.01 mmol) dicyclohexylcarbodiimide and 64 mg (0.57 mmol) dimethylaminopyridine. After addition of 1.10 g (5.38 mmol) methacrylic acid, the solution was stirred overnight and a precipitate of dicyclohexyl-urea was formed. After filtration, the solution was passed through a short silica column to remove the remaining urea. Then the solvent was removed *in vacuo* and the product was recrystallized three times from hot methanol (10 mL) to yield 2.02 g (66%) of **3** as white needles; m.p. 90 °C.

UV-vis (CH<sub>3</sub>CN):  $\lambda_{max}$  ( $\epsilon$ ) = 276.6 (25890), 240.4 (28260) nm (L mol<sup>-1</sup> cm<sup>-1</sup>).

<sup>1</sup>H-NMR (CH<sub>3</sub>CN):  $\delta$  (ppm) = 1.91 (s, CH<sub>3</sub>), 2.19 (tt, 2 H,  $J$  = 6.59 Hz, CH<sub>2</sub>), 4.33 (2t, 4 H,  $J$  = 6.59 Hz, OCH<sub>2</sub>), 5.60 (t, 1 H,  $J$  = 1.47 Hz, H(olefinic)), 6.09 (s, 1 H, H(olefinic)), 7.40 (m, 2 H, H<sub>5,5''</sub>), 7.91 (dd, 2 H,  $J$  = 8.06, 2.20 Hz, H<sub>4,4''</sub>), 7.98 (s, 2 H, H<sub>3,5'</sub>), 8.61 (d, 2 H,  $J$  = 8.06 Hz, H<sub>3,3''</sub>), 8.67 (d, 2 H,  $J$  = 5.86 Hz, H<sub>6,6''</sub>).

Anal. Calcd. For C<sub>22</sub>H<sub>21</sub>N<sub>3</sub>O<sub>3</sub> (375.4): C, 70.38; H, 5.64; N, 11.19. Found: C, 70.18; H, 5.75; N, 11.23.

### Poly(methyl methacrylate)-*co*-(2-methyl-acrylic acid 3-(2,2':6',2''-terpyridin-4'-yloxy)-propyl ester)

#### 4a

400 mg (4 mmol) of methyl methacrylate and 68 mg (0.18 mmol) of **3** were dissolved in 5 mL toluene and heated to 80 °C. Then 20 mg (0.12 mmol) of azo-*bis*(isobutyronitrile) (AIBN) in toluene were added and heating was continued for 5 hours. After analyzing the crude polymer utilizing GPC, the mixture was poured into 10 mL hexane yielding 352 mg (0.10 mmol, 88%) of **4** as a white solid.

UV-vis (CH<sub>3</sub>CN):  $\lambda_{max}$  ( $\epsilon$ ) = 277 (39200), 241 (42900) nm (L mol<sup>-1</sup> cm<sup>-1</sup>).

<sup>1</sup>H-NMR (CHCl<sub>3</sub>):  $\delta$  (ppm) = 0.83 (br, 30 H, CH<sub>3</sub>), 1.01 (br, 16 H, CH<sub>3</sub>), 1.80 and 1.89 (br, 30 H, CH<sub>2</sub>), 2.19 (m (br), 2 H, CH<sub>2</sub>), 3.61 (s, 56 H, OCH<sub>3</sub>), 4.19 (m (br), 2 H, OCH<sub>2</sub>), 4.33 (m (br), 2 H, OCH<sub>2</sub>), 7.40 (m, 2 H, H<sub>5,5''</sub>), 7.91 (dd, 2 H,  $J$  = 8.06, 2.20 Hz, H<sub>4,4''</sub>), 7.98 (s, 2 H, H<sub>3,5'</sub>), 8.61 (d, 2 H,  $J$  = 8.06 Hz, H<sub>3,3''</sub>), 8.67 (d, 2 H,  $J$  = 5.86 Hz, H<sub>6,6''</sub>).

GPC (THF):  $\bar{M}_n$  = 1920 gmol<sup>-1</sup>, PDI = 1.46 ( $\bar{M}_n$  = 3680, PDI = 1.61 in CHCl<sub>3</sub> by GPC).

#### 4b

Methyl methacrylate (426 mg, 4.26 mmol) and 2-methyl-acrylic acid 3-(2,2':6',2''-terpyridin-4'-yloxy)-propyl ester **1** (80 mg, 0.21 mmol) were dissolved in 5 mL *p*-xylene and heated to 70 °C. Then azo-*bis*(isobutyronitrile) (AIBN, 9.2 mg, 0.056 mmol) was added and heating was continued for 6 hours. The polymer was precipitated in 20 mL pentane yielding 346 mg (68%) of **4b** as a white solid.

UV-vis (CH<sub>3</sub>CN):  $\lambda_{max}$  ( $\epsilon$ ) = 278 (93600), 249 (87100) nm (L mol<sup>-1</sup> cm<sup>-1</sup>).

<sup>1</sup>H-NMR (400 MHz; CDCl<sub>3</sub>):  $\delta$  (ppm) = 0.83 (br, 30 H, CH<sub>3</sub>), 1.01 (br, 19 H, CH<sub>3</sub>), 1.80 and 1.89 (br, 32 H, CH<sub>2</sub>), 2.19 (m (br), 2 H, CH<sub>2</sub>), 3.61 (s, 29 H, OCH<sub>3</sub>), 4.19 (m (br), 2 H, OCH<sub>2</sub>), 4.33 (m (br), 2 H, OCH<sub>2</sub>), 7.40 (m, 2 H, H<sub>5,5''</sub>), 7.91 (ddd, 2 H,  $J$  = 8.06, 8.06, 2.20 Hz, H<sub>4,4''</sub>), 7.98 (s, 2 H, H<sub>3,5'</sub>), 8.61 (d, 2 H,  $J$  = 8.06 Hz, H<sub>3,3''</sub>), 8.67 (d, 2 H,  $J$  = 5.86 Hz, H<sub>6,6''</sub>). <sup>13</sup>C-NMR (100.6 MHz; CDCl<sub>3</sub>):  $\delta$  (ppm) = 16.53 (CH<sub>3</sub>), 18.76 (CH<sub>3</sub>), 34.16 (C(PMMA)), 44.58 (CH<sub>2</sub>(PMMA)), 44.90 (CH<sub>2</sub>), 51.82 (OCH<sub>3</sub>), 54.43 (CH<sub>2</sub>), 64.47 (CH<sub>2</sub>), 107.31 (H<sub>3,5'</sub>), 121.35 (H<sub>5,5''</sub>), 123.89 (H<sub>3,3''</sub>), 136.83 (H<sub>4,4''</sub>), 149.05 (H<sub>6,6''</sub>), 156.03 (H<sub>2,2''</sub>), 157.19 (H<sub>2,6''</sub>), 169.30 (H<sub>4'</sub>), 176.94 (COO), 177.80 (COO).

GPC:  $\bar{M}_n$  = 5020 gmol<sup>-1</sup>, PDI = 2.18.

**4c**: See synthesis of **4b**. 400 mg (4 mmol) methyl methacrylate, 68 mg (0.18 mmol) of **1**, 20 mg (0.12 mmol) of azo-*bis*(isobutyronitrile) (AIBN). Yield 352 mg (88%) of **2b**.

<sup>1</sup>H-NMR (400 MHz; CDCl<sub>3</sub>):  $\delta$  (ppm) = 0.83 (br, 30 H, CH<sub>3</sub>), 1.01 (br, 20 H, CH<sub>3</sub>), 1.80 and 1.89 (br, 32 H, CH<sub>2</sub>), 2.19 (m (br), 2 H, CH<sub>2</sub>), 3.61 (s, 48 H, OCH<sub>3</sub>), 4.19 (m (br), 2 H, OCH<sub>2</sub>), 4.33 (m (br), 2 H, OCH<sub>2</sub>), 7.40 (m, 2 H, H<sub>5,5''</sub>), 7.91 (ddd, 2 H,  $J$  = 8.06, 8.06, 2.20 Hz, H<sub>4,4''</sub>), 7.98 (s, 2 H, H<sub>3,5'</sub>), 8.61 (d, 2 H,  $J$  = 8.06 Hz, H<sub>3,3''</sub>), 8.67 (d, 2 H,  $J$  = 5.86 Hz, H<sub>6,6''</sub>).

UV-vis (CH<sub>3</sub>CN):  $\lambda_{max}$  ( $\epsilon$ ) = 278 (46800), 249 (43600) nm (L mol<sup>-1</sup> cm<sup>-1</sup>).

GPC:  $\bar{M}_n$  = 6800 gmol<sup>-1</sup>, PDI = 1.89.

### Preparation of the ruthenium(III)-*mono*-complexes **5 - 8**

The terpyridine containing compounds were diluted in 15 mL ethanol and an excess of ruthenium(III)trichloride in 10 mL ethanol was added. The mixtures were heated to 50 °C for about 2 h. The resulting brown precipitate was collected using a glass filter and washed three times with water, ethanol and diethyl ether (10 mL), respectively. In the case of the terpyridine containing polymers, a mixture of ethanol/THF (1:1, 20 mL) was used for the reaction.

**5:** Yield: 149 mg (78%). UV-vis (DMSO):  $\lambda_{max}(\epsilon) = 311.1$  (21500), 408.1 (6880) nm ( $L \text{ mol}^{-1} \text{ cm}^{-1}$ ).

**6:** Yield: 364 mg (81%). UV-vis (DMSO):  $\lambda_{max}(\epsilon) = 402.2$  (6320) nm ( $L \text{ mol}^{-1} \text{ cm}^{-1}$ ).

**7:** Yield: 1.05 g (99%). UV-vis ( $\text{H}_2\text{O}$ ):  $\lambda_{max}(\epsilon) = 272$  (71700), 375 (11600) nm ( $L \text{ mol}^{-1} \text{ cm}^{-1}$ ).

**8:** Yield: 51 mg (99%). UV-vis ( $\text{CH}_3\text{CN}$ )  $\lambda_{max}(\epsilon) = 277$  (23650), 314 (19160), 323 (19540), 401 (6400), 466 (3460) nm ( $L \text{ mol}^{-1} \text{ cm}^{-1}$ ).

#### General Procedure of the synthesis of the graft copolymers 9 - 12

Copolymer **4** and the ruthenium(III) complexes **5 - 8** (twofold excess) were mixed in 50 mL of a 1:1 mixture of ethanol/THF. Three drops of *N*-ethylmorpholine were added and the mixture was heated to reflux for 5 h (**5**, **6** and **8**), respectively 25 h in the case of **7**. After evaporation of half of the solvent, an excess of ammoniumhexafluorophosphate (500 mg, 3.45 mmol) was added and the mixture cooled to 4 °C. The precipitate was filtered off and washed with a 60:40 mixture of ethanol/water ( $3 \times 10$  mL). Then the precipitate was redissolved in 1.5 mL of dichloromethane and purified by size exclusion chromatography (Bio-beads SX1,  $\text{CH}_2\text{Cl}_2$ ).

**9:** 22 mg ( $5.98 \times 10^{-3}$  mmol) **4**; 4 mg (0.010 mmol) **5**. Yield: 23 mg (81%).

UV-vis ( $\text{CH}_3\text{CN}$ ):  $\lambda_{max}(\epsilon) = 270$  (67800), 306 (82000), 481 (23500) nm ( $L \text{ mol}^{-1} \text{ cm}^{-1}$ ).

$^1\text{H-NMR}$  ( $\text{CD}_3\text{CN}$ ):  $\delta$  (ppm) = 0.79 (br, 22 H, alkyl, PMMA), 0.98 (br, 20 H, alkyl, PMMA), 1.81 (br, 16 H, alkyl, PMMA), 2.41 (tt, 2 H,  $J = 5.86, 5.86$  Hz,  $\text{CH}_2$ ), 3.56, 3.59 (2 s, br, 58 H,  $\text{OCH}_3$ , PMMA), 4.47 (t, 2 H,  $J = 5.86$  Hz,  $\text{OCH}_2$ ), 4.64 (t, 2 H,  $J = 5.86$  Hz,  $\text{OCH}_2$ ), 7.15 (m, 4 H,  $\text{H}_{5,5'}$ ), 7.29 (d, 2 H,  $J = 4.39$  Hz,  $\text{H}_{6,6'}$ ), 7.41 (d, 2 H,  $J = 4.39$  Hz,  $\text{H}_{6,6'}$ ), 7.90 (m, 4 H,  $\text{H}_{4,4'}$ ), 8.31 (s, 2 H,  $\text{H}_{3,5}$ ), 8.36 (dd, 1 H,  $J = 8.06, 8.06$  Hz,  $\text{H}_4$ ), 8.46 (d, 4 H,  $J = 8.06$  Hz,  $\text{H}_{3,3'}$ ), 8.72 (d, 2 H,  $J = 8.39$  Hz,  $\text{H}_{3,5}$ ).

GPC (THF):  $\overline{M}_n = 2100$   $\text{g mol}^{-1}$ , PDI = 1.21.

**10:** 38 mg (0.010 mmol) **4**; 9 mg (0.02 mmol) **6**. Yield: 40 mg (79%).

UV-vis ( $\text{CH}_3\text{CN}$ ):  $\lambda_{max}(\epsilon) = 485$  (23900), 304 (86000), 267 (82800), 241 (87600) nm ( $L \text{ mol}^{-1} \text{ cm}^{-1}$ ).

$^1\text{H-NMR}$  ( $\text{CD}_3\text{CN}$ ):  $\delta$  (ppm) = 0.79 (b, 22 H, alkyl, PMMA), 0.98 (br, 20 H, alkyl, PMMA), 1.81 (br, 22 H, alkyl, PMMA), 2.99 (t, 1 H, OH), 3.61 (s, 52 H,  $\text{OCH}_3$ ), 3.88 (t, 2 H,  $\text{CH}_2$ ), 4.32 (br, 2 H,  $\text{CH}_2$ ), 4.66 (m, 4 H,  $\text{CH}_2$ ), 7.19 (m, 4 H,  $\text{H}_{5,5'}$ ), 7.43 (m, 4 H,  $\text{H}_{6,6'}$ ), 7.93 (m, 4 H,  $\text{H}_{4,4'}$ ), 8.37 (s, 4 H,  $\text{H}_{3,5}$ ), 8.52 (m, 4 H,  $\text{H}_{3,3'}$ ).

GPC (THF):  $\overline{M}_n = 3210$   $\text{g mol}^{-1}$ , PDI = 1.18.

**11a:** 50 mg (0.014 mmol) **4a**; 80 mg (0.024 mmol) **7**. Yield: 71 mg (57%).

UV-vis ( $\text{CH}_3\text{CN}$ )  $\lambda_{max}(\epsilon) = 242$  (64400), 268 (61100), 304 (59800), 485 (15600) nm ( $L \text{ mol}^{-1} \text{ cm}^{-1}$ ).

$^1\text{H-NMR}$  ( $\text{CD}_3\text{CN}$ ):  $\delta$  (ppm) = 0.81 (br, 24 H, alkyl, PMMA), 1.00 (br, 20 H, alkyl, PMMA), 1.82, 1.90 (br, 26 H,  $\text{CH}_2$ , PMMA), 3.33 (s, 3 H,  $\text{OCH}_3$ , PEG), 3.52 (m,  $\text{CH}_3\text{OCH}_2\text{CH}_2$ , PEG), 3.61 (s, 340 H,  $\text{OCH}_3$ , PMMA,  $\text{CH}_2$ , PEG), 3.79 (m, 4 H,  $\text{CH}_2$ , PEG), 3.91 (m, H,  $\text{CH}_2$ , PEG), 4.67 (m, 4 H,  $\text{OCH}_2$ ,  $\text{C}_3$ -alkylspacer), 7.18 (m, 4 H,  $\text{H}_{5,5'}$ ), 7.41 (m, 4 H,  $\text{H}_{6,6'}$ ), 7.92 (m, 4 H,  $\text{H}_{4,4'}$ ), 8.37 (s, 4 H,  $\text{H}_{3,5}$ ), 8.50 (m, 4 H,  $\text{H}_{3,3'}$ ).

GPC (THF):  $\overline{M}_n = 4820$   $\text{g mol}^{-1}$ , PDI = 1.06.

**11b:** 7.5 mg (0.002 mmol) **4b**; 20 mg (0.01 mmol) **7**. Yield: 17.5 mg (64%).

UV-vis ( $\text{CH}_3\text{CN}$ )  $\lambda_{max}(\epsilon) = 242$  (64500), 268 (61100), 304 (59700), 485 (15600) nm ( $L \text{ mol}^{-1} \text{ cm}^{-1}$ ).

$^1\text{H-NMR}$  ( $\text{CD}_3\text{CN}$ ):  $\delta$  (ppm) = 0.80 (br, 16 H, alkyl, PMMA), 0.98 (br, 12 H, alkyl, PMMA), 1.81, 1.88 (br, 10 H,  $\text{CH}_2$ , PMMA), 3.27 (s, 3 H,  $\text{OCH}_3$ , PEG), 3.52 (m,  $\text{CH}_3\text{OCH}_2\text{CH}_2$ , PEG), 3.61 (s, 282 H,  $\text{OCH}_3$ , PMMA,  $\text{CH}_2$ , PEG), 3.79 (m, 4 H,  $\text{CH}_2$ , PEG), 3.91 (m, H,  $\text{CH}_2$ , PEG), 4.67 (m, 4 H,  $\text{OCH}_2$ ,  $\text{C}_3$ -alkylspacer), 7.18 (m, 4 H,  $\text{H}_{5,5'}$ ), 7.41 (m, 4 H,  $\text{H}_{6,6'}$ ), 7.92 (m, 4 H,  $\text{H}_{4,4'}$ ), 8.37 (s, 4 H,  $\text{H}_{3,5}$ ), 8.50 (m, 4 H,  $\text{H}_{3,3'}$ ).

**11c:** 20 mg (0.006 mmol) **4c**; 64 mg (0.019 mmol) **7**. Yield: 49.6 mg (62%).

UV-vis ( $\text{CH}_3\text{CN}$ )  $\lambda_{max}(\epsilon) = 242$  (64400), 268 (61200), 304 (59300), 485 (15700) nm ( $L \text{ mol}^{-1} \text{ cm}^{-1}$ ).

$^1\text{H-NMR}$  (400 MHz,  $\text{CD}_3\text{CN}$ ):  $\delta$  (ppm) = 0.80 and 0.98 (b, 29 H, alkyl, PMMA), 1.81 and 1.88 (b, 10 H,  $\text{CH}_2$ , PMMA), 3.27 (s, 3 H,  $\text{OCH}_3$ , PEG), 3.52 (m,  $\text{CH}_3\text{OCH}_2\text{CH}_2$ , PEG), 3.61 (s, 282 H,  $\text{OCH}_3$ , PMMA,  $\text{CH}_2$ , PEG), 3.79 (m, 2 H,  $\text{CH}_2$ , PEG), 3.91 (m, 2 H,  $\text{CH}_2$ , PEG), 4.67 (m, 4 H,  $\text{OCH}_2$ ,  $\text{C}_3$ -alkylspacer), 7.18 (m, 4 H,  $\text{H}_{5,5'}$ ), 7.41 (m, 4 H,  $\text{H}_{6,6'}$ ), 7.92 (m, 4 H,  $\text{H}_{4,4'}$ ), 8.37 (s, 4 H,  $\text{H}_{3,5}$ ), 8.50 (m, 4 H,  $\text{H}_{3,3'}$ ).

**12:** 20 mg (0.005 mmol) **4**; 67 mg (0.009 mol) **8**. Yield: 139 mg (68%).

UV-vis ( $\text{CH}_3\text{CN}$ ):  $\lambda_{max}(\epsilon) = 480$  (35500), 305 (120300), 272 (138500), 238 (149900) nm ( $L \text{ mol}^{-1} \text{ cm}^{-1}$ ).

$^1\text{H-NMR}$  ( $\text{CD}_3\text{CN}$ ):  $\delta$  (ppm) = 0.79 (br, 38 H, PMMA), 0.99 (br, 30 H, PMMA), 1.51 (d, 260 H,  $J = 6.59$  Hz,  $\text{CH}_3$ , polylactide), 1.81 (br, 26 H, PMMA), 2.05 (s, 6 H, tpy- $\text{CH}_3$ ), 3.57 (s, 58 H,  $\text{OCH}_3$ , PMMA), 5.16 (q, 78 H,  $J = 6.59$  Hz, CH, polylactide), 7.14 (br, 2 H,  $\text{H}_{5,5'}$ ), 7.22 (br, 2 H,  $\text{H}_{3,3'}$ ), 7.30 (br, 2 H,  $\text{H}_{6,6'}$ ), 7.47 (br, 2 H,  $\text{H}_{6,6'}$ ), 7.74 (br, 2 H,  $\text{H}_{3,5}$ ), 7.99 (br, 4 H,  $\text{H}_{4,4'}$ ), 8.40 (br, 2 H,  $\text{H}_{3,3'}$ ), 8.68 (br, 2 H,  $\text{H}_{3,5}$ ).

GPC (THF):  $\overline{M}_n = 9670$   $\text{g mol}^{-1}$ , PDI = 1.16.

#### Preparation of the micelles

The metallo-supramolecular graft copolymers as obtained from the synthesis are poorly soluble in water. Therefore, each copolymer was dissolved in *N,N*-dimethylformamide (DMF) with a concentration of 1 g/L. Then water was stepwise added by increment of 50  $\mu\text{L}$  under vigorous stirring and the scattered intensity of the resulting solution was measured. At a critical concentration of added water, aggregation of the water-insoluble

PMMA block is observed that resulted in an important increase of scattered intensity. The so-called critical water concentration (cwc) was accordingly measured as defined by Eisenberg et al. in ref.<sup>[17]</sup>. Subsequently, the DMF/water solution was dialyzed several times against water (Spectra-Por dialysis bags, cut-off 6000-8000 daltons). The final concentration of the copolymer in pure water was set to 0.5 g/L.

## 4.6 References

- [1] [1a] J. Darnell, H. Lodish, B. Baltimore, *Molecular Cell Biology*, Scientific American Books, New York, **1990**; [1b] D. Philp, F. J. Stoddart, *Angew. Chem.* **1996**, *108*, 1242-1284; *Angew. Chem. Int. Ed.* **1996**, *35*, 1154-1196.
- [2] [2a] J.-M. Lehn, *Supramolecular Chemistry, Concepts and Perspectives*, VCH, Weinheim, **1995**; [2b] U. S. Schubert, in *Tailored Polymers & Applications* (Ed.: M. K. M. Y. Yagci, O. Nuyken, K. Ito, G. Wnek), VSP Publishers, Utrecht, **2000**, 63-85.
- [3] J.-M. Lehn, *Makromol. Chem., Macromol. Symp.* **1993**, *69*, 1-17.
- [4] U. S. Schubert, M. Heller, *Chem. Eur. J.* **2001**, *7*, 5252-5259.
- [5] L. Brunsveld, B. J. B. Folmer, E. W. Meijer, R. P. Sijbesma, *Chem. Rev.* **2001**, *101*, 4071-4097.
- [6] B. G. G. Lohmeijer, U. S. Schubert, *Angew. Chem.* **2002**, *114*, 3980-3984; *Angew. Chem. Int. Ed.* **2002**, *41*, 3825-3829.
- [7] [7a] S. Kelch, M. Rehahn, *Macromolecules* **1999**, *32*, 5818-5828; [7b] O. Hien, C. Eschbaumer, U. S. Schubert, *Macromol. Rapid Commun.* **2000**, *21*, 1156-1161.
- [8] [8a] R. J. Ceresa, *Block and Graft Copolymers*, Wiley, New York, **1976**; [8b] T. Corner, *Adv. Polym. Sci.* **1984**, *62*, 95-142.
- [9] L. R. Rieth, R. F. Eaton, G. W. Coates, *Angew. Chem.* **2001**, *113*, 2211-2214, *Angew. Chem. Int. Ed.* **2001**, *40*, 2153-2156.
- [10] R. Stadler, M. A. de Araujo, M. Kuhrau, J. Rösch, *Makromol. Chem.* **1989**, *190*, 1433-1443.
- [11] F. Ilhan, M. Gray, V. M. Rotello, *Macromolecules* **2001**, *34*, 2597-2601
- [12] X. Schultze, J. Serin, A. Adronov, J. M. J. Fréchet, *Chem. Commun.* **2001**, 1160-1161.
- [13] M. Heller, U. S. Schubert, *Macromol. Rapid Commun.* **2002**, *23*, 411-415.
- [14] [14a] B. P. Sullivan, J. M. Calvert, T. J. Meyer, *Inorg. Chem.* **1980**, *19*, 1404-1407; [14b] T. Togano, N. Nagao, M. Tsuchida, H. Kumakura, K. Hisamatsu, F. S. Howell, M. Mukaida, *Inorg. Chim. Acta* **1992**, *195*, 221-225.
- [15] J. F. Gohy, B. G. G. Lohmeijer, U. S. Schubert, *Macromolecules* **2002**, *35*, 4560-4563.
- [16] P. F. H. Schwab, M. D. Levin, J. Michl, *Chem. Rev.* **1999**, *99*, 1863-1933.
- [17] K. Hanabusa, K. Nakano, T. Koyana, H. Shirai, N. Hojo, A. Kurose, *Makromol. Chem.* **1990**, *191*, 391-396.
- [18] [18a] K. T. Potts, K. C. Usifer, *Macromolecules* **1988**, *21*, 1985-1991; [18b] K. T. Potts, K. C. Usifer, A. Guadalupe, H. D. Abruña, *J. Am. Chem. Soc.* **1987**, *109*, 3961-3967; [20c] K. Hanabusa, A. Nakamura, T. Koyama, H. Shirai, *Makromol. Chem.* **1992**, *193*, 1309-1319.
- [19] M. Heller, U. S. Schubert, *Macromol. Rapid Commun.* **2001**, *22*, 1358-1361.
- [20] [20a] C. D. Eisenbach, A. Gödel, M. Terskan-Reinold, U. S. Schubert, in *Polymeric Materials Encyclopedia, Vol. 10* (Ed.: J. C. Salamone), CRC Press, Boca Raton,

- 1996**, 8162; [20b] A. Goedel, U. S. Schubert, C. D. Eisenbach, *J. Microscopy* **1997**, 186, 67.
- [21] I. W. Hamley, *The Physics of Block Copolymers*; Oxford University Press: Oxford, **1998**.
- [22] M. Yokoyama, T. Okano, Y. Sakurai, H. Ekimoto, C. Shibasaki, K. Kataoka, *Cancer Res.* **1991**, 51, 3329-3336.
- [23] S. Förster, M. Antonietti, *Adv. Mater.* **1998**, 3, 195-217.
- [24] J.-F. Gohy, B. G. G. Lohmeijer, U. S. Schubert, *Macromol. Rapid Commun.* **2002**, 23, 555-560.
- [25] M. A. Twaik, M. Tahan, A. Zilka, *J. Polym. Sci. A* **1969**, 7, 2469-2480.
- [26] G. Bo, B. Wesslén, K. B. Wesslén, *J. Polym. Sci. A* **1992**, 30, 1799-1808.
- [27] I. Berlinova, A. Anzil, I. Panaiotov, *J. Macromol. Sci. A* **1992**, 29, 975-986.
- [28] Y. Ma, T. Cao, S. E. Webber, *Macromolecules* **1998**, 31, 1773-1778.
- [29] J. Y. Chang, P. J. Park, M. J. Han, *Macromolecules* **2000**, 33, 321-325.
- [30] Y. Lin, P. Alexandridis, *J. Phys. Chem. B* **2002**, 106, 10845-10853.
- [31] K. Aoi, A. Takasu, M. Okada, T. Imae, *Macromol. Chem. Phys.* **1999**, 200, 1112-1120.
- [32] U. S. Schubert, H. Hofmeier, *Macromol. Rapid Commun.* **2002**, 23, 561-566.
- [33] [33a] J.-F. Gohy, B. G. G. Lohmeijer, S. K. Varshney, U. S. Schubert, *Macromolecules* **2002**, 35, 7427-7435; [33b] J.-F. Gohy, B. G. G. Lohmeijer, S. K. Varshney, B. Décamps, E. Leroy, S. Boileau, U. S. Schubert, *Macromolecules* **2002**, 35, 9748-9755.
- [34] S. Schmatloch, A. A. Precup, U. S. Schubert, *Design. Monom. Polym.* **2002**, 5, 211-221.
- [35] U. Sampath, W. C. Putnam, T. A. Osiek S. Touami, J. Xie, D. Cohen, A. Cagnoloni, P. Droege, D. Klug, C. L. Barnes, A. Modak, J. K. Bashkin, S. S. Jurisson, *J. Chem. Soc., Dalton Trans.* **1999**, 2049-2058.
- [36] E. C. Constable, *J. Chem. Soc., Chem. Comm.* **1997**, 1073-1080.
- [37] [37a] U. S. Schubert, C. Eschbaumer, *Macromol. Symp.* **2001**, 163, 177; [37b] B. G. G. Lohmeijer, U. S. Schubert, *Pol. Mater.: Sci. & Eng.* **2001**, 85, 460-461.
- [38] [38a] P. Stepanek, in: "Dynamic Light Scattering", W. Brown, Ed., Oxford University Press, London **1972**; [38b] L. Zhang, H. Shen, A. Eisenberg, *Macromolecules* **1997**, 30, 1001-1011.

# 5

## Supramolecular cross-linking

**Abstract:** Cross-linking of polymers in a supramolecular fashion is a promising approach towards reversible glues or coatings. A series of poly(methyl methacrylate) copolymers with terpyridine units in the side chains was obtained by free radical polymerization. The free terpyridine units were complexed by iron(II) and zinc(II) ions and the complexation behavior was studied in detail utilizing UV-vis and viscosity titration experiments. Complexation of the polymer chains could be observed which resulted in the characteristic UV-vis absorption bands and an increase of the solution viscosity. At higher concentration, gel formation was observed. Addition of a strong competitive ligand (hydroxyethyl ethylenediaminetriacetic acid, HEEDTA) resulted in an efficient decomplexation. Continuing experiments included the supramolecular cross-linking in combination with covalent cross-linking. Terpolymers bearing terpyridine as well as oxetane respective epoxide units were synthesized and characterized using NMR, UV-vis and GPC. Subsequently, UV-vis experiments indicated clearly a non-covalent cross-linking of the terpyridine moieties by addition of iron(II) ions. Moreover, the ability of covalent cross-linking was studied by polymerizing the oxetane and epoxide rings utilizing Lewis acids. IR spectroscopy and DSC experiments clearly revealed the success of the combination of both steps when utilizing iron(II) ions and  $\text{AlCl}_3$ . Due to the fact that UV-curing did not show the expected success, acrylates as free-radical curable groups were introduced and investigated. Finally, thermal curing was studied in combination with non-covalent cross-linking. A terpolymer, bearing hydroxy groups and terpyridines, was mixed with a *bis*-isocyanate. The covalent cross-linking as well as the two-step curing could be performed successfully.

*Parts of this work have been published:*

H. Hofmeier, U. S. Schubert, *Macromol. Chem. Phys.* **2003**, *204*, 1391-1397; A. El-Ghayoury, H. Hofmeier, B. de Ruiter, U. S. Schubert, *Macromolecules* **2003**, *36*, 3955-3959; H. Hofmeier, A. El-Ghayoury, U. S. Schubert, *e-polymers* **2003**, no. 053, 1-15; H. Hofmeier, A. El-Ghayoury, U. S. Schubert, submitted.



## 5.1 Introduction

As already shown in the previous chapters, supramolecular polymers represent a highly interesting topic in today's polymer science. For this purpose, non-covalent interactions (see, e.g., ref.<sup>[1]</sup>) are combined with covalent chemistry in order to construct new polymeric systems.<sup>[2,3]</sup> Besides hydrogen bonding units,<sup>[4]</sup> mainly metal-ligand interactions have been utilized.<sup>[5]</sup> As a result, linear high molar mass polymers,<sup>[6-8]</sup> defined block copolymers,<sup>[9]</sup> star-like systems,<sup>[10]</sup> graft copolymers<sup>[11]</sup> and micelles<sup>[12]</sup> as well as networks<sup>[13]</sup> (Figure 5.1) were reported.

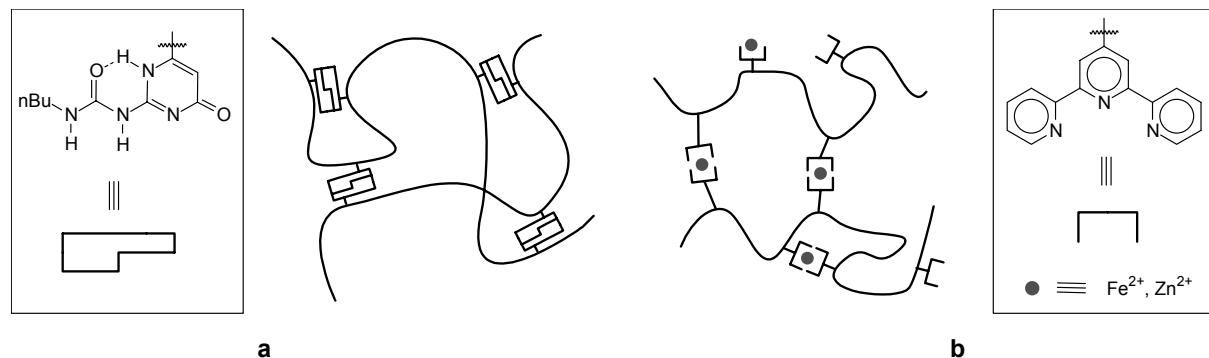


Figure 5.1. Schematic representation of supramolecular cross-linking through self-complementary hydrogen-bonding units (a) or terpyridine metal complexes (b).

In particular, the reversibility of the supramolecular interaction is of special interest due to potential applications such as smart materials, reversible glues or adhesives as well as switchable systems. The binding strength of the non-covalent bond is weaker than a covalent bond and can be reverted under much milder conditions. First examples of thermal and redox reversible hydrogels were already reported in the 1990s by Stadler<sup>[14]</sup> and Chujo.<sup>[15]</sup> Recently, the reversible opening of an iron(II) complex could be shown: the poly(lactide) complex could be opened at 160 °C and reassembled at lower temperatures.<sup>[16]</sup> This procedure could be repeated several times. Iron complexes could also be dis- and reassembled by applying an aqueous  $K_2CO_3$  solution.<sup>[17]</sup> Linear coordinative polymers of *bis*-phenanthrolines with copper(I) or silver(I) form dynamic (small) aggregates in coordinating solvents but stable macromolecules in non-coordinating solvents.<sup>[18]</sup>

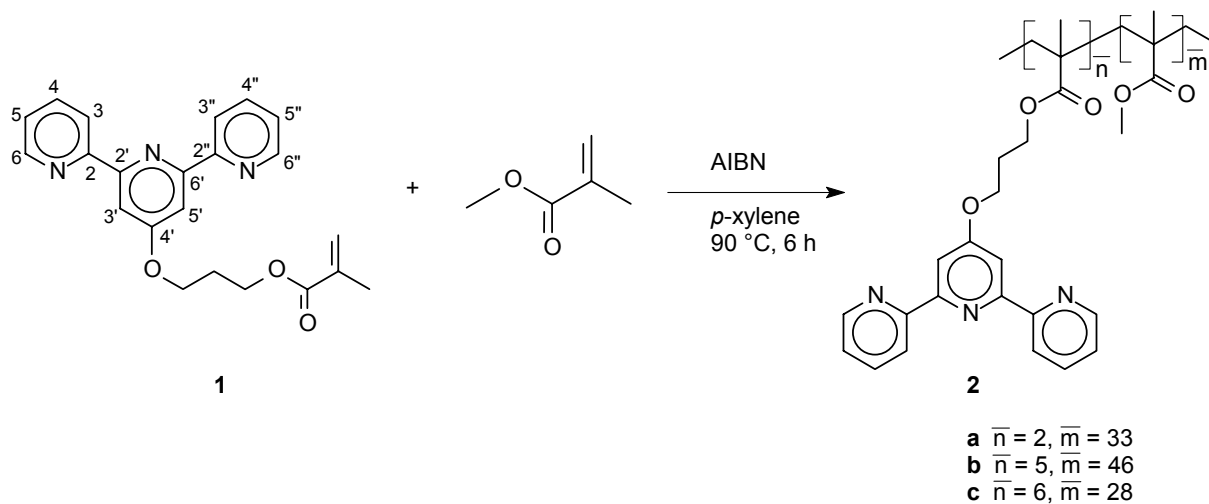
In this chapter, the complexation and decomplexation behavior of terpyridine-containing copolymers containing different ratios of terpyridine units in diluted as well as concentrated solutions will be in the focus. The copolymers were complexed with iron(II) as well as zinc(II) ions and the complexation behavior was studied in detail by means of UV-vis, IR and NMR spectroscopy. Viscosity measurements and gelation studies were performed to study the formation of branching and cross-linking at various concentrations. Moreover, the ability of complete decomplexation of the obtained materials via strong competitive ligands was investigated. Finally, the supramolecular cross-linking was combined with covalent cross-linking in order to design new "smart materials" that might eventually lead to potential applications in coatings technology.

## 5.2 Supramolecular branching and cross-linking of terpyridine-modified copolymers: complexation and decomplexation studies in diluted solution

A powerful building block for reversible supramolecular polymers is 2,2':6',2''-terpyridine,<sup>[19]</sup> as already described in the foregoing chapter. It has been shown in chapter 4 that it can be easily introduced into polymers by copolymerization of a common monomer together with a terpyridine-modified monomer. This has also been demonstrated by the group of Hanabusa,<sup>[20]</sup> who synthesized polystyrene as well as poly(methyl methacrylate)-based systems. Recently, Tew<sup>[21]</sup> and his co-workers also worked on the synthesis of terpyridine-modified poly(methyl methacrylates) and the complexation of the copolymers with copper ions. Another example based on polystyrene was reported recently by Heller and Schubert.<sup>[22]</sup> In the first part of this chapter, the focus will be on the synthesis and characterization of terpyridine-modified copolymers containing different ratios of terpyridine units and their complexation and decomplexation behavior in diluted solution.

### 5.2.1 Synthesis and characterization of the copolymers

Copolymers with supramolecular entities in the side chain have become of special interest during the last years concerning supramolecular polymer modification approaches. In this chapter, reversible supramolecular copolymers, which could find, e.g., future applications as smart materials, are described. For this purpose, 2,2':6',2''-terpyridine was utilized as supramolecular binding unit. This complexing moiety was introduced into the side chain of poly(methyl methacrylate) by free radical copolymerization of commercial methyl methacrylate and a terpyridine-functionalized methacrylate as comonomer (Scheme 5.1). In this manner, copolymers with different molar ratios of terpyridine units (**2a-c**) were obtained (see also refs.<sup>[20,21]</sup> for similar approaches). The comparison of NMR spectra of the comonomer **1** and the resulting copolymers **2a-c** indicate that the terpyridine was successfully incorporated into the copolymer (Figure 5.2).



Scheme 5.1. Copolymerization of **1** with MMA.

From the integral ratios, a terpyridine content of 5% can be calculated for **2a**, whereas polymers **2b** and **2c** showed terpyridine ratios of 10% and 19%, respectively. GPC analysis revealed an  $\overline{M}_n$  of 4 500 g/mol for **2a**, 6 600 g/mol for **2b** and 4 800 for **2c** (Figure 5.3).

PDI's between 1.6 and 2.0 were found for all three polymers (Table 5.1). Two terpyridine units per polymer chain can be calculated for **2a** from the NMR and GPC data. Five terpyridines per chain can be assumed for **2b** and six for **2c**. As a reference experiment for viscosity investigations, also a PMMA homopolymer was synthesized under the same conditions as the copolymer. A molecular weight of 5 200 g/mol and a PDI of 1.65 was obtained. The  $^1\text{H-NMR}$  spectrum is comparable to the PMMA part of the  $^1\text{H-NMR}$  spectrum of **2a** (Figure 5.2).

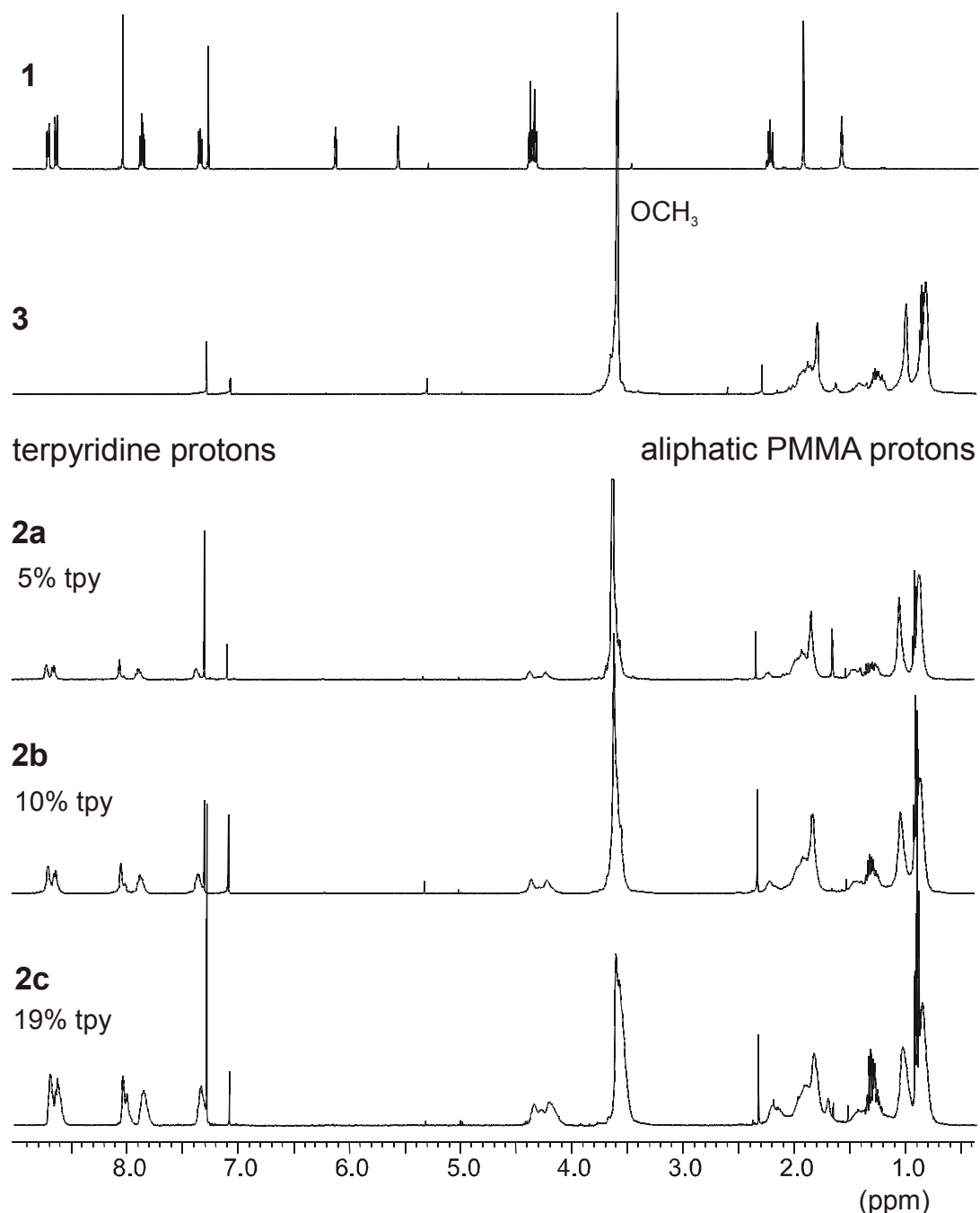


Figure 5.2.  $^1\text{H-NMR}$ -spectra of **1**, **2a-c** and **3** (in chloroform).

After the synthesis of terpyridine-modified PMMAs, the complexation behavior of the terpyridine side chains with transition metal ions was investigated. Previous experiments into this direction, performed by the groups of Hanabusa<sup>[20]</sup> and Tew,<sup>[21]</sup> revealed several open questions. Viscosity experiments by Hanabusa showed a decrease of viscosity by addition of metal ions. The examined polymers had one or two terpyridine moieties per chain, and low concentrations (1.8 mg/mL) were used for the measurements. In this case, the formation of intramolecular complexes or dimers can be assumed. The decrease of viscosity was explained by a shrinkage upon metal addition. Tew's results showed an increase of viscosity even after the 100% ratio of metal ions was reached. The relative viscosity rose to 1.5 at a 4-fold excess of copper nitrate with a polymer concentration of 4 mg/mL. A copolymer bearing an average of six terpyridine units per chain was utilized for the experiment. The observed result was attributed to kinetic effects of the complex formation.

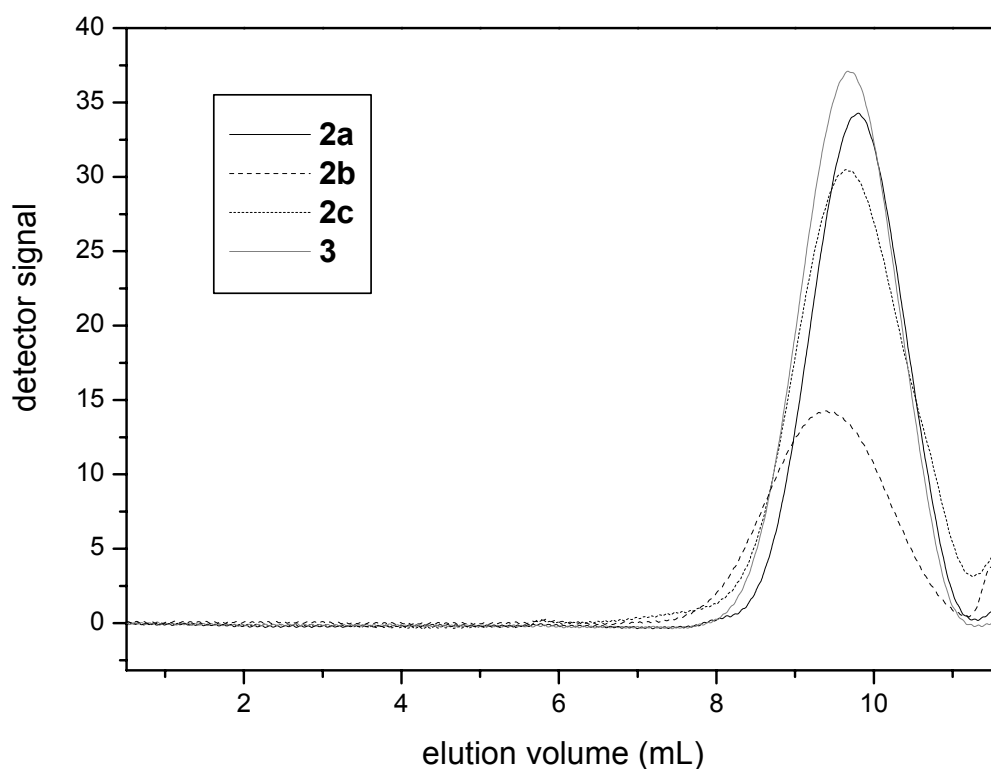


Figure 5.3. GPC curves of **2a-c** and **3** (in chloroform/triethylamine).

Table 5.1. GPC data of the copolymers **2a-c** and PMMA homopolymer **3**.

	$\bar{M}_n$ (RI)	PDI (RI)	Terpyridine content (%)	Average terpyridine per chain
<b>2a</b>	4 500	1.62	5	2
<b>2b</b>	6 600	2.06	10	5
<b>2c</b>	4 800	1.78	19	6
<b>3</b>	5 200	1.65	0	0

UV-vis spectroscopy was the first method used in order to study the complexation behavior of the copolymers. A UV-vis titration of **2b** was performed by means of stepwise addition of iron(II) ions and recording a spectrum after each step (Figure 5.4). The solution was stirred for half an hour after each addition to ensure a complete reaction. By observing the intensity of the metal to ligand charge transfer band (MLCT) at 558 nm, a titration curve was obtained. After a linear increase of the absorption with the concentration, the equivalence point was reached at a 1.02:1 ratio, indicating that the pendant terpyridine groups were complexed completely. No significant change of the absorption bands was observed through overtitration.

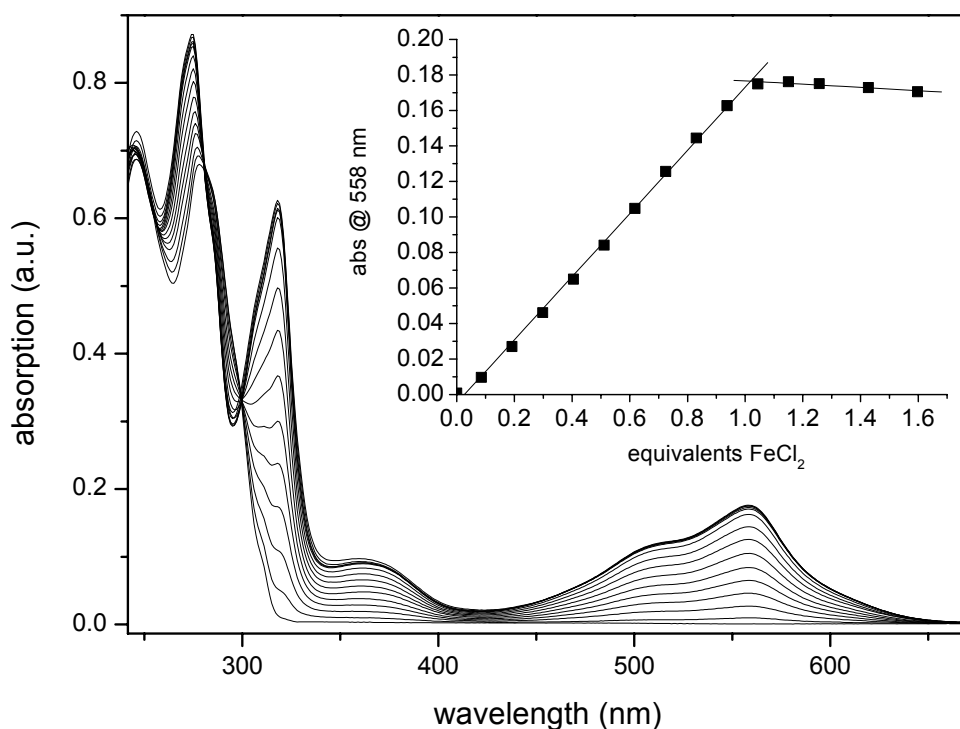
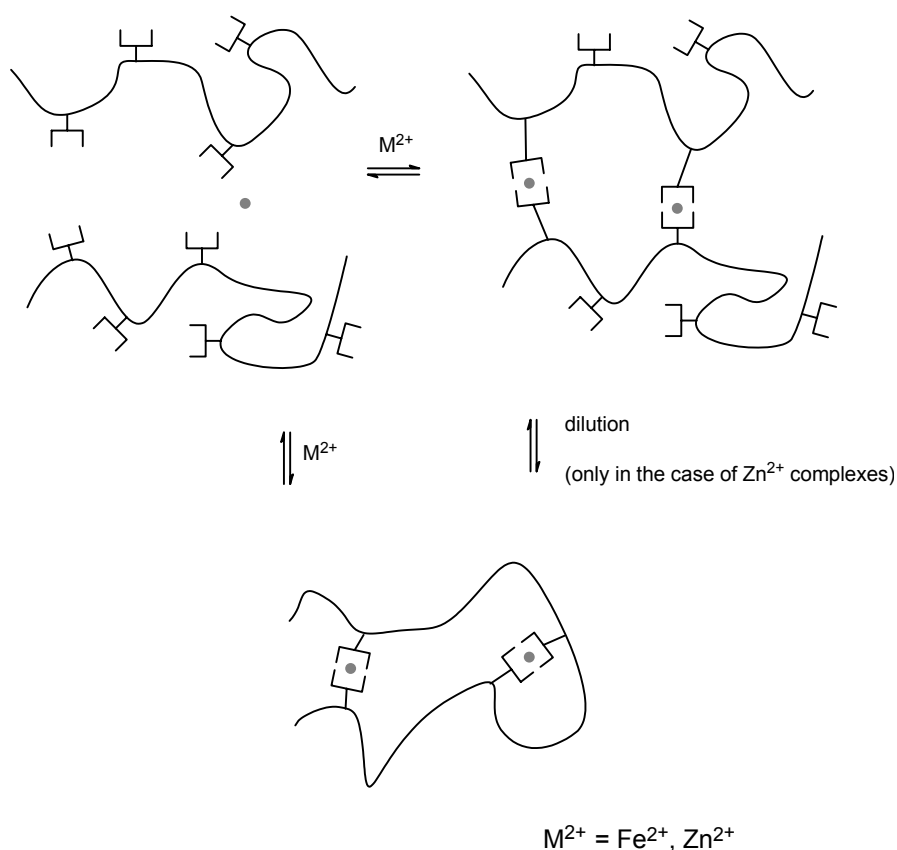


Figure 5.4. UV-vis titration of **2a** with FeCl<sub>2</sub> (in methylene chloride).

### 5.2.2 Solution viscosimetry

From the UV-vis result an intramolecular or intermolecular complex formation cannot be discerned (Scheme 5.2). Therefore viscosity titration experiments at different concentrations and with different metal ions were performed (in a diluted regime). Metal ions were added in stepwise portions to a solution of the (co)polymers **2a**, **2b** and **3** in a 1:1 mixture of chloroform/methanol and the viscosity was measured after each step utilizing an Ubbelohde-viscosimeter. In case of adding Fe(II) ions, the relative viscosity rose ultimately to 2.5 in the case of **2a** and to 1.73 in the case of **2b** (Figure 5.5) at the equivalence point. A concentration of 17.2 mg/mL of polymer was used in both cases. Addition of metal ions to the PMMA homopolymer **3** revealed no color change and no increase in viscosity. Therefore, an interaction of the PMMA backbone with the utilized metal ions can be excluded.



Scheme 5.2. Cross-linking or intramolecular complexation of **2** with metal ions.

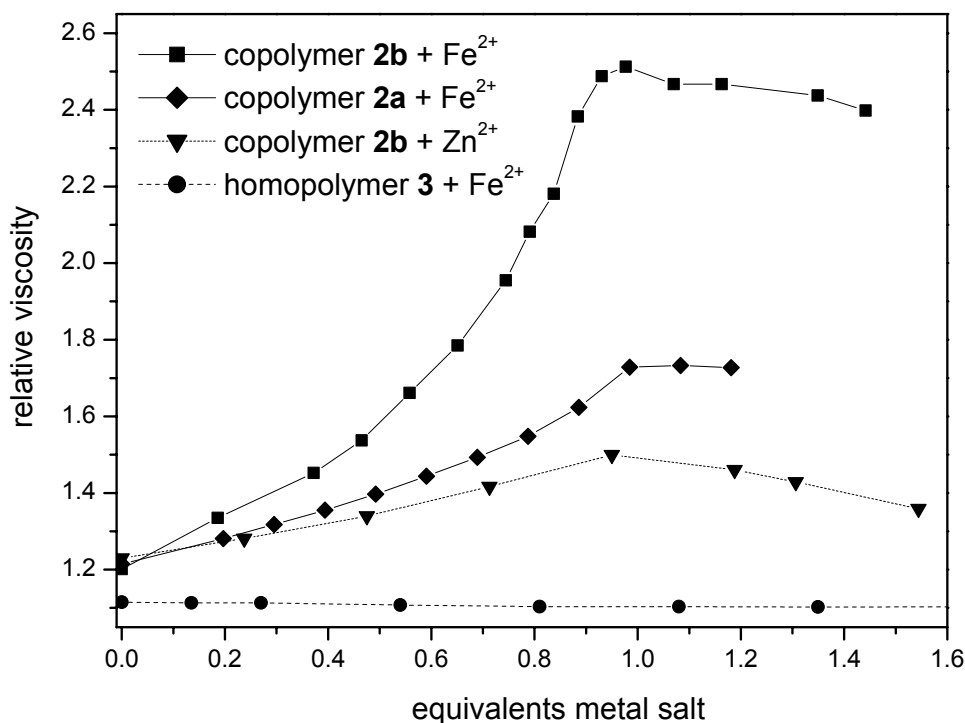


Figure 5.5. Viscosity titration of **2a**, **2b** and **3** ( $FeCl_2$ ,  $ZnCl_2$ ;  $c = 17.2$  mg/mL; chloroform/methanol 1:1).

The correlation of the obtained viscosity values to the terpyridine content of the copolymer suggests a higher degree of cross-linking in the case of the copolymers bearing a higher

number of terpyridine units. Addition of Zn(II) ions at the same concentration to polymer **2a** resulted in much lower viscosity values (1.5 at equivalence point). However, increasing the concentration of the solution by factor 3 led to a viscosity more than 20 times higher as before, giving rise to a honey-like behavior. A relative viscosity of 47 was measured at a concentration of 40 mg/mL. The obtained results seem to support the assumption that at higher concentration the beginning of the formation of network-like aggregates can be observed while at lower concentrations the aggregates are significantly smaller. A more or less symmetrical shape of the titration curve (Zn(II)) was observed by overtitration. *Bis*-complexes are in equilibrium with *mono*-complexes, thus the network breaks apart which results in a decrease of the viscosity. On the other hand, in the case of the iron(II) complexes the curves reveal an asymmetric shape. A plateau could be observed after a maximum. The zinc-terpyridine complexes are weaker than the iron complexes,<sup>[23]</sup> therefore the complex formation can be reversed more easily. Zinc complexes exist in a dynamic equilibrium and thus exchange rapidly. When a solution of the zinc(II)-cross-linked copolymer (starting from a concentration of 34 mg/mL) was stepwise diluted, an exponential decrease of the viscosity was observed, whereas the parent copolymer revealed a linear decrease (Figure 5.6).

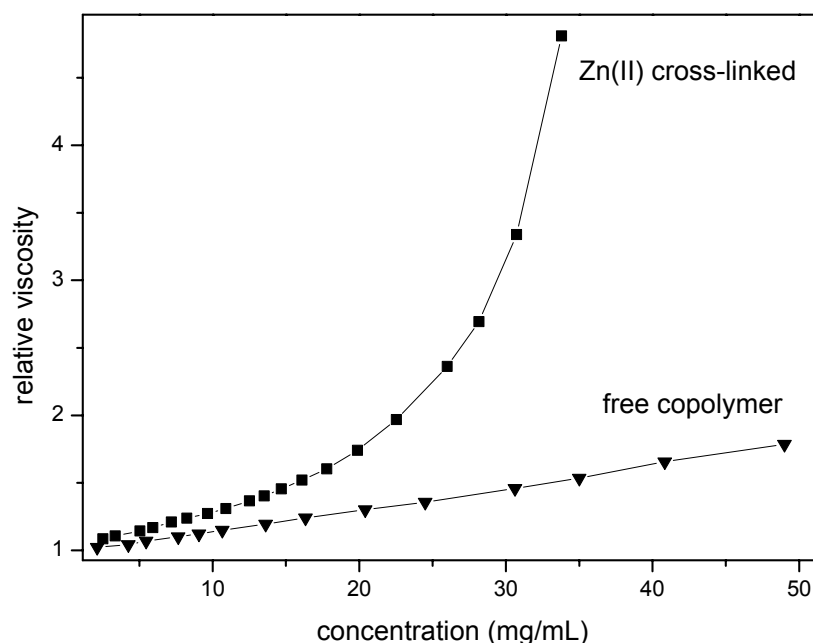


Figure 5.6. Concentration-dependant viscosity of copolymer **2b**, free and cross-linked with zinc(II) ions (in chloroform/methanol 1:1).

For the complexed copolymer, the decrease became also linear at low concentrations (< 15 mg/mL), with values approaching the curve of the free copolymer. This behavior indicates the formation of smaller aggregates through dilution, eventually leading to intramolecular complexes.

### 5.2.3 Gelation studies

Following the experiments described in the last section, higher concentrations of the polymer, where gelation of the cross-linked copolymers occurs, were applied: an appropriate amount of iron(II) ions (calculated from the NMR integral ratios) was added to a solution of copolymer **2b** in chloroform (40 mg/mL), resulting in a deep purple gel (Figure 5.7). A sample of this gel was weighed in the swollen state, subsequently dried and weighed again. Re-swelling in chloroform led to the previous value, showing the reversible nature of the non-covalent cross-linked gel. Zn(II) ions at the same concentration led to a honey-like highly viscous solution and at higher concentrations also gel formation was observed. In contrast to the iron-gel, the Zn(II) gel became completely soluble when more chloroform (5 mL) was added. An explanation for this behavior is the reversible nature of zinc complexes, resulting in smaller aggregates by dilution, as already seen for the viscosity investigations at lower concentrations. The addition of cobalt(II) ions led to a gel similar to that formed by iron(II) ions.

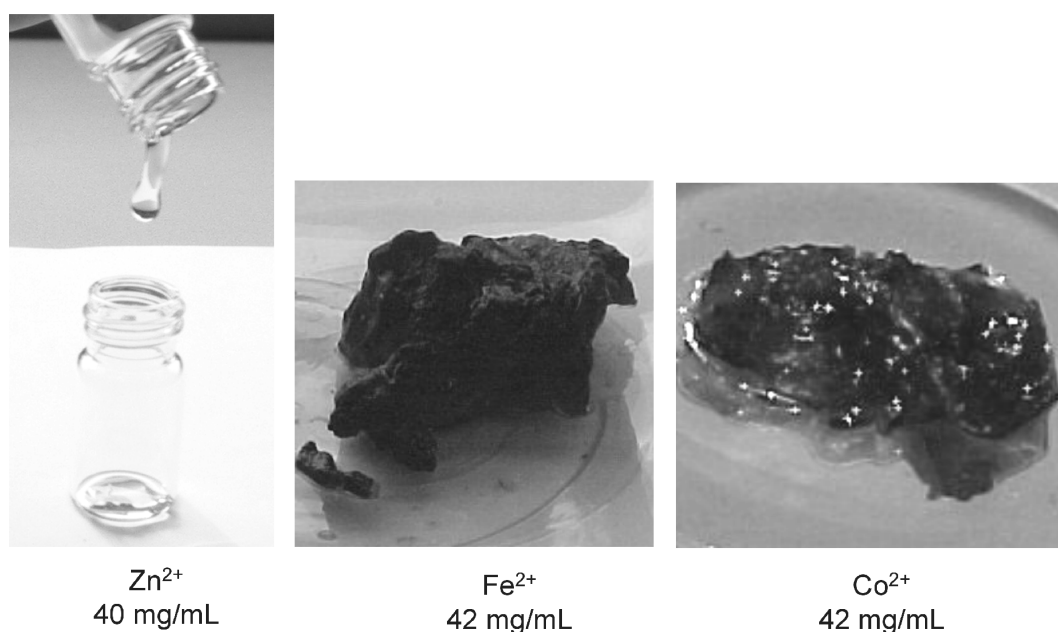
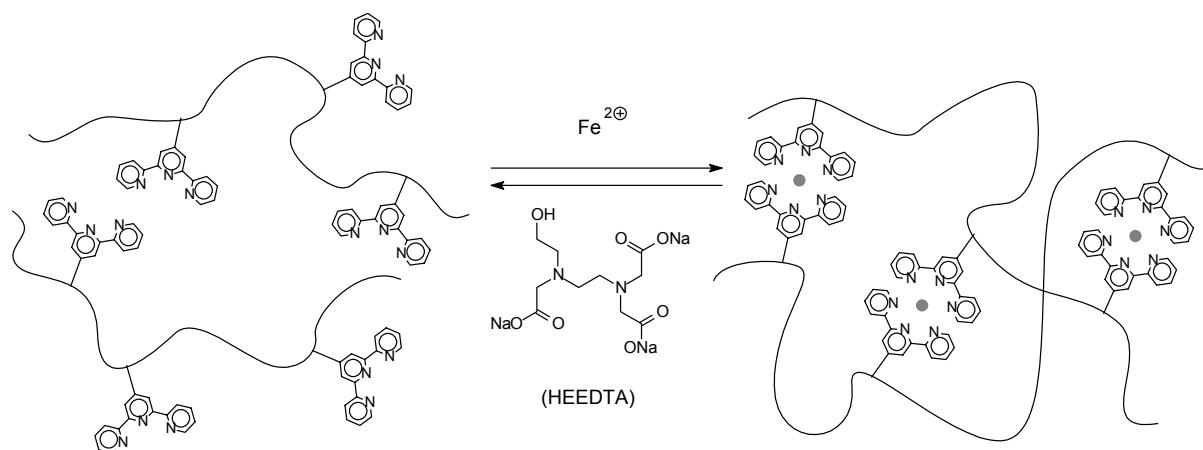


Figure 5.7. Gels of **2b** with zinc(II), iron(II) and with cobalt(II) ions (chloroform).

### 5.2.4 Decomplexation studies

In order to study the reversibility of the complex formation, the solutions from the experiments described in 5.2.2. were treated with HEEDTA (hydroxethyl ethylenediamine-triacetic acid) (Scheme 5.1). HEEDTA is a very strong chelating ligand for transition metal ions with the ability to break up terpyridine metal complexes.<sup>[24]</sup> In the present case, the purple color of the iron(II) complexes as well as the high viscosity of the zinc(II) solutions disappeared.





Scheme 5.3. Decomplexation of polymer **2** with HEEDTA.

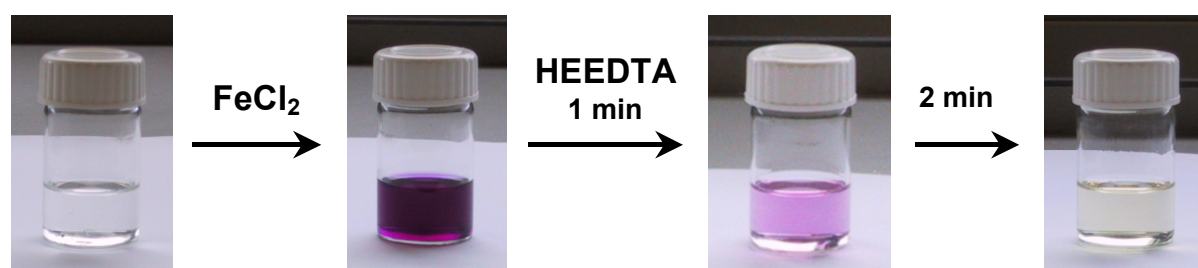


Figure 5.8. Visualization of the complexation and decomplexation of the copolymer **2b** in diluted solution.

The decomplexed iron(II) system was subsequently extracted with a water/dichloromethane mixture. The polymer was precipitated by addition of the organic fraction to pentane. UV-vis spectroscopy showed that the completely uncomplexed polymer could be recovered (Figure 5.9). Furthermore,  $^1\text{H-NMR}$  spectroscopy of the complexed as well as decomplexed samples elucidated the successful decomplexation.

The gel obtained from **2b** at a higher concentration (see 5.2.3.) was also exposed to a HEEDTA solution in a chloroform/methanol mixture. Within one hour the gel dissolved and the purple color vanished. The longer time necessary for decomplexation is probably caused by the less good accessibility of the complex moieties within the gel (higher degree of cross-linking).

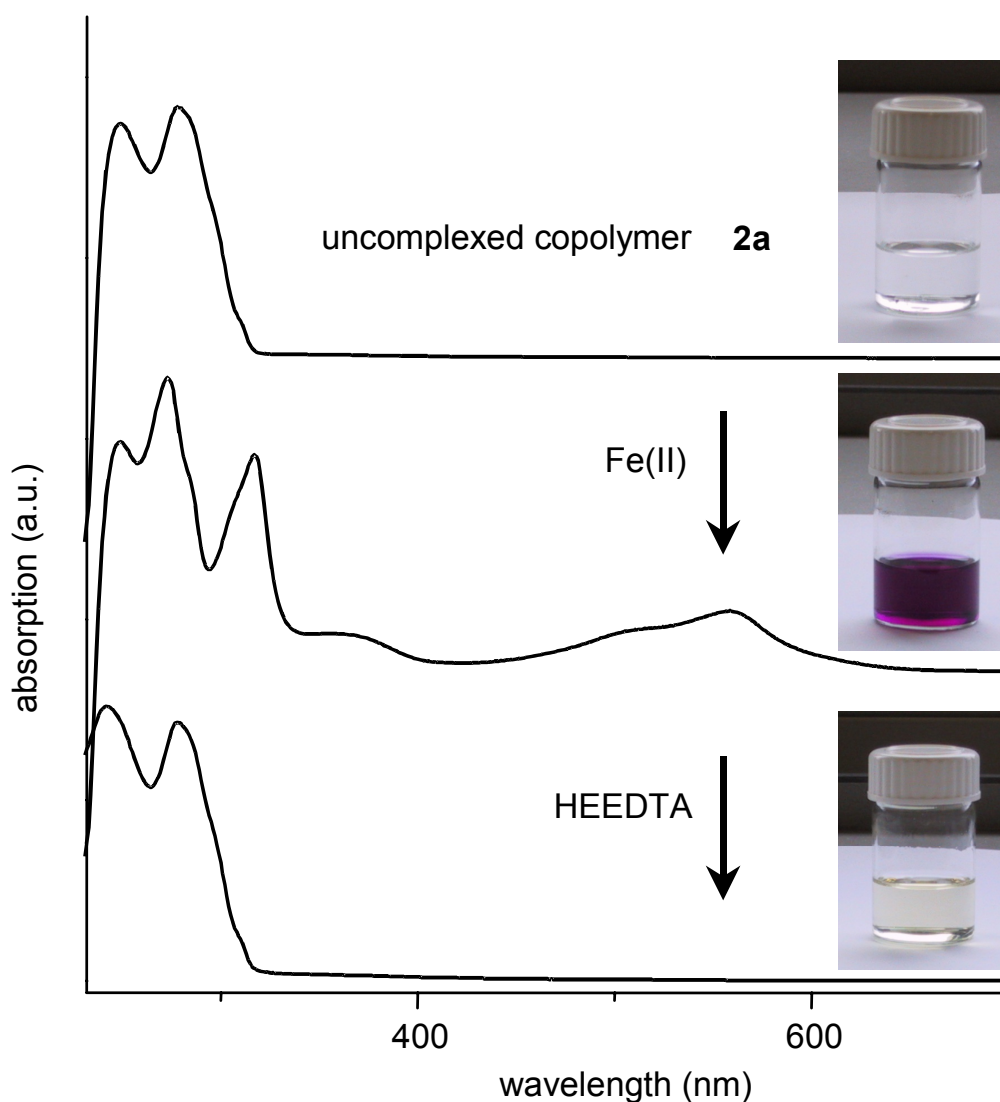


Figure 5.9. UV-vis spectra and photos of **2b** before and after complexation with iron(II)-ions (in chloroform) and after decomplexation with HEEDTA.

### 5.3 Combining covalent and non-covalent cross-linking: a novel terpolymer for two-step curing applications

Copolymers containing supramolecular entities<sup>[13,25]</sup> as well as covalent cross-linking units<sup>[26]</sup> raised special interest during the last years due to their potential to serve for the construction of novel materials with smart or addressable properties, such as switchable adhesives or self-repairing and self-healing materials or coatings.<sup>[27]</sup> For this purpose, the reversible and weaker features of non-covalent interactions have to be combined with the known covalent chemistry in a "two-step curing" process.<sup>[2,28]</sup> The initial application of supramolecular cross-linking leads to materials with adjustable viscosity behavior (as described before), which should be directly tunable by the number of the non-covalent cross-linking units and the kind of metal ions (cross-linkers) used. Applying the covalent cross-linking process after the supramolecular cross-linking step would finally fix the non-covalently cross-linked structure

by the formation of covalent bonds. In addition, the order of the processes could be changed, resulting first in a covalently cross-linked material with the ability to further undergo supramolecular cross-linking and therefore opening the possibility to react on potential changes or damages.

As already described previously, radical polymerization is a versatile method for the rapid and efficient (co)polymerization of a variety of (un)functionalized (meth)acrylate monomers,<sup>[29]</sup> making a large diversity of different functional co- and terpolymers accessible. Besides oxiranes, oxetane is a nicely polymerizable unit that leads to polyethers through a ring-opening-process<sup>[30-32]</sup> and possesses even a higher photoinitiated polymerization ability than oxiranes.<sup>[33]</sup> This behavior makes them in particular attractive for UV-curable processes in coatings technology.<sup>[34]</sup> Therefore, the supramolecular chemistry of terpyridines was combined with the ring-opening polymerization of oxetanes. The approach chosen for this purpose consists of the design of polymeric systems that contain both moieties in the side chain of a terpolymer. In this section, the synthesis, characterization and cross-linking of an acrylate terpolymer bearing terpyridine moieties as a supramolecular unit and oxetane groups as covalent cross-linking units are reported (Figure 5.10).

### 5.3.1 *Synthesis and characterization of an oxetane-terpyridine-terpolymer*

In order to create a suitable polymer system with both terpyridine and oxetane moieties in the main chain, a free radical polymerization process was chosen in combination with acrylate units as polymerizable groups. The terpyridine monomer was synthesized starting from the commercial 4'-chloro-terpyridine.<sup>[39]</sup> A C<sub>3</sub>-spacer was introduced by a nucleophilic substitution reaction in order to avoid any interference of the rather bulky terpyridine unit with the polymerizable group during the terpolymerization process (Scheme 5.4).<sup>[11,38]</sup>

The acrylate was prepared by reaction of acryloyl chloride with the hydroxyl terminated terpyridine **1** in 66% yield. The oxetane monomer **5** was obtained in a four-step reaction introducing a C<sub>2</sub> spacer in between the acrylate and the oxetane ring in order to avoid intramolecular ring-formation during the ring-opening process (see ref.<sup>[26c]</sup> and experimental part). Moreover, butylacrylate **6** was chosen as third monomer due to its low T<sub>g</sub>, which was expected to be of benefit during the cross-linking experiments.

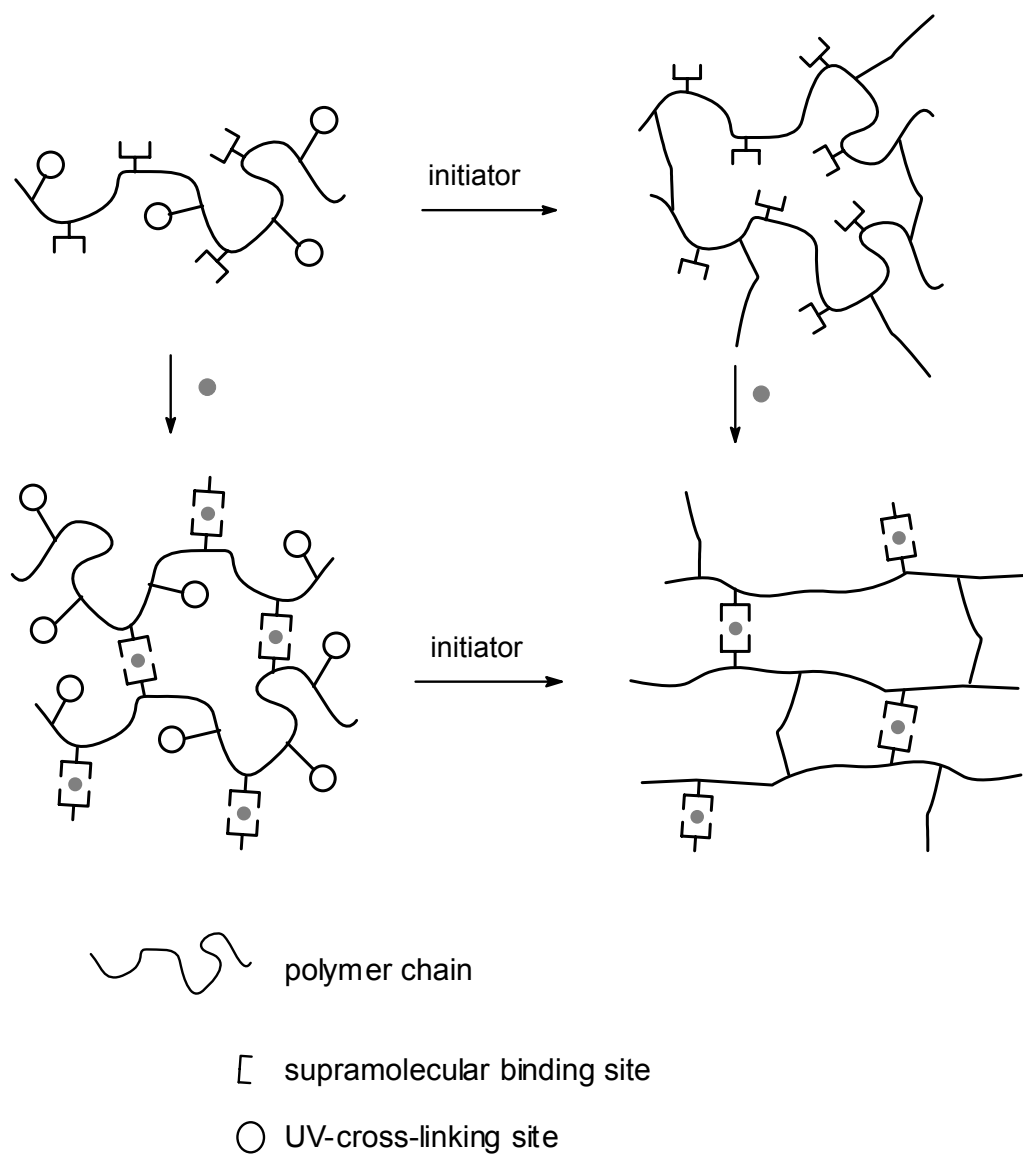
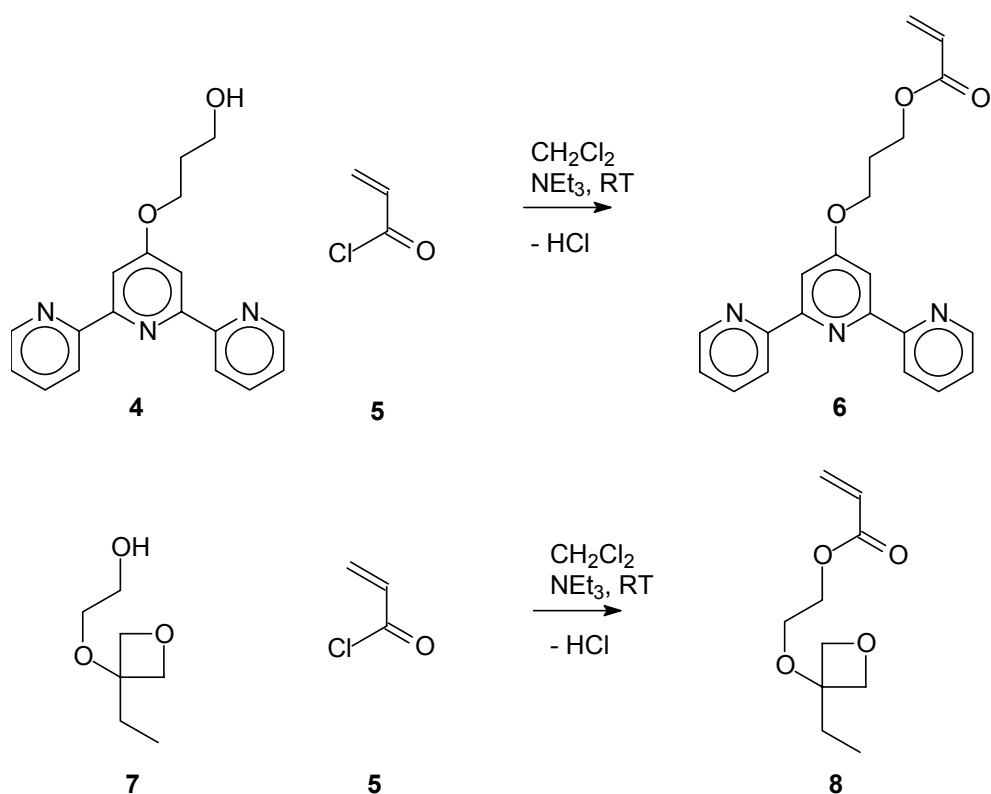
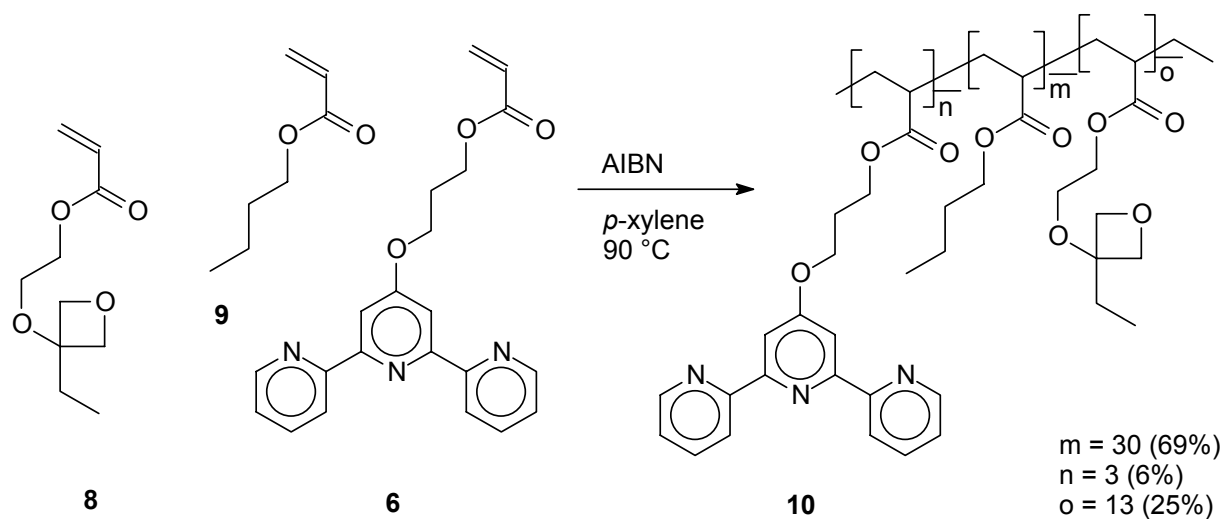


Figure 5.10. Overview of a two-step covalent and supramolecular cross-linking.

Subsequently the monomers **6** (6%), **8** (25%) and **9** (69%) were copolymerized with *N,N*-azobisisobutyronitrile (AIBN) as initiator in order to result the desired butylacrylate terpolymer **7** bearing both terpyridine and oxetane units (Scheme 5.5).



Scheme 5.4. Synthesis of the co-monomers **6** and **8**.



Scheme 5.5. Synthesis of terpolymer **10**.

The polymer was isolated and purified by precipitation and preparative size exclusion chromatography in 70% yield as a white sticky solid. A comparison of the  $^1\text{H-NMR}$  spectra of the corresponding monomers **6** and **8** with the isolated polymer **10** revealed that all functional groups were incorporated into the terpolymer (Figure 5.11).

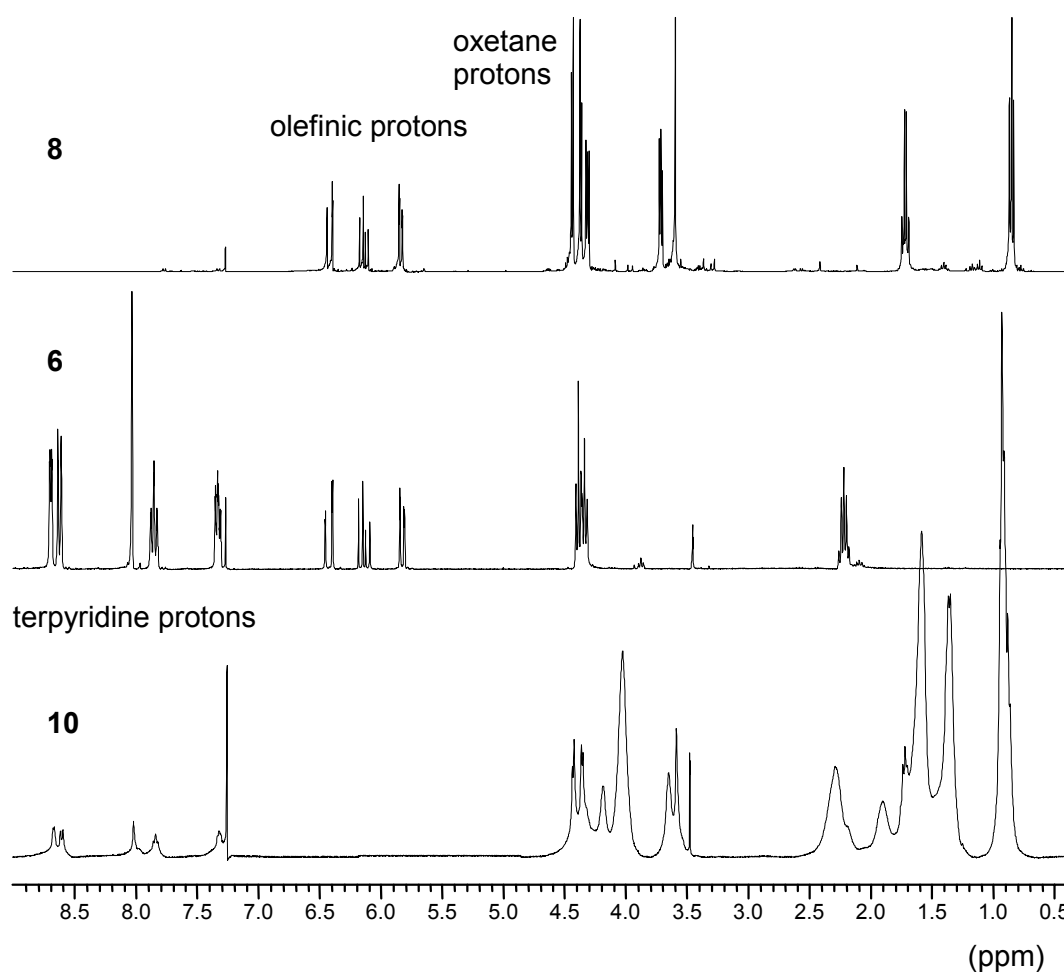


Figure 5.11. NMR spectra of the co-monomers **6**, **8** and the resulting terpolymer **10** (in  $\text{CDCl}_3$ ).

The terpyridine protons could be observed between 7 and 9 ppm and the cyclic  $\text{OCH}_2$ -oxetane signals appeared at 4.36 and 4.43 ppm in combination with the other  $\text{OCH}_2$  signals. In the region from 0.5 to 2.5 ppm the aliphatic protons were detected. The absence of any olefinic signals in the spectrum of polymer **10** underlined the successful isolation and purification procedure. From the integral ratios (combined with the results of the UV-vis titration, see below) a terpyridine content of 5% and an oxetane content of 28% could be calculated. These values are in good agreement with the original composition of the monomer mixture: obviously the three monomers were built into the final terpolymer according to the original monomer feed. GPC analysis (chloroform, polystyrene standards) revealed an  $\bar{M}_n$  of 7 400 g/mol and a polydispersity index of 2.46. It has to be mentioned that the terpyridine units usually interact with the column material resulting in apparent lower molar mass values (see also chapter 4).

In order to gain information regarding the amount of terpyridine units incorporated into each terpolymer chain and to investigate the non-covalent cross-linking behavior, a UV-vis titration with iron(II) ions was performed: a UV-vis spectrum was recorded after each addition of an aliquot of metal salt (in methanol) to polymer **10** (in chloroform, see Figure

5.12). The appearance of the characteristic metal to ligand charge transfer absorption band (MLCT) is a clear proof for the complexation of the terpyridine units with iron(II) ions. By monitoring the intensity of the MLCT band at 558 nm, a titration curve was obtained (Figure 5.12, insert). By this method, a terpyridine content of 2.8 terpyridines per polymer chain was calculated. No change of the absorption bands has been observed with time.<sup>[35]</sup> In addition, the titration results also revealed a successful cross-linking of the terpolymer: when the experiment was conducted in a higher concentration, a precipitation of the colored metal-containing terpolymer could be observed.

### 5.3.2 Covalent and two-step cross-linking of terpolymer **10**

The covalent cross-linking possibilities were investigated utilizing different Lewis acids in order to open the oxetane rings. First, terpolymer **10** was treated with boron trifluorate etherate and heated to 60 °C overnight. A rubber-like, insoluble material was obtained after the reaction. The transmission FTIR spectra depicted in Figure 5.13 showed a significant decrease of the oxetane C-O-C band at 980 cm<sup>-1</sup> indicating that the cationic ring-opening polymerization took place. Moreover, DSC measurements revealed no glass transition anymore indicating that the linear terpolymer **10** was cross-linked via the opening of the oxetane side groups. The DSC curve of the corresponding terpolymer **10** before that treatment is also displayed in Figure 5.14. In this case a glass transition temperature ( $T_g$ ) of -23.5 °C could be observed, caused by the large amount of butylacrylate in the polymer.

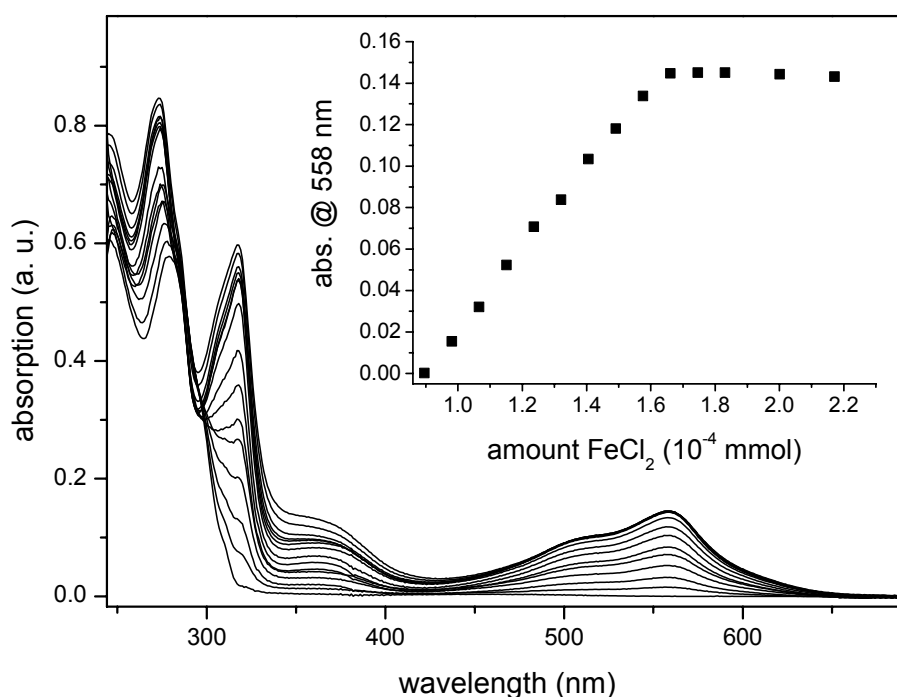


Figure 5.12. UV-titration of **10** with FeCl<sub>2</sub> (in chloroform).

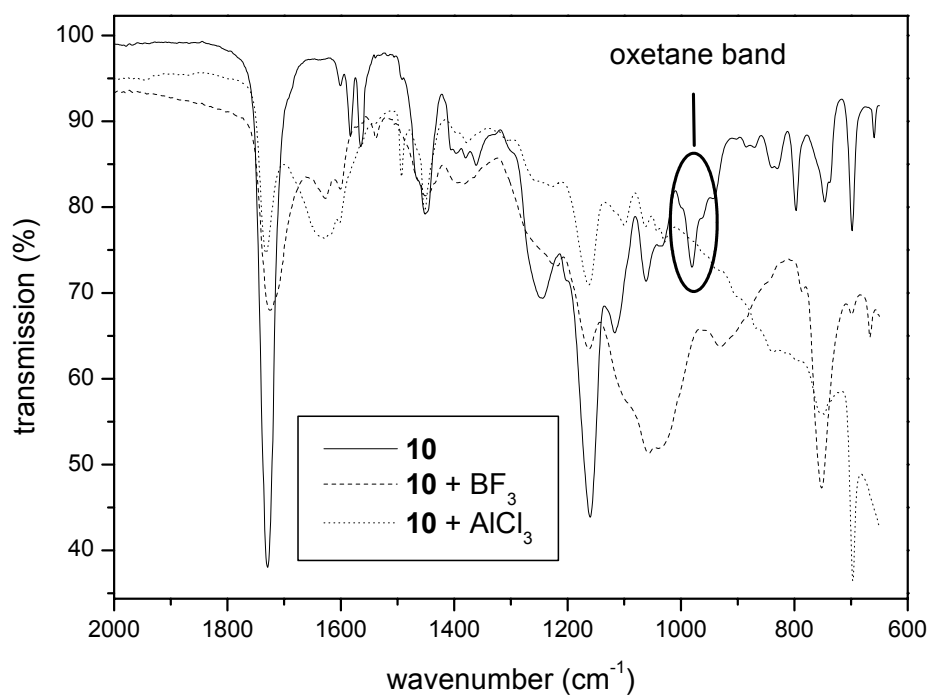


Figure 5.13. IR spectra of **10** before and after cross-linking with  $\text{BF}_3 \cdot \text{Et}_2\text{O}$  and  $\text{AlCl}_3$ .

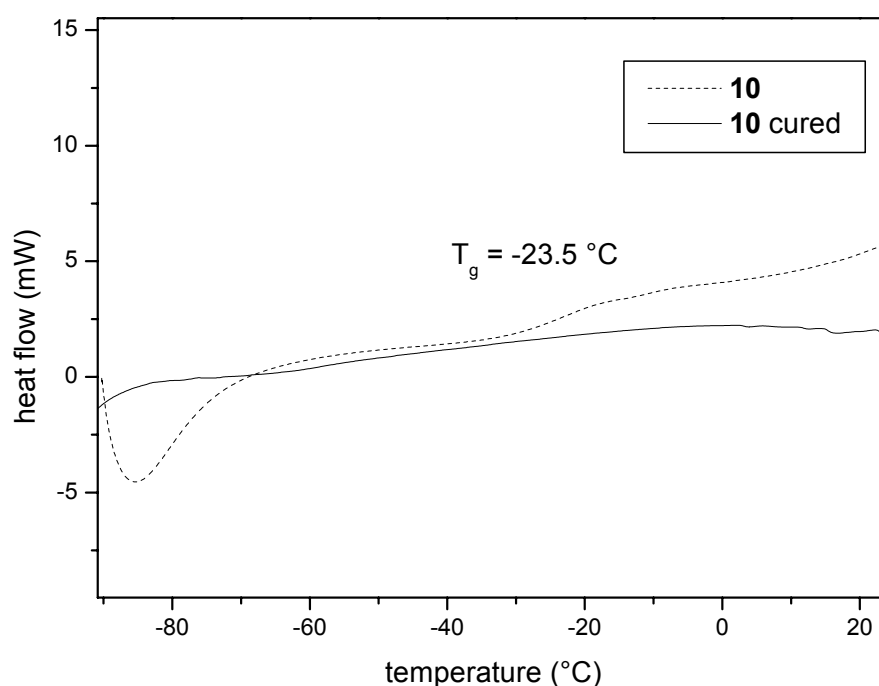


Figure 5.14. DSC curves of **10** before and after cross-linking with  $\text{BF}_3 \cdot \text{Et}_2\text{O}$ .

Subsequently, a first experiment regarding the coupling of supramolecular and covalent cross-linking was performed. The addition of a corresponding amount of iron(II) ions (calculated from the UV-vis titration results) to a diluted solution of terpolymer **10** resulted in a deep purple colored solution (experimental part, route a). This loosely non-covalently cross-linked polymer was then treated in a second step with boron trifluoride etherate to initiate the cationic ring-opening of the oxetane side chains (experimental part, route a). However, this



procedure resulted in a complete disappearance of the purple color indicating a decomplexation of the terpyridine units. These findings can be explained by a reaction of boron trifluorate etherate (strong Lewis acid) and the terpyridine moiety (base), resulting in a decomplexation of the terpyridine metal complexes. In order to circumvent this problem, the initiator was changed as well as the reaction conditions. In the next experiment, the reaction was performed at room temperature in dichloromethane utilizing aluminum trichloride as initiator for the ring-opening polymerization of the oxetane side chains (experimental part, route b). The effect of this treatment to the terpolymer **10** is shown in Figure 5.13.

Also in this case, a significant decrease of the oxetane C-O-C band at  $980\text{ cm}^{-1}$  could be observed indicating a successful ring-opening process. After this positive result,  $\text{AlCl}_3$  was utilized for the two-step cross-linking experiment. A sample of supramolecular cross-linked terpolymer **10** was treated under the above-described conditions with  $\text{AlCl}_3$  (experimental part, route c). This time, the characteristic deep purple color did not fade away. The FTIR spectra shown in Figure 5.15 revealed a significant decrease of the oxetane C-O-C peak at  $980\text{ cm}^{-1}$ . These results indicate that both the supramolecular and covalent cross-linking steps could be combined.

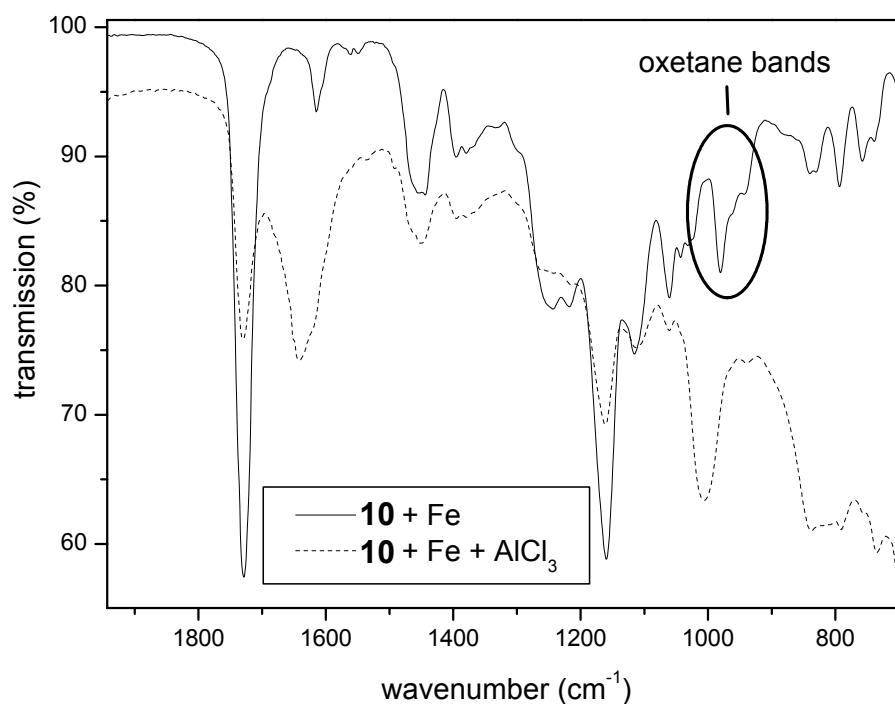


Figure 5.15. IR spectra of the iron(II) complex of **10** before and after cross-linking with  $\text{AlCl}_3$ .

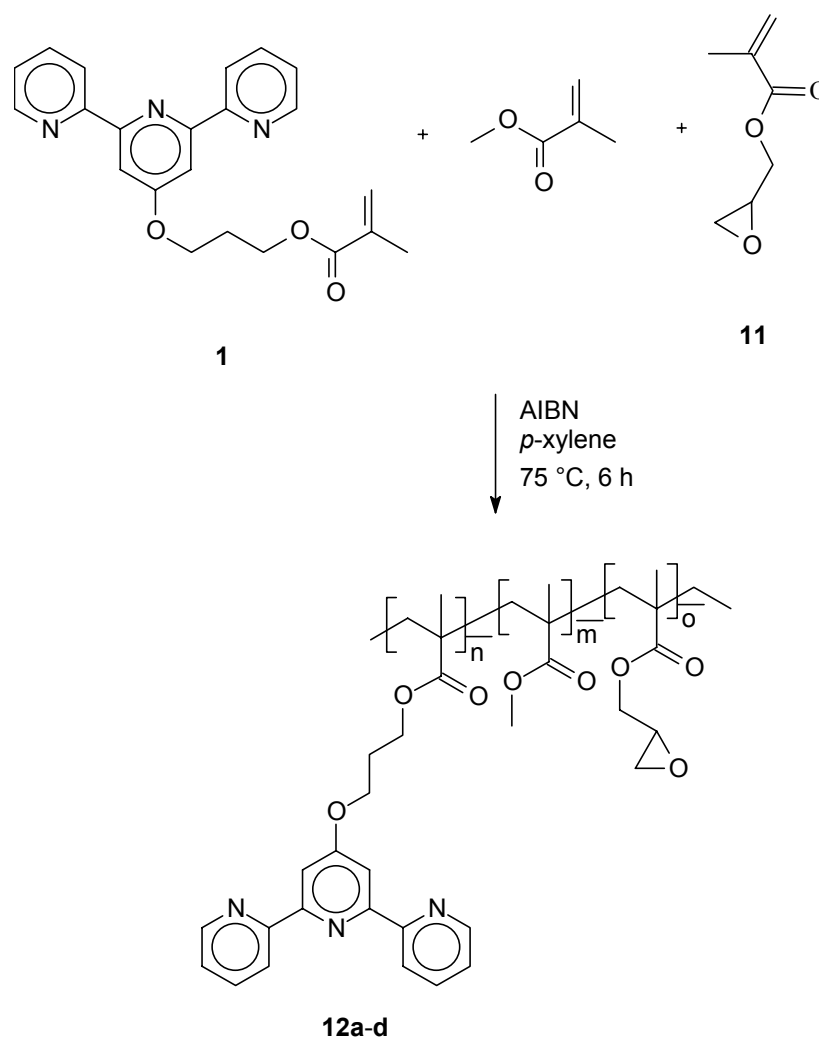
In a second approach the order of the cross-linking reactions was reverted: the rubber-like material obtained from cross-linking of the uncomplexed terpolymer with  $\text{AlCl}_3$  (experimental part, route b) was exposed to a methanolic solution of iron(II) chloride (experimental part, route d). The material immediately turned to purple, which indicated that a complexation of the accessible terpyridine groups took place.

## 5.4 Combination of supramolecular cross-linking with covalent cross-linking through epoxide ring-opening reactions

Another covalently cross-linkable group that has been studied for two-step curing processes is the epoxide unit. The epoxide system is widely industrially used and the corresponding methacrylate monomer is commercially available. In this section, experiments combining the non-covalent cross-linking with covalent curing by ring-opening polymerization of epoxides including studies of the cross-linking density are described.

### 5.4.1 Synthesis and characterization

PMMA-based terpolymers containing terpyridine as supramolecular binding unit and an epoxide group as covalent cross-linking unit<sup>[30]</sup> with two different compositions as well as two model copolymers were synthesized by free radical polymerization utilizing AIBN as initiator (Scheme 5.6 and Table 5.2).



Scheme 5.6. Synthesis of the co- and terpolymers **12a-d**.

The products were precipitated into pentane and characterized by  $^1\text{H-NMR}$ , UV-vis spectroscopy as well GPC. The  $^1\text{H-NMR}$  spectra showed the successful incorporation of all functional groups into the co- and terpolymers **12a-d** (Figure 5.16).

Table 5.2. Characteristics of the co- and terpolymers **12a-b**.

polymer	% MMA*	% epoxide*	% terpy*	Mn	PDI
<b>12a</b>	90	0	10	24 300	2.3
<b>12b</b>	50	50	0	24 700	5.9
<b>12c</b>	59	27	14	17 000	2.7
<b>12d</b>	45	45	10	31 700	5.5

\*mol-% calculated from NMR integral rations

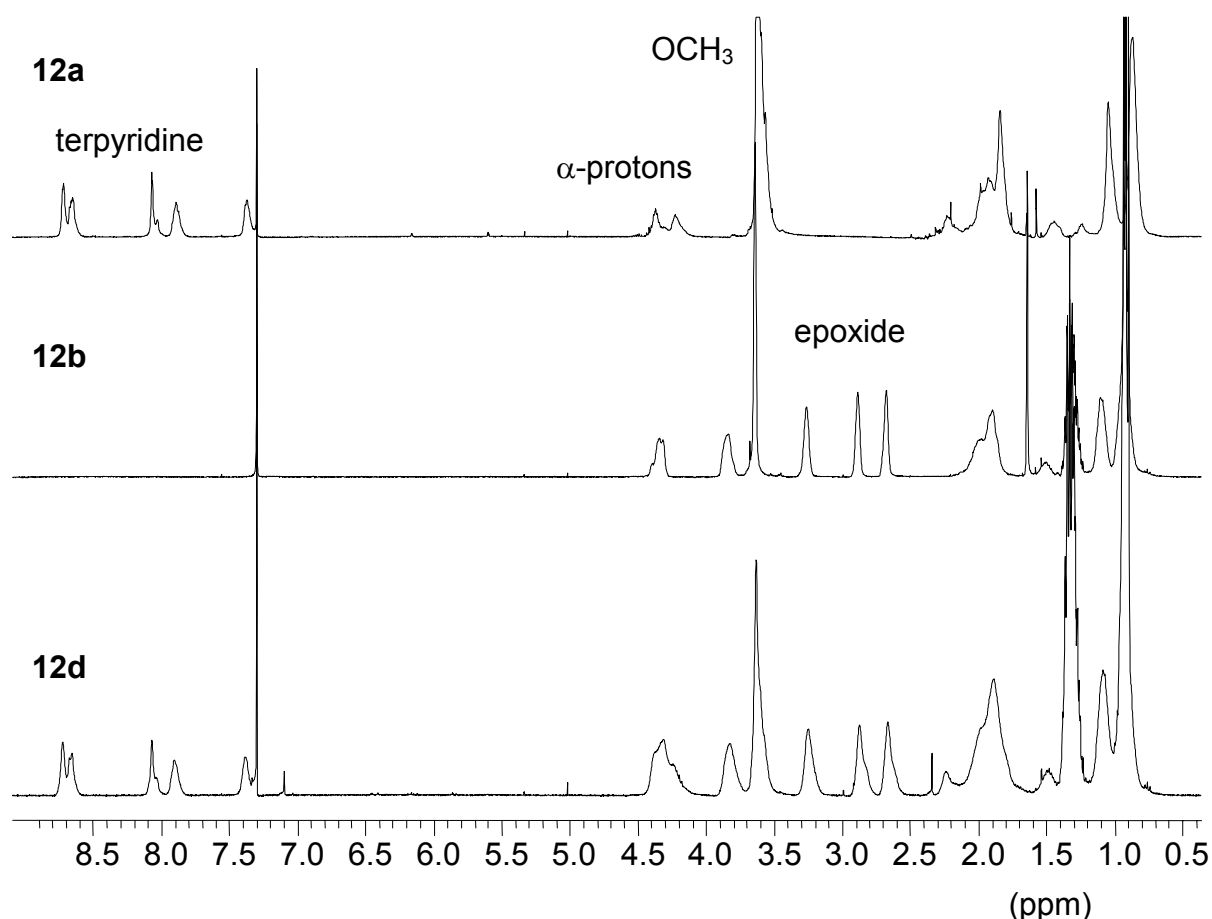


Figure 5.16.  $^1\text{H-NMR}$  spectra of the co- and terpolymers **12a-c** (in chloroform).

The signals in the aromatic region could be assigned to the terpyridine units, the signal at 3.55 ppm to the methyl group of the methyl methacrylate and the signals between 2.5 and 3.5 ppm to the epoxide protons. The main chain resonances were visible between 0.5 and 2 ppm. Furthermore, IR investigations were performed on terpolymer **12d** and the results compared

with the model copolymers containing only terpyridine (**12a**) or epoxide (**12b**), respectively. The spectrum of **12d** revealed clearly both the bands of the terpyridine and the epoxide unit (Figure 5.17): the epoxide signal was located at  $908\text{ cm}^{-1}$  and the bands between  $1540$  and  $1620\text{ cm}^{-1}$  were assigned to the terpyridine unit.

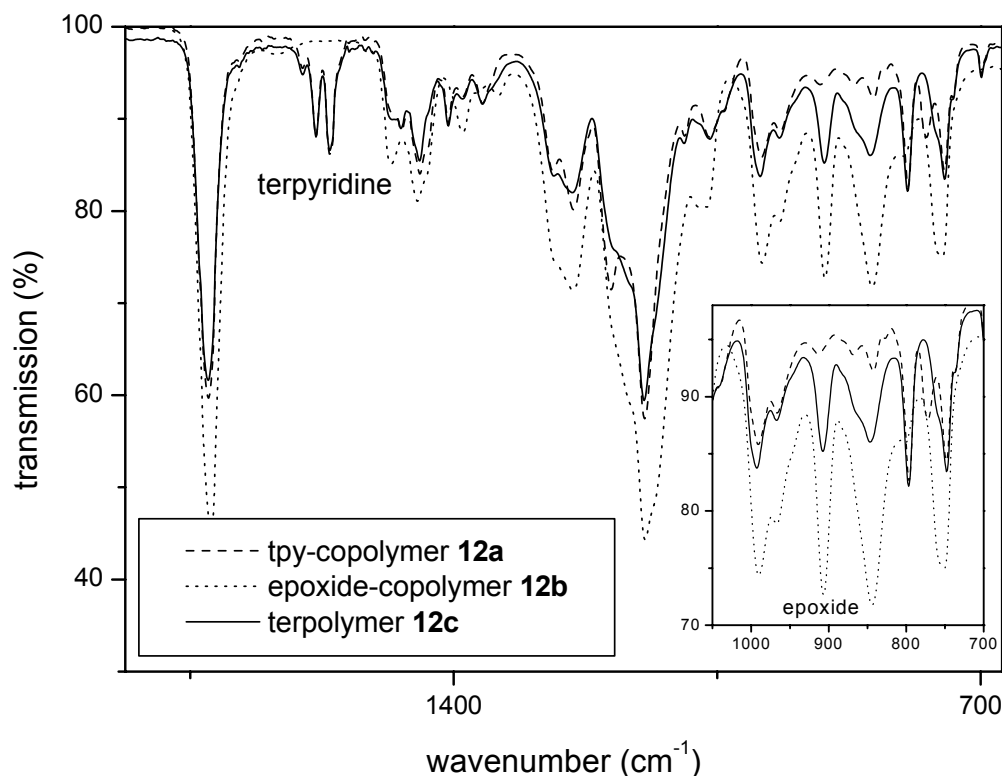


Figure 5.17. IR spectra of copolymers **12a-b** and terpolymer **12c**.

GPC investigations revealed varying polydispersities and a negative tailing for the epoxide-containing polymers **12b-d**. A possible explanation could be a partial polymerization of the epoxide groups initiated by traces of acid during the reaction or the GPC sample preparation. The terpolymer **12d** was studied regarding its ability to combine covalent with supramolecular cross-linking. First, supramolecular cross-linking was studied by complexation of the terpyridine moieties with iron(II) ions. In order to prove the ability and completeness of complexation of the terpyridine units, a UV-vis titration experiment was performed by stepwise addition of an  $\text{FeCl}_2$  solution (in methanol) to a diluted chloroform solution of the terpolymer **12c** and by recording a spectrum 30 minutes after each addition (see, e.g., Figure 5.12 for a similar example). Also in this case a characteristic bathochromic shift of the ligand-centered  $\pi$ - $\pi^*$ -absorption bands from 279 to 317 nm was observed, showing a complexation of the terpyridine moieties. Furthermore, the appearance of the characteristic metal-to-ligand charge transfer (MLCT) band of the iron(II) complex at 558 nm and a metal-centered band at 358 nm was observed in a similar way as for the copolymer **2a** and the oxetane-terpolymer **10**. The equivalence point was reached at an iron(II)/terpyridine ratio of 1:2, demonstrating the complete complexation of all terpyridine units also for the

epoxide-system. However, in diluted solutions where the UV spectra were measured, the formation of intramolecular complexes or small aggregates can be expected. No precipitation was observed. To investigate the actual cross-linking, higher concentrations of the polymer were applied.

#### 5.4.2 Combination with covalent cross-linking and gel-swelling studies

Covalent cross-linking was investigated using  $\text{AlCl}_3$  in order to open the epoxide rings (based on the results with oxetane moieties reported earlier herein). In contrast to boron trifluoride,  $\text{AlCl}_3$  was shown to open oxiranes without affecting the terpyridine ligands or complexes. In the first experiment, a solution of aluminum trichloride in dichloromethane was added to terpolymer **12d** in dichloromethane (route a). A precipitate of rubber-like flakes appeared immediately. The mixture was stirred at room temperature to complete the reaction. The ATR-FTIR spectra shown in Figure 5.18 revealed a significant decrease of the epoxide C-O-C band at  $908\text{ cm}^{-1}$  indicating that the cationic ring-opening polymerization occurred, resulting in a covalently cross-linked material.

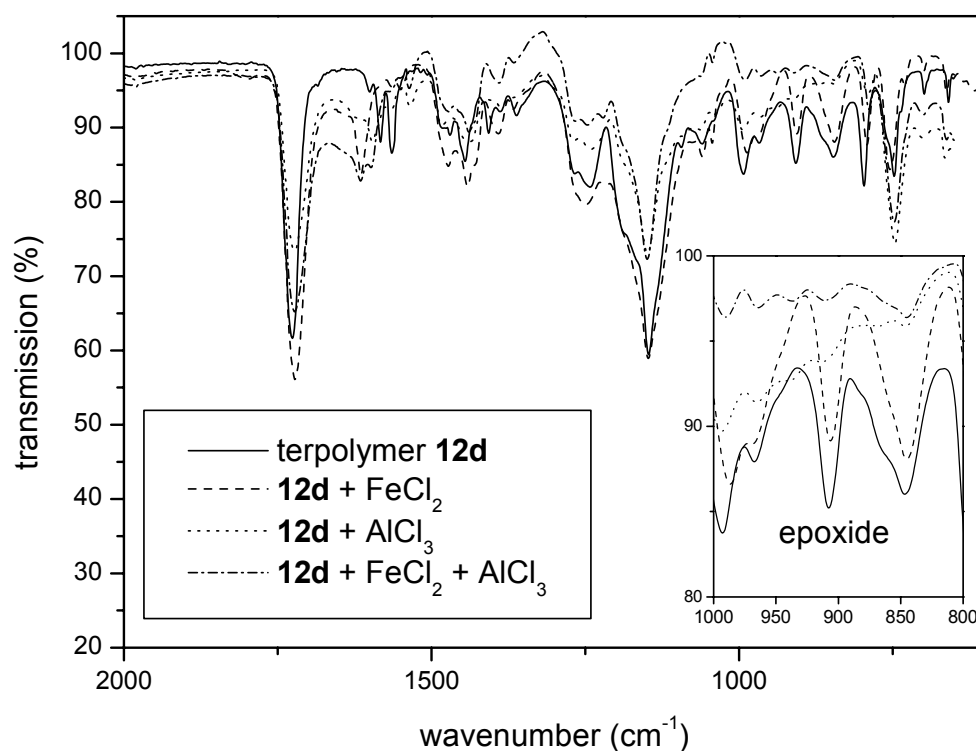


Figure 5.18. IR spectra of the terpolymer **12d** (uncured, non-covalently cross-linked with  $\text{FeCl}_2$ , covalently cross-linked with  $\text{AlCl}_3$  and cross-linked via both methods).

Subsequently, experiments regarding the combination of supramolecular and covalent cross-linking were performed. First, an appropriate amount of iron(II) ions (calculated from the UV-vis titration results) was added to a solution of terpolymer **12d** (30 mg/mL), which led to a deeply purple colored and highly viscous solution (experimental part, route b). This non-covalently cross-linked polymer was treated in a second step with  $\text{AlCl}_3$  to initiate the cationic

ring-opening of the epoxide rings (experimental part, route c), resulting in a purple precipitate of the cross-linked material. As before, a significant decrease of the epoxide C-O-C peak at  $908\text{ cm}^{-1}$  was observed. Another approach included the reversal of the order of the cross-linking reactions: the rubber-like material obtained from cross-linking of the uncomplexed terpolymer with  $\text{AlCl}_3$  (experimental part, route a) was exposed to a methanolic solution of iron(II) chloride (experimental part, route d). The color turned to purple, first on the surface, but a subsequent deepening of the coloration indicated that complexation of the terpyridine groups located inside the material sample took also place. The visual appearance of all the materials is shown in Figure 5.19.

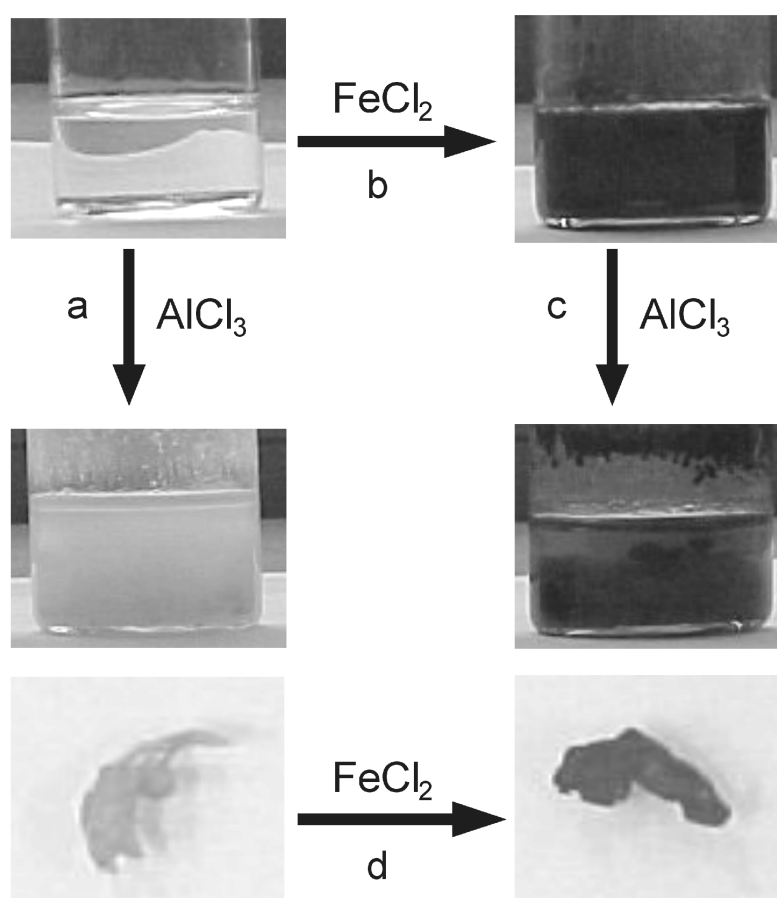


Figure 5.19. Visualization of the terpolymer **12d** and the cross-linked materials.

To investigate the cross-linking density, the swelling behavior of gels was studied. The covalently cross-linked gel from **12d** (route a) as well as the material, which was cross-linked utilizing both covalent and supramolecular processes (route d), were investigated and compared to the gels obtained from **12a**, which contained only cross-links by terpyridine complexation. The gels were weighed in dry state and swollen with chloroform. From the obtained values the  $Q$  factor was calculated applying the following formula:

$$Q = \frac{a - b}{b} \quad (1)$$

( $a$  = weight (swollen gel);  $b$  = weight (unswollen gel)).

The value  $1/Q$  is by the used definition equivalent to the degree of cross-linking.<sup>[36]</sup> The gels derived from copolymer **12a**, consisting of non-covalent cross-links by Fe(II) or Co(II), revealed a  $1/Q$  of 0.08 or 0.04, respectively, whereas a value of 0.30 for the covalent cross-linked material derived from terpolymer **12d** (experimental part, route a) was found. These findings are consistent with the higher amount of epoxide moieties compared to terpyridine moieties in the respective polymers. Finally, in the material containing both covalent and supramolecular cross-links (experimental part, route d), a value of 1.00 was found. These findings suggest that indeed both kinds of cross-links were present in the material and therefore an increased degree of cross-linking is observed.

In order to determine the thermal properties of the initial terpolymer **12d** as well as the corresponding cross-linked products, DSC investigations were performed (Figure 5.20).

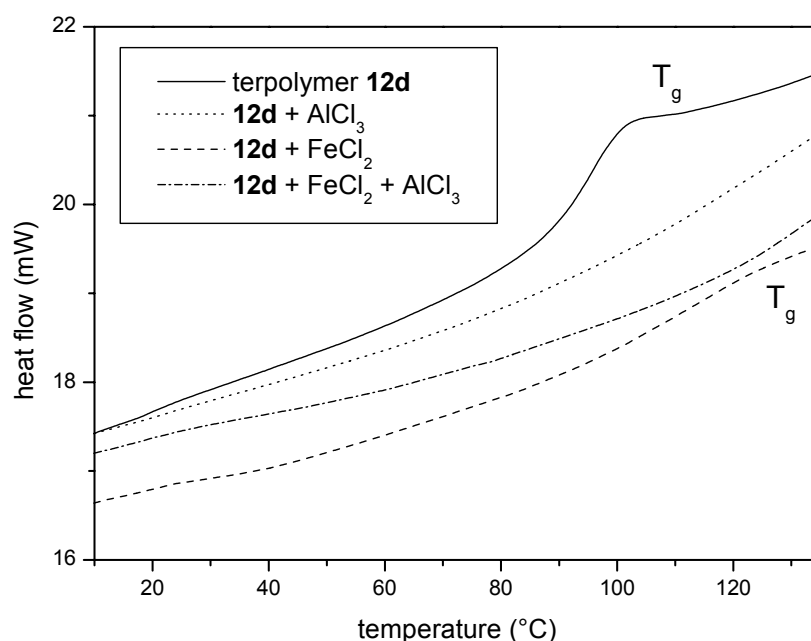


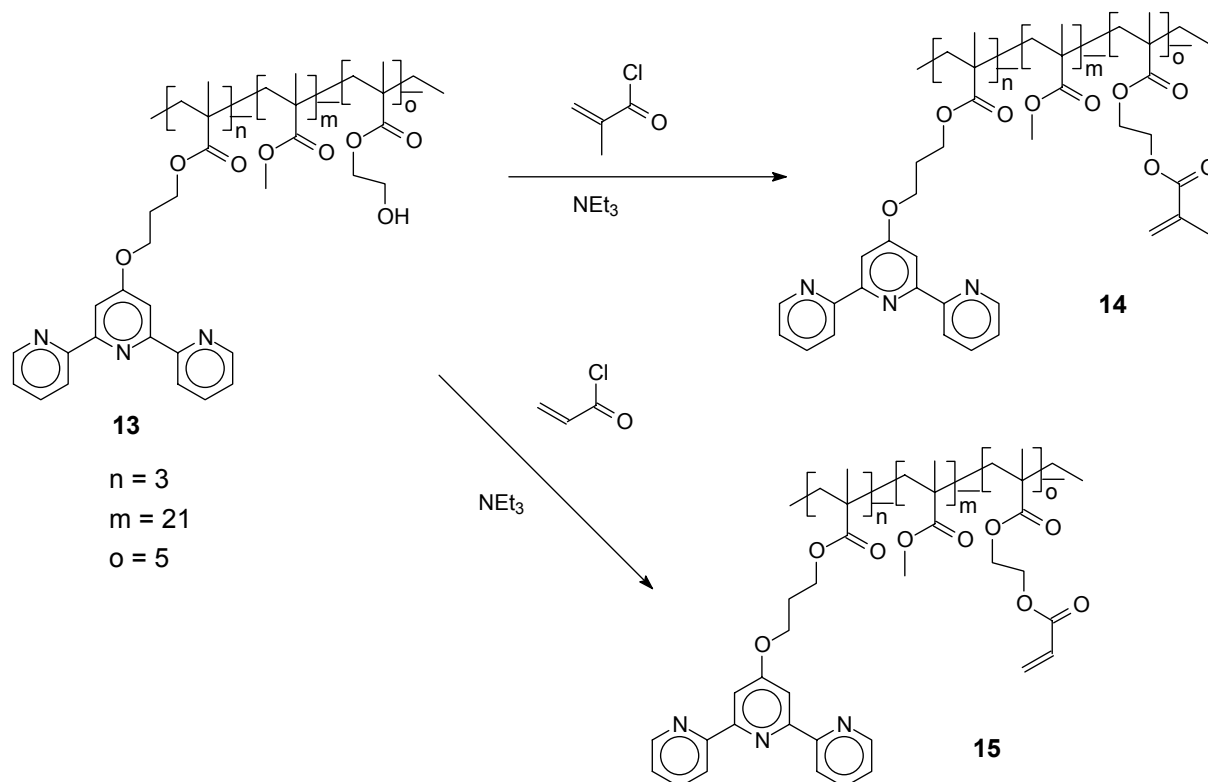
Figure 5.20. DSC thermograms of the terpolymer **12d** and the cross-linked materials.

Whereas terpolymer **12d** revealed a glass transition at 92 °C, a weak transition at 119 °C was found for the terpolymer cross-linked with iron(II) ions. No transition (in the range of the measurement) was found for the covalently cross-linked material, due to the higher degree of cross-linking and the therefore lower mobility of the chain segments. Finally, the material where both cross-linking approaches were combined, was investigated. As expected, also in this case no glass transition was found. The results obtained from IR spectroscopy and DSC clearly indicate that supramolecular and covalent cross-linking steps could be combined successfully for the epoxide/terpyridine system.

## 5.5 Free-radical and thermal curing of terpyridine-modified terpolymers

The previously described terpolymers have been prepared to study the ability for covalent cross-linking in a thin film, initiated by UV-light and a cationic photoinitiator. However, the curing could not be performed successfully if terpyridine moieties were present. IR spectroscopy revealed a change in the terpyridine bands that leads to the conclusion that the generated acid during the composition of the photoinitiator reacts with the terpyridine and therefore the ring-opening of the oxetane or epoxide could not be initiated. Also in the case of a complexation before the curing, no promising results were obtained. Probably there is not enough UV-light available for the activation of the photoinitiator due to the strong absorption of the complex units.

Due to this low efficiency of the UV-curing of epoxides and oxetanes, the strategy was changed from cationic to free-radical UV-curing. Terpolymers containing pendant acrylate (MA) or methacrylate (MMA) groups were prepared. These double bonds should be accessible for UV-curing, initiated by a free-radical-photoinitiator. In a first step, a terpolymer composed of MMA, HEMA and terpyridine-functionalized MA has been synthesized by free-radical terpolymerization, using AIBN as initiator. Subsequently, the hydroxygroups (originating from the HEMA units) were reacted in a polymeranalogous reaction with the acid chlorides of acrylic or methacrylic acid, respectively (Scheme 5.7). The resulting polymers have been precipitated in pentane and purified by preparative size exclusion chromatography (BioBeads SX-1).



Scheme 5.7. Polymeranalogous reactions of **13** to the methacryloyl and acryloyl-functionalized terpyridine-bearing terpolymers **14** and **15**.



$^1\text{H-NMR}$  spectroscopy (Figure 5.21) revealed a successful introduction of the polymerizable units into the polymer. In the range between 5.5 and 6.8 ppm the resonances of the olefinic protons were found, with three signals in the case of the acrylate and two signals for the methacrylate. From the disappearance of the signal of the methylene group adjacent to the hydroxy-group and from the integral ratios of the olefinic resonances an almost complete conversion can be assumed.

IR spectroscopy (Figure 5.22) was performed on the terpolymers **14** and **15** and the results have been compared to the corresponding terpyridine-containing copolymer **12a**. The spectral patterns are very similar. The most distinctive band is a weak peak at  $1636\text{ cm}^{-1}$  that could be assigned to the olefinic groups.

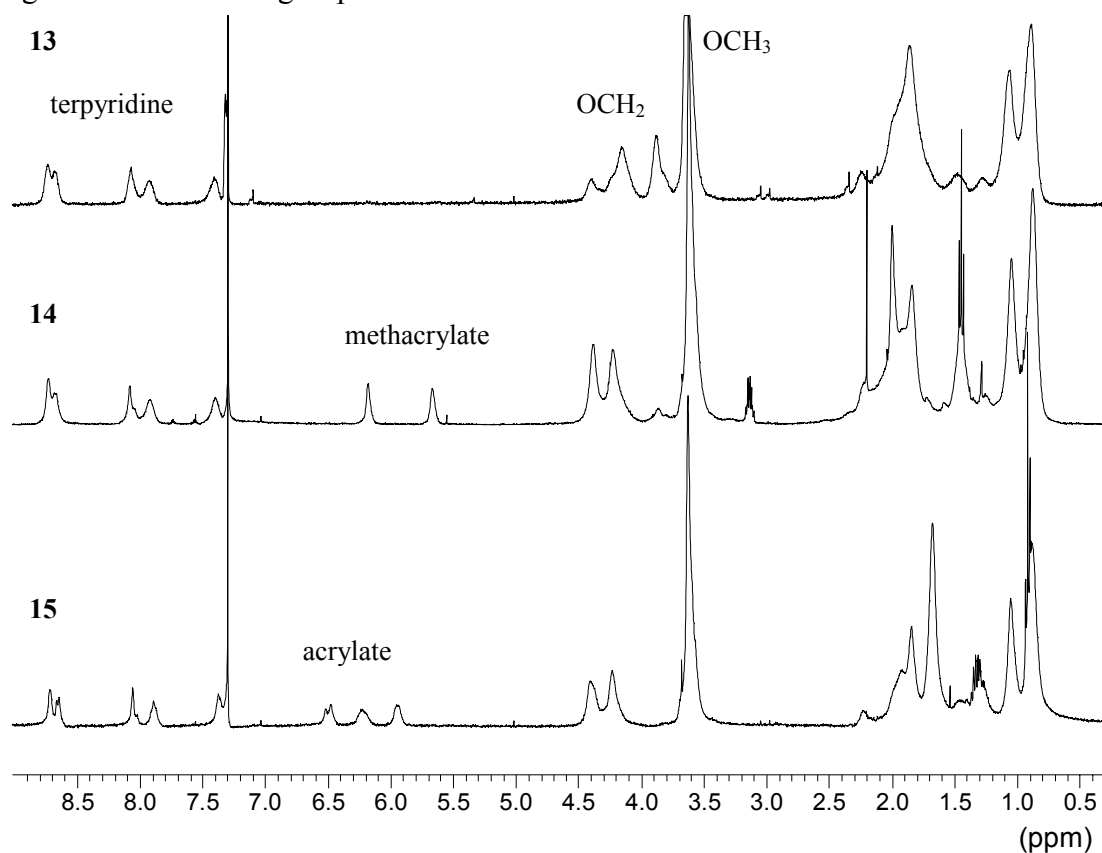


Figure 5.21.  $^1\text{H-NMR}$  spectra of the terpolymers **13-15** (in chloroform).

The pending double bonds of the terpolymers **14** and **15** should be accessible for a covalent cross-linking through free-radical polymerization. To investigate the ability for this reaction in a coating application, a solution of the polymers in dichloromethane was mixed with the photoinitiator Irgacure and a film was applied onto a KBr plate.

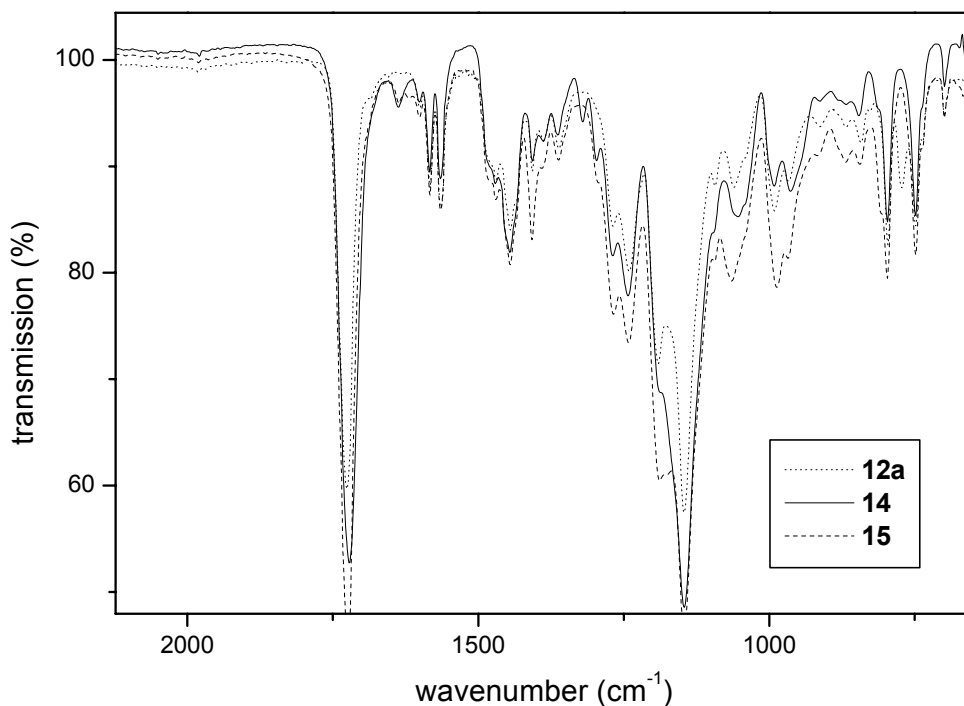


Figure 5.22. IR spectra (ATR) of the terpolymers **13-15**.

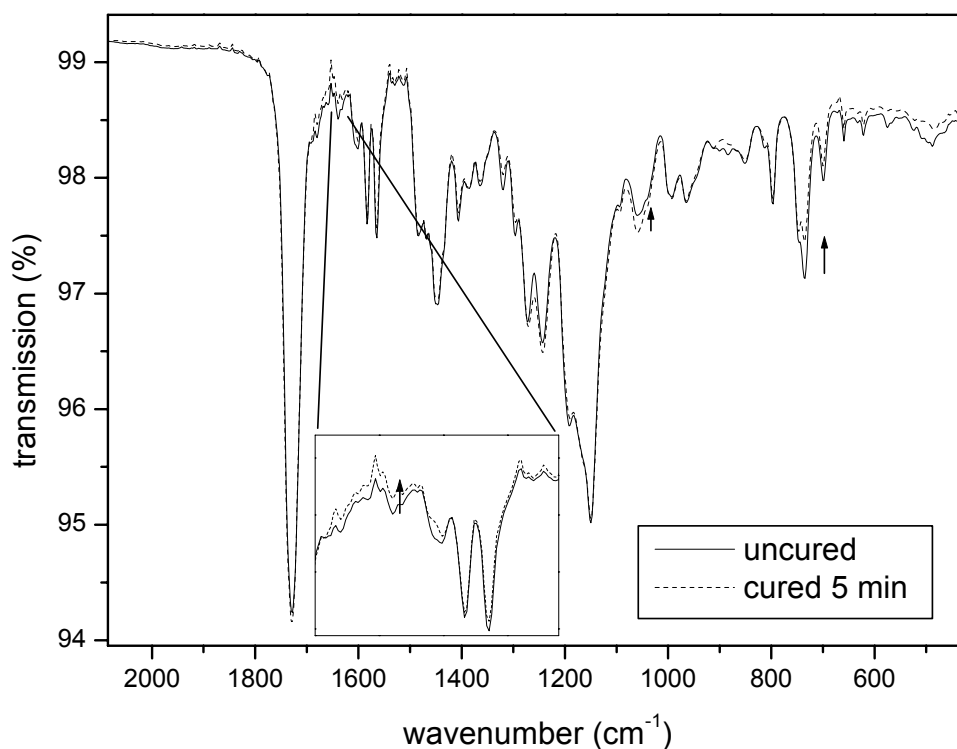
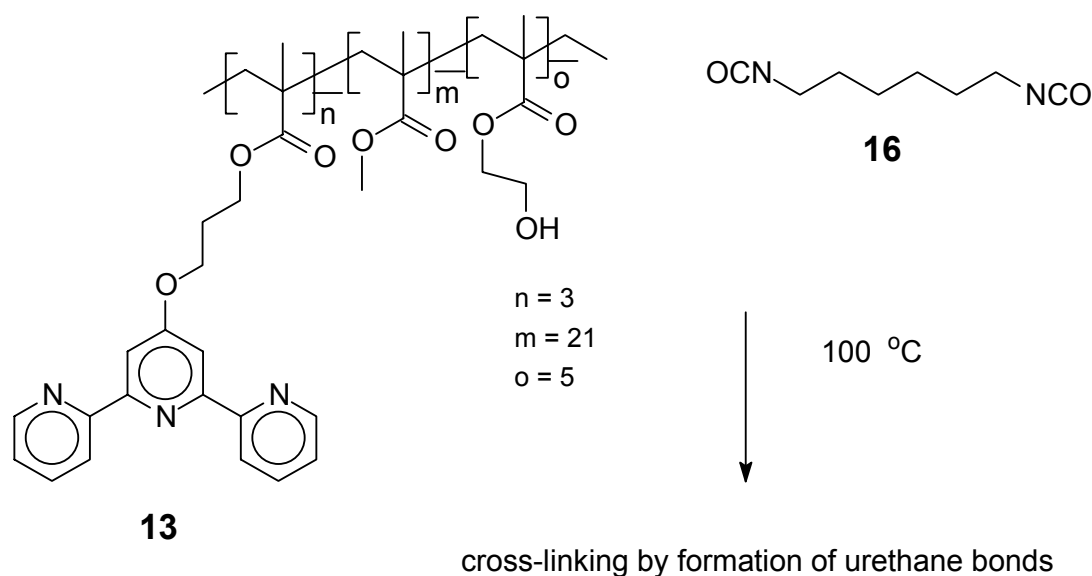


Figure 5.23. IR spectra (KBr-plate) of the acryloyl-terpolymer **15** uncured and UV-cured for 5 minutes.

Subsequently, the film was irradiated by UV-light for 5 minutes. After that treatment, the material was not completely soluble anymore and a swelling was observed, indicating a

covalent cross-linking. Before and after the curing, an IR spectrum was recorded, showing a small decrease of the band at  $1636\text{ cm}^{-1}$  (Figure 5.23). However, due to the relative weakness of the corresponding bands in IR, this interpretation is rather speculative.

Besides the initiation of cross-linking by UV-light, also a thermal initiation was investigated to overcome the mentioned problems. Thermal curing is widely used in coatings technology. Especially the cross-linking of two-component mixtures, utilizing the addition reaction of hydroxy-groups and isocyanates (leading to urethanes) is a standard approach.<sup>[37]</sup> The system chosen here was a two-component system, consisting of the HEMA-terpyridine-terpolymer **13** that has been mixed with a stoichiometric amount of 1,6-hexyl-bis-isocyanate in a dichloromethane solution. A film has been applied onto a glass surface that was subjected to thermal heating at  $100\text{ }^{\circ}\text{C}$  for 15 and 30 minutes (Scheme 5.8).



*Scheme 5.8. Schematic overview over the two-component thermal curing of 13.*

The resulting material was not soluble anymore in chloroform, but a swelling with the same solvent was observed. IR-spectroscopy revealed a decrease of the isocyanate ( $2265\text{ cm}^{-1}$ ) as well as the OH-band (around  $3500\text{ cm}^{-1}$ ), and the appearance of the second urethane band at  $1532\text{ cm}^{-1}$  was observed (Figure 5.24, top). The first one is hidden underneath the ester-band. Moreover, a strong band emerged in the fingerprint region at  $733\text{ cm}^{-1}$ .

After the curing, the obtained particles were covered with chloroform and  $30\text{ }\mu\text{L}$  of a methanolic solution of  $\text{FeCl}_2$  was added. An immediate purple coloration was observed, which deepened within 3 minutes, indicating a complexation of the terpyridine moieties in the cross-linked material. Also IR spectroscopy revealed a complexation of the terpyridines (Figure 5.24, bottom). The isocyanate band disappeared completely, together with an intensification of the urethane bands, probably caused by the used methanol.

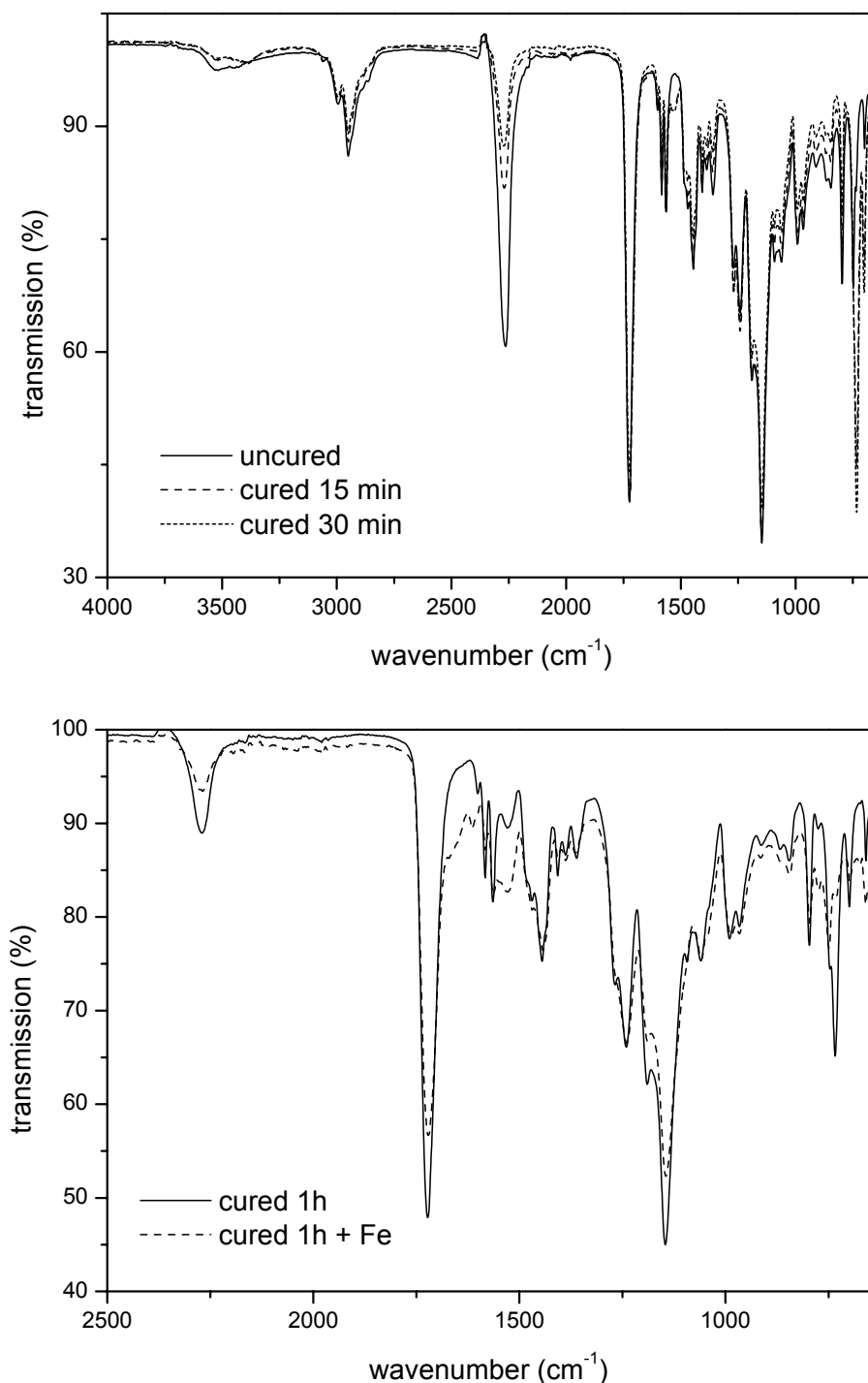


Figure 5.24. Top: IR spectra (ATR) of the two-component mixture (**13** and **16**) uncured and cured for 15 respective 30 minutes. Bottom: thermo-cured mixture **13** and **16** before and after treatment with Fe(II) ions.

In another experiment, the order of the cross-linking steps was changed: first, iron(II) chloride (in methanol) was added to a mixture of the terpolymer **13** (without the *bis*-isocyanate **16**). A solution of the *bis*-isocyanate (in dichloromethane) was added after evaporation of the methanol (in order to avoid a reaction of the methanol with the isocyanate groups). The IR

spectrum revealed indeed an unaffected isocyanate band. Curing of the film for 25 minutes resulted in a decrease of the isocyanate band and the appearance of the urethane band (Figure 5.25).

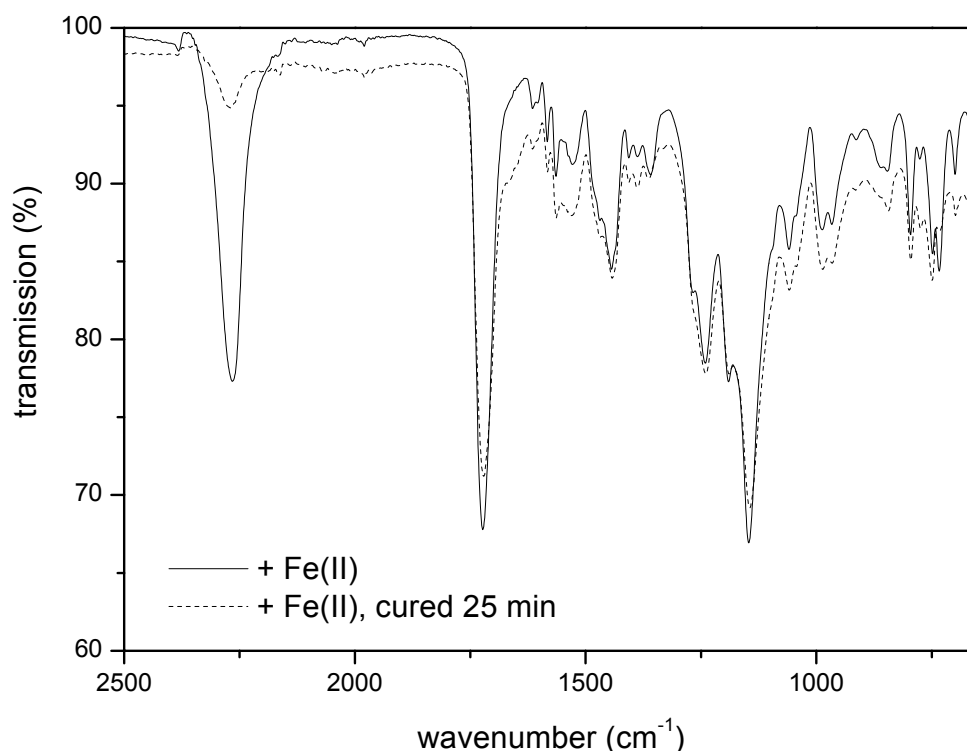


Figure 5.25. IR spectra (ATR) of terpolymer **13**, complexed with iron(II) ions, uncured and thermocured for 15 minutes.

## 5.6 Conclusions

In this chapter, supramolecular cross-linking of terpyridine-containing co- and terpolymers has been investigated. In the first step, poly(methyl methacrylate) based copolymers with different amounts of terpyridine units in the side chain were synthesized utilizing a free radical polymerization process. The addition of transition metal ions (Fe(II) and Zn(II)) was utilized in order to investigate the ability for supramolecular cross-linking in diluted solutions. The complexation reactions were followed in detail by UV- and viscosity titration experiments. Addition of iron(II) ions led to a higher viscosity compared to zinc(II) ions, due to the higher stability of the iron(II)-terpyridine complexes. The complex formation could be reversed completely by addition of HEEDTA as a strong competing ligand, clearly demonstrating the reversible properties of the investigated materials. Subsequently, the preparation of cross-linked materials in higher concentrations has been performed, where intermolecular complexation could be favored. Gels have been obtained and studied regarding their swelling behavior.

The cross-linking studies have been extended to terpolymers bearing terpyridine moieties as well as oxetane or epoxide groups. All polymers have been characterized by  $^1\text{H-NMR}$ , UV-vis, FTIR as well as GPC. Supramolecular cross-linking of the terpolymers through complexation of the pending terpyridine units by addition of metal ions (iron(II), cobalt(II) and zinc(II)) has been successfully combined with covalent cross-linking by opening the oxetane respective epoxide rings, initiated by Lewis acids. The cross-linking behavior has been studied by UV-vis, IR as well as DSC and the swelling behavior of the obtained materials was investigated. Furthermore, the non-covalent cross-linking could be reversed by applying a strong competing ligand. Due to a very low cross-linking efficiency through UV-curing, acrylate groups were introduced into a terpolymer, which have shown the ability for a free-radical initiated UV-curing. Moreover, the thermal curing of a two-component mixture of a terpyridine-terpolymer containing hydroxy-groups and a *bis*-isocyanate could be performed successfully.

These results create multiple possibilities for two-step cross-linking procedures and open new avenues for the development of novel materials, e.g. smart coatings with self-healing properties.

## 5.7 Experimental part

### Materials and characterization

Basic chemicals were obtained from Sigma-Aldrich and hydroxyethyl(ethylenediaminetetraacetic acid) from BASF. 2-Methyl-acrylic acid 3-(2,2':6',2''-terpyridin-4'-yloxy)-propyl ester **1** was synthesized in a two-step reaction (via 4'-hydroxypropyl-2,2':6',2''-terpyridine **1**<sup>[38]</sup>) from 4'-chloro-2,2':6',2''-terpyridine<sup>[39]</sup> as described elsewhere.<sup>[11]</sup> The acrylate-oxetane monomer **5** was prepared in a four steps synthesis as described elsewhere.<sup>[26c]</sup> 2-Bromoethanol was protected according to a literature procedure yielding the protected bromoethanol.<sup>[40]</sup> The protected alcohol was reacted with 3-ethyl-3-hydroxymethylloxetane under phase transfer catalyst conditions to afford the substituted oxetane. The deprotection of the latter compound using pyridinium-*para*-toluenesulfonic salt yielded the hydroxyethylloxetane **4**. This compound was finally reacted with acryloyl chloride **2** and triethylamine in dichloromethane to afford the desired acrylate-oxetane **5**. The butyl acrylate monomer was freshly distilled before use. Preparative size exclusion chromatography was carried out on BioBeads SX1 columns ( $\text{CH}_2\text{Cl}_2$ ).

NMR spectra were measured on a Varian Mercury 400 spectrometer. The chemical shifts were calibrated to the residual solvent peaks or TMS. UV-vis spectra were recorded on a Perkin Elmer Lambda-45 (1 cm cuvettes, methylene chloride) and IR spectra were taken on a Perkin Elmer Spectrum-1 ATR-FT-IR-spectrometer. DSC investigations were performed on a Perkin Elmer Pyris-1 DSC system with a heating rate of 40 K/min ( $T_g$ ). GPC measurements were performed on a Shimadzu GPC-apparatus using a 5  $\mu\text{m}$  PL-gel-mixed-D column (cross-linked polystyrene) with chloroform as eluent and an UV as well as an RI detector. Alternatively, a Waters GPC-apparatus using a Styragel HT column (cross-linked polystyrene) with chloroform containing 4 vol-% triethylamine as eluent, equipped with a 1515 pump, a 717-plus autosampler and a 2414 RI detector, was used. The flow rate was 0.5 mL/min. A poly(ethylene glycol) calibration was utilized. Viscosity investigations were performed on a Schott AVS 350 viscosimetry system using Ubbelohde viscosimeters with a capillary diameter of 0.4 mm and a 1:1 mixture of chloroform/methanol as solvent.

### Poly(methyl methacrylate)-*co*-(2-methyl-acrylic acid 3-(2,2':6',2''-terpyridin-4'-yloxy)-propyl ester) **2a**

Methyl methacrylate (426 mg, 4.26 mmol) and 2-methyl-acrylic acid 3-(2,2':6',2''-terpyridin-4'-yloxy)-propyl ester **1** (80 mg, 0.21 mmol) were dissolved in 5 mL *p*-xylene and heated to 80 °C. Then azo-*bis*(isobutyronitrile) (AIBN, 9.2 mg, 0.056 mmol) was added and heating was continued for 6 hours. After taking a sample for GPC analysis from the crude reaction mixture, the polymer was precipitated in 20 mL pentane yielding 346 mg (68%) of **2a** as a white solid.

UV-vis ( $\text{CH}_3\text{CN}$ ):  $\lambda_{\text{max}}$  ( $\epsilon$ ) = 278 (93400), 249 (87200) nm ( $\text{L mol}^{-1} \text{ cm}^{-1}$ ).

$^1\text{H-NMR}$  (400 MHz;  $\text{CDCl}_3$ ):  $\delta$  (ppm) = 0.83 (br, 30 H,  $\text{CH}_3$ ), 1.01 (br, 20 H,  $\text{CH}_3$ ), 1.80 and 1.89 (br, 32 H,  $\text{CH}_2$ ), 2.19 (m (br), 2 H,  $\text{CH}_2$ ), 3.61 (s, 48 H,  $\text{OCH}_3$ ), 4.19 (m (br), 2 H,  $\text{OCH}_2$ ), 4.33 (m (br), 2 H,  $\text{OCH}_2$ ), 7.40 (m, 2 H,  $\text{H}_{5,5''}$ ), 7.91 (ddd, 2 H,  $J = 8.06, 8.06, 2.20$  Hz,  $\text{H}_{4,4''}$ ), 7.98 (s, 2 H,  $\text{H}_{3,5}$ ), 8.61 (d, 2 H,  $J = 8.06$  Hz,  $\text{H}_{3,3''}$ ), 8.67 (d, 2 H,  $J = 5.86$  Hz,  $\text{H}_{6,6''}$ ).

$^{13}\text{C-NMR}$  (100.6 MHz;  $\text{CDCl}_3$ ):  $\delta$  (ppm) = 16.53 ( $\text{CH}_3$ ), 18.76 ( $\text{CH}_3$ ), 34.16 ( $\text{C}(\text{PMMA})$ ), 44.58 ( $\text{CH}_2(\text{PMMA})$ ), 44.90 ( $\text{CH}_2$ ), 51.82 ( $\text{OCH}_3$ ), 54.43 ( $\text{CH}_2$ ), 64.47 ( $\text{CH}_2$ ), 107.31 ( $\text{H}_{3,5}$ ), 121.35 ( $\text{H}_{5,5''}$ ), 123.89 ( $\text{H}_{3,3''}$ ), 136.83 ( $\text{H}_{4,4''}$ ), 149.05 ( $\text{H}_{6,6''}$ ), 156.03 ( $\text{H}_{2,2''}$ ), 157.19 ( $\text{H}_{2,6}$ ), 169.30 ( $\text{H}_4$ ), 176.94 ( $\text{COO}$ ), 177.80 ( $\text{COO}$ ).

GPC:  $\overline{M}_n = 4500 \text{ g mol}^{-1}$ , PDI = 1.62.

**2b**: See synthesis of **2a** for the general method. 400 mg (4 mmol) methyl methacrylate, 68 mg (0.18 mmol) of **1**, 20 mg (0.12 mmol) of azo-*bis*(isobutyronitrile) (AIBN). Yield 352 mg (88%) of **2b**.

UV-vis ( $\text{CH}_3\text{CN}$ ):  $\lambda_{\text{max}} (\epsilon) = 278 (46800), 249 (43600) \text{ nm (L mol}^{-1} \text{ cm}^{-1})$ .

$^1\text{H-NMR}$  (400 MHz;  $\text{CDCl}_3$ ):  $\delta$  (ppm) = 0.83 (br, 30 H,  $\text{CH}_3$ ), 1.01 (br, 20 H,  $\text{CH}_3$ ), 1.80 and 1.89 (br, 32 H,  $\text{CH}_2$ ), 2.19 (m (br), 2 H,  $\text{CH}_2$ ), 3.61 (s, 48 H,  $\text{OCH}_3$ ), 4.19 (m (br), 2 H,  $\text{OCH}_2$ ), 4.33 (m (br), 2 H,  $\text{OCH}_2$ ), 7.40 (m, 2 H,  $\text{H}_{5,5''}$ ), 7.91 (ddd, 2 H,  $J = 8.06, 8.06, 2.20$  Hz,  $\text{H}_{4,4''}$ ), 7.98 (s, 2 H,  $\text{H}_{3,5}$ ), 8.61 (d, 2 H,  $J = 8.06$  Hz,  $\text{H}_{3,3''}$ ), 8.67 (d, 2 H,  $J = 5.86$  Hz,  $\text{H}_{6,6''}$ ).

GPC:  $\overline{M}_n = 6600 \text{ g mol}^{-1}$ , PDI = 2.06.

**2c**: See synthesis of **2a** for the general method. 273 mg (2.73 mmol) methyl methacrylate, 205 mg (0.055 mmol) of **1**, 6.7 mg (0.041 mmol) of azo-*bis*(isobutyronitrile) (AIBN). Yield 312 mg (65%) of **2c**.

UV-vis ( $\text{CH}_3\text{CN}$ ):  $\lambda_{\text{max}} (\epsilon) = 278 (186700), 249 (174300) \text{ nm (L mol}^{-1} \text{ cm}^{-1})$ .

$^1\text{H-NMR}$  (400 MHz;  $\text{CDCl}_3$ ):  $\delta$  (ppm) = 0.83 (br, 11 H,  $\text{CH}_3$ ), 1.01 (br, 7 H,  $\text{CH}_3$ ), 1.80 and 1.89 (br, 12 H,  $\text{CH}_2$ ), 2.19 (m (br), 2 H,  $\text{CH}_2$ ), 3.61 (s, 18 H,  $\text{OCH}_3$ ), 4.19 (m (br), 2 H,  $\text{OCH}_2$ ), 4.33 (m (br), 2 H,  $\text{OCH}_2$ ), 7.40 (m, 2 H,  $\text{H}_{5,5''}$ ), 7.91 (ddd, 2 H,  $J = 8.06, 8.06, 2.20$  Hz,  $\text{H}_{4,4''}$ ), 7.98 (s, 2 H,  $\text{H}_{3,5}$ ), 8.61 (d, 2 H,  $J = 8.06$  Hz,  $\text{H}_{3,3''}$ ), 8.67 (d, 2 H,  $J = 5.86$  Hz,  $\text{H}_{6,6''}$ ).

GPC:  $\overline{M}_n = 4800 \text{ g mol}^{-1}$ , PDI = 1.78.

### Poly(methyl methacrylate) 3

Methyl methacrylate (800 mg, 8 mmol) was polymerized under the same conditions as compounds **2a-c**. Precipitation in pentane yielded 774 mg (96%) of polymer.

UV-vis ( $\text{CHCl}_3$ ):  $\lambda_{\text{max}} (\epsilon) = 276 (583), 268 (625) \text{ nm (L mol}^{-1} \text{ cm}^{-1})$ .

$^1\text{H-NMR}$  (400 MHz;  $\text{CDCl}_3$ ):  $\delta$  (ppm) = 0.83 (br, 17 H,  $\text{CH}_3$ ), 1.01 (br, 11 H,  $\text{CH}_3$ ), 1.80 and 1.89 (br, 18 H,  $\text{CH}_2$ ), 2.19 (m (br), 2 H,  $\text{CH}_2$ ), 3.61 (s, 27 H,  $\text{OCH}_3$ ).

GPC:  $\overline{M}_n = 5200 \text{ g mol}^{-1}$ , PDI = 1.74.

### UV-vis titration

The solvents were saturated with argon before use. **2a** (3.7 mg) was dissolved in 100 mL of chloroform and stirred under argon. A  $3.76 \times 10^{-4}$  molar solution of iron chloride (in methanol) was added in steps of 50  $\mu\text{L}$ . After every addition, a UV-vis spectrum was recorded after 15 minutes. The absorption value of the maximum of the metal to ligand charge transfer band (MLCT) at 558 nm was used in order to obtain the titration curve.

Equivalence point:  $\lambda_{\text{max}} (\epsilon) = 249 (85300), 273 (109400), 317 (80300), 558 (21300) \text{ nm (L mol}^{-1} \text{ cm}^{-1})$ .

### Viscosity titrations

To 5 mL of a solution of **2a** and **2b** in a chloroform/methanol mixture (1:1) was added stepwise 400  $\mu\text{L}$  of a methanolic solution of  $\text{FeCl}_2$  (in steps of 0.1 or 0.2 equivalents, see Figure 5.5) and the viscosity was measured in an Ubbelohde viscosimeter after each addition. The average of four measurements was taken for each value. The following concentrations were used: Experiment 1: 17.5 mg/mL **2b**,  $\text{FeCl}_2$ . Experiment 2: 17.5 mg/mL **2a**,  $\text{FeCl}_2$ . Experiment 3: 17.5 mg/mL **2b**,  $\text{ZnCl}_2$ . Experiment 4: 17.5 mg/mL **3**,  $\text{FeCl}_2$ .

### Decomplexation of the polymers

0.2 mL of an aqueous solution of HEEDTA (hydroxeethyl(ethylenediaminetetraacetic acid), Trilon D liquid, 39.0–41.0 wt.-%) was added to the polymer-iron-complex solution. After stirring the solution, the purple color of the iron complex disappeared within 2 minutes. The mixture was extracted with 1 mL of dichloromethane and the polymer was recovered by precipitation in pentane. In the same way, 57 mg of the polymer-zinc-complex was treated with 0.4 mL of HEEDTA solution. After extraction and precipitation, 44 mg (85%) of the uncomplexed polymer was obtained.

### Acrylic acid 3-(2,2':6',2''-terpyridin-4'-yloxy)-propyl ester 6

To a solution of 4'-(hydroxypropyloxy)-2,2':6',2''-terpyridine **4** (1.0 g, 3.25 mmol) in 50 mL ice-cooled  $\text{CH}_2\text{Cl}_2$  were added 320 mg (3.57 mmol; 0.288 mL) acryloyl chloride **5** and 493.3 mg (4.88 mmol; 0.5 mL) triethylamine via a syringe. After 30 min, the solution was allowed to warm to room temperature and stirred overnight. The reaction mixture was extracted with an aqueous solution of  $\text{K}_2\text{CO}_3$  ( $3 \times 15$  mL) to neutralize and remove the inorganic salts. The solvent was removed *in vacuo* at room temperature and the product was recrystallized twice from methanol (10 mL) to yield 800 mg (66%) of **6** as white crystals. M.p. 90 °C.

UV-vis (CH<sub>3</sub>CN):  $\lambda_{max}$  ( $\epsilon$ ) = 276 (24200), 240 (26320) nm (L mol<sup>-1</sup> cm<sup>-1</sup>).

<sup>1</sup>H-NMR (400 MHz, CH<sub>3</sub>CN):  $\delta$  (ppm) = 2.23 (tt, 2 H,  $J$  = 6.04, 6.04 Hz, CH<sub>2</sub>), 4.34 (t, 4 H,  $J$  = 6.04 Hz, OCH<sub>2</sub>), 4.39 (t, 4 H,  $J$  = 6.04 Hz, OCH<sub>2</sub>), 5.82 (dd, 1 H,  $J$  = 10.44, 1.10 Hz, H(olefinic)), 6.13 (dd, 1 H,  $J$  = 17.58, 10.44 Hz, H(olefinic)), 6.42 (dd, 1 H,  $J$  = 17.58, 1.10 Hz, H(olefinic)) 7.40 (m, 2 H, H<sub>5,5'</sub>), 7.91 (ddd, 2 H,  $J$  = 8.06, 8.06, 2.20 Hz, H<sub>4,4'</sub>), 7.98 (s, 2 H, H<sub>3,5'</sub>), 8.61 (d, 2 H,  $J$  = 8.06 Hz, H<sub>3,3'</sub>), 8.67 (d, 2 H,  $J$  = 5.86 Hz, H<sub>6,6'</sub>).

GC-MS:  $m/z$  = 361.2 (M<sup>+</sup>).

#### **Poly(butyl acrylate)-*co*-(2-methyl-acrylic acid 3-(2,2':6',2''-terpyridin-4'-yloxy)-propyl ester)-*co*-acryloxetane 10**

437 mg (3.41 mmol) of butyl acrylate **9**, 250 mg (1.25 mmol) of **8** and 106 mg (0.29 mmol) of **6** were dissolved in 2 mL *p*-xylene and heated to 87 °C. Subsequently 12 mg (0.07 mmol) of azo-*bis*(isobutyronitrile) (AIBN) were added and heating was continued for 10 hours. The mixture was precipitated twice in 20 mL pentane followed by preparative size exclusion chromatography yielding 556 mg (70%) of **10** as a white sticky solid.

UV-vis (CHCl<sub>3</sub>):  $\lambda_{max}$  ( $\epsilon$ ) = 279 (52300), 246 (54800) nm (L mol<sup>-1</sup> cm<sup>-1</sup>).

<sup>1</sup>H-NMR (400 MHz, CHCl<sub>3</sub>):  $\delta$  (ppm) 0.97 (br, 57 H, CH<sub>3</sub>), 1.39 (br, 43 H, CH<sub>2</sub>), 1.62 and 1.89 (br, 30 H, CH<sub>2</sub>), 2.19 (m (br), 2 H, CH<sub>2</sub>), 4.03 (s, 28 H, OCH<sub>2</sub>), 4.19 (m (br), 10 H, OCH<sub>2</sub>), 4.36 (d, 10 H,  $J$  = 5.13 Hz, oxetane), 4.43 (d, 10 H,  $J$  = 5.68 Hz, oxetane), 7.32 (m, 2 H, H<sub>5,5'</sub>), 7.83 (dd, 2 H,  $J$  = 8.06, 8.06 Hz, H<sub>4,4'</sub>), 8.02 (s, 2 H, H<sub>3,5'</sub>), 8.61 (d, 2 H,  $J$  = 8.06 Hz, H<sub>3,3'</sub>), 8.67 (d, 2 H,  $J$  = 5.86 Hz, H<sub>6,6'</sub>).

GPC (CHCl<sub>3</sub>):  $\overline{M}_n$  = 7400, PDI = 2.46.

DSC (40 °C/min): T<sub>g</sub> = -23.5 °C.

#### **UV-titration of 10**

4.1 mg of **10** were dissolved in 50 mL of argon-saturated chloroform. A 1.62 × 10<sup>-4</sup> molar solution of iron(II) chloride (in argon-saturated methanol) was added in steps of 40 μL while the mixture was stirred. 30 minutes after every addition a UV-vis spectrum was recorded. The absorption value of the maximum of the metal to ligand charge transfer band (MLCT) at 558 nm was used in order to obtain the titration curve.

#### **Cross-linking of the terpolymer 10**

**Route a:** 24 mg of terpolymer **10** were dissolved in 2 mL of nitromethane and saturated with argon. Subsequently 5 drops of borontetrafluoride etherate were added and the mixture was heated to 60 °C overnight. The resulting material was dried in vacuum. Yield: 18 mg.

**Route b:** 16 mg of **10** were dissolved in 1 mL of dichloromethane. Then 1 mL of a solution of AlCl<sub>3</sub> in dichloromethane was added and the mixture was allowed to react overnight.

**Route c:** To 18 mg of **10** in dichloromethane were added 1 mg of iron(II) chloride in 0.2 mL FeCl<sub>2</sub>. Half of this solution was treated as described in (b).

**Route d:** The material obtained from (a) was covered with dichloromethane and 3 drops of a methanolic solution of FeCl<sub>2</sub> were added.

#### **Poly(methyl methacrylate)-*co*-(methacrylic acid 3-(2,2':6',2''-terpyridin-4'-yloxy)-propyl ester) 12a**

1.33 g (13.3 mmol) of methyl methacrylate and 500 mg (1.33 mmol) of **1** were dissolved in 2 mL *p*-xylene and heated to 75 °C. Then 12 mg (0.07 mmol) of azo-*bis*(isobutyronitrile) (AIBN) was added and heating was continued for 6 hours. The mixture was precipitated twice in 20 mL pentane yielding 1.11 g (62%) of **12a** as a white solid.

UV-vis (CHCl<sub>3</sub>):  $\lambda_{max}$  ( $\epsilon$ ) = 279 (445600), 245 (488100) nm (L·mol<sup>-1</sup>·cm<sup>-1</sup>).

IR (ATR) 1/λ (cm<sup>-1</sup>) = 2994 (m), 2950 (m), 1726 (s), 1601 (w, tpy), 1583 (m, tpy), 1565(m, tpy), 1470 (m), 1445 (m), 1407 (m), 1384 (w), 1362 (w), 1268 (m), 1241 (m), 1191 (s), 1146 (s), 1060 (m), 991 (m), 968 (m), 913 (w), 868 (w), 842 (w), 796 (m), 772 (m), 748 (m), 699 (w), 660 (w).

<sup>1</sup>H-NMR (400 MHz, CHCl<sub>3</sub>):  $\delta$  (ppm) = 0.83 and 1.01 (br, 26 H, CH<sub>3</sub>), 1.80 and 1.86 (br, 18 H, CH<sub>2</sub>), 2.19 (m (br), 2 H, CH<sub>2</sub>), 3.58 (s, 26 H, OCH<sub>3</sub>), 4.19 and 4.33 (m (br), 4 H, OCH<sub>2</sub>), 7.33 (m, 2 H, H<sub>5,5'</sub>), 7.85 (m, 2 H, H<sub>4,4'</sub>), 8.01 (s, 2 H, H<sub>3,5'</sub>), 8.61 (m, 2 H, H<sub>3,3'</sub>), 8.67 (m, 2 H, H<sub>6,6'</sub>).

GPC (DMF):  $\overline{M}_n$  = 24330, PDI = 2.29.

#### **Poly(methyl methacrylate)-*co*-methylepoxidyl methacrylate 12b**

465 mg (4.65 mmol) of methyl methacrylate and 283 mg (1.99 mmol) of **11** were dissolved in 2 mL *p*-xylene and heated to 75 °C. Then 5.45 mg (0.03 mmol) of azo-*bis*(isobutyronitrile) (AIBN) was added and heating was continued for 6 hours. The mixture was precipitated twice in 20 mL pentane yielding 732 mg (97%) of **12b** as a white solid.

UV-vis (CHCl<sub>3</sub>):  $\lambda_{max}$  ( $\epsilon$ ) = 269 (3100), 2276 (2900) nm (L·mol<sup>-1</sup>·cm<sup>-1</sup>).

IR (ATR) 1/λ (cm<sup>-1</sup>) = 2994 (m), 2950 (m), 1726 (s), 1470 (m), 1445 (m), 1407 (m), 1384 (w), 1362 (w), 1268 (m), 1241 (m), 1191 (s), 1146 (s), 1060 (m), 991 (m), 968 (m), 908 (m, epoxide), 847 (m, epoxide), 796 (m), 748 (m), 699 (w), 660 (w).



$^1\text{H-NMR}$  (400 MHz,  $\text{CHCl}_3$ ):  $\delta$  (ppm) = 0.87 and 1.03 (br, 6 H,  $\text{CH}_3$ ), 1.84 and 1.93 (m (br), 4 H,  $\text{CH}_2$ ), 2.64 (s, 1 H, epoxide), 2.85 (s, 1 H, epoxide), 3.22 (s, 1 H, epoxide), 3.60 (s, 3 H,  $\text{OCH}_3$ ), 3.80 (m (br), 1 H,  $\text{OCH}_2$ ), 4.30 (m (br), 1 H,  $\text{OCH}_2$ ).

GPC (DMF):  $\overline{M}_n = 24660$ , PDI = 5.85, negative tailing.

**Poly(methyl methacrylate)-*co*-(methacrylic acid 3-(2,2':6',2''-terpyridin-4'-yloxy)-propyl ester)-*co*-methyl-epoxidyl methacrylate 12c**

437 mg (3.41 mmol) of methyl methacrylate, 250 mg (1.25 mmol) of **1** and 106 mg (0.29 mmol) of **11** were dissolved in 2 mL *p*-xylene and heated to 65 °C. Then 12 mg (0.12 mmol) of benzoylperoxide (BPO) was added and heating was continued for 10 hours. The mixture was precipitated twice in 20 mL pentane followed by size exclusion chromatography yielding 556 mg (70%) of **12c** as a white solid.

UV-vis ( $\text{CHCl}_3$ ):  $\lambda_{\text{max}}$  ( $\epsilon$ ) = 279 (52300), 246 (54800) nm ( $\text{L}\cdot\text{mol}^{-1}\cdot\text{cm}^{-1}$ ).

IR (ATR)  $1/\lambda$  ( $\text{cm}^{-1}$ ) = 2994 (m), 2950 (m), 1726 (s), 1601 (w, tpy), 1583 (m, tpy), 1565 (m, tpy), 1470 (m), 1445 (m), 1407 (m), 1384 (w), 1362 (w), 1268 (m), 1241 (m), 1191 (s), 1146 (s), 1060 (m), 991 (m), 968 (m), 908 (m, epoxide), 847 (m, epoxide), 796 (m), 748 (m), 699 (w), 660 (w).

$^1\text{H-NMR}$  (400 MHz,  $\text{CHCl}_3$ ):  $\delta$  (ppm) = 0.87 and 1.03 (br, 24 H,  $\text{CH}_3$ ), 1.84 (br, 17 H,  $\text{CH}_2$ ), 2.19 (m (br), 2 H,  $\text{CH}_2$ ), 2.63 (s, 2 H, epoxide), 2.84 (s, 2 H, epoxide), 3.21 (s, 2 H, epoxide), 3.59 (s, 16 H,  $\text{OCH}_3$ ), 4.43 (m (br), 4 H,  $\text{OCH}_2$ ), 7.36 (m, 2 H,  $\text{H}_{5,5''}$ ), 7.88 (dd, 2 H,  $J = 7.32, 7.32$  Hz,  $\text{H}_{4,4''}$ ), 8.06 (s, 2 H,  $\text{H}_{3,3''}$ ), 8.63 (d, 2 H,  $J = 7.32$  Hz,  $\text{H}_{3,3''}$ ), 8.70 (d, 2 H,  $J = 5.86$  Hz,  $\text{H}_{6,6''}$ ).

GPC ( $\text{CHCl}_3$ ):  $\overline{M}_n = 17000$ , PDI = 2.7, negative tailing.

**Poly(methyl methacrylate)-*co*-(methacrylic acid 3-(2,2':6',2''-terpyridin-4'-yloxy)-propyl ester)-*co*-methyl-epoxidyl methacrylate 12d**

478 mg (4.78 mmol) of methyl methacrylate, 300 mg (0.67 mmol) of **1** and 340 mg (2.39 mmol) of **11** were dissolved in 2 mL *p*-xylene and heated to 75 °C. Then 6.5 mg (0.03 mmol) of azobisisobutyronitrile (AIBN) was added and heating was continued for 6 hours. The mixture was precipitated twice in 20 mL pentane yielding 1.08 g (96%) of **12d** as a white solid.

UV-vis ( $\text{CHCl}_3$ ):  $\lambda_{\text{max}}$  ( $\epsilon$ ) = 279 (421100), 246 (427600) nm ( $\text{L}\cdot\text{mol}^{-1}\cdot\text{cm}^{-1}$ ).

IR (ATR)  $1/\lambda$  ( $\text{cm}^{-1}$ ) = 2994 (m), 2950 (m), 1726 (s), 1601 (w, tpy), 1583 (m, tpy), 1565 (m, tpy), 1470 (m), 1445 (m), 1407 (m), 1384 (w), 1362 (w), 1268 (m), 1241 (m), 1191 (s), 1146 (s), 1060 (m), 991 (m), 968 (m), 908 (m, epoxide), 847 (m, epoxide), 796 (m), 748 (m), 699 (w), 660 (w).

$^1\text{H-NMR}$  (400 MHz,  $\text{CHCl}_3$ ):  $\delta$  (ppm) = 0.87 and 1.03 (br, 27 H,  $\text{CH}_3$ ), 1.85 (br, 20 H,  $\text{CH}_2$ ), 2.19 (m, 2 H,  $\text{CH}_2$ ), 2.63 (s, 4.5 H, epoxide), 2.84 (s, 4.5 H, epoxide), 3.21 (s, 4.5 H, epoxide), 3.59 (s, 13H,  $\text{OCH}_3$ ), 4.43 (m (br), 4 H,  $\text{OCH}_2$ ), 7.34 (m, 2 H,  $\text{H}_{5,5''}$ ), 7.86 (m, 2 H,  $\text{H}_{4,4''}$ ), 8.03 (s, 2 H,  $\text{H}_{3,3''}$ ), 8.63 (m, 2 H,  $\text{H}_{3,3''}$ ), 8.69 (m, 2 H,  $\text{H}_{6,6''}$ ).

GPC (DMF):  $\overline{M}_n = 31650$ , PDI = 5.47, negative tailing.

**UV-vis titration of 12c**

4.1 mg of **12c** were dissolved in 50 mL of chloroform. A  $1.62 \times 10^{-4}$  molar solution of iron(II)chloride (in methanol) was added in steps of 40  $\mu\text{L}$  while the mixture was stirred. 15 minutes after every addition a spectrum was recorded.

**Covalent cross-linking of the terpolymer 12d**

**Route a:** 65 mg of **12d** were dissolved in 10 mL of dichloromethane. Subsequently 1 mL of a solution of  $\text{AlCl}_3$  in dichloromethane was added and the mixture was allowed to react for 2 hours.

**Route b:** 3 mg of iron(II) chloride in 1 mL of methanol were added to 65 mg of **12d** in 10 mL of dichloromethane.

**Route c:** The product obtained from (b) was treated with  $\text{AlCl}_3$  as described in (a).

**Route d:** A sample of the material obtained from (a) was covered with dichloromethane and 30  $\mu\text{L}$  of a methanolic solution of  $\text{FeCl}_2$  ( $8 \times 10^{-3}$  M) were added.

**Gel formation studies**

Solutions of  $\text{FeCl}_2$ ,  $\text{ZnCl}_2$  and  $\text{Co}(\text{NO}_3)_2$  (0.5 mL of 0.14 mol/L solutions in methanol) were added to solutions (2 mL, 42 mg/mL) of copolymer **12a** in chloroform. The obtained gel and the gels yielded from **12d** (routes b and d) were weighed in the swollen state (chloroform) as well as dry state and the swelling factors  $Q$  were calculated.

**Poly(methyl methacrylate)-*co*-(hydroxyethyl methacrylate)-*co*-(methacrylic acid 3-(2,2':6',2''-terpyridin-4'-yloxy)-propyl ester) 13**

0.48 mL (4.51 mmol) of methyl methacrylate, 0.07 mL (0.58 mmol) of hydroxyethyl methacrylate and 213 mg (0.568 mmol) of **1** were dissolved in 2 mL *p*-xylene and heated to 75 °C. Then 18 mg (11.32 mmol) of

azobis(isobutyronitrile) (AIBN) was added and heating was continued for 4 hours. The mixture was precipitated twice in 20 mL pentane yielding 688 mg (93%) of **13** as a white solid.

UV-vis (CHCl<sub>3</sub>):  $\lambda_{max}$  ( $\epsilon$ ) = 279 (53600), 243 (52000) nm (L·mol<sup>-1</sup>·cm<sup>-1</sup>).

IR (ATR) 1/ $\lambda$  (cm<sup>-1</sup>) = 3523 (br, OH), 2994 (m), 2950 (m), 1726 (s), 1601 (w, tpy), 1583 (m, tpy), 1565 (m, tpy), 1470 (m), 1445 (m), 1407 (m), 1384 (w), 1362 (w), 1268 (m), 1241 (m), 1191 (s), 1146 (s), 1060 (m), 991 (m), 968 (m), 913 (w), 868 (w), 842 (w), 796 (m), 772 (m), 748 (m), 699 (w), 660 (w).

<sup>1</sup>H-NMR (400 MHz, CHCl<sub>3</sub>):  $\delta$  (ppm) = 0.83 and 1.02 (br, 36 H, CH<sub>3</sub>), 1.67 and 1.81 (br, 24 H, CH<sub>2</sub>), 2.40 (m, 2 H, OH), 3.59 (s, 24 H, OCH<sub>3</sub>), 3.84 (4 H, OCH<sub>2</sub>, HEMA), 4.12 and 4.35 (m (br), 8 H, OCH<sub>2</sub>), 7.32 (m, 2 H, H<sub>5,5''</sub>), 7.86 (m, 2 H, H<sub>4,4''</sub>), 8.02 (s, 2 H, H<sub>3',5'</sub>), 8.60 (m, 2 H, H<sub>3,3''</sub>), 8.67 (m, 2 H, H<sub>6,6''</sub>).

GPC (chloroform):  $\overline{M}_n$  = 3800, PDI = 3.98.

#### **Poly(methyl methacrylate)-co-(methacryloyl methacrylate)-co-(methacrylic acid 3-(2,2':6',2''-terpyridin-4'-yloxy)-propyl ester) 14**

100 mg (0.026 mmol) of the HEMA-terpolymer **1** were dissolved in dichloromethane and 14.6 mg (0.30 mL, 0.14 mmol) of methacryloylchloride and 0.45 mL of triethylamine were added under ice-cooling and stirring. After defrosting, stirring was continued overnight. Subsequently, 30 mL of an aqueous solution of potassium carbonate was added and the mixture was extracted three times. After drying of the organic phase, the solvent was removed in vacuum under ambient temperature. The product **14** was purified by preparative size-exclusion chromatography utilizing a BioBeads SX-1 column. Yield: 84 mg (81%).

UV-vis (CHCl<sub>3</sub>):  $\lambda_{max}$  ( $\epsilon$ ) = 243 (47000), 279 (46200) nm (L·mol<sup>-1</sup>·cm<sup>-1</sup>).

IR (ATR) 1/ $\lambda$  (cm<sup>-1</sup>) = 2994 (m), 2950 (m), 1726 (s), 1636 (w, olefinic), 1601 (w, tpy), 1583 (m, tpy), 1565 (m, tpy), 1470 (m), 1445 (m), 1407 (m), 1384 (w), 1362 (w), 1268 (m), 1241 (m), 1191 (s), 1146 (s), 1060 (m), 991 (m), 968 (m), 913 (w), 868 (w), 842 (w), 796 (m), 772 (m), 748 (m), 699 (w), 660 (w).

<sup>1</sup>H-NMR (400 MHz, CHCl<sub>3</sub>):  $\delta$  (ppm) = 0.83 and 1.02 (br, 36 H, CH<sub>3</sub>), 1.67 and 1.81 (br, 24 H, CH<sub>2</sub>), 3.59 (s, 24 H, OCH<sub>3</sub>), 4.19 (m, 6 H, OCH<sub>2</sub>), 4.37 (m, 6 H, OCH<sub>2</sub>), 5.63 (s, 2 H, olefinic), 6.14 (s, 2 H, olefinic), 7.32 (m, 2 H, H<sub>5,5''</sub>), 7.86 (m, 2 H, H<sub>4,4''</sub>), 8.02 (s, 2 H, H<sub>3',5'</sub>), 8.60 (m, 2 H, H<sub>3,3''</sub>), 8.67 (m, 2 H, H<sub>6,6''</sub>).

GPC (chloroform):  $\overline{M}_n$  = 8200, PDI = 1.58 after BioBeads size-exclusion column.

#### **Poly(methyl methacrylate)-co-(acryloyl methacrylate)-co-(methacrylic acid 3-(2,2':6',2''-terpyridin-4'-yloxy)-propyl ester) 15**

100 mg (0.026 mmol) of the HEMA-terpolymer **1** were dissolved in dichloromethane and 12.6 mg (0.32 mL, 0.14 mmol) of methacryloylchloride and 0.45 mL of triethylamine were reacted analogous to the synthesis of polymer **15**. Yield: 79 mg (77%).

UV-vis (CHCl<sub>3</sub>):  $\lambda_{max}$  ( $\epsilon$ ) = 245 (50800), 279 (49100) nm (L·mol<sup>-1</sup>·cm<sup>-1</sup>).

IR (ATR) 1/ $\lambda$  (cm<sup>-1</sup>) = 2994 (m), 2950 (m), 1726 (s), 1636 (w, olefinic), 1601 (w, tpy), 1583 (m, tpy), 1565 (m, tpy), 1470 (m), 1445 (m), 1407 (m), 1384 (w), 1362 (w), 1268 (m), 1241 (m), 1191 (s), 1146 (s), 1060 (m), 991 (m), 968 (m), 913 (w), 868 (w), 842 (w), 796 (m), 772 (m), 748 (m), 699 (w), 660 (w).

<sup>1</sup>H-NMR (400 MHz, CHCl<sub>3</sub>):  $\delta$  (ppm) = 0.83 and 1.02 (br, 36 H, CH<sub>3</sub>), 1.67 and 1.81 (br, 24 H, CH<sub>2</sub>), 3.59 (s, 24 H, OCH<sub>3</sub>), 4.19 (m, 6 H, OCH<sub>2</sub>), 4.37 (m, 6 H, OCH<sub>2</sub>), 5.90 (m, 2 H, olefinic), 6.18 (m, 2 H, olefinic), 6.47 (m, 2 H, olefinic), 7.32 (m, 2 H, H<sub>5,5''</sub>), 7.86 (m, 2 H, H<sub>4,4''</sub>), 8.02 (s, 2 H, H<sub>3',5'</sub>), 8.60 (m, 2 H, H<sub>3,3''</sub>), 8.67 (m, 2 H, H<sub>6,6''</sub>).

GPC (chloroform):  $\overline{M}_n$  = 10500, PDI = 1.70 after BioBeads size exclusion column.

#### **Thermal curing of terpolymer 13**

**Route a:** 20 mg of **13** were dissolved in 0.2 mL of dichloromethane. Subsequently 0.38  $\mu$ L 1,6-hexanebisocyanate **16** was added. A film was applied onto a glass surface and heated to 100 °C for 15 and 30 minutes, respectively. The materials (after removing from the surface) were investigated by ATR-IR spectroscopy. Also the uncured polymer was measured for comparison.

**Route b:** A particle of the cured material of **13** (route a) was covered with 0.1 mL of dichloromethane and 0.2 mg of iron(II) chloride in 1 mL of methanol was added.

**Route c:** To a solution of **13** in dichloromethane (a) FeCl<sub>2</sub> was added as described in (b). After evaporation of the solvent, a solution of **16** was added. A film of the complexed terpolymer was cured at 100 °C. The uncured as well as the cured samples were investigated by IR spectroscopy.

#### **UV-curing of polymers 14 and 15**

The terpolymers (solution in dichloromethane) were mixed with 5 mass-% Irgacure-photoinitiator. A film was applied onto a KBr plate and a transmission-IR spectrum was recorded. The film was cured for 5 minutes.

## 5.8 References

- [1] [1a] J.-M. Lehn, *Supramolecular Chemistry, Concepts and Perspectives*, VCH, Weinheim, **1995**; [1b] U. S. Schubert, in *Tailored Polymers & Applications* (Ed.: M. K. M. Y. Yagci, O. Nuyken, K. Ito, G. Wnek), VSP Publishers, Utrecht, **2000**, 63-85.
- [2] J.-M. Lehn, *Makromol. Chem., Macromol. Symp.* **1993**, *69*, 1-17.
- [3] U. S. Schubert, M. Heller, *Chem. Eur. J.* **2001**, *7*, 5252-5259.
- [4] L. Brunsveld, B. J. B. Folmer, E. W. Meijer, R. P. Sijbesma, *Chem. Rev.* **2001**, *101*, 4071-4097.
- [5] U. S. Schubert, C. Eschbaumer, *Angew. Chem.* **2002**, *114*, 3016-3050, *Angew. Chem. Int. Ed.* **2002**, *41*, 2892-2926.
- [6] [6a] S. Kelch, M. Rehahn, *Macromolecules* **1999**, *32*, 5818-5828; [6b] S. Kelch, M. Rehahn, *Chem. Commun.* **1999**, 1123-1124; [6c] U. S. Schubert, O. Hien, C. Eschbaumer, *Macromol. Rapid Commun.* **2000**, *21*, 1156-1161.
- [7] R. P. Sijbesma, F. H. Beijer, L. Brunsveld, B. J. Folmer, J. H. Hirschberg, R. F. Lange, J. K. Lowe, E. W. Meijer, *Science* **1997**, *278*, 1601-1604.
- [8] C. D. Eisenbach, U. S. Schubert, *Macromolecules* **1993**, *26*, 7372-7374.
- [9] B. G. G. Lohmeijer, U. S. Schubert, *Angew. Chem.* **2002**, *114*, 3980-3984, *Angew. Chem. Int. Ed.* **2002**, *41*, 3825-3829.
- [10] [10a] X. Wu, J. E. Collins, J. E. McAlvin, R. W. Cutts, C. L. Fraser, *Macromolecules* **2001**, *34*, 2812-2821; [10b] C. L. Fraser, A. P. Smith, X. Wu, *J. Am. Chem. Soc.* **2000**, *122*, 9026-9027; [10c] P. S. Corbin, M. P. Webb, J. E. McAlvin, C. L. Fraser, *Biomacromolecules* **2001**, *2*, 223-232; [10d] G. Hochwimmer, O. Nuyken, U. S. Schubert, *Macromol. Rapid Commun.* **1998**, *19*, 309-313.
- [11] U. S. Schubert, H. Hofmeier, *Macromol. Rapid Commun.* **2002**, *23*, 561-566.
- [12] J.-F. Gohy, B. G. G. Lohmeijer, U. S. Schubert, *Macromolecules* **2002**, *35*, 4560-4563.
- [13] L. R. Rieth, R. F. Eaton, G. W. Coates, *Angew. Chem.* **2001**, *113*, 2211-2214, *Angew. Chem. Int. Ed.* **2001**, *40*, 2153-2156.
- [14] R. Stadler, M. A. de Araujo, M. Kuhrau, J. Rösch, *Makromol. Chem.* **1989**, *190*, 1433-1443.
- [15] [15a] Y. Chujo, K. Sada, T. Saegusa, *Macromolecules* **1993**, *26*, 6315-6319; [15b] Y. Chujo, K. Sada, T. Saegusa, *Macromolecules* **1993**, *26*, 6320-6323.
- [16] M. Heller, U. S. Schubert, *Macromol. Rapid Commun.* **2001**, *22*, 1358-1363.
- [17] J. J. S. Lamba, C. L. Fraser, *J. Am. Chem. Soc.* **1997**, *119*, 1801-1802.
- [18] B. Lahn, M. Rehahn, *e-polymers* **2002**, *001*, 1-33.
- [19] U. S. Schubert, C. Eschbaumer, P. R. Andres, H. Hofmeier, C. H. Weidl, E. Herdtweck, E. Dulkeith, A. Morteani, N. E. Hecker, J. Feldmann, *Synth. Met.* **2001**, *121*, 1249-1252.
- [20] K. Hanabusa, K. Nakano, T. Koyana, H. Shirai, N. Hojo, A. Kurose, *Makromol. Chem.* **1990**, *191*, 391-396.
- [21] K. J. Calzia, G. N. Tew, *Macromolecules* **2002**, *35*, 6090-6093.
- [22] M. Heller, U. S. Schubert, *Macromol. Rapid Commun.* **2002**, *23*, 411-415.
- [23] R. H. Holyer, C. D. Hubbard, S. F. A. Kettle, R. G. Wilkins, *Inorg. Chem.* **1966**, *5*, 622-625.
- [24] S. Schmatloch, M. F. Gonzalez, U. S. Schubert, *Macromol. Rapid Commun.* **2002**, *23*, 957-961.
- [25] K. Chino, M. Ashiura, *Macromolecules* **2001**, *34*, 9201-9204.

- [26] [26a] C. C. Roffey, *Photopolymerization of Surface Coatings*; Wiley: Chichester, England, **1982**; [26b] S. P. Pappas, *UV-curing science and Technology*; Technology Marketing: Stanford, CT, **1978** and **1985**, vols. 1 and 2; [26c] A. El-Ghayoury, C. Boukaftane, B. de Ruyter, R. van der Linde, *J. Polym. Sci. A* **2003**, *414*, 469-475.
- [27] L. Brunsveld, B. J. B. Folmer, E. W. Meijer, *MRS Bulletin* **2000**, *25(4)*, 49-54.
- [28] [28a] Abstracts of the Smart Coatings Conference **2002**, Berlin; [28b] H. Hofmeier, U. S. Schubert, *Polym. Preprints* **2003**, *44*, 91-92.
- [29] G. Moad, D. H. Solomon, *The Chemistry of Free Radical Polymerization*, Elsevier Science: Oxford, England, **1995**.
- [30] Reviews on the cationic ring-opening polymerization of oxetane: [30a] Dreyfuss, M. P.; *Oxetane polymers*, in: *Encyclopedia of Polymer Science and Engineering*, 2nd edition, Mark, H. F.; Bikales N. M.; Overberger, C. G.; Menges, G.; Eds. John Wiley and Sons, New York, **1987**, p. X/751; [30b] S. Penzek, P. Kubisa, *Cationic Ring-Opening Polymerization: Ethers*, in: *Comprehensive Polymer Science*, G. Allen, Ed., Pergamon Press, Oxford **1989**, p. III/751; [30c] H. Desai, *Telechelic Polyoxetanes*, in: *Polymeric Materials Encyclopedia*, J. C. Salamone, Ed., CRC Press, New York **1996**, p. XI/8286.
- [31] Y. Xu, H. Ogawa, S. Kanoh, M. Motoi, *Polym. J.* **1999**, *31*, 143-149.
- [32] C. Decker, *Macromol. Symp.* **1999**, *143*, 45-63.
- [33] H. Sasaki, *Design and Application of Photo-Curable Oxetane System*, Ph. D. Thesis, **1996**, Hokkaido, Japan.
- [34] H. Sasaki, J. V. Crivello, *J. Macromol. Sci., Pure Appl. Chem.* **1992**, *A29*, 915-930.
- [35] H. Hofmeier, U. S. Schubert, *Macromol. Chem. Phys.* **2003**, *204*, 1391-1397.
- [36] [36a] H.-J. Tai, J. B. Wang, J.-H. Chen, H.-L. Chou, *J. Appl. Polym. Sci.* **2001**, *79*, 652-661; [36b] P. J. Flory, *Principles in Polymer Chemistry*, Cornell Univ. Press, Ithaca, New York, 1953.
- [37] [37a] D. A. Wicks, Z. W. Wicks Jr., *Progr. Org. Coatings* **1999**, *36*, 148-172; [37b] D. A. Wicks, Z. W. Wicks Jr., *Progr. Org. Coatings* **2001**, *41*, 1-83.
- [38] U. Sampath, W. C. Putnam, T. A. Osiek, S. Touami, J. Xie, D. Cohen, A. Cagnolini, P. Droege, D. Klug, C. L. Barnes, A. Modak, J. K. Bashkin, S. S. Jurisson, *J. Chem. Soc., Dalton Trans.* **1999**, 2049-2058.
- [39] U. S. Schubert, S. Schmatloch, A. A. Precup, *Design. Monom. Polym.* **2002**, *5*, 211-221.
- [40] M. Arisawa, C. Kato, H. Kaneko, A. Nishida, M. Nakagawa, *J. Chem. Soc., Perkin Trans 1* **2000**, 1873-1876.



## Summary

The aim of this thesis is to contribute to the development of new functional metallo-supramolecular polymers, in particular with respect to potential applications, e.g. in coatings technology. To achieve that goal, covalent polymer chains were combined with the metallo-supramolecular chemistry of functionalized terpyridine moieties. These chelate ligands have excellent complexation abilities with a large variety of transition metal ions and have therefore evolved to one of the major building blocks for the construction of supramolecular materials. In particular terpyridine ruthenium(II) complexes play an important role, since they support the directed synthesis of asymmetric complexes, allowing the construction of extended functional hetero-structures. The basis of the ruthenium-terpyridine supramolecular chemistry is presented in the second part of this thesis (following an extensive review in the first chapter), focussing on the preparation and properties of model complexes of functionalized terpyridine ligands. Among these are also complexes bearing chiral groups, which form chiral aggregates in apolar solvents.

In the third part, the gained knowledge was applied to the construction of linear metallo-supramolecular polymers. Small organic as well as polymeric precursors with terpyridine functions at the chain ends were used. Film-forming coordination polymers of high molecular weight could be obtained, which were investigated in detail by viscosity measurements. Moreover, the visco-elastic properties were studied which represent, to the best of our knowledge, the first rheological investigations of such metallo-supramolecular polymers. Finally, thermogravimetric analysis revealed an improved stability of the coordination polymers compared to the analogous conventional polymers. Moreover, we combined the chemistry of terpyridine metal complexes for the first time with the supramolecular chemistry of ureidopyrimidinone moieties, resulting in a new class of supramolecular polymers, containing alternating metal coordination units and quadruple hydrogen bonds.

The fourth part of the thesis describes the design of metallo-supramolecular graft copolymers. Poly(methyl methacrylate) copolymers containing pendant terpyridine moieties were prepared for this purpose. The ligands were subsequently used for grafting reactions utilizing ruthenium(III)/(II)-chemistry. The prepared materials include amphiphilic systems, which formed spherical micelles in aqueous solution. These nano-objects have been studied in detail by dynamic light scattering, transmission electron microscopy and atomic force microscopy both in solid state and solution.

Finally, the possibility of supramolecular cross-linking through metal coordination was investigated. Various metal ions were added to solutions of terpyridine-containing copolymers. Cross-linking was studied in diluted solution by means of viscometry as well as at higher concentrations where gels could be obtained. Subsequently, supramolecular cross-linking was combined with the widely-used covalent cross-linking. To this end, terpolymers were synthesized, containing a covalent cross-linkable functionality besides a terpyridine

ligand. Cross-linking by ring-opening of epoxides and oxetanes as well as free radical cross-linking and thermal curing (urethane formation) was also studied.

The obtained results represent a first step towards potential applications as "smart materials" in coatings technology, including reversible or "switchable" coatings and glues, which could finally be permanently cured by covalent cross-linking. Supramolecular polymers based on terpyridine ruthenium(II) complexes also possess "switchability", as was demonstrated recently. Moreover, the photophysical properties of the ruthenium(II) complexes might allow application of the corresponding metallopolymers in solar cells.

In conclusion, the knowledge of metallo-supramolecular polymers has been extended successfully and the way to potential applications of such materials has been paved.

## Zusammenfassung

Das Ziel dieser Doktorarbeit ist ein Beitrag zur Entwicklung neuer funktioneller metallo-supramolekularer Polymere, insbesondere in Hinsicht auf neuartige Anwendungen. Hierfür wurden klassische Polymere mit der metallo-supramolekularen Chemie von funktionalisierten Terpyridinen kombiniert. Diese Chelatliganden besitzen vorzügliche Komplexbildungseigenschaften für eine große Bandbreite verschiedener Übergangsmetall-Ionen und entwickelten sich deswegen zu einem der wichtigsten Bausteine für supramolekulare Materialien. In diesem Gebiet spielen Terpyridin-Ruthenium(II)-Komplexe eine besondere Rolle, denn sie ermöglichen die gerichtete Synthese asymmetrischer Komplexe und erlauben deshalb den Aufbau ausgedehnter funktioneller Heterostrukturen. Die Grundlagen zur supramolekularen Chemie der Ruthenium-Terpyridin-Komplexe sind im zweiten Kapitel beschrieben (einem ausführlichem Review im ersten Kapitel nachfolgend). Der Fokus liegt in der Präparation und Charakterisierung von Modellkomplexen funktionalisierter Terpyridinliganden. Darunter befinden sich auch Komplexe, welche chirale Liganden tragen und chirale Aggregate in apolaren Lösemitteln bilden.

Im dritten Kapitel wurde das gewonnene Wissen für die Konstruktion linearer metallo-supramolekularer Polymere angewendet. Hierfür wurden kleine organische und auch polymere Vorstufen eingesetzt, welche Terpyridin-Funktionalitäten an den Kettenenden trugen. Als Ergebnis konnten filmbildende hochmolekulare Koordinationspolymere erhalten werden, welche im Detail mittels Viskositätsmessungen analysiert wurden. Darüber hinaus wurden nach unserem Wissenstand zum erstenmal die viskoelastischen Eigenschaften derartiger Systeme erforscht. Zuletzt konnte eine erhöhte Stabilität dieser Koordinationspolymere im Vergleich zu den analogen konventionellen Polymeren mittels thermogravimetrischer Analyse nachgewiesen werden. Darüberhinaus wurde die Chemie der Terpyridinkomplexe erstmals mit der supramolekularen Chemie von Ureidopyrimidinon-Einheiten kombiniert. Das Ergebnis ist eine neue Klasse supramolekularer Polymere mit abwechselnden Metallkoordinations-Gruppen und Vierfach-Wasserstoffbrückenbindungen.

Der vierte Teil dieser Dissertation beschreibt das Design von metallo-supramolekularen Graft-Copolymeren. Zu diesem Zweck wurden Poly(methyl methacrylat) Copolymere mit freien Terpyridineinheiten in der Seitenkette hergestellt und nachfolgend unter Anwendung der Ruthenium(III)/(II)-Chemie für Grafting-Reaktionen benutzt. Unter den synthetisierten Materialien befand sich ein amphiphiles System, aus welchem sphärische Mizellen in wässriger Lösung erhalten wurden. Diese Nano-Objekte wurden im Detail mittels dynamischer Lichtstreuung, Transmissionselektronenmikroskopie und Rasterkraftmikroskopie in Festphase und in Lösung studiert.

Im letzten Teil dieser Arbeit wurden die Möglichkeiten zur supramolekularen Vernetzung untersucht. Terpyridin-haltige Copolymere wurden mit verschiedenen Metall-Ionen versetzt und die Vernetzung in verdünnter Lösung mittels Viskosimetrie untersucht. Weiterhin wurde die Gelbildung bei höheren Konzentrationen studiert. Danach wurde die supramolekulare



Vernetzung mit der weitverbreiteten kovalenten Vernetzung kombiniert. Hierfür wurden Terpolymere synthetisiert, welche eine kovalent vernetzbare Funktionalität neben einem Terpyridinliganden enthalten. Vernetzung durch Ringöffnung von Epoxiden und Oxetanen als auch radikalische Vernetzung und thermische Vernetzung mittels Urethanbildung wurde untersucht.

Die erhaltenen Ergebnisse stellen einen ersten Schritt in Richtung potentieller Anwendungen als "intelligente Materialien" in der Lacktechnologie dar, beispielsweise reversible oder "schaltbare" Beschichtungen und Klebstoffe, welche in einem zweiten Vernetzungsschritt fixiert werden können. Auch die auf Terpyridin-Ruthenium(II)-Komplexen basierenden supramolekularen Polymere besitzen eine potentielle "Schaltbarkeit", wie unlängs beschrieben wurde. Darüberhinaus sollten die photophysikalischen Eigenschaften der Ruthenium(II)-Komplexe zukünftige Anwendungen der entsprechenden Metallopolymere in Solarzellen ermöglichen.

Zusammenfassend wurde das Wissen über metallo-supramolekulare Polymere mit dieser Dissertation erfolgreich erweitert und der Weg zu potentiellen Anwendungen geebnet.

## Acknowledgement

I especially acknowledge

### **Professor Dr. Ulrich S. Schubert**

for admission in his research group, the assignment to this interesting research project and for a personal and friendly supervision of this work, giving me a lot of motivation.

Furthermore, I would like to thank all people who helped for making this thesis possible:

*Prof. Dr. Matthias Rehahn, Prof. Dr. Roeland J. M. Nolte, Prof. Dr. J.-F. Gohy and Dr. Alan Rowan* for reading the thesis as members of the commission.

*Dr. Abdelkrim El-ghayoury and Prof. Dr. Jean-François Gohy* for fruitful collaborations resulting in several joined publications.

*Christian Eschbaumer, Philip Andres and Michael Meier* for MALDI-TOF-measurements.

*Marcel Heller, Bas Lohmeijer, Richard Hoogenboom, Christian Eschbaumer, Philip Andres, Stefan Schmatloch, Gaby van Gemert and Dr. Michel Franssen* for the synthesis of precursors.

*Dr. Marielle Wouters* for rheological measurements.

*Daan Wouters and Dr. Alexander Alexeev* for AFM measurements.

*Philip Andres, Bas Lohmeijer, Richard Hoogenboom, Dr. Stefan Schmatloch and especially Nico Adams* for proof-reading of manuscripts.

*Dr. Eberhardt Herdtweck* for X-ray structure analysis.

*Eric Dulkeith and Arne Morteani* for low-temperature fluorescence measurements.

*Dr. Nikhil Singha, Sachin Jain and Dr. Berend-Jan de Gans* for helpful discussions.

*Prof. Dr. Oskar Nuyken* for providing me a space in his laboratories in Munich.

All colleagues in Munich and Eindhoven for a helpful and friendly atmosphere.

The Deutsche Forschungsgemeinschaft (SFB 486), the Fonds der Chemischen Industrie and the TU Eindhoven for financing this project.

## Curriculum vitae



Harald Hofmeier was born on 6 September 1972 in Heidelberg (Germany). After finishing his Abitur in 1992 in Heidelberg, he started studying chemistry at the *Universität Heidelberg* in 1992, where he received his diploma in 1999 under the supervision of Prof. Dr. H. Irgartinger. His diploma thesis dealt with "Spacerkontrollierte Fernfunktionalisierung von Fullerenen". In the same year, he started his Ph.D. program at the *Technische Universität München* (Germany) under supervision of Prof. Dr. U. S. Schubert. In 2001 he moved to Eindhoven University of Technology, the Netherlands, to complete his Ph.D program. The results of his research are presented in this thesis.

## List of publications

### Refereed publications

U. S. Schubert, C. Eschbaumer, P. Andres, H. Hofmeier, C. H. Weidl, E. Herdtweck, E. Dulkeith, A. Morteani, N. E. Hecker, J. Feldmann: "2,2':6',2"-Terpyridine metal complexes as building blocks for extended functional metallo-supramolecular assemblies and polymers", *Synth. Met.* **2001**, *121*, 1249-1252.

U. S. Schubert, H. Hofmeier: "Metallo-supramolecular graft copolymers: a novel approach for polymeranalogous reactions", *Macromol. Rapid Commun.* **2002**, *23*, 561-566.

A. El-Ghayoury, H. Hofmeier, B. de Ruyter, U. S. Schubert: "Combining covalent and non-covalent cross-linking: a novel terpolymer for two-step curing applications", *Macromolecules* **2003**, *36*, 3955-3959.

H. Hofmeier, U. S. Schubert: "Supramolecular branching and cross-linking of terpyridine-modified copolymers: complexation and decomplexation studies in diluted solution", *Macromol. Chem. Phys.* **2003**, *204*, 1391-1397.

J.-F. Gohy, H. Hofmeier, A. S. Alexeev, U. S. Schubert: "Aqueous micelles from supramolecular graft copolymers", *Macromol. Chem. Phys.* **2003**, 1524-1530.

H. Hofmeier, S. Schmatloch, D. Wouters, U. S. Schubert: "Linear terpyridine-ruthenium(II) poly(ethylene glycol) coordination polymers", *Macromol. Chem. Phys.* **2003**, *204*, 2197-2203.

U. S. Schubert, G. Hochwimmer, S. Schmatloch, H. Hofmeier: "A novel class of smart materials", *Europ. Coatings J.* **2003**, 28-34.

H. Hofmeier, A. El-Ghayoury, U. S. Schubert: "Combination of supramolecular cross-linking with covalent cross-linking through epoxide ring-opening including gel-studies", *e-polymers* **2003**, *no. 053*, 1-15.

P. R. Andres, H. Hofmeier, B. G. G. Lohmeijer, U. S. Schubert: "Synthesis of 4'-functionalized 2,2':6',2"-terpyridines *via* the pyridone route: symmetric and asymmetric *bis*-complex formation", *Synthesis*, **2003**, 2865-2871.

S. Schmatloch, A. M. J. v. d. Berg, A. S. Alexeev, H. Hofmeier, U. S. Schubert: "Soluble high molecular mass poly(ethylene oxide)s *via* self-organization", *Macromolecules*, **2003**, *36*, 9943-9949.

A. El-Ghayoury, H. Hofmeier, A. P. H. J. Schenning, U. S. Schubert: "Self-assembled chiral terpyridine ruthenium complexes", *Tetrahedr. Lett.* **2004**, *45*, 261-264.

H. Hofmeier, A. El-Ghayoury, A. P. H. J. Schenning, U. S. Schubert: "New supramolecular polymers containing both terpyridine metal complexes and quadruple hydrogen bonding units", *Chem. Commun.* **2004**, in press.

S. Schmatloch, A. M. J. v. d. Berg, H. Hofmeier, U. S. Schubert: "Linear coordination polymers: synthetic strategies and solution viscosities", *Design. Monom. Polym.* **2004**, in press.

H. Hofmeier, S. Schmatloch, D. Wouters U. S. Schubert: "Metallo-supramolecular polymers: towards new functional materials with controlled nanostructures", *Trans. Mater. Res. Soc. J.* **2004**, in press.

H. Hofmeier, E. Herdtweck, U. S. Schubert: "Asymmetric bipyridine-terpyridine-copper(II) complexes: an approach for new supramolecular architectures", *Zeitschr. Anorg. Allg. Chem.* **2004**, *630*, in press.

H. Hofmeier, P. R. Andres, R. Hoogenboom, E. Herdtweck, U. S. Schubert: "Terpyridine metal complexes as building blocks for new metallo-supramolecular architectures", submitted.

H. Hofmeier, U. S. Schubert: "Recent developments in the supramolecular chemistry of terpyridine metal complexes", submitted.

H. Hofmeier, A. El-Ghayoury, A. P. H. J. Schenning, U. S. Schubert: "Synthesis and optical properties of (a)chiral terpyridine-ruthenium complexes", submitted.

H. Hofmeier, A. El-Ghayoury, U. S. Schubert: "Free-radical and thermal curing of terpyridine modified terpolymers", submitted.

### **Non-refereed publications**

U. S. Schubert, P. R. Andres, H. Hofmeier, "Terpyridine ruthenium(II) complexes: towards new metallo-supramolecular architectures", *Polym. Mat. Sci. Eng.* **2001**, 85, 510-511.

U. S. Schubert, H. Hofmeier: "Metallo-supramolecular graft copolymers", *Polym. Mat. Sci. Eng.* **2002**, 87, 209-210.

H. Hofmeier, J.-F. Gohy, U. S. Schubert: "Metallo-supramolecular graft copolymers: micelle formation", *Polym. Mat. Sci. Eng.* **2003**, 88, 193-194.

H. Hofmeier, A. El-Ghayoury, U. S. Schubert: "Supramolecular polymers containing terpyridine complex and hydrogen bonding units", *Polym. Prepr.* **2003**, 44, 711-712.

H. Hofmeier, S. Schmatloch, U. S. Schubert: "Supramolecular polymers based on poly(ethylene glycol)-terpyridine ruthenium systems", *Polym. Prepr.* **2003**, 44, 709-710.

H. Hofmeier, U. S. Schubert: "Supramolecular terpolymers for covalent and non-covalent cross-linking", *Polym. Prepr.* **2003**, 44, 91-92.